



UNIVERSITE BLAISE PASCAL
Clermont-Ferrand, France

UFR Lettres Langues et
Sciences Humaines
GEOLAB UMR 6242 - CNRS



UNIVERSIDAD NACIONAL DEL SUR
Bahía Blanca, Argentina

Departamento de Geografía
y Turismo

HUMAN IMPACTS AND FLUVIAL METAMORPHOSIS

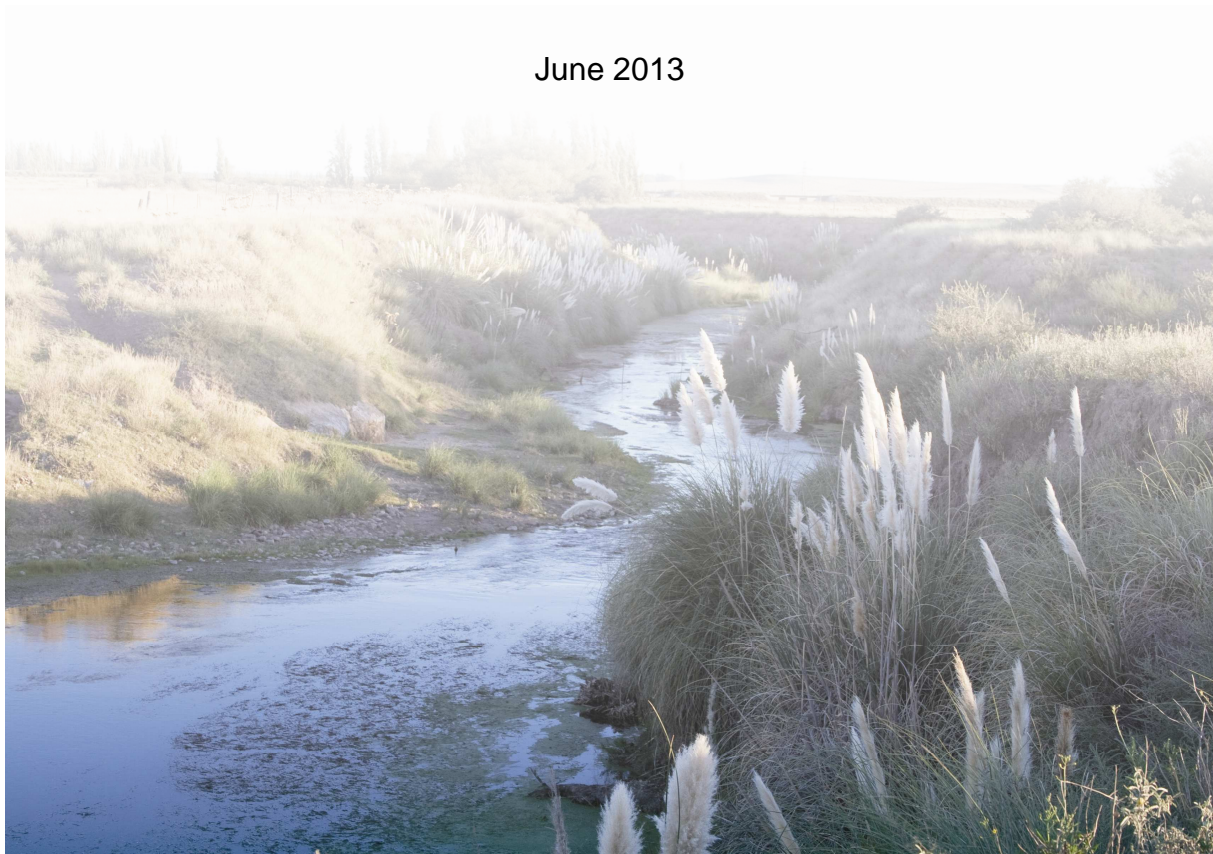
The effects of flow regulation on the hydrology, morphology
and water temperature of the Sauce Grande River, Argentina

by

Ana CASADO

A thesis submitted in partial fulfilment of the requirements for the degree of
Doctor of Philosophy in Geography

June 2013





UNIVERSITE BLAISE PASCAL
Clermont-Ferrand, France

UFR Lettres Langues et Sciences Humaines
GEOLAB UMR 6242 - CNRS



UNIVERSIDAD NACIONAL DEL SUR
Bahía Blanca, Argentina

Departamento de Geografía
y Turismo

IMPACT ANTHROPIQUE ET METAMORPHOSE FLUVIALE

Effets de la régulation du débit sur
l'hydrologie, la morphologie et la
température de l'eau de la Sauce
Grande, Argentine

IMPACTO HUMANO Y TRANSFORMACIÓN FLUVIAL

Efectos de la regulación de caudal
sobre la hidrología, la morfología y
la temperatura del agua del río
Sauce Grande, Argentina

Ana CASADO

Thèse soumise pour l'obtention du
Doctorat de Géographie

Tesis de
Doctorado en Geografía

Juin 2013

Junio 2013

THESIS COMMITTEE

Prof. Laurent Schmitt
Université de Strasbourg, France

Prof. M. Cintia Piccolo
Universidad Nacional del Sur, Argentina

Prof. David M. Hannah
University of Birmingham, UK

MCF Dov Corenblit
Université Blaise Pascal, France

Prof. Jean-Luc Peiry
Université Blaise Pascal, France

Prof. Alicia M. Campo
Universidad Nacional del Sur, Argentina

PARA USO DE LA UNIVERSIDAD NACIONAL DEL SUR

Esta Tesis se presenta como parte de los requisitos para optar al grado Académico de Doctor en Geografía, de la Universidad Nacional del Sur (UNS), en el marco del Programa de Cotutela firmado entre este establecimiento y la Université Blaise Pascal (UBP), Francia y no ha sido presentada previamente para la obtención de otro título en estas Universidades u otras. La misma contiene los resultados obtenidos en investigaciones llevadas a cabo en el área de Geografía Física, dependiente del Departamento de Geografía y Turismo de la UNS y en el laboratorio GEOLAB UMR 6042, dependiente de la UBP, durante el período comprendido entre el 16 de septiembre de 2008 y el 7 de mayo de 2013 bajo la dirección de la Dra. Alicia M. Campo, Profesora Titular de Geografía de la UNS e Investigadora Independiente del CONICET y del Dr. Jean-Luc Peiry, Professeur des Universités de la UBP e Investigador del CNRS.

Ana Casado

18 de junio de 2013

Departamento de Geografía y Turismo - GEOLAB UMR 6042

UNIVERSIDAD NACIONAL DEL SUR - UNIVERSITE BLAISE PASCAL



UNIVERSIDAD NACIONAL DEL SUR
Secretaría General de Posgrado y Educación Continua

La presente tesis ha sido aprobada el .../.../..... , mereciendo
la calificación de (.....)

A

ACKNOWLEDGEMENTS

The following paragraphs are addressed to those that have contributed to this thesis work. The text is written in three languages; far from being pretentious, this section aims to acknowledge all the French, Argentinean and English people that have helped to the progression and accomplishment of this research. I sincerely apologize for any grammar and/or spelling mistake in my French or English writing; regarding the bits in Spanish, I have no excuses.

Je remercie très sincèrement mon directeur de thèse en France, **Jean-Luc Peiry**, pour son soutien inconditionnel, autant sur le plan académique que personnel. Malgré mes connaissances plutôt légères sur la dynamique des systèmes fluviaux, il s'est chargé de mon encadrement depuis mon arrivée en France et c'est grâce à ses encouragements, ses conseils et ses suggestions toujours avisées que j'ai réussi à achever mon parcours doctoral. Autre que ses qualités scientifiques indéniables, ses qualités humaines font l'objet de ma plus grande admiration. Sans son encadrement et son soutien, cette thèse n'aurait sûrement pas la forme qu'elle a aujourd'hui. J'espère, très sincèrement, avoir été à la hauteur de la confiance qu'il m'a accordée.

La **Dra. Alicia Campo**, mi directora de tesis en Argentina, es sin duda la piedra fundamental de mi carrera de postgrado. Desde las tareas de archivo hasta las tesis defendidas, ya suman más de 10 años de formación constante y desinteresada. Seguramente, esta tesis no hubiera existido sin la confianza que me tuvo desde los inicios, sin sus enseñanzas, tanto científicas como de la vida en general y sin su estímulo permanente para crecer y perfeccionarme. Esta tesis tampoco hubiera existido sin su fuerza, convicción y empuje en las etapas de creación del programa de tesis en co-tutela internacional. Por estas y por un sinnúmero de razones, le estoy y le estaré eternamente agradecida. Espero sinceramente que este trabajo de tesis esté a la altura de sus expectativas.

This thesis would not have been possible without the support of **Prof. David Hannah** on water temperature analysis. I sincerely thank him for his generous help, for the hospitality he showed to me during my visits to England, for the time he has spent editing countless revisions of manuscripts and for letting me join his research group on many exciting activities. His good advice and suggestions were decisive to the accomplishment of the chapter on river water temperature, and his teachings inspired me to redefine my research interests. I sincerely hope that this thesis work is up to his expectations.

I would like to extend my sincere thanks to the remaining members of the thesis committee, **Prof. Laurent Schmitt** (Université de Strasbourg, France), **Prof. Cintia Piccolo** (Universidad Nacional del Sur, Argentina), and **MCF Dov Corenblit** (Université Blaise Pascal), for spending their time on careful reading of the thesis manuscript as well as for their insightful comments and questions.

Je remercie également tous les membres du laboratoire GEOLAB - les doctorants, les permanents, ceux qui sont partis et ceux qui sont arrivés - pour leur accueil toujours chaleureux, leur aide précieuse dans les domaines où je suis moins compétente, leurs conseils toujours judicieux, la passion qu'ils transmettent dans leur discours scientifique, le dépannage géomatique, informatique et (notamment) linguistique et les moments de convivialité partagés autour de table, pendant les pauses café-cigarette ou

autour d'une bière, plus tard. Malgré mon absence régulière pendant la période de rédaction de thèse, l'ensemble du laboratoire fait l'objet de ma plus sincère amitié et de ma plus grande reconnaissance.

Igualmente, quiero expresar mi más sincera gratitud a los decanos, secretarios, personal administrativo y profesores del Departamento de Geografía y Turismo por la buena predisposición y la ayuda constante que me brindaron para poder cumplir con los requisitos de postgrado, lo cual estando lejos una buena parte del tiempo no fue nada fácil. Muchísimas gracias también por la confianza y el apoyo para la creación de la cotutela con Francia y por el recibimiento siempre afectuoso que me acordaron.

Agradezco enormemente a la Autoridad del Agua de la provincia de Buenos Aires por permitir el acceso a las instalaciones del Dique Paso de las Piedras y alrededores, por su colaboración para la instalación de material de campo y por la provisión de datos de caudal. Muchas gracias igualmente al Ministerio de Agricultura de la Nación y al Centro de Información Meteorológica por la provisión gratuita de datos de temperatura y precipitación.

Ces remerciements ne seraient pas complets sans adresser un petit mot à **Fabienne, Cathy** et à tous les responsables et enseignants du Lycée La Présentation Notre Dame. Leur soutien et la flexibilité qu'ils m'ont accordée pendant les derniers mois de rédaction de la thèse ont été décisifs pour que je puisse achever mon travail dans les meilleures conditions.

Je n'ai jamais eu des doutes sur le parcours choisi, mais des moments de découragement et de grosse fatigue que j'ai surmonté grâce au soutien de mes amis. Un grand merci donc à **Erwan, Marion, Greg, Charlotte, Nico, Alex, Guille, Yoann, Naman, Rouquin, Clément, Mymi, Willy, Elise** pour m'avoir permis faire partie de leurs vies et pour être toujours là, malgré une thèse qui sur la fin est devenue très preneuse de temps.

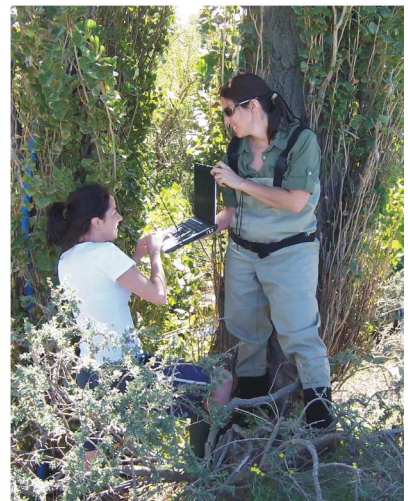
Un millón de gracias también a **Yanina, Fernanda, el Negro, Mariana, Eri, Fede, Lucho, Euge, Martín, Fabri** por el aguante antes, después y durante cada viaje a Argentina. Saber que siguen ahí, al pie del cañón, después de tanto tiempo y de tantas ausencias me ayuda a seguir con mis objetivos por mas difícil que a veces pueda volverse el desarraigo.

Also, I would like to thank some great people who made my stay in England unforgettable. **James F., James H., Grace, Kieran, Phil, Sunisa, Dario, Vangelis, Isabella**, many thanks to all of you for make me feel so welcome in Birmingham, for helping with my horrible English, for providing me a place to stay so many times and for sharing so many nice moments around a pint.

Je dédie cette thèse à ma famille française : **Mado, Serge, Fabien** et **Guillaume Guerra**. Un grand merci à eux tous pour m'avoir accueilli comme l'une de leurs. Notamment, j'adresse un grand merci à Fabien pour m'avoir soutenue et encouragée depuis le tout début. Muchas gracias igualmente a mi papá por el apoyo económico, a mi mama por el apoyo moral y a mi hermano por un millón de razones.

Finalmente, quisiera agradecer a todos aquellos que me acompañaron y ayudaron durante las campañas de campo. Sin su ayuda y buena predisposición permanentes esta tesis no podría haber sido finalizada. Un millón de gracias a mis directores, **Jean-Luc** y **Alicia**, a mis amigos y compañeros geógrafos, **Verónica, Paula, Jorge, Mariana** y **Julia**, a mi hermano **Horacio** y a mis amigos que nada tienen que ver con la geografía pero que vinieron a hacer el aguante igual: **Fernanda** y **el Negro**.

Muchísimas gracias a todos.





INTRODUCTION.....	1
CHAPTER 1: Research Context	
1. The effects of dams on alluvial fluvial systems	13
2. The Paso de las Piedras Dam on the Sauce Grande River	32
3. Research Purpose, Hypothesis and Structure.....	57
CHAPTER 2: Generation of baseline data	
1. Methods.....	68
2. Results	84
2.1. The terrain model of the river basin	84
2.2. Climatic data series	87
2.3. The hydrological model of the upper river basin	96
2.4. Daily flow rates for the unregulated river	101
2.5. Daily flow rates for the regulated river	104
3. Discussion and Conclusions.....	107
CHAPTER 3: The Water Balance of the Dam Reservoir	
1. Methods.....	121
2. Results	128
2.1. The Water Balance Model of the Paso de las Piedras Reservoir	128
2.2. Patterns in the reservoir hydrology	134
2.3. Reservoir size-yield-performance	140
2.4. The degree of impoundment	144
3. Discussion and Conclusions.....	146
CHAPTER 4: Dam Impacts of First Order	
1. Methods.....	165
2. Results	175
2.1. Dam impacts on the river flow regime.....	175
2.2. Dam impacts on the river water temperature	185
3. Discussion and Conclusions.....	206

CHAPTER 5: Dam Impacts of Second Order

1. Methods.....	231
2. Results.....	240
2.1. Changes in the river morphology.....	240
2.2. Changes in the fluvial landscape.....	259
3. Discussion and Conclusions.....	272
CONCLUSIONS AND PERSPECTIVES	287
Résumé.....	293
Resumen.....	303
Reference List	313
List of Figures	341
List of tables.....	349

This thesis work evaluates the degree to which the Paso de las Piedras Dam and its reservoir (water supply) have disrupted the hydrologic continuity of the Sauce Grande River, and quantifies the impacts of flow regulation on the hydrology, morphology and water temperature of the river downstream. Building upon the existing literature on regulated rivers, this thesis provides an integrated and systemic assessment of the broad-scale impacts of the dam based on the understanding of ‘natural’, unregulated fluvial processes upstream from the impoundment. Besides yielding new information on the hydrology, water temperature and morphology of the Sauce Grande River, this study generates new climatic and hydrological data achieved from physical and regression modelling and implements a methodological framework to hydrogeomorphological assessment of ungauged basins.

1. JUSTIFICATION OF THE STUDY

The hydrological, thermal and morphological effects of the Paso de las Piedras Dam on the Sauce Grande River are the focus of this study. The river and the dam are located in the central portion of the south-western Buenos Aires province (SWBA), Argentina (Fig. I.1). The Sauce Grande collects its waters on the eastern slope of the Sierra de la Ventana Range and flows down into the Atlantic Ocean draining a basin area of about 4600 km² (Luque *et al.*, 1979). It constitutes one of the most important freshwater resources within the central SWBA (Borromei, 1991; Zavala and Quattrocchio, 2001; Schefer, 2004), and has been at the basis of the agricultural and urban development of the region.

Despite that the climate type is temperate sub-humid (Campo *et al.*, 2004), inter-annual variability in moisture is strong and linked to El Niño Southern Oscillation and other large-scale atmospheric phenomena related to anomalous circulation within the South Atlantic Convergence Zone (Scian, 2000; Labraga *et al.*, 2002; Scian *et al.*, 2006). Episodes of drought (or flooding) are frequent (Campo *et al.*, 2009; Bohn *et al.*, 2011) and impact very seriously on the regional economy (Troha and Forte Lay, 1993; Andrade *et al.*, 2009), which is based on rainfed agriculture and livestock grazing of unimproved grasslands (Scian, 2000).

The central SWBA has known qualitative and quantitative deficiencies for drinking water supply periodically (Andrés *et al.*, 2009). Recurrence of drought and increased water demand subsequent to population growth led to a number of water crises which, in turn, led to systematic advances in local practices of water management. The Paso de las Piedras Dam has impounded the middle river section since 1978 for water supply to a population that today reaches about 350 000 people mainly concentrated in the cities of Bahía Blanca and Punta Alta. At full supply, its reservoir has a surface area of 30 km², depth of 25 m and active storage capacity of 325 hm³ (Schefer, 2004). Climate variability and population growth combine to generate low resilience to deficiencies in local water resources; accordingly, dam operational procedures seek to store and conserve a maximum volume of water to assure supply in periods of drought.

impoundment on the Sauce Grande River specifically, this study generates spatial, climatic and hydrologic data and implements a methodological framework to hydrological assessment of ungauged basins. The new climatic, hydrologic and morphologic information yielded herein has triple applicability: (i) it informs dam managers about the complex behaviour of the river system, (ii) it contributes to improve reservoir operation policies while maintaining the overall integrity of the river system, and (iii) it provides a consistent scientific platform on which to base further research efforts conducting to an interdisciplinary framework of river restoration. Furthermore, the methods implemented in this research are widely transferable to hydrological assessment of ungauged basins worldwide with special applicability to semiarid regions.

2. BACKGROUND

Rivers exist as a *continuum* of linked physical and biological processes (Vannote *et al.*, 1980) dependent on longitudinal, lateral and vertical transfers of energy, material and biota (Petts and Amoros, 1996). Despite the unquestionable value of dams for water resources management (Magilligan and Nislow, 2005; Petts and Gurnell, 2005), dam construction and reservoir operation disrupts strongly the longitudinal continuity of fluvial processes along the river system (Petts, 1984), inducing serial discontinuities in the river *continuum* (Ward and Stanford, 1983; 1995a; Stanford and Ward, 2001).

Concern about the impacts of dams on fluvial systems has grown as the rate of dam building increased worldwide (Brandt, 2000). The works of Graff (2005) and Petts and Gurnell (2005), for example, provide an exhaustive review of advances in the scientific understanding of the effects of river impoundment. At present, literature on hydrologic, geomorphic and ecologic impacts of dams is abundant, and the number of studies that inspired this research is too large to be cited herein. This study builds clearly on the concept of discontinuity (Ward and Stanford, 1983; 1995a; Stanford and Ward, 2001) in the continuity of the fluvial hydrosystem (Petts and Amoros, 1996), and is inspired strongly in the work of Petts (1979; 1984) based on the idea of orders of response to disruption in the equilibrium of fluvial processes (Schumm, 1969). We certainly forget to cite many study cases and baseline works that inspired this research; for example, the ecology-related concept of *hydrological alteration* introduced by Richter *et al.* (1996), based on the concept of *natural flow regime* developed by Poff *et al.* (1997), among many others.

The conceptual basis of our research may be simplified as shown in Figure I.2. In their natural state, rivers are three-dimensional systems in dynamic equilibrium dependent on climatic, topographic and geologic drivers at the scale of the river basin. River impoundment by dams is seen as the greatest source of hydrological disruption by human activities. Sediment and water detention in reservoirs modify three critical elements of the fluvial system downstream (i) the river ability to transport sediment, (ii) the amount of sediment available to transport, and (iii) the quality of the running waters, all of which ultimately triggers a series of adjustments until the system either accommodates the disturbance or reaches a new equilibrium state.

Studies on impounded rivers worldwide have documented a wide range of morphologic

and ecologic adjustments to altered hydrologic conditions including changes in the channel geometry (cross-sectional shape, planform and slope), in the diversity and patterns of succession of riparian communities and in the structure and function of aquatic organisms. However, the direction, magnitude, temporal rate and spatial extent of morphologic and ecologic change were reported to vary substantially from one regulated river to another. The fluvial response to upstream impoundment is complex and depends on a number of factors related to the dam size, purpose and operation history imposing specific patterns of flow regulation, and on the environmental setting of the river system imposing a greater or lesser resistance to change. Quoting Phillips (2003b), *it may be that the only generalization is that the downstream effects of dams are usually significant and frequently extensive, and that the effects vary from one stream or reach to another, and over time and downstream.*

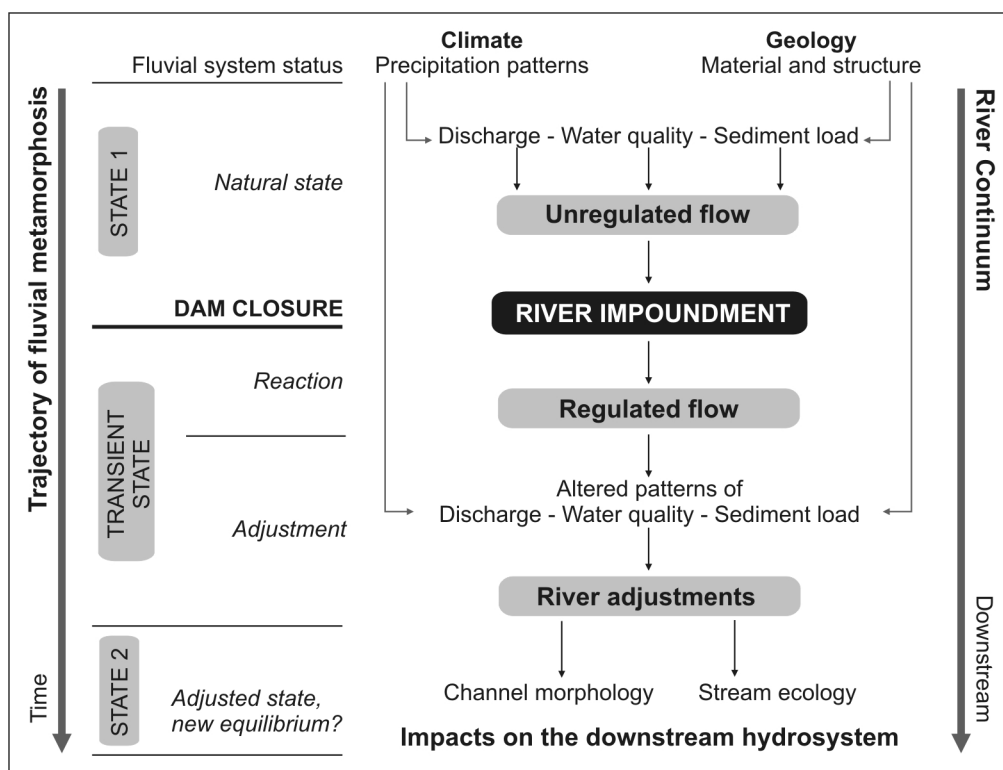


Figure I.2: Conceptual scheme of fluvial response to river impoundment.

3. RESEARCH CONTEXT AND OBJECTIVES

This research has been motivated by the need for (i) an integrated assessment of the hydrology of the dam reservoir and of the broad-scale effects of the dam on the river environment, and (ii) generation of climatic, hydrologic and spatial data to hydrological assessment of the river basin itself as well as of the dam reservoir and its impacts over time. The purpose of this research is then double and consists in (i) assessing the degree of flow regulation induced by the dam and its impacts on the hydrology, water temperature and morphology of the river downstream (ii) based on prior generation of

baseline data that permits to assess spatiotemporal variations in hydrological, water temperature and morphological processes accurately.

Accordingly, the methods selected for analysis, the corresponding results and the discussion of the key findings from this investigation were grouped into two principal sets discriminating (i) generation of spatial, climatic and hydrologic data, and (ii) assessment of the effects of flow regulation on the river environment downstream. As shown in Figure I.3, the structure of the thesis manuscript is driven by this main separation relative to the research motivations.

The first chapter of the present manuscript synthesizes the current knowledge on impounded rivers. Mechanisms of flow regulation relative to the dam size and purpose and impacts of flow regulation on the river system downstream are revisited based on the orders of fluvial change presented by Petts (1984). Examples of hydrological and morphological change below dams are provided based on a number of studies on regulated rivers worldwide. Afterwards, the chapter explores the interconnections between the use and management of water resources within the Sauce Grande Basin and its regional environment. It provides an integrated understanding of the complex behaviour of local water resources face to the natural climate variability, and its implications for water management face to the evolving needs of the involved society. Finally, the research objectives and hypothesis are delineated based on the literature review.

Chapter 2 presents the procedures performed to generate spatial, climatic and hydrological data and the corresponding results. The terrain model of the river basin is introduced first because the configuration of the terrain surface is a key factor controlling climatic and hydrological processes. Afterwards, the chapter describes the procedures performed to derive climatic and hydrologic data required to simulate and calculate river flow data. A model for runoff simulation from rainfall within ungauged basins is developed and evaluated.

The hypothesis to test in this research states that the dam disrupts the longitudinal continuity of fluvial processes strongly. As a result, the overall hydrology of the river downstream is altered and the channel morphology and the riverine landscape change in response to altered hydrologic conditions. This logic guides the research objectives and governs the structure of the thesis results. Accordingly, results from this investigation are articulated into three chapters that test each component of the hypothesis enunciate separately (Chapters 3 to 5).

Chapter 3 quantifies the degree of flow regulation induced by the dam. This quantification is achieved based on the prior understanding of the water balance of the dam reservoir. Temporal patterns in the hydrologic components of the water balance equation are inspected to identify dynamics in the reservoir hydrology over time, and a Reservoir Water Balance Model is developed as tool for dam management. Analysis of the reservoir water balance provides the basis to further assessment of the relationships between reservoir size, yield and performance. The degree to which the dam impounds the middle river section is evaluated by quantifying the dam potential to interrupt water fluxes from the headwater sources relative to the reservoir capacity and performance to meet human requirements for water supply.

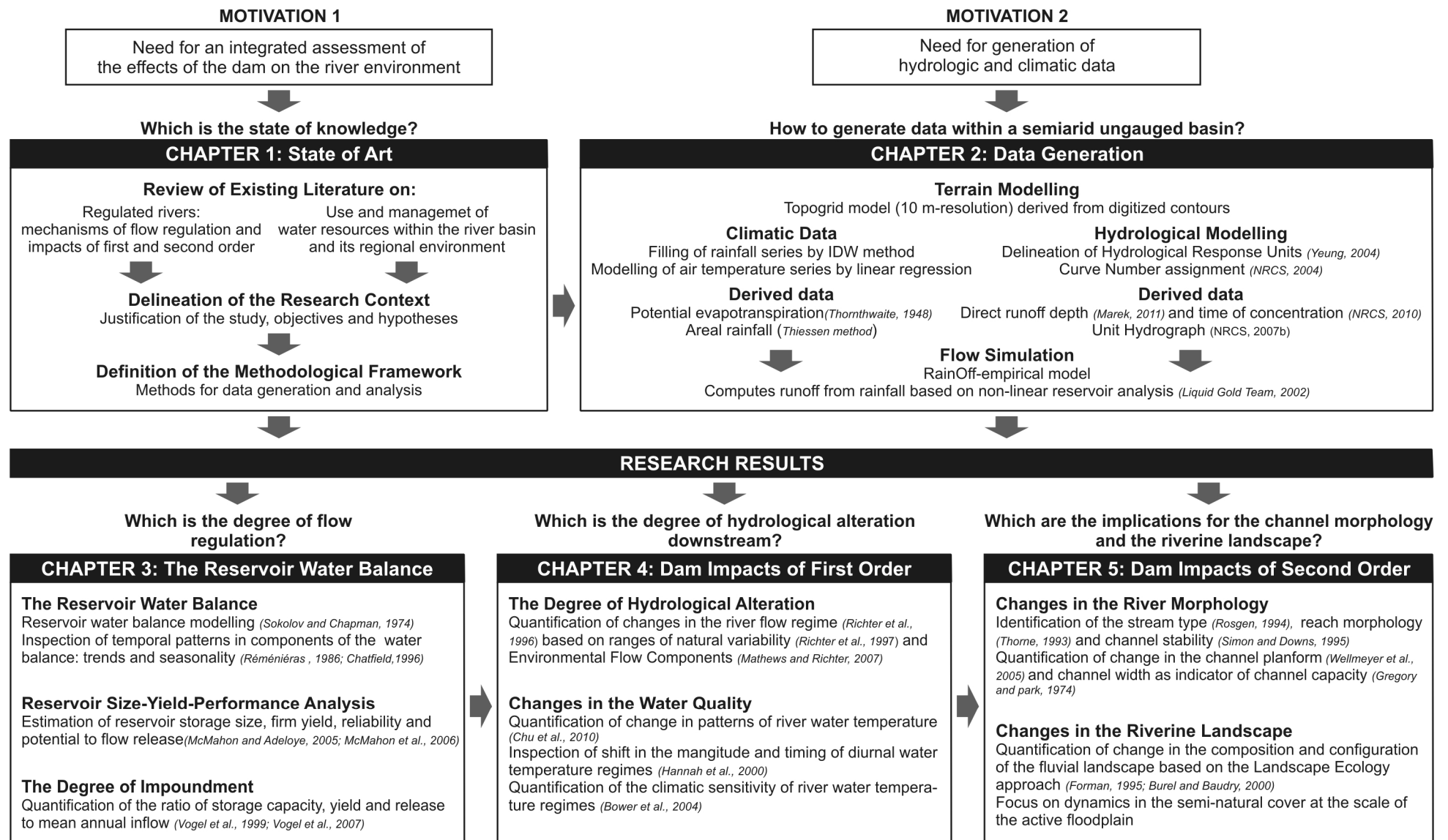


Figure I.3: Scheme of the structure of the thesis manuscript relative to the research purposes.

Chapter 4 evaluates the dam impacts of first order, i.e. the impacts that occur immediately after the dam closure and that depend directly on the dam operational procedures. Analysis focuses on two of the three primary changes recognized by Petts (1984) namely changes in the river flow regime and the river water quality with focus on the river thermal regime. The magnitude and distance of change in the river flow regime and water temperature after dam construction are quantified based on the comparison of river flow and thermal conditions occurring synchronically upstream and downstream from the impoundment over time. Results are structured into two sections assessing changes in the river flow regime and the river water temperature separately. Interconnections between both variables are examined in the Discussion section.

Finally, Chapter 5 evaluates the dam impacts of second order, i.e. the response of the river channel morphology and the associated riparian zone to altered patterns of flow and sediment over time. Analysis is structured into two linked subsections exploring (i) morphologic changes below the dam with focus on the lateral mobility and the channel capacity at the scale of the river segment, and on the channel stability at the scale of the river reach, and (ii) the evolution of the fluvial landscape at the scale of the active floodplain with especial regard on the riparian zone. As the river Sauce Grande is an agricultural stream, special attention is given to the dynamics in land use types within the river environment to identify their potential effects on the river channel morphology regardless of the effects of the dam. Methods use coupled diachronic and synchronic analysis based on comparison of land cover types and fluvial forms between the regulated and the unregulated river over time. This permits to quantify rates of change in two dimensions: the trajectory of changes since dam closure (time) and the distance of changes with respect to the dam (space).

4. DEVELOPMENT OF THE RESEARCH WORK

This thesis work is the result of six years of research efforts (Fig. I.4). The first year was dedicated almost exclusively to establish the international collaborations involved in the development of the research project, which builds under the joint supervision of France and Argentina. A 2-month field campaign was effectuated during austral winter 2008 (1, Fig. I.4) to delineate the research project relative to the overall state of knowledge on the topic; field works included stream reconnaissance surveys, gathering of existing information and data and establishment of contact with dam managers. These activities provided the basis to delineate the research objectives and to postulate the research hypothesis.

The phase of data collection took about a year and a half. Two 3-month field campaigns were effectuated during austral summer 2009 (2, Fig. I.4) and austral winter 2010 (3, Fig. I.4) to install instrumental of measure and to survey the hydrogeomorphologic and water quality characteristics the stream. The period of time comprised between both field campaigns was used to generate the set of spatial, climatic and hydrologic data that were missing for analysis.

After the overall set of data required to analysis was achieved, the phase of data treatment spanned about 6 months. Errors in prior data calculation and modelling were

detected, so that some parameters required to be recalibrated. A supplementary field campaign was effectuated in early 2011 (4, Fig. I.4) to collect new data required to parameterize the models. The present manuscript is written in English to meet concomitant requirements of the two countries involved in the development of the thesis project.

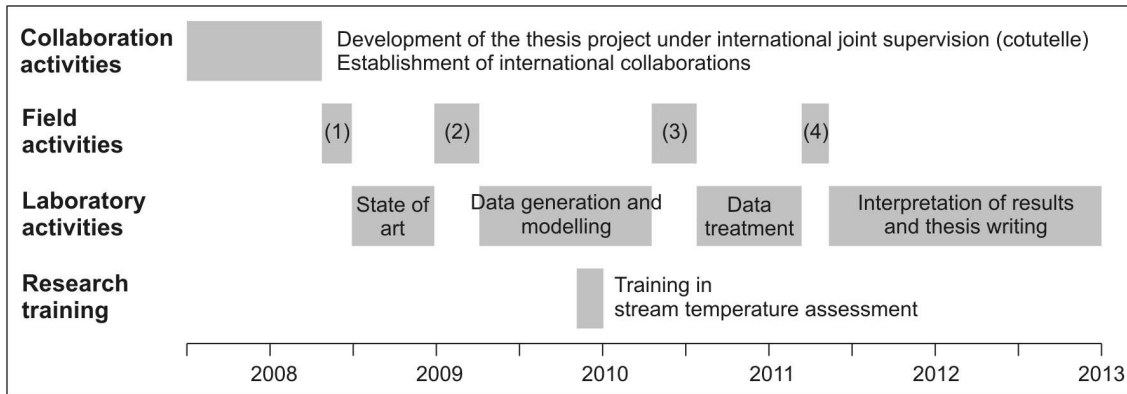


Figure I.4: Gantt chart showing the progress of the research project

CONTENTS

- 1 Dam effects on alluvial fluvial systems
 - First-order impacts: regulated inputs below dams
 - Second-order impacts: the river channel response
- 2 The Paso de las Piedras dam on the Sauce Grande River
 - The vulnerability of local water resources
 - The water demand: agriculture, population and industry
 - Practices and policies of water management
- 3 Research purpose and hypothesis

SECTION

1

THE EFFECTS OF DAMS ON ALLUVIAL FLUVIAL SYSTEMS

River regulation for water management has been the key for the advancement of human civilizations (Petts and Gurnell, 2005). Dams have been built for centuries, although the construction of large dams, i.e. dams having an influence on fluvial processes, initiated in the 20th Century and accelerated strongly since the 1950's (Brandt, 2000; Graf, 2005; Petts and Gurnell, 2005; Wang *et al.*, 2007). As shown in Figure 1.1, rivers of the world are impounded by more than 45 000 large dams (W.C.D., 2000) and to present, few rivers are in a natural or semi-natural state (Surian and Rinaldi, 2003). According to the *Comité Argentino de Presas* (National Commission on Dams), Argentina accounts for 110 large dams. Most Argentinean dams are multipurpose, with hydropower (53 %), flood control (40 %) and water supply (21 %) as primary functions; recreation is an important secondary function to all dam types.

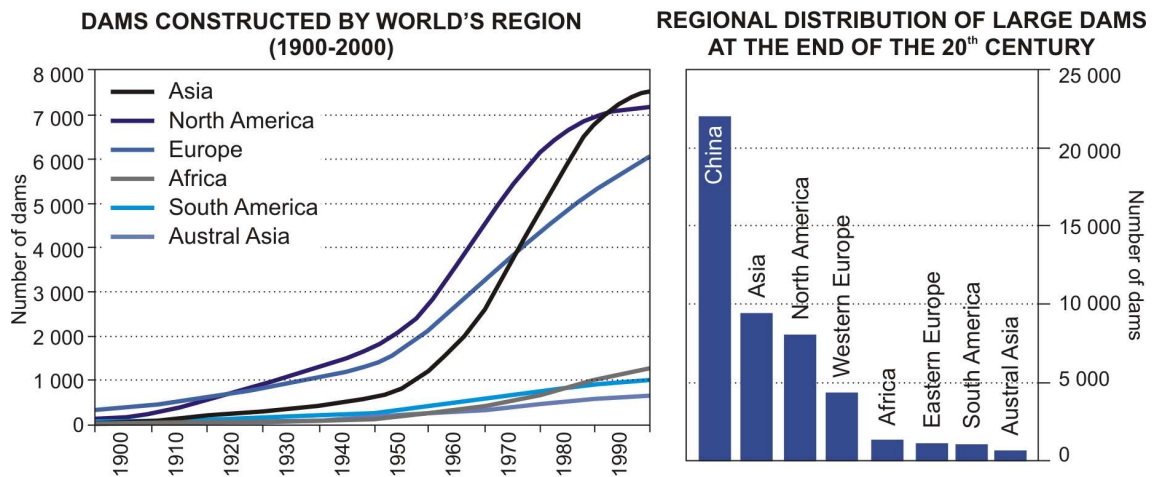


Figure 1.1: Dams constructed by world's region over the period 1900-2000 and regional distribution of large dams at the end of the 20th Century. After the World Commission on Dams (2000).

In spite of the unquestionable socioeconomic value of dams, dams represent the greatest source of fluvial disturbance induced by human activities (Petts, 1984; Graf, 2005; Magilligan and Nislow, 2005; Petts and Gurnell, 2005; Wang *et al.*, 2007). Most scientific concern about the hydrologic, geomorphic and ecologic impacts of river impoundment emerged during the 1960-1970's where the impacts of large dams became visible, and rapidly grown as the rate of dam building increased worldwide (Petts, 1980a; Brandt, 2000). However, the environmental impacts of Argentinean dams remain poorly evaluated, especially within small- and middle-size basins. Furthermore, programs for integrated management of water resources in Argentina are incipient.

This section introduces a brief review of the current knowledge on fluvial changes following dam construction and reservoir operation. It is structured into two linked subsections accounting for dam impacts of first and second order (*sensu* Petts, 1980a; 1984). Whilst the *impacts of first order* occur immediately after dam closure and

include changes in flow and sediment inputs into the river downstream, the *impacts of second order* are associated with the response of the channel morphology and primary vegetal communities to regulated quantities of water and material (Fig. 1.2). Third-order impacts (i.e. changes in fish and invertebrate populations, Petts, 1980a; 1984) are beyond the scope of this research and hence they are not discussed herein.

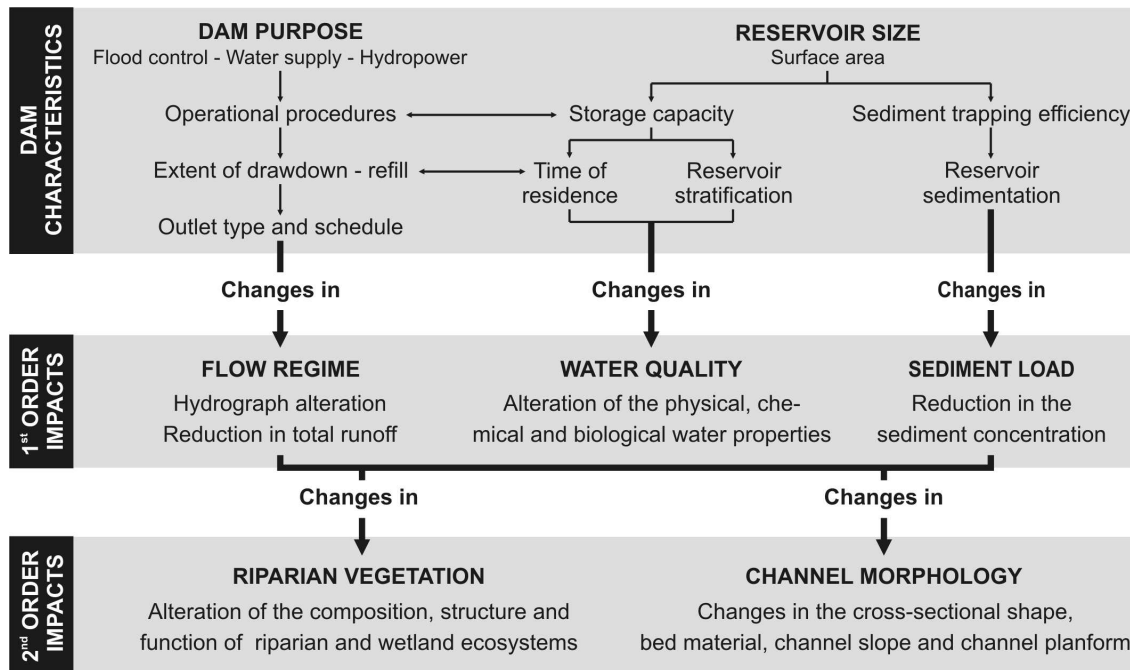


Figure 1.2: Orders of change of impounded river systems relative to the dam purpose and the reservoir size. Based upon Petts (1984), McCartney (2001) and Graf (2006).

1.1. FIRST-ORDER CHANGES: REGULATED INPUTS BELOW DAMS

According to Petts (1984), the effects of dams on the downstream river environment are primarily related to the reservoir size and to the dam purpose (Fig. 1.2). The *reservoir size* is a primary indicator of the potential impacts of dams on fluvial systems (Poff and Hart, 2002), because it determines the potential of the reservoir to (i) store and retain water and sediment (storage capacity and sediment trapping efficiency), and (ii) alter the quality of the stored water (residence time and stratification of the water column). On the other hand, the *dam purpose* (e.g. dams operating for hydropower, irrigation, water supply, flood and/or sediment control) influences the relationship between the volume of water stored within the reservoir and the magnitude, frequency and timing of flow release (release schedule) for a given outlet type. Water and sediment detention in large reservoirs ultimately alters the hydrology of the river system downstream.

1.1.1. Changes in the river flow regime

Dams intercept flow from headwater source areas (Kondolf, 1997) and control the

patterns of flow discharge within the river downstream (Petts, 1979; 1984). Mechanisms of flow regulation may differ substantially from one dam to another relative to the dam size and purpose; however, common to all dams is that they induce a different, artificial distribution of flows over time (Petts, 1984; Williams and Wolman, 1984).

Petts (1984) argued that there are three primary types of flow regulation: peak absorption, peak attenuation and release manipulation (Fig. 1.3). The first two types are strongly related to dams operating for *supply purposes* (e.g. water, energy, etc), which seek to store a maximum volume of water to assure supply in times of drought (conservation storage procedures). Peak flows from headwaters are either absorbed within the reservoir or reduced and delayed due to reservoir attenuation.

On the other hand, release manipulation is associated to dams designed for *flood control*, which keep the reservoir volume as low as possible so that floods can be attenuated or absorbed within the reservoir. Peaks may be fully or partially absorbed, and controlled reservoir evacuation may occur prior the flood arrival, behind the flood wave if it generates water excess, or in both cases. Because most dams are multipurpose, a wide range of controlled patterns of flow may occur downstream; some examples are given in Table 1.1.

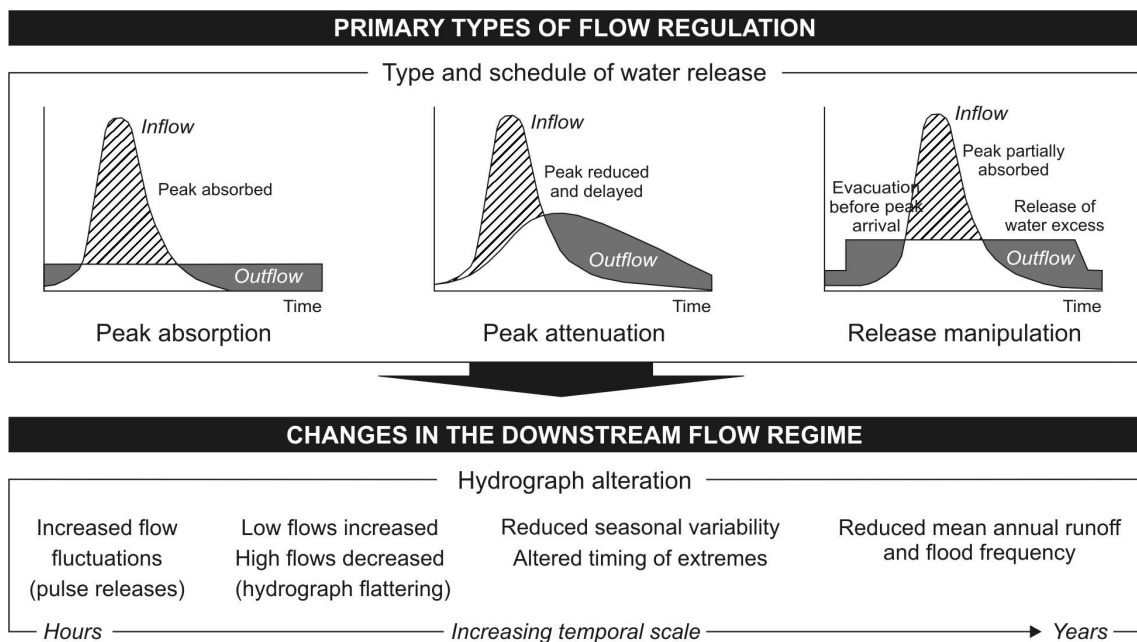


Figure 1.3: Common types of flow regulation and implications for the flow regime of the river downstream. Based upon Petts (1984).

The most common effect of dams is the attenuation (flattering) of the downstream hydrograph: high-flows are reduced, and the permanence of base-flows is consequently increased. Reduction of the magnitude and frequency of peak flows and floods is a common (logic) impact below dams operating for flood control (e.g. Yellow River below Sanmenxia Dam, Chien, 1985; Río Grande below Cochiti Dam, Richard and Julien, 2003). However, reduction of the magnitude and frequency of peak flows and floods has been documented below many dams, regardless of their purpose (Table 1.1).

Table 1.1: Hydrologic impacts of dams reported worldwide by dam purpose.

Country	Impoundment	Size	Opening	Hydrologic impacts	Citation
<i>Hydropower dams and multipurpose dams with hydropower as primary function</i>					
Belgium	Butgenbach Dam on Warche River	Large	1932	Major floods eliminated; frequency of large and medium floods reduced; low-flows increased.	Assani and Petit (2004)
Norway	Power stations on Fortun River	Large	1963	Mean flow reduced (from 20 to 7 m ³ s ⁻¹); peak flows reduced (from 140 to 86 m ³ s ⁻¹); low-flows increased.	Fergus (1997)
Scotland	Spey Dam on Spey River	Small	1942	Major floods reduced (60 %); minor floods absorbed; low-flows increased.	Gilvear (2004)
France	Several dams on the upper Rhône and tributaries	Large	Since 1960	High flows decreased; low flows increased; mean flow increased; altered seasonality.	Edouard and Vivian (1984) Vivian (1986; 1994)
USA, Montana	Fort Peck Dam on Missouri River	Large	1940	High-flows reduced; low-flows increased; timing of extremes altered.	Shields <i>et al.</i> (2000)
USA, Texas	Toledo Bend on Sabine River	Large	1967	Pulse-releases smoothed; no evidence of decline in annual peak flows after dam closure.	Phillips (2003b)
<i>Water supply dams</i>					
Australia	Mangrove Creek Dam on Mangrove creek	Large	1981	Mean daily flow and peak flows reduced; floods reduced (94 %).	Sherrard and Erskine (1991)
USA, Texas	Livingston Dam on Trinity River	Large	1968	No evidence of significant changes after dam closure.	Phillips <i>et al.</i> (2005)
<i>Irrigation dams</i>					
USA, California	Several dams on Sacramento-San Joaquin	Many	Since 1940	Winter peak flows eliminated; summer base flows increased; Q ₂ and Q ₁₀ decreased (94 % and 90 %).	Kondolf and Batalla (2005)
USA, Wyoming	Jackson Lake Dam on Snake River	Large	1916	Dramatic decrease in the frequency and magnitude of summer peak flows.	Marston <i>et al.</i> (2005)
<i>Flood control dams and multipurpose dams with flood control as primary function</i>					
USA, New Mexico	Cochiti Dam on Río Grande	Large	1973	Annual floods reduced (38 %); high-pulses duration increased; mean annual flow increased.	Richard and Julien (2003)
China	Sanmenxia Dam on Yellow River	Large	1960	Peak flows reduced (60 %); duration of medium flows increased (57 %).	Chien (1985)
Korea	Hapchon Dam on Hwang River	Large	1988	Major floods reduced; minor floods increased.	Choi <i>et al.</i> (2005)

According to Petts (1977), conservation reservoirs may be responsible for a reduction of 98 % in flood events if no overflow occurs. For example, Assani and Petit (2004) found that the major floods in the Warche River below Butgenbach Dam (hydropower) were fully eliminated and minor floods were reduced considerably. In Australia, Sherrard and Erskine (1991) documented a flood reduction of 94 % in Mangrove creek below Mangrove Creek Dam (water supply). Similarly, Kondolf and Batalla (2005) documented a reduction of 94 % and 90 % in annual and decadal floods, respectively, within the Sacramento – San Joaquin River Basin (irrigation).

Another common impact of dams is the increase in the magnitude of low flows, especially in rivers below dams operating for hydropower (e.g. Fortun River, Fergus, 1997; Missouri River, Shields *et al.*, 2000; Spey River, Gilvear, 2004). In some cases, increased low-flow magnitude below hydropower dams may entrain an increase of the river module (e.g. Upper Rhône, Edouard and Vivian, 1984; Vivian, 1986; 1994). Below dams designed for flood control, increase of the river module (e.g. Río Grande, Richard and Julien, 2003) or even increased magnitude of small floods (e.g. Hwang River, Choi *et al.*, 2005) is a common consequence of controlled flow release before and after the flood arrival.

Controlled patterns of flow release ultimately disrupt the natural seasonality of flows over the annual cycle. Seasonal maxima are frequently reduced (e.g. summer peaks in the Snake River below Jackson Lake Dam, Marston *et al.*, 2005) and/or dramatically altered in timing (e.g. Missouri River below Fort Peck Dam, Shields *et al.*, 2000). In the long term, water detention within the reservoir contributes to reduce the total volume of runoff downstream (Petts, 1984; McCartney *et al.*, 2001).

1.1.2. Changes in the river water quality

River impoundment by large reservoirs may lead to changes in the physical, chemical and biological properties of the stored water (Petts, 1984; McCartney *et al.*, 2001). Such changes occur as a result of two linked processes: (i) concentration of organic and inorganic materials within the reservoir, and (ii) reservoir stratification. As this research focuses on the dam effects on the river water temperature, the latter process is of particular interest.

As shown in Figure 1.4, water stored in deep reservoirs (i.e. more than 10 m-depth, Chapman, 1992) has a tendency to become thermally stratified and deoxygenated (Wetzel, 1975; Petts, 1984; McCartney *et al.*, 2001). Stratification of the water column is a natural consequence of variations in the water density with depth; water in the bottom (hypolimnion) is colder and denser than water in the surface of the lake (epilimnion). In deep temperate reservoirs that do not freeze such as Paso de las Piedras overturn occurs in autumn; water temperature in the epilimnion decreases due to cool weather and the vertical variations in water density decrease (Meybeck *et al.*, 1996). If temperatures fall below 4 °C, a cold inverse stratification may develop during the winter months (Chapman, 1992).

Thermal stratification influences the distribution of dissolved substances within the reservoir lake such as nutrients, metals and oxygen (Boehrer and Schultze, 2008). Whilst water in the epilimnion is well oxygenated and nutrient-rich (Petts, 1984;

McCartney *et al.*, 2001), water properties in the hypolimnion depend on the trophic status of the lake (Wetzel, 1975; Walker, 1979). The diagram shown in Figure 1.4 assumes a temperate eutrophic reservoir, where the deepest layers may be anoxic or oxygen-reduced during much of the year.

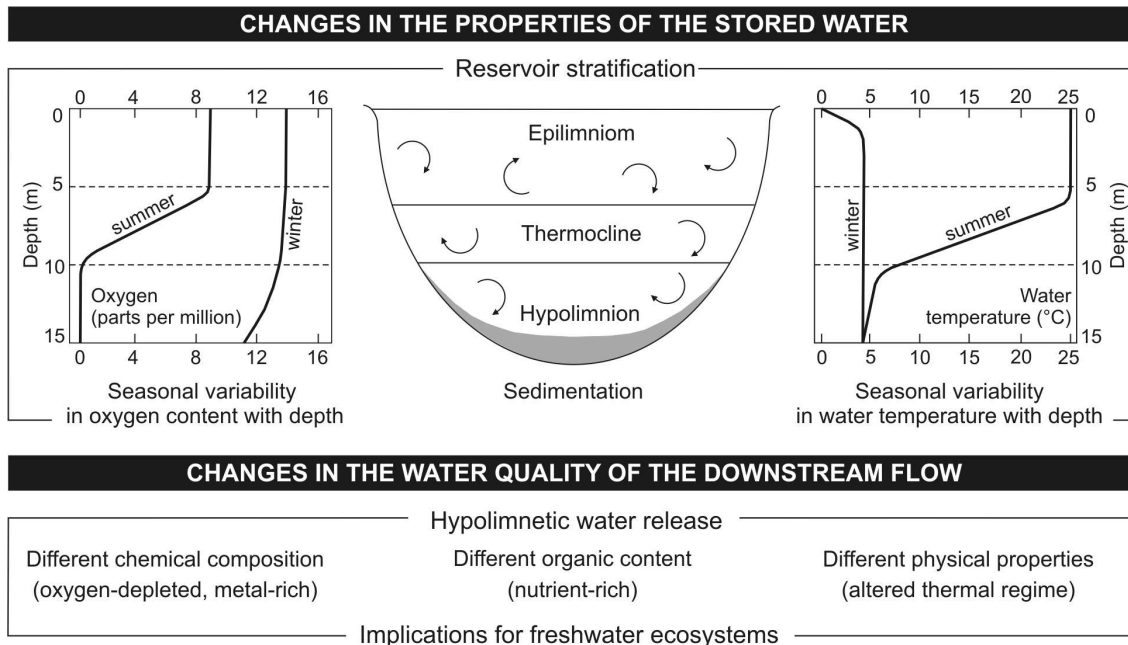


Figure 1.4: Stratification of deep temperate reservoirs and implications for the water quality of the river downstream. Based upon Wetzel (1975), Petts (1984) and McCartney (2001).

A special regard on river water temperature

River water temperature (RWT) is the most important physical property of streams and rivers (Webb, 1996; Caissie, 2006; Bonacci *et al.*, 2008; Webb *et al.*, 2008). It influences strongly the hydrological, chemical and biological processes within the river system (Hannah *et al.*, 2008b), and therefore has great ecological and water quality significance (Webb and Walling, 1992; Poole and Berman, 2001; Caissie, 2006).

The water temperature of streams and rivers is a measure of the concentration of heat energy in a stream relative to the volume of water (Poole and Berman, 2001). Under natural conditions, the thermal regime of rivers is driven by a number of physical factors (Fig. 1.5) affecting the heat exchange and the heating capacity of the stream (Ward, 1985; Webb, 1996; Poole *et al.*, 2001; Hannah *et al.*, 2004; Caissie, 2006). Atmospheric conditions and flow discharge influence river thermal patterns at a meso-scale (Ward and Stanford, 1979; Webb, 1996; Caissie, 2006), whilst the channel characteristics (topography and morphology) act as thermal buffers at the micro-scale (Poole *et al.*, 2001) moderating heat exchange at the water-streambed interface (e.g. hyporheic flow, Hannah *et al.*, 2009), and/or at the water-air interface (e.g. riparian vegetation shading, Moore *et al.*, 2005; Hannah *et al.*, 2008a). Whilst external thermal drivers determine the heat load capacity of the stream (volume of water) and the heat energy added to the stream, the structural stream components ultimately determine the stream resistance to warming or cooling.

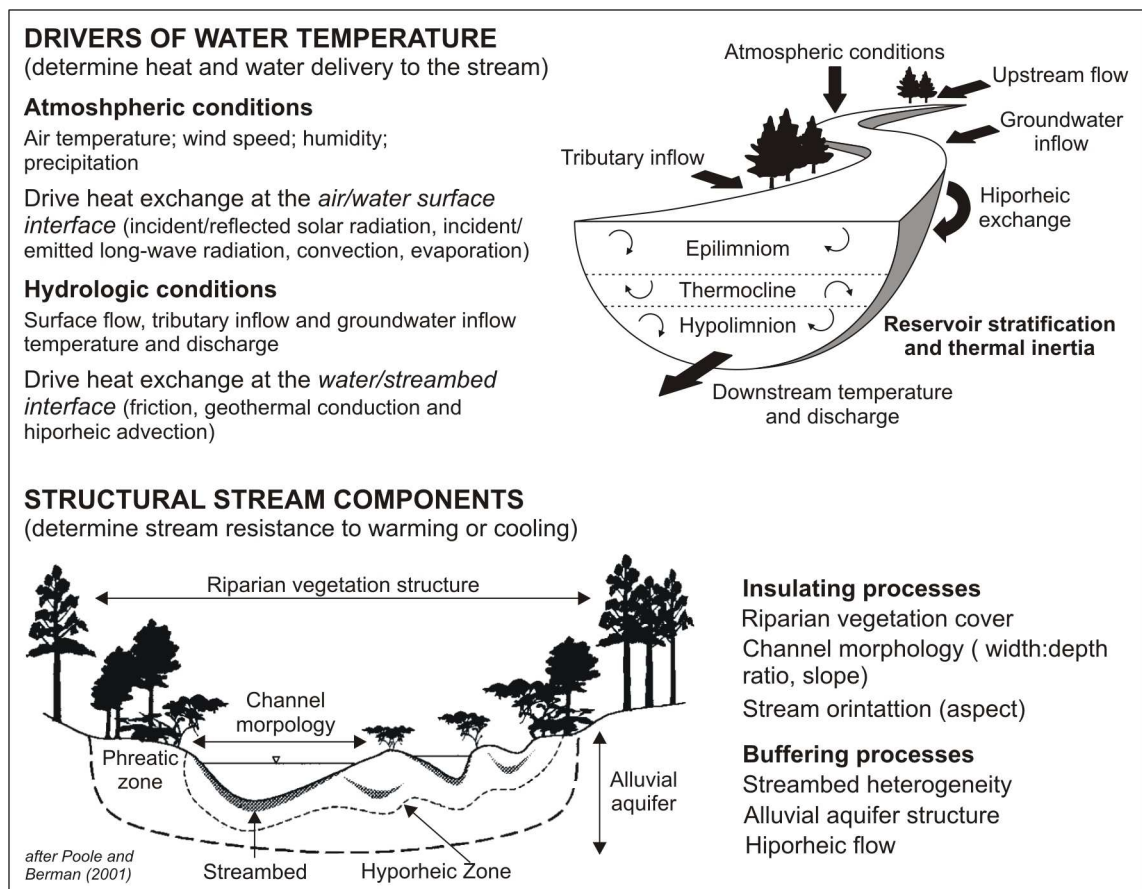


Figure 1.5: Drivers of river water temperature and insulating/buffering processes within a hypothetical stream. Based on Poole and Berman (2001), Hannah *et al.* (2004), Moore *et al.* (2005) and Caissie (2006).

Since flow regulation by dams represents the greatest source of hydrologic alteration of stream and rivers (Petts and Gurnell, 2005), it has direct implications for the thermal regime of the river downstream (Olden and Naiman, 2010). Depending on the release depth, the thermal stratification of the reservoir and the retention time (Ward and Stanford, 1979), dams may induce substantial changes in both key thermal attributes of streams and rivers: the heat load and the thermal capacity of flow (Webb, 1996; Poole and Berman, 2001). The effects of dams on the thermal regime of regulated rivers have received very early attention (e.g. Lavis and Smith, 1972; Lehmkuhl, 1972; Smith, 1972; Ward and Stanford, 1979; 1982; Petts, 1984; Cowx *et al.*, 1987; Crisp, 1987; Webb and Walling, 1988; Anderson, 1989). These studies revealed that changes may occur to all aspects of the *natural thermal regime* (sensu Olden and Naiman, 2010), affecting the magnitude and the timing of the thermographs, the frequency and duration of temperature extremes, and the rate of thermal change over a range of temporal scales.

The most common thermal impact of deep-release dams is the homogenization (flattening) of the annual thermograph related to decreased summer maxima and increased winter minima (Table 1.2). Except extreme cases (e.g. Colorado River below Glen Canyon Dam, Wright *et al.*, 2009), most studies report summer maxima decreased by 3 to 5 °C and winter minima increased by 4 to 6 °C.

Table 1.2: Examples of changes in the thermal regime of regulated rivers worldwide.

Country	Impoundment	Release type	Thermal impacts	Downstream persistence	Citation
USA, Utah	Flaming Gorge Dam on Green River	Hypolimnetic	Summer temperature decreased (11.5 °C); winter temperature increased (5 °C); frequency and duration of low and high temperatures decreased; annual cycle delayed	-	Olden and Naiman (2010)
USA, Arizona	Glen Canyon Dam on Colorado River	Hypolimnetic	Summer temperature decreased (15 °C); winter temperature increased (8 °C)	400 km	Wright <i>et al.</i> (2009)
USA, Oregon	Several dams on Willamette Basin	Hypolimnetic, epilimnetic	Summer temperature decreased (3 °C); regime variability over small temporal scales decreased by 75 %	-	Steel and Lange (2007); Angilletta <i>et al.</i> (2008)
France	Vouglans Dam on Ain River	Hypolimnetic	Summer temperature decreased (2 °C); winter temperature increased (1 °C); daily fluctuations decreased (6 °C); annual cycle delayed	35 km	Poirel <i>et al.</i> (2010)
UK	Kielder Dam on Tyne River	Hypolimnetic	Summer temperature decreased (3 °C); winter temperature increased (4 °C)	60 km	Archer (2008)
UK	Wimbleball Dam on the Haddeo River	Hypolimnetic	Summer temperature decreased (3 °C); daily fluctuations decrease by 60 %; annual cycle delayed	20 to 40 km	Webb and Walling (1993a; 1995; 1997)
Spain	Ascó Power Plant and upstream reservoirs on the Ebro River	Hypolimnetic, epilimnetic	Summer temperature decreased (3.5 °C); winter temperature increased (6 °C); daily fluctuations increased; annual cycle delayed Seasonal patterns reverse below the lowest reservoir and the power plant due to epilimnetic release (summer increase and winter decrease)	186 km	Prats <i>et al.</i> (2010; 2011; 2012)
China	Xinanjiang Dam on Qiantang River	Hypolimnetic	Mean temperature decreased (5 °C); maximum temperature decreased (12 °C); minimum temperature increased (4 °C)	260 km	Zhong and Power (1996)
South Africa	Clanwilliam Dam on Olifants River	Hypolimnetic, epilimnetic	Spring temperatures rose during epilimnetic release; summer maxima and minima decreased (8 °C; 5 °C) due to hypolimnetic release	7 km	King <i>et al.</i> (1998)
Australia	Keepit Dam on Naomi River	Hypolimnetic	Summer temperature decreased (5 °C); winter temperature increased; annual cycle delayed	100 km	Preece and Jones (2002)

Besides altering the magnitude of the downstream thermograph, dams alter the thermal seasonality of flow by increasing the seasonal constancy, reducing the frequency and duration of temperature extremes (e.g. Green River below Flaming Gorge Dam, Olden and Naiman, 2010), and delaying the annual cycle (e.g. Naomi River below Keepit Dam, Preece and Jones, 2002; Ebro River below several dams, Prats *et al.*, 2010; 2011; 2012). As for the natural variability of river water temperature, studies on impounded rivers have shown that dams may reduce thermal fluctuations over daily (Webb and Walling, 1993a; 1995; 1997), 3- to 7-day (Steel and Lange, 2007) and seasonal (Poirel *et al.*, 2010) time scales.

In many regulated rivers, such changes were recognised to be significant immediately below the dam (e.g. 7 km, King *et al.*, 1998), and persisted over some tens of kilometres downstream (e.g. 30 km, Cowx *et al.*, 1987; 20 km, Webb and Walling, 1993a; Webb and Walling, 1995; 1997; 60 km, Archer, 2008; 35 km, Poirel *et al.*, 2010). However, the distance for thermal recovery below dams has been reported to vary considerably (260 km, Zhong and Power, 1996; 100 km, Preece and Jones, 2002; 60 km, Archer, 2008; 400 km, Wright *et al.*, 2009) as it depends primarily on the dam structure and operational procedures (Ward and Stanford, 1979; Petts, 1984), on the energy contributions from the atmosphere, tributaries and the phreatic zone (Webb, 1996; Hannah *et al.*, 2004; Caissie, 2006; Webb *et al.*, 2008), and on a number of structural factors moderating heat exchange to and from the river (Fig. 1.5).

1.1.3. Changes in the sediment load

Most natural rivers are in dynamic equilibrium between erosion, transport and deposition (Schumm, 1977). As illustrated in Figure 1.6, dams and reservoirs disrupt sediment transfer from headwater source areas (Rausch and Heinemann, 1975; Morris and Fan, 1997) and so may dramatically alter the sedimentary balance of the regulated river. According to Petts and Gurnell (2005), the headwater areas provide more than 75 % of the river's sediment load; depending on the size of the reservoir, dams can isolate all or a significant proportion of the sediment delivered by the upper zones (Chien, 1985; Morris and Fan, 1997). Sediment control is a specific purpose for many dams, although for most dams sediment trapping is a consequence of the dam's structure (Williams and Wolman, 1984).

From measurements made below 21 large dams across United States, Williams and Wolman (1984) showed that the trapping efficiency of large reservoirs is commonly greater than 99 %. Similar values were documented by a number of studies on regulated American rivers; for example, Richard and Julien (2003) revealed that the trapping efficiency of the Cochiti Dam on the Río Grande, New México, was also of 99 % and a smaller percentage although not less significant was documented by Phillips *et al.* (2005) within the Livingston Dam on the Trinity River, Texas (81 %). In China, Chien (1985) estimated that the proportion of sediment retention within the Sanmenxia Reservoir on the Yellow River was of 93 %. In UK, Petts (1977) reported that 80 to 90 % of the sediment delivered from the headwaters of the Derwent River was trapped within the Ladybower Dam. In Australia, Sherrard and Erskine (1991) found that the trapping efficiency of the Mangrove Creek Dam was nearly 100 %.

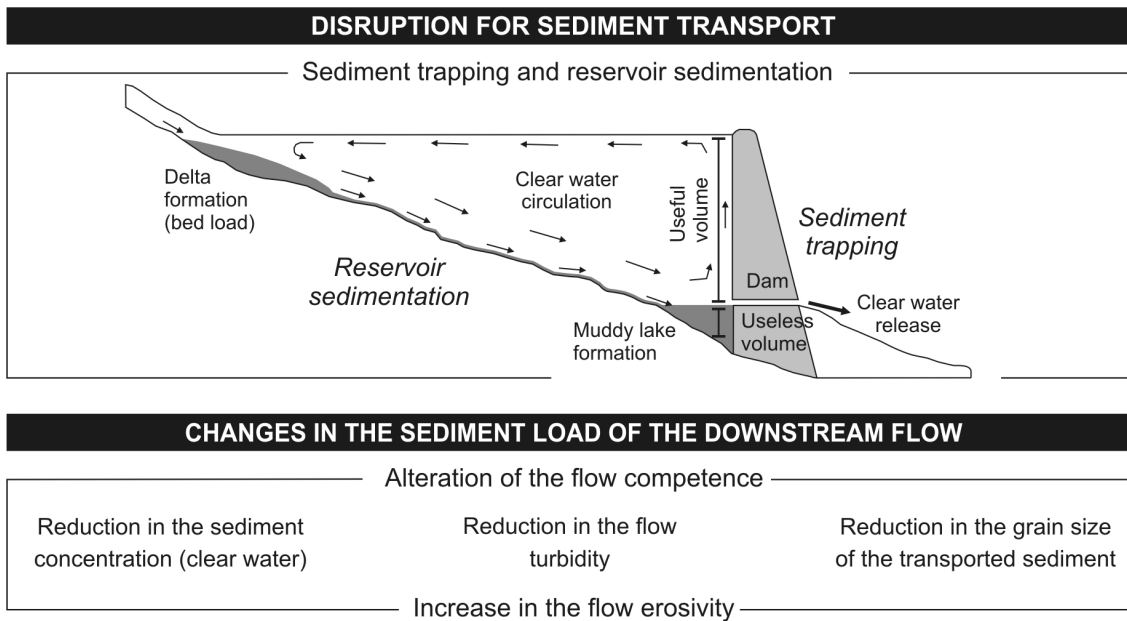


Figure 1.6: Dam-induced disruption for sediment transport. Based upon Petts (1984), Morris and Fan (1997) and (Rausch and Heinemann, 1975).

Sediment isolation within the reservoir involves a reduction in the turbidity (Petts and Gurnell, 2005) and sediment concentration (Petts, 1979; Chien, 1985; Kondolf, 1997; Wang *et al.*, 2007) of the downstream flow, as well as a reduction in the grain size of the fraction of the sediment delivered (Brandt, 2000). Reduction in the sediment load downstream involves changes in the flow competence (Petts, 1979) because the reduction in the amount of material available to transport is usually greater than the reduction in the transport capacity of the flow.

Clear water releases (or ‘hungry water’ *sensu* Kondolf, 1997) have an unfilled capacity to transport sediment, which increase their erosive power regardless of the potential reduction of the effective flow (Petts, 1977; 1979; Petts and Lewin, 1979; Phillips, 2003b; Wang *et al.*, 2007). The relationship between the transport capacity and the sediment concentration of the flow, together with the relationship between the flow erosivity and the erodibility of the channel materials determines morphological changes that, in the long term, produce new stable conditions (Xu, 1996; Brandt, 2000).

1.2. SECOND-ORDER CHANGES: THE RESPONSE OF THE RIVER MORPHOLOGY

As it was discussed above, dams may modify three critical elements of the fluvial system downstream: (i) the river flow regime (ii) the relationship between the flow capacity to transport sediment and the amount of sediment available to transport, and (iii) the quality of the flowing water. As a result, changes in the channel morphology and in the composition of the riparian communities are expected to occur (Fig. 1.2). This section examines the complex response of the channel morphology and its riverine

landscape to altered quantities of water and material below dams.

As reviewed by Knighton (1998), studies on regulated rivers subject to altered hydrologic conditions indicate that the river channel morphology is the most adjustable physical component of the fluvial system. Furthermore, variation in natural flow conditions after river impoundment represents the most serious and continuous threat to the ecological sustainability of rivers and their associated wetlands (Bunn and Arthington, 2002), through influences on the reproductive success, the natural disturbance and the biotic competition (Petts, 1980b; Nilsson and Berggren, 2000; Batalla *et al.*, 2004; Kondolf and Batalla, 2005).

Bed degradation is usually the most immediate channel adjustment after dam closure, although bed aggradation processes and bank stabilisation by vegetation encroachment have been also widely documented. Nevertheless, the geomorphic response to altered patterns of flow and sediment below dams may reflect a wide range of channel adjustments which, in the long term, will not only affect the shape and the size of the river channel but also the overall morphology and diversity of the river system.

1.2.1. The direction of geomorphic change

A number of conceptual models have been developed to predict channel metamorphosis in response to flow regulation. Based on the sedimentary balance of Lane (1955) and/or the qualitative model of Schumm (1969), these approaches may vary in their quantitative and qualitative predictions, although they are all consistent on the concept of equilibrium between flow discharge [Q], sediment load [L] and channel morphology.

a) Schumm-based approaches

The qualitative model of Schumm (1969) has provided the broadest basis for predicting the direction of channel metamorphosis following changes (increase or decrease) in flow discharge and sediment load. According to the model, eight combinations of change are possible, each of which involves specific channel adjustments. Since dams are expected to reduce both Q and L , the Schumm's relationship that better represents the direction of channel metamorphosis below dams is expressed as follows:

$$Q^-, L^- \rightarrow w^-, d^\pm, (w:d)^-, \lambda^-, S^+, s^\pm \quad (1.1)$$

where [w] is the channel width, [d] is the channel depth, [λ] is the wavelength, [S] is the channel sinuosity, and [s] is channel slope.

Although Schumm's model is rather effective to predict the final outcome of channel metamorphosis, it limits the understanding of the intermediate phases of such channel changes (Petts and Lewin, 1979). Accordingly, a number of Schumm-based models have been developed to predict the direction, style and trajectory of geomorphic changes in response to river impoundment.

Based on the previous work of Petts (1979), Petts and Gurnell (2005) developed a model that includes both the *space* and *time* dimensions (Fig. 1.7). The model considers four styles of channel adjustment dependent on two scenarios of relative variations [Δ] in flow discharge and sediment load as expressed below.

Scenario 1 groups the geomorphic effects of clear water release leading to channel degradation. If flow discharge is unchanged (Scenario 1a), then the flow erosivity increases and all morphological variables will increase except for the channel slope, which decreases as a result of bed incision. If flow discharge is reduced (Scenario 1b) then the flow competence decreases; flow will concentrate within the main channel, leading to an overall decrease in the channel capacity by channel aggradation and narrowing.

Scenario 2 groups the geomorphic effects of extreme reduction in the flow capacity relative to the flow competence leading to channel aggradation. If the sediment load is reduced (Scenario 2a), then some bed degradation may occur, although the channel capacity will decrease by lateral aggradation. If the sediment load is unchanged (Scenario 2b) then the flow erosivity decreases and all morphological variables will decrease due to the extreme decrease in the transport capacity of flow.

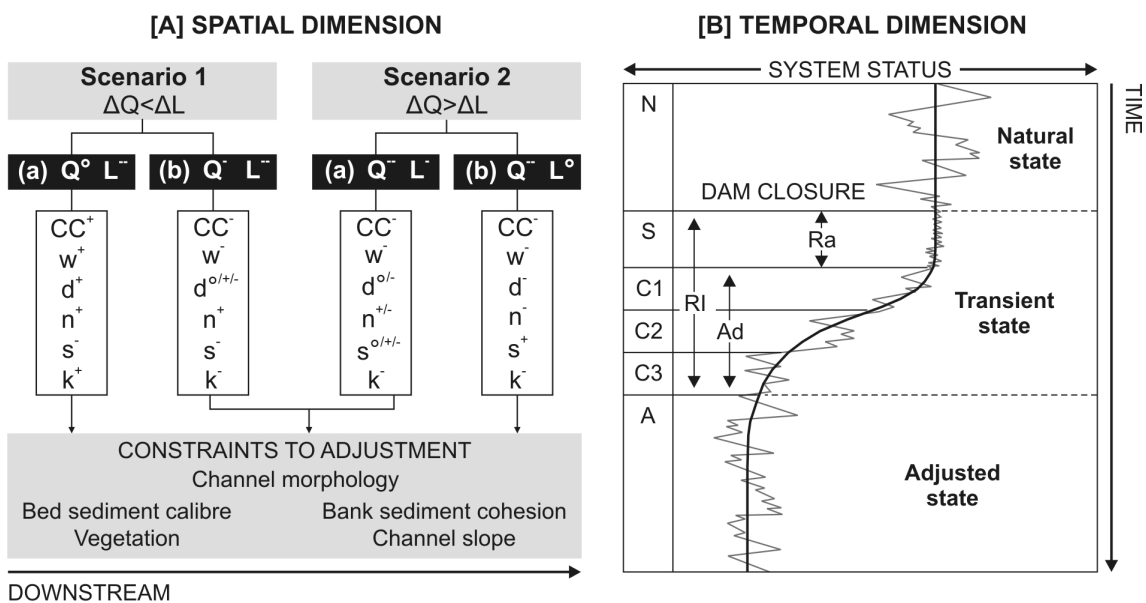


Figure 1.7. [A] Scenarios of channel adjustment in response to relative changes in flow discharge and sediment load, and [B] trajectory of geomorphic changes following dam closure. Morphologic variables include [CC] channel capacity, [w] channel width, [d] channel depth, [n] channel roughness, [s] slope, and [k] conveyance; the magnitude of change is indicated by [o] no significant change, [+] increase, [-] decrease, and [--] major decrease. After dam closure, the relaxation period [RI] includes a reaction phase [Ra] involving an accommodation state [S] and a phase of adjustment [Ad] involving different channel states [C]. After Petts (1979) and Petts and Gurnell (2005).

The four styles of channel metamorphosis may be combined into different sequences of change with distance below the dam (Fig. 1.7 [A]). For example, the sequence 1a→1b→2a→2b hypothesizes channel changes in the downstream direction as the dam impacts decline and the river recovers its discharge (groundwater and tributary inflows) and sediment load (channel degradation and load from tributaries). The trajectory of channel changes (Fig. 1.7 [B]) from a natural regime state [N] to an adjusted regime state [A] involves a sequence of transient states. After dam closure, the fluvial system enters into a relaxation period [RI] comprising two transitory phases: (i) a reaction phase

[Ra] involving an accommodation state [S] where regulated flows are accommodated within the former channel, and (ii) a phase of adjustment [Ad] to regulated flows involving a range of channel states ($C_1, C_2, C_3 \dots C_n$). Temporal lags for both reaction and adjustment periods reflect the magnitude and frequency of geomorphologically-effective floods below the dam and the channel conditions at the time of dam closure.

Based on observations made for more than 25 regulated Italian rivers, Surian and Rinaldi (2003) proposed a qualitative classification scheme that considers the direction of change in the fluvial style (Fig. 1.8). Changes in the fluvial style are hypothesized based on increasing rates of channel incision and narrowing; hence, the scheme can be seen as an extension of the qualitative model described above.

The classification starts with three initial channel morphologies: single thread (case A), braided (case C), and transitional (case B) morphologies. The channel response to altered hydrologic conditions within *braided rivers* will involve channel narrowing. Increasing channel narrowing may reduce the braiding intensity (Case G) or induce dramatic changes in the fluvial style from braided to wandering (case F). Such changes may be intensified strongly if channel incision occurs (case H). The geomorphic response of *single-thread* channels to regulated patterns of flow is clearly dominated by bed incision. Depending on the hydrologic conditions and channel materials, bed incision may range from moderate (case D) to extremely severe (case I). Channel adjustments from initial *transitional* morphologies are more complex, as both narrowing and incision may occur (case E).

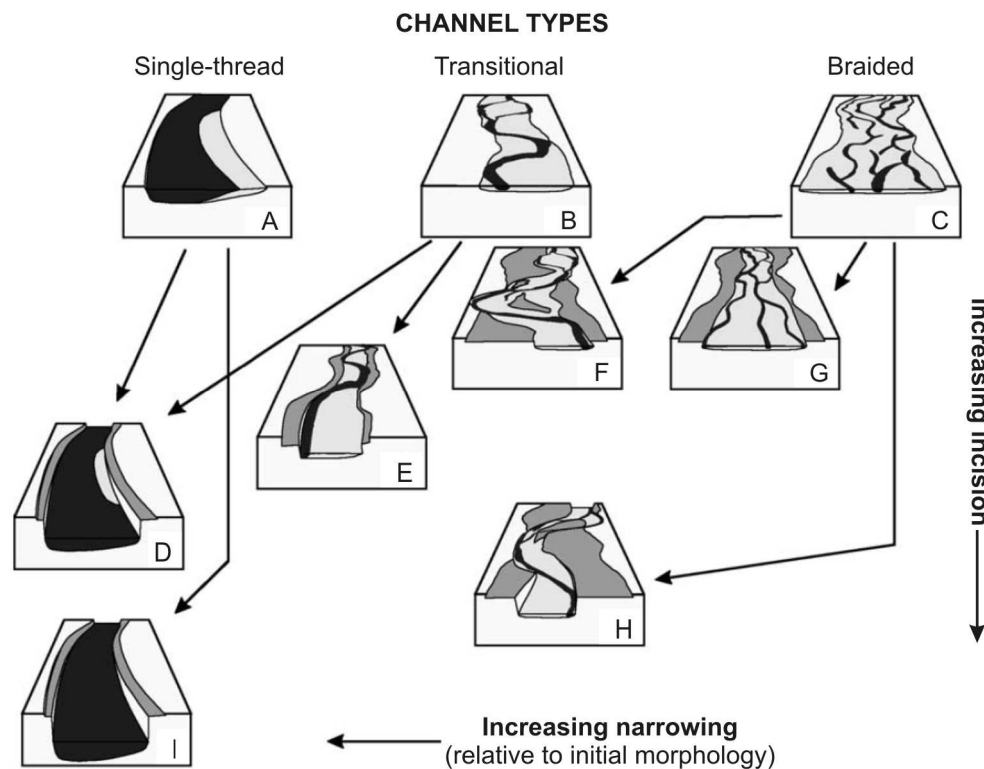


Figure 1.8: Qualitative scheme of change in the fluvial style. After Surian and Rinaldi (2003).

This review showed that the channel geometry (cross-section, slope and planform) is a function of flow discharge and sediment load. Consistently with the empirical framework of Schumm (1969), any change in both key hydrological parameters, Q and L , will initiate changes in the channel form and size; the direction and magnitude of geomorphic will depend on (i) the patterns of flow regulation affecting the geomorphic effectiveness of downstream flow over time, and (ii) the morphological setting of the river system prior to dam closure providing a greater or lesser resistance to change.

b) Lane-based approaches

Lane (1955) conceptualized the balance between grain size, sediment load, flow discharge and channel slope as follows:

$$Qs = \int L_b D \quad (1.2)$$

where the flow discharge [Q] and the channel slope [s] are a function of the bed load [L_b] and grain size of the bed material [D].

Upon this basis, Brandt (2000) developed an alternative approach grouping two determinants for the geomorphic response below dams: relative changes in flow discharge, Q (i.e., increase, decrease or no change), and relative changes in the relationship between sediment load, L , and sediment transport capacity, K (i.e. smaller, equal, or greater). From combination of all of these parameters, nine cases of channel change are possible (Fig. 1.9); the most common morphologic changes following river impoundment correspond to cases 1, 2 and 4 (Brandt, 2000).

Case 1: decreased Q and $L < K$

Reduction in flow discharge involves a reduction in the flow capacity. The flow is not longer able to erode and transport the pre-dam material, and tends to concentrate within the main channel. However, because the load is also reduced, bed and/or bank degradation may occur within erodible channels. Bed degradation may lead to bed coarsening, channel narrowing and terrace formation, whilst bank degradation may lead to channel scour. In all cases, the channel capacity is reduced.

Case 2: decreased Q and $L = K$

Same as for Case 1, reduction in flow discharge leads to a reduction in the channel capacity. However, deposition processes are expected to be more extensive than in Case 1 because the sediment concentration of the flow equals its transport capacity. Riffle scour should not be much intense, and deposition in pools should increase.

Case 4: equal Q and $L < K$

Clear water release implies an increase in the flow erosivity. Depending on the channel morphology and materials, channel changes may involve two different mechanisms: (i) bed degradation and bend down cutting leading to formation of straight and narrowed channels, or (ii) bank scour and undercutting leading to channel widening and wandering. In both cases, floodplain rebuilding processes decrease because of the reduction in the frequency of floods downstream.

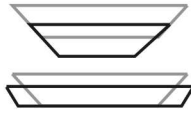
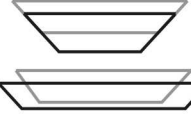
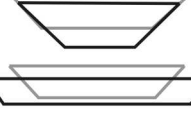
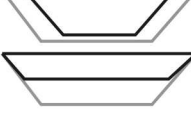
CHANGES	L < K	L = K	L > K
-Q	<p>Case 1</p>  <p>-CC; ±w; ±d; o-BL Terrace formation Riffles erosion Pools erosion/deposition</p>	<p>Case 2</p>  <p>-CC; -w; -d; oBL Terrace formation Riffles erosion Pools deposition</p>	<p>Case 3</p>  <p>-CC; ±w; ±d; +BL Terrace formation Riffles erosion/deposition Pools deposition</p>
oQ	<p>Case 4</p>  <p>+CC; ±w; ±d; -BL Terrace formation Riffles erosion Pools erosion</p>	<p>Case 5</p>  <p>No change</p>	<p>Case 6</p>  <p>-CC; ±w; ±d; +BL Terrace disappearance Riffles deposition Pools deposition</p>
+Q	<p>Case 7</p>  <p>+CC; ±w; ±d; -BL Terrace disappearance Riffles erosion/deposition Pools erosion</p>	<p>Case 8</p>  <p>+CC; +w; +d; oBL Terrace disappearance Riffles deposition Pools erosion</p>	<p>Case 9</p>  <p>+CC; ±w; ±d; +BL Terrace disappearance Riffles deposition Pools erosion/deposition</p>

Figure 1.9: Potential changes in the channel morphology following altered inputs of flow and sediment below dams. (Pre-) post-dam conditions are illustrated in (grey) black.

Morphological variables are indicated by [CC] channel capacity, [w] channel width, [d] channel depth, and [BL] bed level; the magnitude of change is indicated by [+] increase, [-] decrease, and [o] no change. After Brandt (2000).

1.2.2. The magnitude of geomorphic change

Studies on regulated rivers worldwide have documented a wide range of channel adjustments (Table 1.3). Vertical erosion is the most immediate impact of dams, and persists until the reduced flow is no longer able to remove the bed material (Petts, 1979). The magnitude of channel incision may vary widely from one river to another, ranging from some tens of centimetres (e.g. Fortun River, Fergus, 1997) to up to 4 m (e.g. Rhône River, Peiry *et al.*, 1994). Both examples account for bed level changes below hydropower facilities, suggesting that the magnitude of channel incision depends on the geomorphic effectiveness of flow for a given channel morphology and materials more than on the reservoir operational procedures.

A common consequence of channel incision is bed coarsening as the finest material is removed downstream (e.g. Chien, 1985; Peiry *et al.*, 1994; Church, 1995; Sear, 1995; Richard and Julien, 2003; Phillips, 2003b; Assani and Petit, 2004; Choi *et al.*, 2005). Yet, studies on regulated rivers with pool-riffle bed morphologies have documented

coupled bed aggradational-degradational processes (e.g. river Tyne below Kielder Dam, Sear, 1995; river Warche below Butgenbach Dam, Assani and Petit, 2004).

Another common change below dams is the reduction in the channel width (channel narrowing) due to lateral accretion and terrace formation within the former floodplain (e.g. Church, 1995; Surian, 1999; Shields *et al.*, 2000; Richard and Julien, 2003; Gilvear, 2004). Studies reporting channel narrowing document reduction in the channel width of 40 to 50 %; in some cases, these proportions decrease in the downstream direction (Table 1.3).

Channel incision and narrowing involve a reduction in the channel capacity. Except for extreme cases (e.g. 94 %, Gordon and Meentemeyer, 2006), most studies document reduction in the channel capacity of 30 to 60 % (Table 1.3). If the grain-size of the load exceeds the flow capacity, then the channel capacity decrease due to sediment deposition in bars, islands, pools and riffles (e.g. river Tyne below Kielder Dam, Sear, 1995).

These processes are frequently benefited by the persistence of low-flows leading to vegetation encroachment within the active channel, which increases the channel roughness and stabilizes the channel materials (e.g. river Derwent below Ladybower Dam, Petts, 1977; Mangrove Creek below Mangrove Creek Dam, Sherrard and Erskine, 1991; river Hwang below Hapchon Dam, Choi *et al.*, 2005; Dry Creek below Warm Springs Dam, Gordon and Meentemeyer, 2006). Vegetation plays a key role in reducing channel width, particularly where the pre-dam channels are wide and shallow and where increased base flows provide moist environments suitable for vegetation growth (Petts and Gurnell, 2005).

Furthermore, reduction in the frequency, extent and duration of overbank flooding contributes to isolate the river channel from its floodplain (Nilsson and Berggren, 2000) and to lowering the groundwater table (Petts, 1984; McCartney *et al.*, 2001), all of which disrupts the pathways of lateral and vertical connectivity of the fluvial system (Ward and Stanford, 1995b; Poff *et al.*, 1997; Ward, 1998). Such disruption will induce significant changes in the structure of riparian communities (Collier *et al.*, 1996; Richter *et al.*, 1996; Nilsson and Berggren, 2000; Bunn and Arthington, 2002; Magilligan and Nislow, 2005). Changes may involve from invasion of exotic, drought-tolerant species (e.g. Green River below Flaming Gorge Dam, Merritt and Cooper, 2000) to the establishment of new patterns of vegetal succession (e.g. Snake River below Jackson Lake Dam, Marston *et al.*, 2005).

On the other hand, lateral erosion and scouring may lead to channel widening if the material is not erosion-resistant (e.g. Sabine River below Toledo Bend dam, Phillips *et al.*, 2005). The most evident consequence of channel widening is the increase in the channel capacity (Xu, 1996), with a consequent loss of riparian habitats (Chien, 1985). Increase in the channel width have been observed to range from 2 to 40 m (Table 1.3); however, channel widening appears to be less common than channel narrowing and mostly related to rivers impounded for hydropower generation (e.g. Fortun River, Fergus, 1997; Warche River, Assani and Petit, 2004).

Table 1.3: Examples of dam-induced geomorphic changes by world region.

EUROPE					
Region	Impoundment	Dam purpose	Opening	Channel adjustments	Citation
Belgium	Butgenbach Dam on Warche River	Hydropower	1932	d ^o ; w ⁺ (7.4 m); bed coarsening; number of pools & riffles reduced; bars & islets increased; meander cut-off; braidering	Assani and Petit (2004)
Norway	Several dams on Fortun River	Hydropower	1963	d ⁺ (0.2-0.4 m); w ⁺ (2-3 m); CC ⁺ (40m ²); channel aggradation and degradation	Fergus (1997)
Italy	Several dams on Piave River	Hydropower; irrigation	1930/ 1960	d ⁺ (2-3 m); w ⁻ (50 %); planform from braided to wandering	Surian (1999)
France	Several dams on the upper Rhône	Hydropower	1960	d ⁺ (3-4 m); w ⁻ ; CC ⁻ ; bed coarsening; river entrenchment	Peiry <i>et al.</i> (1994)
UK, England	Clatworthy Dam on Tone River	Water supply	1959	CC ⁻ (54 %)	Gregory and Park (1974)
UK, England	Ladybower Dam on Derwent River	Water supply; hydropower	1943	CC ⁻ (40 %)	Petts (1977)
UK, England	Kielder Dam on Tyne River	Hydropower	1981	Riffle degradation and pool aggradation; Bars on tributary confluence; vegetation on former deposits	Sear (1995)
UK, Scotland	Spey Dam on Spey River	Hydropower	1942	w ⁻ (50 to 20 % in downstream direction)	Gilvear (2004)
AMERICA					
Region	Impoundment	Dam purpose	Opening	Channel adjustments	Citation
Canada	Bennett Dam on Peace River	Hydropower	1968	w ⁻ ; s ⁻ ; bed coarsening; terrace formation in former floodplain	Church (1995)
USA, California	Warm Springs Dam on Dry Creek	Water supply; hydropower; flood control	1982	d ⁺ (0.9 to 0.5 m); w ⁻ (45 to 21 m); CC ⁻ (94 %); reduction in lateral migration (64 %); increase in riparian vegetation (72 %)	Gordon and Meentemeyer (2006)
USA Great Plains	Several	Muliple	-	w ⁻ in braided rivers; reduced migration of meandering rivers; vegetation growth/decrease relative to fluvial style	Friedman <i>et al.</i> (1998)
USA, Montana	Fort Peck Dam on Missouri River	Hydropower; flood control	1940	w ⁻ (80 m); S ⁺ (4 km); decrease in lateral migration (6.6 to 1.8 m yr ⁻¹)	Shields <i>et al.</i> (2000)

Table 1.3: *Cont.*

Region	Impoundment	Dam purpose	Opening	Channel adjustments	Citation
USA, New Mexico	Cochiti Dam on Rio Grande	Flood/sediment control	1973	w ⁻ ; S ⁺ ; bed coarsening; bars and islands reduced	Richard and Julien (2003)
USA, Texas	Toledo Bend Dam on Sabine River	Hydropower; water supply	1967	Bed coarsening; bank scarp; little evidence of changes further downstream	Phillips (2003b)
USA, Texas	Livingston Dam on Trinity River	Water Supply	1968	d ⁺ (2 to 3 m); w ⁺ (40 m); CC ⁺ (43 %); s ⁻ ; pointbar migration; coupled bank erosion and lateral accretion; no changes in planform	Phillips <i>et al.</i> (2005) Wellmeyer <i>et al.</i> (2005)
USA, Wyoming	Flaming Gorge Dam on Green River	Hydropower	1964	Planform changes from meandering to shallow braided; Rapid vegetation growth and invasion of drought-tolerant species	Merritt and Cooper (2000)
USA, Wyoming	Jackson Lake Dam on Snake River	Irrigation	1916	S ⁺ ; increase in lateral migration; terrestrial-like patterns of vegetal succession	Marston <i>et al.</i> (2005)
ASIA					
Region	Impoundment	Dam purpose	Opening	Channel adjustments	Citation
China	Sanmenxia Dam on Yellow River	Flood control; irrigation; hydropower	1960	d ⁺ ; CC ⁻ (65 %); S ⁺ ; bed coarsening	Chien (1985)
				Planform changes from braided to wandering and from wandering–braided to wandering–meandering	Wang <i>et al.</i> (2007)
Korea	Hapchon Dam on Hwang River	Flood control; hydropower; water supply	1988	d ⁺ (1.8 to 3.5 m); bed coarsening; vegetation growth over sandbars (33 %)	Choi <i>et al.</i> (2005)
OCEANIA					
Region	Impoundment	Dam purpose	Opening	Channel adjustments	Citation
Australia	Mangrove Creek Dam on Mangrove Creek	Water supply	1981	d [±] ; w ⁻ ; CC ⁻ ; S ⁺ ; channel stabilisation by vegetation growth	Sherrard and Erskine (1991)
Australia	Two adjacent locks and associated weirs	Navigation; irrigation; water supply	1925; 1928	d+/-; w+; s ^o / cohesive bank materials restrict the initiation of channel metamorphosis	Thoms and Walker (1993)

Changes in the channel planform may take much longer before any transformation takes shape (Chien, 1985). As shown in Table 13, planform changes may involve either slight modifications in the planform such as reduction in the number of bars and islands (e.g. Rio Grande below Cochiti Dam, Richard and Julien, 2003) and reduction in the lateral mobility (e.g. Missouri River below Fort Peck Dam, Shields *et al.*, 2000; Dry Creek below Warm Springs Dam, Gordon and Meentemeyer, 2006) or dramatic changes in the fluvial style from braided to wandering (e.g. Piave River, Surian, 1999; Yellow River below Sanmenxia Dam, Wang *et al.*, 2007) or from meandering to braided (e.g. Green River below Flaming Gorge Dam, Merritt and Cooper, 2000; Warche River below Butgenbach Dam, Assani and Petit, 2004). The magnitude and direction of change in the channel planform will depend on the initial fluvial style (Surian and Rinaldi, 2003) and on the channel slope (Brandt, 2000) for a given pattern of flow regulation over time (Wellmeyer *et al.*, 2005). Whilst the degree of braiding increases as water discharge is increased for a given slope (or as the slope is increased for a given discharge), the degree of wandering increases as the load decreases and the channel becomes narrower, deeper and flow concentrates within a single thread (Brandt, 2000).

1.2.3. Variability of changes with time and distance from the dam

Besides assessing the direction and the magnitude of geomorphic changes, there is a held opinion about the importance of evaluating the temporal trends and spatial extent of river channel metamorphosis below dams. Whilst the magnitude and direction of geomorphic changes vary in space for a given time step (e.g. the impacts of dams were observed to decline in the downstream direction), geomorphic changes vary with time for a given cross-section (Williams and Wolman, 1984). Alluvial fluvial systems subject to altered hydrologic conditions may exhibit very short reaction times (Surian and Rinaldi, 2003), although the relaxation time may be considerably longer (Xu, 1996). Geomorphic changes usually begin as early as the dam construction begins, and were observed to be significant immediately below the impoundment (Petts, 1984; Williams and Wolman, 1984; Knighton, 1998; Brandt, 2000). However, the effective transformation of the downstream river morphology is usually a long-term process, needing sometimes several tens or even more than 100 years before to stabilize (Petts, 1984).

THE PASO DE LAS PIEDRAS DAM ON THE SAUCE GRANDE RIVER

The complexity of the regional environment

Dams and reservoirs may induce dramatic disruptions in the river hydrology, with significant implications for the channel morphology and the ecology of the river downstream. However, the impacts of dams may vary considerably from one dam to another, as each dam has a unique operation history according to its purpose and each river has a unique environmental setting providing a greater or lesser resistance to change.

The assessment of the effects of the Paso de las Piedras Dam upon the Sauce Grande River requires a prior understanding of the uniqueness and unpredictability of linked environmental processes affecting the use and management of local water resources over time. Figure 1.10 returns to the simplified scheme of fluvial response to river impoundment (Figure I.2, p. 4), and includes the complexity of processes playing within the regional scenario.

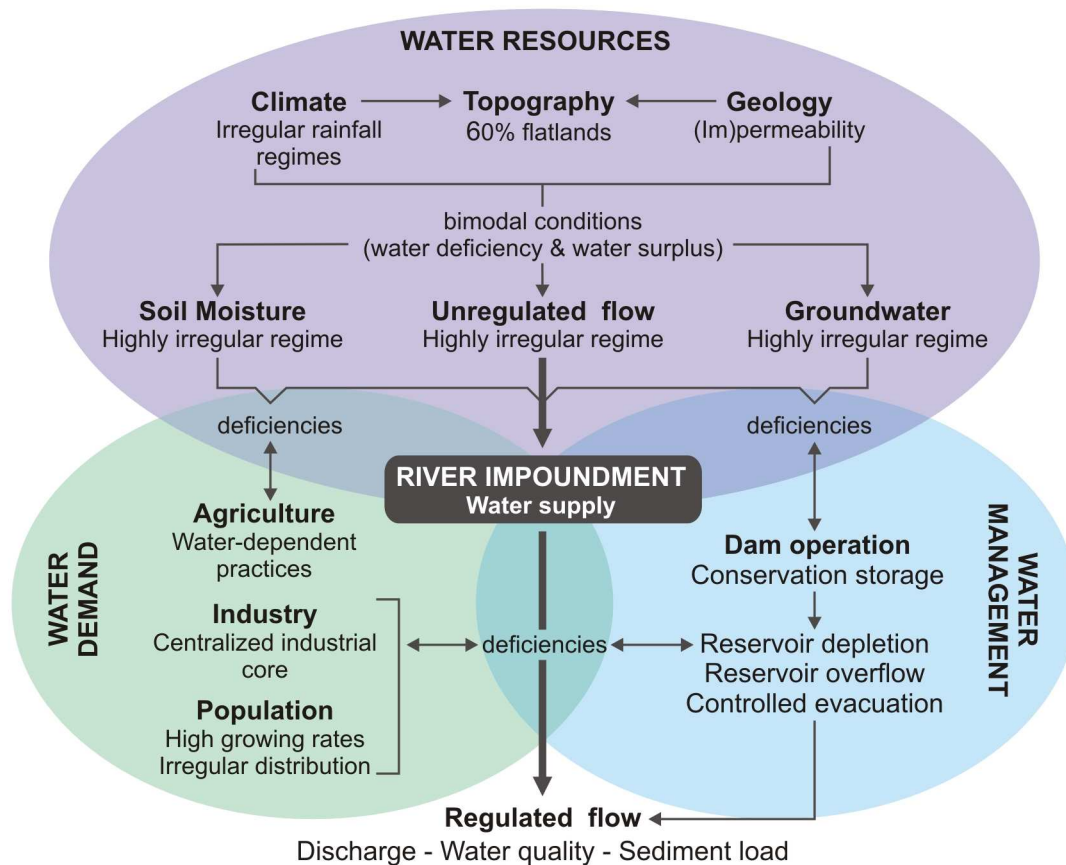


Figure 1.10: Linked processes influencing the relationship between use and management of water resources within the Sauce Grande River Basin and its regional context.

The following sections assemble the existing knowledge on physical and human processes contributing to the regional environmental complexity. They include (i) the climate variability, topography and materials inducing strong fluctuations in regional water resources in terms of availability, (ii) the evolving water needs of the involved society inducing an increase in the water demand, and (iii) the history of water management practices reflecting different patterns of hydrologic regulation.

2.1. THE VULNERABILITY OF LOCAL WATER RESOURCES

Water resources within the south-western Buenos Aires region (SWBA) comprise an array of water courses, water bodies and aquifers. Figure 1.11 illustrates the distribution of surface and underground water resources within the central part of the SWBA region; the Sauce Grande Basin situated on the east side of the region.

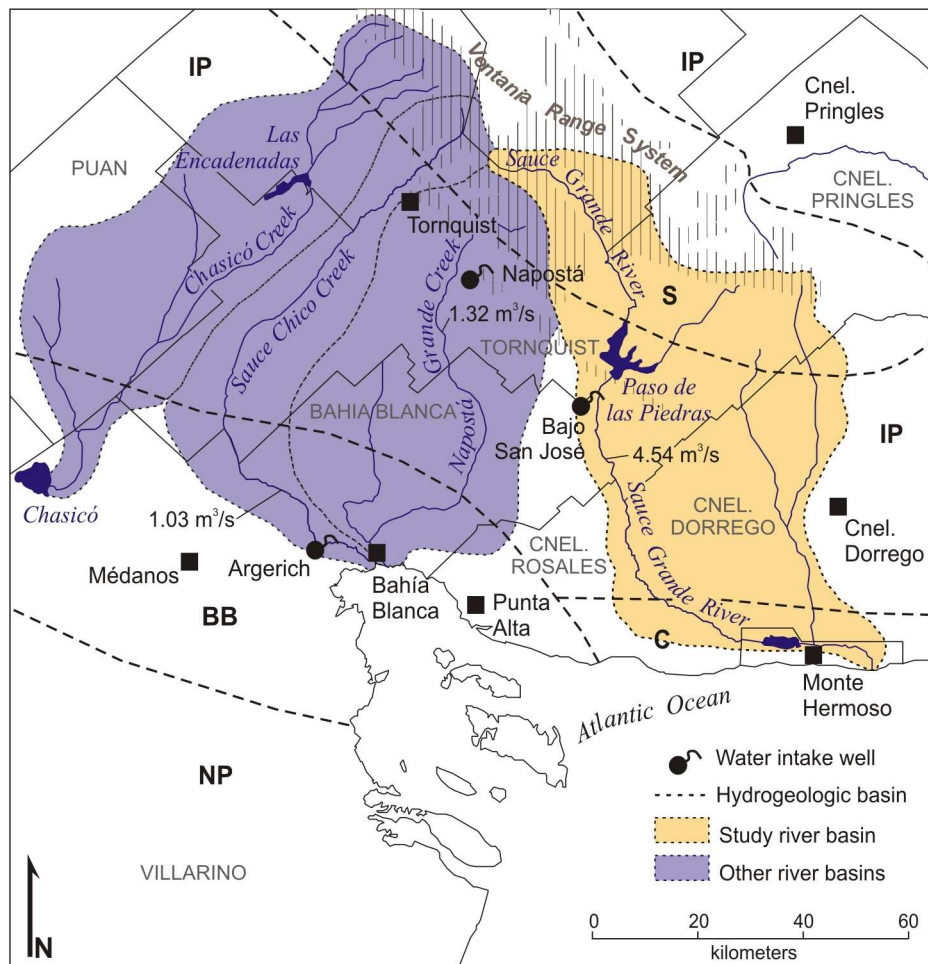


Figure 1.11: Spatial distribution of surface and underground water resources within the central south-western Buenos Aires. Based upon Auge (2004) and Schefer (2004). Legend of symbols in text.

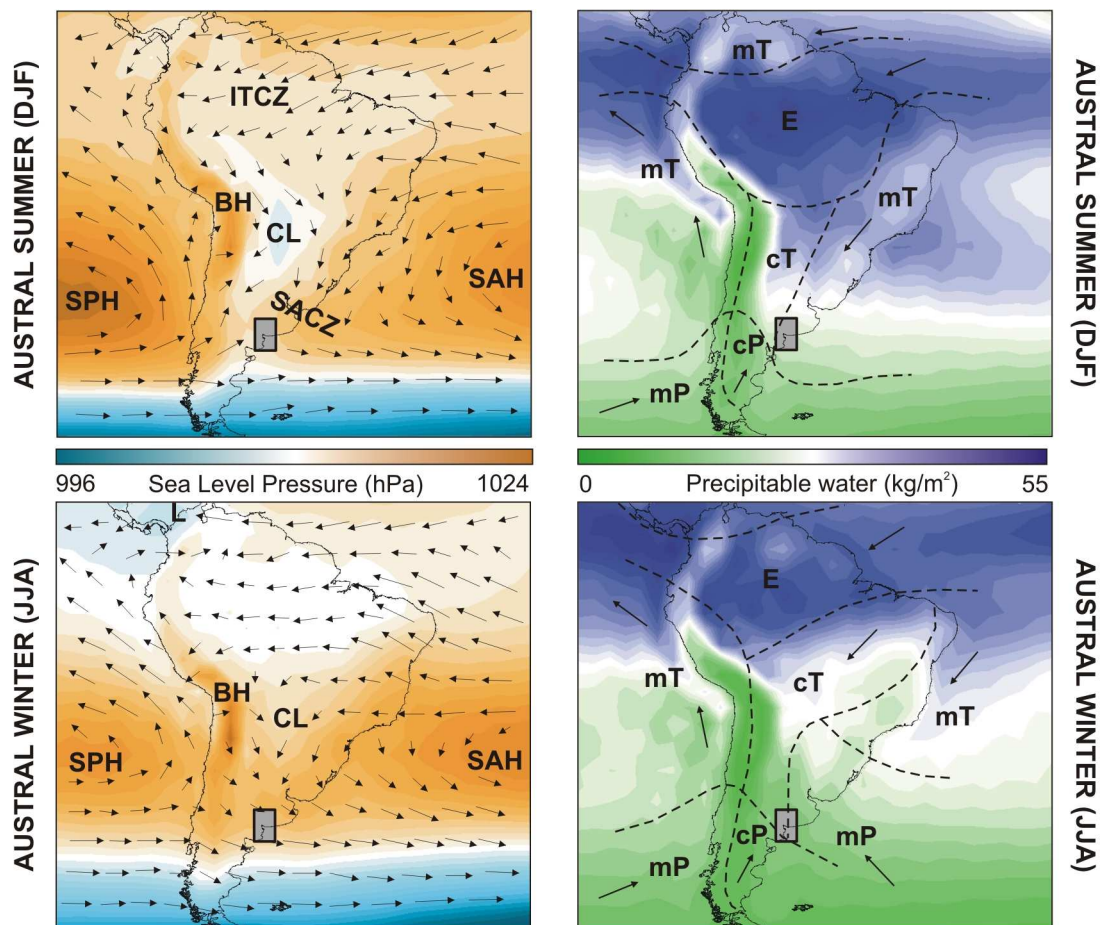
According to Auge (2004), the region comprises five hydrogeologic basins: Nord Patagonia [NP], Bahía Blanca [BB], Interserrana y pie de monte [IP], Costera [C], and Serrana [S]. Except for the deep aquifer within the Bahía Blanca hydrogeologic basin, the overall inaccessibility of the regional aquifers, their composing materials and/or their salinity content have historically constrained their use for drinking water purposes. Surface sources for freshwater include multiple streams and water bodies of varying hierarchy (Fig. 1.11). Mean annual runoff is 217 hm³, from which the Sauce Grande River contributes in 66 % (143 hm³). The remaining volume is supplied by the Sauce Chico creek (42 hm³) and by the Napostá Grande creek (32 hm³). Given the unsteady character of most of the water courses and the elevated salinity content of the water bodies, the Sauce Grande River emerges as the major source for freshwater within the region (Borromei, 1991; Zavala and Quattrocchio, 2001; Schefer, 2004).

The strong rainfall variability inherent to the local climate induces high instability for regional water resources. This is reflected by a succession of periods of water deficiency (or excess) which, coupled with the smooth topography, may turn rapidly into episodes of extended drought (or flooding). Based upon the existing literature, the following sections explore the interconnections between rainfall variability, topography and materials having implications for regional water resources in terms of availability over time.

2.1.1. The climate variability within SWBA

The regional climate is temperate with thermal and rainy seasons well defined (Campo *et al.*, 2004). However, the geographical situation of the area leads to strong climate fluctuations in space and time dependent on the effects of continentality, topography and synoptic patterns of large-scale atmospheric flow (Bruniard, 1982; Capelli-de-Steffens and Campo, 1994). Assessing large-scale phenomena as origin of local climate variability is way beyond the scope of this research. Nevertheless, we introduce a brief description of the main features influencing climate variability to help the understanding of the singularities of the regional climate. More detailed information on South American climates can be found in the reviews of Garreaud and Aceituno (2007), Garreaud *et al.* (2009), and Zamboni *et al.* (2010), among others.

The major South American atmospheric features are summarized in Figure 1.12; the grey box illustrates the situation of SWBA within the continental scale. Counter-clockwise low-level divergence from the South Atlantic and the South Pacific semi permanent high-pressure cells is responsible for most flow circulation over the continent (Zhou and Lau, 1998; Garreaud *et al.*, 2009), although patterns of atmospheric flow differ greatly between low and high latitudes due to the continental topography (Garreaud and Aceituno, 2007). In addition, the advance of air masses and the position of fronts reveal seasonal and inter-annual oscillations dependent on the seasonal drift of major atmospheric features (Grimm *et al.*, 2005; Vera *et al.*, 2006; Garreaud *et al.*, 2009) and on large-scale phenomena such as El Niño Southern Oscillation (Aceituno, 1988; Grimm *et al.*, 2000). These phenomena are at the basis of the regional climate variability. Such variability attains all climatic parameters, although it becomes evident regarding precipitation regimes involving spatial and temporal fluctuations over a range of spatial and time scales.

**FEATURES**

[ITCZ] Inter-tropical Convergence Zone; [SACZ] South Atlantic Convergence Zone; [SPH] South Pacific High; [SAH] South Atlantic High; [BH] Bolivian High; [CL] Chaco Low.

AIR MASSES

[E] Equatorial; [mT] maritime Tropical; [cT] continental Tropical; [mP] maritime Polar; [cP] continental Polar

Figure 1.12: Patterns of atmospheric circulation and rainfall over South America and adjacent oceans during austral summer (DJF) and austral winter (JJA). Left: Sea level pressure (SLP) and 850 hPa wind vectors. Right: air masses, fronts and precipitable water (PW). SLP and PW data was achieved from long-term (1981-2010) monthly means of the NCEP/NCAR Reanalysis. Wind vectors were modified from Garreaud *et al.* (2009). Fronts and air masses were based on Campo *et al.* (2004).

a) The spatial variability in rainfall regimes

Patterns of flow circulation over South America are highly constrained by the continental topography. The Andes ridge constitutes a massif wall for Pacific flow (Marengo and Seluchi, 1998) and so the continental tropics and subtropics are influenced by easterly winds originating from the Atlantic Ocean (SAH; Fig. 1.12). The Atlantic flow brings large amounts of moisture to the northern and central parts of the continent and its influence extends to the extra-tropics. Within the mid-latitudes, the flow pattern reverses and low-level Pacific westerlies penetrate into the continent in connection with a poleward decrease in pressure (Garreaud and Aceituno, 2007;

Garreaud *et al.*, 2009). The Pacific flow carries large amounts of moisture to the southwestern coasts, although subsidence over the eastern side of the Andes forces the penetration of very dry air masses across the Argentinean Patagonia (Castañeda and Gonzalez, 2008). Westerlies and north-easterlies converge over the western South Atlantic Ocean forming a diagonal band of precipitation maxima (Nogués Paegle and Mo, 1997) known as the South Atlantic Convergence Zone (SACZ; Fig. 1.12).

SWBA is situated in a transitional zone for the action of subtropical Atlantic flow and mid-latitude Pacific flow imposing sub-humid and sub-arid conditions, respectively (Fig. 1.12). Most moisture is supplied by maritime Tropical air masses originating from the Atlantic Ocean (Campo *et al.*, 2004); these air masses release their humidity progressively as they penetrate into the continent, and so rainfall amounts decrease southwestward (Campo *et al.*, 2004; Scian *et al.*, 2006). Mean annual precipitation within the north-eastern departments of SWBA is 900 mm (Fig. 1.13 [B]), this is twice the mean annual precipitation within the departments situated south-west (Kruse and Laurencena, 2005). The sub-arid conditions inherent to the south-western SWBA are frequently enhanced by the northward advancement of dry continental Polar air (Gil, 2009).

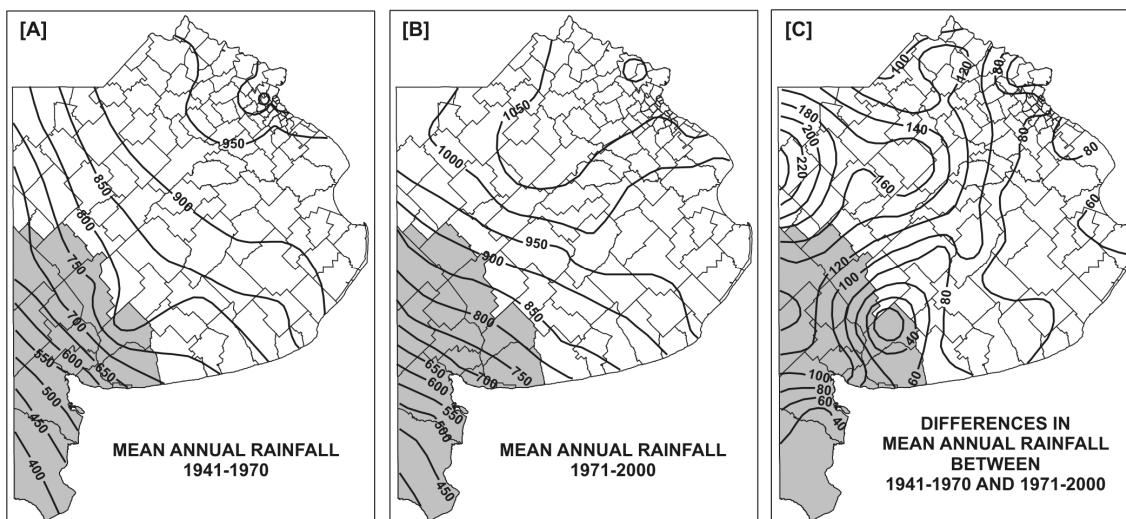


Figure 1.13: Distribution of mean annual rainfall for the periods 1941-1970 and 1971-2001 across the Buenos Aires province (SWBA in grey). After Kruse and Laurencena (2005).

In addition, mean annual rainfall for the period 1971-2000 revealed a westward displacement of the isohyets with respect to the period 1941-1970 (Kruse and Laurencena, 2005). Differences in mean annual rainfall between the two periods were positive across the entire province; within SWBA, precipitation increased by between 20 and 160 mm (Fig. 1.13 [C]). Positive trends in annual precipitation since 1970 have been documented by many studies across the entire La Pampa region and other parts of the country (e.g. Scian, 2000; Penalba and Vargas, 2004; Penalba and Robledo, 2005; Forte-Lay *et al.*, 2008). At the scale of South Eastern South America, Liebmann *et al.* (2004) found that positive rainfall anomalies occur mostly during the summer season in connection to positive anomalies in the sea surface temperature within the nearby Atlantic Ocean.

b) The seasonality of rainfall regimes

Seasonal patterns of atmospheric circulation over South America¹ (Fig. 1.12) define distinct rain and dry seasons for many areas from the equator south to 35°S (Gan *et al.*, 2004). During *austral summer* (DJF), the major heating zone drifts southward (Grimm *et al.*, 2005), the Subtropical Jet penetrates into extra-tropical latitudes (Marengo and Seluchi, 1998; Saulo *et al.*, 2004) and the South American Convergence Zone (SACZ) intensifies strongly, leading to intense frontal convective rainfall over much of south-eastern South America (Nogués Paegle and Mo, 1997). During *austral winter* (JJA), the heating zone drifts equatorward, the SACZ weakens significantly (Nogués Paegle and Mo, 1997), and the central part of the continent exhibits its dry season (Garreaud *et al.*, 2009). Accordingly, rainfall regimes across SWBA exhibit strong seasonality (Scian *et al.*, 2006; Barrucand *et al.*, 2007; Forte-Lay *et al.*, 2008; Gabella *et al.*, 2010); the wet season extends from October through April and the dry season extends from May through September (Fig. 1.14).

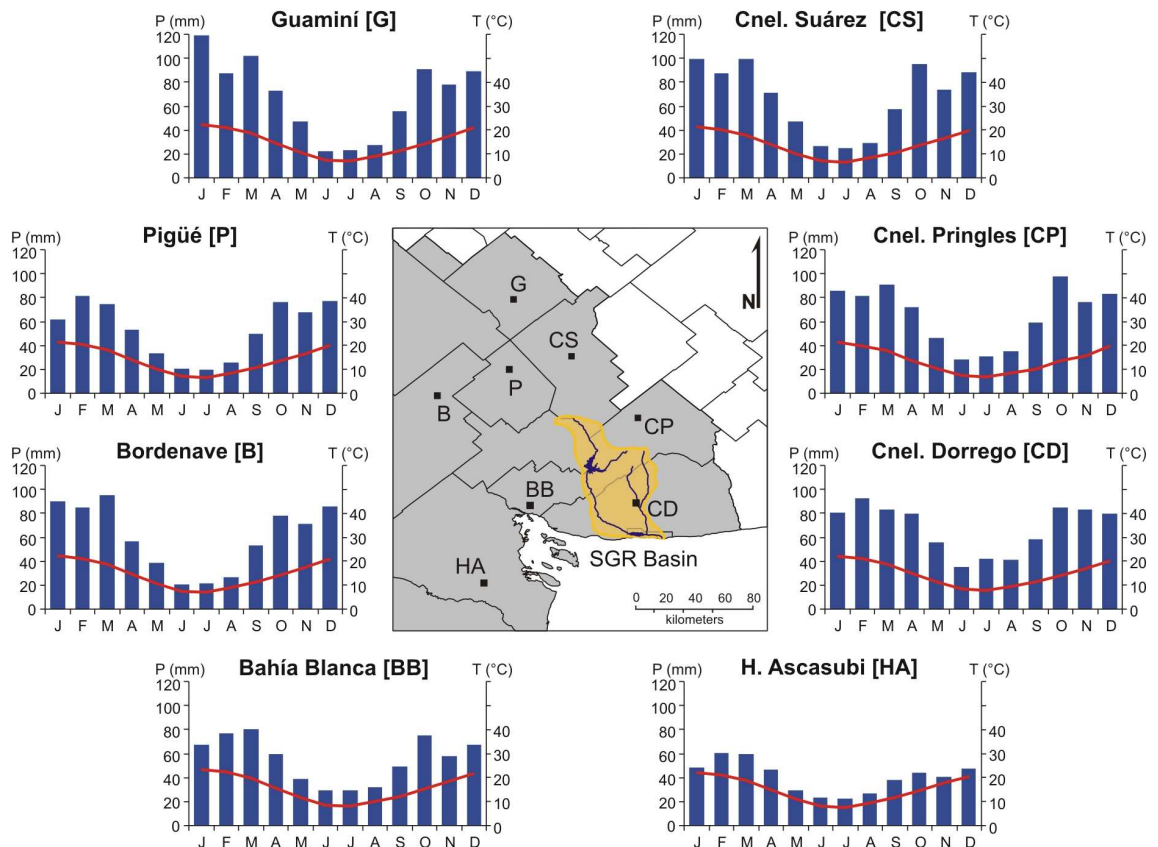


Figure 1.14: Long-term (1971-2010) climographs for eight locations across SWBA. Rainfall and temperature data were achieved from MinAgri (Ministerio de Agricultura, Ganadería y Pesca de la Nación Argentina) and INTA (Instituto Nacional de Tecnología Agropecuaria).

¹ More information on synoptic patterns of atmospheric flow circulation in South America can be found in Lenters and Cook (1996) for the Bolivian High; in Saulo *et al.* (2004) for the Subtropical Jet; and in Nogués-Paegle and Mo (1997), Marengo and Seluchi (1998), Liebmann *et al.* (1999), Barros *et al.* (2000), Robertson and Mechoso (2000), Carvalho *et al.* (2004; 2010) for the South American Convergence Zone.

During the *wet season*, rainfall is originated from heavy frontal storms within the SACZ (Barros *et al.*, 2000; Barrucand *et al.*, 2007; Forte-Lay *et al.*, 2008). The strengthening of thermal low-pressure continental cells (Zhou and Lau, 1998) allows for penetration of maritime Tropical air masses from the Atlantic Ocean (Liebmann *et al.*, 2004; Penalba and Vargas, 2004), which lift in contact with cooler and denser air from higher latitudes (cold front) and cause heavy showers (Zapperi *et al.*, 2007; Gil *et al.*, 2008). On the other hand, Campo *et al.* (2004) and Gil (2009) reported that penetration of continental Tropical air masses may be responsible for very warm and dry weather conditions, especially during the summer season.

During the *dry season*, rainfall is mainly related to warm frontal systems originating from continental Polar air masses blowing from higher latitudes (Zapperi *et al.*, 2006; Barrucand *et al.*, 2007; Gil *et al.*, 2008). During winter, anticyclogenesis over the Atlantic Ocean may lead to rainy episodes over the Atlantic coast; locally known as *Sudestada*, these events may persist over a week or more (Campo *et al.*, 2004; Gil, 2009).

Even if the low-level winds never reverse their direction (as it occurs with the Asian monsoon), synoptic flow circulation over South America reveals a monsoon-like seasonality (Grimm *et al.*, 2005). Accordingly, several authors refer to the effects of a South American Monsoon System (SAMS) based on the seasonal migration of major atmospheric features (Zhou and Lau, 1998; Nogués Paegle *et al.*, 2002; Gan *et al.*, 2004; Grimm *et al.*, 2005; Vera *et al.*, 2006; Marengo *et al.*, 2010).

c) The inter-annual variability of rainfall regimes

Considerable research has evaluated the relationship between rainfall anomalies and *El Niño* Southern Oscillation (ENSO) over a range of spatial scales (e.g. globally: Ropelewski and Halpert, 1987; 1989; 1996; in South America: Aceituno, 1988; Nogués Paegle and Mo, 1997; Grimm *et al.*, 2000; and Grimm, 2011; in South Eastern South America: Almeida and Scian, 2006 and Zamboni *et al.*, 2010; in La Pampa region: Scian, 2000 and Holzman and Rivas, 2011; in SWBA: Campo *et al.*, 2009 and Bohn *et al.*, 2011). The ENSO phenomenon consists of an irregular strengthening and weakening of the trade winds related to coupled interactions of both the ocean (anomalies in the sea surface temperature) and the atmosphere (anomalies in the surface pressure) within the tropical Pacific (Trenberth, 1997; Dijkstra, 2006). According to Trenberth (1997), such anomalies or *oscillations* are the source for inter-annual climate variability worldwide.

Southern South America (which comprises southern Brazil, Argentina, Chile, Uruguay, and Paraguay) is one of the extra-tropical regions most affected by the ENSO phenomenon (Grimm *et al.*, 2000). ENSO events occur roughly every four years (Dijkstra, 2006) and even if their effects have been recognized in all seasons, they seem to be stronger during the austral summer (Grimm *et al.*, 2000; Scian, 2000; Almeida and Scian, 2006; Holzman and Rivas, 2011).

Either in the warm or the cold phase (i.e. *El Niño* or *La Niña*, respectively), the ENSO phenomenon impacts on the frequency and magnitude of rainfall extremes (Grimm *et al.*, 2000). It induces episodes of drier- or wetter-than-normal conditions which,

depending on their magnitude and duration, may conduct to episodes of severe drought or flooding. A number of studies demonstrated that negative and positive rainfall anomalies in South Eastern South America were strongly associated with cold and warm phases of ENSO, respectively (e.g. Ramusson and Wallace, 1983; Ropelewski and Halpert, 1987; Aceituno, 1988; Ropelewski and Halpert, 1989; 1996; Grimm *et al.*, 2000; Grimm, 2011). Whilst the *El Niño* episodes may be responsible for wetter-than-normal conditions occurring in spring and summer, *La Niña* events may be responsible for severe drought occurring during winter, spring and early summer.

The relationship between ENSO episodes and rainfall anomalies within the region of interest has been firstly evaluated by Scian (2000), who correlated oceanic indices (SOI and SST) with long-term series (1911-2000) of precipitation for different sectors of La Pampa (physiographic) region. Later, Campo *et al.* (2009) and Bohn *et al.* (2011) applied a similar methodology in order to identify sequences of dry and wet episodes within SWBA. The years identified as wet or dry by the studies cited above were compared graphically with the SST index for EL Niño 3.4 region (Fig. 1.15).

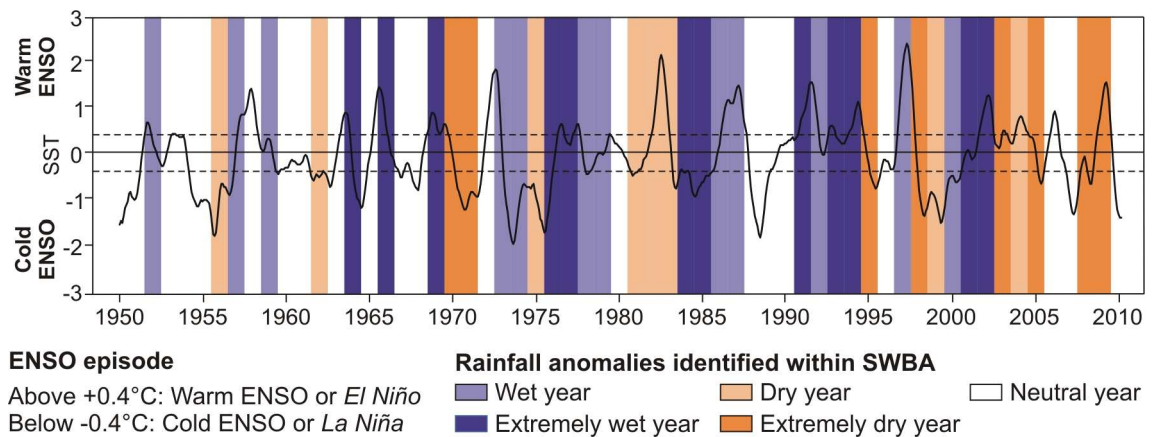


Figure 1.15: Recurrence of dry (or wet) years within SWBA and ENSO episodes for the period 1950–2010. ENSO episodes are defined by 5-month running means of the SST 3.4 (black line) exceeding a threshold of ± 0.4 °C (dashed line) over 6 consecutive months or more (Trenberth, 1997). Dry (or wet) years were identified based on the findings of Scian (2000), Campo *et al.* (2009) and Bohn *et al.* (2011).

Overall, inter-annual variations in annual precipitation over the last six decades were consistent with warm and cold phases of ENSO (Fig. 1.15). Twelve years exhibited extreme positive rainfall anomalies; eight cases were associated with *El Niño* (1964, 66, 69, 77, 91, 93, 94 and 2002) and three cases were related to *La Niña* (1976, 84, 85). Years extremely dry were less frequent, and only one case was coincident with cold phases of ENSO (1971).

Several years revealed anomalous conditions in moisture, positive or negative, without ENSO connections; for example, the extreme wet conditions recorded in 2001 occurred under neutral conditions, and from 2003 through 2009 there was a strong tendency to dry conditions regardless of the ENSO phase. Many studies found that rainfall anomalies within South Eastern South America were also related to anomalies in the sea surface temperature of the nearby Atlantic Ocean (e.g. Barros *et al.*, 2000; Labraga *et*

al., 2002; Liebmann *et al.*, 2004; Scian *et al.*, 2006; Barrucand *et al.*, 2007; Rusticucci *et al.*, 2010). Such anomalies modulate the inter-annual position and intensity of the SACZ, affecting the distribution of precipitable water and vapour fluxes over the region.

Either under ENSO or neutral conditions, the region is severely affected by rainfall extremes inducing water deficiency or water surplus. The significance of rainfall anomalies lies in their cumulative progression (Llano and Penalba, 2011) and on their implications for major human activities such as water management and agriculture (Holzman and Rivas, 2011).

2.1.2. The topographic setting: landforms and materials

From the headwaters to the mouth, the Sauce Grande River flows through multiple structural and lithological units. According to González Uriarte (1984), topography, structure and materials define three major geomorphologic units: (i) the Mountain System, which includes the Ventana and Pillahuinco ranges and series of confined and longitudinal valleys, (ii) the Flatlands, which constitute a large plain by their form and a sediplain by their origin, and (iii) the Coastal Environments dominated by dune alignments and lagoon systems. Altitude, terrain slope and dominant materials impose great contrast for runoff and infiltration processes along the river course, defining three distinct river sections: the upper, middle and lower section (Fig. 1.16).

The *Upper Section* extends from the eastern slopes of the Ventana range to the confluence of El Divisorio creek. This area is currently covered by the Paso de las Piedras Lake so that the upper section closes on the top of the lake. Even if the southern sectors comprise the northern portion of the sediplain, the geomorphologic feature that influences the behaviour of the Sauce Grande River within the upper basin is the mountain system. The Ventana and Pillahuinco Ranges exhibit mean elevation ranges of between 700 and 800 m and maximum height of 1 240 m in Cerro Tres Picos (Gil, 2009). The folding phase affected distinct sedimentary sequences of conglomerates, sandstone and pelites of Palaeozoic age (Rabassa, 1989); intense metamorphism led to formation of quartzite, gneiss and shale. Together with outcrops of Precambrian granite, these materials constitute the most characteristic rocks of the system (Gonzalez Uriarte, 1984).

The Sauce Grande River dissects the eastern slopes of the Ventana Range and the western slopes of the Pillahuinco range by a dense drainage network of dendritic to sub-parallel design ($Dd = 1.2 \text{ km/km}^2$; Table 1.4). The collectors are deep, V-shaped and describe torrential unsteady regime ($FI = 1.1$; Table 1.4). Large amounts of material are carried down to the foothills, forming a highly permeable alluvial fill (Luque *et al.*, 1979; Rabassa, 1982). As shown in Figure 1.16, the frequency of collectors decreases significantly with distance from the source areas. Over the foothill, the channel slope is 0.009 and the main collector (stream order 6; Gil, 2009) forms a wide channel that separates longitudinally the two mountain ranges (Paoloni *et al.*, 1972; Luque *et al.*, 1979; Rabassa, 1982).

The *Middle Section* extends integrally over the post-Miocene plain which, in terms of surface, is the most representative geomorphologic feature of the river basin. Elevation ranges from 300 m over the foothills to 60 m over the frontal scarp that separates the

plain from the coastal zone (Gonzalez Uriarte, 1984). Mean channel slope is 0.003, and the general topography is rather flat and homogeneous (Fig. 1.16).

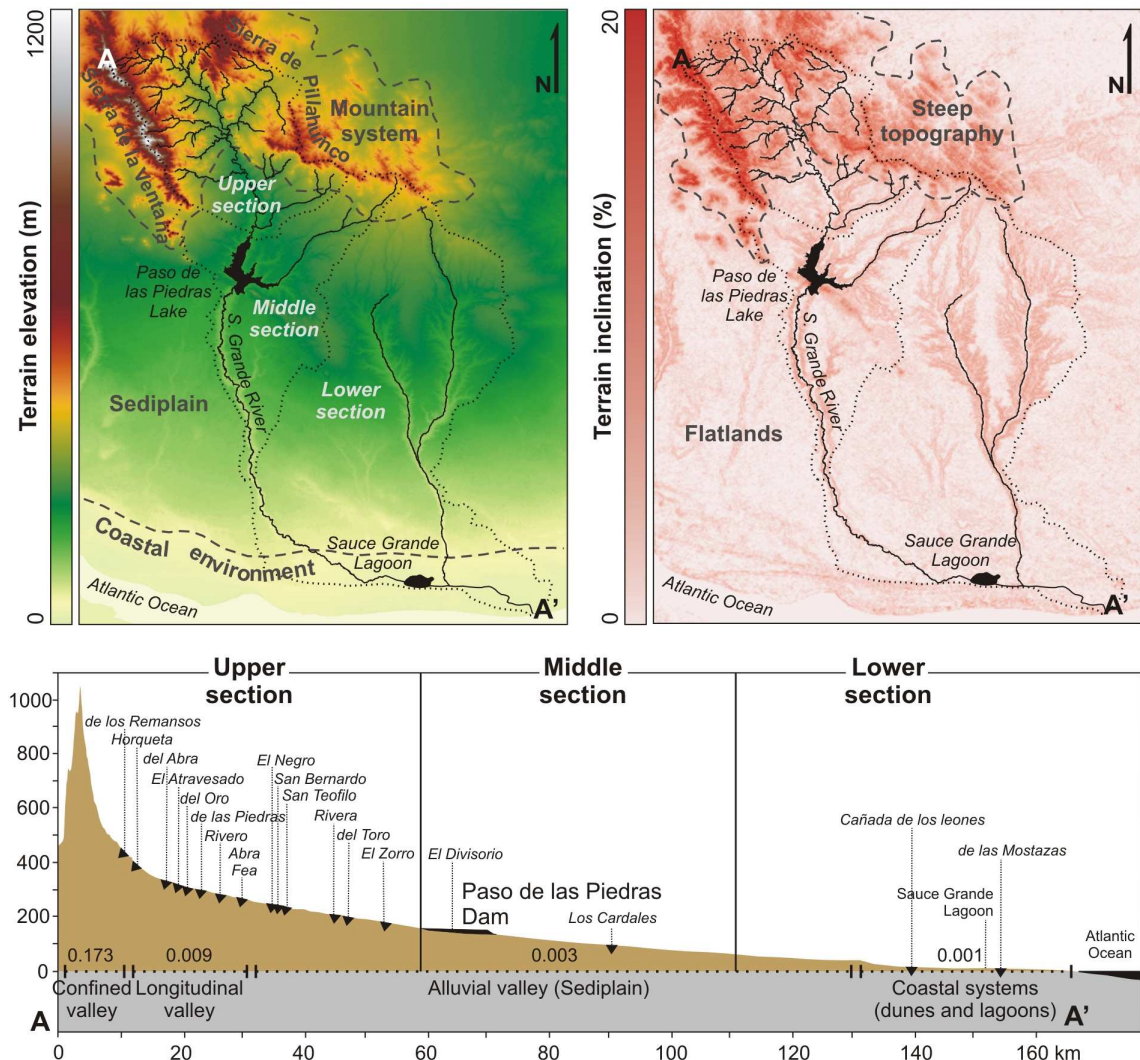


Figure 1.16: Major geomorphologic features within the Sauce Grande Basin based on elevation ranges and terrain slope, and longitudinal profile of the river from the headwaters to the mouth. Altitude and slope maps were achieved by reanalysis of the USGS DEM90 within ArcGIS. Geomorphologic features were based on González Uriarte (1984).

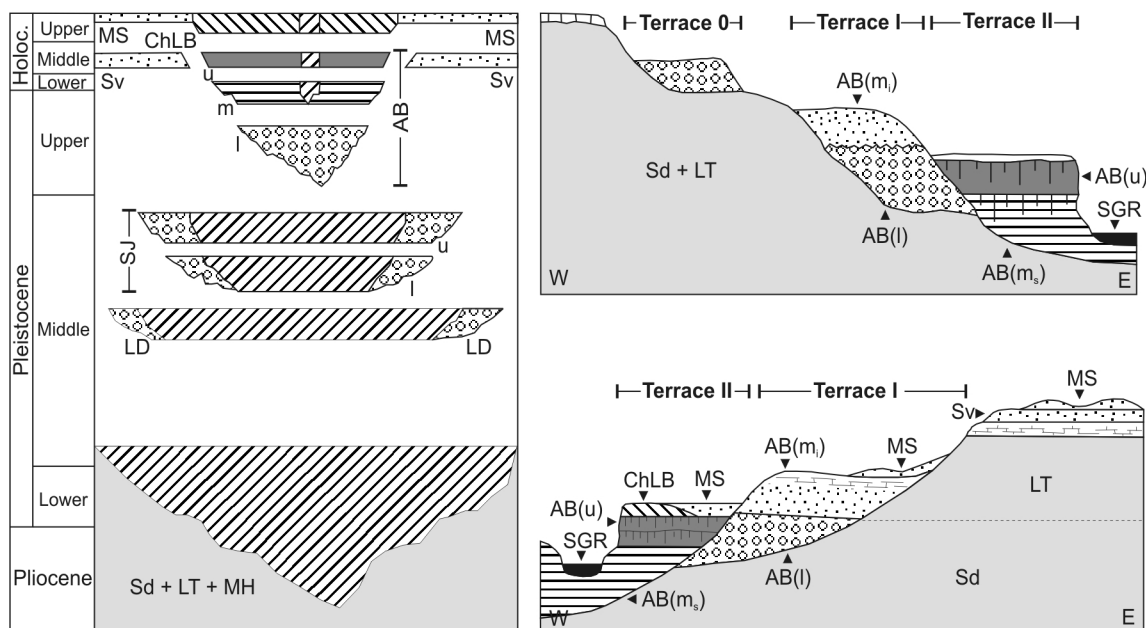
In the top portion, the river excavates fine aeolian and fluvial deposits and flows confined within a deep channel that exhibit vertical banks of up to 8 m height (Borromei, 1991). Down southward, the canyons lose altitude, the channel slope decreases and the flow sinuosity increases (Paoloni *et al.*, 1972; Luque *et al.*, 1979). The drainage density and regime flashiness decrease notably ($Dd = 0.27$; $FI = 0.01$; Table 1.4).

Three different terrace levels give evidence of at least three diachronic episodes of fluvial incision and filling (Fig. 1.17, Zavala and Quattrocchio, 2001). The Terrace 0 is the oldest fluvial feature and hence, it is extremely eroded. It integrates facies of

conglomerates and sand (La Delta Fm.), sitting discordantly upon sandy-silty Pampean sediments of Plio-Pleistocene age (Saldungaray and La Toma Fms). The basis of Terrace 0 is, on average, 12 m higher than the ceiling of Terrace II (current floodplain), and the remnants have been only observed over the right bank (Borrromei, 1991).

Table 1.4: Morphometric characteristics of the Sauce Grande Basin for the upper, middle and lower river sections. Based upon Luque *et al.* (1979), Rabassa (1982), and Gil (2009).

Metric		Abbrev.	Upper section	Mid section	Lower section
Shape	Area	A (km ²)	1020.2	992.7	2644.7
	Perimeter	P (km)	153.4	205.1	260.7
Topography	Maximum altitude	H _{max} (m)	1228	638	523
	Minimum altitude	H _{min} (m)	161	60	0
	Mean altitude	H _{mean} (m)	362	204	133
Drainage	Drainage density	D _d (km/km ²)	1.19	0.27	0.15
	Flashiness Index	FI	1.10	0.01	0.0
	Main channel long.	L _C (km)	71.98	68.79	77.47
	Main channel slope	S _C (°)	0.009	0.003	0.001



References

- | | | | |
|---------------------------------------|--------------------------------------|-------------------------------|------------------------|
| Eolian and flooding deposits | Conglomerates | ChLB - Ch. La Blanqueada Fm. | Sd - Saldungaray Fm. |
| Fine 'spring' deposits | Eolian and paleofluvial deposits | MS - Matadero Saldungaray Fm. | LT - La Toma Formation |
| Ephemeral fluvial and eolian deposits | Erosive hiatus | Sv - Saavedra Formation | MH - Monte Hermoso Fm. |
| Eolian deposits | Non-deposition hiatus (soil genesis) | AB - Agua Blanca Sequence | |
| | | SJ - San José Sequence | |
| | | LD - La Delta Sequence | |

Figure 1.17: Quaternary geology of the Sauce Grande River. After Borrromei (1991), Quattrocchio *et al.* (1993; 2008), and Zavala and Quattrocchio (2001).

Terraces I and II show similar evolutionary stages consisting of erosive episodes alternated by events of filling. Filling integrates both aeolian and fluvial sediments, and the grain size of the layers decreases with time (Zavala and Quattrocchio, 2001; Quattrocchio *et al.*, 2008). The Terrace I comprise two members of the Sequence Agua Blanca linked by a regional discontinuity. The lowest member [AB(l)] contains layers of gravel and sand; the lowest-medium member [AB(mi)] is composed by silt and sand. The Terrace II includes Holocene fluvial deposits composed of sand, silt and clay (Chacra La Blanqueada Fm; ChLB) laying upon sandy and silty deposits of the upper members of the Sequence Agua Blanca [AB(ms) and AB(u)]. On the left banks, aeolian deposits associated with Saavedra and Matadero Saldungaray Formations [Sv; MS] have been also observed (Borromei, 1991).

Within the *Lower Section* the slope decreases significantly (0.001; Fig. 1.16) and the river channel exhibit high sinuosity. In the lowest portions, the river flows parallel to the coastline, forced by dune alignments with elevation ranges of between 10 and 15 m (Borromei, 1991). It forms several lagoon systems over hydro-aeolian depressions of varying size, the most important being the Sauce Grande lagoon (Paoloni *et al.* 1972, Luque *et al.* 1979).

2.1.3. Linked physical processes and fluctuations in water resources

Studies on regional climate have demonstrated that the duration and frequency of rainfall anomalies may be highly variable in space and time, although their magnitude is frequently severe. Given the steep-flat topography of the river basin and the varying geology, cumulative rainfall shortages (or excesses) may have an immediate effect on the volume of water available for runoff, infiltration and storage.

According to Luque *et al.* (1979), about 34 % of the river basin corresponds to mountain areas where the steep topography and the impervious geology contribute to runoff dominate over infiltration processes (Gaspari *et al.*, 2008; Gil, 2009). In periods of precipitation shortages, tributaries remain dry and the main collector describes low residual flows (Paoloni *et al.*, 1972). Surface flow during wet periods is torrential-like, and cumulative water excess may lead rapidly to overflowing of streams and rivers (Gil, 2009). Nevertheless, peak flows and floods exhibit a short duration as water is quickly evacuated downstream where it is currently intercepted by the Paso de las Piedras Reservoir.

The remaining 66 % of the total basin surface corresponds to flatlands. The smooth topography and the permeable geology contribute to decrease the rate and extent of runoff and to increase the vertical water exchange, i.e. infiltration and evaporation. In addition, the water table is relatively shallow (Luque *et al.*, 1979) and so surface and underground flow are closely related (Kruse *et al.*, 2001; Kruse and Laurencena, 2005).

Topography and materials within the river basin increase the vulnerability of water resources face to rainfall extremes inducing disruptions for the water exchange over the horizontal and the vertical axis. Rainfall shortages may turn rapidly into agricultural droughts, or into hydrological droughts if cumulative, because the shallow streams and aquifers are particularly vulnerable to evaporation. On the other hand, episodes of heavy rainfall may contribute to quickly saturate the water table and hence lead to flooding.

Concern on the impacts of rainfall anomalies upon regional water resources has motivated a number of studies, although most of them focus on the recurrence of drought (e.g. Troha and Forte-Lay, 1993; Piccolo *et al.*, 2002; Penalba and Vargas, 2004; Penalba and Robledo, 2005; Barrucand *et al.*, 2007; Minetti *et al.*, 2007; Penalba and Llano, 2008; Andrade *et al.*, 2009; Llano and Penalba, 2011). Literature on the effects of water excess is less frequent, probably due to the shorter duration and minor extent of the local floods. The overall lack of knowledge about the complex dynamics in local water resources is evidenced by the current deficiencies in drinking water supply. Rainfall shortages and population growth have always been of major concern for water management practices. The following sections explore the relationship between use and management of local water resources, with focus on the history of the Sauce Grande River as main source for water supply.

2.2. THE WATER DEMAND: AGRICULTURE, POPULATION, AND INDUSTRY

Despite the considerable size of the river basin (4 600 km²), the Sauce Grande River is linked to a larger area due to its environmental service. The river has been historically at the basis of the agricultural and urban development of the central SWBA; today, the Paso de las Piedras Dam provides drinking water to a population of about 400 000 people mainly concentrated in the cities of Bahía Blanca and Punta Alta (Fig. 1.18 [A]). Primary production is at the heart of the regional development (Sili, 2000). More than 50 % of the surface area is used for livestock-related activities such as forage crops and farming on natural grasslands (Fig. 1.18 [B]); the remaining surface is used for rainfed agriculture (cereal and oilseeds). Agricultural practices depend strongly on natural sources for water (Serio *et al.*, 2010), so that annual and inter-annual rainfall variability are the major threat for agricultural production and farming (Penalba and Robledo, 2005; Forte Lay *et al.*, 2008).

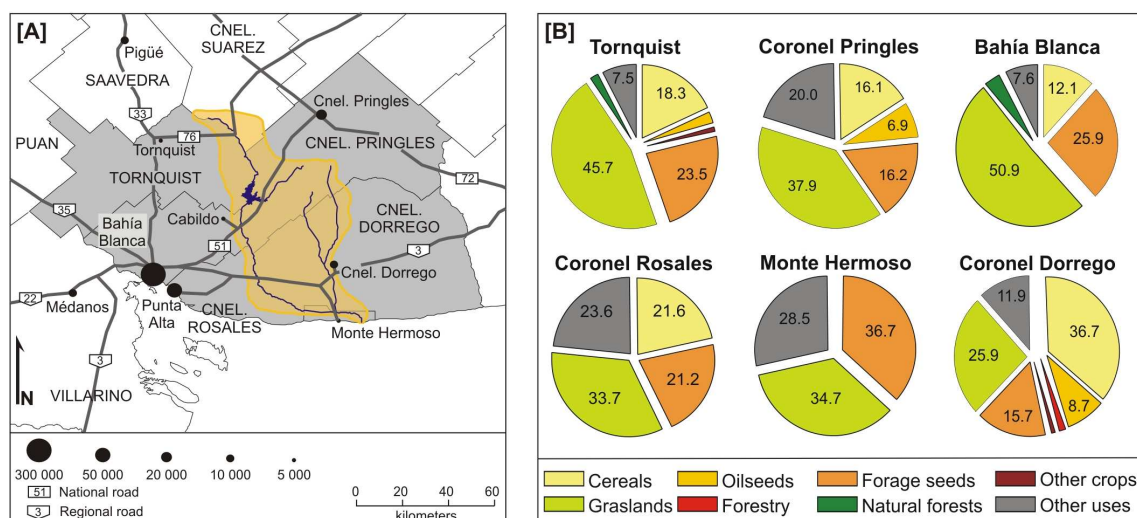


Figure 1.18: [A] Urban centres and [B] major land uses within the six departments (grey area) linked to the Sauce Grande River Basin (yellow area). Data were achieved from INDEC.

The number and size of urban centres is much reduced, and population density is very low (Fig. 1.18 [A]). For example, the departments of Tornquist, Coronel Dorrego and Coronel Pringles reveal less than 5 inhab.km² and very low (even negative) rates of population growth, at least during the last decades (Fig. 1.19). In contrast, the departments of Bahía Blanca and Coronel Rosales emerge as core of the regional economy. They support major primary-related services such as agro-industry and commercialization (Grippe and Visciarelli, 2005), concentrate the highest population density (more than 130 and 45 inhab.km² in 2010, respectively) and reflect the highest rates of population growth. The steepest increase in population took place between 1881 and 1948 with a growing rate of 4 400 % in 67 years. Population growth during the second half of the 20th Century was more gradual, although population duplicated its number increasing from 150 000 to 346 000 inhabitants.

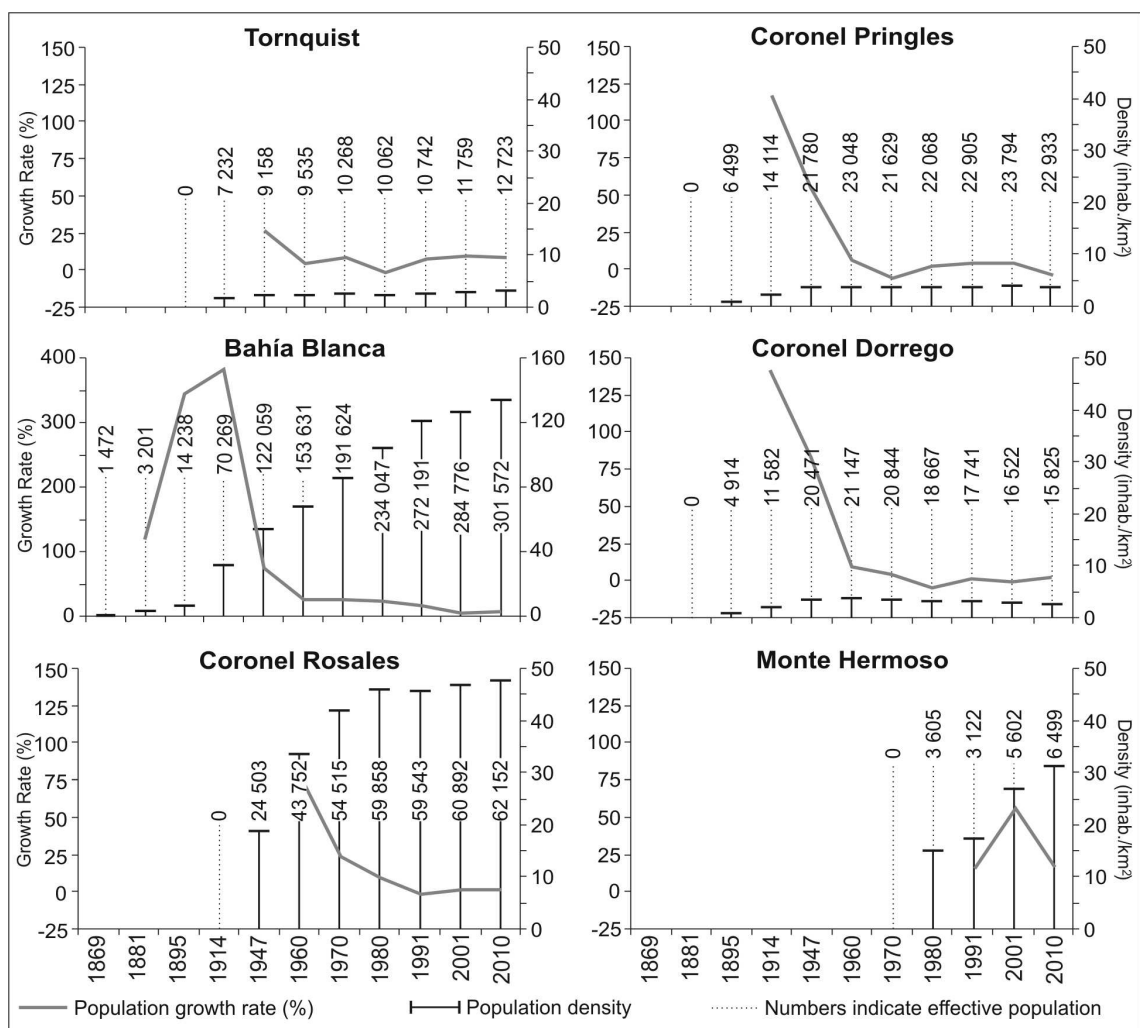


Figure 1.19: Population density and rates of population growth by department for 11 time steps between 1869 and 2010. Data were achieved from INDEC.

High rates of population growth all along the 20th Century entrained, logically, an increase in the demand for drinking water (Table 1.5). Between 1909 and 2009, the annual water use rose from 0.57 hm³ to 94.6 hm³; this is more than 160 times increase

for a population that increased 9 times over the same period. Domestic and industrial water needs during the first half of the century were considerably lower than those related to modern life; therefore, an increase of 244 litres per inhabitant per day between 1909 and 1967 is not much surprising. However, the annual water usage between 1967 and 2009 increased by 275 % and today, a person consumes 713 litres of water per day.

Table 1.5: Water use within the departments of Bahía Blanca and Coronel Rosales along the 20th Century. The volume of daily water use for each time step was calculated based on the corresponding population number.

Year	Population		Water Use			
	Inhabitants ^(a)	Growth rate (%)	Daily (l/in/d)	Daily (m ³)	Annual (m ³)	Growth rate (%)
1909	~42 254	-	36	1 550	565 750 ^(b)	-
1919	70 269	66.3	36	2 540	927 100 ^(b)	63.9
1931	146 562	108.6	77	11 240	4 102 600 ^(b)	342.5
1967	246 139	67.9	280	69 000 ^(c)	25 185 000	513.9
1986	293 905	19.4	408	120 000 ^(c)	43 800 000	73.9
1994	331 734	12.9	531	176 000 ^(c)	64 240 000	46.7
2000	345 668	4.2	600	207 400 ^(c)	75 701 000	17.8
2009	363 724	5.2	713	259 200 ^(d)	94 608 000	25.0

Data source: (a) INDEC (Instituto Nacional de Estadística y Censo); (b) Grippo and Visciarelli (2005); (c) Plan Estratégico Bahía Blanca (MBB, 2000); (d) Raskovsky (2009).

The question that emerges in this context is: how much water does a person need? According to most international agencies, a volume of 50 litres per person per day should cover basic human water requirements for drinking, sanitation, bathing and food preparation (WCD, 2000). This implies that the current water usage in Bahía Blanca and Coronel Rosales is surpassing by more than 10 times the international standards. Conceivably, a considerable proportion of such volume is related to the expansion of heavy agro-industries which consume large volumes of water (Grippo and Visciarelli, 2005; Ferrera and Alamo, 2010); however, Raskovsky (2009) documented that the proportion of industrial water use in 2009 was only of 20 % the current water use (52 800 m³ per day).

2.3. PRACTICES AND POLICIES OF WATER MANAGEMENT

The central SWBA has known qualitative and quantitative deficiencies for drinking water supply periodically. Recurrence of drought and increase in the water demand subsequent to population growth led to a number of water crises which, in turn, led to systematic advances in local practices of water management.

2.3.1. Advances in water management practices

Advances in practices of water management (Fig. 1.20; 1.21) may be grouped into three different periods: (a) building the city, (b) the city expansion, and (c) the dam era. The figures and the text were based upon the contributions of the Plan Estratégico Bahía Blanca (MBB, 2000), Schefer (2004), Grippo and Visciarelli (2005), Andrés *et al* (2009) and Ferrera and Alamo (2010).

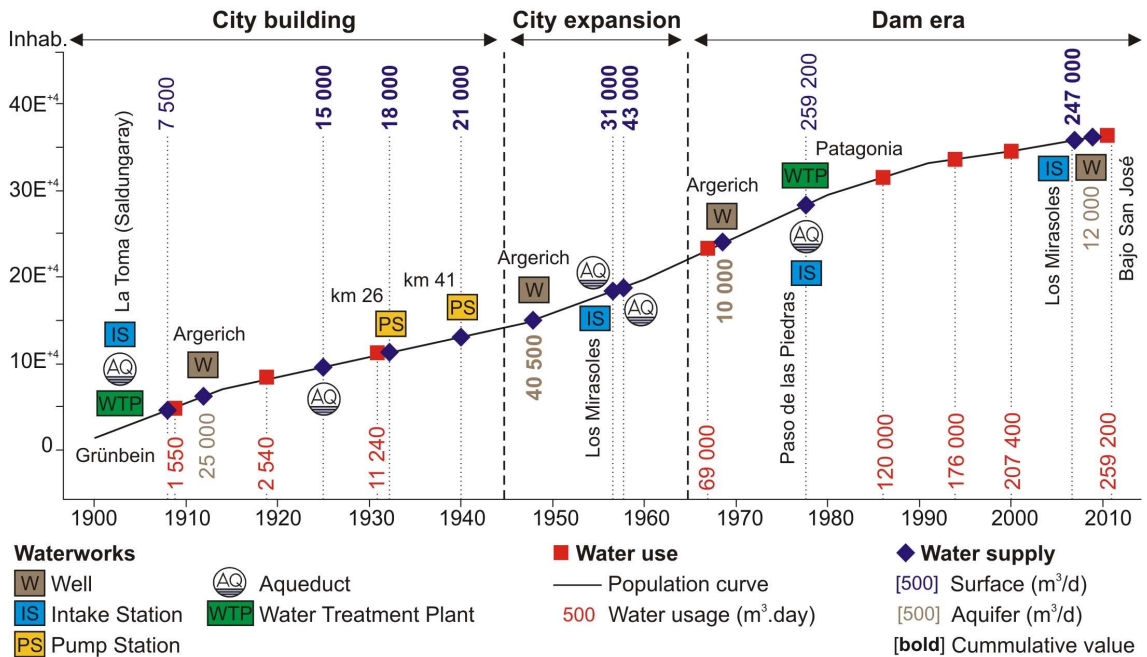


Figure 1.20: Population growth and advances in water management practices along the 20th Century.

a) 1900-1945 → Building the city

The first aqueduct and the associated urban distributing pipes were built during the early steps of the city foundation. This was motivated by the drought of 1905 (which depleted the local cisterns) and by the steep increase in the population number (more than 50 000 people in 15 years). With a capacity of 7 500 m³ per day, the aqueduct transported water by gravity from La Toma intake station upon the Sauce Grande River to a water treatment plant located in Grünbein near the city of Bahía Blanca. Additionally, the deep aquifer within the Bahía Blanca hydrogeologic basin, discovered in 1912, provided 25 000 m³ per day from a well situated near Argerich town. Between 1915 and 1945 population increased by twice its number and other waterworks were assembled to the network. A new aqueduct and two pump stations increased three times the capacity for water supply; by the end of the period, Grünbein was processing a total volume of 21 000 m³ per day.

b) 1945-1965 → The city expansion

In response to the drought of the year 1947, series of supplementary wells were

constructed near Argerich. Although they provided a total volume of 40 500 m³ per day, their capacity decreased rapidly with time and a new water crisis took place by late 1950's. An auxiliary intake station, Los Mirasoles, was constructed in 1957 upon the Napostá Grande Creek; it was connected to Grünbein plant through an aqueduct of 10 000 m³.day capacity. By 1958, a new aqueduct was assembled to incorporate a volume of 12 000 m³ per day from La Toma.

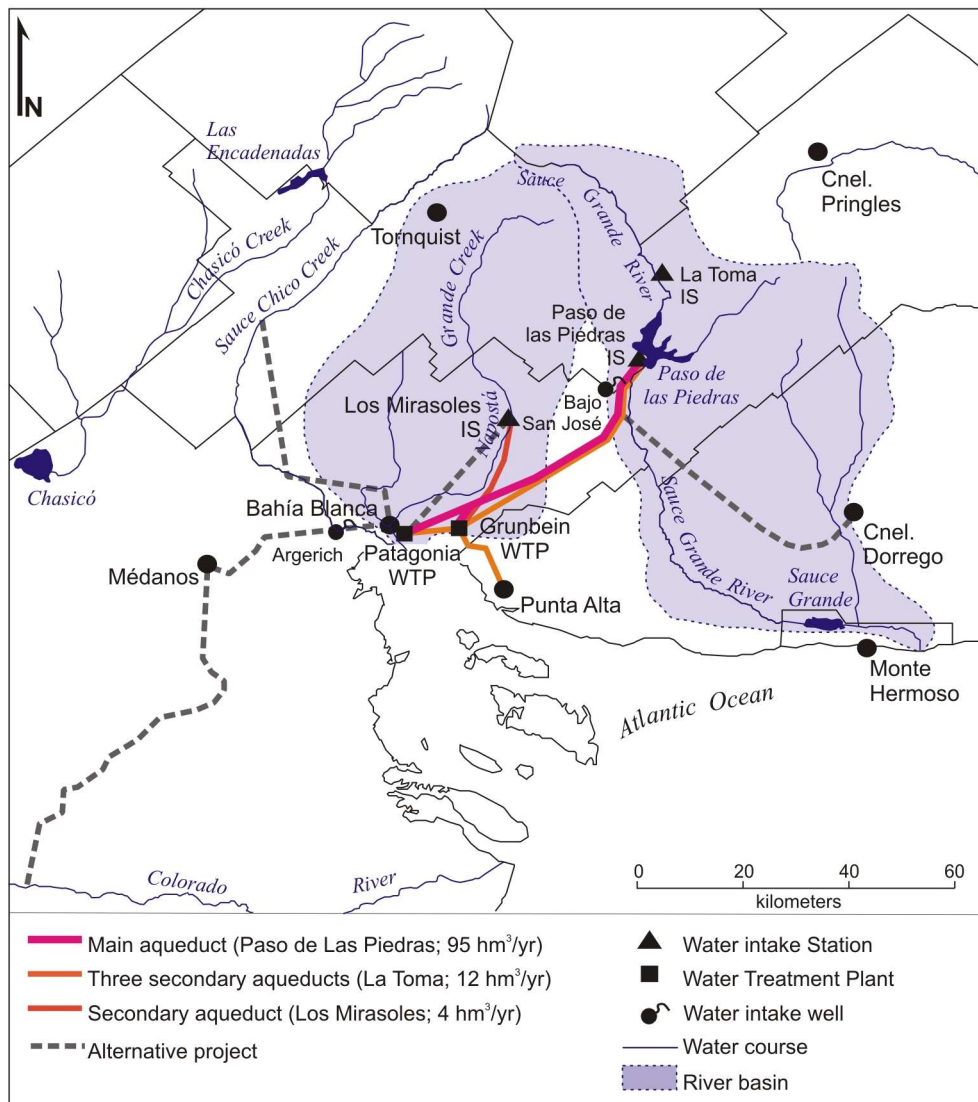


Figure 1.21: Waterworks for water supply in central SWBA.

c) 1965-2010 → The Dam era

By mid 1960's, Grünbein was processing a total volume of 43 000 m³ per day for drinking water supply to Bahía Blanca and Punta Alta. This volume was assembled to the groundwater extracted from the deep aquifer in Argerich, although its resources were declining with time. The water demand by 1967 was of about 69 000 m³ per day; as this volume exceeded largely the supply capacities of Grünbein and Argerich, the

provincial government announced the construction of the Paso de las Piedras Dam to give a definitive solution to the increasing water demand. The dam and its reservoir were completed in 1978 replacing all the pre-existing features except by the Grünbein plant, which is still in use. The dam was designed to assure 500 litres of water per day to a population of 500 000 people; waterworks included an aqueduct of $259\,200\text{ m}^3\cdot\text{day}^{-1}$ capacity and a new water treatment plant located in Patagonia neighbourhood, western Bahía Blanca.

The Paso de las Piedras Dam has satisfied urban and industrial water needs for 30 years. To date, the water demand exceeds largely the supply capacities of the dam. The current water crisis began in 2007 and peaked dramatically in 2009, in connection to a hydrological drought that caused the depletion of surface and underground water resources. Several actions were undertaken to increase water supply capacities. For example, Los Mirasoles station upon the Napostá Grande Creek was reactivated in 2007, and new wells for groundwater extraction were built within both the Napostá Grande Basin (2008) and the Sauce Grande Basin (2009). In addition, three projects for multipurpose dam building were announced over the long-term; they include (i) impoundment of the Napostá Grande Creek for flood control, irrigation and water supply to the industrial core, (ii) impoundment of the Sauce Chico Creek for flood control, irrigation and drinking water supply to the city of Bahía Blanca, and (iii) impoundment of the Colorado River for irrigation and water supply to the department of Villarino and the city of Bahía Blanca (Fig. 1.21).

2.3.2. The Paso de las Piedras Complex

The Paso de las Piedras Dam classifies as large. The main features integrating the dam complex are illustrated in Figure 1.22; the characteristics of the dam and its reservoir, and the type and capacity of the dam outlets are summarized in Table 1.6. Both the table and the figure were based on the contributions of Buraschi *et al.* (1999), Schefer (2004), and Raskovsky (2009).

As discussed above, the main purpose of the Paso de las Piedras Dam is water supply to a population of about 350 000 people centred in the departments of Bahía Blanca and Coronel Rosales. Fishing and recreation were important secondary functions, although the current public entrance is restricted as the reservoir was declared Protected Area in 2009. The impoundment was not designed for flood control; however, it highly regulates flow between the upstream and the downstream reaches.

The reservoir lake extends over 3 600 ha and has a total capacity of 328 hm^3 for 25 m depth. It lies over heterogeneous and unconsolidated alluvial deposits composed of gravel, sand, silt, and clay. The high permeability of the underlying materials led to high rates of infiltration feeding the river downstream by subsurface flow (Buraschi *et al.*, 1999). However, infiltration rates are currently controlled by an artificial impermeable layer which, in some areas, exceeds 50 cm thickness (Schefer, 2004).

An aqueduct with maximum capacity of $3\text{ m}^3\cdot\text{s}^{-1}$, i.e. $259\,200\text{ m}^3\cdot\text{day}$, transports water by gravity from the dam chamber (160 m.s.l.) to the water treatment plant situated in Patagonia (83 m.s.l.). The plant may process a maximum volume of $200\,000\text{ m}^3$ per day for water supply to the city of Bahía Blanca. The remaining volume is conducted to

Grünbein plant and assembled to the volume extracted from Los Mirasoles (reactivated in 2007). Grünbein supplies drinking water to the city of Punta Alta and its associated Naval Base, and contributes to increase the water supply to Bahía Blanca during summer (MBB, 2000; Ferrera and Alamo, 2010).

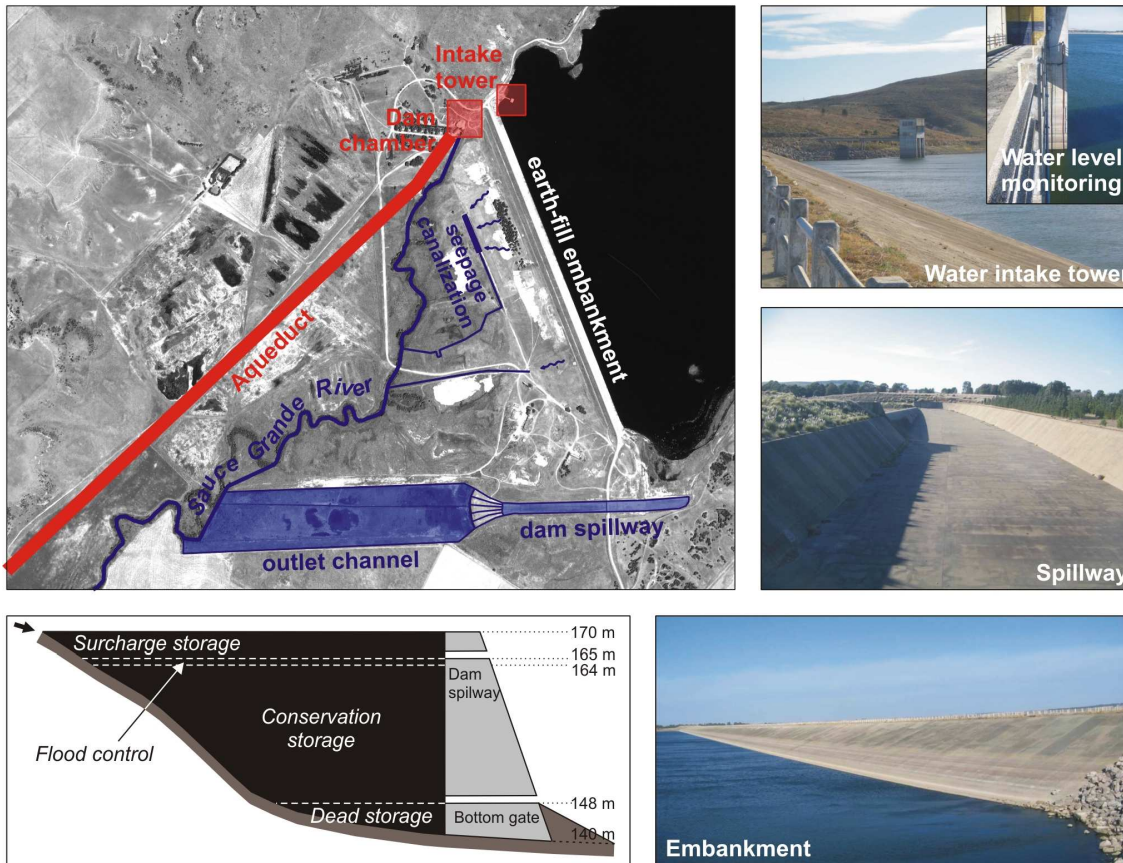


Figure 1.22: Paso de las Piedras Complex scheme.

a) Water level monitoring

The standards for reservoir management are established by consensus within the Sauce Grande Basin Committee. The Committee is composed by ADA authorities (Autoridad del Agua de la Provincia de Buenos Aires) and the mayors of each of the departments related to the river basin. The Water Code of the Buenos Aires Province sets the legislative framework for reservoir cleaning and evacuation, water withdrawal, control of pesticides, and channel freedom zone; there are no regulations concerning the flow maintenance downstream.

Given its purpose for drinking water supply, dam management tends to maximize water storage within the reservoir. According to Petts (1984), such dam operation procedures may be described as *conservation storage* procedures, where water is stored and conserved for use without special regard for flow maintenance downstream. Reservoir evacuation occurs only in periods of water excess where the water levels are near or surpassing 164 m.s.l. (i.e. full reservoir). Water diversions are conducted either through

the bottom gate (controlled hypolimnetic release) or through the overflow spillway (uncontrolled epilimnetic release). Since the main function of the reservoir is to store and conserve water, controlled water release occurs mostly for reservoir cleaning or flood control purposes.

Table 1.6: Characteristics and main features integrating the Paso de las Piedras Complex.



Paso de las Piedras Complex	
Opening date	1978
Owner	Government of the Buenos Aires Province
Regulator	ADA (Autoridad del Agua de la Provincia de Buenos Aires)
Inflow	Sauce Grande River; El Divisorio Creek
Outflow	Sauce Grande River
Dam	
Type	
<i>By purpose</i>	Water supply
<i>By operation procedure</i>	Conservation storage
<i>By size</i>	Large
Structure	Earth-fill embankment
Length	1 700 m
Height	170 m.s.l. (30 m)
Base width	200 m
Crest width	20 m
Outlets	
Overflow spillway	
<i>Type</i>	Chute-spillway
<i>Capacity</i>	2 000 m ³ .s ⁻¹
<i>Height</i>	165 m.s.l. (25 m)
Bottom gate	
<i>Capacity</i>	10 m ³ .s ⁻¹ for 15 cm opening
<i>Height</i>	148 m.s.l. *
Reservoir	
Capacity	328 hm ³ (active capacity: 310 hm ³)
Surface area	3 600 ha
Maximum height	165 m.s.l.
Maximum depth	25 m

(*) These values were based upon the work of Schefer (2004). Raskovsky (2009) allocates an active storage of 321 hm³ for a minimum height of 145 m.s.l.

High evaporation rates ($1 \text{ m}^3 \cdot \text{s}^{-1}$), strong inter-annual variability in climate-driven reservoir inflows and growing water demand combine to generate low resilience to declines in water reserves. Accordingly, Raskovsky (2009) devised a warning system based on lowering water levels within the reservoir (Fig. 1.23). The system uses the ratio of water levels to active storage to define three benchmarks that represent a threat for water reserves as follows:

- The *Yellow Warning* indicates that the reservoir water level lowered to 155 m.s.l. (25 % of the active storage) and lowers;
- The *Orange Warning* indicates that the reservoir water level lowered to 152 m.s.l. (15 % of the active storage) and lowers;
- The *Red Warning* indicates that the reservoir water level lowered to of 150 m.s.l. (10 % of the active storage) and lowers.

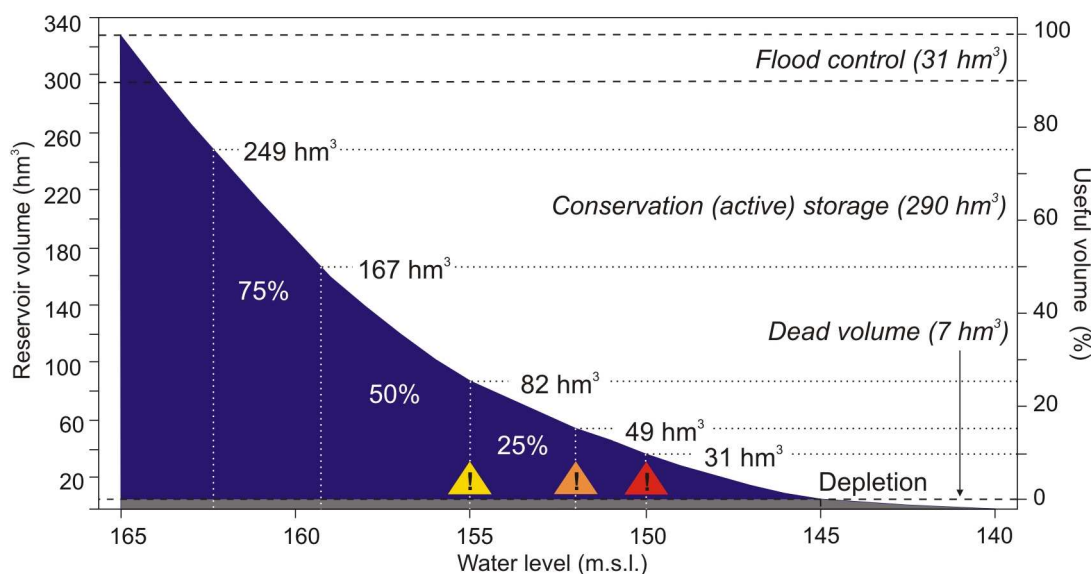


Figure 1.23: Reservoir volume by water level and level-related threats for water reserves. Based upon Raskovsky (2009).

The decline in the reservoir's volume and the corresponding warning levels is projected considering long-standing precipitation shortfalls, high evaporation rates and maximum volumes of water withdrawal. Once the water level enters into the yellow warning, it may take less than one year before the reservoir depletes.

b) Reservoir trophic state

Maximization of water storage within the reservoir implies long water residence times. After maturation, reservoirs act as nutrient sinks, particularly for nutrients associated with sediments (Petts and Gurnell, 2005); nutrient concentration and long water detention times leads to eutrophication (McCartney *et al.*, 2001), with significant implications for the quality of the water stored (Estrela *et al.*, 1996).

The trophic level of the Paso de las Piedras Reservoir is currently eutrophic-

hypereutrophic (Fernández *et al.*, 2011), and undergoes algae blooms dominated by potentially toxic cyanobacteria such as *Anabaena circinalis* and *Microcystis aeruginosa*, especially during warm months (Estrada *et al.*, 2002; Fernández *et al.*, 2009). Such trophic state may have great implications for the quality of the water supplied for drinking purposes (Echenique *et al.*, 2007); however, inspecting these implications is way beyond the scope of this research. For more information on the biological composition, limnology and trophic state of the Paso de las Piedras Reservoir see Parodi *et al.* (2004), Ruibal Conti *et al.* (2005) and Fernández *et al.* (2009; 2011); for more information on algae blooms within the reservoir, see Echenique *et al.* (2001); for more information on restoration policies and actions, see Estrada *et al.* (2002; 2008) and López *et al.* (2006).

2.4. WATER USE AND MANAGEMENT FACE TO THE VARIABILITY OF WATER RESOURCES

The overall lack of knowledge about the complex behaviour of regional water resources became evident in recent years due to the dramatic impacts that rainfall extremes have had on the local society. During the last decade, a succession of episodes of drought and flooding affected not only the local agricultural practices but also the relationship between water use and water available for use, putting into question deficiencies in water management practices. The recurrence and the severity of these events was such that was documented by countless articles within the local press. This provided a rich baseline to assess the recurrence of extreme rainfall events and their economic and social implications.

Figure 1.24 reconstructs the succession of extreme dry (or wet) events documented by the local newspaper, *La Nueva Provincia* (LNP), over a timeline ranging from the year 2000 to 2010. Within the wet events, *Heavy Storms* refer to episodes of large rainfall amounts recorded in a short period of time (few hours or few days) causing urban and rural flooding, road blockades, landslides, falling trees and power lines, etc. Where these storms entrained saturation of the water table and overflowing of streams and rivers for one day or more, they are referred to as *Flooding*. On the other hand, the dry events were defined separately as agricultural or hydrological drought. *Agricultural Drought* refers to precipitation shortages causing water deficits that affect the agricultural practices, whilst the *Hydrological Drought* occurs following long periods of precipitation shortfalls that affect not only the soil moisture but also the sources for freshwater such as streams, groundwater and reservoir storage.

According to the local newspaper, the early years 2000's revealed an array of heavy storms which, depending on the degree of severity, affected many communities all across SWBA. The storm of biggest magnitude took place in November 2002, recording more than 210 mm in several sectors of the river basin and peaking in the headwaters (e.g. 416 mm in Villa Ventana). Given the humidity cumulated from previous months, the hydrological system could not absorb such water mass and collapsed. The storm caused damage in several departments, although the most serious consequence of the storm was the overflowing of the Paso de las Piedras Dam (Fig. 1.24-a).

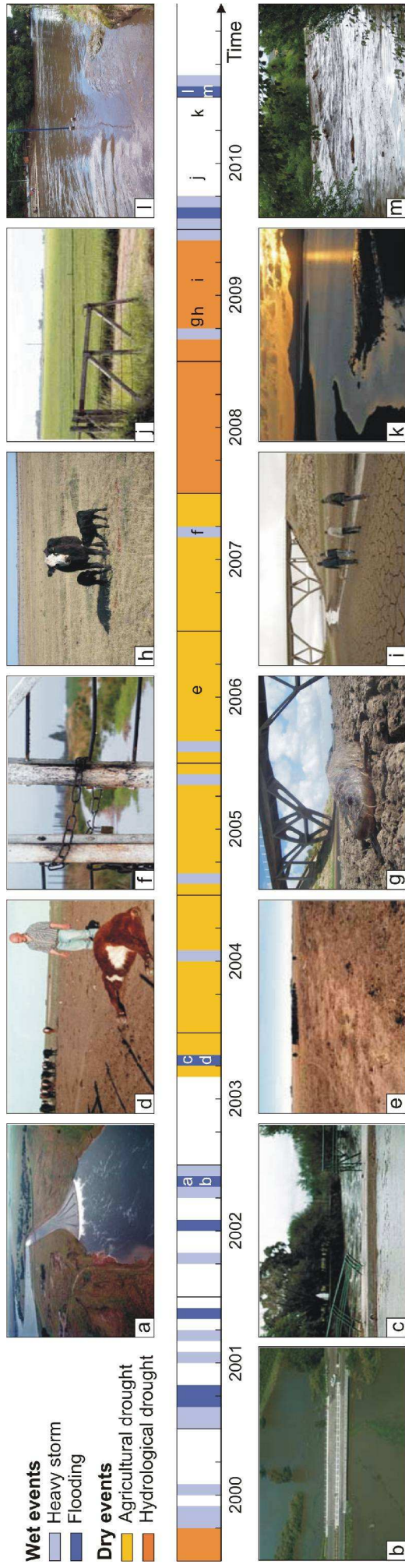


Figure 1.24: Sequence of extreme dry (wet) events documented within the area of interest during the last decade. Data source: La Nueva Provincia Newspaper online (<http://www.lanueva.com.ar>).

Photo items:

- (a) Overflow over dam spillway. LNP, 12/11/2002 "Panorama después de las lluvias: Paso de las Piedras está superando bien la prueba".
- (b) Road 78 upon Sauce Grande River (about 40 km below the dam). LNP, 14/11/2002 "La Ruta 78 está cortada por una corriente de 500 metros de ancho. Monte, en alerta por el Sauce Grande".
- (c) Broken bridge in Sierra de la Ventana caused by overflow of the Sauce Grande River. LNP, 8/10/2003 "Temporal: En la ciudad pasó sin consecuencias, pero en Sierra hizo desastres".
- (d) Livestock losses in the district of Coronel Dorrego. LNP, 07/10/2003 "Los registros en la zona no resultaron significativos. La escasa lluvia de ayer no alcanzó para alimentar a los productores".
- (e) The drought in SWBA. LNP, 09/07/2006 "Opinan los especialistas: La sequía, cada vez más dura".
- (f) Rainfall came too late for farming. LNP, 14/09/2007 "Las condiciones no se modificarían hasta, por lo menos, la mañana de este domingo. La lluvia sigue cambiando la cara de los productores".
- (g) El Divisorio Creek below Road 51. LNP, 19/04/2009 "La sequía que mata".
- (h) Hard times for farming. LNP, 05/05/2009 "La naturaleza por dos".
- (i) Technicians walking over a land previously covered by the Paso de las Piedras Lake. LNP, 09/08/2009 "Dramática situación: El dique tiene agua para menos de un año".
- (j) Fields of green wheat. LNP, 20/05/2010 "Comienza a definirse la suerte del trigo en la zona. La gota que falta".
- (k) The reservoir recovers its volume. LNP, 02/11/2010 "Paso de las Piedras: El dique alcanzó ayer la cota más elevada del año".
- (l) Overflow of the Sauce Grande River. TN y la Gente, 07/01/2011 "Creciente por fuertes lluvias en Sierra de la Ventana".
- (m) Overflow of the San Bernardo Creek. LNP, 31/01/2011 "Histórica crecida en Sierra de la Ventana".

Reservoir inflows peaked in more than $1\,000\text{ m}^3\cdot\text{s}^{-1}$ and the exceeding volume reached 80 hm^3 that were evacuated downstream over four consecutive days. Besides the dam overflow, the heavy rains recorded in the departments of Coronel Dorrego, Monte Hermoso and Coronel Rosales caused flooding by overflowing of local streams (e.g. Las Mostazas and Bajo Hondo creeks) and saturation of the water table. As a result, more than 200 000 ha were submerged under almost 60 cm of water (Fig. 1.24-b); the city of Monte Hermoso remained isolated during three consecutive days and the district of Coronel Rosales was declared in state of emergency. The economic losses were inestimable, although according to LNP they reached several millions of US Dollars.

During the austral spring of 2003, a heavy storm recorded more than 300 mm in six hours within the headwaters; overflow of the Sauce Grande River and the San Bernardo Creek caused serious damage in Sierra de la Ventana (Fig. 1.24-c). Urban flooding reached more than 1.2 m height, and 200 people were evacuated. In spite of this wet event, an agricultural drought was declared within several departments; Coronel Dorrego being the most affected by crop and livestock losses (Fig. 1.24-d).

The agricultural drought of the spring of 2003 set the beginning of a severe drought that will affect the whole SWBA during several years (Fig. 1.24-e). From 2004 through 2007, precipitation shortfalls were alternated by a number of heavy storms that came too late or were too heavy for agricultural practices (Fig. 1.24-f). LNP published countless drought-related articles all along this period; the beginning of the hydrological drought was arbitrarily fixed in January 2008 as LNP first publishes “*Bahía Blanca is facing a lack of drinking water*”.

By early 2009, the consequences of the drought were dramatic: water courses and aquifers were depleted (Fig. 1.24-g), farming activities were seriously damaged (Fig. 1.24-h) and the reservoir water levels were almost 7 m below the optimal mark (Fig. 1.24-i). Concerned authorities from the Autoridad del Agua (ADA) declared to the local newspaper that the reservoir’s volume was declining since 2005; the Yellow Warning was declared in May. The year 2010 was rainy as expected; the soil recovered its moisture (Fig. 1.24-j) and the reservoir’s volume increased (Fig. 1.24-k). However, ADA authorities remained attentive and announced that the Yellow Warning would persist until the reservoir water levels reach 155 m.s.l.

This mark was largely exceeded in January 2011, where a heavy storm recorded more than 250 mm in several sectors of the headwater areas causing a flood wave (Fig. 1.24-l, m) that contributed in 3 m increase in the water level. On the 27th of January, LNP published “*Water crisis: the solution came in the month the less expected*” and the article continues “*According to the unpredictability of the local climate, the reservoir has recovered its volume outside the rainy season, during a month of January not less surprising...*”.

In this context, the question that emerges is: what do we know about the complex relationships between physical and human processes affecting the water management within the river basin? Considerable research has assessed the recurrence, magnitude and extent of episodes of drought and their implications for agricultural practices; however, few studies have evaluated the effects of rainfall variability over the long term. These aspects underline the need of understanding the complex behaviour of the local water resources face to the natural climate variability, and its implications for

water management practices face to the evolving needs of the involved society. Such understanding is at the basis of the assessment of the hydrological, morphological and ecological impacts of the dam upon the river system.

The previous review has demonstrated clearly that flow regulation induced by dams is the greatest source for hydrologic alteration of river systems, with great implications for the river morphology and for the composition of aquatic and riverine ecosystems downstream. The effects of the Paso de las Piedras Dam on the Sauce Grande River are the focus of this study. Strong variability in climate-driven reservoir inflows, dam operational procedures highly dependent on its vital purpose for water supply and a growing population demanding for water and water-related services combine to generate low resilience to fluctuations in local water resources. Periods of water excess, where large volumes of water were evacuated downstream, were succeeded systematically by periods of water deficiency which in some cases were so severe that represented a threat for water storage.

In spite of the importance of the Sauce Grande River as main source for drinking water supply and the large capacity of the impoundment, hydrological processes within the river basin remain poorly evaluated and the effects of the dam upon the downstream river environment require to be investigated directly. These facts are conceivably related to the overall lack of climatic and hydrologic data over the long-term. In this regard, this research is motivated by two interrelated aspects: (i) the need for generation of *hydrologic and climatic data* and for making these data available to managers of flows to contribute to improve the dam management practices, and (ii) the need for an *integrated assessment* of the causal relationship between human impacts and fluvial metamorphosis over time in the context of reservoir operational procedures that are climate-dependent and purpose-constrained. This understanding is at the basis of an overall diagnosis of impact that underlies further efforts for river restoration.

3.1. RESEARCH PURPOSE

This research aims to answer three essential questions:

- i. Which is the hydrological balance of the dam reservoir and how the dam has regulated the balance between inflows and outflows over time?
- ii. Which is the degree of flow regulation and how this regulation has affected the river flow regime and water quality within the river downstream?
- iii. Which are the implications of altered flow regime and water quality for the river channel and its riparian zone?

Accordingly, the aim of this research is (1) to assess the degree of flow regulation induced by the Paso de las Piedras Dam upon the middle section of the Sauce Grande River (2) to quantify its impacts upon the hydrology of river downstream, and (3) to evaluate the effects of altered hydrologic conditions upon the river channel and its floodplain. The need for generation of baseline data that permit to assess spatiotemporal variations in hydrological processes demarcates the second purpose of this research.

3.2. RESEARCH HYPOTHESIS

The literature review revealed a wide range of mechanisms in which dams may alter the hydrologic regime of impounded rivers and showed that the direction and magnitude of fluvial change depend strongly on the purpose of the dam and on the natural setting of the river system exerting a greater or lesser resistance to change. The response of the Sauce Grande River to upstream impoundment is hypothesized assuming (i) sub-arid to sub-humid climate conditions with strong annual, inter-annual and inter-decadal variations in the water available for runoff and storage processes, (ii) a river *continuum* consisting of three well-defined sections along the river course, (iii) a disruption of the river *continuum* by damming the middle section (stream order 6), (iv) a large dam with a deep-release storage reservoir, stratified and oxygen depleted, (v) a reservoir sediment trapping efficiency greater than 99 %, and (vi) a reservoir capacity at least two times the annual runoff yield from the upper basin.

Upon the basis of these assumptions, the hypothesis to test in this research states that the Paso de las Piedras Dam disrupts the hydrologic continuity of the Sauce Grande River strongly by maximizing water storage within its reservoir to assure water supply in periods of drought. In periods of drought, which are recurrent and ENSO-related, reduction of the frequency and magnitude of peak flows and floods exerts the greatest influence on the river environment downstream. Changes occur to all variables of the river system and involve alteration of the water quality by increased exposure to groundwater inflows, reduction in the channel capacity by channel aggradation, bank stabilisation by vegetation growth within the main stream channel and disruption of the river-floodplain connectivity. In periods of humidity, the frequency and magnitude of downstream peak flows and floods increase and the direction of fluvial adjustment resets. Changes in the water quality occur because flow inputs are oxygen-depleted and thermally out-of-phase with respect to the unregulated river, the channel capacity increases due to channel degradation, in-channel vegetation is removed and the river-floodplain connectivity is re-established.

The following paragraphs explain the relations of causality between the variables expressed above.

3.2.1. Dam-induced hydrological regulation

The degree of flow regulation induced by the Paso de las Piedras Dam is hypothesized relative to (i) the large storage capacity of the reservoir, and (ii) the dam function for water supply in the context of varying climate conditions (Figure 1.25 [A]). The primary mechanisms of flow regulation induced by the dam are related to reservoir storage procedures. Large volumes of water are withdrawn annually and the remaining volume is conserved for periods of drought. The capacity of the reservoir to store water and sediment is large, and so the volume of runoff and sediment delivered downstream may be very small relative to the volume of runoff and sediment yielded from headwater sources. Furthermore, conservation storage procedures imply long times of water residence which, combined to reservoir sedimentation and stratification (relative to the reservoir depth), may conduct to formation of cold and oxygen-depleted layers on

the bottom of the reservoir, to eutrophication of the water column and to algae blooms, especially in periods of drought.

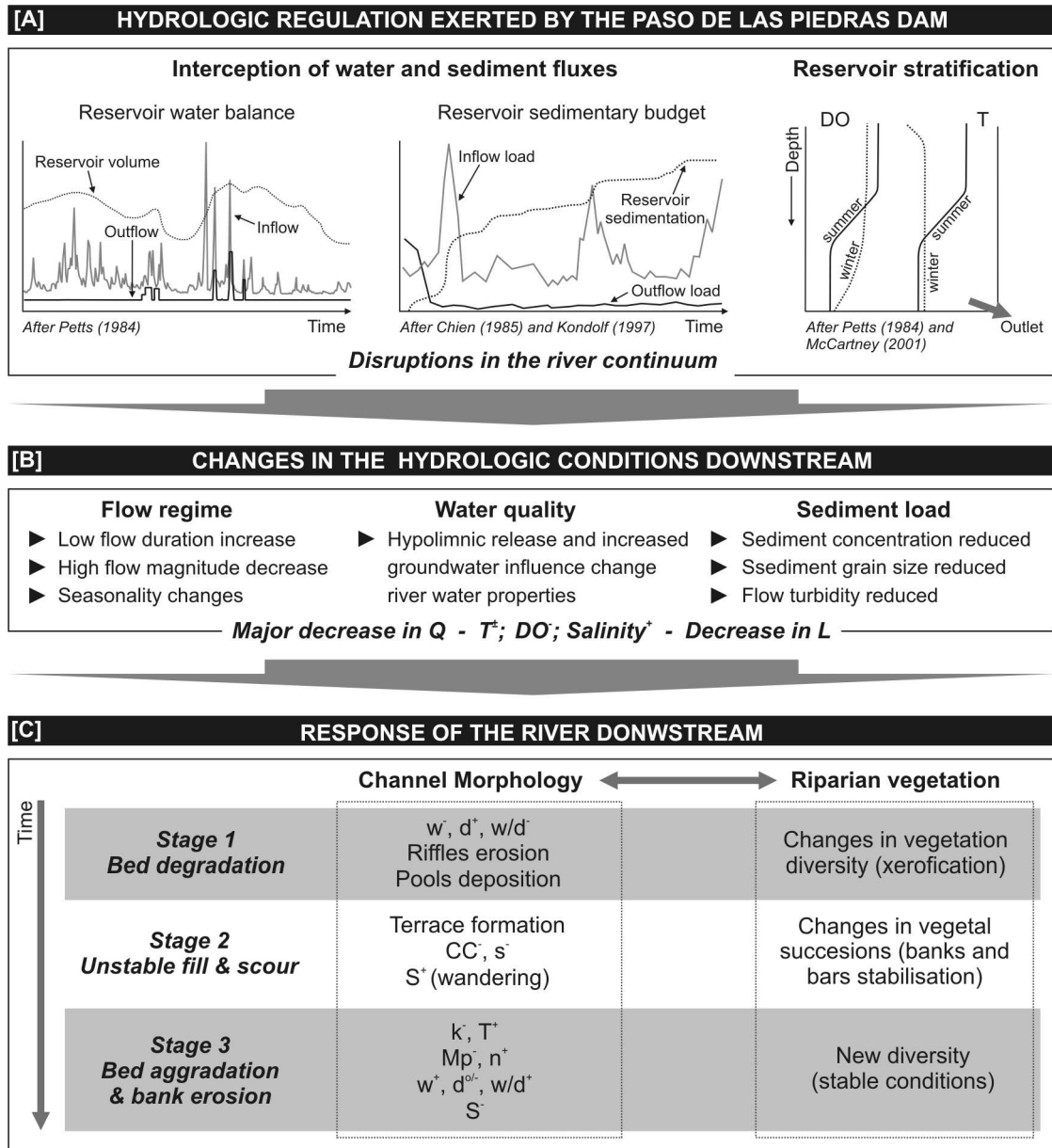


Figure 1.25: Hypothesized effects of the Paso de las Piedras Dam on the hydrology of the Sauce Grande River downstream and expected response of the river environment.

3.2.2. Changes in hydrological conditions downstream

The Paso de las Piedras Dam disrupts the longitudinal continuity of the Sauce Grande River by intercepting water and sediment fluxes from the headwaters and by altering the properties of the water stored within the reservoir. Ultimately, these processes alter the overall hydrology of the river downstream (Fig. 1.25 [B]). In periods of water deficiency, peak flows and floods are eliminated or dramatically reduced, the sediment

concentration of flow is negligible, and increased influence of groundwater inflows alters the river thermal regime and the chemistry of the flowing waters (dissolved oxygen and salinity content). In periods of water surplus, the frequency and magnitude of flow release increase and the sediment concentration of flow may increase due to sediment recovery from the channel bed and/or banks. However, peak flows and floods will be delayed and reduced respect to the unregulated river, and the thermal regime of flow will differ substantially from that of the river upstream due to the effects of hypolimnetic release from a thermally stratified reservoir. Over the long term, the river downstream will reflect a flattered hydrograph with altered seasonality and water quality. The fraction and size of the sediment load will be reduced, although the sediment concentration may equal the flow transport capacity due to major decrease in flow discharge.

3.2.3. The response of the river downstream

A number of conceptual models were developed to hypothesize the fluvial response to altered inputs of flow discharge and sediment load. Three models were retained for the purpose of this research: the models of channel metamorphosis of Petts and Gurnell (2005) and Brandt (2000), and the model of changes in the fluvial style of Surian and Rinaldi (2003). Changes in the channel morphology and the riverine landscape of the Sauce Grande River were hypothesized by combination of the three models cited above (Figure 1.25 [C]). Three different stages of adjustment were assumed:

Stage 1 spans the phase of reaction (accommodation) immediately after dam closure and defines the initial direction of channel metamorphosis. The immediate morphological response to reduced flow and sediment inputs is degradation of the channel bed. If the transport capacity exceeds the sediment load, then the channel depth [d] increases by erosion in riffles. The channel width [w] decreases, and the width:depth ratio [w/d] is consequently reduced. Reduction of the frequency and magnitude of bank overflowing causes the composition of riparian vegetation to change by invasion of species more adapted to xeric conditions.

Stage 2 (current channel state) corresponds to the initial states of relaxation. The finer material has been removed by base flows, and unstable processes of fill and scour occur as a consequence of persistence of base flows alternated by flood episodes. If the persistence of base flows dominates over the flood frequency, then the channel capacity [CC] is reduced by channel aggradation and terraces form within the former floodplain. Bank stabilisation may occur by vegetation encroachment. The balance between channel aggradation-degradation may entrain a reduction in the channel slope [s] and an increase in the flow sinuosity [S].

Stage 3 spans the final states of relaxation before a new equilibrium takes place. The flow conveyance [k] and consequently the shear stress [T] decrease, and the channel roughness [n] increases due to bed armouring and vegetation encroachment. Aggradation of the channel bed may be reset by episodes of flood. If lateral erosion occurs, then the channel width and subsequently the channel capacity increase. Cut-offs may occur, and so the channel sinuosity decreases. As for riparian communities, new and more stable patterns of succession and diversity take place.

3.3. ARTICULATION OF THE THESIS MANUSCRIPT

The hypothesis to test in this research states a logic sequence of causality between independent and dependent variables as follows:

The dam disrupts the longitudinal continuity of fluvial processes → the overall hydrology of the river downstream is altered → the river channel and its riparian zone change in response to altered hydrologic conditions.

This logic guides the research objectives and governs the structure of the thesis manuscript. Accordingly, the methods used to accomplish the research objectives and the corresponding results are articulated into chapters that test each component of the hypothesis enunciate separately (Fig. 1.26).

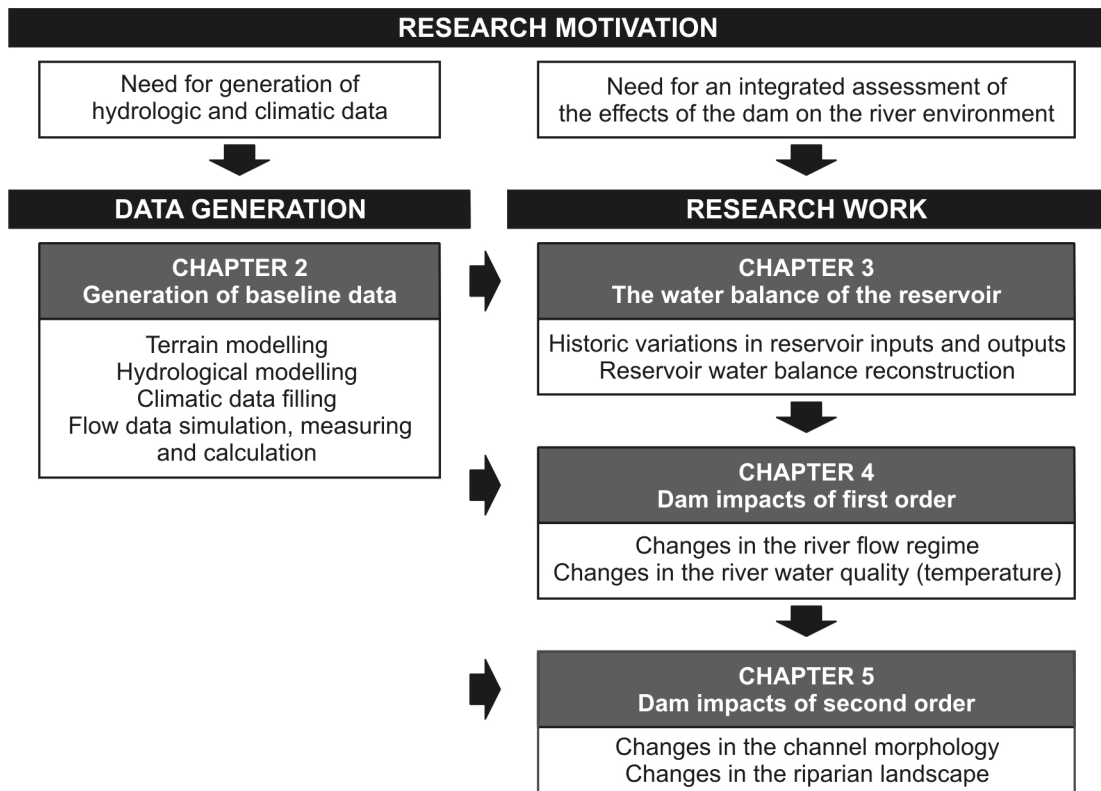


Figure 1.26: Scheme of the structure of the thesis manuscript.

Prior to articulate and discuss the thesis results (Chapters 3 to 5), Chapter 2 presents the results of a number of procedures performed to generate spatial, climatic and hydrologic data required for analysis. Chapter 3 looks into the historical relationships between runoff processes and reservoir operation procedures to identify the degree of hydrological regulation relative to the water balance of the dam reservoir. The implications of flow regulation for the flow regime and the water quality of the river downstream are evaluated in Chapter 4. Chapter 5 quantifies the response of the river channel and its riparian zone to altered hydrologic conditions.

3.4. WORKING SCALES

To assess and quantify the impacts of the Paso de las Piedras Dam on the Sauce Grande River, this research considers two key aspects: (i) the history of dam management inducing a disruption for longitudinal fluvial processes, and (ii) the complex response of the fluvial system over time. These fundamentals evidence the need of conducting analysis at different spatial and temporal scales hierarchically delineated by linked processes of cause and effect.

3.4.1. The spatial dimension

Rivers may be seen as three-dimensional systems being dependent on longitudinal, lateral and vertical transfers of energy, material and biota (Petts and Amoros, 1996; Ward, 1998). From the drainage basin to the microhabitats, fluvial systems involve a nested hierarchy of functional units controlled by different links of biotic and abiotic processes. This study considers three spatial levels of analysis defined by (i) the upper-middle river basin, (ii) two river segments above and below the impoundment, and (iii) a set functional sectors (or reaches) within each river segment.

The effects of river impoundment were evaluated firstly on the scale of the river basin through analysis of dam effects upon the longitudinal continuity of the river system. The impacts of flow regulation upon the river downstream were assessed on the scale of a river segment extending over a straight distance of about 25 km (~ 40 km river distance) from the dam closure. A secondary river segment of about 15 km-length (~ 25 km river distance) was selected upstream from the impoundment as sample for unregulated conditions. River segments upstream and downstream from the dam were divided into functional sectors of 1 km-length to inspect for fluvial forms and associated ecological units affecting the diversity of changes within the river system.

3.4.2. The temporal dimension

Time was addressed through a double perspective: retrospective-prospective analysis of causation, and diachronic analysis of synchronic conditions (Petts, 1989). The longitudinal and transverse dimensions were included in both perspectives implicitly; the difference was in the temporal continuity of the observational scale.

The causation perspective was used to assess the degree of flow regulation induced by the dam, where the present degree of flow regulation is seen as the outcome of historic relationships of causality between climate variability and water-related human needs affecting the dam operational procedures. This inductive understanding provided the basis for predictive scenarios of flow regulation according to prospective scenarios of reservoir inflows and outflows.

Assessment of the fluvial response to flow regulation used both historic and diachronic analysis of synchronic conditions. The historic perspective was used to inspect for patterns of flow within the river upstream (unregulated) and the river downstream (regulated) to detect (a)synchrony. Analysis of (a)synchrony was also used to quantify

the dam impacts on the river water quality based on observations at multiple sites along the unregulated and the regulated rivers.

Finally, diachronic analysis was used to reconstruct the trajectory of fluvial metamorphosis from the pre-dam natural state to the post-dam regulated state (Fig. 1.27). The static conditions observed for a given river segment (e.g. R2) or functional sector (e.g. S1) for a given time step were evaluated based on chronological sequences of change (e.g. $S1 \rightarrow S1' \rightarrow S1''$). Differences in static conditions along the river corridor (synchronic analysis) were also inspected to discriminate for changes related to dam operation and those related to the natural variability of the river system over time.

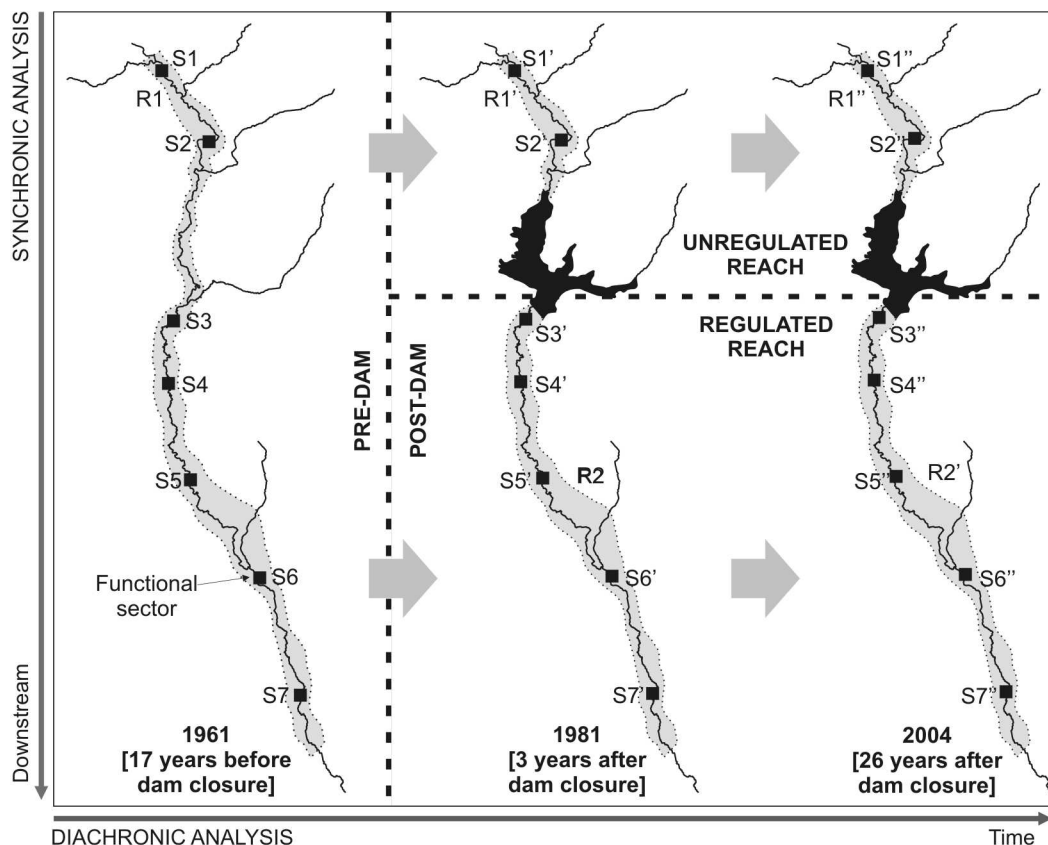


Figure 1.27: Conceptual scheme of synchronic and diachronic analysis.

CONTENTS

- 1 Methods
- 2 Results
 - Terrain modelling
 - Climatic data filling and simulation
 - Hydrological modelling of the upper river basin
 - Flow simulation
- 3 Discussion and Conclusions

The overall lack of climatic and hydrologic data over the long term has limited strongly previous studies assessing the hydrology of the Sauce Grande Basin. This chapter presents the results of a number of procedures achieved to generate baseline data to hydrological assessment of the river basin itself as well as of the dam reservoir over time.

The methods include a large set of metrics performed to model terrain and hydrologic parameters of the river basin, and to calculate climatic and hydrologic data over the long term. The main purpose of data modelling and calculation was to generate baseline data that permit to assess spatiotemporal variations in hydrological processes accurately.

Terrain modelling of the river basin provided the basis to assemble series of climatic data and to model hydrologic parameters within the upper drainage basin; in turn, climatic data series and hydrological modelling provided the basis to simulate flow rates within the unregulated river upstream. Calculation of flow rates within the regulated river downstream was based on empirical models derived from field-gauged data.

The models and data series presented herein are made available to dam managers as tool for reservoir management. Methods used in data generation are widely transferable to other ungauged basins as presented and discussed in the following sections.

A number of data series were required for analysis (Fig. 2.1). The methods used to generate and to assemble data include: (i) assemblage of pre-existing data, (ii) terrain modelling of the river basin, (iii) filling and assemblage of climatic data series, (iv) hydrological modelling of the upper drainage basin, (v) simulation of flow rates within the upper, unregulated Sauce Grande River, and (vi) calculation of flow rates within the middle, regulated Sauce Grande River.

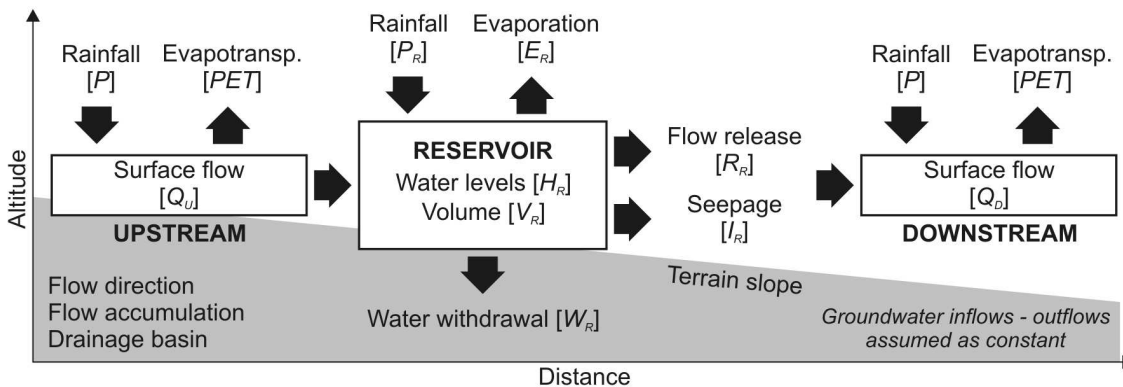


Figure 2.1: Terrain parameters and series of climatic and hydrologic data required for analysis.

1.1. ASSEMBLAGE OF PRE-EXISTING DATA

Documents and time series were obtained from a variety of agencies (Table 2.1; Figure 2.2). Given the great volume of records, the temporal irregularity of the time series and the heterogeneity of the data sources, the data sets required of exhaustive procedures of assembling, correcting and formatting prior to use in analysis. Data treatment varied depending on the primary type of data, i.e. documents or time series. In all cases, data were projected to UTM 20 South (WGS84), adjusted to the local time (-3 GMT) and converted into the International Metric System.

1.1.1. Processing and classification of documents and imagery

Document rectification

Scanned topographic and geologic maps (800 dpi) were corrected by polynomial restitution within ERMMapper. The restitution process used 30 control checkpoints by map resulting from intersections of the projection grid. Geologic maps provided the source for information on surface geology within the river basin, whereas topographic maps were used as main source for river basin altimetry.

Table 2.1: Set of documents used in analysis.

Document type	Description	Scale / Resolution	Source
Topographic maps	Gauss-Krüger Conformal Projection (Campo Inchauspe); contour intervals vary with altitude from 50 m to 5 m (15 maps)	1 : 50 000	IGN
Geologic maps	Maps of surface geology derived from field observations (8 maps)	1 : 50 000	Borromei (1991)
Aerial photography	Mission 1961 (16 photographs)	1 : 35 000	IGN
	Mission 1981 (29 photographs)	1 : 20 000	MOSP
Imagery	Ikonos 2004	1 m	GeoEye
	Landsat ETM 2003	30 m	USGS
Terrain model	SRTM90 (3 arcsec; filled and finished)	90 m	USGS (2000)

IGN (Instituto Geográfico Nacional); MOSP (Ministerio de Obras y Servicios Públicos); USGS (US Geological Survey).

Aerial photographs covering the river channel and its floodplain were available for 1961 (prior to dam construction) and for 1981 (immediately after dam closure). Distortions in the geometry of the photographs were corrected using control point rectification in ERMMapper. The river and its floodplain were placed in the centre of most photographs there where the geometric distortions are most reduced; despite the bad quality of some photographs, errors from rectification were very small ($0.1 < RMSE < 1.2$).

Ikonos imagery (2004) was rectified in Envi based on the Rational Polynomial Coefficients (RPC) attached to the image files. The geoid height was calculated using the Buenos Aires Geoid Calculator Software devised by the Departamento de Astrometría, Facultad de Ciencias Astronómicas y Geofísicas of the Universidad de La Plata. Ikonos imagery provided the basis for rectification of aerial photography and completes the chronological sequence to inspect for fluvial changes over time.

Image and terrain model classification

Landsat imagery and the SRTM90 terrain model were classified in ArcGIS to derive spatial data at a coarse spatial scale. Landsat imagery provided information on land cover and soil types within the entire river basin; the SRTM90 was used to test the quality of contour-derived terrain models for the river basin. Imagery and terrain model classification was at the basis of terrain and hydrological modelling of the river basin and so its applicability to the research context is described in further sections.

1.1.2. Time series assemblage

The reliability of hydrologic and climatic data was inspected before to assemble the time series for analysis. Unreliable commas and unreasonable readings were corrected

as detected; the phase of detection of invalid data was based on time series analysis and used statistical software (XLStat for MS Excel and PASW Statistics of SPSS Inc.). Time series corrected for analysis are presented in Figure 2.2; time series with low reliability were dismissed.

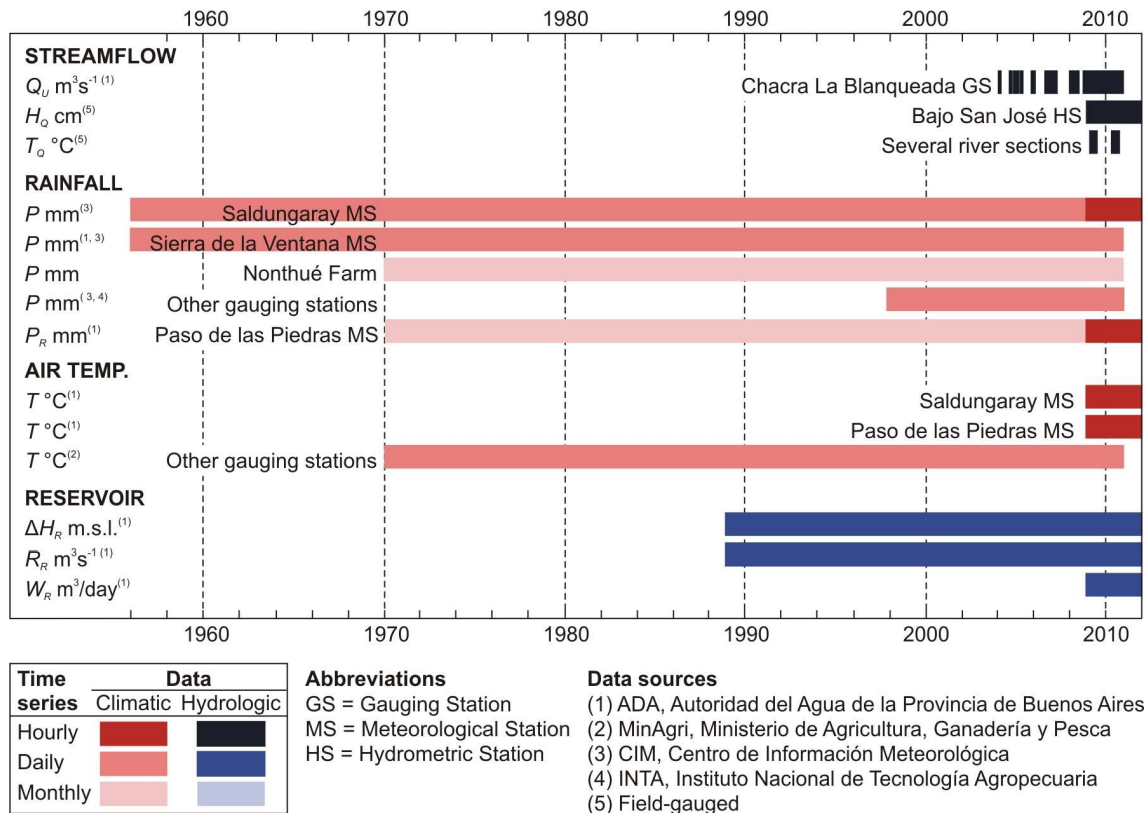


Figure 2.2: Series of climatic and hydrologic data available for analysis.

The overall reliability of series of hydrologic data was intermediate to low, and there was great inconsistency in the temporal extent of the datasets (Fig. 2.2). Series of river flow data were reduced in terms of both gauging stations available and temporal length of the observations. Other series of flow data available for the upper river (not shown in Figure 2.2) include long-term series (1910-1947) of monthly runoff depth measured at La Toma Gauging Station (Fig. 2.3) by the Ministerio de Obras y Servicios Públicos (MOSP). Reservoir water levels and rates of water release were available over the period 1989-2010, so that data are lacking over 12 consecutive years since dam closure in 1978. Water withdrawal data were available for a 3-yr period only (2009-2011). Supplementary series of hydrologic data were field-gauged. They include stream water temperatures measured at multiple river sites during austral summer 2009 and austral winter 2010, and hourly stream stages gauged in Bajo San José Hydrometric Station over the period 2009-2012 (regulated river).

Climatic data were achieved from a variety of sources, so that the resolution and the accuracy of the time series vary notably; in addition, climatic data were spatially scarce and temporally discontinuous (Fig. 2.2). Long-term series of rainfall data were obtained for the upper river basin (Nonthue Farm, Sierra de la Ventana and Saldungaray) and for

the Paso de las Piedras Reservoir (Fig. 2.3), although with varying temporal extent and resolution. Supplementary rainfall series (1998-2010) were achieved for multiple sites across the river basin and nearby locations. Series of air temperature data were available for Paso de las Piedras and Saldungaray, although the period of observation was much reduced (2009-2011). Supplementary series of air temperature over the long term (1971-2010) were obtained for three locations in the vicinity of the river basin (Bahía Blanca, Pigüé and Tres Arroyos; Fig. 2.3).

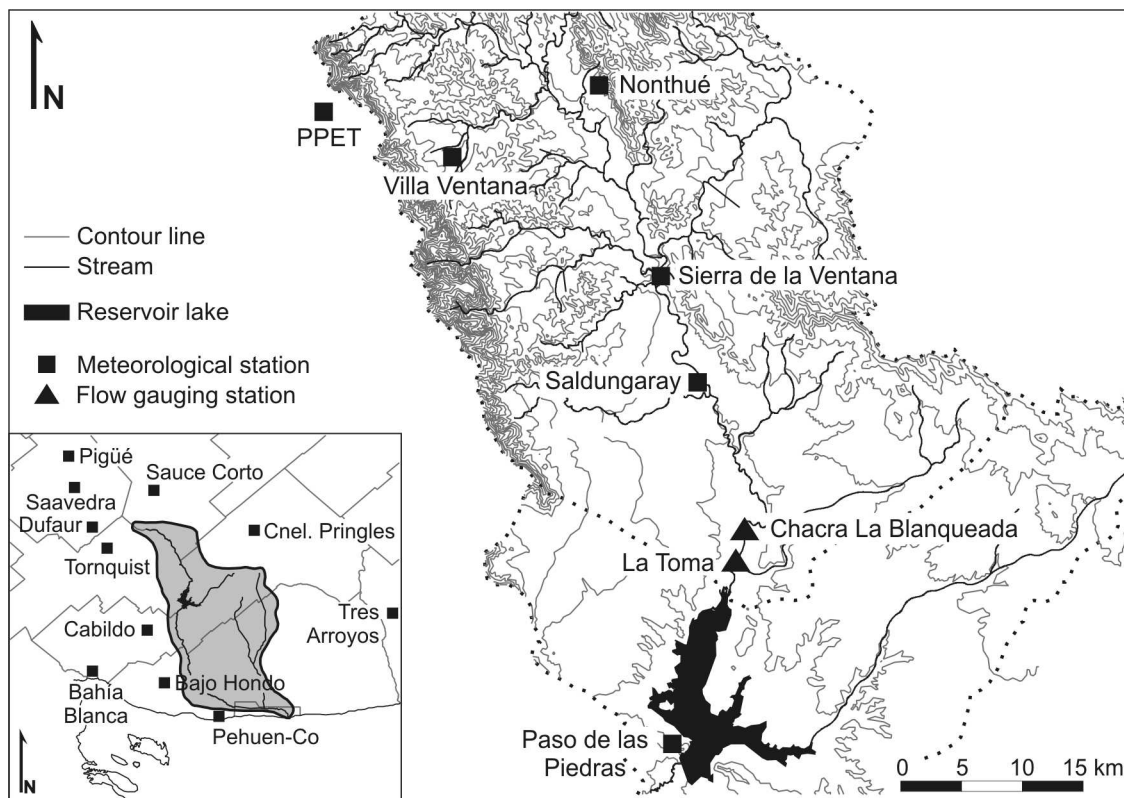


Figure 2.3: Distribution of meteorological and flow gauging stations within the upper river basin and nearby areas.

1.2. TERRAIN MODELLING

Definition of surface terrain parameters within the river basin was required to (i) assemblage of climatic data series, and (ii) hydrological modelling. Hence, we generated a Digital Terrain Model (DTM) from digitized contour lines based on the set of topographic maps (Table 2.1). Despite the suitable vertical accuracy of topographic maps in Argentina (del Cogliano *et al.*, 1998), the use of contour lines to derive terrain models has been recognized widely as source of error and uncertainty relative to (i) the vertical spacing of the contours, (ii) the algorithm used in interpolation, (iii) the model resolution, and (iv) the configuration of the terrain surface to model.

Accordingly, we have created and evaluated twelve contour-derived DTMs for a sample area of 1470 km² located within the middle river basin (Casado *et al.*, 2010). The twelve

models were generated in ArcGIS using four of the most common interpolating algorithms: (i) Triangulated Irregular Network (TIN), (ii) Inverse Distance Weighting (IDW), (iii) TopoGrid (TG), and (iv) Ordinary Kriging (OK). The output from each interpolating method was produced for 10, 25 and 50 m-resolution. In addition, each model was overlaid to a slope map (SRTM90-derived) discriminating for four zones with different degree of terrain inclination: (i) flat lands (0° to $0^\circ 30'$), (ii) terrain slightly inclined ($0^\circ 30'$ to 2°), (iii) terrain gently inclined (2° to 5°), and (iv) terrain steeply inclined (more than 5°).

Assessment of the quality of the terrain models

First, the models were inspected for their *absolute accuracy* (i.e. vertical precision). The measure of error was based on error residuals [e_i] between estimated values of elevation and a sample of 350 digitized trigonometric checkpoints. Descriptive statistics of error used the error range, the Mean Error (ME) and the Standard Deviation (SD), and the Root Mean Square Error (RMSE). The ME, SD and RMSE are expressed as follows:

$$ME = \frac{1}{n} \cdot \sum_{i=1}^n e_i \quad SD = \sqrt{\frac{1}{n-1} \cdot \sum_{i=1}^n (e_i - ME)^2} \quad RMSE = \sqrt{\frac{1}{n} \cdot \sum_{i=1}^n e_i^2} \quad (2.1)$$

Second, the models were inspected for their *relative accuracy* (i.e. precision in the representation of landforms). Methods considered the visual quality of the models and two types of error: (i) artifacts, defined as artificial flat areas where all pixels have the same elevation value, and (ii) outliers, defined as isolated pixels with anomalous elevation values (sinks).

Artifacts were detected using Equation 2.2 (Hengl *et al.*, 2004), which quantifies the number of neighbouring pixels [NB_c] having elevation values [z] that equal the elevation value of the central pixel [CP]. Outliers were detected from high error residuals between the weighed mean elevation of the central pixel [z_{CP}^{NB}] and its original elevation value (Eq. 2.3, Felicísimo, 1994). In both cases, the measure of error was performed in ArcGIS based on simple neighbourhood analysis for sampling windows of 3 x 3 pixels.

$$artifacts \leftarrow [\forall c z_{NB_c} = z_{CP}] \quad (2.2)$$

$$e_i = z_{CP}^{NB} - z_{CP} \quad (2.3)$$

Terrain model selection and model running

The interpolating method that produced the model of best quality for a given output grid size was used to generate the terrain model of the entire river basin. After generation, the accuracy of the model was improved by detecting and reducing absolute and relative errors. Artifacts and outliers were corrected manually by adding auxiliary contours and control points derived from the SRTM90 DTM. Afterwards, the model was filtered for sinks (outliers) and stream-adjusted by using HecGEO HMS tool for ArcGIS.

1.3. GENERATION OF CLIMATIC DATA

Besides containing invalid records (e.g. unreliable commas, false zeroes, spurious numbers, etc), climatic data series were incomplete. Rainfall data were missing for many days (or months) and temperature data were missing for almost the entire period of observation. Filling of missing data required of more sophisticated procedures than correction of invalid data as described below.

1.3.1. Filling of rainfall series

Missing observations of rainfall were estimated using the Inverse Distance Weighting method based on Silva *et al.* (2007). Missing rainfall data for a single day (or month) and for a single location were estimated based on the data gauged in nearby stations as follows:

$$P_x = \frac{\sum_{i=1}^n \frac{1}{d^2} P_i}{\sum_{i=1}^n \frac{1}{d^2}} \quad (2.4)$$

where $[P_x]$ is the rainfall value to estimate, $[P_i]$ is the rainfall value gauged in a nearby station, and $[d]$ is the distance that separates P_i from P_x .

Estimation of missing rainfall data on a daily scale (i.e. Sierra de la Ventana and Saldungaray series; Fig. 2.2) used rainfall data recorded in seven auxiliary sites (Bajo Hondo, Cabildo, Coronel Pringles, Dufaur, Pehuen-Co, Saavedra and Sauce Corto; Fig. 2.3) over the period 1998-2010. Interpolation beyond this period was not viable because of the reduced number of auxiliary time series on which to base an accurate interpolation.

Estimation of missing rainfall data on a monthly scale (i.e. Nonthue and Paso de las Piedras series; Fig. 2.2) for a single month and for a single location used rainfall data recorded in the remaining site and in Sierra de la Ventana and Saldungaray. When available, the process of interpolation was strengthened using three supplementary sites (PPET -Parque Provincial Ernesto Tornquist-, Villa Ventana and Tornquist; Fig. 2.3).

1.3.2. Assemblage of rainfall series

Series of monthly rainfall (1971-2010) for Nonthue, Sierra de la Ventana, Saldungaray and Paso de las Piedras were evaluated to inspect the spatial differentiation (or homogeneity) in rainfall regimes across the river basin. Rainfall regimes were evaluated in terms of magnitude (central values and dispersion), timing (pluviometric coefficients) and frequency (normal probability distribution) over annual and inter-annual time scales using common descriptive statistics based on Roche (1963) and Réménérias (1986). Rainfall time series within areas of rainfall homogeneity were averaged using the Thiessen method; the definition of Thiessen polygons was topography-based and used the HEC GeoHMS module for ArcGIS.

1.3.3. Filling of air temperature series

Air temperature data were available for two sites: Saldungaray and Paso de las Piedras; however, the temporal extent of the time series was much reduced (2009-2011; with blanks). Long-term series (1971-2010) of daily temperature were simulated for both sites using linear regression analysis. Regression models were based on maximum and minimum daily temperature data for three sites (Bahía Blanca, Pigüé and Tres Arroyos, Fig. 2.2) situated between 60 and 130 km from the area of interest. Linear regressions were run by site and for maximum and minimum daily temperatures separately; mean daily temperatures were calculated by averaging estimates to compensate for errors in the estimation of temperature extremes. Concurrent and continuous temperature data were available for the year 2010 only; hence model running and verification used the same period of time. The accuracy of the regression models was evaluated using the R^2 values, and the metrics of error expressed in Equation 2.1.

1.3.4. Estimation of potential evapotranspiration and evaporation

Long-term series (1971-2010) of monthly rainfall and mean monthly air temperature for Paso de las Piedras and Saldungaray were used to calculate potential evapotranspiration [PET] by Thornthwaite method (Thornthwaite, 1948). Calculation of monthly PET was latitude-based and used the USGS's Water Balance program devised by McCabe and Markstrom (2007).

Evaporation rates from the surface of the reservoir lake were calculated based on daily series of evaporation estimated from air temperature, air pressure, relative humidity and wind speed data recorded in Paso de las Piedras MS over the period 2009-2011. Calculation of daily evaporation [E] used the Penman method (Chow, 1994) expressed as follows:

$$E(\text{mm/day}) = 0.35(e_s - e) * (1 + \mu 10^{-2}) \quad (2.5)$$

where $e = Rh * e_s$ and $e_s = \log^{10} e_s = 0.02604T + 0.82488$

where [e_s] is the saturated vapour pressure, [e] is the vapour pressure, [μ] is the wind speed, [Rh] is the relative humidity.

1.4. HYDROLOGICAL MODELLING OF THE UPPER RIVER BASIN

Hydrological modelling of the upper river basin provided the basis to runoff analysis within the headwater areas. The methods evaluated (i) the physiographic characteristics of the contributing basin defining different units of hydrological response, and (ii) the depth of runoff rates and their temporal distribution within the drainage basin.

1.4.1. Delineation of Hydrologic Response Units (HRU)

The physiographic characteristics of the upper river basin were inspected using three

layers of spatial data: terrain slope, soil types and land cover. The land cover map was achieved by simple classification of Landsat ETM 2003 Imagery. The same classification technique was used to produce a map of soil types based on the findings of Gil (2009). Finally, the slope layer was derived from the contour-derived DEM for the river basin.

The areas having similar physiographic characteristics were assumed to delineate basin units having similar hydrological response to runoff processes (Yeung, 2004). The hydrological response of each unit was estimated using the Curve Number method of the U.S. Soil Conservation Service now NRCS (Mockus, 1972; NRCS, 1986; 2004; Marek, 2011). A runoff Curve Number (CN) was assigned to each unit depending on combinations of land cover types and hydrologic soil characteristics; the CN value for the entire drainage basin was derived from the weighted mean of the CN values corresponding to all units.

1.4.2. Estimation of direct runoff rates

The next step of the CN method consists in deriving runoff depths [Q] from empirical relationships between rainfall [P] and soil retention. After rainfall has started, a proportion of rainfall is retained before runoff starts [I_a]; after runoff has started, a proportion of rainfall is lost by infiltration. Infiltration increases as rainfall increases up to a maximum value defined by the maximum potential retention [S]. The value of maximum potential retention is found from the runoff Curve Number as follows:

$$S(mm) = z \left(\frac{100}{CN} - 1 \right) \quad (2.6)$$

where [z] is a constant factor equal to 254, and [CN] is the areal weighted mean of the CN values of all units integrating the drainage basin. The fraction of initial abstraction is found as $I_a = 0.2S$.

Based on the depth of potential retention and initial abstraction, the runoff depth that corresponds to a given rainfall depth is found by:

$$Q(mm) = \frac{(P - I_a)^2}{P + 0.8S} \quad \text{for } P > 0.2S \quad (2.7)$$

The runoff coefficient [C] is derived from the ratio of runoff to rainfall (Eq. 2.8, Ferrer, 1993). Calculations used 1 mm-increase rainfall depths from 16 mm (given an initial retention of 15.8 mm) to 190 mm (1000-yr rainfall).

$$C = \frac{Q}{P} \quad (2.8)$$

1.4.3. Estimation of the time of concentration

The temporal distribution of runoff rates was estimated based on the time of concentration of the drainage basin, i.e. the time required for runoff to travel from the most hydraulically remote point of the drainage basin to the basin outlet (Marek, 2011).

A number of formulas exist to derive the time of concentration from physical characteristics of the drainage basin; according to several authors (e.g. Boonstra, 1994; Roussel *et al.*, 2005; Marek, 2011), the TR55 method (NRCS, 1986) and the Kirpich-Kerby equation (Kirpich, 1940; Kerby, 1959) are the most preferable. We have evaluated the accuracy of both approaches relative to the physical characteristics of the upper Sauce Grande basin.

The Kirpich-Kerby equation calculates the time of concentration based on empirical relationships between channel length and channel slope for two flow components: the channel flow [T_{ch}] and the overland flow [T_{ov}]. The Kerby-Kirpich equation is expressed as follows:

$$Tc = T_{ch} + T_{ov} \quad \text{where} \quad T_{ch} = 0.02 * L^{0.77} * s^{-0.385} \\ T_{ov} = 1.44 * (0.4 * L)^{0.467} * s^{-0.2352} \quad (2.9)$$

where [L] is the longest flow path (m) for the channel flow (or the overland flow), and [s] is the slope (dimensionless). The values 0.02 and 1.44 are correctional factors for SI units, and the value of 0.4 is a retardance coefficient for grasslands and pastures. The slope was computed as H/L , where H is the difference in elevation between the most remote point in the drainage basin and the basin outlet.

The TR55 method was available in ArcGIS through the Hec-GeoHMS module. The time of concentration was calculated by routing travel times for three flow components: the sheet flow (or headwaters flow), the shallow concentrated flow, and the channel concentrated flow. Besides considering the length and slope of each flow component, computation of travel times used additional parameters such as 2-yr rainfall depth, percentage of pervious surfaces, flow velocity and bankfull channel conditions (e.g. Manning's roughness and hydraulic radius). For more information on the equations used in calculation see the report of the NRCS (1986) or the Chapter 4 in the manual of Marek (2011).

1.5. SIMULATION OF FLOW WITHIN THE UNREGULATED RIVER

The lack of flow data over the long term has limited strongly previous studies assessing the river flow regime. Available flow data include hourly flow rates for Chacra La Blanqueada Gauging Station over the period 2004-2011 (with blanks). We have simulated daily flow rates over the long-term (1956-2011) using physically-based hydrological modelling. The model and the parameters used in flow simulation are described below.

1.5.1. The RainOff-empirical model

Among the wide number of popular models used in flow simulation, the model that best fitted to simulate the *timing* and *duration* (recession) of both low and high flows was the RainOff model (Liquid Gold Team, 2002). However, simulation results regarding the *magnitude of high flows* were unsatisfactory. To solve this problem, we combined the

RainOff model to empirical equations to calculate the magnitude of high daily flows and the peak intensity separately. The coupled RainOff-empirical model simulates runoff from rainfall using a five-step procedure (Fig. 2.4). The model considers transient discharge-recharge relations between two reservoirs, and is based on the continuity (non-linearity) of a water balance equation and on a reaction factor dependent on the volume of recharge.

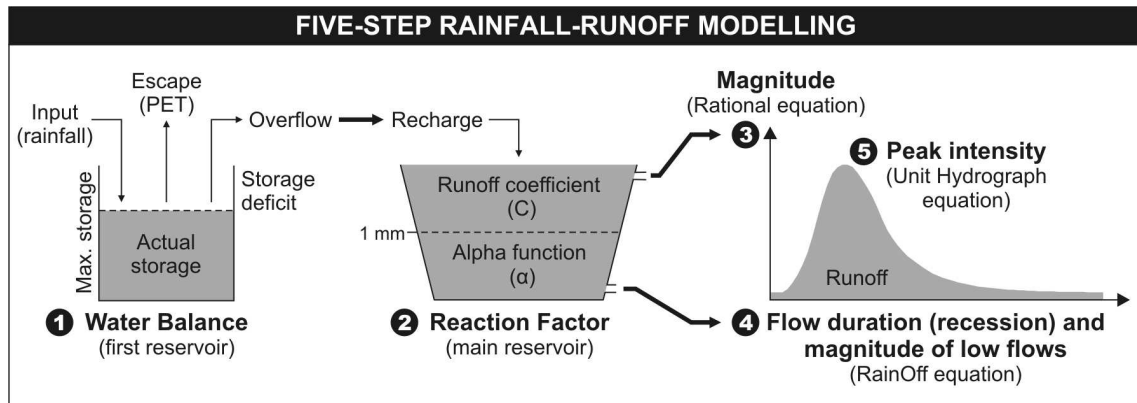


Figure 2.4: RainOff-empirical model for streamflow simulation.

Step 1: the water balance of the first reservoir

Rainfall-runoff relationships within the upper river basin were firstly evaluated by non-linear reservoir analysis based on the RainOff model. Model inputs used long-term (1956-2010) series of averaged daily rainfall for Sierra de la Ventana and Saldungaray (Thiessen method). Daily rates of maximum escape were derived from dividing long-term (1970-2010) mean monthly potential evapotranspiration for Saldungaray by the number of days of a given month. The hydrologic abstractions within the contributing basin (i.e. I_a and S) were estimated using the CN method as described above.

The water balance of the first reservoir was run to convert rainfall into recharge (Fig. 2.4) on a continuous day-to-day basis. The total recharge for a time interval t_2 was determined from the difference between rainfall and storage deficiency as expressed in Equation 2.10; where the recharge value was negative (i.e. where no overflow occurred), the recharge value was set to zero.

$$Rech_2 \text{ (mm)} = P_2 - StoDef_2 / \Delta t \quad (2.10)$$

The value of storage deficiency was found from the relationship between the maximum storage [$MaxSto$], the rate of actual escape and the actual storage [$ActSto$]. The initial value of storage deficiency used the difference between the potential retention, S , and the initial abstraction, I_a ; the storage deficiency at time t_2 was calculated as:

$$StoDef_2 \text{ (mm)} = MaxSto + ActEsc_2 * t - ActSto_2 \quad (2.11)$$

The value of maximum storage used the value of potential retention and was invariant for all time intervals. The initial value of actual storage used the value of initial

abstraction; the actual storage at time t_2 was found from the relationship between rainfall, recharge, escape and actual storage at time t_1 as follows:

$$ActSto_2 \text{ (mm)} = ActSto_1 + (P_1 - Rech_1 - ActEsc_1) * \Delta t \quad (2.12)$$

The rate of actual escape at each time interval was found from the ratio [r] of actual storage to maximum storage and the rate of maximum escape [$MaxEsc$] as expressed below:

$$ActEsc \text{ (mm/t)} = r * MaxEsc \quad (2.13)$$

Step 2: the reaction factor of the main reservoir

The recharge from the first reservoir was routed into a second reservoir from which runoff depths were calculated based on a reaction factor (Fig. 2.4). High-flow simulation by RainOff modelling was inconsistent in terms of magnitude (see above), so that two different coefficients of reaction were used depending on the recharge depth: (i) the runoff coefficient, and (ii) the alpha function from the RainOff model. The recharge depth (i.e. the depth of effective rainfall) determining the use of one or other reaction factor was defined by 1 mm, this arising from Unit Hydrograph analysis (see Steps 3 and 5).

The runoff coefficient was calculated empirically from the ratio of runoff to rainfall (Eq. 2.8) using rainfall depths of 1 mm-increase ranging from 16 mm to 190 mm. The alpha function was calculated based on concurrent and continuous daily observations of rainfall and runoff over a period ranging from September 2008 to December 2010. The relationship between rainfall depths and alpha coefficients for runoff depths (Eq. 2.14) was evaluated using linear and non-linear regression analysis; the regression function that produced the best data fit gave the alpha function to use in runoff computation.

$$Alpha \text{ coefficient} = \ln(Q_{t1} / Q_{t2}) \quad (2.14)$$

The alpha function was adjusted by trial and error according to two criteria: (i) the rate of minimum flow should fall below the rate of low flows (25^h percentile) and above the rate of minimum flows calculated from observed flow data, and (ii) the recession curve should not exceed the maximum base time calculated for the entire river basin (4.5 days; Paoloni *et al.*, 1972).

Step 3: daily flow simulation for Recharge > 1 mm

Recharge depths greater than 1 mm were assumed to generate a peak on the runoff hydrograph (Fig. 2.4). As the magnitude of such peak is dependent on the ratio of runoff to recharge (i.e. the runoff coefficient), the runoff depth resulting from a given recharge depth and the corresponding daily flow rate were calculated based on the rational equation as follows:

$$Q_2 \text{ (m}^3 \cdot \text{s}^{-1}\text{)} = \frac{Rech_2 * C * A}{86.4} + Q_b + 0.13Q_1 \quad (2.15)$$

where $[Q_2]$ is the flow rate occurring at the time interval t_2 ; $[Rech_2]$ is the recharge from the first reservoir during the time interval t_2 ; $[C]$ is the runoff coefficient corresponding to a given recharge depth; $[A]$ is the area of the drainage basin (km^2); 86.4 is the time unit (in fraction of seconds); and $[Q_b]$ is the base flow rate. The use of the fraction $0.13Q_1$ accounted for antecedent runoff conditions; the coefficient of 0.13 arises from Unit Hydrograph analysis and denotes the ratio Q/Q_p for the 24th hour (see Step 5).

Step 4: daily flow simulation for Recharge < 1 mm

The runoff depth for episodes of zero or very little recharge (less than 1 mm) and the corresponding rate of daily flow were calculated using the alpha function $[\alpha]$ as follows:

$$Q_2 (m^3 .s^{-1}) = \frac{|Q_1 (mm) * \exp(-\alpha_2) + Rech_2 * [1 - \exp(-\alpha_2)]| * A}{86.4} \quad (2.16)$$

Equation 2.16 was used to simulate daily flows either during periods of rainfall shortages (i.e. low flows) or during periods of little rainfall following rainy episodes (i.e. recession flows).

Step 5: simulation of daily peak discharge

We use the Dimensionless Unit Hydrograph method (NRCS, 2007b) to calculate daily rates of peak discharge. To adjust the dimensionless unit hydrograph to the river basin, we estimated the runoff response, in terms of peak discharge and time to peak, to rainfall excess of 1 mm-depth. The time unit was expressed in hours and the discharge units were expressed in cubic meters per second. The inflection point on the recession limb was assumed to occur at 1.67 times the time to peak, and the maximum base time was defined as five times the time to peak.

The time to peak $[t_p]$ was calculated based on the rainfall duration $[\Delta t]$ and the lag time $[t_L]$, both time values arising from the time of concentration $[T_c]$ of the river basin as follows:

$$tp (hours) = \frac{\Delta t}{2} + t_L \quad \text{where } t_L = 0.6Tc \quad \text{and } \Delta t = 0.133Tc \quad (2.17)$$

The peak discharge $[Q_p]$ generated by a given recharge depth was calculated based on the relationship between the drainage area $[A, \text{mi}^2]$ and the time to peak $[t_p, \text{minutes}]$ as expressed in Equation 2.18. The value of 0.0283 is a correction factor for international units.

$$Q_p (m^3 s^{-1}) = \frac{484 * A * Rech}{t_p} * 0.0283 \quad (2.18)$$

1.5.2. Model calibration and verification

Concurrent and continuous daily observations of rainfall and streamflow were much reduced and so model calibration and verification used basically the same period of

time. The period of calibration extends from the 1st September 2008 through the 31st December 2010; daily flow rates over the year 2007 (May to November) were used to strengthen the process of model verification. In spite of their short duration, these periods encompass episodes of low and high flows and so were suitable to both model calibration and verification.

The purpose of model calibration was to estimate parameters and coefficients that simulate low flows (< 25th percentile), median flows (25th > 75th percentile) and high flows (> 75th percentile) accurately. The measure of error was based on residuals [e_i] between simulated [S_i] and observed [O_i] daily flow rates. The measure of error used common metrics (ME, SD, RMSE; Eq. 2.1) and three additional metrics based on Yeung (2004):

- the overestimation rate [OE] was simply calculated as the proportion (%) of overestimated values (i.e. positive error residuals);
- the relative error [RE], or prediction error, was computed based on the ratio of error values to observed values as follows:

$$RE = \frac{\sum_{i=1}^n (e_i / O_i)}{N} * 100 \quad \text{where } e_i = S_i - O_i \quad (2.19)$$

- the coefficient of efficiency (CE, Nash and Sutcliffe, 1970) was used to compare the accuracy of the modelled data to the mean of the observed data as follows:

$$CE = 1 - \left(\frac{\sum_{i=1}^n e_i^2}{\sum_{i=1}^n e_{mi}^2} \right) \quad \text{where } e_{mi} = O_i / O_m \quad (2.20)$$

1.6. ESTIMATION OF FLOW WITHIN THE REGULATED RIVER

Available flow data for the river below the dam included long-term series (1989-2012) of daily rates of flow release from the dam and short-term series (2009-2011) of hourly stream stages gauged in Bajo San José (Fig. 2.2, 2.5). The following sections summarize the methods used in estimation of flow discharge within the regulated river; the methods and techniques used in flow computation were based on André *et al.* (1976), Réménérias (1986) and Chow (1994).

1.6.1. Computation of the downstream hydrograph

Stream stage readings in Bajo San José were the only source of information for flow states in periods of zero water release, i.e. periods of low flow. Hence the importance of calculating the hydrograph, $Q=f(t)$, that corresponded to the limnograph measured, $H=f(t)$. Two different issues related to the drought of 2005-2010 affected the calibration of the hydrometric station: (1) flow gauging for high flows is lacking because the river described very low flow variability over the entire period of observation, and (2) the number of flow measurements is much reduced. The latter aspect was related to the

construction in 2010 of a small dam (1.5 m height) about 1 km downstream from the original hydrometric station (hereinafter referred to as BSJ-1). As the dam caused an artificial rise in the stream stage, BSJ-1 had to be displaced about 2 km upstream after one year of recording data, giving origin to BSJ-2 (Fig. 2.6 [A]).

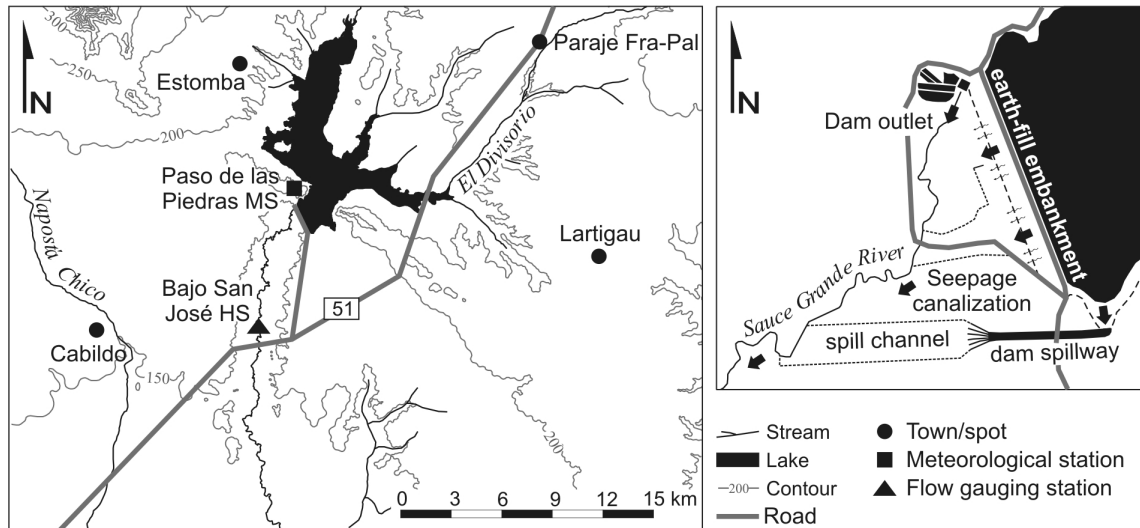


Figure 2.5: Distribution of meteorological and flow gauging stations within the river basin downstream from the dam and nearby areas.

Flow gauging used the velocity-area method. The cross-sectional area and the velocity field were explored from a number of measures made along verticals equidistantly spaced across the channel (Fig. 2.6 [B]). Flow velocity was measured using a current meter (TECMES Model TS 1001); the velocity sensor was set to give mean flow velocity [ms^{-1}] per point of measure every 30 seconds.

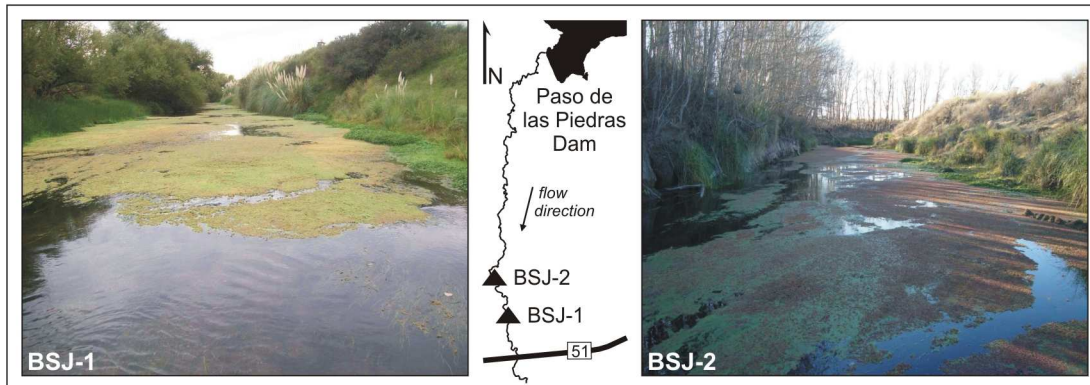
Flow discharge for episodes of high flow was estimated empirically using the Manning's equation:

$$Q = \frac{1}{n} * A * R^{2/3} * s^{0.5} \quad (2.21)$$

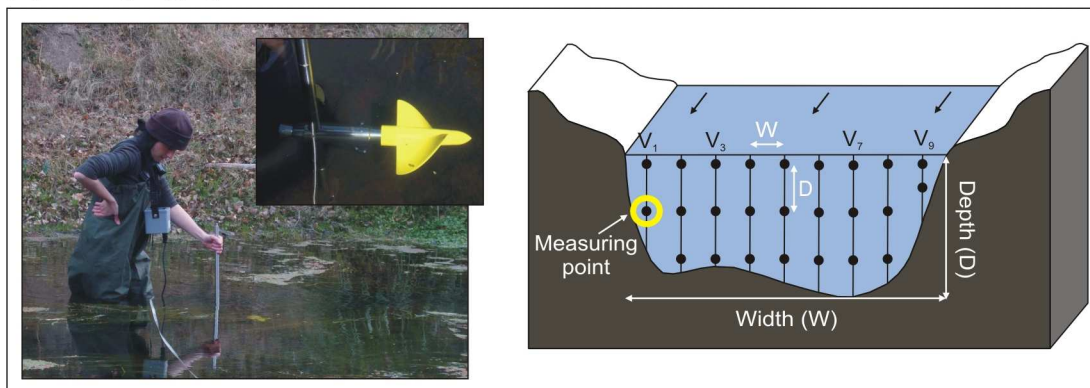
where [n] is the channel roughness; [A] is cross sectional area; [R] is the hydraulic radius; and [s] is the channel slope. The principle of Manning's equation is that the factor $A * R^{2/3}$ is a function of the stream stage [H]. Thus, for a given channel slope and roughness, flow discharge was estimated from the multiplicative derivative of the function $A * R^{2/3} = f(H)$, where H is the stream stage.

The parameters used in the Manning's equation were field-measured (Fig. 2.6 [C]) by using laser rangefinder of centimetre precision (Impulse Laser tech). The channel cross section for each hydrometric station (i.e. a-a') was plotted in ArcGIS; the hydraulic radius for increasing stages of 10 cm was simply calculated from the ratio of the wetted area to the wetted perimeter. The channel roughness was determined upon the basis of Arcement and Schneider (1989).

[A] Hydrometric stations



[B] Flow gauging



[C] Channel geometry measurement

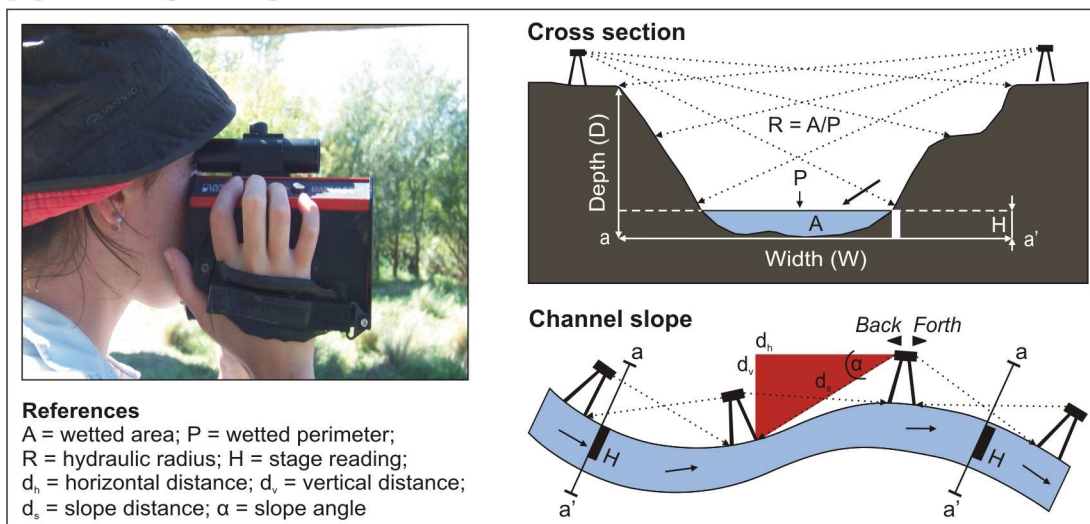


Figure 2.6: [A] Overview and spatial situation of the river sections selected for stream stage reading (hydrometric stations); [B] field techniques used to flow gauging; [C] field techniques used to measurement of the channel geometry.

Daily rates of downstream flow were calculated for the entire period for which stream stage data were available (2009-2012). Since reservoir flow release did not occur, mean flow rates over the period were assumed to represent low flow conditions below the

dam and were used to fill blanks within the long-term series of daily rates of flow release.

1.6.2. Inspection of rates of reservoir seepage

When no flow release occurs, a significant proportion of downstream flow is provided by reservoir seepage below the dam structure (Fig. 2.5). In order to determine such proportion, a number of measures were effectuated within the weir draining reservoir seepage into the main channel. Rates of reservoir seepage were estimated by using the formula of Kindsvater-Carter for rectangular weirs:

$$Q(m^3 s^{-1}) = C_e \frac{2}{3} \sqrt{2g} (b + K_b) (h + K_h)^{3/2} \quad (2.22)$$

where $[C_e]$ is the discharge coefficient, $[g]$ is the acceleration of gravity (9.81 m/s^2), $[b]$ is the notch width, and $[h]$ is the weir head. The sum $b+K_b$ gives the effective width, and the sum $h+K_h$ gives the effective head. K_h and K_b account for effects of viscosity and surface tension; the value for K_h is 0.001 m, and K_b is a function of b/B . Finally, $[C_e]$ is a function of b/B and h/P .

2.1. THE TERRAIN MODEL OF THE RIVER BASIN

We have evaluated the quality of twelve contour-derived Digital Terrain Models (DTMs) to inspect the interpolating algorithm and model resolution that best adjusted to the terrain configuration of the river basin (see Section 1.2, p. 71). The twelve models were reproduced for a sample area of 1470 km² within the middle river section (Fig. 2.7). Criteria for selecting the sample area involved (i) its spatial extent, which was large enough to reduce the influence of micro-topography and small enough to accelerate the speed of processing, and (ii) the complexity of the terrain surface, which included series of ridges, plains and valleys providing a variety of landforms on which to test the quality of the models. Besides corresponding to both criteria, this area was of particular interest because it comprises the great depression currently occupied by the Paso de las Piedras Reservoir and so it constitutes the main source of information of reservoir bathymetry.

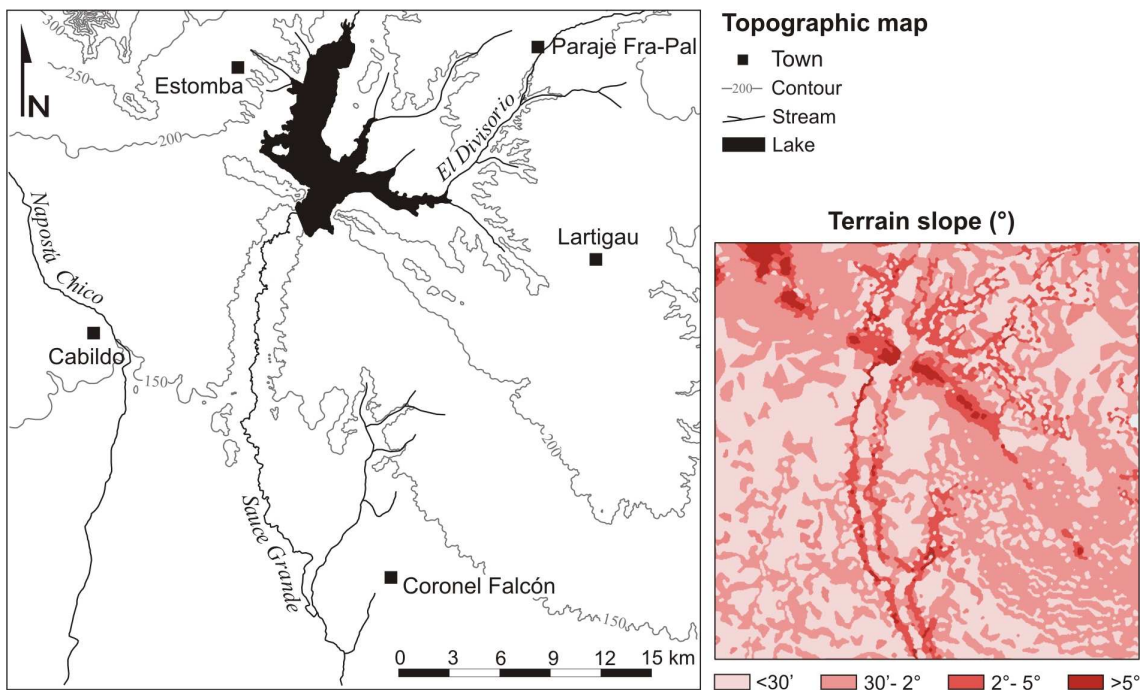


Figure 2.7: Sample area for the twelve contour-derived Digital Elevation Models.

2.1.1. The quality of the sample models

Evaluation of the quality of the digital terrain models measured their absolute accuracy (i.e. their vertical precision) and their relative accuracy (i.e. the quality in the representation of landforms) separately. Results are presented below.

Absolute quality of the models

Results showed that the absolute accuracy of the models (i.e. vertical precision) decreased significantly as the terrain slope increased regardless of the method used to interpolation or the resolution of the output model (Table 2.2). Intercomparison between interpolation techniques revealed that Inverse Distance Weighting (IDW) provided the coarsest errors for all terrain inclinations ($2.12 < \text{RMSE} < 8.13$), whereas TopoGrid (TG) provided the most accurate results for terrain inclinations until 5° ($1.13 < \text{RMSE} < 2.34$); in areas steeply inclined, the interpolation method the most accurate was Triangulated Irregular Network ($5.22 < \text{RMSE} < 5.81$). The effects of the output grid size on the vertical accuracy of the models were of less importance, although the models of 10 m-resolution exhibited overall better quality, notably the model derived from TopoGrid ($1.13 < \text{RMSE} < 4.52$).

Table 2.2: Absolute error (m) of the terrain models by interpolating method (TIN, IDW, TG, OK) and output grid size (50, 25 and 10 m resolution). Errors were discriminated by degree of terrain inclination. Best results per metric in bold.

<i>Flat lands (0° a $0^\circ 30'$)</i>						<i>Terrain slightly inclined ($0^\circ 30'$ a 2°)</i>					
Metric	Res.	TIN	IDW	TG	OK	Metric	Res.	TIN	IDW	TG	OK
ME (m)	50	-0.20	-0.26	-0.21	-0.13	ME (m)	50	-0.07	-0.16	0.04	-0.03
	25	-0.21	-0.27	-0.17	-0.12		25	-0.07	-0.23	0.05	-0.03
	10	-0.17	-0.27	-0.26	-0.12		10	-0.07	-0.26	0.06	-0.03
SD (m)	50	1.45	2.11	1.35	1.25	SD (m)	50	2.48	3.27	1.73	2.24
	25	1.35	2.13	1.21	1.24		25	2.48	3.29	1.71	2.23
	10	1.12	2.14	1.12	1.24		10	2.48	3.29	1.80	2.23
RMSE (m)	50	1.45	2.12	1.36	1.25	RMSE (m)	50	2.47	3.26	1.81	2.23
	25	1.36	2.14	1.23	1.24		25	2.47	3.29	1.73	2.22
	10	1.13	2.15	1.13	1.25		10	2.47	3.28	1.73	2.23
<i>Terrain gently inclined (2° a 5°)</i>						<i>Terrain steeply inclined (more than 5°)</i>					
Metric	Res.	TIN	IDW	TG	OK	Metric	Res.	TIN	IDW	TG	OK
ME (m)	50	0.31	1.12	-0.14	0.42	ME (m)	50	-3.54	-4.82	-7.89	-6.28
	25	0.29	1.16	-0.40	0.41		25	-3.15	-4.42	-4.43	-5.98
	10	0.27	1.12	-0.42	0.40		10	-3.08	-4.34	-3.24	-5.87
SD (m)	50	3.51	4.47	2.39	3.36	SD (m)	50	4.83	6.86	8.70	7.40
	25	3.48	4.51	2.27	3.32		25	4.52	6.74	4.36	7.00
	10	3.49	4.50	2.30	3.32		10	4.42	6.62	3.31	6.90
RMSE (m)	50	3.45	4.52	2.34	3.32	RMSE (m)	50	5.81	8.13	11.45	9.45
	25	3.42	4.57	2.29	3.28		25	5.33	7.80	6.08	8.96
	10	3.43	4.55	2.26	3.28		10	5.22	7.66	4.52	8.82

Relative quality of the models

First, the relative quality of the models was evaluated by inspection of their *qualitative accuracy*, that is, the graphic quality of the models relative to the real configuration of the terrain surface. Results evidenced the effects of resolution on the graphic quality of the output model, which increased notably as the resolution decreased. Accordingly and building on previous results, the models of 25 and 50 m-resolution were dismissed.

Broad differences were evidenced between models of 10 m-resolution, these arising from the interpolation technique used to generate the model (Fig. 2.8). Models derived from Inverse Distance Weighting (IDW) and Triangulated Irregular Network (TIN) revealed the less suitable qualitative accuracy; landforms were blurred by excessive terracing resulting from the horizontal spacing between contour lines. Conversely, the models derived from Ordinary Kriging (OK) and TopoGrid (TG) reproduced terrain forms that, qualitatively, were closer to reality.

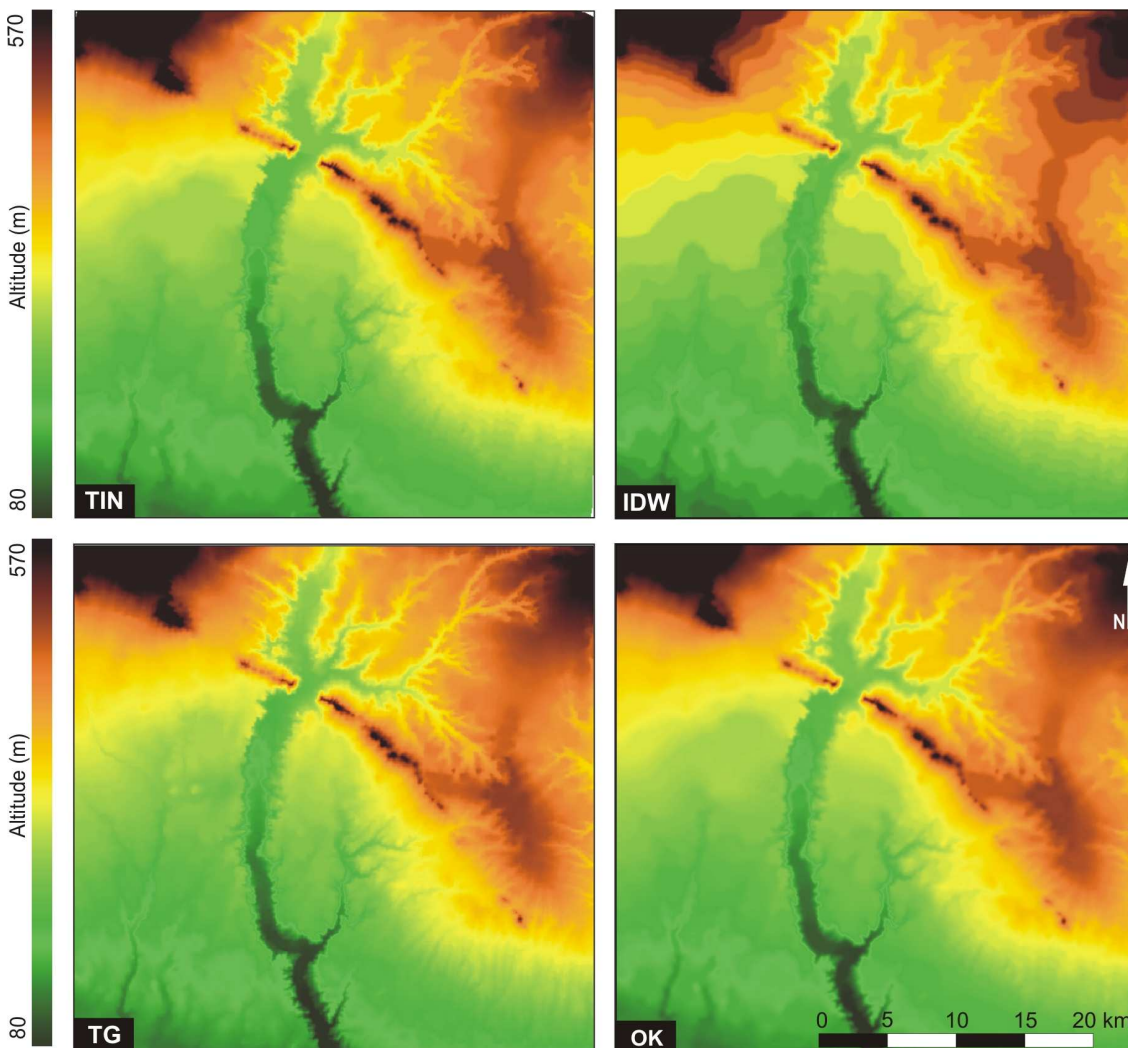


Figure 2.8: Overview of the 10 m-resolution DTMs by interpolation technique (TIN, IDW, TG, OK).

Second, the relative quality of the models was evaluated by inspection of artifacts and outliers (Fig. 2.9). Neighbourhood analysis revealed that the proportion of *artifacts* (i.e. surfaces where all pixels have the same elevation value) was greater for IDW- and TIN-derived models (35 to 40 %). Such proportion is very unlikely to occur in reality, so that both models were dismissed. Conversely, the proportion of artifacts within the TG- and OK-derived models was negligible (less than 1 %), and more than 98 % of the pixels had unique elevation values. Inspection of *outliers* (i.e. relative pixel elevation with respect to its neighbours) revealed similar results. TG- and OK-derived models were the models the most accurate, the TopoGrid model showing the smaller error range (3.4 m) and RMSE (0.012 m).

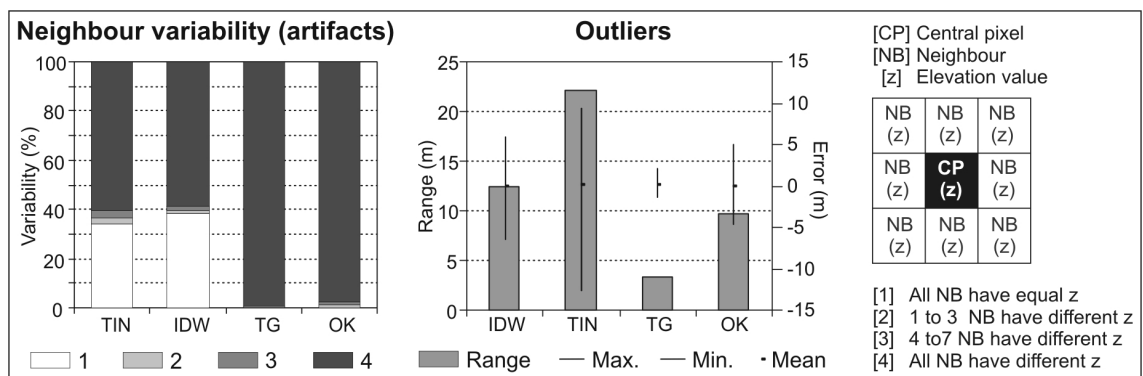


Figure 2.9: Relative accuracy of the 10-m resolution DEMs by interpolation technique (TIN, IDW, TG, OK).

2.1.2. Model selection and running

Analysis of the absolute and relative quality of the 12 digital terrain models revealed that the TopoGrid model of 10 m-resolution (TG10) was the model of better quality; absolute errors were small, the graphic quality of the model was suitable, and relative errors were negligible. The TopoGrid command was run in ArcGIS to generate a terrain model of 10 m-resolution for the entire river basin. The interpolation process used digitized contours with horizontal spacing ranging from 5 m within the lowest areas to 50 m in the headwaters (except for the Las Mostazas catchment and the lowest section, areas that were interpolated based on contour lines derived from the SRTM90). In addition, interpolation used digitized trigonometric points and streamflow lines. Prior to calculation of derived terrain parameters (i.e. terrain slope) and hydrologic parameters (i.e. flow direction, flow accumulation, stream definition and catchment delineation), the accuracy of the model was improved by detecting and reducing absolute and relative errors.

2.2. CLIMATIC DATA SERIES

As discussed in the Methods section, climatic data required of exhaustive procedures of correcting and filling before being used in analysis. Missing records of rainfall were

estimated using the Inverse Distance Weighting interpolation technique; air temperature data were missing for almost the entire period of analysis, so that filling of temperature data used more sophisticated procedures (see Section 1.3, p. 73).

2.2.1. Long-term series of rainfall

Long-term series (1971-2010) of monthly rainfall for Nonthue, Sierra de la Ventana, Saldungaray and Paso de las Piedras were corrected, filled, and inspected for spatial differentiation (or homogeneity) in rainfall regimes within the river basin. Nonthue, Sierra de la Ventana and Saldungaray account for the water precipitated within the upper river basin, whereas Paso de las Piedras is situated near the dam reservoir and so accounts for direct rainfall upon the surface of the lake (Fig. 2.10).

Distribution of annual rainfall

The distribution of annual rainfall modules over the period 1971-2010 (Fig. 2.10 [A]) revealed a decline in mean annual rainfall south-southwestward; mean (median) annual rainfall in Nonthue was +118 mm (+124 mm) compared to that in Paso de las Piedras. Conversely, the dispersion around the central values increased south-southwestward, suggesting that the magnitude and the recurrence of rainfall extremes were greater for the southern sites. In order to assess these aspects, annual rainfall series were inspected based on (i) the frequency of annual rainfall modules of a given magnitude (using normal probability density functions), and (ii) the inter-annual variability of annual rainfall modules relative to the historic mean (using pluviometric coefficients).

Annual modules were standardized, and then adjusted to a normal probability distribution to inspect the probability of exceedance [$p(x > x_r)$] and the recurrence period [Tr] of years classed as drier- or wetter-than-normal rainfall by site. Probability plots showed strong linear correlations for all sites, with correlation coefficients higher than 0.98. This suggested that the normal distribution provided a good model of the data. Nevertheless, all sites but Sierra de la Ventana (which gave the best probability fit) revealed outliers in the upper and lower sides of the plot revealing significant deviations of rainfall extremes relative to the normal distribution. Positive skew values ($0.14 < \gamma < 0.76$) indicated that most values lied to the left of the mean (i.e. drier-than-normal years) in all sites with maximum skewness in Paso de las Piedras.

The distribution of annual rainfall modules relative to their probability of exceedance (Figure 2.11 [A]) evidenced the decline in annual rainfall SSW clearly: the fitted line (and so all parametric values) displaces progressively to the left of the plot as the sites are located southward. Precipitation series for the northern sites revealed that annual rainfall may reach about 955 mm every 10 years, and more than 1000 mm every 100 years; the probability of exceedance for the dry year threshold (~550 mm) was of between 82 and 85 %. The magnitude of annual rainfall modules in Paso de las Piedras for return periods of 10 and 100 years was considerably lower (900 mm and 960 mm, respectively), although the probability of exceedance for dry years was greater than that for the northern sites (88 %).

Annual pluviometric coefficients [PC] revealed strong inter-annual variations in annual

rainfall modules relative to the normal precipitation for all sites, with maximum variability in Paso de las Piedras (Fig. 2.11 [B]). However, annual *PC* showed spatial differentiation in the timing of the highest values (i.e. years of high humidity); the most humid years within the headwaters were 1976 and 1985, whereas most humid years in Paso de las Piedras were 2001 and 2002. Conversely, the lowest annual pluviometric coefficients (i.e. years of high dryness) were consistent in timing (1995, 2005, 2008 and 2009) and magnitude ($0.5 < PC < 0.7$) for all sites.

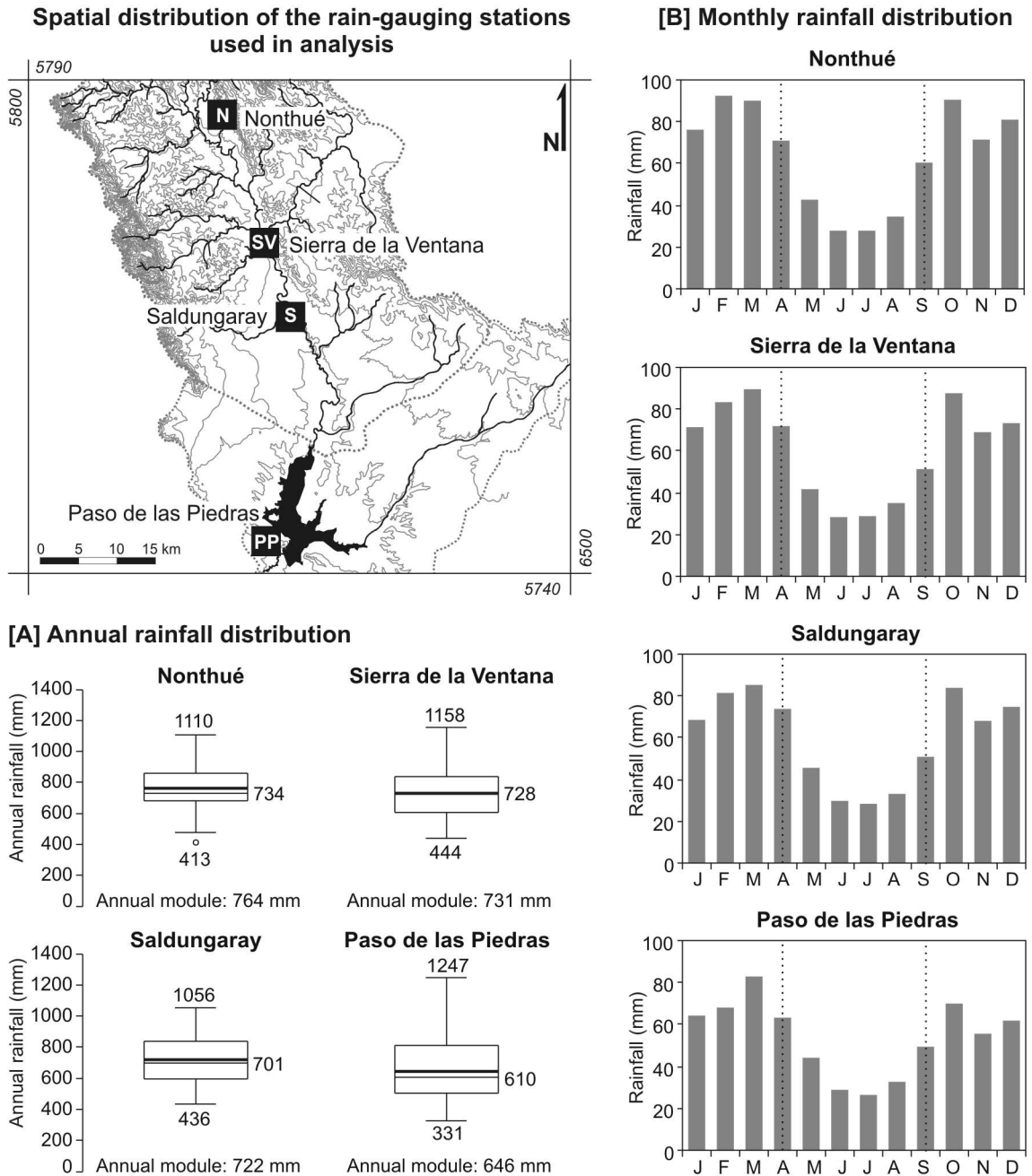
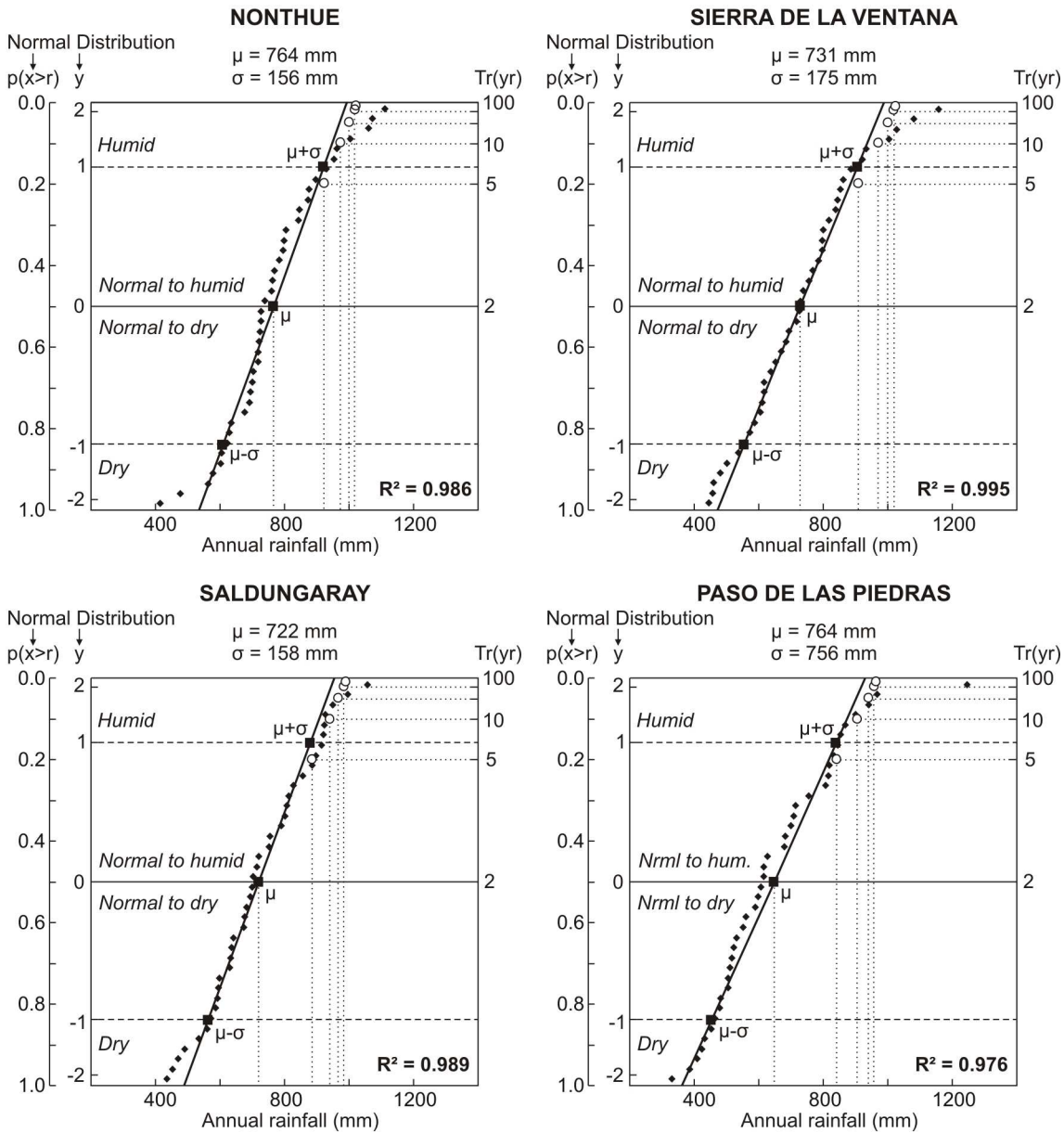


Figure 2.10: [A] Annual rainfall distribution and [B] monthly rainfall distribution in Nonthué, Sierra de la Ventana, Saldungaray and Paso de las Piedras over the period 1971-2010. The map shows the situation of the four rain-gauging stations within the river basin.

[A] Frequency of annual rainfall modules by site



[B] Annual pluviometric coefficient by site

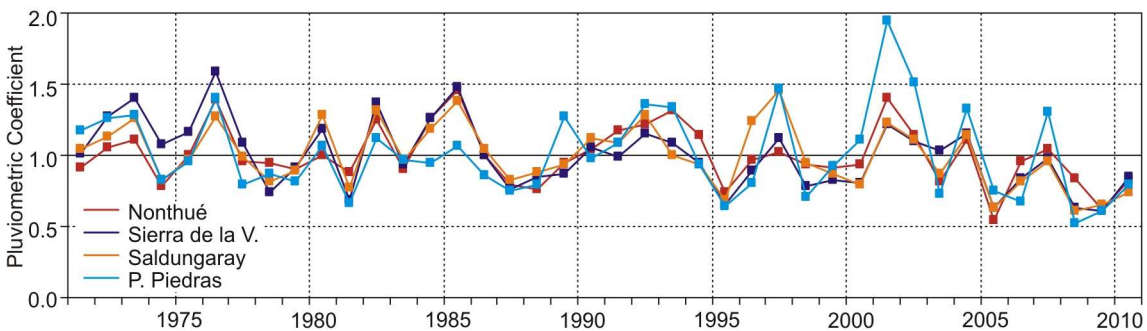


Figure 2.11: Frequency, return period and inter-annual variability of annual rainfall modules by site over the period 1971-2010. [A] Normal probability plots of rainfall to exceedance probability with a fitted line based on the standardized normal distribution (based on Oosterbaan, 1994); [B] Annual pluviometric coefficient by site (based on Réménieras, 1986). The correlation values (probability fit) were derived from the p-p plot (not shown).

Distribution of monthly rainfall

The annual distribution of monthly rainfall exhibited similar timing for all sites (Fig. 2.10 [B]), although the magnitude of mean monthly rainfall declined SSW (differences between Nonthue and Paso de las Piedras were of up to 25 mm in February). The use of monthly pluviometric coefficients permitted to inspect the spatial differentiation in the annual distribution of monthly rainfall regardless of the absolute magnitude of the hyetographs (Table 2.3).

Table 2.3: Monthly pluviometric coefficients (%) for Nonthue [N], Sierra de la Ventana [SV], Saldungaray [S] and Paso de las Piedras [PP] based on long-term (1971-2010) averaged monthly rainfall. Black bold numbers indicate the month of maximum contribution to the annual module.

Site	J	F	M	A	M	J	J	A	S	O	N	D	Module (mm)
N	9.9	11.8	12.1	9.3	5.6	3.6	3.6	4.5	7.9	11.9	9.3	10.6	764
SV	9.8	11.4	12.3	9.8	5.7	3.9	3.9	4.8	7.0	12.0	9.4	10.0	731
S	9.5	11.3	11.8	10.2	6.3	4.1	3.9	4.6	7.0	11.6	9.4	10.3	722
PP	9.9	10.5	12.8	9.8	6.8	4.4	4.0	5.0	7.7	10.8	8.6	9.5	646

The distribution of monthly rainfall over the annual cycle defined clearly a dry season extending from May through September and a wet season extending from October through April. Rainfall during the wet season accounted for between 72 and 75 % the annual module for all sites; these proportions correspond to averaged rainfall amounts declining from 570 mm in the headwaters to 460 mm in Paso de las Piedras. Rainfall during the dry season averaged between 200 mm and 180 mm, respectively. As the wet season is coincident with austral summer and spring, both calendar seasons revealed logically the highest monthly pluviometric coefficients (Table 2.3) with peak in March and a secondary peak in October. The driest months were June and July.

Regions of rainfall homogeneity

Previous results showed that rainfall regimes within the river basin differed in the absolute magnitude of the hyetographs but not in the timing of the rain seasons neither in the relative contribution of monthly rainfall to the annual module. Furthermore, rainfall regimes within the upper river basin were poorly differentiated by absolute magnitude, the biggest differences in the magnitude of rainfall regimes were evidenced relative to Paso de las Piedras series.

Accordingly, long-term series of monthly rainfall for Nonthue, Sierra de la Ventana and Saldungaray were assembled into a single dataset accounting for mean areal rainfall within the upper river basin (using the Thiessen method). This procedure summarized rainfall observations into two distinct rainfall series accounting for spatial homogeneity in rainfall regimes: monthly areal rainfall for the upper river basin and monthly rainfall for Paso de las Piedras (Fig. 2.12).

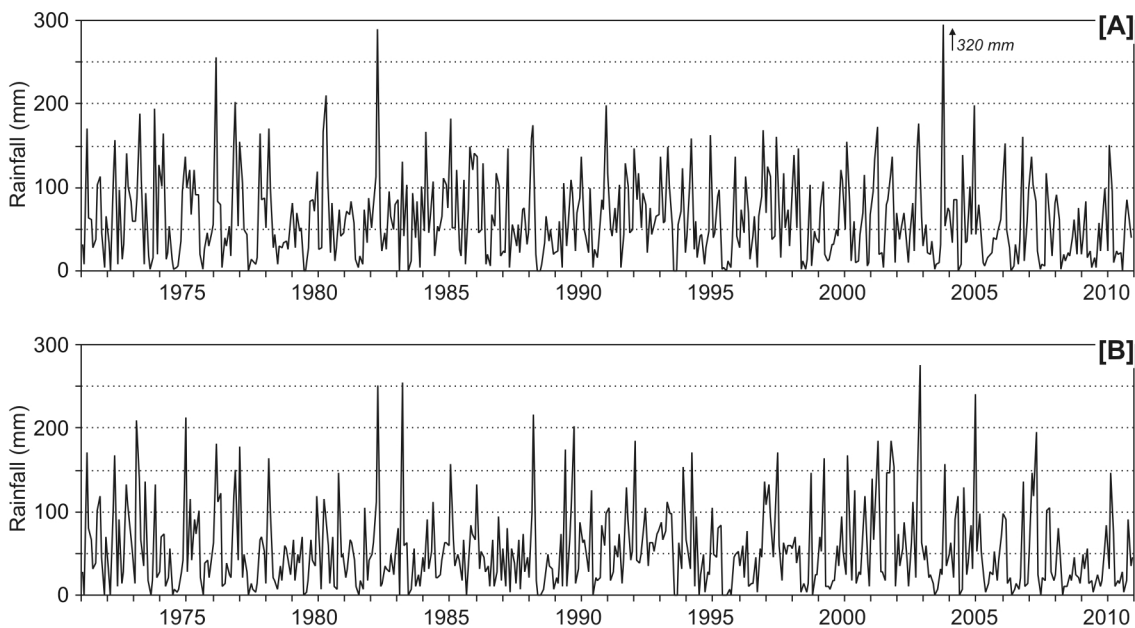


Figure 2.12: Long-term series (1971-2010) of monthly rainfall for [A] the upper river basin and [B] Paso de las Piedras. Rainfall series for the upper river basin were averaged using the Thiessen method (areal rainfall).

2.2.2. Long-term series of air temperature

Long-term series (1971-2010) of maximum and minimum daily temperature in Paso de las Piedras and Saldungaray were estimated using linear regression analysis. Regressions were based on temperature data for three nearby stations: Bahía Blanca, Pigüé and Tres Arroyos (Fig. 2.3).

Model verification

The R^2 values obtained from regression (Fig. 2.13) indicated that the models explained between 90 and 99 % of variations in maximum and minimum daily temperature for both sites (confidence interval of 95 %). About 90 % of error residuals were between ± 1.6 °C, with maximum in ± 3.6 °C. The mean error [ME] was 0.01 °C in all cases with high variation ($0.85 < SD_{T_{max}} < 1.25$; $1.31 < SD_{T_{min}} < 1.64$), which indicated that mean errors were affected by errors of opposite sign. Hence, verification of the results used preferably the annual RMSE. Small to moderate RMSE values indicated that the regression models fitted better for estimation of maximum daily temperature in both sites ($0.85 < RMSE < 1.25$).

The accuracy of the regression models was evaluated by comparison between observed and estimated mean daily temperatures over the year 2010. Correlations coefficients were 0.97 for both Saldungaray and Paso de las Piedras series, which revealed the suitable accuracy of the regression models on a daily scale. Comparison between observed and estimated temperatures averaged on a monthly scale showed very little differences between measured and estimated temperature data in both sites (-0.3 °C > T > 0.6 °C), and very small annual RMSE values (0.2 °C in Saldungaray and 0.3 °C in

Paso de las Piedras). Overall, the verification process indicated that the models simulate temperature data accurately for both sites, although fit better for Saldungaray series.

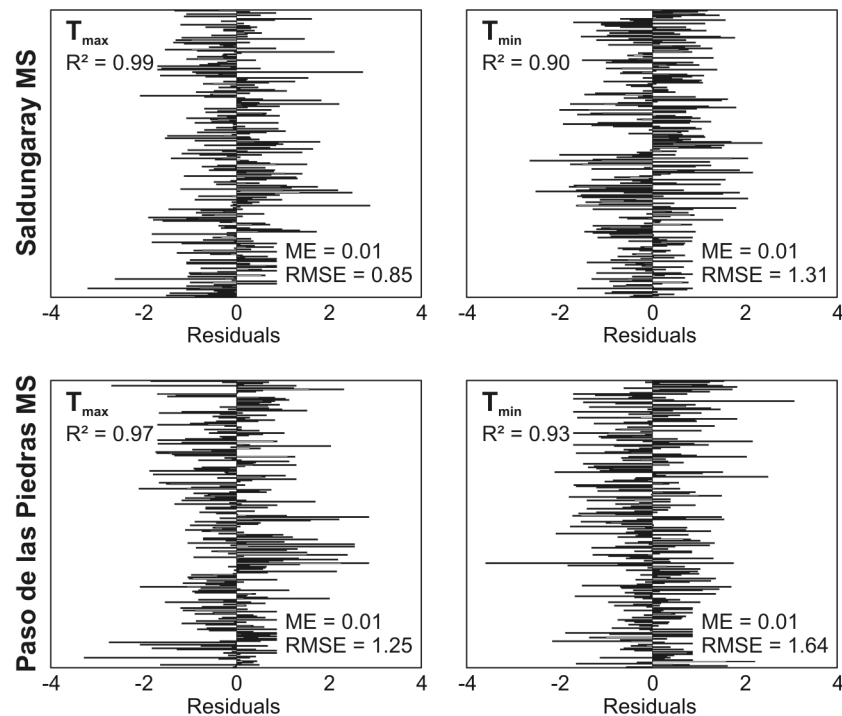


Figure 2 13: Error residuals from estimation of maximum daily temperature [T_{max}] and minimum daily temperature [T_{min}] in Saldungaray and Paso de las Piedras over the year 2010. Descriptive statistics of error from regressions are shown along.

Model running

The regression models were run on a continuous daily basis from 1971 to 2010; mean daily temperatures by site were calculated by averaging estimates of daily maximum and minimum temperature (Fig. 2.14). Inspection of thermal patterns in Saldungaray and Paso de las Piedras revealed notable inter-site differences. Mean daily temperatures in Saldungaray were colder than in Paso de las Piedras, and so the value of mean annual temperature was lower (13.7 °C and 15.0 °C, respectively). However, annual thermal ranges in Saldungaray were higher than in Paso de las Piedras (28.6 °C and 26 °C, on average) and diurnal fluctuations were considerably higher as well (12.8 °C and 9.3 °C, on average). Such differences are conceivably related to the higher topographic situation (+100 m) and greater wind exposure of Saldungaray MS with respect to Paso de las Piedras MS.

2.2.3. Temperature-derived time series

Depths of potential evapotranspiration

Series of mean monthly temperature for Paso de las Piedras and Saldungaray were combined with corresponding series of monthly rainfall to calculate series of mean

monthly potential evapotranspiration (PET) over the long-term (1971-2010). Similarly, series of maximum monthly temperature were used to derive series of maximum monthly potential evapotranspiration.

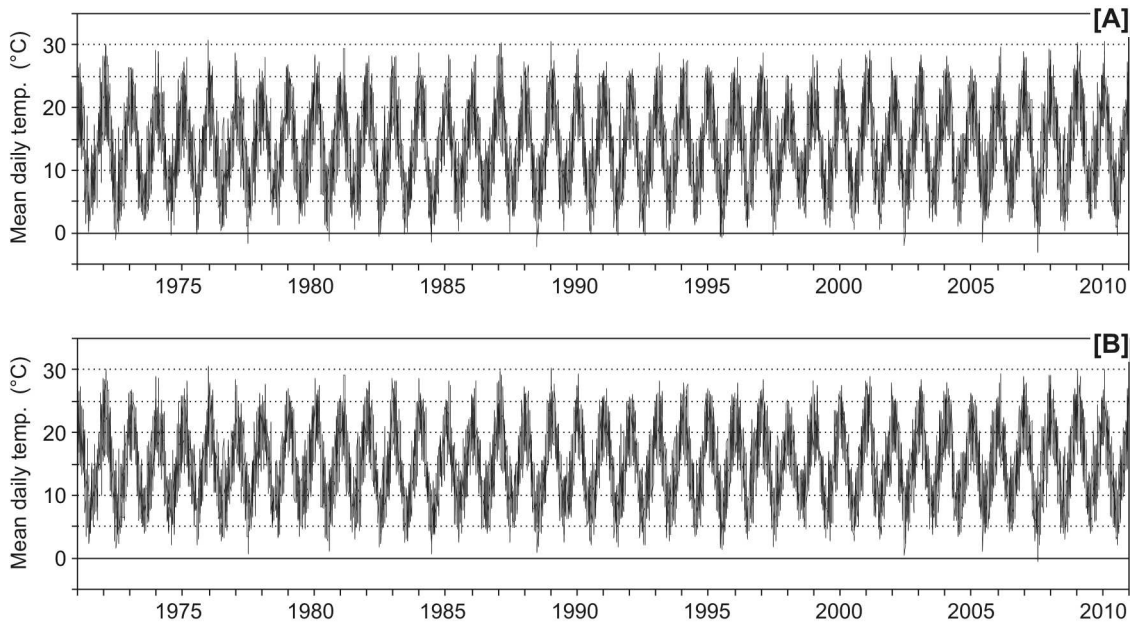


Figure 2.14: Long-term series (1971-2010) of mean daily temperature in Saldungaray and Paso de las Piedras. Mean daily temperatures by site were averaged from maximum and minimum daily temperature estimates.

Series of mean monthly PET (Fig. 2.15) revealed that the march of potential evapotranspiration over the annual cycle followed similar patterns in both sites: PET was almost negligible during the winter months with minimum in June (20 mm, on average) and peaked significantly during the summer months with maximum in January (120 mm, on average). Mean monthly PET in Paso de las Piedras was notably higher than in Saldungaray, this arising from the higher temperatures recorded by the former site. Mean annual PET was $690 \text{ mm}\cdot\text{yr}^{-1}$ in Saldungaray and $740 \text{ mm}\cdot\text{yr}^{-1}$ in Paso de las Piedras.

Rates of evaporation from the reservoir surface

Evaporation rates from the surface of the reservoir lake were calculated on a daily basis from 2009 to 2011 (with blanks) using the Penman method (See Section 1.3.4, p. 74); note that evaporation rates in $\text{m}^3\cdot\text{s}^{-1}$ were calculated using the maximum reservoir surface area (36 km^2). Mean daily evaporation rates over the 3-yr observation period (Fig. 2.16) ranged from $1.8 \text{ m}^3\cdot\text{s}^{-1}$ in January ($4.3 \text{ mm}\cdot\text{day}^{-1}$) to $0.44 \text{ m}^3\cdot\text{s}^{-1}$ in July ($1.1 \text{ mm}\cdot\text{day}^{-1}$); the mean annual evaporation rate was $0.9 \text{ m}^3\cdot\text{s}^{-1}$ ($2.2 \text{ mm}/\text{day}$).

Evaporation rates calculated by Penman method were highly consistent with previous studies; for example, the hydrologic study of the MOSP reported mean annual rates of reservoir evaporation of $1 \text{ m}^3\cdot\text{s}^{-1}$ (cited by Schefer, 2004). Nevertheless, computation of evaporation rates depend on a range of atmospheric conditions (e.g. wind speed, relative

humidity, and air pressure) for which data were lacking over the long term. Hence the need to validate the accuracy of series of potential evapotranspiration calculated by Thornthwaite method (above).

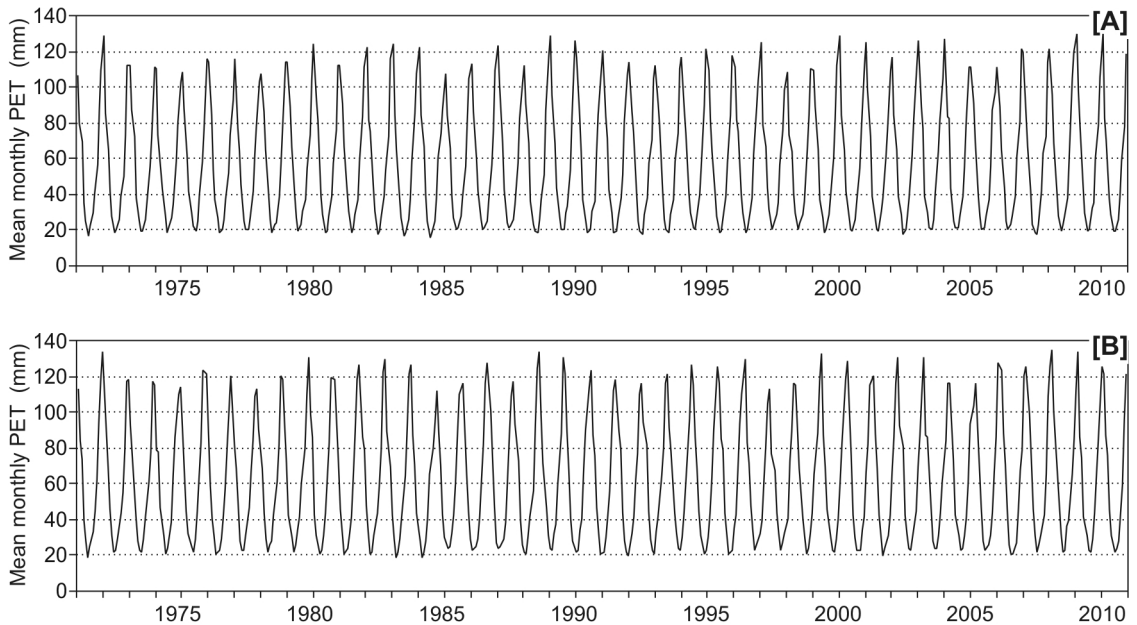


Figure 2.15: Long-term series (1971-2010) of mean monthly potential evapotranspiration for [A] Saldungaray and [B] Paso de las Piedras. PET was calculated using Thornthwaite method.

Series of monthly evaporation over the period 2009-2011 were compared to corresponding series of mean and maximum monthly potential evapotranspiration for Paso de las Piedras to inspect the correlation in the depth of water losses calculated using one or other method (Fig. 2.17). Results showed that variations in monthly evaporation were highly correlated to variations in monthly PET, with maximum correlation to series of maximum monthly PET (84 %). This indicates that the use of series of maximum potential evapotranspiration instead than evaporation should not be a source for high error in hydrologic analysis of the reservoir.

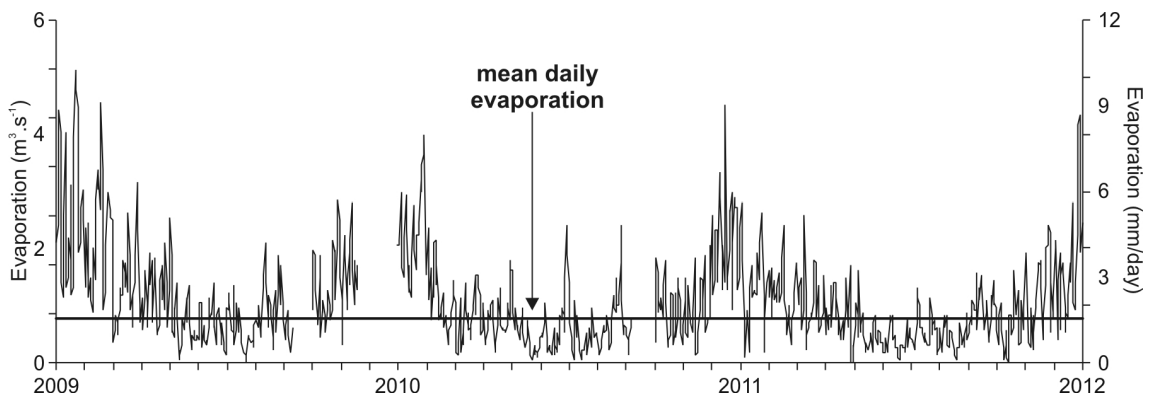


Figure 2.16: Short-term series (2009-2011, with blanks) of daily evaporation from the surface of the reservoir lake. Daily evaporation rates were calculated using Penman method.

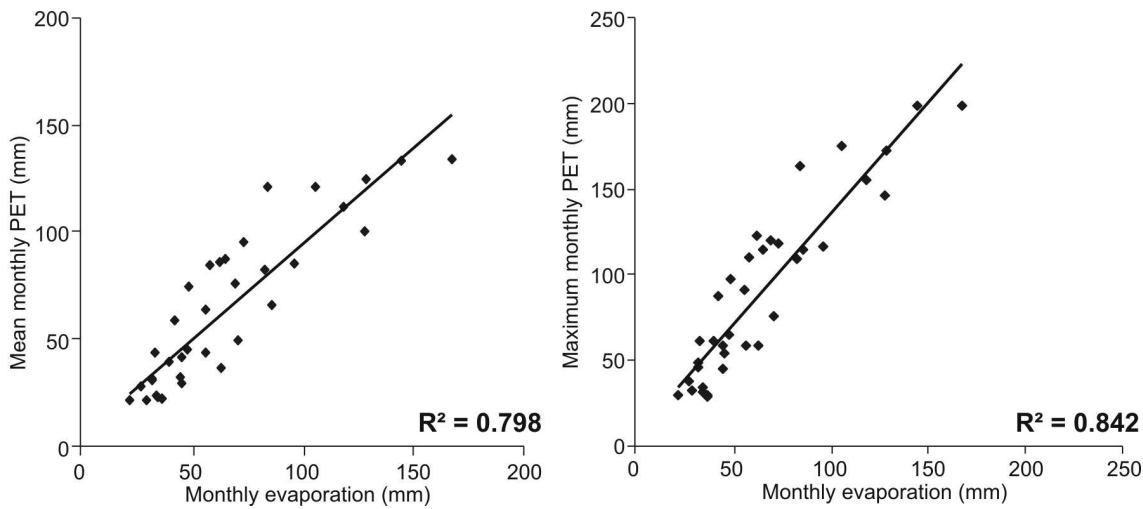


Figure 2.17: Correlation between monthly evaporation and monthly potential evapotranspiration for Paso de las Piedras over the period 2009-2011.

2.3. THE HYDROLOGICAL MODEL OF THE UPPER RIVER BASIN

2.3.1. Physiographic characteristics of the drainage basin

The effective rainfall (i.e. the fraction of precipitation available for runoff processes) within a basin depends primarily on its physiographic characteristics affecting the sub-surface and underground water retention (Marek, 2011). Soil types, land cover and terrain slope combine to delineate different units of homogeneous hydrologic response to runoff processes (Yeung, 2004).

Land use types

Satellite imagery revealed that land use types within the upper basin may be assembled into three major types of land cover: cultivated lands, grasslands, and areas of exposed rock with none or little vegetation (Fig. 2.18). Cultivated lands are dominated by rainfed wheat and corn production, and natural grasslands are frequently used for pasture (Gil, 2009). The heterogeneity within each category (e.g. crop types) was considered of less importance because of the little difference in the values of hydrologic response across sub-categories.

Soil types

Soil classification in Argentina uses the Soil Taxonomy of the U. S. Department of Agriculture (USDA, 1999). According to Gil (2009), the principal soil types within the upper river basin integrate the group of the Argiudolls (Typic subgroup) and of the Hapludolls (Typic and Lithic subgroups), both within the order of the Molisolls (Fig. 2.18). The main characteristics of these soil types are defined as follows:

- Typic Argiudolls [A_T] have clay loam to loam texture and are relatively deep (80

to 120 cm). They constitute the loess supporting grasslands and croplands within the lower lands.

- Lithic Hapludolls [H_L] are very shallow (27 cm) and develop over the basement rock within the mountain areas; even if they have clay loam texture, the horizon A1 contains boulders and pebbles.
- Typic Hapludolls (H_T) are deep (130 cm) with sandy clay loam to loam texture; they occupy a much reduced extension within the intermountain areas.

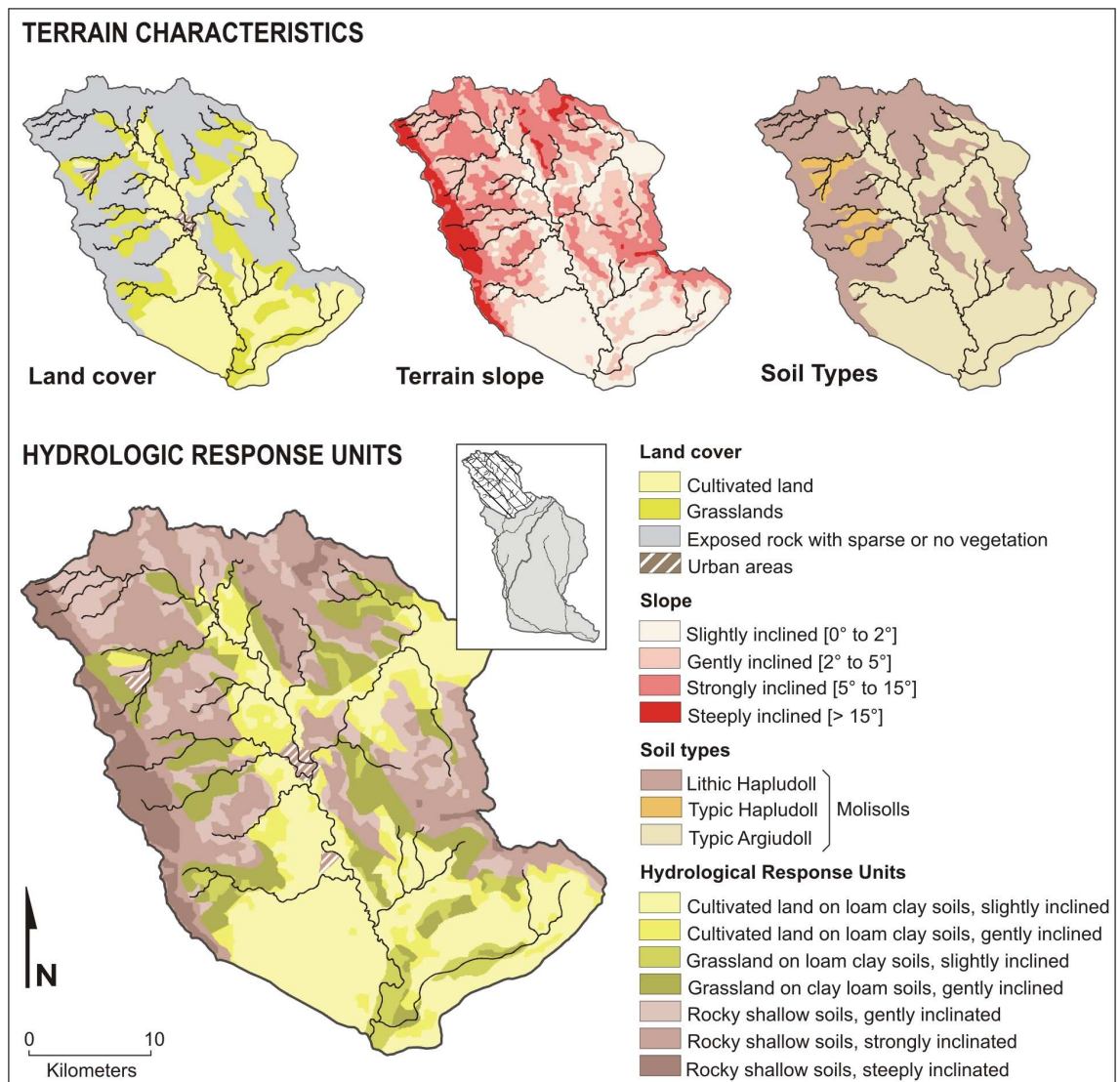


Figure 2.18: Hydrological Response Units (HRU) within the upper Sauce Grande Basin. HRUs were merged in ArcGIS from intersection of three layers of spatial data: land cover, terrain slope and soil types. Land cover and soil type data were derived from imagery classification (Landsat ETM 2003) upon the basis of the work of Gil (2009). The slope layer was derived from the TG10 digital terrain model.

According to Luque *et al.* (1979), A_T and H_L fall within the *C* and *D* categories of the hydrologic soil group classification of the NRCS (NRCS, 2007a), respectively; the latter

being categorized as *C* where the slope is less steep (Gil, 2009). The hydrologic characteristics of the *C* and *D* soil groups are expressed as follows:

- Soils in the *C* group have between 20 and 40 % clay, less than 50 % sand, and loam to clay loam texture with moderately high runoff potential when thoroughly wet. The saturated hydraulic conductivity in the transmissive layer between the surface and 50 cm is between 0,36 cm.h⁻¹ per hour and 3,61 cm.h⁻¹. The depth to any water impermeable layer is greater than 50 cm, and the depth to the water table is greater than 60 cm.
- Soils in the *D* group have more than 40 % clay, less than 50 % sand, and clayey textures with high runoff potential when thoroughly wet. For soils with a water impermeable layer at a depth between 50 cm and 100 cm, the saturated hydraulic conductivity in the least transmissive soil layer is less than or equal to 0,36 cm.h⁻¹.

Terrain slope

The slope layer derived from the TG10 DTM was classified into four categories of terrain inclination according to Pedraza (1996). Each slope class was closely related to specific ranges of terrain elevation. The steepest areas extended between 1 200 and 500 m.s.l.; below the contour line of 500 m the slope declined notably, although the terrain remained strongly inclined between 500 and 400 m.s.l. The lower lands were gently (300 to 400 m) to slightly (200 to 300 m) inclined.

2.3.2. Hydrological Response Units

The areas having similar physiographic characteristics were assumed to delineate basin units having similar hydrological response. As shown in Figure 2.18, terrain slope, land cover and soil types discriminated eight different Hydrological Response Units for the upper river basin (HRU; Table 2.4). The runoff curve number (CN) assigned to each HRU considered Antecedent Moisture Conditions of Type II based on Boonstra (1994) and included the effects of the terrain slope based on Luque *et al.* (1979). The hydrologic condition was considered along with the CN values. A good (or poor) hydrologic condition indicates that the soil usually has a low (or high) runoff potential for a specific hydrologic soil group, cover type, and treatment (NRCS, 1986).

The HRU 1 corresponds to urban areas with very little influence on runoff processes because of their rural character and reduced size (9.5 km²). The remaining HRUs may be assembled into two major groups of similar hydrologic response:

i) The higher, steeper areas (HRUs 6 to 8) are dominated by impermeable structures with little and sparse vegetation developing upon shallow rocky soils. In terms of surface, this group represents 43 % of the upper basin (434 km²). The overall hydrologic condition is fair to poor; impermeable rock and steep topography contribute to runoff dominate over infiltration.

ii) The second group integrates the HRUs 2 to 5 and is coincident with the lower, gently to slightly inclined lands (574 km²; 57 %). Land use is dominated by pastures and agriculture. The smooth topography together with the permeable geology contributes to

decrease the rate and extent of runoff and to increase the vertical water exchange (i.e. infiltration and evapotranspiration); the hydrologic condition is fair to good.

Table 2.4: Runoff Curve Number (CN) by Hydrological response Unit (HRU) identified within the upper river basin.

HRU	Slope (°)	Cover type	Soil type	Hydrol. Condition	Soil group	CN
1	---	Urban area	Clay loam	Fair to Poor	C	85
2	$0 \geq 2$	Cultivated land	Clay loam	Good	C	64
3	$2 \geq 5$	Cultivated land	Clay loam	Good	C	69
4	$0 \geq 2$	Grasslands	Clay loam	Fair to Good	C	74
5	$2 \geq 5$	Grasslands	Clay loam	Fair	C	79
6	$2 \geq 5$	Bare rock	Rocky soil	Poor	D	86
7	$5 \geq 15$	Bare rock	Rocky soil	Poor	D	90
8	> 15	Bare rock	Rocky soil	Poor	D	95

2.3.3. Direct runoff depth

Rainfall-runoff relationships are at the basis of flow simulation for the headwaters. Since flow simulation uses flow data gauged at Chacra La Blanqueada GS, rainfall-runoff analysis focuses on the drainage area contributing to this gauging station (Fig. 2.19). The issue to be solved at this point was related to the spatial distribution of the rainfall data series available to simulate streamflow on a daily basis; rainfall data were available for Saldungaray and Sierra de la Ventana locations only, so that rainfall processes within a considerable proportion of the upper basin were unknown.

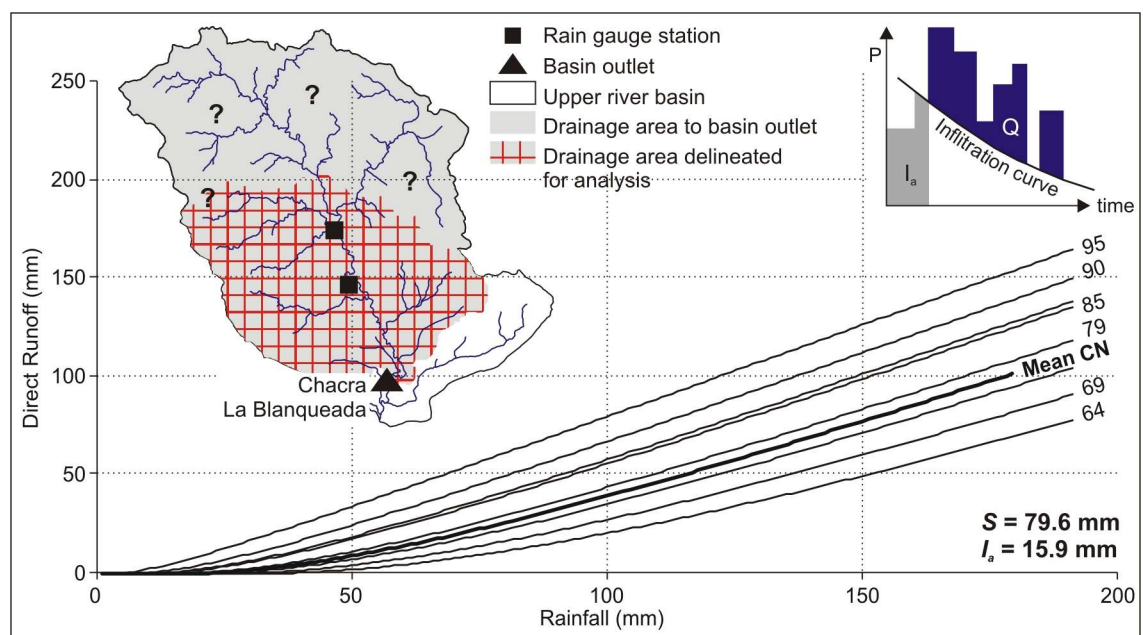


Figure 2.19: Rainfall-runoff relationships by runoff curve number. The thick black line indicates average rainfall-runoff relationships for the upper drainage basin (red squared area).

Two different possibilities were involved in the delineation of the contributing drainage area: (i) delineation by the watershed boundary assuming rainfall uniformity across the entire contributing area, or (ii) delineation by the ratio of influence of the rain gauge stations for which data were available. Given the evidence of strong spatial variability of rainfall across the upper basin (Gaspari *et al.*, 2008; Gil, 2009) and given the extreme importance of rainfall uniformity in space and time to accurate rainfall-runoff calculations (Boonstra, 1994; Marek, 2011), the second possibility was considered more suitable (Fig. 2.19). Implications of this decision for the final outcome of hydrological modelling are discussed in the Discussion section. Hereinafter, the term ‘upper drainage basin’ refers implicitly to the drainage area that extends from Sierra de la Ventana to Chacra La Blanqueada GS (basin outlet).

Delineation of the upper drainage basin (Fig. 2.19) was based on maps of flow direction, flow accumulation and watershed delineation created in ArcGIS using the HEC-GeoHMS module. The hydrologic heterogeneity within the drainage basin was accounted for by averaging CN values (Table 2.5); the potential soil retention was calculated in 79.6 mm with an initial abstraction of 15.9 mm. Runoff depths within the upper drainage basin were derived from empirical relationships between rainfall and soil retention by runoff curve number (Fig. 2.19). Rainfall-runoff relationships for the mean CN value revealed that runoff depths may reach up to 18 mm for 2-yr rainfall (63 mm) and 43 mm for 10-yr rainfall (100 mm). The ratio of runoff to rainfall (i.e. the runoff coefficient) was solved for rainfall depths increasing from 16 mm to 190 mm (1000-yr rainfall); the runoff coefficient of the drainage basin averaged 0.35.

Table 2.5: Areal-weighted runoff curve number (CN) by Hydrological Response Unit (HRU). Values for the entire drainage basin in bold.

HRU	CN	Area (km ²)	Area (%)	Weighted CN
1	85	6.9	1.6	1.3
2	64	79.7	18.1	11.6
3	69	154.9	325.2	24.3
4	74	39.5	9.0	6.6
5	79	18.0	4.1	3.2
6	86	30.4	6.9	5.9
7	90	82.0	18.6	16.8
8	95	35.6	8.1	7.7
Sum	-	439.9	100	76.1

2.3.4. Temporal distribution of runoff

The time that takes to runoff to travel across the drainage basin was estimated calculating the time of concentration [T_c] of the drainage basin. Two different methods were evaluated: the Kerby-Kirpich equation and the TR55 method of the NRCS (See Section 1.4.3, p. 75):

- The Kerby-Kirpich equation provided a basin time of concentration of 10.7 hours, this arising from runoff travel times of 2.5 hours (overland flow) and 8.7 hours

(channel flow).

- The TR55 method provided a basin time of concentration of 14.5 hours, this arising from runoff travel times of 0.1 hours (sheet flow), 0.9 hours (shallow concentrated flow), and 13.6 hours (channel flow).

The difference between the two estimates was notably high (3.8 hours), which indicates that at least one estimate is inaccurate to computation of derived hydrologic parameters. According to Mareck (2011), the accuracy of the estimates can be evaluated using an *ad hoc* methodology that simply computes the time of concentration as the square root of the drainage area (in mi^2). Results indicated that the time of concentration of the upper drainage basin should be close to 13 hours (given a surface area of 170 mi^2); hence the use of a basin time of concentration of 14.5 hours (TR55 method) was considered more suitable.

2.4. DAILY FLOW RATES FOR THE UNREGULATED RIVER

Hydrological modelling of the upper drainage basin provided the basis to compute the Unit Hydrograph of the upper Sauce Grande River; in turn, the Unit Hydrograph provided the hydrologic parameters required to river flow simulation (See Section 1.5, p. 76). As shown in Figure 2.20, rainfall excess of 1 mm-depth generates a hydrograph peak that reaches $4 \text{ m}^3 \cdot \text{s}^{-1}$ in 9.7 hours, this arising from a drainage area of 440 km^2 and a time of concentration of 14.5 hours. The base time is 26 hours with maximum duration of 2 days. The inflexion point on the recession limb occurs after 16 hours, which gives a base flow rate of $2.0 \text{ m}^3 \cdot \text{s}^{-1}$.

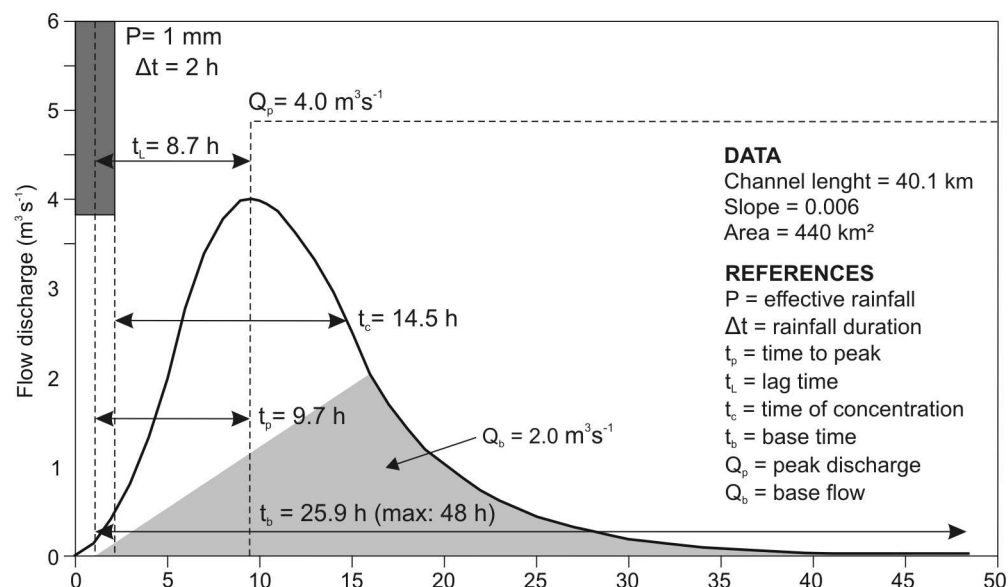


Figure 2.20: Unit Hydrograph for 1 mm-depth rainfall excess within the upper Sauce Grande Basin.

The period selected for calibration of the RainOff-empirical model spans concurrent observations of rainfall and flow discharge over 852 days ranging from the 1st

September 2008 through the 31st December 2010. The purpose of model calibration was to estimate parameters and coefficients that simulate low, median and high flows accurately. Prolonged dry conditions increased the permanence of subsidence flows ($3.17 \text{ m}^3 \cdot \text{s}^{-1}$) over almost the entire year 2009; by late 2009 and over the year 2010, minimum flow rates increased to $3.28 \text{ m}^3 \cdot \text{s}^{-1}$ and random events of heavy rainfall led to high-flow pulses and small floods.

A trial-and-error adjustment of the parameters to which the model was sensitive was performed to regulate the magnitude and timing of the hydrograph simulated. The alpha function was fitted to give a minimum flow rate of $3.22 \text{ m}^3 \cdot \text{s}^{-1}$, i.e. a base flow rate falling between the minimum flow rate and low-flow rates observed over the entire period for which data were available ($2.90 \text{ m}^3 \cdot \text{s}^{-1}$ and $3.30 \text{ m}^3 \cdot \text{s}^{-1}$, respectively). Errors in the simulation process were measured separately considering low flows ($< 3.30 \text{ m}^3 \cdot \text{s}^{-1}$), median flows ($3.30 \text{ m}^3 \cdot \text{s}^{-1} > 3.85 \text{ m}^3 \cdot \text{s}^{-1}$) and high flows ($> 3.85 \text{ m}^3 \cdot \text{s}^{-1}$). Low- and high-flow rates were calculated based on the series of flow data available; median flow was $3.42 \text{ m}^3 \cdot \text{s}^{-1}$.

The measure of error during the *calibration period* revealed good correspondence between simulated and observed flow data (Table 2.6), although coefficients of efficiency for high flows were low ($CE = 0.22$). Metrics of absolute error (ME, RMSE) and relative error (RE) showed very low values for all flow ranges and indicated that the model fitted better for median and low flows. Overestimation rates showed that the magnitude of median and high flows was underestimated by between 87 and 90 %, which was less suitable than expected (50 %). Despite some random error residuals related to overestimation of evaporation rates and to bias in rainfall series used as input data, comparison between curves of observed and simulated flow data showed that the model fitted suitably to simulate the timing, the magnitude and the recession of mean daily flows (Fig. 2.21).

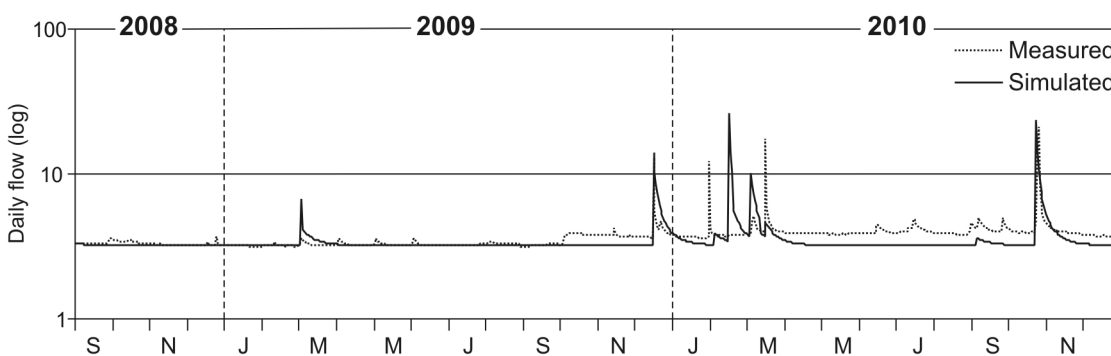


Figure 2.21: Comparison between measured and simulated daily flow rates for the upper Sauce Grande River over the calibration period (01/09/2008 to 31/12/2011).

The efficiency of the model to simulate daily flows was evaluated over an independent *verification period* ranging from the 1st March 2007 to the 30th November 2007 (Table 2.6). Coefficients of efficiency revealed that the model fitted better for low flows ($CE = 0.99$) than for median and high flows ($0.48 < CE < 0.58$), even if absolute and relative errors were relatively small. Overall, results indicated that the model simulated flows suitably; the highest error ranges were related to simulation of high flows and revealed

to respond to bias in the rainfall series used as input data.

Table 2.6: Errors from simulation of daily flow rates for the upper Sauce Grande River over (a) the calibration period (01/09/2008 to 31/12/2011), and (b) the verification period (01/03/2007 to 30/11/2007). Best results per metric in bold.

<i>(a) Calibration period</i>							
Flow magnitude	n	ME	SD	RMSE	RE	OE	CE
Low flows	277	0.01	0.07	0.07	0.39	46.9	1.00
Median flows	289	-0.09	1.57	1.57	-2.59	9.7	0.70
High flows	286	-0.49	1.79	1.85	-10.58	12.6	0.22
<i>(b) Verification period</i>							
Flow magnitude	n	ME	SD	RMSE	RE	OE	CE
Low flows	66	-0.02	0.06	0.05	-0.70	0.62	0.99
Median flows	161	0.37	1.57	1.60	10.31	38.5	0.48
High flows	48	0.70	2.44	2.52	17.01	56.3	0.58

[n] number of individuals; [ME] Mean Error ($\text{m}^3 \cdot \text{s}^{-1}$); [SD] Standard Deviation ($\text{m}^3 \cdot \text{s}^{-1}$); [RMSE] Root Mean Squared Error ($\text{m}^3 \cdot \text{s}^{-1}$); [RE] Relative Error (%); [OE] Overestimation rate (%); [CE] Coefficient of Efficiency.

The RainOff-empirical model was run on a continuous daily basis from 1956 through 2011. Two separated series of flow data were achieved: mean daily flow rates (Fig. 2.22) and daily rates of peak discharge (see Section 1.5.1, p. 76). These data series provided a robust basis on which to base further analysis of the natural river flow regime. River flow regime assessment was required prior to evaluate the effects of the dam upon the river hydrology system.

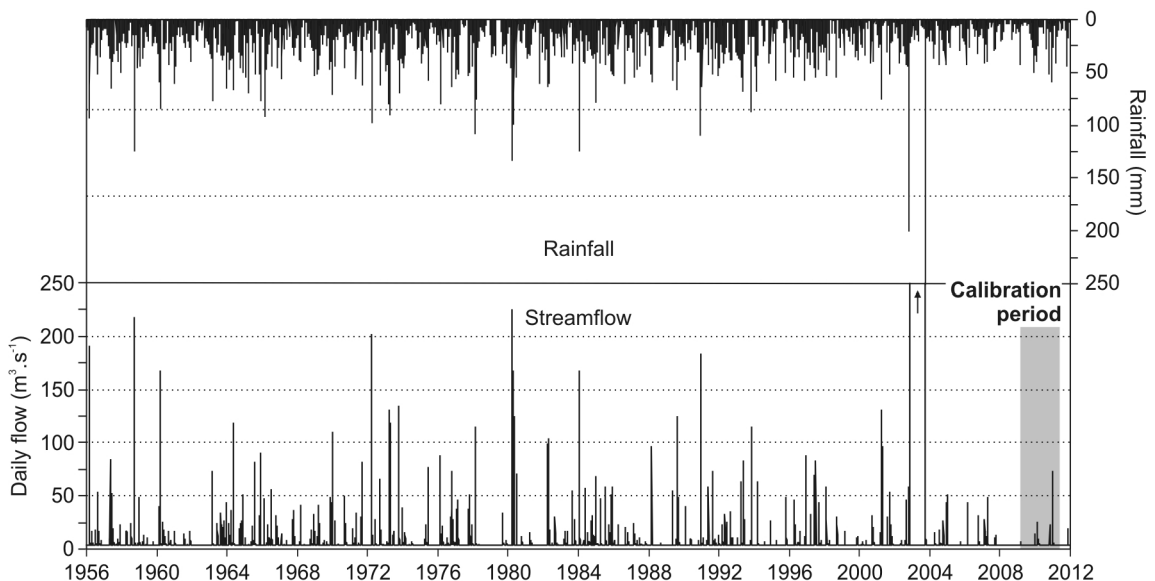


Figure 2.22: Rates of daily flow simulated from daily rainfall over the period 1956-2011.

2.5. DAILY FLOW RATES FOR THE REGULATED RIVER

Long-term series of daily streamflow within the river below the dam were estimated by combining three different sources of hydrologic data: (i) mean daily flow rates derived from stream stage readings, (ii) mean daily rates of reservoir flow release, and (iii) mean daily rates of reservoir seepage. Procedures performed to calculate flow rates within the river downstream are described below.

2.5.1. Daily flow rates over the period 2009-2012

The hydrometric stations located upon Bajo San José, BSJ-1 and BSJ-2, were calibrated using 5 and 4 measures of flow discharge, respectively. Measures of flow discharge were effectuated during periods of low flow, so that the function $Q = f(H)$ derived from these measures was used to calculate daily flows below the low flow threshold ($0.4 \text{ m}^3 \cdot \text{s}^{-1}$). Flows higher than this rate were calculated using derivative functions based on the Manning's equation.

R^2 values from the derivative functions revealed perfect model fit in both cases ($R^2 = 1$), and absolute errors resulting from daily flow estimations were very small for both hydrometric stations ($-0.03 < \text{RMSE} < -0.01$). Therefore, the stations can be said to be calibrated accurately and the parameters used in computation of the Manning's equation can be said to be precisely estimated. For a given stream stage, the error in estimates of the corresponding flow is expected to be less than 1 % in periods of base flow and between 1 and 5 % during high-flow events.

Hydraulic parameters used in empirical modelling

The *channel slope* was very low for both hydrometric stations ($0.0001 < s < 0.0008$) and the *hydraulic radius* for 5 m channel depth (bankfull stage) was moderate in BJS-1 ($R = 1.1$) to low in BSJ-2 ($R = 2.8$). The *channel roughness* was determined using the Manning's-Cowan coefficient [n] upon the basis of Arcement and Schneider (1989).

Overall channel conditions for both hydrometric stations were good (Fig. 2.23); as the river excavates fine materials (silt and clay; $n_b = 0.02$), the channel is mainly regular ($n_1 = 0.005$) with little obstructions ($n_3 = 0.015$). Variations in the channel cross-section along the river section were gradual in both cases; large and small cross sections alternate occasionally ($n_2 = 0.005$). As for the obstructions caused by vegetation, both sections revealed medium vegetation cover on the channel bed ($n_4 = 0.025$) and large vegetation cover over the channel banks, the vegetation cover over the channel banks being greater for BSJ-1 ($n_4 = 0.045$) than for BSJ-2 ($n_4 = 0.035$).

2.5.2. Daily flow rates over the long term

Daily flow rates were calculated over the entire period for which stream stage data were available (Fig. 2.24). Daily flow rates over the observation period (2009-2012) averaged $0.28 \text{ m}^3 \cdot \text{s}^{-1}$ with very little fluctuation ($0.03 \text{ m}^3 \cdot \text{s}^{-1}$); reservoir flow release did not occur,

and the response of flows to episodic rainfall was negligible compared to that of the river upstream.

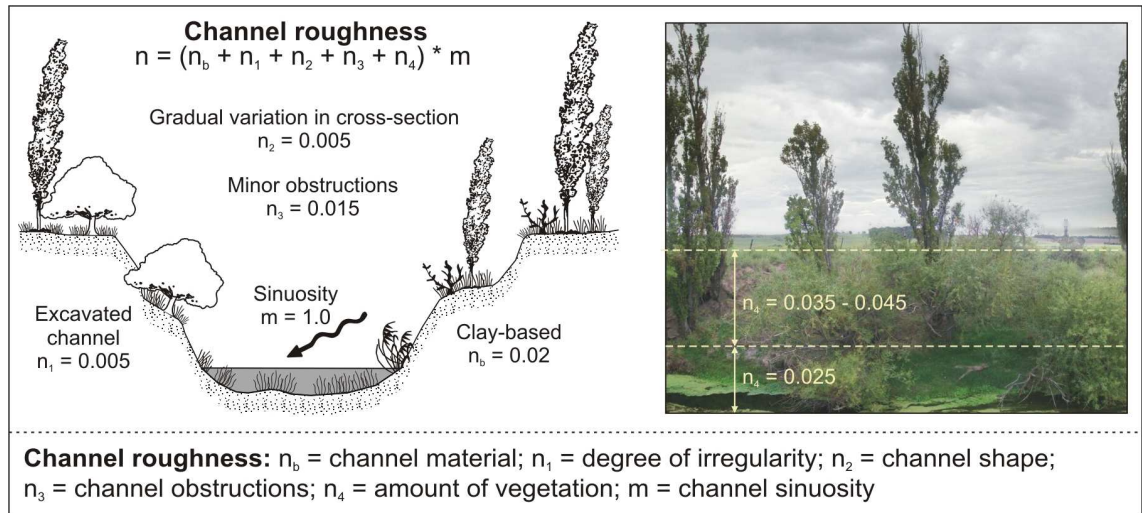


Figure 2.23: Scheme of the parameters used in estimation of the channel roughness (n).

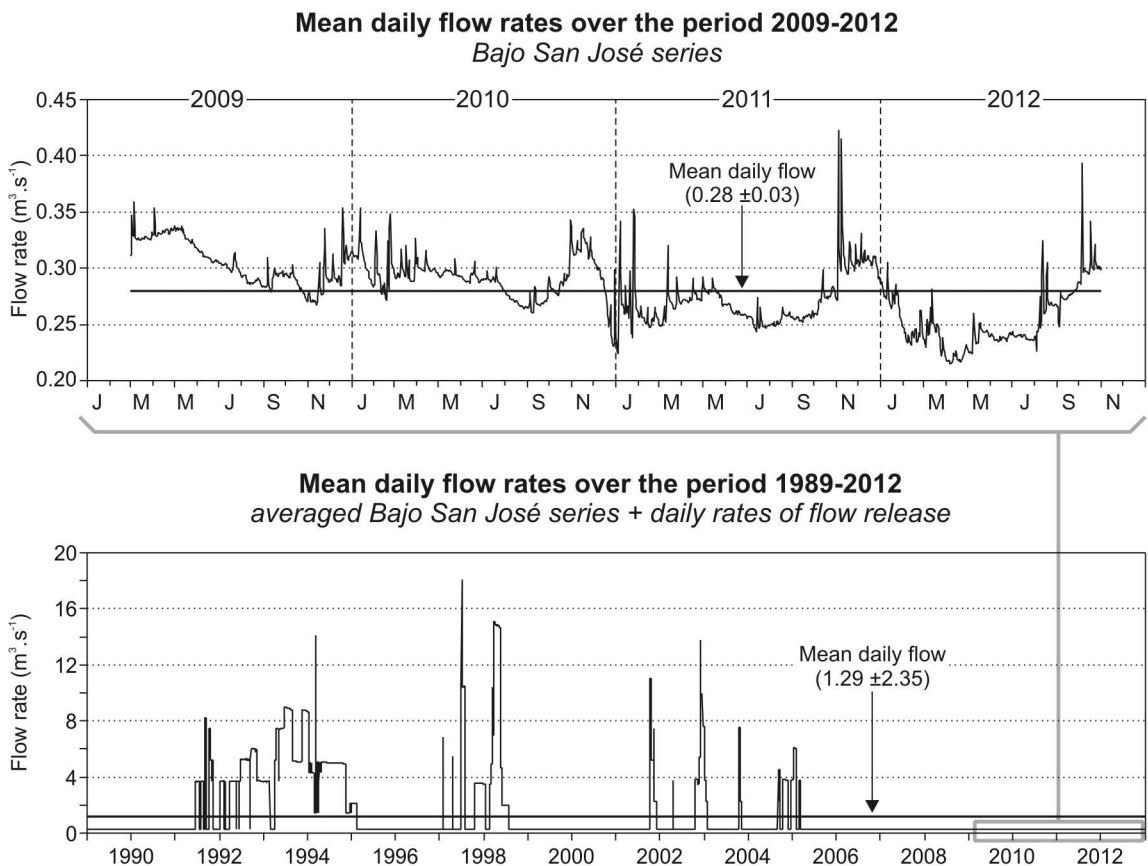


Figure 2.24: Mean daily flow rates for Bajo San José over the period 2009-2012 (above) and long-term series (1989-2012) of daily flow rates estimated for the river downstream.

Accordingly, we assumed that mean daily flow rates for the period 2009-2012 were characteristic of downstream conditions during periods of zero flow release from the dam reservoir; mean daily flow rates were then used to fill blanks within the series of daily rates of flow release (1989-2011). As shown in Figure 2.24, this procedure permitted to reconstruct long-term series of daily streamflow within the Sauce Grande River below Paso de las Piedras Dam.

2.5.3. The sources for downstream flow

Where no reservoir release occurs, downstream flow originates from (i) reservoir seepage below the dam structure, and (ii) leakage from the bottom gate; further downstream, groundwater inflows contribute to increase flow discharge significantly. Rates of reservoir seepage were calculated to discriminate the contribution of the dam reservoir to the downstream flow in periods of zero flow release (See Section 1.6.2, p. 83). Parameters used in calculations were measured *in situ* within the weir draining reservoir seepage into the main channel (Fig. 2.25). The current rate of reservoir seepage were averaged in $0.034 \text{ m}^3 \cdot \text{s}^{-1}$ (1.1 hm^3 per year) with very little variation between measures ($\text{SD} = 0.0001$).

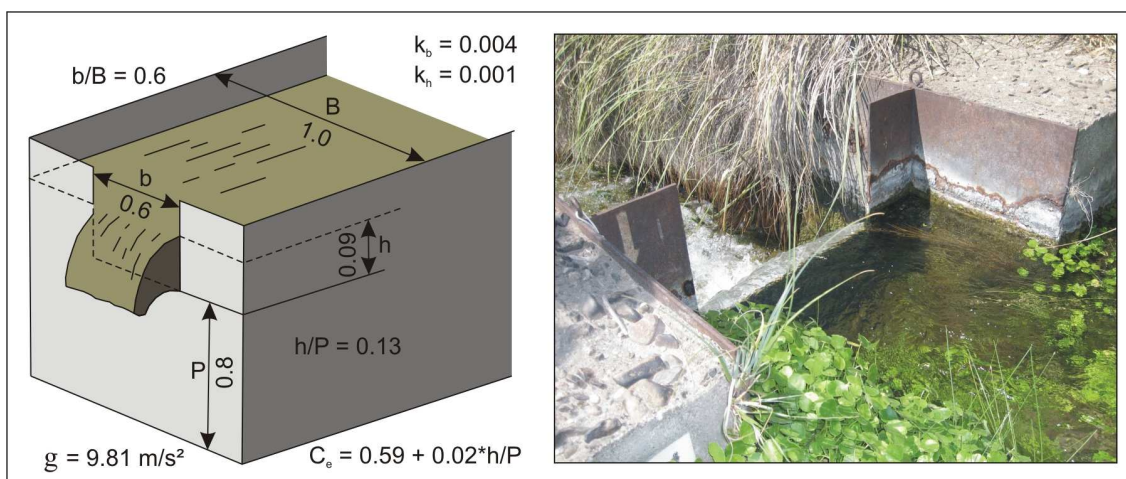


Figure 2.25: Parameters and measures used in estimation of rates of reservoir seepage. Based on André *et al.* (1976).

Flow discharge at Bajo San José averages $0.28 \text{ m}^3 \cdot \text{s}^{-1}$; this implies that reservoir seepage contributes to downstream flow by 12 %. A second weir drains reservoir seepage into the main channel (Fig. 2.5), although field observations revealed that the volume of water conducted is negligible. Another source for downstream flow observed (but not measured) is the reservoir leakage through the bottom gate. Assuming that the bottom gate is open by 1 mm, the rate of reservoir leakage should average $\sim 0.07 \text{ m}^3 \cdot \text{s}^{-1}$ (25 % of mean downstream flow). These measures suggest that the reservoir contributes to downstream flow by about 37 %; the remaining proportion is provided by groundwater inflow. Except for some short gullies, the Sauce Grande River receives no tributary inputs until its confluence with Cañada de los Leones creek (unsteady) in the lowest section.

The lack of climatic and hydrologic data over the long term has limited strongly earlier studies assessing the hydrology of the river basin. As a result, the hydrologic and geomorphic effects of river impoundment remain poorly evaluated. This chapter has presented in detail the procedures performed to generate baseline data for hydrological analysis of both the unregulated and the regulated Sauce Grande River. As well as yielding new spatial, climatic and hydrologic data made available to dam managers (Fig. 2.26), this chapter has tested applicability of a number of methods to spatial, climatic and hydrological modelling of ungauged basins. The methods presented herein are widely transferable to other ungauged basins as discussed below.

3.1. SPATIAL DATA

As the configuration of the terrain surface is a key factor controlling hydrological processes, Digital Terrain Models (DTM) are a valuable tool for hydrological assessment (Wise, 2000; Wu *et al.*, 2008). Examples of hydrological applications of DTMs include drainage basin definition (e.g. Rieger, 1998; Wang *et al.*, 2000; Mazvimavi *et al.*, 2006) and morphometry (e.g. Wang and Yin, 1998; Tucker *et al.*, 2001; Drogue *et al.*, 2002; Maestro Cano *et al.*, 2003; Hancock, 2005; Ozdemir and Bird, 2008; Matsunaga *et al.*, 2009), runoff modelling (e.g. Kim and Lee, 2004; Ko and Cheng, 2004; Wise, 2007), and flood hazard modelling (e.g. Gilard and Oberlin, 1998; Sanders, 2007; Lastra *et al.*, 2008; Merwade *et al.*, 2008), among many others. Within the context of the present research the DTM has triple applicability:

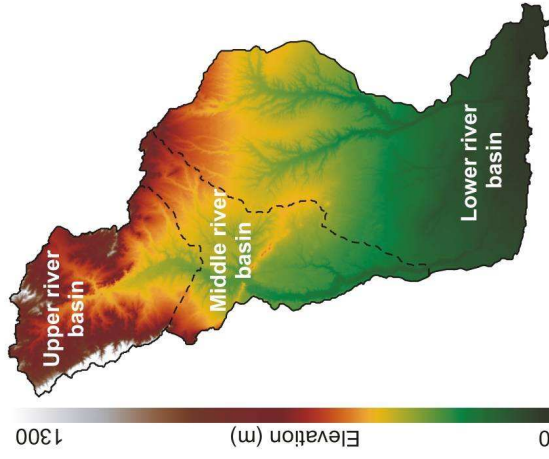
- i) it constitutes the source of elevation for rectification of aerial photography and imagery,
- ii) it provides information on the configuration of the terrain surface from which terrain and terrain-related products such as slope maps and Thiessen polygons are derived, and
- iii) it represents the basis on which to delineate the river watershed, create flow direction and flow accumulation maps, define the drainage network and the sub-catchments, and delimitate the contributing drainage basin to predict hydrological response.

Although the prime today is the generation of high-resolution DTMs based on remote sensing (e.g. photogrammetry, Walker and Willgoose, 1999; satellite imagery, Endreny *et al.*, 2000; LIDAR, Hilldale and Raff, 2008), the cost of these techniques and the time required for processing were too elevated relative to the large size of the river basin. The DTM used within the context of this research (Fig. 2.26) was derived from digitized contour lines; besides being the source for elevation most widely available (and affordable), contour lines provide additional information on the characteristics of the terrain surface to model (Felicísimo, 1994; van Kreveld, 1997; Wise, 2000; Selvi and Bildirici, 2008) that are hydrologically important (Wise, 2000; Wu *et al.*, 2008).

SPATIAL DATA REQUIRED FOR ANALYSIS

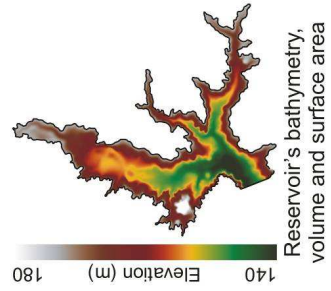
TERRAIN PARAMETERS
Elevation (h)
Slope (s)

Terrain modelling
Topogrid 10 m-resolution

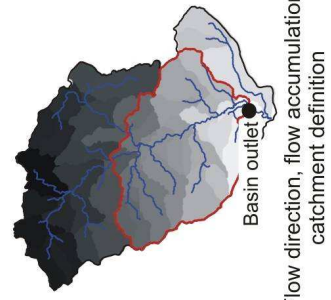


APPLICATIONS

RESERVOIR MODELLING



HYDROLOGICAL MODELLING



TIME SERIES REQUIRED FOR ANALYSIS

CLIMATIC DATA
Rainfall (P)
Air temperature (T)
Potential evapotransp. (PET)

Correction - Filling
Point interpolation
IDW^(P) - Linear Regression^(T)
Calculation^(PET)
Thornthwaite's method

FLOW DATA
River flow upstream (Q_u)
River flow downstream (Q_d)
River water temp. (T_o)

Field gauging^(OD,TO)
Modelling^(OU)
RainOff-empirical model
Calculation^(OD)
Manning's method

RESERVOIR DATA
Reservoir outputs (W_R , R_R , I_R , E_R)
Reservoir's water levels (H_R)

Field gauging^(R)
Correction - Filling
Point interpolation
Calculation^(ER)
Penman method

TIME SERIES ASSEMBLED FOR ANALYSIS

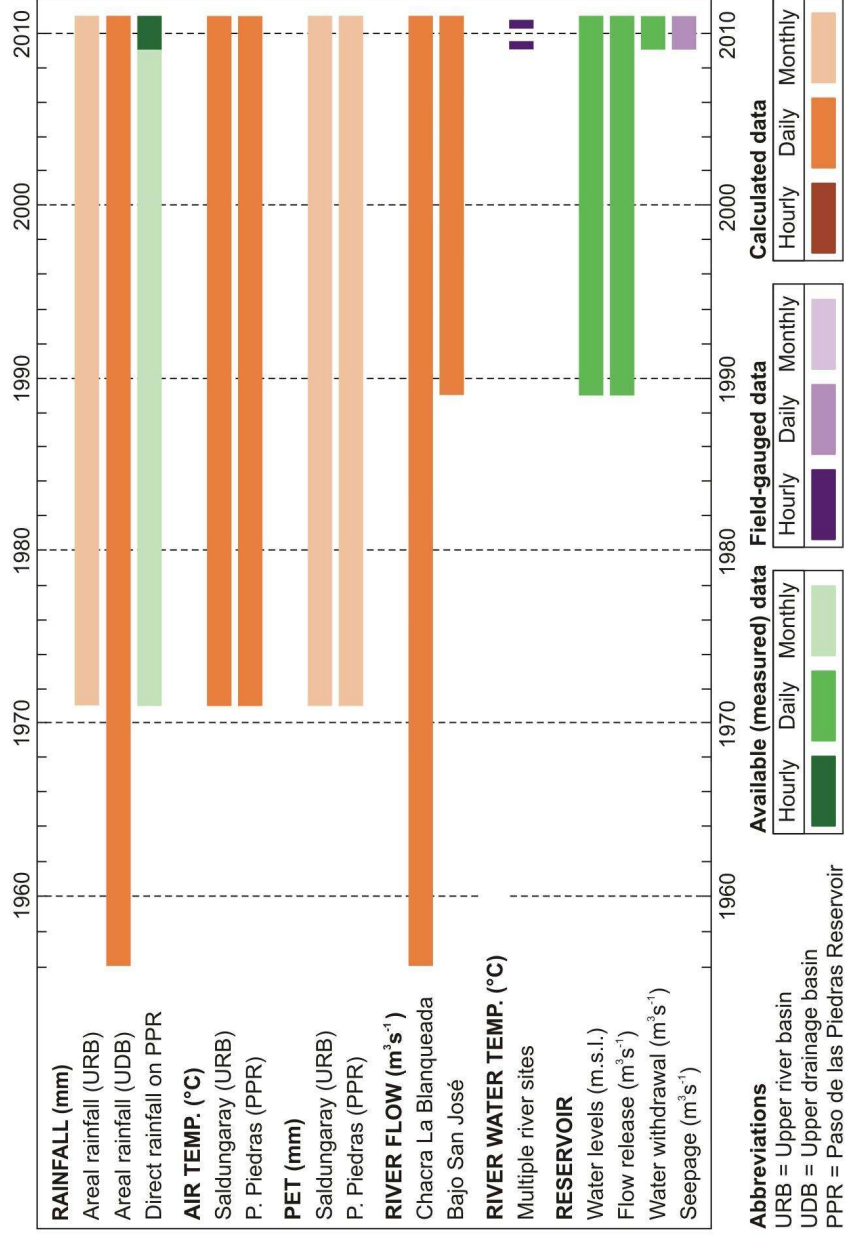


Figure 2.26: Overview of the procedures performed to generate data for hydrological assessment of the Sauce Grande River and series of data achieved.

Despite these benefits, contour lines do not provide information between levels of terrain elevation and, depending on the configuration of the terrain surface, they may give very little information on which to base an accurate interpolation (Wise, 2000). In this regard, contour-derived DTMs are subject to a certain degree of error relative to the quality of the data source and to the algorithm used in interpolation, and to a certain degree of uncertainty relative to the lack of vertical information between contours (Fisher and Tate, 2006). Error and uncertainty have direct implications for terrain-derived products and DTM applications (Hengl *et al.*, 2004), and hence the need of assessing and improving the quality of the contour-derived model.

A number of studies have evaluated different interpolation techniques (e.g. Wood and Fisher, 1993; Carrara *et al.*, 1997; Wise, 2000; Pardo Pascual *et al.*, 2002; Selvi and Bildirici, 2008) and output model resolutions (Gao, 1997; Ziadat, 2007; Sharma *et al.*, 2009) to derive DTMs from contour lines accurately. These studies revealed that whilst the absolute accuracy of the model (i.e. altimetry) depends on the quality of the elevation source, the interpolation technique and the resolution of the output model, the qualitative accuracy of the model (i.e. the degree of similarity between the model and the real topography) depends strongly on the configuration of the terrain surface to model.

We have evaluated the absolute and the relative quality of 12 contour-derived DTMs (four different interpolation techniques for three different output resolutions) considering four different degrees of terrain complexity. Intercomparison between models revealed that there were great variations in the quality of the DTMs derived from the same source of data. The vertical accuracy of the models, measured in terms of ME and RMSE, was closely related to the terrain complexity in all cases; the highest errors were detected in areas steeply inclined regardless of the algorithm used in interpolation and the resolution of the output model. The impact of the interpolating method and the model resolution were stronger regarding the relative quality of the models; TG and OK interpolators provided the best results.

Although none of the models was clearly superior relative to the others, the model generated using the TopoGrid interpolator for 10 m-resolution (TG10) was the model the most reasonable in terms of both vertical accuracy and precision in the relative representation of landforms. Similar results were reported by Wise (2000) and by Sharma *et al.* (2009) from comparison among a wide range of interpolators and software. These results were expected, as the TopoGrid command in ArcGIS was specially designed to work intelligently with contours, point elevation data, streamflow lines and water bodies (Hutchinson, 1988; 1989; Hutchinson and Dowling, 1991).

In spite that the TG10 model qualified as the model of best quality, results revealed that the vertical accuracy of the model decreased considerably as the inclination of the terrain surface increased; the RMSE ranged from 4.5 m in areas steeply inclined to 1.1 m in areas of low relief. Large errors in areas steeply inclined were strongly related to the presence of isolated peaks, which are represented by closed contours. Even if the TopoGrid algorithm is non-linear (i.e. it extrapolates beyond the elevation value of closed contours), errors may occur relative to the lack of data on which to base an accurate extrapolation (Hengl *et al.*, 2004). Differences in elevation in areas of low relief are less significant, and hence errors from interpolation were smaller. Results

regarding the relative accuracy of the model were more than suitable. As the algorithm checks for outliers during interpolation and corrects them (Hutchinson, 1988; 1989; Hutchinson and Dowling, 1991), error ranges were very small (less than 3.4 m). In addition, the interpolation process is non-linear and so artifacts were much reduced (less than 1 %).

Overall, the relative accuracy of the TG10 was comparatively better than its vertical accuracy. From a hydrological point of view, precision in the reproduction of the terrain forms is largely more important than precision in the reproduction of absolute elevation values, as any error in the former may lead to large errors in hydrological estimates derived (Kenward *et al.*, 2000; Fisher and Tate, 2006). In addition, the vertical accuracy of the model may be improved using simple techniques based on auxiliary contour and stream line data (Hengl *et al.*, 2004) derived from DTMs of wide availability (e.g. the SRTM90 of the USGS). Also, most terrain-related programs integrate commands that correct DTMs for sinks automatically (e.g. ArcHydro Tools and HEC GeoHMS for ArcGIS). These procedures contribute to improve the plausibility of the model notably (Felicísimo, 1994; Wise, 2000; Hengl *et al.*, 2004), and hence the hydrological analysis derived.

3.2. CLIMATIC DATA

Invalid and missing data within climatic data sets were abundant. As complete and accurate sources of climatic data are fundamental to model environmental processes efficiently (Jeffrey *et al.*, 2001), climatic data series required of exhaustive efforts of correction and filling before being used in analysis. Random and systematic invalid data were surrogated once detected; estimation of missing data required of more sophisticated techniques, as simple and arbitrary replacement of missing records may lead to unrealistic and discontinuous results (Islam *et al.*, 2000).

3.2.1. Rainfall data

Incomplete sources of rainfall data have restricted many research efforts worldwide, so that a number of studies have evaluate the accuracy of different techniques to estimate rainfall data for a variety of environments and applications (e.g. Bennett *et al.*, 2007; Silva *et al.*, 2007; Modallaldoust, 2010; Mair and Fares, 2011; Chen and Liu, 2012). These studies concluded that the Inverse Distance Weighting (IDW) interpolation technique provided the most suitable results, although demonstrated that the method depended strongly on the density and spatial scarcity of the network of observational stations used in interpolation of missing data for a given location.

The main advantage of using the IDW technique to estimate missing observations of rainfall was its simplicity for computation and its flexibility to calculate missing records over either discrete and long periods or short and intermittent periods. However, there is a high degree of uncertainty in the accuracy of the estimations relative to the strong variability in rainfall regimes across the river basin.

Assessment of rainfall regimes in Nonthue, Sierra de la Ventana, Saldungaray and Paso de las Piedras revealed variations in the magnitude of the hyetographs and similarity in timing. Rainfall modules described a clear decline south-southwestward, although the magnitude of rainfall extremes was higher for the southern sites. The decline in annual rainfall amounts southwestward is characteristic of the south-western Buenos Aires Province (Capelli de Steffens and Campo, 1994; Campo *et al.*, 2004; Kruse and Laurencena, 2005; Scian *et al.*, 2006). However, bias between the northern and the southern sites were significant relative to the short distance that separates them (about 40 km). Such variations were conceivably related to topographic forcing. Rainfall amounts within the headwaters are enhanced by the effect of the Sierra de la Ventana Range, which imposes wetter-than-normal conditions in the higher areas and precipitation maxima over the north-eastern slopes (Gaspari *et al.*, 2008; Gil, 2009). Gil (2009) found that annual rainfall modules between nearby locations (7 to 10 km apart) may increase by 200 mm and 400 mm as the sites are more exposed to the effects of north-easterly winds uplifting the windward slopes. On the lee side, rainfall amounts decrease considerably; for example, the mean annual rainfall module in Paso de las Piedras (situated southwestward from the mountain system) was up to 120 mm smaller than that mean annual module of the upper sites.

These results permitted to assemble the four series of rainfall observations into two data sets accounting for zones of relative rainfall homogeneity: the upper river basin and the area near the Paso de las Piedras Reservoir (Fig. 2.26). This procedure contributed to reduce the number of rain-gauging stations available and hence facilitated further analysis. Nevertheless, the spatial distribution of rain-gauging stations for which data were available over the long term (1971-2010) was scarce relative to the complexity of rainfall regimes within the river basin. Rainfall amounts for a great proportion of the river basin remain unknown, especially within the headwater areas which record the largest rainfall amounts. Hence, there is high degree of uncertainty in the use of these data series as source for hydrological assessment of the upper river basin.

3.2.2. Air temperature data

Air temperature data was lacking for almost the entire period of observation, and hence the need of estimating air temperature data over the long term. During the last decades, researchers have developed and used a variety of procedures to estimate missing temperature data. According to many studies (e.g. Kemp *et al.*, 1983; Islam *et al.*, 2000; Schneider, 2001), regression-based techniques provide the most accurate results.

Long-term series (1971-2010) of daily air temperature for Saldungaray and Paso de las Piedras (Fig. 2.26) were estimated using linear regression analysis. Temperature data used in regressions were available for three sites (Bahía Blanca, Pigüé and Tres Arroyos) situated between 60 and 130 km from the area of interest. Campo *et al.* (2004) demonstrated that the area is subject to notable differences in air temperature due to the coupled effect of the ocean and the continental topography; hence, multiple regression using temperature records for these sites may lead to error resulting from the thermal gradient between stations. Networks of climatic observational stations are usually sparse, and climatic data is not always available for stations nearest than several hundred kilometres; however, sparse networks may be not representative of the

climatology of the area for which data need to be estimated (Jeffrey *et al.*, 2001).

To solve this problem, regressions were run for maximum and minimum daily temperatures separately; mean daily temperatures were calculated averaging estimates to compensate for errors in the estimation of temperature extremes. Error analysis revealed that the regression models fitted suitably to simulate both maximum and minimum daily temperatures and for the two sites of interest. Consistently, errors in estimation of mean daily temperatures were very small, and errors in estimation of mean monthly temperature were negligible.

3.3. HYDROLOGIC DATA

Hydrologic data available for the river basin included: (i) historical records of monthly runoff for La Toma Gauging Station (1910-1947), and (ii) hourly flow rates for Chacra La Blanqueada Gauging Station (2004-2011; with blanks). The limitation of using these time series to assess the river hydrology are clear: the former series, besides lacking of daily observations, do not account for the effects of wetter climate conditions reported for the last decades, and the latter series, besides being incomplete, span a period of time too short to effectuate an accurate hydrologic characterization of the river basin. As a result, the overall hydrology of the river basin remains poorly evaluated.

Assessing the river basin hydrology is not the main objective of this study; however, the understanding of hydrological processes within the river basin was required prior to assessment of the effects of dam impoundment upon the hydrologic continuity of the river system. The greatest limitation for hydrological assessment of the river basin was the overall lack of hydrologic data; hence, we used a set of physically-based empirical models to generate long-term series of river flow data for both the unregulated river and the regulated river (Fig. 2.24).

3.3.1. The hydrology of the river basin

Hydrologic data for the river basin was generated based on simple empirical methods widely available in literature such as the Curve Number method and the Unit Hydrograph method of the NRCS (1986; 2004; 2007a; 2007b; 2010). In addition to their simplicity to calculate hydrologic parameters, the greatest benefit of using these methods is that they require a relatively reduced number of input data and yet they provide accurate results. These aspects explain their wide applicability to hydrological assessment of ungauged basins.

Within the area of interest, these methods were applied by Paoloni *et al.* (1972) and by Luque *et al.* (1979) to assessment of the entire upper Sauce Grande Basin. These studies reported potential soil retention of 75 mm, initial abstractions of 15 mm, mean runoff coefficient of 0.32, and basin time of concentration of 13.8 hours. These values are very close to those estimated for the drainage area contributing to Chacra La Blanqueada (80 mm, 16 mm, 0.35 and 14.5 hours, respectively), which validates the accuracy of our results.

3.3.2. Rainfall-runoff modelling

Empirical modelling of the upper drainage basin provided the set of hydrologic data required for rainfall-runoff modelling. Among the wide range of popular models used to flow simulation from rainfall, few models were adapted to the local conditions. The biggest limitation was the lack of data to use as input for several components of the hydrological balance (e.g. infiltration and groundwater flow rates). On the other hand, most models have been developed to work with rivers within oceanic climates, and hence having flow regimes that differ substantially from the Sauce Grande flow regime which is more characteristic of dry climates (i.e. flashy regime). For example, we have tested the TOPMODEL (TOPography based hydrological MODEL (Beven and Kirkby, 1979; Beven, 2001), which have a friendly interface and requires few input parameters to run such as rainfall data, evapotranspiration data and GIS-derived basin topography. However, simulation results were unsatisfactory; peaks were underestimated and recession curves were longer and gentler than those described by observed flow data. Indeed, it has been demonstrated that the model works poorly in Mediterranean climates (Beven, 2001; Saulnier and Le-Lay, 2009; Vincendon *et al.*, 2010), and so a specific version of TOPMODEL called TOPODYN was developed by the Observatoire Hydrométéorologique Méditerranéen Cévennes-Vivarais (Pellarin *et al.*, 2002; Vincendon *et al.*, 2010). However, TOPODYN has been used principally to simulate single flood events, and its accuracy to simulate flow within the Sauce Grande Basin over the long term is subject of further research.

The model that provided the best fit in terms of flow timing, recession and duration was the RainOff model of the Liquid Gold Team (2002). It provided three major benefits:

- (i) Simplicity in calculations, as the model requires only four input parameters to run (rainfall, runoff, evapotranspiration, and soil retention).
- (ii) Non linearity of processes, as the model accounts for the effects of antecedent moisture conditions by running the water balance of the first reservoir on a continuous day-to-day basis. This is particularly important to consider the effects of dry periods (where the soil has an unfilled retention capacity) and wet periods (where the soil is saturated) on runoff processes.
- (iii) Non stationary of processes, as the runoff reaction function of the second reservoir depends on the depth of recharge from the first.

The greatest disadvantage of the RainOff model was that it worked poorly to simulate the magnitude of high flows, conceivably related to the flashiness of peak flows and floods within the Sauce Grande Basin. However, as the RainOff model is flexible, the magnitude of high flows could be calculated easily by using empirical equations based on the rational method and unit hydrograph analysis. A similar physically-based empirical model was devised by Ibrahim and Cordery (1995) to estimate runoff in an ungauged flashy basin in eastern Australia, which evidences the applicability of the model to simulate flow in dry climates.

The biggest weakness of the RainOff-empirical model was its high sensitivity to variations in rainfall and evapotranspiration data. Although Sensitivity Analysis (*sensu* McCuen, 1973) was not performed, this fact was evidenced clearly during the phase of model calibration. For example, variations of 10 mm for recharge depths greater than 50

mm may lead to variations of up to 4 mm in runoff depths dependent on the runoff coefficient, and overestimation of 0.5 mm in evaporation rates during summer days may contribute to eliminate small flow fluctuations. Similarly, as the model works with rainfall inputs only, flow variations during periods of zero rainfall remain unknown because the model does not account for the effects of groundwater inputs feeding subsidence flows.

Model uncertainties

Despite streamflow simulation results were likely suitable, results are subject to various sources of uncertainty. First, the complexity of hydrologic processes interacting within the upper river basin has been simplified; for example, the initial abstractions used in computations do not necessarily account for the entire heterogeneity of the basin characteristics recognized by Gil (2009). Other sources of uncertainty are probably related to the inconsistency and discontinuity of input rainfall data and to inaccuracies of potential evapotranspiration estimates. Second, the availability of daily observations of rainfall at different sites across the upper river basin was limited. Series of daily rainfall used in flow simulation (i.e. Sierra de la Ventana and Saldungaray) account for precipitation in the mid-lower sectors of the upper basin; rainfall amounts within the highest areas remain unknown. Probably, the river module and the magnitude and frequency of high-flow events were underestimated because contributions from the upper areas and tributaries were not considered. Given the evidence of heavy rainfall events inducing flash-floods from the highest areas (Gaspari *et al.*, 2008; Gil, 2009), simulation results should be read carefully. Third, the accuracy of the model relies on proper estimates of hydrologic parameters for the river basin (e.g. soil retention and time of concentration of the contributing area), and on the uniformity of rainfall in terms of intensity and duration across the entire basin. Finally, it also should be noted that the applicability of the model outside the range of flow conditions that occurred during the calibration and verification periods is highly uncertain (Yeung, 2004).

3.4. CONCLUSIONS

This chapter has presented in detail the procedures performed to generate baseline data for hydrological assessment of the Sauce Grande Basin. Despite that the main purpose of this research is to quantify the hydrogeomorphological effects of river impoundment, hydrological processes within the river basin have been poorly evaluated in the past and hence the need for understanding these processes prior to assess dam-induced disruptions in the river hydrology.

The spatial, hydrologic and climatic data yielded herein (Fig. 2.26) serves as an important platform to further hydrological assessment of both the unregulated and the regulated rivers. In addition, these data are made available of managers of flows to contribute to the overall understanding of the behaviour of local water resources; this understanding is at the basis of future planning and improvement of dam management practices. As well as yielding new information to underpin further research, this chapter has evaluated the application of a number of physical models to hydrological

assessment of the river basin. The methods presented herein are widely transferable to generate hydrological data within other ungauged basins, especially those situated within dry regions of the globe.

CHAPTER

3

THE WATER BALANCE OF THE DAM RESERVOIR

CONTENTS

- 1 Methods
- 2 Results
 - The Water Balance Model of the reservoir
 - Patterns in the reservoir hydrology
 - Reservoir size and performance
 - The degree of impoundment
- 3 Discussion and Conclusions

The Paso de las Piedras Dam and its reservoir were designed to store and yield mean annual inflow volumes of 143 hm³ (4.54 m³.s⁻¹) to water supply purposes (Fig. 3.1). Mean annual inflow volume was calculated based on historic series of flow data (1910-1947) gauged at the Paso de las Piedras Station below the confluence of El Divisorio Creek (Ministerio de Obras y Servicios Públicos –MOSP–; cited by Schefer, 2004). The aqueduct was designed to withdraw up to 87 hm³ of water per year (3 m³.s⁻¹; maximum capacity), the annual volume of evaporation from the surface of the reservoir lake was estimated in 32 hm³ (1.0 m³.s⁻¹) and the remaining volume (24 hm³) was allocated to conservation storage and water release downstream (compensation flow).

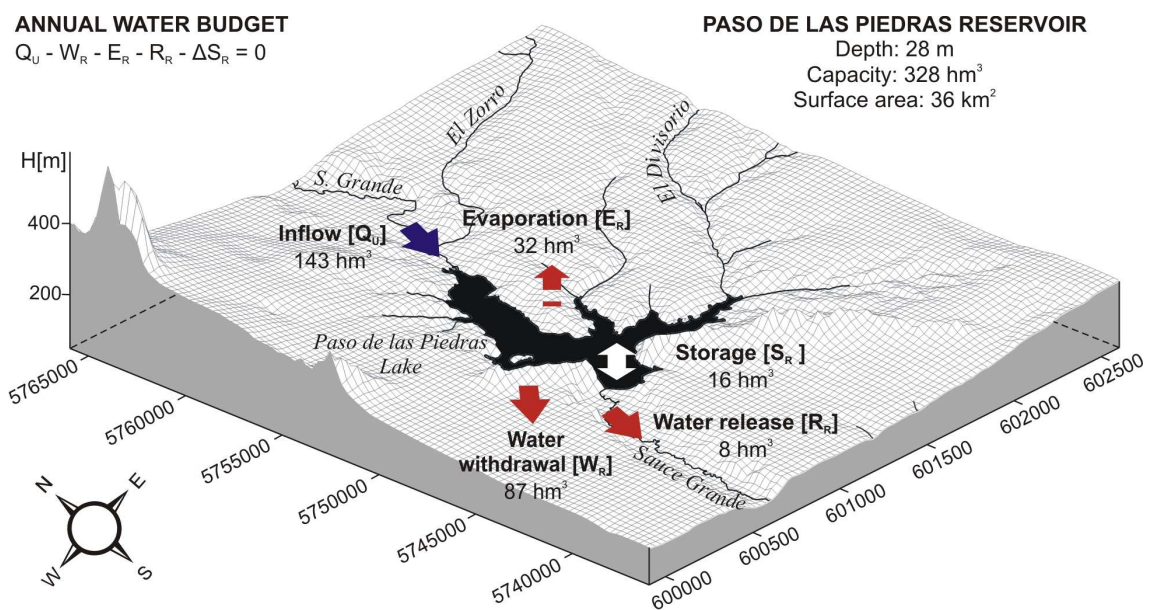


Figure 3.1: Annual water budget of the Paso de las Piedras Reservoir. Input and output volumes were based on Schefer (2004).

Despite the unquestionable hydrological value of the study of the MOSP, there are a number of reasons for which the water balance of the Paso de las Piedras reservoir requires to be re-evaluated. First, the study of the MOSP was conducted prior to dam construction and reservoir operation, and the water balance of the reservoir since dam closure in 1978 has been poorly evaluated. Second, a number of studies reported strong spatial and temporal variability in local rainfall regimes related to the ENSO phenomenon and other large-scale phenomena (e.g. Scian, 2000; Labraga *et al.*, 2002; Scian *et al.*, 2006; Campo *et al.*, 2009; Bohn *et al.*, 2011); as the hydrologic system is rainfed, inter-annual variations in rainfall have direct influence on the annual volume of water available for runoff and storage processes. Third, the actual water demand has exceeded substantially the reservoir yield capacity for water supply and to date, the reservoir volume declines alarmingly due to the recurrence of drought and high rates of water withdrawal.

The first objective of this research is to quantify the degree of flow regulation induced by the Paso de las Piedras Dam on the Sauce Grande River. To meet this purpose, this

chapter examines how the reservoir volume responds to variations in inflow components over time, and quantifies the predictability of flow release relative to such variations. Temporal patterns in the hydrologic components of the water balance equation are inspected, and a Reservoir Water Balance Model is proposed as tool for dam management. The degree to which the dam impounds the Sauce Grande River is evaluated by quantifying the dam potential to interrupt water fluxes from the headwater sources relative to the capacity of its reservoir and human requirements for water supply.

1.1. THE WATER BALANCE MODEL OF THE RESERVOIR

The reservoir water balance equation for a given time interval states that the relationship between inflows, outflows and changes in the water storage equals zero (Sokolov and Chapman, 1974). Accordingly, any change in the water storage equals the difference between inflows and outflows. Assuming that groundwater inflows and outflows are equal, the water balance of the Paso de las Piedras reservoir may be expressed as follows:

$$\Delta S_R = (Q_U + P_R * A_R) - (E_R * A_R + R_R + W_R + I_R) + \eta \quad (3.1)$$

where $[\Delta S_R]$ are changes in water storage; $[Q_U]$ is the surface inflow; $[P_R]$ is the direct precipitation on the surface of the reservoir lake; $[E_R]$ is the evaporation from the surface of the reservoir lake; $[R_R]$ is the water released downstream; $[W_R]$ is the water withdrawal; $[I_R]$ is the storage loss by seepage below the dam embankment; $[A_R]$ is the surface of the reservoir lake; and η is the error term.

Building on this assumption, we developed a Water Balance Model (WBM) for the Paso de las Piedras Reservoir. The main purpose of the model is to verify the viability of the variables used in the water balance equation; if variations in water storage are simulated accurately, then any component of the balance equation may be estimated based on the relationships between the remaining components.

1.1.1. Time series assemblage

The Water Balance Model of the Paso de las Piedras Reservoir was computed on a monthly scale. Outside the fact that daily data were missing for various components of the balance equation, the monthly scale was considered most appropriate for the purpose of this research because it allows to explore relations between water storage, water supply yield and flow release relative to annual and inter-annual variations in inflow components. All components of the water balance equation were expressed in volumetric units (hm^3) and were independently measured or independently calculated.

Concurrent and continuous measured data for all components of the balance equation were available over the period 2009-2010 only (see Figure 2.2, p. 70); beyond this period, at least one component required to be estimated. Note that climatic and flow data were available since dam closure in 1978, whilst reservoir data were available over the period 1989-2010. Hence, the period used for analysis of the reservoir water balance extends over the 22-yr period for which data were available; the reservoir hydrology from dam closure to the year 1988 remains unknown.

Reservoir volume and surface area

Daily series of reservoir water levels over the period 1989-2010 were the only source of

information available on water storage; hence, the relationships of reservoir volume and surface area to water elevation required to be solved prior to assemble the data series for analysis. Information on reservoir volume was required to inspect variations in water storage, whereas information on reservoir surface was required to estimate rainfall and evaporation volumes to and from the reservoir.

Volume- and surface area-elevation relationships were calculated in ArcGIS using the HEC-GeoRAS module. Input data used the map of reservoir bathymetry derived from the TG10 DTM (see section 2.1 in Chapter 2, p. 84). The reservoir volume [V_R] and the corresponding surface area [A_R] were calculated for water levels [H_R] increasing by 0.25 m from 139 m.s.l. (bottom of the reservoir) to 170 m.s.l. (crest of the dam barrage).

The functions $V_R = f(H_R)$ and $A_R = f(H_R)$ were derived from GIS-measured data using non-linear regression analysis. The accuracy of the regression models to simulate reservoir volume and surface area from water level data was inspected using common descriptive metrics of error (mean error, standard deviation and root mean squared error; Eq. 2.1, p. 72) and the coefficient of efficiency of Nash and Sutcliffe (Eq. 2.20, p. 80).

Inflow components

Series of monthly direct rainfall volume (1989-2010) were calculated based on monthly rainfall observations for Paso de las Piedras MS times the surface area of the reservoir at spillway level (30 km²). Input data for surface inflow volume [Q_U] used daily flow rates of the Sauce Grande River [Q_{SG}] over the period 1978-2010 (i.e. since dam closure in 1978). Concurrent flow data for the El Divisorio Creek (tributary) over the period 2004-2007 (with blanks) was used to derive a correction factor ($R^2 = 0.99$) for inflow volumes from the sauce Grande River expressed as follows:

$$Q_U \text{ (} hm^3 \text{)} = 1.0143 (Q_{SG}) + 0.0357 \quad (3.2)$$

This procedure was performed to account for the entire volume of surface inflow from headwater sources and tributaries (i.e., Q_U). Note that inflow volumes from the Sauce Grande River and the corresponding correction factor were computed on a daily scale as daily data were available; monthly volumes of surface inflow were calculated from the sum of daily inflow volumes over the month.

Outflow components

Measure of dam-controlled outflow volumes used daily rates of water release measured by the dam managers (ADA), and daily rates of water withdrawal measured by the water shipping company (ABSA). Long-term series (1989-2010) of monthly volume of water release were calculated based on the sum of corresponding daily volumes over the month; monthly volumes of water withdrawal were calculated similarly although data were available over the period 2009-2010 only.

Monthly volumes of reservoir evaporation used series of maximum potential evapotranspiration for Paso de las Piedras MS (1989-2010) times the surface area of the reservoir over the month considered. Monthly volumes of reservoir seepage were

calculated based on mean seepage rates of $0.034 \text{ m}^3 \cdot \text{s}^{-1}$ (for more information on calculation of seepage rates, see section 2.5.3 in Chapter 2, p. 106). Monthly seepage volumes were assumed as constant over the entire period of observation.

1.1.2. Model running

The WBM of the Paso de las Piedras Reservoir was computed on a continuous monthly basis following a series of steps based on Yeung (2004):

- Step 1 Determine the initial reservoir volume [V_{Rini}] and surface area [A_{Rini}] for the month from the reservoir volume and surface area at the end of the preceding month.
Note: V_{Rini} and A_{Rini} for the first month of the series are calculated based on water level data for the last day of the month.
- Step 2 Determine the monthly volume of direct rainfall on the reservoir [P_R] based on the surface area of the reservoir at spillway level.
- Step 3 Estimate the daily volume of runoff from the headwaters based on gauged flow data for the Sauce Grande River [Q_{SG}]. And determine the daily volume of surface inflow [Q_U] based on a correction factor for Q_{SG} (Eq. 3.2).
Note: monthly Q_U is calculated from the sum of daily Q_U over the month.
- Step 4 Estimate the monthly volume of reservoir evaporation [E_R] based on the initial surface area times the evaporation rate estimated for the month.
- Step 5 Determine the monthly volume of water release [R_R] from the sum of daily R_R over the month.
- Step 6 Estimate the monthly volume of water withdrawal [W_R] from the sum of daily W_R over the month.
- Step 7 Determine the reservoir volume at the end of the month [V_{Rend}] based on the water balance equation (Eq. 3.1) as follows:

$$V_{Rend} = V_{Rini} + (P_R + Q_U) - (E_R + R_R + W_R + I_R) \quad (3.3)$$

Note: water losses by reservoir seepage [I_R] were assumed as constant over the entire period of observation.

1.2.3. Model verification

The ability of the WBM to simulate month-end water storage was verified over the period for which measured data was available for all components of the water balance equation (2009-2010). The phase of model verification involved the measure of error between estimates of reservoir volume and actual reservoir volume at the end of each month. Errors in simulation were inspected using a set of metrics of error including (i) common error statistics such as the mean error, the standard deviation of the mean error and the root mean square error (Eq. 2.1, p. 72), (ii) the relative error (Eq. 2.19, p. 80), (iii) the overestimation rate, and (iv) the coefficient of efficiency of Nash and Sutcliffe (Eq. 2.20, p. 80).

1.2. TIME SERIES ASSESSMENT

Temporal patterns in the hydrologic components of the reservoir water balance were inspected to explore dynamics in the reservoir hydrology over time. Analysis was performed on a monthly scale and used simple descriptive metrics of the central tendency (mean and median) and dispersion from the central tendency (standard deviation, minimum and maximum, kurtosis and skewness) based on Réménieras (1986). The tendency of each variable to change over time was measured by fitting a linear function to the data series.

Furthermore, seasonal patterns in each hydrologic component were detected based on autocorrelation analysis (Kendall and Dickinson-Gibbons, 1990). Equations to obtain autocorrelation functions (ACF) are complex, and are best explained in text books of time series analysis (e.g. Chatfield, 1996). Autocorrelation functions for each variable considered in the water balance equation were calculated automatically using the PASW Statistics program.

Autocorrelation analysis used time lags ranging from 1 to 66. The maximum number of lags was defined by $N/4$ (Box and Jenkins, 1970), where N equals 264 (12 months times 22 years). Correlograms were examined graphically and numerically. Seasonality in the time series was detected based on significant deviations of residuals of the autocorrelation function, i.e. residuals exceeding two standard errors above the zero mean (positive threshold) or two standard errors below the zero mean (negative threshold). Significant deviations repeating every n lags defined the seasonality of the time series.

Partial autocorrelations were evaluated to inspect for results after removing the dependence between consecutive lags. However, partial autocorrelation analysis provided similar results to autocorrelation analysis and so its use for inspection of seasonality was considered unnecessary.

1.3. DETERMINING THE RESERVOIR SIZE AND PERFORMANCE

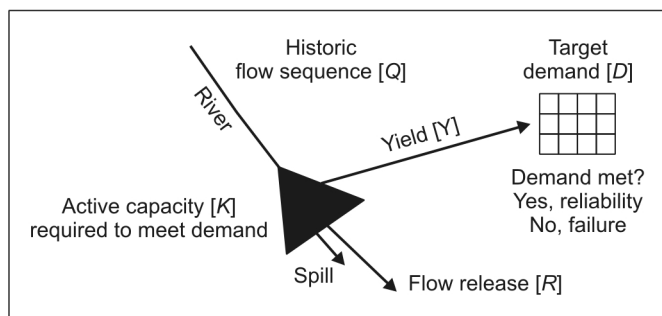
The Water Balance Model provided the basis to perform reservoir size-yield-performance analysis (McMahon and Mein, 1978; McMahon and Adeloje, 2005; McMahon *et al.*, 2006). This approach permitted to estimate (1) the active storage size required to meet a target demand at some level of reliability given historic inflow volumes, (2) the reservoir firm yield given the maximum reservoir capacity required to meet demand, and (3) the dam potential to release water downstream given the reservoir yield and capacity (Fig. 3.2). Analysis was performed on an annual scale so that results were not affected by the effects of seasonality in the different components of the reservoir hydrology.

The terms, and hence the notation used to refer to the variables involved in reservoir size-yield-performance analysis may vary considerably across English speaking countries. The terms used within the context of this research were defined as follows:

- the term *yield* refers to controlled water release from the reservoir to meet human

water requirements, where the *firm yield* is the yield that can be provided 100 % of times over the life operation history of the reservoir;

- the term *release* refers to controlled reservoir evacuation downstream feeding the hydrological requirements of the river below the impoundment;
- when such evacuation occurs through the dam spillway (uncontrolled), it is referred to as *spills*;
- the term *demand* refers to the amount of water required by the demand centre; and
- the term *reliability* refers to the potential of the reservoir to meet such demand (performance).

**Question 1**

Given Q , which is the maximum K required to meet D ?

Question 2

Given Q and K , which is the firm yield of the reservoir?

Question 3

Given K and Y , which is the Q magnitude required to produce R ?

Figure 3.2: Conceptual scheme of the reservoir capacity-yield-performance approach. Based on (McMahon and Mein, 1978; McMahon and Adeloye, 2005).

1.3.1. Question 1: measuring storage-yield relationships

The storage-yield relationships for the Paso de las Piedras Reservoir were explored using sequent peak analysis (Thomas and Burden, 1963). The Sequent Peak Algorithm technique (SPA) is based on the mass curve procedure (Rippl, 1883), and assumes that the storage required to meet a given demand $[D]$ equals the maximum difference between the reservoir yield $[Y]$ and inflow $[Q]$ during a critical period. The critical period is defined as the longest period ranging from full conditions through emptiness (critical drawdown period) and to full conditions again (recovery period).

The active storage capacity requirement for a given year was calculated based on the balance equation as follows:

$$K_t = (Y - Q_t) + K_{t-1} \quad \text{if } K_{t-1} > 0, \quad K_{t-1} = 0 \text{ otherwise} \quad (3.4)$$

where $[K_t]$ is the storage at end of the current month; $[K_{t-1}]$ is the storage at end of the previous month; $[Y]$ is the reservoir yield; and $[Q_t]$ is the total inflow for the month. The reservoir has a given storage capacity $[S]$, so that K_t should be less than S for each time interval. The maximum (or minimum) of all K_t is the maximum (or minimum) storage capacity required to meet the specified yield given the historic inflow record.

1.3.2. Question 2: measuring the reservoir performance

Sequent peak analysis provided the basis to explore the reservoir performance, i.e the

range of conditions that may be expected to occur during the operating life of the reservoir (McMahon *et al.*, 2006). Performance analysis determined whether the annual inflow was sufficient to meet the demand rate without leaving the reservoir below its minimum capacity.

Among the wide range of metrics of reservoir performance available in literature, we selected three comparative metrics based on (Vogel *et al.*, 1999; McMahon *et al.*, 2006): reliability (inverse frequency of reservoir failures), resilience (ability of the reservoir to recover from a failure) and vulnerability (magnitude of potential failures).

Reliability [*Rel*] measures the probability that the reservoir meets the target demand in any given time interval [*i*] over a sample period [*n*] as follows:

$$Rel = \frac{Rel_t}{n} * 100; \quad 0 < Rel < 100 \quad (3.5)$$

Resilience [*Res*] measures how quickly the reservoir recovers from a failure as the ratio of the total duration of all failures [*fd*] to the number of failure sequences [*fs*] as follows:

$$Res = fd / fs; \quad fd \neq 0 \quad (3.6)$$

Vulnerability [*Vul*] measures the average volumetric severity of failure [*fv*] during *j*th failure sequences as follows:

$$Vul = \frac{\sum_{j=1}^{fs} \max(fv)}{fs} \quad (3.7)$$

1.3.3. Predicting scenarios of inflow volume and reservoir response

The dam potential to release water downstream depends on the relationship between inflow volumes, reservoir storage capacity and reservoir yield. Whilst storage capacity and annual yield are constant, inflow volumes may vary considerably from one year to another. Hence, the dam potential to water release will depend primarily on (i) the magnitude of inflow volumes for a given year, and (ii) the reservoir operation policies.

Different inflow scenarios were predicted based on series of annual inflow volume over the long-term (1956-2010). The magnitude of annual inflow volume for return periods from 2 to 1000 years was estimated using frequency analysis based on normal probability distribution. The ability of the dam to release water according to varying inflow conditions was measured considering two scenarios of reservoir operation based on Vogel *et al.* (2007):

Fraction of Inflow (FOI). The fraction of annual inflow that is not used to meet the annual demand is released downstream so that $R = Q - Y$.

Drought management (DM). Flow release occurs only if annual storage is above the buffer zone defined by the maximum storage capacity required to meet annual demand at 100 % reliability level. Hence, $R = Q - Y$, if $S > K_{max}$.

Estimation of the reservoir response to varying inflow conditions was based on three

initial water levels assumed as critical: (i) 150 m.s.l. (red warning for active storage), (ii) 155 m.s.l. (yellow warning for active storage), and (iii) 164 m.s.l. (flood control storage). For more information on the warning system for water storage within the Paso de las Piedras Reservoir, see Section 2.3.2 in Chapter 1 (pp. 49).

1.4. QUANTIFICATION OF THE DEGREE OF IMPOUNDMENT

We used the index m of Hazen (Vogel *et al.*, 1999) to explore the operational behaviour of the reservoir for water supply. The m index is the standardized net inflow to the reservoir system and is expressed as:

$$m = \frac{(1 - \alpha) * \mu}{\sigma} = \frac{(1 - \alpha)}{CV} = \frac{(\mu - Y)}{\sigma} \quad (3.8)$$

where $[\alpha]$ is the annual yield as a fraction of the mean annual inflow to the reservoir $[\alpha = Y/\mu]$; $[\mu]$ and $[\sigma]$ are the mean and standard deviation of annual inflows, respectively; and $[CV]$ is the coefficient of variation of annual inflows $[CV = \sigma/\mu]$. High values of m correspond to over-year operating reservoirs, i.e. systems that accumulate storage over humid periods to assure supply during dry periods. Low m values designate reservoir systems operating on within-year (seasonal) storage requirements (Vogel *et al.*, 1999).

The impact of the reservoir operation on the hydrologic conditions downstream will depend primarily upon the ratio of storage capacity to mean annual inflow $[S:\mu]$ (Batalla *et al.*, 2004; Kondolf and Batalla, 2005; Graf, 2006). However, in reservoirs operating for water supply within semiarid regions, the magnitude and the frequency of flow release downstream will be highly constrained by the ratio of reservoir yield to mean annual inflow $[Y:\mu]$ (Vogel *et al.*, 1999; Vogel *et al.*, 2007). All the water that is not yielded to meet human needs may be considered to be released downstream (Vogel *et al.*, 2007). Hence, $\mu = Y + R$, which implies that the yield ratio and downstream flow ratio sum to one so that $Y/\mu + R/\mu = 1$.

The degree of impoundment exerted by the Paso de las Piedras Reservoir was quantified based upon these relationships. The ratio of storage capacity to mean annual inflow was referred to as Impounded Runoff Index $[QI]$ (Batalla *et al.*, 2004; Kondolf and Batalla, 2005), the ratio of reservoir yield to mean annual inflow was referred to as Yield Index $[YI]$, and the ratio of reservoir release to mean annual inflow was referred to as Release Index $[RI]$. Input data to compute QI , YI and RI used the reservoir firm yield and series of annual inflow volume from headwater sources and tributaries since dam closure (1978-2010). To avoid overestimations of the hydrologic effects of the dam, QI used the active storage capacity (i.e. the volume of water that can actually be released from the reservoir) instead than the total reservoir capacity. Note, the storage capacity of the reservoir $[S]$ is different from the storage capacity to meet yield requirements $[K]$.

2.1. THE WATER BALANCE MODEL OF THE PASO DE LAS PIEDRAS RESERVOIR

The Water Balance Model (WBM) for the Paso de las Piedras Reservoir assumed that any change in water storage should equal the difference between a set of inflow and outflow components (Fig. 3.3). Inflow components considered in the balance equation include surface inflow from headwater sources and tributaries and direct rainfall on the surface of the lake; outflow components include flow release, reservoir seepage and evaporation, and water withdrawal. The overall lack of hydrologic data for the river basin and the limited understanding of subsurface and underground processes of water exchange prevent to consider the influence of groundwater inflows and outflows in the water balance equation.

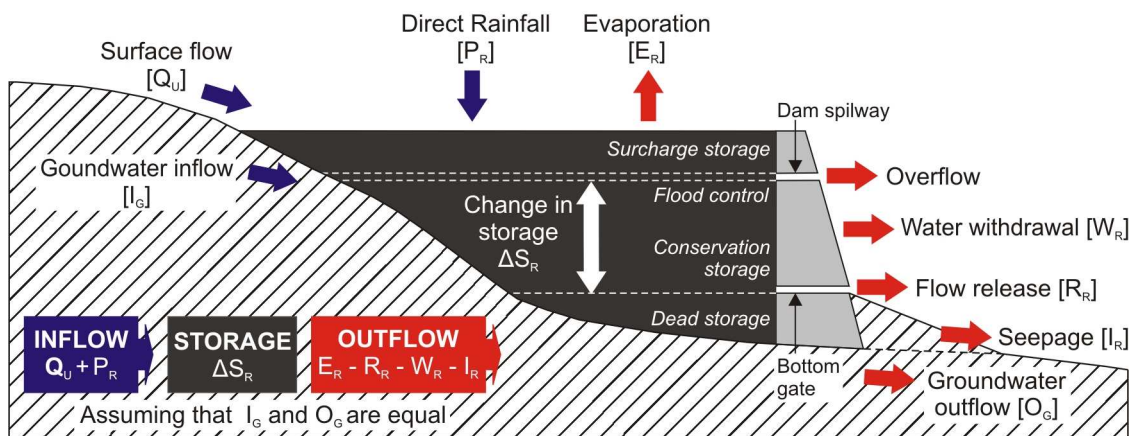


Figure 3.3: Components of the water balance of the Paso de las Piedras Reservoir.

The Sauce Grande River is the main inflow component; inflow from the El Divisorio Creek and direct rainfall upon the surface of the lake are also important hydrologic inputs, although their contribution to variations in the water storage was assumed of minor importance. Outflows from the reservoir were classified into outflows controlled by the dam managers to assure requirements of water supply (i.e. water withdrawal) and water release downstream, and outflows that occur without human intervention such as evaporation and seepage from the reservoir. From all outflow components, water withdrawal and reservoir evaporation were assumed to account for the greatest volume of storage loss per year.

2.1.1. Reservoir volume-surface area-elevation relationships

The first step prior to compute the WBM involved calculating the reservoir volume and surface area corresponding to water level elevations (Fig. 3.4). Note that the absolute height of the bottom of the reservoir lake is ~140 m.s.l., and the absolute height of the

top of the dam embankment is 170 m.s.l. (MOSP). According to Schefer (2004), the height of the dam outlet is 147.9 m.s.l. and the height of the dam spillway is 165 m.s.l.

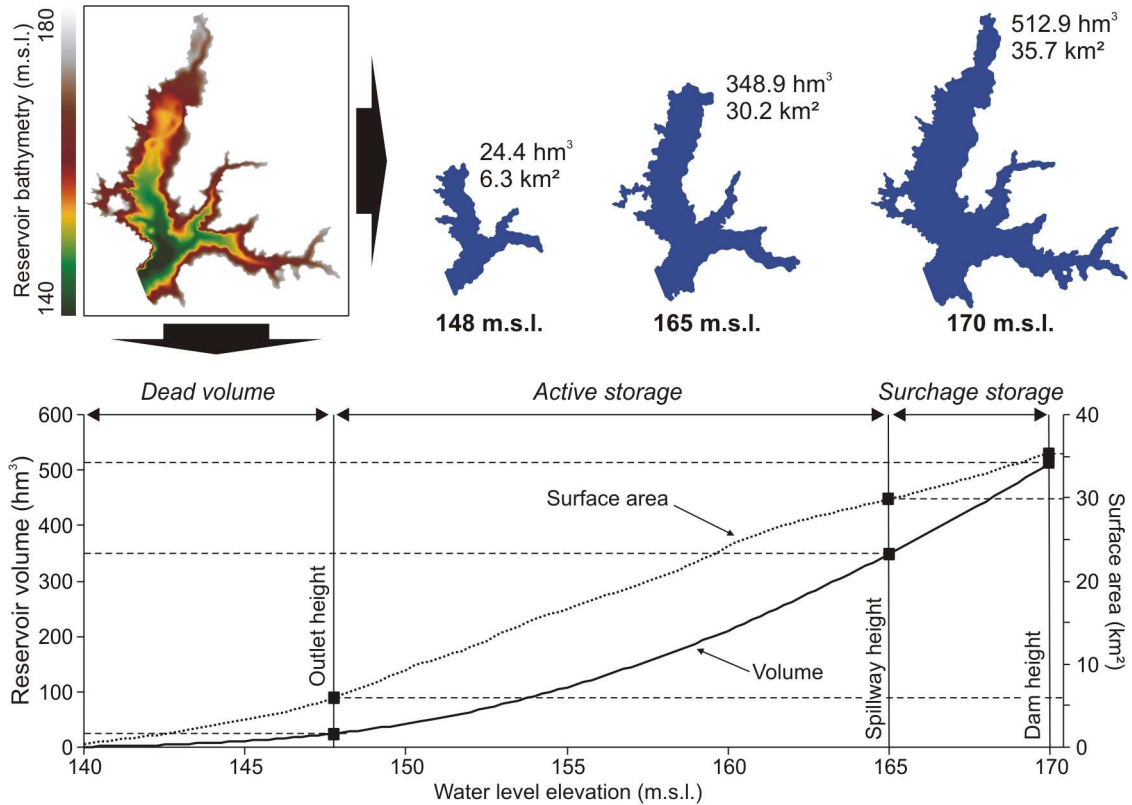


Figure 3.4: Reservoir volume as function of water level and maps of reservoir coverage for three water level heights. The figure presents the regression functions $V_R = f(H_R)$ and $A_R = f(H_R)$ used to calculate each variable.

Regression functions derived from the relationship of reservoir volume [V_R] and surface area [A_R] to water level elevation [H_R] (Eq. 3.9 and 3.10, respectively) gave a perfect fit in both cases ($R^2=1$). Error residuals between measured and estimated reservoir volume and surface area averaged 0.4 hm^3 (± 1.5) and 0.1 km^2 (± 0.9). Coefficients of efficiency were 0.84 (reservoir volume) and 0.81 (surface area), respectively, which indicates that regression functions explain variations in the data series suitably.

$$V_R \text{ (hm}^3\text{)} = 13441 - 188.9 H_R + 0.664 H_R^2 \quad (3.9)$$

$$A_R \text{ (km}^2\text{)} = 13.424 - 0.879 H_R + 0.007 H_R^2 \quad (3.10)$$

The dead volume of the reservoir (i.e. the volume of water stored below the dam outlet) was calculated in 24.4 hm^3 for 9 m-depth, and the surplus storage capacity (i.e. the volume of water that may be retained between the crest of the dam spillway and the crest of the dam barrage) was calculated in 164.0 hm^3 for 5 m-depth. The remaining volume constitutes the active reservoir storage capacity and was calculated in 324.5 hm^3 for 17 m-depth (Fig. 3.4). The storage capacity and surface area of the reservoir for 31 m depth were 512.9 hm^3 and 35.7 km^2 , respectively; the reservoir surface area at spillway level (165 m.s.l.) was 30.2 km^2 . Note, these values assume absence of reservoir

sedimentation.

The relationship of reservoir volume and surface area to reservoir water level elevation was non-linear, so that rates of variation in the former two variables for increasing (or decreasing) water levels were very different depending on the initial elevation of the water surface. For example, a raise of 1 m in the reservoir water level starting in 150 m.s.l. (red alert for active storage) represents an increase of 10.4 hm³ in water storage, whereas the volume gained for 1 m-increase in water level elevation starting in 164 m.s.l. (flood control height) is 29.7 hm³. Knowing these relationships is very important from a dam management perspective.

2.1.2. Model running and verification

Building on volume-surface area-elevation relationships, the Water Balance Model was run on a continuous monthly basis over a 2-yr period (2009-2010). This period was dictated by the availability of concurrent gauged data for all components of the water balance equation. In spite of its short duration, the period encompasses decreasing trends in water storage alternated by episodes of rapid water storage increase; the ability of the water balance model to simulate steep declines (or raises) in water storage accurately is decisive to its utility as management tool. It should be noted that the accuracy of the WBM beyond this period remains uncertain, as measured data over the long term are either discontinuous or lacking for one or more components of the balance equation (See Figure 2.2, p. 70).

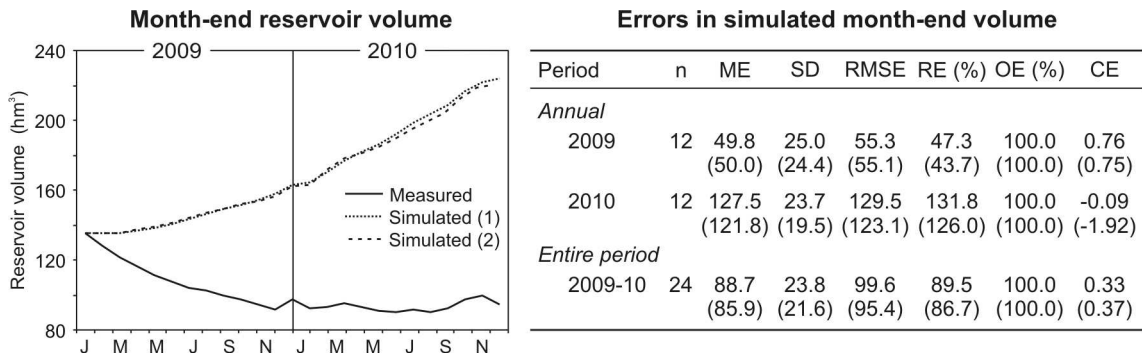
Simulation of monthly water storage used two different data sets: (1) gauged data for all components of the balance equation (Simulated scenario 1), and (2) gauged data for all components of the balance equation except for surface inflow data that was calculated based on streamflow data simulated by RainOff-empirical modelling (Simulated scenario 2). For more information on the procedures performed to simulate flow data, see section 2.4 in Chapter 2 (p. 101).

Scenario 1 tests the ability of the model to simulate variations in water storage over time and verifies the viability of the variables used in the water balance equation. Accuracy in both parameters is essential to further assessment of the reservoir hydrology; if variations in water storage are simulated accurately, then the model allows estimating any component of the water balance equation based on the interactions between the remaining components. Scenario 2 tests the accuracy of flow data simulation for the upper sauce Grande River; this procedure was of extreme importance because simulated series of flow data are the only source of hydrologic information available over the long term.

Results of the WBM over the verification period (Fig. 3.5) revealed that the model works very poorly to simulate monthly variations in water storage for both scenarios. Errors from simulation were very high and increased steeply with time, and so the coefficients of model efficiency were low and lowered steeply with time. Errors for the entire verification period were of about 90 % and the model efficiency was 0.33 for Scenario 1 and 0.37 for Scenario 2. Interestingly, Scenario 1 and Scenario 2 provided similar results. This suggested that patterns in simulated series of flow were very similar to those described by gauged flow data, which indicated suitable reliability of results

from rainfall-runoff modelling.

Visual inspection of results (Fig. 3.5) showed that simulated month-end storage increased with time clearly, whereas actual month-end storage described an opposite tendency to decrease. This suggested that at least one component of the balance equation was underestimated (if outflow) or overestimated (if inflow). The viability of the variables used in the balance equation and the accuracy of the time series used in calculations were revisited.



References:

n = number of months considered; ME = Mean Error; RMSE = Root Mean Square Error; RE = relative error; OE = Overestimation rate; CE = Efficiency Coefficient. (1) Simulated from measured data; (2) Simulated from calculated flow data.

Figure 3.5: Measured and simulated month-end reservoir volume over the period 2009-2010 (verification period). Errors in simulated month-end volume are shown in the table to the right; errors in simulation using series of simulated flow data are presented in parentheses.

Viability of the variables used in the water balance equation

All variables used in the water balance equation were assumed to contribute to variations in water storage in a greater or lesser extent. Assuming that the inflow components were not overestimated, model results suggested underestimation of at least one outflow component, i.e. at least one variable of storage loss was not considered in the balance equation.

The model assumed that the volume of water losses by infiltration below the reservoir lake was equal to the volume of water gained by groundwater inflow. Previous studies gave evidence of substantial infiltration rates due to the high permeability of underlying materials (gravel, sand and silt); however, these studies reported that restoration actions were achieved in 1996 involving the installation of an impervious panel to prevent water losses and to preserve the stability of the dam structure (Buraschi *et al.*, 1999; Schefer, 2004). Hence, the magnitude of actual infiltration volumes is expected to be small relative to the magnitude of other volumes of reservoir outflow.

Other component of water loss observed (although not measured) was the water flowing out through the bottom gate, even in periods of zero water release. Assuming that mean flow rates observed downstream ($0.28 \text{ m}^3 \text{ s}^{-1}$) originate exclusively from reservoir seepage and leakage, then water losses through seepage and leakage should equal 0.72 hm^3 per month. The initial volume of seepage used in calculations was replaced by this value and the model was run again. Results did not reveal improvements relative to the

original model, indicating that no actions were required regarding the viability of the variables considered for the outflow components.

Reliability of estimated data series

Among all components of the water balance equation, three components required to be estimated: the reservoir volume (and surface area), the evaporation volume and the surface inflow volume. The remaining components used gauged data as input and were, comparatively, well known. Although estimations were based on gauged data, the phase of detection of error in computations involved revisiting the accuracy in the estimation of these three components.

Reservoir volume and surface area. Regression functions to derive reservoir volume and surface from water level elevation gave a perfect fit, and coefficients of efficiency indicated that the regression models simulated variations in reservoir volume and surface area accurately. Hence, no actions were required regarding this variable.

Volume of reservoir evaporation. The original model used monthly data of maximum PET for Paso de las Piedras MS. To inspect the reliability of PET series, we used the Penman method to calculate rates of evaporation on a daily basis over the period 2009-2010. Other methods commonly used to calculate evaporation such as the aerodynamic method were tested to verify the accuracy of the original estimations. The model was run in a trial-and-error mode in which different evaporation rates were entered as input. Results revealed no improvements respect to the original model and hence indicated that no actions were required regarding this variable.

Surface inflow. The model was run using monthly inflows from the Sauce Grande River only (i.e. without using the correction factor) to inspect for overestimations in the original inflow volumes. Results showed the same increasing trend in simulated reservoir volumes, indicating that no actions were required regarding this variable.

Reliability of series of gauged data

If the variables considered in the balance equation are relevant and if the series of estimated data are accurate, then the source of error have to be related to the reliability of gauged data series. Among all series of gauged data, flow data for the upper Sauce Grande River emerges as the most spurious data series.

Inspection of historic flow records showed that flow rates never declined below $2.90 \text{ m}^3 \cdot \text{s}^{-1}$, not even in years of extreme drought such as the year 2009. Yet, studies based on field-gauged flow data reported that streamflow rates could reach about $0.7 \text{ m}^3 \cdot \text{s}^{-1}$ during summer days (Gil, 2009). Such inconsistency suggests a potential difference in the magnitude of base flows of 0.2 hm^3 per day (or 7.5 hm^3 per month), which may modify substantially the results from water balance modelling. The following section describes the procedures performed to correct gauged series of flow data.

2.1.3. Flow data recalibration

Series of flow data for the upper Sauce Grande River were obtained into two separated

spreadsheets; one contains hourly readings of stream stage, the other contains all the parameters necessary to solve compute flow discharge based on the Manning's equation. The fact that stream stage data were available facilitated the process for correcting flow data.

We assumed that the source of error was in the hydraulic parameters (i.e. channel slope, roughness and cross section) and derivative functions provided in the spreadsheets more than in the stream stage readings. Hence, these parameters were re-calculated based on empirical relationships and GIS analysis for a hypothetical river cross-section building on previous field observations. Although these measures should be performed on the field and for the channel cross section where the stream stage readings are collected, these actions were not viable given the substantial distance between us (France) and the study area (Argentina) when the problem arose.

The relationship $A \cdot R^{2/3}$ was solved for stream stages increasing by 0.1 m from 0 to 7 m; the coefficients of channel roughness were estimated as 0.070 up to 1 m, as 0.055 from 1 to 2 m, as 0.045 from 2 to 3 m, and as 0.040 from 3 to 7 m. Variations in the channel roughness with channel depth build on field recognisance of vegetation cover within the channel and bank materials. The channel slope was estimated in 0.0015.

Hourly streamflow rates were re-calculated using the parameters described above. Comparison between original and re-calculated flow data revealed significant differences of magnitude, especially during periods of low flow (Fig. 3.6). Inspection of annual flow volumes showed that calculated flow series were reduced by 74 hm³ (2009) and 77 hm³ (2010) relative to the original flow data. Such a difference clearly explains the errors in the original Water Balance Model. At this point, it should be noted that simulation of streamflow data was based on erroneous gauged data, so that the RainOff-empirical model required be re-parameterized and run again.

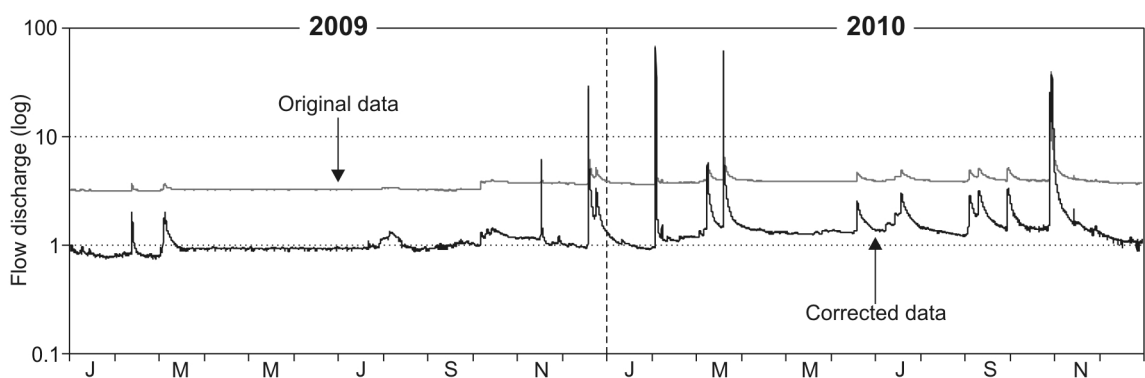


Figure 3.6: Original and corrected series of hourly flow data (gauged) for the upper Sauce Grande River over the years 2009 and 2010.

2.1.4. Water Balance Model re-running

Series of corrected flow data were used to re-calculate monthly volumes of surface inflow as originally (see Section 1.1.2, p. 123) and the Water Balance Model was run again (Fig. 3.7). Visually and statistically, simulation of month-end volume was suitable for both scenarios. Trends in simulated month-end volume were similar to those of

measured data, so that errors from simulation were very small (less than 4 %). Furthermore, the coefficient of efficiency revealed perfect model fit for both scenarios. This indicated that the new series of streamflow data were re-calculated and re-simulated accurately.

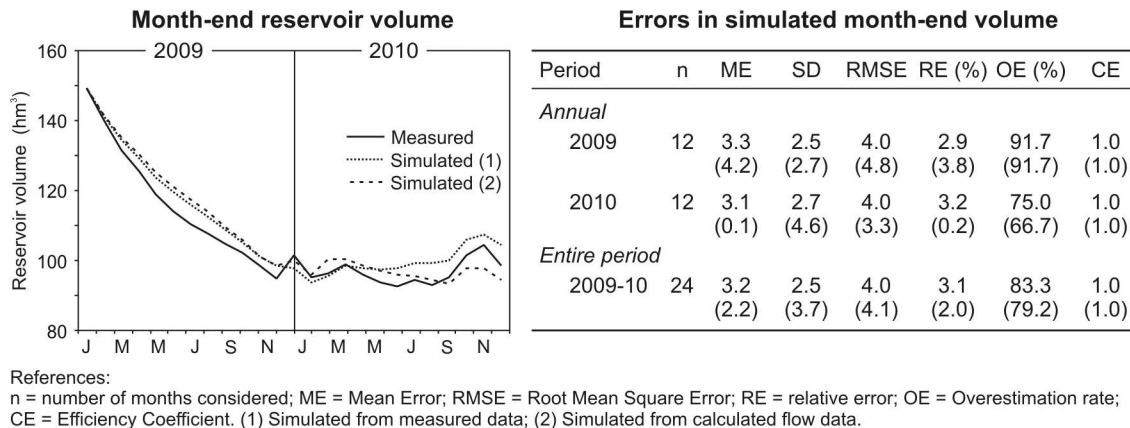


Figure 3.7: Measured and simulated month-end reservoir volume over the period 2009-2010 (verification period) based on corrected series of gauged and simulated streamflow data. Errors in simulated month-end volume are shown in the table to the right; errors in simulation using series of simulated flow data are presented in parentheses.

2.2. PATTERNS IN THE RESERVOIR HYDROLOGY

Building on previous results, storage variations in the Paso de las Piedras reservoir depend on the interactions between rainfall and surface inflow entering the reservoir and storage losses by evaporation, seepage, water withdrawal and flow release downstream. Time series for each of these hydrologic components were inspected to explore dynamics in the reservoir hydrology over time. Note, time series assessment was effectuated over the period for which data were all available for all components of the balance equation (1989-2010) to facilitate further comparisons.

2.2.1. Patterns in inflow components

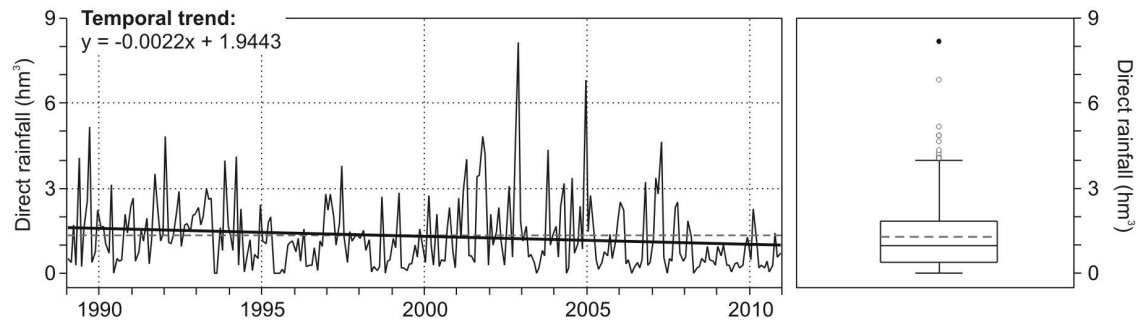
Monthly volumes of direct rainfall averaged 1.7 hm³ with maximum in 8.2 hm³ (Fig. 3.8). Time series described high deviations from the historic mean; rainfall volumes were twice the mean for 12.5 % of months, and were three times the mean for 3.8 % of months. However, the distribution was skewed to the right (skewness = 1.8); 61.4 % of months remained below the mean and 4.5 % of months recorded zero rainfall.

Series of surface inflow from headwater sources and tributaries described high deviations from the historic mean as well, although the magnitude of such deviations was notably higher than that for series of direct rainfall. Surface inflow averaged 7.2 hm³ with minimum in 3.3 hm³ and maximum in 83.4 hm³; this was more than 10 times the historic mean. In spite of the high magnitude of the deviations, the distribution was notably right-tailed (skewness = 6.8); surface inflow for 72.3 % of months remained

below the historic mean.

Inspection of linear trends in the data series revealed that inflow volumes declined with time. The slope value of the linear function was negative for both series, although the decreasing trend was sensibly higher for the series of surface inflow (-0.01 hm^3 per month) than for the series of direct rainfall (-0.002 hm^3 per month).

Direct rainfall upon the surface of the reservoir lake



Surface inflow from headwater sources and tributaries

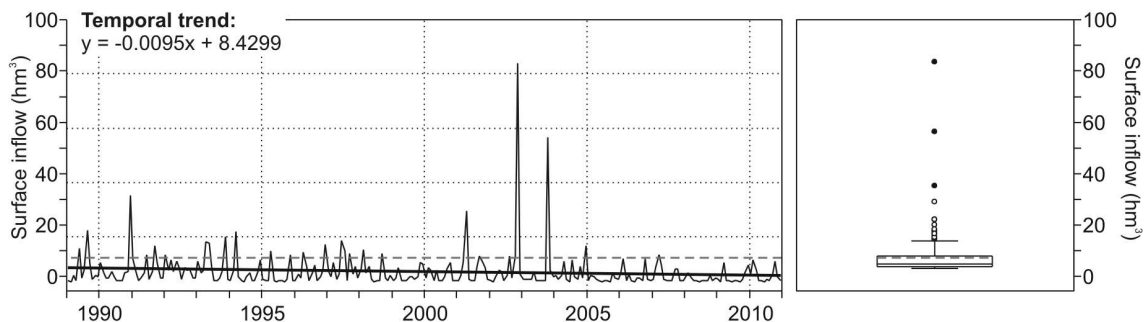


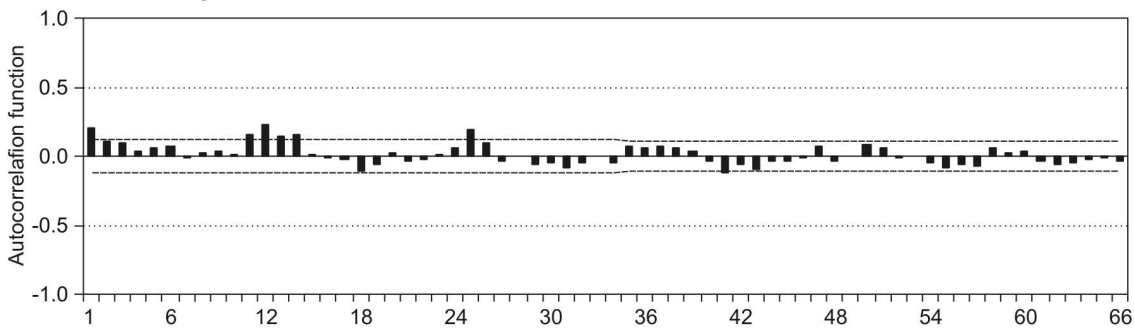
Figure 3.8: Temporal trends and descriptive statistics of monthly series of inflow volume by inflow component over the period 1989-2010.

Patterns of seasonality

Autocorrelations for series of direct rainfall (Fig. 3.9) showed significant positive deviations from zero at lags 1, 11-14 and 25, and significant negative deviations from zero at lags 18 and 41. Deviations were close to the positive threshold at lags 35-38 and close to the negative threshold at lags 43 and 55. This indicates a tendency to 6-month seasonality with rainfall maxima (rain season) from November to February (late spring-early summer) and rainfall minima (dry season) from May to August (late autumn-winter). However, significant deviations from zero did not occur cyclically over the years, suggesting notable inter-annual variations in the magnitude of rainfall amounts for both the rainy and the dry seasons.

Patterns of seasonality in series of surface inflow were less clear (Fig. 3.9). Autocorrelations showed significant positive deviations from zero at lags 11 and 25, and deviations were close to the positive threshold at lags 14, 19 and 30. This suggests that there is two annual maxima that tend to occur preferably in summer (February) and in late spring (November), although large volumes of surface inflow may occur randomly during winter months (June and July). Seasonality in monthly minima was unclear.

Direct rainfall upon the surface of the reservoir lake



Surface inflow from headwater sources and tributaries

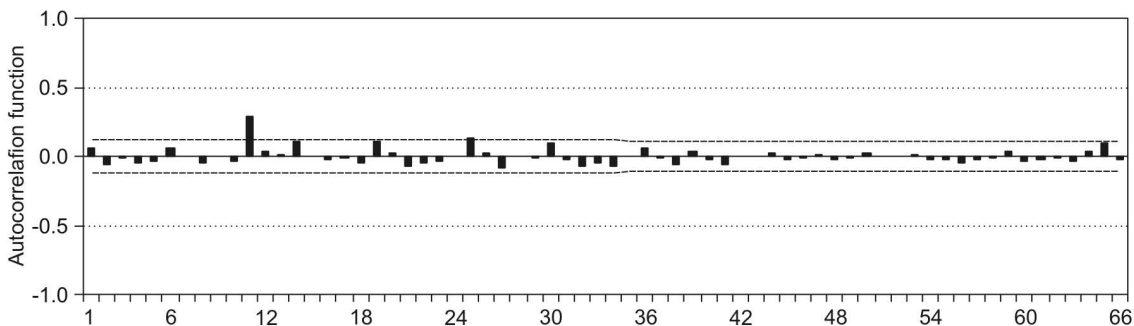


Figure 3.9: Correlograms of monthly series of inflow volume by inflow component showing autocorrelation functions at 66 lags. Thresholds for significant autocorrelations were defined by two standard errors above and below the zero mean.

2.2.2. Patterns in outflow components

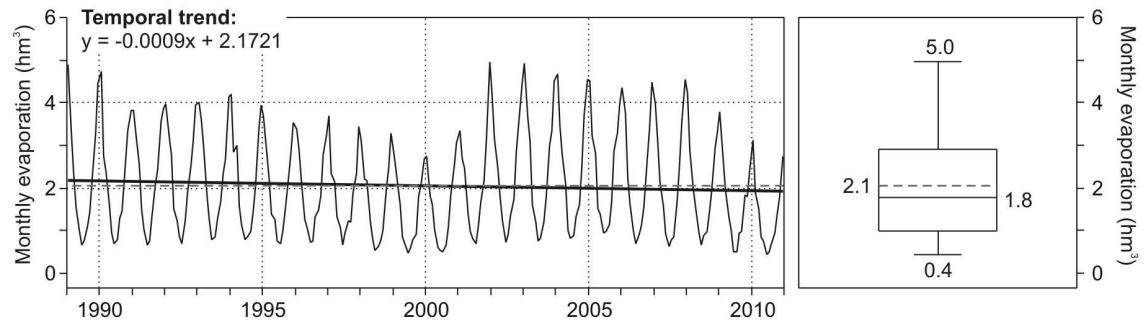
Inspection of time series of reservoir evaporation revealed yearly cyclic variations with maximum in January (up to 5.0 hm^3) and minimum in June (0.4 hm^3); mean monthly evaporation was 2.1 hm^3 (Fig. 3.10). Dispersions from the historic median (1.8 hm^3) remained within the inter-quartile limits indicating absence of evaporation extremes; however, the historic mean was 0.3 hm^3 greater than the historic median indicating greater occurrence of high evaporation rates. Note, inter-annual variations in the magnitude of annual evaporation maxima responded to variations in the surface of the reservoir lake (i.e. the greater the surface of the lake, the greater the volume of evaporation) more than to variations in the effective rates of evapotranspiration.

Time series of water release were highly scattered in magnitude and in time, with no clear periodicity (Fig. 3.10). The historic mean (3.3 hm^3) was exceeded by three times for 12.9 % of months, and the maximum volume observed (November of 2002) was more than 23 times the mean (78.6 hm^3). Despite random episodes of water release where large volumes of water were evacuated downstream, monthly volumes of water release were equal to zero for 72 % of months.

The temporal extent of the time series of the remaining two outflow components was too reduced to effectuate an accurate characterization. Mean monthly volumes of water withdrawal over the period 2009-2010 averaged 5.6 hm^3 with maximum in January (6.9 hm^3) and minimum in June and July (5.0 hm^3 ; Table 3.1); extreme values were not observed. Note, these values were averaged based on two years of data so that they

should be read carefully. Rates of reservoir seepage were measured *in situ* over the years 2009 and 2010 and averaged $0.034 \text{ m}^3 \cdot \text{s}^{-1}$, this is 0.09 hm^3 per month (for a 30-day month) and 1.1 hm^3 per year. Variations between measures were negligible ($\text{SD} = 0.0001 \text{ m}^3 \cdot \text{s}^{-1}$).

Evaporation from the surface of the reservoir lake



Water release from the dam reservoir

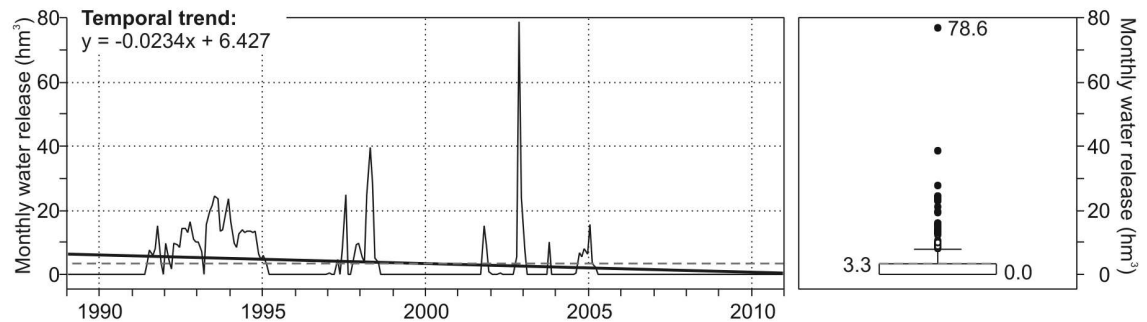


Figure 3.10: Temporal trends and descriptive statistics of monthly series of outflow volume by outflow component over the period 1989-2010.

Table 3.1: Monthly and annual volumes of water withdrawal (hm^3) over the period 2009-2010. Mean monthly and annual volumes in bold.

Year	J	F	M	A	M	J	J	A	S	O	N	D	Annual
2009	7.8	6.9	7.4	6.8	6.1	5.6	5.7	6.3	5.4	6.0	5.3	5.8	75.3
2010	5.9	5.2	5.5	4.7	4.8	4.4	4.3	4.2	4.5	4.8	4.4	5.4	58.4
Mean	6.9	6.0	6.5	5.8	5.5	5.0	5.0	5.3	5.0	5.4	4.8	5.6	66.8

Series of reservoir evaporation and water release revealed decreasing trends with time (Fig. 3.8). Yet, the slope value of the linear functions indicated that the decreasing trend in monthly volumes of water release was significant (0.02 hm^3 per month), whilst the decreasing trend in monthly volumes of evaporation was negligible (0.0009 hm^3 per month).

Decreasing trends with time were also observed for series of monthly water withdrawal over the period 2009-2010 (Fig. 3.11). These findings oppose those of Raskovsky (2009), who found that water withdrawals were increasing since 2006 at rates of 0.01

hm^3 per month. Similarly, inspection for temporal trends based on historic rates of water demand showed clear increasing tendency with time. Conceivably, decreasing trends in water withdrawal by the end of the observation period are related to the water crisis of 2009, where the reservoir water levels reached the yellow warning for active reserves.

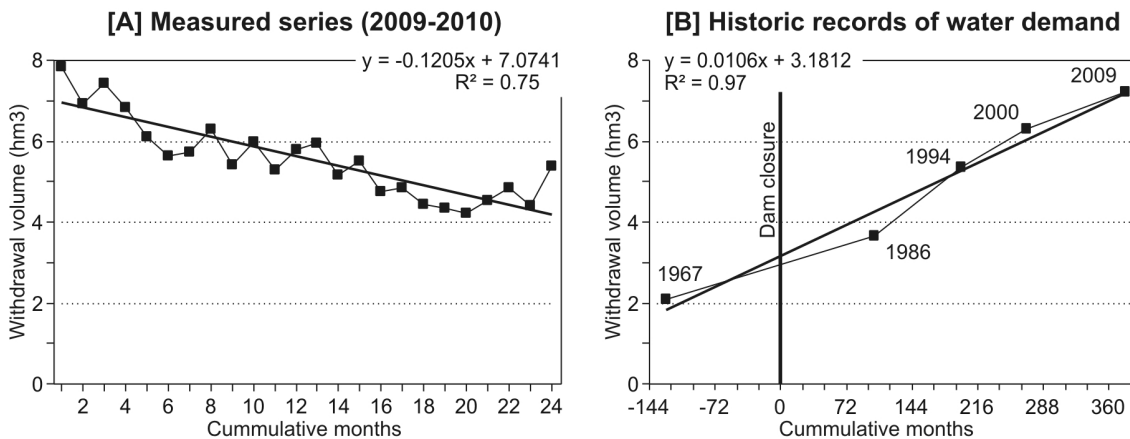


Figure 3.11: Temporal trends in water withdrawal based on [A] series of measured data over the period 2009-2010, and [B] historic records of annual water demand.

Variations in rates of reservoir seepage between measures were negligible, even if the reservoir volume varied notably across the year 2009 (steep decline) and 2010 (gradual increase). Furthermore, mean rates of reservoir seepage over the observation period were highly consistent with previous measurements made on the base of the dam embankment for maximum conditions of water storage (34 litres per second; Buraschi *et al.*, 1999). This suggested that the pressure exerted by the reservoir water column exerts very little influence on the rates of reservoir seepage. Hence, mean monthly seepage volumes (0.09 hm^3) were assumed as constant for the entire period of observation.

Patterns of seasonality

Autocorrelations for series of monthly evaporation revealed clear 6-month seasonality (Fig. 3.12). The most significant positive deviations from zero occurred cyclically at lags 12, 24, 36, 48 and 60, indicating that evaporation maxima occur once per year during the spring-summer months with peak in December (month 12). The most significant negative deviations from zero occur cyclically at lags 6, 18, 30, 42, 54 and 66, indicating that evaporation minima occur once per year during the autumn-winter months with minimum in June (month 6).

Similar patterns were found for series of water withdrawal (Table 3.1), which described relative 6-month seasonality in response to varying water needs throughout the year. Annual maxima occurred during the warmest months (December to March) with peak in January where water needs are the highest. Annual minima occurred during the coldest months (June to September) with minimum in June-July where the water needs are the lowest.

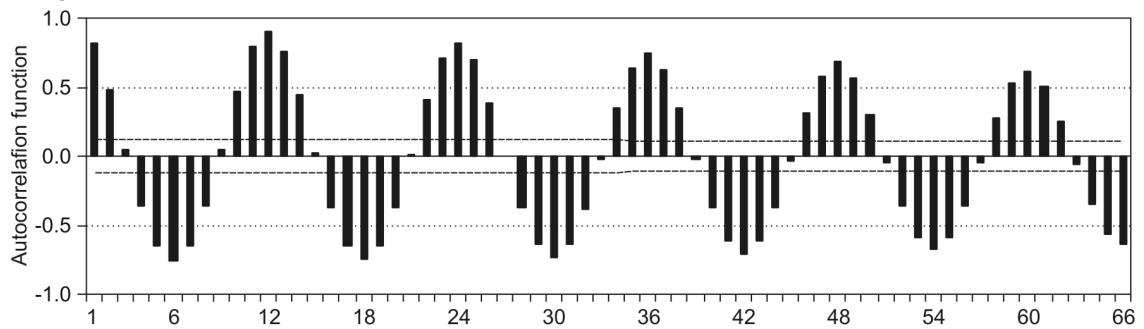
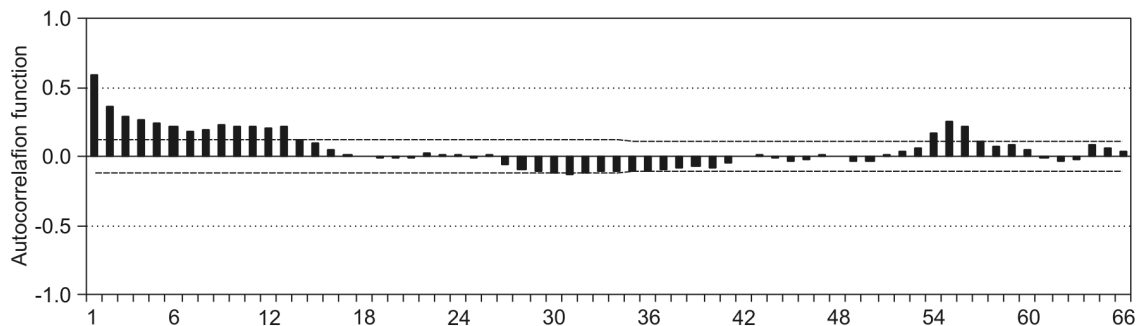
Evaporation from the surface of the reservoir lake**Water release from the dam reservoir**

Figure 3.12: Correlograms of monthly series of outflow volume by outflow component showing autocorrelation functions at 66 lags. Thresholds for significant autocorrelations were defined by two standard errors above and below the zero mean.

Series of water release described unclear patterns of seasonality (Fig. 3.12). Significant correlations occurred at lags 1-13, 31 and 54-56, indicating that water release occurs randomly, and that the frequency, duration and magnitude of episodes of water release is highly variable over time.

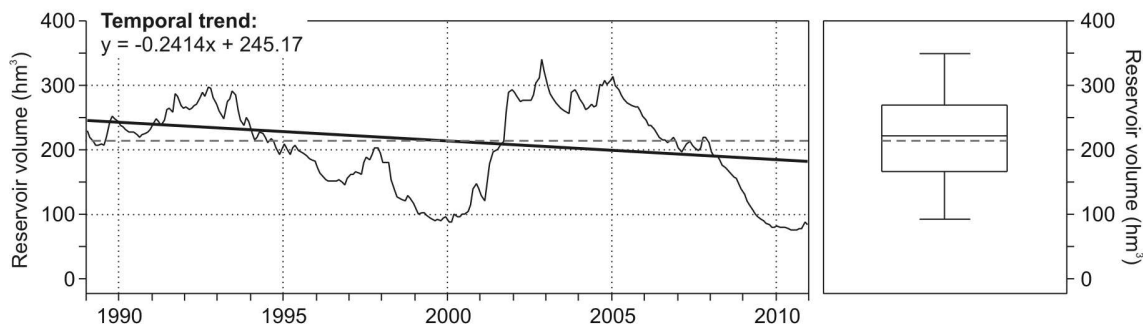
2.2.3. Patterns in water storage

Series of mean monthly reservoir volume described wide variations between years (Fig. 3.13). The reservoir was nearly full over two marked periods (1991-93 and 2001-04), and remained near 25 % its active capacity over the periods 1999-2000 and 2009-10. Mean monthly reservoir volumes over the monitoring period averaged 213.2 hm^3 , with maximum in 343.0 hm^3 and minimum in 93.1 hm^3 . Trend analysis indicated that the reservoir volume decline with time significantly (0.2 hm^3 per month).

Although monthly reservoir volume showed clear periodicity over time (Fig. 3.13), autocorrelation functions at 66 lags did not show clear patterns of seasonality. This suggested that seasonal patterns of reservoir volume were longer than 66 months, and hence autocorrelations were run over the entire period of observation (264 months). Interpretation of results suggested two seasonal episodes of water storage (high and low) spaced of about 5 and 7 years (Fig. 3.8). Maximum negative deviations from the zero mean at lags 69 and 208 indicate that minimum water storage occurs 139 months apart (~ 12 years); maximum positive deviations from the zero mean at lag 125 indicate that maximum water storage occurs 56 months (~ 5 years) apart from episodes of

minimum water storage. Residuals of the autocorrelation function indicated that the duration of episodes of high and low waters was approximately equal (66 months, on average, or 5.5 years); however, maximum significant deviations from the zero mean revealed that raising trends were steeper and shorter (~5 years) than declining trends (~7 years).

Monthly series of reservoir volume



Autocorrelations at 264 lags (entire period)

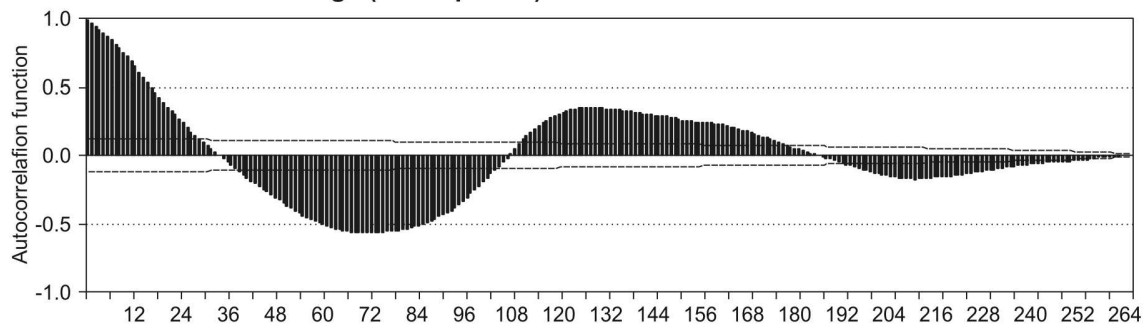


Figure 3.13: Temporal trends, descriptive statistics and correlogram of series of monthly reservoir volume over the period 1989-2010. The correlogram shows autocorrelation functions at 264 lags (entire period).

2.3. RESERVOIR SIZE-YIELD-PERFORMANCE

The Water Balance Model permitted to respond three principal questions: (1) Given historic inflow volumes, which is the active storage size required to meet a target demand at some level of reliability? (2) Given the reservoir capacity required to meet demand, which is the firm yield of the reservoir? (3) Given the storage capacity of the reservoir and the firm yield, which is the dam potential to release water downstream?

These relationships were evaluated on an annual scale based on reservoir size-yield-performance analysis (see Section 1.3, p. 124). Results are presented below.

2.3.1. Storage-yield relationships

Simulation of annual active storage requirements used sequent peak analysis based on the 33-yr period (1978-2010) since dam closure (Fig. 3.14). The sample series was

repeated once to assure that the critical period was comprised entirely within the observational period; this provided a sample series of 66 years. The minimum reservoir storage (i.e. the minimum volume required to the reservoir operates, S_{\min}) used in simulation was equivalent to the dead volume (24.4 hm^3); simulations were solved to give low volumes of initial storage [S_{init}] because the first years of the series represent initial conditions of water storage after dam closure in 1978.

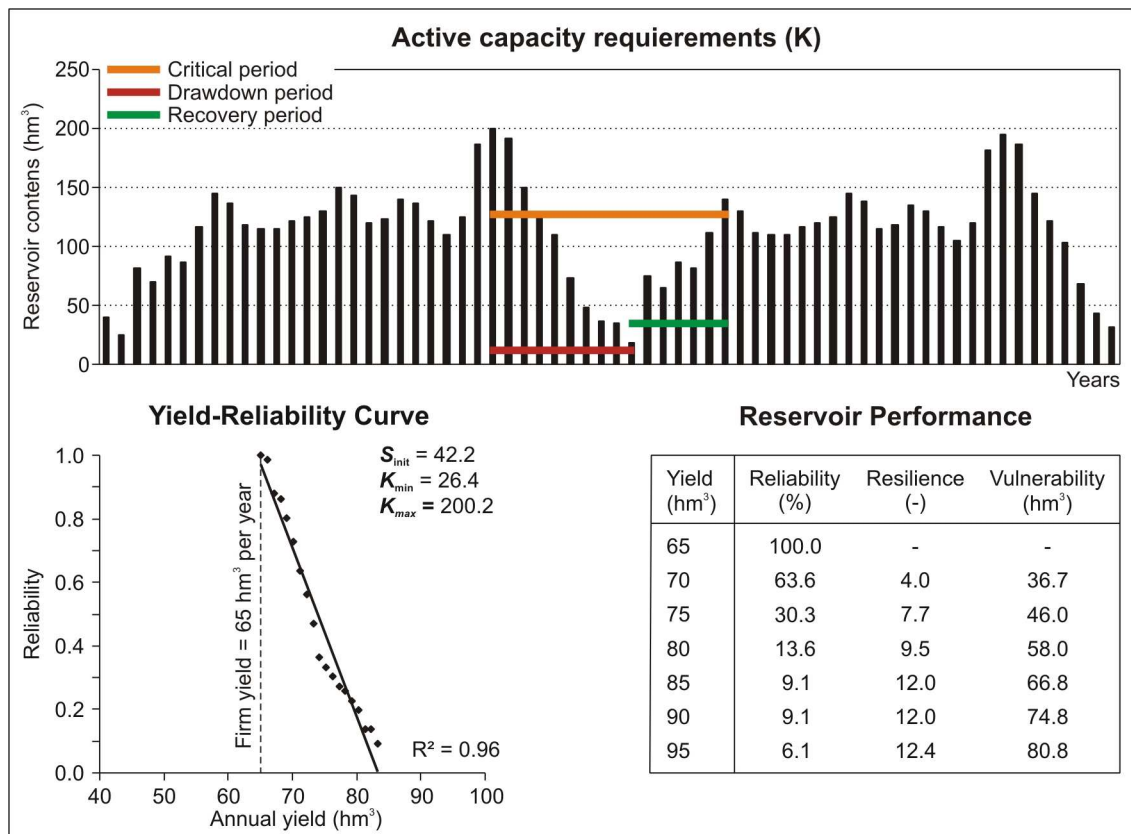


Figure 3.14: Storage-yield relationships for the Paso de las Piedras Reservoir based on historic inflow data over the year 1978-2010. The sample series was repeated one time to assure that the critical period was comprised within the observational period.

The sequence of annual active storage requirements [K] is illustrated in Figure 3.14. The critical period for reservoir operation was about 14 years; the period for reservoir drawdown took 8 years and the period for reservoir refill took 6 years. Maximum [K_{\max}] and minimum [K_{\min}] storage requirements during the critical period permitted to size the reservoir in 200.2 hm^3 and 26.4 hm^3 , respectively. Note, the critical period fell at the end of the first sequence, which suggest that it may take about 30 years before critical declines occur; this is highly consistent with the inter-decadal patterns of rainfall variability reported for the area of interest (see Section 2.1.1 in Chapter 1, p. 34) and is discussed in the Discussion section. Furthermore, the length of periods of reservoir drawdown and refill is highly coincident with the reservoir seasonality (see above).

Inspection of annual yield reliability (i.e. years where storage requirements K were greater than S_{\min}) revealed that the firm yield for water supply (i.e. the yield that can be

delivered without failure over the 66-year period) was 65 hm^3 per year; this is 73 % the mean annual inflow volume (89.3 hm^3). The resulting reliability associated with the firm yield was consequently 100 % (Figure 3.14). Above 65 hm^3 , the reservoir can not assure water supply without failure. Actual reservoir yield is below this value (58.4 hm^3 in 2010) and so the actual reservoir performance can be said to be 100 % reliable. Nevertheless, annual yield in 2009 reached 75 hm^3 ; the yield reliability for such volume is only 30 % and it may take about 8 years before the reservoir recovers from a failure. Assessing these relationships is essential from a management perspective and requires to be investigated directly.

2.3.2. Storage-release relationships

Storage-release relationships were explored to estimate the inflow volume required to assure water release downstream given the maximum storage capacity required to meet water demand. Estimations were based on two scenarios of reservoir operation policies for water release based on Vogel *et al.* (2007): fraction of inflows (FOI) and drought management (DM) policies.

Scenario 1: Fraction of Inflow policy (FOI)

The FOI scenario assumed that any fraction of annual inflow exceeding the reservoir firm yield will be released downstream; annual volumes of direct rainfall and reservoir evaporation were not considered. Mean annual inflow over the observation period [μ] was 89.3 hm^3 ; given a firm yield of 65 hm^3 , the FOI scenario indicates that, on average, 24.3 hm^3 could be released downstream every year. Inspection of the difference between annual inflow and firm yield [$Q-Y$] over the period of record revealed that inflow volumes exceeded the firm yield by 91 %. Exceeding volumes ranged from 91.0 hm^3 to 1.2 hm^3 , and averaged 27.8 hm^3 ($\pm 19 \text{ hm}^3$).

Based on historic inflow records, the FOI scenario indicates that the reservoir performance to yield up to 65 hm^3 per year should not be compromised by operations of downstream flow maintenance. However, FOI scenario did not consider initial conditions of water storage or evaporation processes, which may induce substantial variations in water levels.

Scenario 2: Drought Management policy (DM)

Scenario 2 combines the FOI policy with the DM policy, which implies that flow release will occur only if the reservoir storage is above a buffer zone defined by some critical level from a management perspective. Level-based processes of water loss are considered herein, and annual inflow volume includes the entire range of hydrologic inflows. Scenario 2 assumed:

- a firm yield of 65 hm^3 per year and mean annual evaporation losses of 25.2 hm^3 per year,
- a variety of total annual inflow volumes (i.e. surface inflow and direct rainfall) that could be expected to occur for return intervals of 2 to 1000 years, and

- a storage threshold for water release defined by the flood control level (164 m.s.l.). The 164 m-level defines ideal storage conditions from a management policy perspective. Above this threshold, water levels are controlled by flow release (or spills if water levels exceed 165 m.s.l.); below this threshold, storage is conserved for periods of drought and hence no water release occurs.

Simulation assumed that annual release downstream occurs only if (i) annual inflow volume exceeds the annual volume of storage losses (98.1 hm^3), and (ii) the fraction of inflow contributes to exceed the 164 m-level threshold. Initial storage conditions used three levels that are critical for dam management: (i) 150 m.s.l. (10 % of active storage; red warning), (ii) 155 m.s.l. (25 % of active storage; yellow warning), and (iii) 163 m.s.l. (82 % of active storage; 1-m below the flood control level). Additionally, simulation used initial storage levels based on mean storage conditions over the period of record (160 m.s.l.).

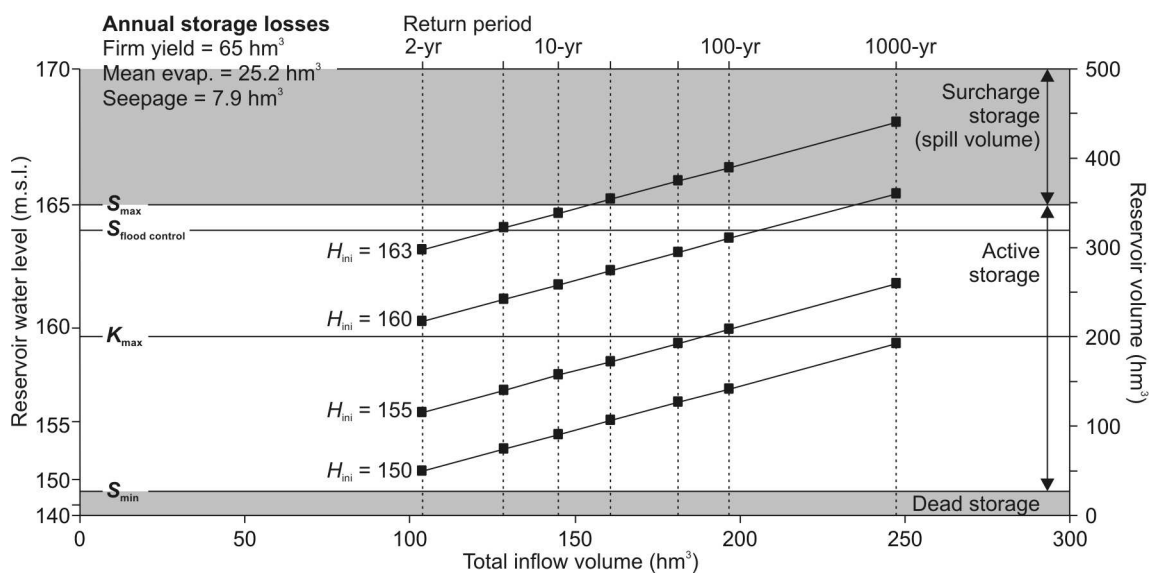


Figure 3.15: Storage-release relationships for the Paso de las Piedras reservoir as fraction of varying annual inflow volumes. The contribution of varying inflow volumes to variations in water storage is simulated based on different levels of initial storage.

As shown in Figure 3.15, results indicated that any positive variation in water storage entraining reservoir release requires of inflow volumes higher than 2-yr inflow (103.9 hm^3); in other words, 2-yr inflow was nearly equal the annual outflow volume and hence it will unlikely entrain reservoir release whatever the initial conditions of reservoir storage. Furthermore, simulation revealed that reservoir release will occur only under initial conditions of high reservoir storage and for inflow volumes higher than 5-yr inflow (128.8 hm^3); below 163 m-level, the probability of water release to occur is very low regardless of the inflow magnitude. Previous results revealed that the reservoir recovery period was about 6 years. Hence, storage-release simulation for the Drought Management scenario suggests that it could take more than 6 years before reservoir release occurs whether initial storage conditions are low.

2.4. THE DEGREE OF IMPOUNDMENT

The ability of the Paso de las Piedras Dam to store inflow volumes within its reservoir and to control patterns of flow downstream was evaluated using a suite of indices widely available in literature: the m index, the Impounded Runoff Index [QI], the Yield Index [YI] and the Release Index [RI] (see Section 1.4, p. 127). Input parameters to calculate the indices used:

- active storage capacity [S] equal to 324.5 hm^3 , and
- mean annual inflow volume [μ] equal to 89.3 hm^3 with 23.8 hm^3 standard deviation [σ].

The reservoir behaviour for water supply

The estimates μ and σ were used to compute the standardized net inflow [m] for a given reservoir yield [Y] as expressed in Equation 3.8. The m index provided information on whether the reservoir operates on within-year or carryover yield requirements relative to the historic behaviour of inflow volumes. Given a coefficient of variation of annual inflow volume equal to 0.3, the net inflow for the firm yield was $m = 1.0$; this indicates that the reservoir may yield up to 65 hm^3 per year without failure or, in other words, that variations in inflow volumes over time do not compromise the reservoir to meet annual requirements for water supply.

However, a standardized net inflow volume equal to unity is on the limit between within-year and carryover yield requirements so that any variation in the water demand may determine very different reservoir operational procedures. For example, the net inflow volume for actual yield requirements (58.4 hm^3) is $m = 1.3$; this implies that inflow volumes are large enough to the reservoir meets the annual demand and releases the exceeding volume downstream. If the water demand increases to 75 hm^3 per year (as in 2009), then $m = 0.6$; this implies that inflow volumes are not enough to meet annual yield requirements, so that water demand is met using water stored in preceding years. In cases where $m \leq 1$, water release downstream is very unlikely to occur.

The dam potential for river impoundment

The potential of the dam to disrupt the longitudinal continuity of water fluxes was evaluated based on the ratio of active reservoir capacity [S] and supply yield [Y] to mean annual inflow [μ]. Estimations used the maximum volume of reservoir yield without failure over the historical record (firm yield) so that $m = 1$.

Results indicated that the hydrologic magnitude of the dam was almost four times the magnitude of inflow volumes ($QI = S/\mu = 3.63$), and that the proportion of annual yield for water supply relative to mean annual inflow was very high ($YI = Y/\mu = 0.73$). S/μ and Y/μ relationships for the Paso de las Piedras Reservoir imply great dam potential to disrupt the longitudinal continuity of the sauce Grande River. First, the active capacity of the reservoir allows to store inflow volumes over more than three years and a half; considering mean annual volumes of storage loss by evaporation and yield, the reservoir potential for impoundment will be even greater ($QI = 4.64$). Second, if reservoir

evacuation occurs, the fraction of inflow available to flow release once the annual yield requirements were met is only 27 % the mean annual inflow ($R = \mu - Y = 24.3 \text{ hm}^3$).

Figure 3.16 illustrates the Impounded Runoff Index [QI] and the Yield Index [YI] on an annual basis so that $QI = S/Q$ and $YI = Y/Q$, where Q = annual surface inflow. Note that annual release [R] equals the difference of annual yield to annual inflow so that $RI = 1 - YI$ only if $YI \leq 1$, as no water release will occur if the annual reservoir yield is greater than the annual inflow volume. Results showed that annual yield requirements were met for 91 % of years ($YI \leq 1$), which implies that the degree of impoundment relative to the reservoir function was of 9 % over the 33-yr of record. Nevertheless, annual QI were above unity for all years of record and were above the mean QI for 58 % of years, which evidences the great potential of the dam to absorb annual floods and peak flows within its reservoir.

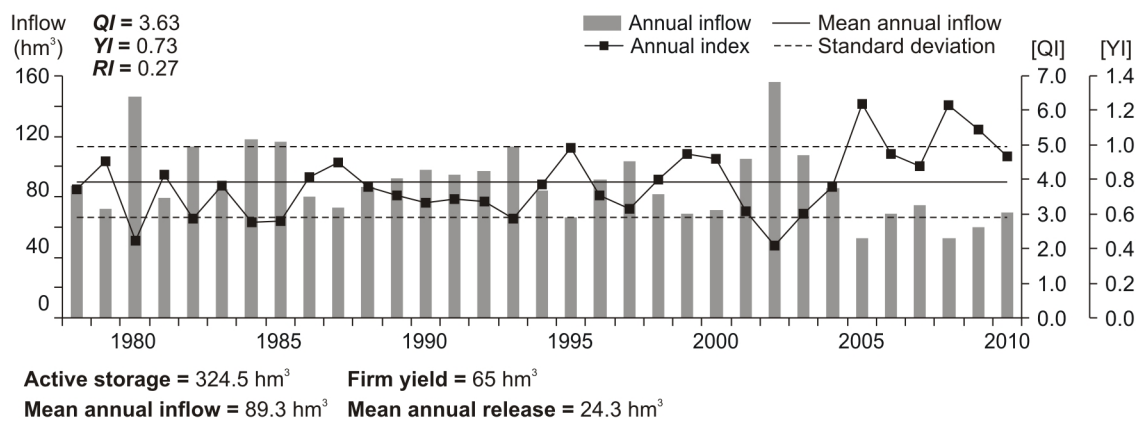


Figure 3.16: Annual Impounded Runoff Index [QI] and Yield Index [YI] showing the degree of hydrologic regulation of the Sauce Grande River after closure of the Paso de las Piedras Dam in 1978. Annual volumes of surface inflow are also illustrated.

SECTION

3

DISCUSSION AND CONCLUSIONS

This chapter has assessed the hydrology of the Paso de las Piedras Reservoir robustly. It determined the dam potential to store inflow volumes within its reservoir and to control patterns of flow downstream relative to the reservoir capacity and the human requirements for water supply. The assessment of these relationships provided the basis to quantify the degree of disruption of the hydrological continuity of the Sauce Grande River induced by the dam. The results from this investigation are discussed below.

3.1. PATTERNS IN THE RESERVOIR HYDROLOGY

The Water Balance Model for the Paso de las Piedras Reservoir indicated that the reservoir hydrology depends on the interactions between surface flow and direct rainfall entering the reservoir, water losses by evaporation and seepage, reservoir yield for water supply, and flow release for downstream maintenance. From Table 3.2, it is clear that the most important components of the reservoir water balance are the surface inflow from headwaters and tributaries and the reservoir yield to meet human water requirements. The relative magnitude of reservoir release, whether occurs, is moderate.

Table 3.2: Patterns in inflow and outflow components of the water balance of the Paso de las Piedras Reservoir

Hydrologic component		Relative magnitude	Annual seasonality	Inter-annual variability	Temporal trend
INFLOW	Surface inflow	Very high (82 % of total inflow)	2 annual peaks (summer and spring)	High	Low decrease
	Direct rainfall	Low (18 % of total inflow)	6-month (max. in spring-summer)	High	Low decrease
OUTFLOW	Evaporation	Low (18 % of total outflow)	6-month (max. in summer)	Storage-dependent	Relatively constant
	Seepage	Very low (6 % of total outflow)	Relatively constant	Relatively constant	Relatively constant
	Yield (withdrawal)	High (47 % of total outflow)	6-month (max. in summer)	Demand-dependent	High increase
	Release	Moderated (29 % of total outflow)	Unclear	Very high	High decrease

3.1.1. Synchrony in the seasonality of inflows and outflows

Except for reservoir release which was highly scattered in time without clear

periodicity, major inflow and outflow components revealed similar patterns of seasonality (Table 3.2). Annual patterns of reservoir inflow were synchronized to those of water demand: annual maxima of direct rainfall and surface inflow tended to occur by late spring and summer, there where human and environmental water needs are highest.

The distribution of monthly rainfall over the annual cycle described high monthly totals from November to February (rain season) and low monthly totals from May to August (dry season). Such pattern of seasonality is characteristic of the South-western Buenos Aires and La Pampa regions (Labraga *et al.*, 2002; Penalba and Robledo, 2005; Scian *et al.*, 2006; Forte-Lay *et al.*, 2008; Gabella *et al.*, 2010). Furthermore, low monthly totals in late autumn and winter and high monthly totals in spring and summer indicate a **summer monsoon rainfall regime** consistent with the tropical and subtropical sections of South Eastern South America (Zhou and Lau, 1998; Nogués-Paegle *et al.*, 2002; Gan *et al.*, 2004; Grimm *et al.*, 2005; Vera *et al.*, 2006; Grimm, 2011). Even if the area situates within an extra-tropical temperate zone (38°S), we consider appropriate to refer to a monsoon regime influenced by the strengthening of the South Atlantic Convergence Zone during summer (Marengo and Seluchi, 1998; Liebmann *et al.*, 1999; Barros *et al.*, 2000; Barros and Doyle, 2002).

The hydrological system within the river basin is rainfed, so that the seasonality of surface inflow is influenced by the seasonal cycle of rainfall. However, there were two clear annual maxima, one in mid spring (November) and one in mid summer (February), and annual minima were unclear. Unclear patterns of annual minima were strongly related to the high inter-annual variability of inflow volumes (see next section); low inflow volume in December and January may be explained by rates of evapotranspiration that were higher than rainfall contributions during the rain season.

Similar patterns of flow seasonality were found, for example, within dry regions of eastern Australia (Haines *et al.*, 1988; McMahon *et al.*, 2007c; Kennard *et al.*, 2010). The most interesting fact within these regions is that annual maxima of rainfall and surface flow occurs during the spring and summer seasons, in opposition to other dry regions of the world, like Mediterranean climates, where summers are dry (Strahler, 1981) and so water availability is out-of-phase with respect to the water demand (Batalla *et al.*, 2004; Kondolf and Batalla, 2005).

3.1.2. Inter-annual variability vs inter-annual reliability

Despite the overall synchrony in seasonal patterns of reservoir inflows and outflows, there was great contrast in the inter-annual behaviour of such patterns (Fig. 3.17). Reservoir outflows (except for water release) repeated cyclically year after year; inter-annual variations in magnitude were related to gradual and linear variations in water storage and human water demand, respectively, and so were hardly noticeable from one year to another. In opposition, inflow components described high inter-annual fluctuations in both the magnitude and the timing of annual maxima and minima.

Inflow variability and outflow reliability (constancy) combine to generate high fluctuations in the effective water available to storage (Fig. 3.17). Inflow volumes were higher than outflow volumes for 37.1 % of months, which contributed to monthly

increase of up to 40 hm³ in reservoir volume; in some cases, inflows were so high that entrained large volumes of reservoir evacuation. These episodes are evidenced by steep declines in the monthly water storage curve (Fig. 3.17).

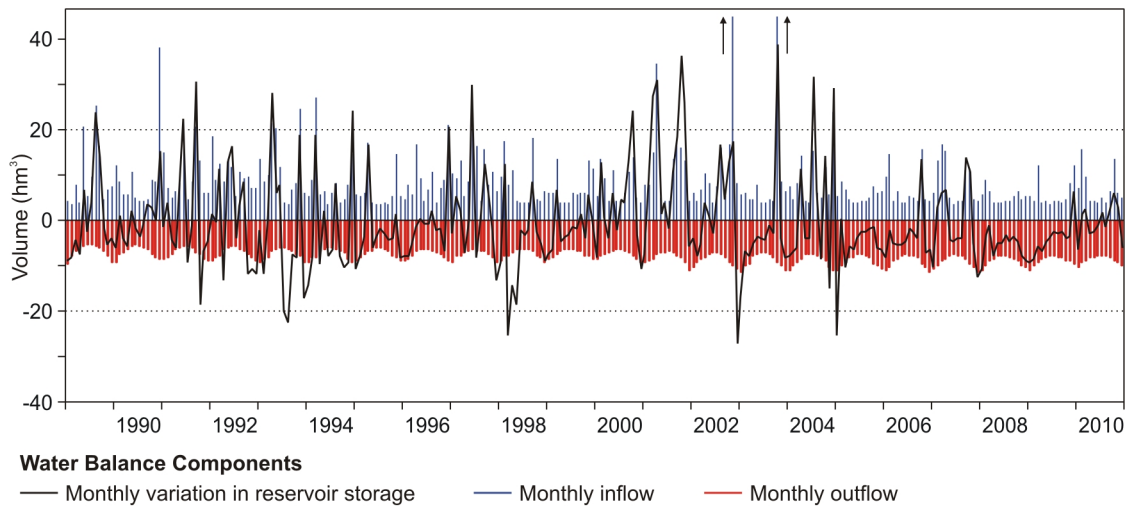


Figure 3.17: Monthly variations in the components of the reservoir water balance over the period 1989-2010.

Correlation analysis (Table 3.3) indicated that about 30 % of variations in water storage were driven by fluctuations in inflow components ($0.557 < r < 0.642$). Surprisingly, correlation coefficients between water storage and controlled patterns of reservoir outflow were non significant. This suggested that monthly decrease in water storage over the long term was related to reservoir evaporation more than to dam operations to water yield or storage control. In addition, significant correlations indicated that the magnitude, frequency and duration of episodes of dam release were highly driven by inflow volumes relative to the actual storage within the reservoir ($r = 0.492$).

Table 3.3: Correlation coefficients between components of the reservoir water balance

	Direct rainfall	Surface inflow	Evaporation	Yield	Release	Change in storage
Direct rainfall	1.000					
Surface inflow	0.631	1.000				
Evaporation	0.253	0.137	1.000			
Yield	-0.112	-0.102	-0.059	1.000		
Release	0.248	0.492	0.092	-0.228	1.000	
Change in storage	0.642	0.557	-0.172	-0.053	-0.060	1.000

Inter-annual variability in the effective water available to storage and supply purposes is a common characteristic of reservoir systems operating within sub-humid and semiarid regions (Graf, 1999; Vogel *et al.*, 1999; Güntner *et al.*, 2004; Wurbs, 2005; Hoff *et al.*, 2007; McMahon *et al.*, 2007c). Water availability depends on the relationship between

rainfall, soil retention and evapotranspiration for a given time interval (Thornthwaite, 1948), so that inter-annual fluctuations in this relationship were explored based on the Thornthwaite's water balance. The water balance was computed monthly over the period 1978-2010 for the upper river basin (source for surface inflow) and for the Paso de las Piedras Reservoir itself (Fig. 3.18) to investigate both temporal variations in moisture since dam closure and spatial variations in moisture relative to the situation of sources for direct rainfall and surface flow. The latter aspect was of particular interest because reservoirs in semiarid areas are usually fed by surface flow that originates in more humid upland areas (Schmandt, 2010).

Annual moisture conditions were estimated using the Moisture Index [*MI*] based on the Thornthwaite's monthly water balance as follows:

$$MI = \frac{100 * \text{Water surplus} - 60 * \text{Water deficiency}}{PET} \quad (3.11)$$

Mean annual *MI*s indicated that the climate type for the upper river basin is moist sub-humid, whereas the climate type within the lowest areas near the Paso de las Piedras Reservoir is dry sub-humid. These climate types are equivalent to semiarid (BSk) and humid subtropical (Cfa) climates in Köppen classification (Strahler, 1981), and are comparable to the central-western portions of the United States and eastern Australia, respectively (Feddema, 2005). Higher moisture conditions for the upper river basin are conceivably related to the effect of the Ventania Mountain System, which imposes wetter-than-normal conditions within the higher areas and precipitation maxima over the north-eastern slopes (Gaspari *et al.*, 2008; Gil, 2009). Since surface inflow from headwaters and tributaries represents 82 % of the total inflow, patterns of water storage within the reservoir will be influenced by moist climate in spite that moisture conditions near the reservoir lake are dry.

Sequential analysis of annual *MI*s revealed high variability in water availability over time, which has direct implications for the sustainability of human, agricultural and industrial water requirements. Annual moisture conditions fluctuated between humid-B₂ climate (e.g. the climate type of Uruguay) and semiarid climate (e.g. the climate type of North Patagonia) in both sites. Within the upper river basin, inter-annual variations in moisture described clear humid trends from 1980s to early 2000s, and a clear tendency to dryness during the last years of record; variations in annual moisture in Paso de las Piedras revealed similar patterns, although the 1980s were notably dryer.

These results match the findings of Gil (2009) on rainfall anomalies within the upper river watershed, and are highly consistent with rainfall anomalies observed on the regional scale (Scian, 2000; Campo *et al.*, 2009; Bohn *et al.*, 2011). For example, these studies reported cyclic periods of humidity that peaked in intensity during the mid 1980's, early 1990's and early 2000's; the years 2001 and 2002 were identified as extreme humid in the central parts of the region. The driest events occurred from 2005 to 2009, the year 2008 identified as the driest year across the entire region.

A number of studies at the regional and national scales (e.g. Scian, 2000; Penalba and Vargas, 2004; Kruse and Laurencena, 2005; Núñez *et al.*, 2005; Penalba and Robledo, 2005; Forte-Lay *et al.*, 2008; Penalba and Llano, 2008) reported that the frequency of extreme drought declines since 1940, and that rainfall increase since the 1970s. Very

few studies documented the actual tendency to dry conditions (e.g. Andrés *et al.*, 2009; Campo *et al.*, 2009; Bohn *et al.*, 2011), conceivably because the temporal length of the time series used by most studies rarely exceeds the year 2000.

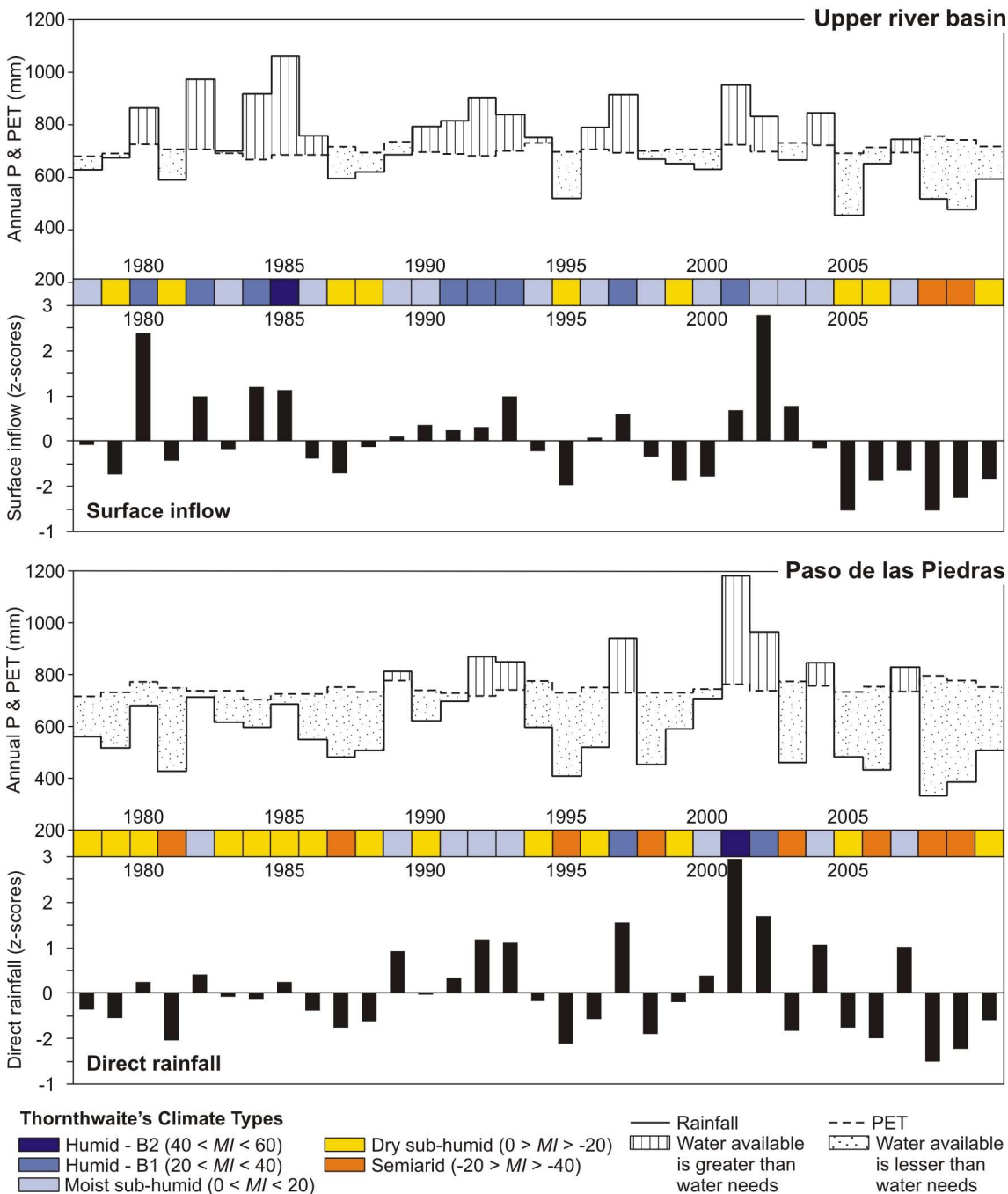


Figure 3.18: Relationship between annual rainfall [P] and evapotranspiration [PET] for the upper river basin and the area near the Paso de las Piedras Reservoir. Annual climate types were defined based on the Moisture Index [MI] of Thornthwaite (1948).

Inspection of rainfall trends over the period of record (1971-2010) clearly suggested the *beginning of a dry climate cycle* since 2005. Inter-decadal rainfall variability explains

the reason for which the critical period for active storage capacity occurred by the end of the observational period since dam closure (1978-2010). Despite water storage within the reservoir described clear 5- to 7-yr seasonality, the storage decline observed during recent years is the strongest over the entire reservoir history.

3.1.3. The causes of inter-annual variability in inflow components

Patterns in reservoir inflows over the observation period described strong inter-annual variability. Although such variability may result from the combination of a number of large-scale phenomena (Garreaud *et al.*, 2009), most studies argue that the *El Niño*-Southern Oscillation (ENSO) phenomenon is the greatest source for rainfall variability in South Eastern South America (Ropelewski and Halpert, 1987; Aceituno, 1988; Ropelewski and Halpert, 1989; 1996; Barros *et al.*, 2000; Grimm *et al.*, 2000; Andreoli and Kayano, 2005; Kayano and Andreoli, 2007; Zamboni, 2008; Grimm, 2011). Hence, we confronted monthly variations in inflow components to ENSO episodes to assess the degree of correlation between both phenomena within the area of interest.

An array of ENSO definitions has been formulated by different researchers worldwide; the ENSO definition used within this research is equivalent to that of Trenberth (1997) and is summarized in Table 3.4. *El Niño* episodes were defined by 5-month running means of the SST Index for the Niño 3.4 region (5°N-5°S, 120°-170°W) exceeding 0.4 °C for at least 6 consecutive months (positive anomaly); conversely, *La Niña* episodes were defined by 5-month running means of the SST Index remaining below -0.4 °C for at least 6 consecutive months (negative anomaly). As the *El Niño* (or *La Niña*) episodes are related to a basinwide warming (or cooling) of the tropical Pacific Ocean, they are referred to as Warm (or Cold) ENSO.

Ropelewski and Halpert (1987; 1989; 1996), hereinafter referred to as RH87, RH89 and RH96, respectively, examined and documented seasons and regions of strong and consistent ENSO-rainfall relationships for both ENSO phases. For the region of La Pampa, the authors found that Warm ENSO-rainfall relationships are positive and tend to occur from November through February. Conversely, Cold ENSO-rainfall relationships are negative and stronger from June through December. These periods are referred to as WE and CE seasons, respectively.

To analyze variability in rainfall and surface flow we used the Standardized Precipitation Index (SPI) of McKee *et al.* (1993) and its equivalent version for flow analysis which we decided to call Standardized Runoff Index (SRI). The SPI (or SRI) simply consists in the standardization of rainfall (or runoff) observations based on probability density functions ($Z \sim N [0,1]$), so that any significant deviation from the zero mean is assumed as anomalous (McKee *et al.*, 1993; Guttman, 1999; Lloyd-Hughes and Saunders, 2002).

The SPI and SRI were computed on a monthly scale based on series of rainfall for Paso de las Piedras and series of runoff from the headwaters; time series span the period 1971-2010 as data were available for both variables. ENSO-rainfall (-runoff) relationships were inspected separately for the WE and CE seasons identified by RH87, 89, and 96 for La Pampa region. Monthly SPI and SRI values were averaged for each season over the entire period of record; seasonal anomalies were identified from mean

SPI (SRI) deviations from the zero mean exceeding the $\pm 0.5\sigma$ threshold. Analysis of correspondence between ENSO episodes and rainfall (runoff) anomalies was performed by simply computing the frequency of associations. Note that this procedure matches that used by Scian (2000) to give continuity to previous studies on regional ENSO-rainfall relationships.

Table 3.4: Recurrence and duration (in months) of Warm and Cold ENSO episodes since 1970. The ENSO definition was based on Trenberth (1997). Shaded cases indicate coupled events where the SST Index remained of the same sign.

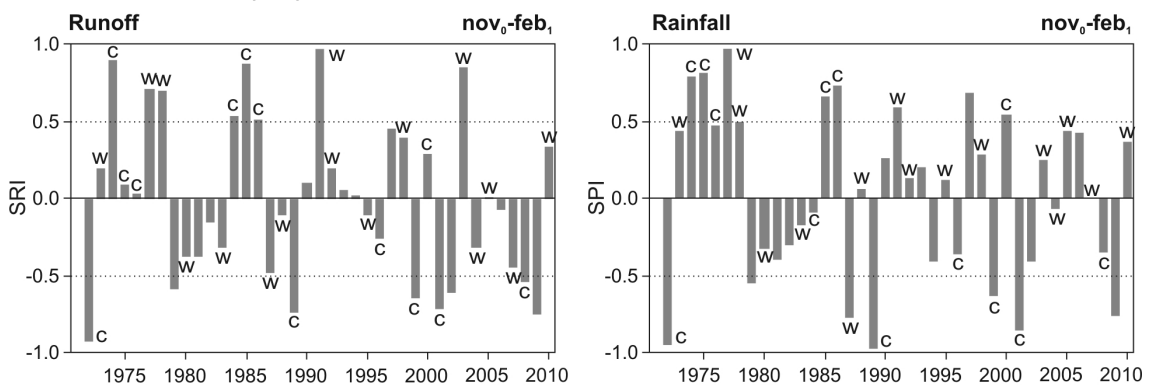
Cold ENSO or <i>La Niña</i>			Warm ENSO or <i>El Niño</i>		
Begin	End	Duration	Begin	End	Duration
Jul 1970	Jan 1972	19	Apr 1972	Mar 1973	12
Jun 1973	Jun 1974	13	Aug 1976	Mar 1977	8
Sep 1974	Apr 1976	20	Jul 1977	Jan 1978	7
Sep 1984	Jun 1985	10	Oct 1979	Apr 1980	7
May 1988	Jun 1989	14	Apr 1982	Jul 1983	16
Sep 1995	Mar 1996	7	Aug 1986	Feb 1988	19
Aug 1998	Mar 2001	32	Mar 1991	Jul 1992	17
Jul 2007	May 2008	11	Feb 1993	Sep 1993	8
Jul 2010	Apr 2011	10	Jun 1994	Mar 1995	10
			Apr 1997	May 1998	14
			Apr 2002	Mar 2003	12
			Aug 2003	Feb 2004	7
			May 2004	Jul 2005	15
			Jul 2006	Feb 2007	8
			Jun 2009	Apr 2010	11

Deviations of averaged series of the SPI and SRI for the WE season (Nov₀-Feb₁) and for the CE season (Jun-Dec) are illustrated in Figure 3.19. Deviations during the *WE season* showed certain inconsistency between runoff and rainfall series in terms of frequency, intensity and timing. Ten seasons revealed positive anomalies simultaneously for both series (67 to 83 % of the positive anomalies observed in both series), from which only five occurred under warm ENSO (1977, 1978, 1991, 1998 and 2010). SPI and SRI deviations during the *CE season* revealed similar patterns; eleven seasons revealed significant negative deviations simultaneously (73 to 85 % of the negative anomalies observed in both series), from which only 6 were coincident with Cold ENSO (1988, 1995, 1998, 2000, 2007 and 2010).

In opposition to what was expected, ENSO-rainfall and ENSO-runoff relationships during the WE and the CE seasons were unclear. As shown in Table 3.5, the frequency of occurrence of positive anomalies [A^+] under Warm ENSO was similar during both the WE season (39 to 70 %) and the CE season (55 to 58 %) for both series; in the case

of rainfall series, WE-A⁺ relationships were stronger during the CE season. The correspondence between negative anomalies [A⁻] and Cold ENSO was of between 36 and 53 % and was slightly stronger during the CE season. The proportion of rainfall (or runoff) anomalies occurring under non-ENSO conditions was notable during both seasons (27 to 43 %).

Warm ENSO season (WE)



Cold ENSO season (CE)

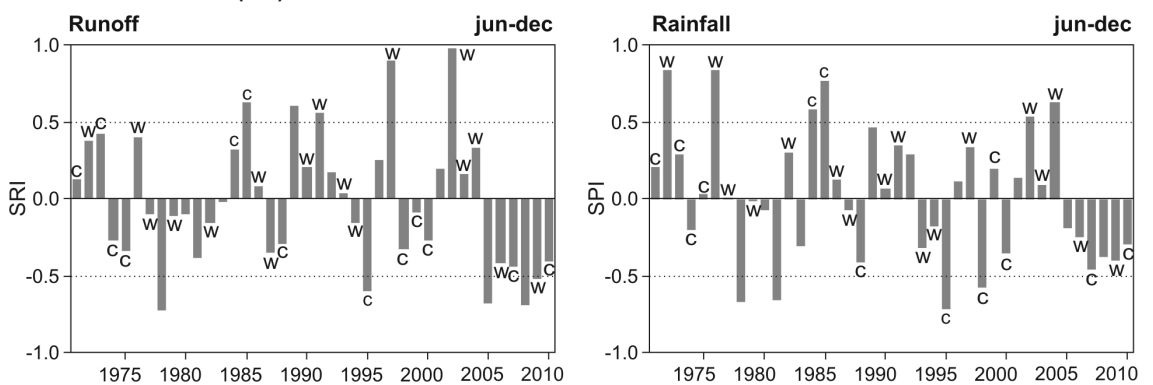


Figure 3.19: Deviations of averaged series of the SPI and SRI for the WE season (Nov0-Feb1) and the CE season (jun-dec). Years WE (*El Niño*) and CE (*La Niña*) are indicated with 'w' and 'c', respectively.

Building on these findings, we can not affirm the existence of strong response of local rainfall variability and ultimately, runoff variability, to the ENSO phenomenon, at least during the WE and CE seasons defined by RH87, RH89 and RH96. WE-A⁺ relationships during the WE season and CE-A⁻ relationships during the CE season were moderate to weak, and there were significant inverse ENSO-rainfall (-runoff) correlations during both seasons. WE-A⁻ relationships accounted for 14 to 36 % of the associations for both series; CE-A⁺ relationships were slightly weaker (10 to 27 %). Furthermore, there were significant deviations either positive (e.g. 1997 during the WE season, Fig. 3.19) or negative (e.g. 1978 during the CE season, Fig. 3.19) occurring under non-ENSO conditions (Table 3.5).

Inspired on the results of Labraga *et al.* (2002), Scian *et al.* (2006) investigated positive and negative rainfall anomalies (wet and dry extreme events) occurring in La Pampa region under non-ENSO conditions. The authors found that a great proportion of

extreme dry and wet events were connected to anomalies in horizontal patterns of water vapour transport occurring at the scale of South Eastern South America (SESA). A number of studies reported a complexity of atmospheric processes involved in the natural variability of rainfall regimes across SESA, e.g. the seasonal displacement of the South Atlantic Convergence Zone (SACZ), anomalies in the sea surface temperature of the nearby Atlantic Ocean, and turbulent disturbances associated with the subtropical jet (Nogués-Paegle and Mo, 1997; Liebmann *et al.*, 1999; Barros *et al.*, 2000; Barros and Doyle, 2002; Liebmann *et al.*, 2004).

Table 3.5: Frequency (%) of positive and negative anomalies of averaged SPI and SRI values occurring under ENSO conditions (WE, CE) and non-ENSO conditions (N) during (a) the WE season and (b) the CE season. Frequency analysis encompasses the period 1971-2010.

	Positive anomalies (+0.5 σ)			Negative anomalies (-0.5 σ)		
	WE	CE	N	WE	CE	N
<i>(a) WE season</i>						
SRI	38.5	23.0	38.5	35.7	35.7	28.6
SPI	70.0	10.0	20.0	14.3	42.9	42.9
<i>(b) CE season</i>						
SRI	54.5	27.3	18.2	20.0	53.3	26.7
SPI	58.3	25.0	16.7	23.0	46.2	30.8

These findings indicate that inter-annual variability in the effective water availability within the river basin respond to anomalies in the atmospheric circulation associated with both ENSO and non-ENSO events. This implies a complexity of processes affecting the magnitude, timing and frequency of rainfall regimes and runoff processes year after year, and such complexity remains to be investigated directly. The low predictability of extreme dry and wet events within the area is the greatest threat for water availability from a management perspective.

3.2. DROUGHT AND WATER DEMAND: CONSTRAINTS FOR RESERVOIR MANAGEMENT

Inter-annual fluctuations in the effective water available for supply purposes are the greatest threat for water storage management in semiarid regions (Graf, 1999; Vogel *et al.*, 1999; Güntner *et al.*, 2004; Wurbs, 2005; Hoff *et al.*, 2007; McMahon *et al.*, 2007c). To inspect how dry and wet episodes have influenced reservoir storage over time, mean annual SPIs and SRIs calculated over a 12-month scale over the period 1971-2010 were compared to mean annual water level elevation over the period 1989-2010 (Fig. 3.20).

Despite the overall low predictability of flow and rainfall anomalies within the river

basin, results revealed clear tendency to dryness (or wetness) every five to six years, especially during the last decades (Fig. 3.20). Nevertheless, negative (or positive) anomalies showed high inter-annual variations in magnitude and hence in severity. For example, 5 to 6 years revealed significant negative deviations ($SRI/SPI < -1$) over the period of record, although only one year classified as extreme dry ($SRI/SPI < -2$; 2009). Similarly, 5 to 7 years classified as wet ($SRI/SPI > 1$) but only 2002 and 2003 described deviations close to the extreme wet threshold ($SRI/SPI > 2$). This indicates that droughts (or floods) may be expected to occur with certain seasonality, yet the severity of such events is less predictable.

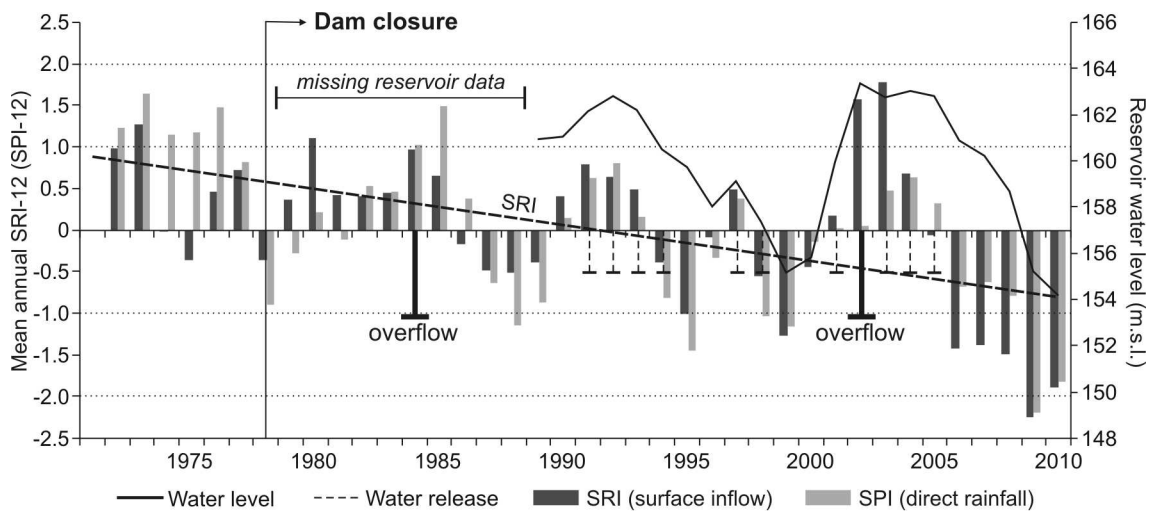


Figure 3.20: Deviations of mean annual SRI/SPI indices (1971-2010) and mean annual reservoir water level elevation (1989-2010). SRI/SPI deviations between the ± 1 threshold indicate normality. The SPI and SRI indices were computed monthly over a 12-month time scale, where each monthly value is standardized based on the values recorded over the 12 preceding months and relative to the same 12-month period over the entire period of record.

From Figure 3.20, the influence of flow and rainfall anomalies on reservoir storage is clear. The early 1990's and 2000's were very humid, so that reservoir storage increased close to (or beyond) the maximum capacity. Increasing water levels were managed by operations of controlled flow release (except for the year 2002 where the reservoir overflowed; Fig. 3.20); during the early 1990's, flow release downstream was substantial and related to dam operations to lowering reservoir levels prior to initiate actions of restoration to prevent infiltration (Schefer, 2004). On the other side of the scale, mid and late 1990's and late 200's were dry to extreme dry, and so the reservoir storage declined. Logically, flow release during these periods did not occur.

At this point, it should be noted that both SRI and SPI deviations described clear decreasing trends with time (only SRI trend shown in Figure 3.20). The recurrence of drought during the second half of the observation period increased, and attained maximum severity by the end of the period where reservoir levels declined alarmingly. These aspects evidence the beginning of a drier climate cycle as discussed above.

The last decade of the reservoir history is of particular interest because it encompasses the reservoir overflow in 2002 and the steep decline in water storage since 2005 (Fig.

3.20). Reservoir overflow occurred in response to inflow volumes that peaked in more than $1000 \text{ m}^3 \cdot \text{s}^{-1}$ and entered into a reservoir already top full (La Nueva Provincia, 11 November 2002). According to the local news paper, the exceeding volume would have reached more than 80 hm^3 , surpassing notably that of October 1984 where the reservoir overflowed for the first time in its history. Regardless of this extreme wet event, the actual reservoir volume declines since 2005 (See section 2.4 in Chapter 1, p. 53). Marini (2009) reported that the reservoir surface area between January 2005 and January 2009 decreased by 1145 ha, this is 35.6 % the initial surface area; the equivalent decrease in reservoir volume was 174 hm^3 (53.6 % the active capacity). Such decrease in the reservoir volume may be explained by surface inflow volumes that were between 59 and 83 % the mean annual inflow volume and between 65 and 92 % the mean annual water losses by evaporation and yield.

In the context of increasing water demand due to population growth and increased recurrence of drought, how do dam managers deal with declining water storage? Conservation storage procedures seem to be not longer effective. An alert system to lowering storage reserves has been implemented by late 2000's, and many actions were undertaken to reduce volumes of reservoir yield (See Chapter 1). Yet, the water demand during the last decade increased by 25 % (MBB, 2000; Raskovsky, 2009) and at present, reservoir yield is near the maximum volume that the reservoir can supply at 100 % reliability.

Maintaining reservoir reliability to meet water needs during drought or low flow conditions with low predictability is a key consideration in water supply management (USACE, 1991). Results from this investigation showed that the reservoir may yield up to 65 hm^3 per year without failure (i.e. firm yield); above this volume, the reservoir reliability decreases significantly (e.g. 30 % reliability for 75 hm^3 annual yield) and so the reservoir requires of carryover procedures to meet the annual water demand. If the annual yield equals 95 hm^3 (maximum yield capacity), the period of time required to the reservoir recovers from a failure could take up to 12 years. Increasing water demand combines to the scarcity and variability of water resources to generate low resilience to reservoir storage. These aspects impose the greatest challenge to management of the Sauce Grande River, and so require further attention in order to delineate alternatives for reservoir optimization.

3.3. THE DEGREE OF IMPOUNDMENT OF THE SAUCE GRANDE RIVER

Building on reservoir size-yield-performance analysis (McMahon and Mein, 1978; McMahon and Adeloje, 2005; McMahon *et al.*, 2006), this chapter has evaluated the dam potential to release water downstream based on the relationships between historic inflow volumes and the reservoir yield required to meet water demand. The firm yield is 73 % the mean annual inflow volume (89.3 hm^3) and the net inflow equals 1 given annual inflow CV equal to 0.3 (characteristic of temperate regions, McMahon *et al.*, 2007b); this indicates that the reservoir may yield up to 65 hm^3 per year without failure or, in other words, that variations in inflow volumes over time should not compromise

the reservoir to meet annual requirements for water supply.

However, a standardized net inflow volume [m] equal to unity is on the limit between within-year and carryover yield requirements. Storage conservation over time increases significantly as the net inflow decreases below unity (Vogel *et al.*, 1999), so that any variation in the water demand may determine very different reservoir operational procedures alternating between (i) within-year storage procedures (where the reservoir releases a fraction of inflow every year) characteristic of temperate regions, and (ii) carryover storage procedures (where water is conserved to use in further years) more characteristic of semiarid regions (Vogel *et al.*, 1999; McMahon *et al.*, 2007b; McMahon *et al.*, 2007d).

The ratios of reservoir storage and yield to mean annual inflow (S/μ and Y/μ , respectively) for the Paso de las Piedras Reservoir indicated great dam potential to disrupt the longitudinal continuity of the sauce Grande River. First, the active capacity of the reservoir is 3.6 times the mean annual inflow volume; second, the fraction of inflow available to flow release once the annual yield requirements are met is only 0.27 the annual inflow (24.3 hm^3). High storage capacity relative to the hydrologic magnitude of the river and a reservoir yield near 75 % mean inflow volumes are characteristic of water supply reservoirs within semiarid regions of the world (e.g. Australia and South Africa, McMahon *et al.*; 2007d, western USA, Graf, 1999; Vogel *et al.*, 1999; Kondolf and Batalla, 2005; Graf, 2006; Mediterranean countries, Batalla *et al.*, 2004; Hoff *et al.*, 2007; Lorenzo Lacruz *et al.*, 2010; and semiarid regions of Brazil, Güntner *et al.*, 2004), where carryover storage procedures are most likely to occur due to the water scarcity, the high rates of evaporation, the unpredictability of climate and the recurrence of drought.

Results from storage-release analysis revealed that the volume of annual reservoir yield coupled to water losses by evaporation and seepage is greater than the mean annual runoff volume (91.2 hm^3). This indicates that, on average, downstream runoff is fully eliminated due to water retention in the reservoir. Furthermore, simulation for the Drought Management Scenario revealed that reservoir release will occur only under initial conditions of high reservoir storage and for inflow volumes higher than 5-yr inflow (128.8 hm^3); in conditions of low initial storage, it could take more than 6 years before any flow release occurs. Elimination or extreme reduction of runoff below the impoundment has greatest implications for the overall hydrology and morphology of the river downstream; these implications are revisited robustly in the following chapters.

3.4. APPLICABILITY OF THE METHODS USED IN ANALYSIS

The objective of this chapter was to quantify the degree of flow regulation induced by the Paso de las Piedras Dam on the Sauce Grande River. To meet this purpose, this chapter has examined how the reservoir volume responds to variations in inflow components over time, and has quantified the predictability of flow release relative to such variations. The ultimate purpose of this investigation was to identify the dam potential to disrupt the hydrological continuity of the Sauce Grande River relative to the capacity of its reservoir and human requirements for water supply.

A simple Water Balance Model based on the model of Yeung (2004) for the Fena Valley Reservoir has been developed for the Paso de las Piedras Reservoir to capture dynamics in the reservoir hydrology over time. In the context of the present research, the model had triple applicability. First, it permitted to verify the viability of the variables used in the water balance equation implemented (Sokolov and Chapman, 1974), as well as the reliability of the data series used in analysis. Second, as the model simulates variations in water storage relative to interactions between inflow and outflow components, any component of the balance equation may be estimated based on the relationships between the remaining components. Third, the relationships between inflows, outflows and water storage for the Paso de las Piedras Reservoir provided the basis to simulate scenarios of flow release as a function of the reservoir size, function and performance. The model performance to simulate variations in reservoir storage, yield and release was suitable, and the results provided meaningful information on the reservoir dynamics relative to its function for water supply. These aspects validate the applicability of the model as tool for dam management.

Although the balance equation used in the Water balance Model is fairly simple, the measure of the reliability of hydrologic variables was more complex. Model results during the calibration period were very low (2 to 4 %); however, large errors were detected in series of measured flow data. Furthermore, the reliability of climatic data was moderate to low and evaporation processes were estimated; understanding the magnitude of evaporation from water supply reservoirs in semiarid regions is an important component of reservoir management (Lowe *et al.*, 2009). These aspects impose a high degree of uncertainty relative to (i) the viability of the variables involved in the balance equation, and (ii) the reliability of the model results outside the period used for calibration. This investigation provided a consistent basis on which to base further research efforts to improve the model performance, especially based on series of gauged data over the long term.

Despite the high degree of uncertainty relative to the accuracy of the results, the Water Balance Model provided a consistent platform to perform reservoir size-yield-performance analysis (McMahon and Mein, 1978; McMahon and Adeloje, 2005; McMahon *et al.*, 2006). Although investigating these relationships is way beyond the scope of the present research, the interest of this approach was that it permitted to estimate the dam potential to flow release as a function of the reservoir reliability to meet its vital purpose for water supply. Assessing these relationships is very important from a dam management perspective; such understanding is at the basis of future planning to improve the reservoir performance to meet both yield and release requirements.

Storage-yield analysis provides information on three key variables defining the reservoir performance to meet a target demand: the active reservoir capacity, the firm reservoir yield, and the reservoir reliability (McMahon *et al.*, 2007d). Meaningful information on the impounding potential of the dam was obtained building on these relationships. Evaluation of the degree of impoundment exerted by the Paso de las Piedras dam used three simple statistics: (i) the ratio of storage capacity to mean annual inflow, (ii) the ratio of reservoir yield to mean annual inflow, (iii) and the ratio of reservoir release to mean annual inflow.

The impact of the reservoir operation on the hydrologic conditions downstream will depend primarily upon the ratio of storage capacity to mean annual inflow (Batalla *et al.*, 2004; Kondolf and Batalla, 2005; Graf, 2006). However, in reservoirs operating for water supply within semiarid regions, the magnitude and the frequency of flow release downstream will be highly constrained by the ratio of reservoir yield to mean annual inflow (Vogel *et al.*, 1999; Vogel *et al.*, 2007). Ultimately, the fraction of inflow that is not yielded to meet human needs may be considered to be released downstream (Vogel *et al.*, 2007). In spite of their simplicity, these metrics provide an essential comparison between the hydrologic magnitude of the river and the hydrologic magnitude of the dam, and hence on the dam potential to reduce runoff downstream (Graf, 2006).

3.5. CONCLUSIONS

This chapter provided substantial information on the overall hydrology of the Paso de las Piedras reservoir and on the dam potential to disrupt hydrological processes along the Sauce Grande River. Analysis revealed that reservoir inflows describe relative annual seasonality with high inter-annual variations, whereas reservoir outflows (except for water release) describe marked annual seasonality with high-inter-annual constancy. Inspection for variations in water storage revealed high fluctuations from month-to-month, and correlation analysis suggested that such variations were strongly related to variations in inflow components; the magnitude, frequency and duration of episodes of dam release were highly dependent on inflow volumes relative to the actual storage within the reservoir.

The patterns of flow regulation exerted by the Paso de las Piedras Dam are intrinsic to the dam purpose for water supply within a dry sub-humid climate region, where droughts are recurrent and severe with low predictability. Water storage is conserved for periods of drought, and reservoir evacuation occurs almost exclusively during sequences of humid climate. Inter-annual variations in water availability to storage impose the greatest challenge to reservoir operation, and so the assessment of processes underlying climate variability requires special attention.

CHAPTER

4

DAM IMPACTS OF FIRST ORDER

CONTENTS

1 Methods

2 Results

Dam impacts on the river flow regime

Changes in the attributes of the river flow regime

Changes in the environmental components of flow

Flow predictability

Dam impacts on the river water temperature

Changes in temporal patterns of river water temperature

Changes in the magnitude and timing of water temperature regimes

Climatic sensitivity of water temperature regimes

Other factors influencing river thermal variability

3 Discussion and Conclusions

Previous results revealed that reservoir inflows are driven by varying climate conditions inducing strong intra- and inter-annual fluctuations in the effective water available for storage purposes. On the other hand, reservoir outflows are constrained by the dam purpose for water supply; large volumes of water are withdrawn annually (73 % of the mean annual runoff) and the remaining volume is conserved within the reservoir for periods of drought.

The reservoir storage capacity is four times the mean annual inflow volume. This implies great dam potential to absorb the full range of flows within its reservoir, and hence to disrupt longitudinal fluvial processes over a range of time scales. In addition, large reservoir storage capacity combines to dam operational procedures (conservation storage) to generate long water residence times, which lead to changes in the water properties by reservoir stratification and eutrophication. Regulation and alteration of running waters from headwater sources will impact very seriously on the hydrology and water quality of the river downstream.

This chapter evaluates the dam impacts of first order, i.e. the impacts that occur immediately after dam closure and that depend directly on the dam operational procedures and the outlet type. Analysis focuses on two of the three primary changes recognized by Petts (1984) namely changes in the river flow regime and the river water quality with focus on the river thermal regime. The assessment of these variables was strongly motivated by the actual river state below the impoundment (Fig. 4.1). Changes on the sediment load of the river downstream were considered of less concern relative to the magnitude of changes in the former two variables; note, the sediment trapping efficiency of the dam was assumed nearly as great as 100 % of the sediment delivered from headwater sources.

Analysis of change in the river flow regime and in the river water temperature builds on the quantification of two key parameters based on Ward and Stanford (1993; 1995a):

- (i) the magnitude of change, i.e. the intensity of change relative to natural conditions, and
- (ii) the discontinuity distance, i.e. the distance over which changes are apparent.

Quantification of changes in terms of magnitude and distance from dam closure was based on the comparison of river flow and thermal conditions occurring synchronically upstream and downstream from the impoundment over time.

Results are structured into two sections assessing changes in the river flow regime and the river water temperature separately. Interconnections between both variables are examined in the Discussion section.



Figure 4.1: Actual state of the Sauce Grande River for two reference reaches located upstream and downstream from the Paso de las Piedras Dam.

1.1. QUANTIFYING DAM IMPACTS ON THE RIVER FLOW REGIME

Dam impacts on the downstream river flow regime were assessed using a methodological suite including (i) the Indicators of Hydrologic Alteration approach (IHA, Richter *et al.*, 1996), (ii) the Range of Flow Variability approach (RVA, Richter *et al.*, 1997), and (iii) the Environmental Flow Components approach (EFC, Mathews and Richter, 2007). Combined, these approaches allow inspecting the degree to which the river flow regime below the dam has been altered relative to the ‘natural’ unregulated flow regime over time.

For the purpose of this research, the IHA, RVA and EFC methods were adapted to provide a comparison between unregulated (upstream) and regulated (downstream) daily flow conditions over the period 1989-2010. This period was dictated by the availability of concurrent streamflow data for both river systems; the use of the same period of time in comparisons was considered more suitable due to the effects that climate variability may have on the results. Synchronic comparison of flow conditions permitted to determine unregulated attributes flow that should be repeated downstream in case of absence of hydrological alteration.

Series of flow data used in analysis include (i) daily flow discharge at Chacra La Blanqueada GS (upstream), and (ii) daily flow discharge at Bajo San José (downstream). Flow data for the river upstream was simulated using RainOff-empirical modelling, and flow data for the river downstream was estimated based on rates of flow release (see Chapter 2 for detailed information on simulation and estimation procedures). As unregulated flow data were available over the period 1956-2010, this series were used to characterize major attributes of flow such as the magnitude of characteristic flows, the thresholds for bankfull flow and overbank flooding and the distribution of flows over the water year, among other variables.

The properties of the IHA, RVA and EFC methods are explained below. In all cases, analysis was performed using the IHA Program of The Nature Conservancy and Smythe (2001).

1.1.1. Computing flow statistics

Flow attributes for the regulated and the unregulated rivers were quantified using the Indicators of Hydrologic Alteration approach (IHA). IHA is based on a set of descriptive statistics of flow based on the paradigm of natural flow regime (Poff *et al.*, 1997). Hence, the method considers the five attributes of the river flow regime that are critical for the geomorphic and ecologic integrity of the river system: the magnitude, the timing, the frequency, the duration and the rate of change of flows. As shown in Table 4.1, flow regime attributes are described using five groups of metrics.

Groups 2, 3 and 4 focus on the magnitude, duration, timing, and frequency of extreme flow events having the greatest influence on the river morphology and the stream

ecosystems, whereas Groups 1 and 5 measure the overall behaviour of flows decisive to the geomorphic and ecologic structure of the river system. In spite of the simplicity of these metrics, they encapsulate the overall hydrologic behaviour of the river (Graf, 2006) face to the lack of previous studies on the river flow regime, and hence have great potential to quantify dam impacts on the river hydrology downstream. Most of the metrics presented in Table 4.1 were computed twice (i) to characterize the main attributes of the natural flow regime (*sensu* Poff *et al.*, 1997) over the long term (1950-2010), and (ii) to quantify shifts in each attribute between regulated and unregulated flow conditions over the period 1989-2010.

Table 4.1: Descriptive statistics of flow included within the IHA method and implications of each metric for the river morphology and the stream ecology. After Richter *et al.* (1996) and Graf (2006).

IHA group	Hydrologic metrics	Geomorphic implications	Ecologic implications
<i>Group 1:</i> Magnitude of monthly water conditions	Mean (or median) for each calendar month	Size of active channel Channel pattern Geomorphic complexity and functional surfaces	Habitat availability or suitability Environmental constancy and/or contingency
<i>Group 2:</i> Magnitude and duration of annual extremes	1-, 3-, 7-, 30-, 90-day annual maximum flow 1-, 3-, 7-, 30-, 90-day annual minimum flow	Space available for river processes: floodplain size and overall channel morphology Dominant particle size of bed materials Limit for sediment transport and storage Channel maintenance Particle size distributions of bed material	Environmental stress and disturbance (or species triggers) Structure of physical habitat conditions, plant species distribution and colonization
<i>Group 3:</i> Timing of annual extremes	Julian date of 1-day maximum (or minimum)	Interactions between erosive flows, stabilizing vegetation and deposition processes	Seasonal nature of environmental stress and/or life-cycles strategies
<i>Group 4:</i> Frequency and duration of high and low pulses	No. of high (or low) pulses per year Mean duration of high (or low) pulses	Channel mobility, change in functional surfaces and depositional regimes Magnitude of erosive and depositional processes	Pulsing behaviour of environmental variation Lateral (channel-floodplain) exchange
<i>Group 5:</i> Rate and frequency of changes in water conditions	Mean of positive (or negative) differences between consecutive days No. of raises (or falls)	Spatial extent of active area of functional surfaces Overall erosion/stability of channel and banks	Rate and frequency of intra-annual cycles of environmental variation Entrapment of organisms and drought stress

1.1.2. Assessing the range of flow variability

The Range of Variability Approach (RVA) determines the hydrological requirements of a river system (Richter *et al.*, 1997) based on ranges of natural variability for each flow attribute measured in Table 4.1. Ranges of variability are calculated using parametric (or non parametric) measures of central tendency and deviation ($\pm 1\sigma$ or inter-quartile range). These values, expressed as a range of acceptable values for each flow attribute, represent the *targets* for flow management (Fig. 4.2). The fundamental concept of RVA is that the regulated river should be managed in such way that the annual value of each flow attribute falls within the range of variation of such attribute under natural conditions (Richter *et al.*, 1998).

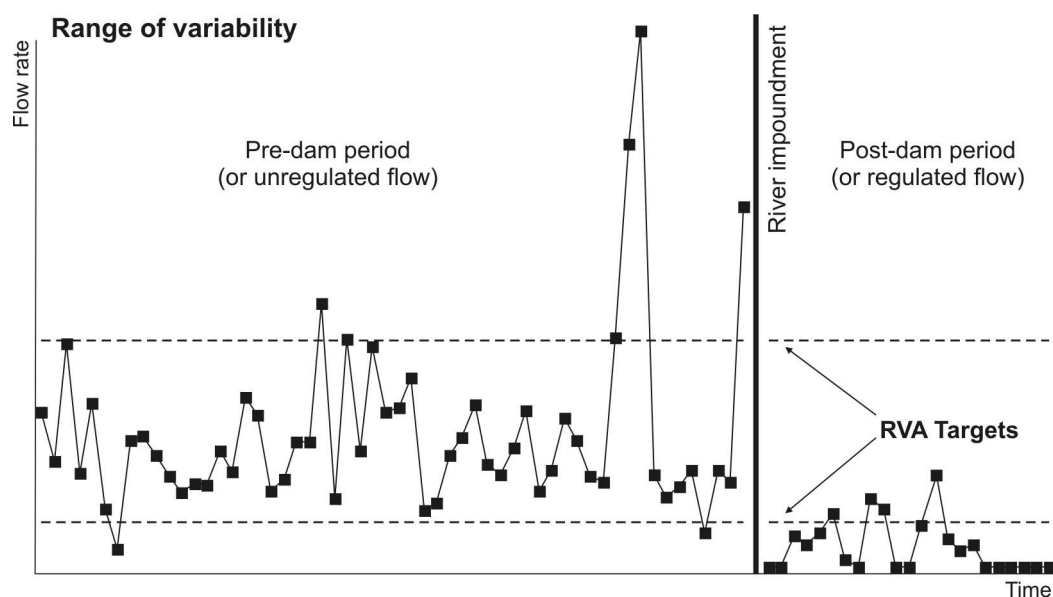


Figure 4.2: Conceptual scheme of the Range of Variability Approach (RVA). Modified from Richter *et al.* (1997).

1.1.3. Evaluating Environmental Flow Components

The Environmental Flow Components approach (EFC) is the latest component included in the IHA methodological suite. EFC was developed by Mathews and Richter (2007) to provide an additional hydrological characterization based on five major flow states that are critical for the river morphology, ecology and water quality (Fig. 4.3; Table 4.2). The interest of the EFC approach relies on its double applicability. First, the method divides and classifies the hydrograph into sets of geomorphic and ecologically significant flow conditions. Second, the method permits to calculate the magnitude, frequency, duration, timing and rate of change of a given flow state over time.

The threshold for each EFC category was calculated based on long-term series (1956-2010) of daily flow discharge for the unregulated river upstream. The magnitude of high flows for a given return period (i.e. the flood frequency) was estimated by fitting series of annual maximum daily flow to the Gumbel extreme value distribution (Gumbel, 1958).

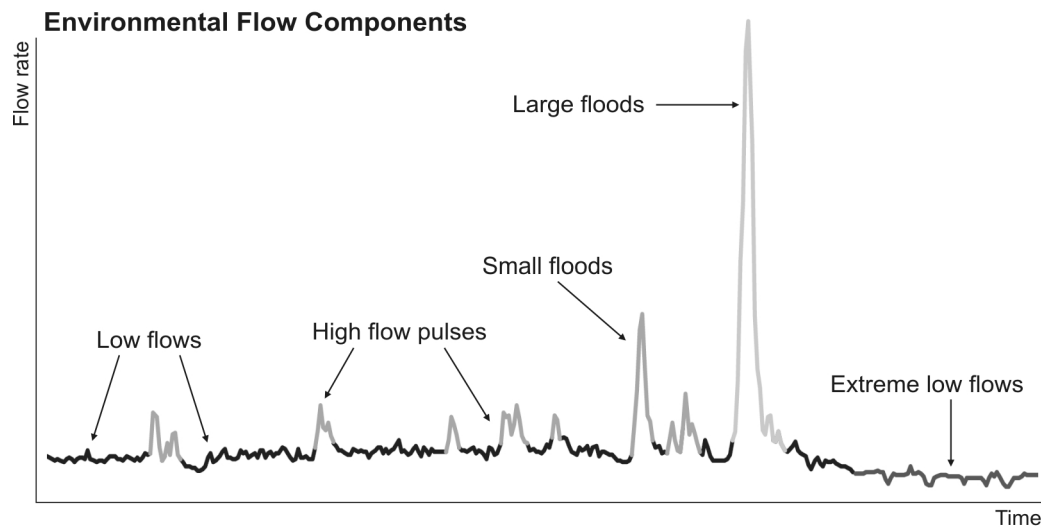


Figure 4.3: Conceptual scheme of the Environmental Flow Components approach (EFC). After Mathews and Richter (2007).

Table 4.2: Environmental Flow Components and implications for the river morphology, ecology and water quality. After Hersh and Maidment (2006) and Mathews and Richter (2007).

	EFC	Hydrologic definition	Geomorphic implications	Ecologic implications	Water quality implications
LOW FLOWS ($< 50^{\text{th}}$ percentile)	Extreme low flows (subsidence flows)	Infrequent low flows (10^{th} percentile of all low flows)	Deposition of small-sized material	Restricted aquatic habitat with limited connectivity	Unsuitable in-channel water quality
	Low flows (base flows)	Median flow conditions, with variability	Soil moisture and groundwater table maintenance	Suitable aquatic habitat with longitudinal connectivity	Suitable in-channel water quality
HIGH FLOWS ($> 75^{\text{th}}$ percentile)	High flow pulses	In-channel high flows of short duration	Channel maintenance, prevent vegetation encroachment	Lateral connectivity (near-channel water bodies)	Restore in-channel water quality after prolonged low flow
	Small floods	Flows greater than the Q_2 (overbank flooding)	Floodplain maintenance, lateral mobility	Lateral connectivity (river-floodplain), riparian maintenance	Restore water quality in floodplain water bodies
	Large floods	Flows greater than the Q_{10} (floodplain flooding)			

1.1.4. Assessment of the river flow predictability

The metrics used to quantify the predictability of natural variations in daily flows were based on Poff and Ward (1989) and were computed using the IHA program. The flow predictability index was used to measure the temporal predictability of flow states using two additive components: the flow constancy (measure of the flow invariance; C) and the flow contingency (measure of the flow periodicity; M). The flow predictability index ranges from 0 to 100 %, where 100 % indicates either fairly uniform flows where the constancy proportion (C) is high, or variable flows with fixed periodicity where the contingency proportion (M) is high.

The flood regime (i.e. the regime of flows falling above the Q_2 threshold) was evaluated using three metrics: (i) the flood frequency, calculated as the mean number of floods per year, (ii) the flood predictability, calculated as the maximum proportion of all floods falling in any 60-day period common to all years in the record, and (iii) the flood-free season, calculated as the maximum number of 365 days over all the water years during which no floods occurred.

1.1.5. Quantification of the degree of hydrologic alteration

The set of flow statistics presented in Table 4.1 were calculated for the unregulated and the regulated river based on concurrent series of daily flow data over the period 1989-2010. The natural ranges of variability in each flow attribute were estimated based on series of unregulated flow upstream.

The degree of hydrological alteration downstream was estimated depending on whether the values of regulated flow fall within the range of natural variability calculated for a given flow attribute. The equation used is expressed as follows:

$$HA = \frac{F_O - F_E}{F_E} \quad (4.1)$$

where $[HA]$ is the degree of hydrological alteration for a given flow attribute, $[F_O]$ is the frequency of years in which the flow value observed downstream fell within the target range, and $[F_E]$ is the frequency of years for which such value was expected to fall within the target range. The hydrological alteration for a given attribute equals zero if $F_O = F_E$; positive deviations of HA indicate that flow values fall inside the RVA target more often than expected, and negative deviations indicate the opposite.

To quantify the magnitude of hydrological alteration we used simple measures of dispersion or variation, depending on whether flow statistics were computed using non-parametric (medians) or parametric (means) statistics, respectively. The coefficient of dispersion $[CD]$ for each flow attribute were calculated as follows:

$$CD = \frac{(75^{th} \text{ percentile} - 25^{th} \text{ percentile})}{median} \quad (4.2)$$

The coefficient of variation $[CV]$ and the magnitude of change $[MC]$ are the analogous measures of deviation for parametric statistics, where CV is expressed as shown in Equation 4.3.

$$CV = \frac{\sigma}{\mu} \quad (4.3)$$

1.2. QUANTIFYING DAM IMPACTS ON THE RIVER WATER TEMPERATURE

Assessment of the dam impacts on the water quality of the river downstream focuses on the river water temperature, a fundamental parameter of water quality and stream ecology (e.g. Webb, 1996; Poole and Berman, 2001; Caissie, 2006; Webb *et al.*, 2008; Hannah *et al.*, 2008b). Longitudinal patterns of other important water properties such as dissolved oxygen, pH, electrical conductivity and diatom composition were evaluated by Beauger (2012) and are discussed briefly.

1.2.1. Temperature data collection

Eight temperature data loggers (Hobo Pendant Temperature, ONSET Computer Corporation) were deployed within the main river channel above and below the impoundment. Water temperature sampling sites were selected based on distance from the dam, site accessibility, channel morphology and riparian vegetation. Additionally, one logger was installed in the weir draining reservoir seepage into the main channel, and two loggers were installed in two oxbow lakes below the impoundment. All the data loggers were cross-calibrated and clocks synchronised (Hannah *et al.*, 2009) to record water temperature every 15 minutes during summer 2009 and winter 2010.

Hourly observations of air temperature were provided by ADA for two meteorological stations (Saldungaray MS and Paso de las Piedras MS) located upstream and adjacent to the reservoir, respectively. The use of two stations was considered appropriate to highlight any meteorological variability due to differences in altitude and exposure along the river. Rainfall and river flow discharge records were also provided by ADA. However, these data were excluded from the analysis because of the very low variability of river flow across the two monitoring periods.

Two 30-day data sets of continuous hourly records were assembled for all air and water temperature gauging sites. The time series span a hot period recorded during austral summer 2009 ranging from late February (day 58) to late March (day 87), and a cold period recorded during austral winter 2010 ranging from late June (day 173) to late July (day 202). These periods of high quality data were chosen to assess water temperature sensitivity under strong meteorological influence.

1.2.2. Time series assessment and thermal metrics

Patterns of air and water temperature were inspected by absolute differences in daily temperatures during the summer and winter sample periods. The descriptive statistics used for thermal characterization of the time series (Table 4.3) were adapted from Chu *et al.* (2010). They include a set of temperature metrics equivalent to those proposed by

Poff *et al.* (1997) to characterize the five critical components of the river flow regime. Note, high and low daily temperature in Table 4.3 correspond to the 75th and 25th percentiles, respectively. Additionally, station-to-station differences in water temperature were inspected by plotting the seasonal mean, maximum and minimum temperature for each site *versus* distance from the dam. Seasonal maximum and minimum values correspond to the daily means recorded on the hottest and the coldest days of each series, respectively.

Table 4.3: Metrics used in the characterization of air and water temperature series.

Thermal regime component	Temperature metric	Ecological and water quality relevance
Magnitude	Mean daily temperature (°C)	Absolute thermal values defining specific biological, physical and chemical reactions/responses
	Maximum daily temperature (°C)	
	High daily temperature (°C)	
	Median temperature	
	Low daily temperature (°C)	
	Minimum daily temperature (°C)	
Frequency	Area under the mean seasonal temperature of all gauging stations (°C)	How often thermal events of a particular magnitude occur
Timing	Day of maximum (Julian day)	When do temperatures of a certain magnitude occur, having specific ecological and water quality implications
	Day of minimum (Julian day)	
	Start of high daily temperature (Julian day)	
	Start of low daily temperature (Julian day)	
Duration	Length of high temperature (number of days)	Period of time associated with temperature of a certain magnitude
	Length of low temperature (number of days)	
Rate of change	Mean daily range (°C)	How quickly temperature changes in magnitude
	Maximum daily range (°C)	
	Minimum daily range (°C)	

1.2.3. Classification of diurnal regimes of air and water temperature

Daily patterns in air and water temperature were inspected using a cluster-based classification based on relative differences in the shape (timing) and the magnitude (size) of diurnal regimes. The Regime Shape and Magnitude Classification technique (RSMC) was developed by Hannah *et al.* (2000) for hydrograph classification, and has been widely evaluated in many studies assessing river flow, air temperature and rainfall regimes over a range of time scales (e.g. Harris *et al.*, 2000; Bower and Hannah, 2002; Bower *et al.*, 2004; Kansakar *et al.*, 2004; Hannah *et al.*, 2005). This study represents the first application of the RSMC approach to the assessment of river water temperature regimes.

To classify the *regime shape* regardless of the absolute magnitude of the thermographs, hourly air and water temperature records for both seasons were standardized by day and

by station using z-scores ($\mu = 0$, $\sigma = 1$). This gave a data matrix with 24 columns (hourly temperature observations) times 570 lines (station-days); 300 station-days corresponded to the summer period (10 gauging stations x 30 days) and 270 station-days corresponded to the winter period where one data logger was lost (9 gauging stations x 30 days). Station-days for air and water temperature during summer and winter were classified together into groups of similar diurnal regime form.

The *magnitude classification* was based upon four indices: the daily mean, maximum, minimum, and variance of hourly temperatures. These indices were calculated daily for each station and season, regardless of the timing of the thermographs. Within-station differences in each index were standardized separately for each 30-day observation period using z-scores. Station-days of air and water temperature during summer and winter were classified together into groups of similar regime magnitude, i.e. similarities in the behaviour of the four indices.

For both regime shape and magnitude, classification was achieved using Hierarchical Cluster Analysis (HCA) and Ward's linkage method. Ward's algorithm was selected because it produced relatively dense clusters with small within-group variance (c.f. Hannah *et al.*, 2005). The structure of the cluster dendrogram and breaks of slope in the agglomeration schedule plot were used to estimate the appropriate number of clusters (regime classes).

1.2.4. Quantification of the climatic sensitivity of diurnal water temperature regimes

We used the novel Sensitivity Index [*SI*] to evaluate the sensitivity of water temperature regimes to air temperature conditions during the summer and winter periods. The *SI* was devised by Bower *et al.* (2004) to complete the conditional entropy analysis developed by Krasovskaia (1996) and Krasovskaia and Saelthun (1997). The index works with any previous regime classification, and permits to consider regime shape and magnitude attributes separately. Same as the RSMC approach, this study represents the first application of the *SI* to water temperature assessment.

The computation of the *SI* uses a set of six equations calculated in two stages. First, the *stability* of air and water temperature regimes by site is quantified using an Equitability Index [*EI*]. Based on the concept of entropy (Krasovskaia, 1995), *EI* considers the probability of occurrence of one regime class against all the possible regime classes as expressed in Equation 4.4. Second, the associations between water and air temperature regime classes are evaluated as the *conditional probability* [$P(Y_j|X_i)$] of observing a particular water temperature regime [Y_j] as conditioned by each air temperature regime [X_i] and vice versa, i.e. $P(X_i|Y_j)$.

$$EI = \frac{-\sum_{i=1}^n P_i \ln P_i}{\ln n} \quad (4.4)$$

The *SI* is computed based upon the ratio of *equitability* [*E*] between water and air temperature regimes ($E[Y]:E[X]$). The ratio of equitability defines two different scenarios of sensitivity as follows:

- If $E(Y) > E(X)$, then Equation 4.5 is used to produce a value between 0 and +1 (positive scenario).

$$SI = \frac{1}{2(n_x n_y)} \left(- \sum_{i=1}^{n_x} \left(\frac{P(Y_j/X_i) \ln P(Y_j/X_i)}{\ln n_y} \right) + \left(\frac{P(X_i/Y_j) \ln P(X_i/Y_j)}{\ln n_x} \right) \right) \quad (4.5)$$

- If $E(Y) < E(X)$, then Equation 4.6 is used to give a value between -1 and 0 (negative scenario).

$$SI = -1 - \frac{1}{2(n_x n_y)} \left(\sum_{i=1}^{n_x} \left(\frac{P(Y_j/X_i) \ln P(Y_j/X_i)}{\ln n_y} \right) + \left(\frac{P(X_i/Y_j) \ln P(X_i/Y_j)}{\ln n_x} \right) \right) \quad (4.6)$$

Positive and negative scenarios represent the direction of sensitivity (Fig. 4.4). Negative SI values indicate that a limited number of water temperature regimes occur under a variety of air temperature conditions. Conversely, positive SI values indicate that a variety of water temperature regimes occur under similar air temperature conditions. SI values approaching -1 or +1 both designate levels of insensitivity; the difference is in the direction of the associations. Values closer to zero indicate a sensitive situation, where a single water temperature regime is observed under particular air temperature conditions (Bower *et al.*, 2004).

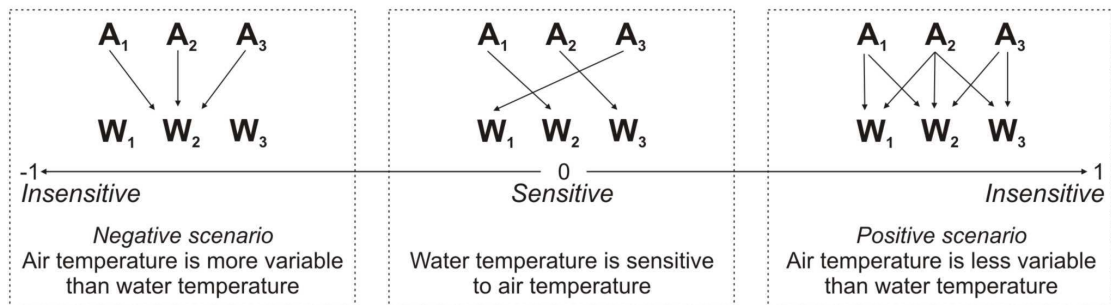


Figure 4.4: Conceptual illustration describing the direction and the level of meteorological sensitivity of water temperature regimes. Modified from Bower *et al.* (2004).

1.2.5. Inspection of structural characteristics of the stream

The influence of the stream structure on seasonal and spatial variations in river water temperature was determined using principal component analysis (PCA). In spite of the reduced size of the population data (eight water temperature sites), PCA was performed to reduce variables of potential influence into a set of linear combinations of uncorrelated factors reflecting a fraction of variability in water temperature regimes.

The variables selected to use in PCA involve a set of indicators of topographic influence (riparian vegetation cover, stream orientation and site elevation), morphologic influence (bed channel slope, number of upstream pools and riffles, wetted area and the width:depth ratio), and groundwater influence (electrical conductivity of running waters).

The value assigned to each control variable was calculated as mean of observations

made *in situ* or percentage of surface area within riparian zones. Riparian zones were digitized in ArcGIS over a straight river section of 1500 m-length upstream of each water temperature site; this length was selected relative to the total length of the sample reach (15 km) and based on common distances used in other studies linking riparian buffers to stream temperature (e.g. Frimpong *et al.*, ; Moore *et al.*, 2005; Malcolm *et al.*, 2008; Hannah *et al.*, 2008a; Chu *et al.*, 2010; Groom *et al.*, 2011). The optimal width of the riparian zone depends on many variables such as dominant tree species, channel morphology and stream style (Moore *et al.*, 2005); as the overall river morphology exhibits a single meandering channel, the lateral limits of the riparian zone were defined by the boundaries of the active (bankfull) channel.

2.1. DAM IMPACTS ON THE DOWNSTREAM RIVER FLOW REGIME

Dams interrupt the hydrologic continuity of streams and rivers by intercepting flow from the headwater areas (Kondolf, 1997) and by controlling the patterns of flow discharge within the river downstream (Petts, 1984). Studies assessing the effects of dams on the river flow regime downstream document reduction in the magnitude and frequency of floods, increase in the permanence of base flows and alteration of the flow seasonality (e.g. Batalla *et al.*, 2004; Kondolf and Batalla, 2005; Magilligan and Nislow, 2005; Graf, 2006).

This section evaluates the impacts of the Paso de las Piedras Dam on the flow regime of the Sauce Grande River based on the understanding of the upstream 'natural' flow regime (*sensu* Poff *et al.* 1997). The degree of hydrological alteration induced by the dam is examined based on comparisons between concurrent flow conditions for the unregulated and the regulated rivers.

2.1.1. Changes in the attributes of the river flow regime

We used a set of metrics describing the flow regime magnitude, timing, frequency, duration and rate of change (Table 4.1) to quantify upstream-downstream shifts in the river hydrology. The *magnitude* of flows refers to the quantity of water per unit time at any given time interval. Flows of a given magnitude occur with a certain regularity (*timing*) and have an associated *frequency* (or recurrence) and *duration* (or persistence). The degree to which flow *changes* from one magnitude to another indicates the regime (in)stability throughout the annual cycle (Richter *et al.*, 1996; Poff *et al.*, 1997).

Magnitude and timing of monthly flows

The distribution of mean monthly flow over the water year (Fig. 4.5) indicated a complex river flow regime (*sensu* Pardé, 1933) in spite that it originates exclusively from rainfall. The hydrograph peaked in spring (Oct.-Nov.) and in late summer-early autumn (Mar.-Apr.), in connection to the rainiest months of the rainy season. The period of low flow was coincident with the dry season (late autumn and winter) and recorded the lowest levels in July. A secondary episode of low flow was observed during the rainy season in connection to high evaporation rates characteristic of early summer months (Jan.-Dec.).

Mean monthly flow was $2.5 \text{ m}^3 \cdot \text{s}^{-1}$ with high variability ($CV = 1.1$). Mean monthly flows over the monitoring period were highly scattered, especially during the spring season ($1.0 < CV < 1.4$); the magnitude of median flows and monthly coefficients of dispersion were low for all months ($0.4 < CD < 0.5$). High coefficients of variation and low coefficients of dispersion suggest coupled variability and constancy in the behaviour of the unregulated river, where episodes of low flow with long duration are alternated by episodes of high flow with short duration and high magnitude.

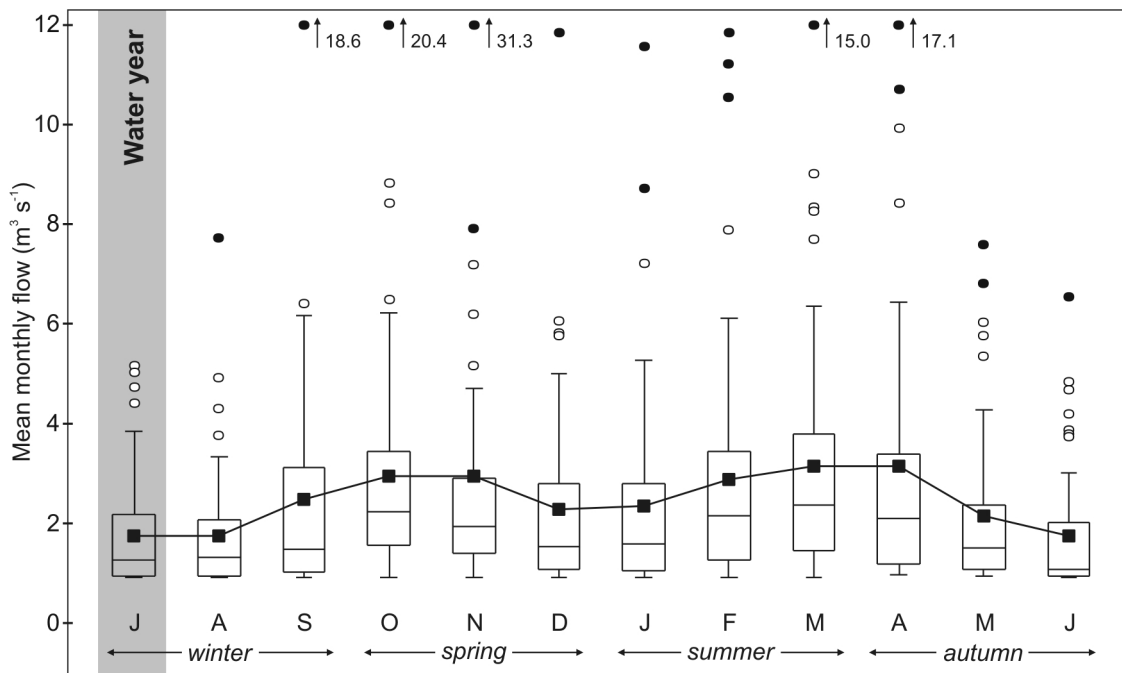


Figure 4.5: Annual distribution of mean monthly flow within the unregulated Sauce Grande River over the period 1956-2010. The water year starts in July.

The annual hydrograph below the dam was clearly depressed (Fig. 4.6; Table 4.4). Mean monthly flow was reduced near to or below the lowest threshold of natural variability for most months, except for the month of July where mean monthly flow was increased by 10 %. Flow reduction was moderated to low during spring months (e.g. 20 % in November) and peaked during late summer months (66 %). In addition, monthly means fell outside the natural range of variability for many years and, as a result, indices of hydrologic alteration (HA) were negative for all months.

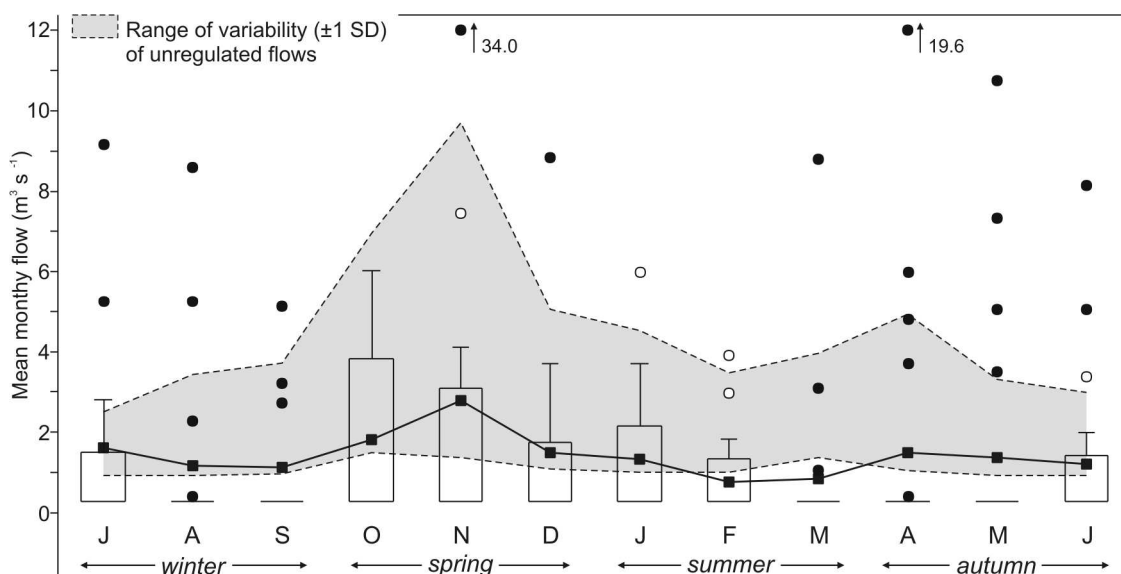


Figure 4.6: Annual distribution of mean monthly flow within the regulated river over the period 1989-2010. Ranges of variability were calculated using the same period of time.

Median flow was equal to minimum flow ($0.28 \text{ m}^3 \cdot \text{s}^{-1}$) for all months (Fig. 4.6), and the inter-annual persistence of minimum flow during autumn and late winter months was greater than 75% (i.e. the third quartile). This indicated notable increase in the low-flow duration relative to the unregulated river upstream.

Persistence of low flows within- and between-years ultimately contributes to alter the hydrograph seasonality by suppression of flow variability throughout the water year. Long-term monthly means revealed that summer peaks were suppressed, spring peaks were reduced and delayed, and winter minima were increased. Conceivably, mean monthly flows provide a better expression of change in the flow seasonality because they are equally affected by episodes of flow release during humid years and persistence of low flows during dry years.

Table 4.4: Changes in the magnitude of mean monthly flow ($\text{m}^3 \cdot \text{s}^{-1}$) from the unregulated river upstream to the regulated river downstream over the period 1989-2010. Significant values per metric in bold.

Month	Unregulated river		Regulated river		Rate of Change		Hydrological Alteration
	Means	C. Var.	Means	C. Var.	Magnitude	%	
Jul	1.48	0.69	1.63	1.69	0.15	10.2	-0.94
Aug	1.88	0.84	1.15	1.87	-0.72	-38.5	-0.94
Sep	2.18	0.70	1.13	1.52	-1.05	-48.0	-0.86
Oct	3.08	1.27	1.81	1.21	-1.27	-41.2	-0.47
Nov	3.48	1.79	2.78	2.54	-0.70	-20.2	-0.59
Dec	2.41	1.10	1.48	1.71	-0.93	-38.6	-0.73
Jan	2.23	1.03	1.33	1.37	-0.90	-40.2	-0.71
Feb	2.25	0.55	0.78	1.26	-1.47	-65.5	-0.71
Mar	2.43	0.63	0.83	2.21	-1.60	-65.8	-0.94
Apr	2.56	0.93	1.51	2.19	-1.05	-40.9	-0.86
May	1.91	0.74	1.39	1.96	-0.52	-27.4	-1.00
Jun	1.59	0.89	1.22	1.63	-0.37	-23.3	-0.87

Magnitude, timing and duration of annual flow extremes

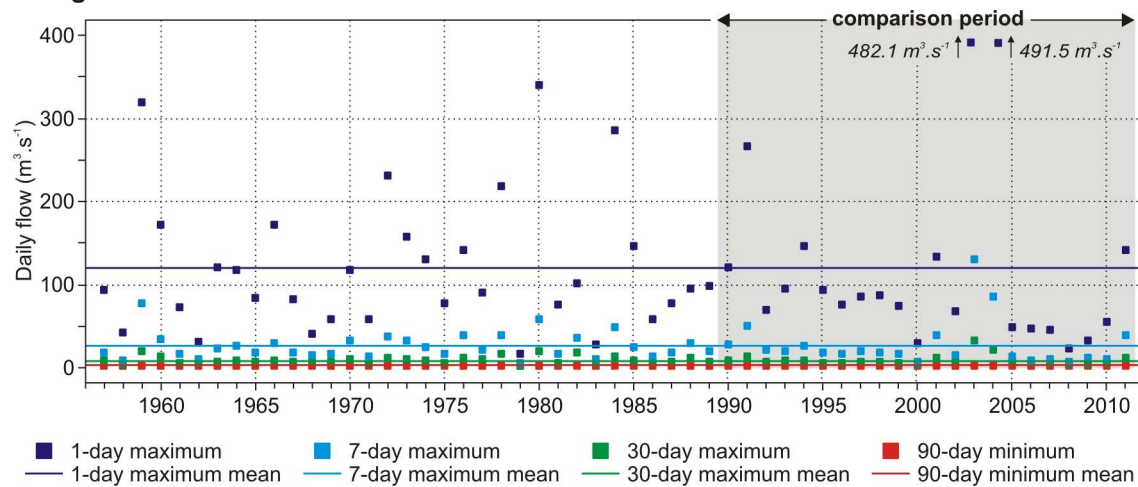
The magnitude and timing of annual flow extremes were inspected for various flow durations including daily (1-day), weekly (7-day), monthly (30-day) and seasonal (90-day) time scales. For a given year, 1-day maximum (or minimum) flow is the highest (or lowest) daily flow; multi-day maximum (or minimum) flow is the highest (or lowest) flow averaged over the multi-day scale of duration.

The distribution of annual flow extremes over the entire monitoring period (1956-2010) gave evidence of strong intra- and inter-annual variability in the flow regime magnitude (Fig. 4.7). Annual maxima were highly scattered for most years; the ratio of annual maxima to annual means averaged 44.6 and peaked to 157.7 in 2003. The flashy character of flows was evidenced by the reduced magnitude of 7- day maxima relative

to 1-day maxima; differences in magnitude of 1-day maxima respect to 30-day maxima were notable, and 90-day maxima (not shown in figure) were nearly as low as 90-day minima for most years of record. Annual minima were invariant for all the durations considered in analysis, which indicated that the base flow season has very long duration.

The mean date of maximum flow was day 80 (21st March) and the mean date of minimum flow was day 207 (26th July). Overall, dates of maximum and minimum flow were synchronized with the timing of the annual hydrograph; however, dates of annual extremes were highly scattered in time so that these statistics must be read with caution.

Unregulated river - annual extremes



Regulated river - annual extremes

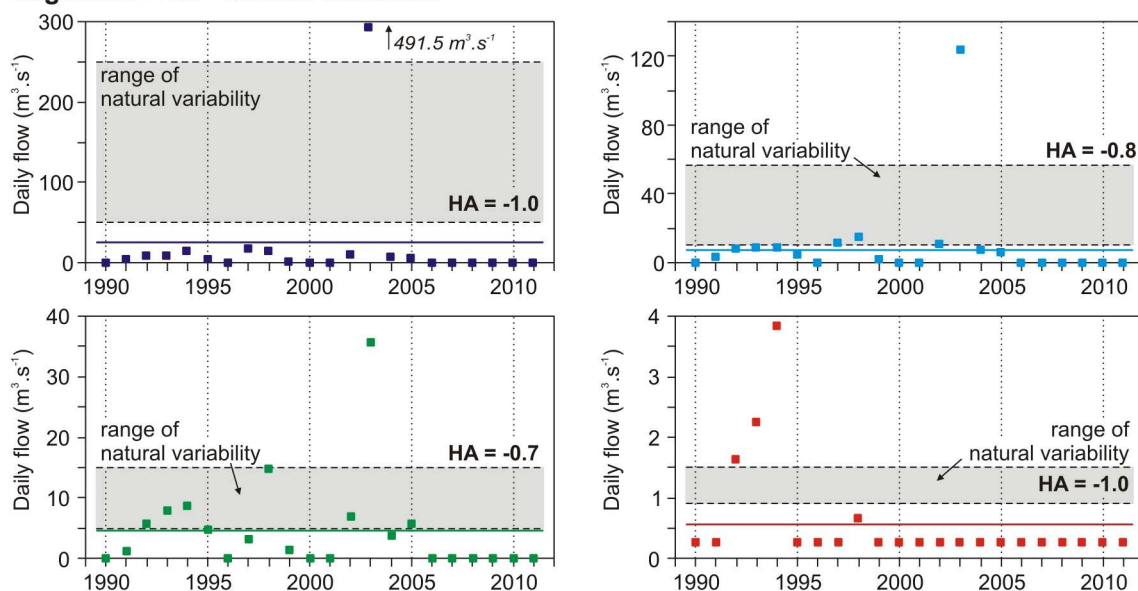


Figure 4.7: Magnitude of annual flow extremes for different durations within the unregulated river (1956-2010) and the regulated river (1989-2010). Ranges of natural variability for each flow duration were calculated based on the comparison period.

Comparison between unregulated and regulated flow conditions over the period 1989-2010 revealed that the dam was very effective to reduce annual flow extremes of all

durations (Fig. 4.7; Table 4.5). The most dramatic shift occurred in the magnitude of annual maxima: 1-day maximum flows were reduced by 79 %, on average, and fell outside the range of natural variability in all years of record ($HA = -1$). Note, the magnitude of 1-day maxima remained notably below the lowest threshold of natural variability for all years of record except for one single episode of extreme-high flow. The degree of hydrological alteration and the magnitude of change in annual maxima for the remaining flow durations declined as the analysis window expanded and more and more years fell within acceptable ranges of variability ($-0.8 < HA < -0.7$).

Table 4.5: Changes in the magnitude of annual extreme flows ($\text{m}^3 \cdot \text{s}^{-1}$) from the unregulated river upstream to the regulated river downstream over the period 1989-2010. Significant values per metric in bold.

<i>High extremes</i>	Unregulated river		Regulated river		Rate of Change		Hydrological Alteration
	Means	C. Var.	Means	C. Var.	Magn.	%	
1-day maximum	121.6	1.04	25.4	3.92	-96.1	-79.1	-1.00
7-day maximum	26.9	1.05	9.3	2.71	-17.5	-65.2	-0.81
30-day maximum	8.3	0.77	4.6	1.72	-3.7	-44.8	-0.75
90-day maximum	4.3	0.58	2.8	1.46	-1.5	-34.2	-0.69
<i>Low extremes</i>	Unregulated river		Regulated river		Rate of Change		Hydrological Alteration
	Means	C. Var.	Means	C. Var.	Magn.	%	
1-day minimum	0.9	0.01	0.3	0.73	-0.6	-64.3	-1.00
7-day minimum	0.9	0.01	0.3	0.73	-0.6	-64.3	-1.00
30-day minimum	0.9	0.03	0.4	1.25	-0.5	-59.6	-1.00
90-day minimum	1.1	0.28	0.6	1.44	-0.5	-47.9	-1.00

Shifts in annual minimum extremes were similar to those in annual maximum extremes, although the degree of hydrological alteration was extreme for all flow durations ($HA = -1$). Mean 90-day minimum flow was reduced by 48 %; the reduction of annual minima increased with decreasing duration up to -64 % for 1-day minima.

Significant changes occurred in the timing of annual extremes, and especially in annual maxima. The mean date for 1-day maximum within the river downstream was day 186 (5th July); this was 106 days delayed relative to 1-day maximum within the regulated river and was almost the date of 1-day minimum flow upstream. Mean date for 1-day minimum downstream was day 178 (27th June); despite annual minimum downstream was advanced of 29 days, both dates fell within the same calendar season (winter).

Frequency and duration of hydrologic pulsing

This section quantifies the number of times that high- and low-flow pulses occurred within a given year and measures the mean duration of such pulsing. High- and low-flow pulses were identified from daily flows exceeding the 75th percentile threshold or remaining below the 25th percentile threshold, respectively. Quantification of the frequency and duration of flow pulsing gives an expression of environmental and geomorphic variability within the river system (Richter *et al.*, 1996; Magilligan and

Nislow, 2005).

The unregulated river revealed relatively high flow constancy throughout the water year (Table 4.6). Results showed that, on average, episodes of subsidence flow (flows lower than $1.0 \text{ m}^3 \cdot \text{s}^{-1}$) may occur twice per year and have long duration (40 days), whereas episodes of high flow (flows higher than $12.8 \text{ m}^3 \cdot \text{s}^{-1}$) may occur four times per year with very short duration (1.4 days).

Table 4.6: Changes in the frequency and duration of high- and low-flow pulses from the unregulated river upstream to the regulated river downstream over the period 1989-2010. Significant values per metric in bold.

	Unregulated river		Regulated river		Rate of Change		Hydrological Alteration
	Means	C. Var.	Means	C. Var.	Magn.	%	
<i>Low pulses</i>							
Count (per year)	2.3	0.5	1.0	1.9	-1.4	-59.3	-0.75
Duration (days)	40.0	0.8	228.7	1.6	188.8	472.5	-0.84
Threshold ($\text{m}^3 \cdot \text{s}^{-1}$)	1.0	-	-	-	-	-	-
	Unregulated river		Regulated river		Rate of Change		Hydrological Alteration
	Means	C. Var.	Means	C. Var.	Magn.	%	
<i>High pulses</i>							
Count (per year)	4.3	0.5	0.2	2.4	-4.1	-95.0	-0.95
Duration (days)	1.4	0.3	6.6	2.7	5.1	353.0	-1.00
Threshold ($\text{m}^3 \cdot \text{s}^{-1}$)	12.8	-	-	-	-	-	-

The effects of the dam in increasing the flow constancy were clear (Table 4.6). Both low and high flow pulses were reduced in frequency and increased in duration notably. The most critical shift in low-flow pulsing was related to increased pulse duration ($HA = -0.85$) more than to reduced pulse frequency ($HA = -0.75$). In the case of high-flow pulsing, changes were significant for both the frequency ($HA = -0.95$) and the duration ($HA = -1.0$) of high pulses.

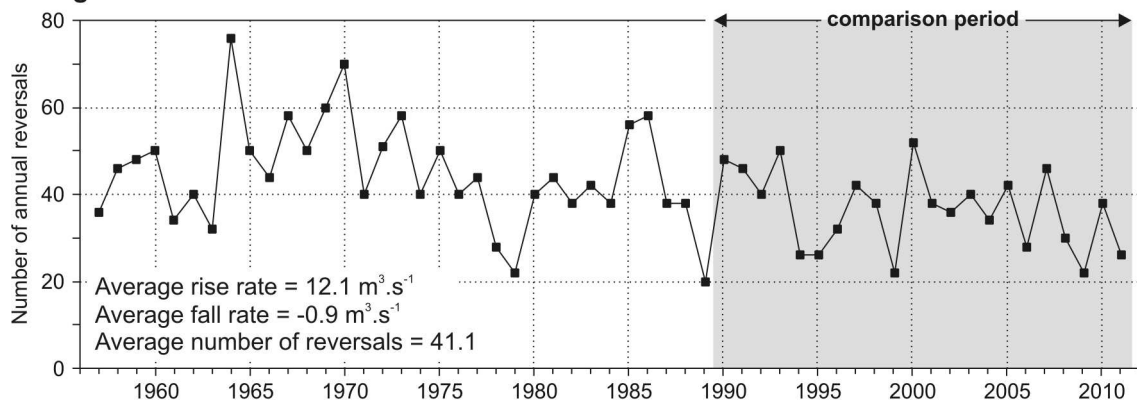
Rate of change in daily flows

This final section evaluates shifts in the variability of daily flow conditions over the water year. The most common technique used to inspect annual flow variability is the coefficient of variation of daily flows [CV]. Annual CVs within the unregulated river (1956-2010) ranged from 0.5 to 8.7 and averaged 4.0 with high deviation ($SD = 1.6$). Annual CVs were greater than 1 for 95 % of years of record indicating strong within-year variability; yet, annual CVs were highly scattered and so suggested that the magnitude of annual flow variations may vary considerably from year to another. Downstream, annual CVs (1989-2010) ranged from 0.1 to 6.8 and averaged 4.2 with high variability ($SD = 1.5$). Despite apparent similarity in the variability of upstream and downstream flows, coefficients of variation downstream were near zero for 55 % of years of record and hence indicated great frequency of stagnant downstream flow conditions.

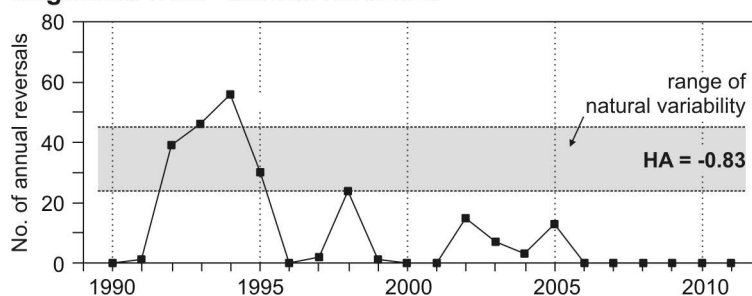
Inspection of the number of annual flow reversals (i.e. how many times flow changes from a rising trend to a falling trend, or *vice versa*) permitted to quantify relative

variations in annual flow regardless of the absolute magnitude of such variations (Fig. 4.8). Long-term (1956-2010) flow variability analysis within the unregulated river showed that the natural annual hydrograph was composed of about 40 flow reversals (on average) with moderate to low inter-annual variability ($CV = 0.29$). This indicated that daily flows over the water year tend to rise and fall with a certain seasonality common to all years, in spite that variations in the magnitude of such flows may vary considerably from one year to another. The latter aspect was evidenced by relatively high coefficients of variation for mean rise rates (0.60) and mean fall rates (-0.54).

Unregulated river - annual reversals



Regulated river - annual reversals



Reversal counting

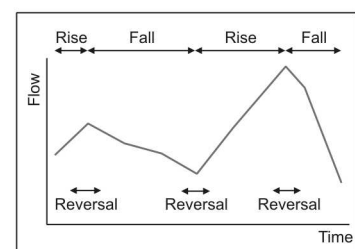


Figure 4.8: Number of annual flow reversals within the unregulated river (1956-2010) and the regulated river (1989-2010). Ranges of natural variability for flow reversals were calculated based on the comparison period.

The most statistically significant upstream-downstream shift over the comparison period (1989-2010) occurred in rising flow rates, which described an average decrease of 61 % and a value of hydrologic alteration close to unity (-0.94). Reduction in recession rates was negligible (0.6 %), although fall rates fell outside the range of natural variability by 90 % ($HA = -0.89$). The average number of reversals decreased by 71 %, and annual reversals remained below the suitable threshold of variability 83 % of times over the 22-yr observation period.

Reduction in the number of annual reversals implies a flattered hydrograph, where the duration of flows of similar magnitude was increased notably after river impoundment. It should be noted that in years where large volumes of water were evacuated from the dam, the number of reversals of the downstream hydrograph was significantly greater than that for the unregulated flow upstream (e.g. see years 1993, 1994 in Figure 4.8).

This gives evidence of the pulsing character of flow releases inducing artificial variations in daily flows which frequency throughout the year is notably higher than that for the natural flows.

2.1.2. Changes in environmental flow components

This section summarizes major hydrologic changes after river impoundment using the Environmental Flow Components (EFC) approach based on prior flood frequency analysis (See Section 1.1.3, p. 167). The purpose of flood frequency analysis was to estimate the recurrence interval of high flows that are determinant for (i) the ecologic and geomorphic integrity of the river system, and (ii) dam management and design. Flood frequency analysis used series of annual maximum daily flow discharge and annual maximum daily peak discharge for the unregulated river over the period 1956-2010; results are illustrated in Figure 4.9.

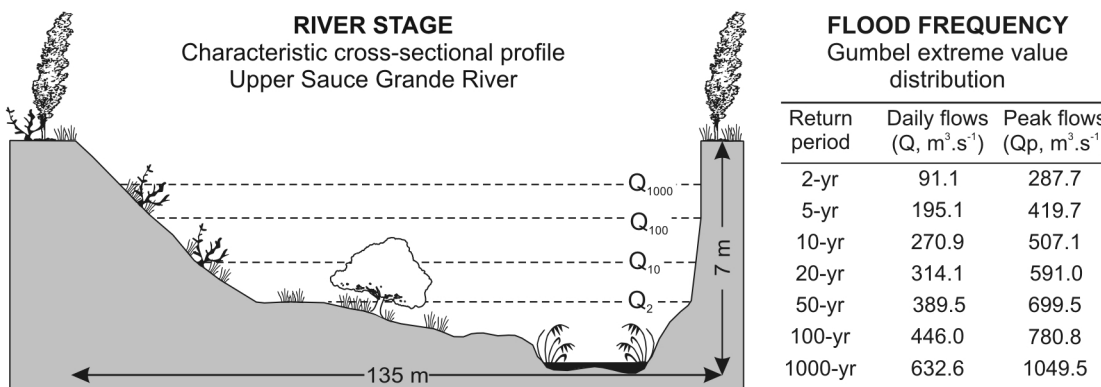


Figure 4.9: Flood magnitude and frequency within the upper Sauce Grande River (1956-2011).

River stages by flood frequency were inspected based on a characteristic channel cross-section for the upper river. The upper river flows through a slightly entrenched valley that averages 135 m width and 7 m depth (ceiling of the Terrace II, or active floodplain). Canyons in some river sections are considerable lower and so the width of the active floodplain enlarges; in other sections, the canyons are so deep that the width of the active floodplain matches that of the active channel. Despite the channel geometry defining different channel widths for overbank flooding, the bankfull stage in terms of discharge at which the channel maintenance is most effective was defined by daily flows of 91.1 m³.s⁻¹ with peak in 287.7 m³.s⁻¹ (2-yr return interval). Flows above this threshold were categorized as floods; the difference between *small floods* and *large floods* was defined by the flow magnitude for 10-yr return interval (271 m³.s⁻¹ with peak in 507 m³.s⁻¹).

Environmental flow components within the unregulated river are illustrated in Figure 4.10. The upstream river exhibited low flows over 64.5 % of days during the 55-yr period of monitoring; the frequency of extreme low flows was 10.3 %. The remaining proportion corresponded to episodes of high flow, from which the frequency of small and large floods was much reduced (1.6 and 0.2 %, respectively).

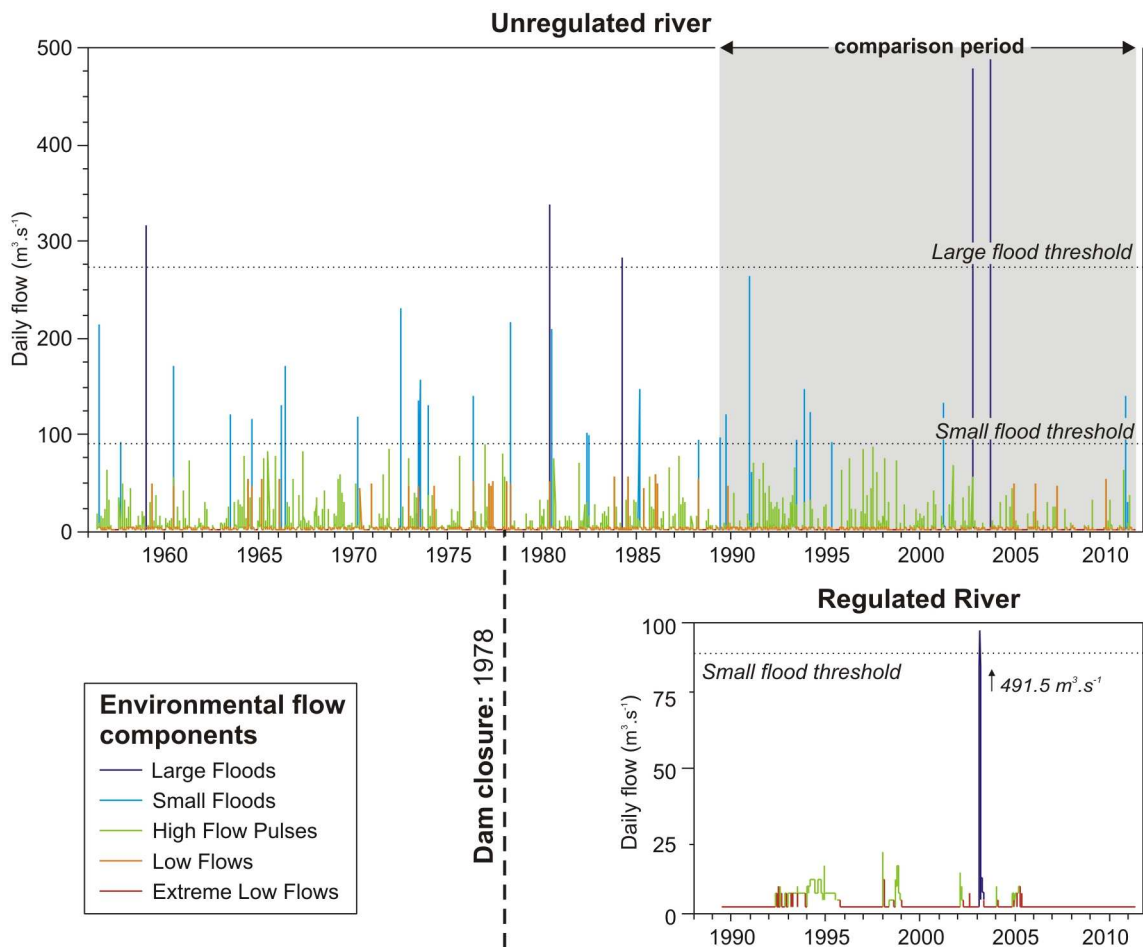


Figure 4.10: Environmental flow components within the unregulated river (1956-2011) and the regulated river (1989-2011). Thresholds for EFC were calculated based on the entire observation period; quantification of changes used the comparison.

Inspection of EFC for the unregulated and regulated rivers over the period of comparison (1989-2010) revealed that the greatest impact of the dam was the suppression of *floods* (Fig. 4.10; Table 4.7). Small floods were fully eliminated, and only one episode of flooding was observed over the 22-yr period of observation. Such episode was related to the large flood of November 2002 (greater than the Q_{100}), which caused the reservoir overflows for the second time in its history. A second impact related to this episode was the extreme increase in the flood duration (624 %) due to dam-controlled flood recession. The largest flood recorded upstream occurred in October 2003, although in that case the flood was fully absorbed within the dam reservoir.

On the other side of the scale, results showed that the magnitude of *extreme low flows* was dramatically reduced by 70 %, whereas extreme low flow duration was increased notably (821 %); increased duration led to reduction in the extreme low-flow frequency (-33 %) due to increased persistence of similar flow conditions over time. Changes in *high flows* were similar to those observed for low flows (Table 4.7). The major upstream-downstream shift was the increased high-flow persistence (+468 %) with dramatic decrease in the high-flow frequency (-88 %).

Table 4.7: Changes in the attributes of Environmental Flow Components (EFC) from the unregulated river upstream to the regulated river downstream over the period 1989-2010. Significant values per metric in bold.

EFC	Unregulated river		Regulated river		Rate of Change		
	Means	C. Var.	Means	C. Var.	Magn.	%	
<i>Ext. low flows</i>	Magnitude	0.9	0.0	0.3	0.0	-0.6	-69.6
	Duration	41.4	0.7	381.2	1.1	339.8	821.2
	Timing	238.8	0.2	331.8	0.2	93.0	50.8
	Frequency	1.4	0.8	1.0	1.9	-0.5	-33.3
	<i>Threshold (m³.s⁻¹)</i>	<i>0.9</i>					
<i>High flow</i>	Magnitude	16.3	0.4	7.2	0.6	-9.1	-55.7
	Duration	10.9	0.2	63.9	0.9	53.0	485.9
	Timing	338.3	0.2	289.2	0.3	49.1	26.8
	Frequency	8.7	0.3	1.1	1.6	-7.7	-87.6
	<i>Threshold (m³.s⁻¹)</i>	<i>1.8</i>					
<i>Small flood</i>	Magnitude	134.7	0.4	-	-	-	-
	Duration	12.4	0.3	-	-	-	-
	Timing	134.9	0.3	-	-	-	-
	Frequency	0.4	1.5	0.0	0.0	-0.4	-100.0
	<i>Threshold (m³.s⁻¹)</i>	<i>91.1</i>					
<i>Large flood</i>	Magnitude	486.8	0.0	482.1	0.0	-4.7	-1.0
	Duration	14.5	0.1	105.0	0.0	90.5	624.1
	Timing	298.0	0.1	315.0	0.0	17.0	9.3
	Frequency	0.1	3.3	0.0	4.8	0.0	-50.0
	<i>Threshold (m³.s⁻¹)</i>	<i>270.9</i>					

Flood suppression, reduction in the magnitude and frequency of low and high flows, and increased duration in all flow components imply reduced flow variability below the impoundment. The timing of episodes of low and high flow over the annual cycle was altered significantly, especially regarding episodes of extreme low flow (Table 4.7). Interestingly, shifts in the timing of extreme-high flows were not much significant, as large floods entering the reservoir entrain some proportion of flow released downstream.

2.1.3. Flow predictability

Previous results indicated high constancy of low flow conditions alternated by episodes of high flow with short duration. Furthermore, analysis of annual flow extremes revealed that the magnitude, frequency and timing of extreme-high flows were highly scattered respect to average flow conditions. These aspects suggest a flashy flow regime and an event-driven river configuration. This section evaluates the degree of predictability of the river flow regime based on long-term series of flow for the unregulated river.

The flow predictability index [Pr] revealed that unregulated flows were moderately to highly predictable (58 %). Yet, flow predictability was influenced by the frequency of fairly uniform episodes of low flow, where the constancy component [C] was notably higher than the flow contingency or periodicity ($C/Pr = 0.94$). Accordingly, the predictability of overbank flooding (i.e. the predictability of flows greater than the Q_2) was very low (28 %). This indicated that there is no clear flood seasonality or, in other words, that floods are seasonally unpredictable. The average flood-free season was 7 consecutive years, and so the flood frequency, calculated as the mean number of floods per year, was below unity (0.7).

2.2. DAM IMPACTS ON THE RIVER WATER TEMPERATURE

This section evaluates the influence of flow regulation on the thermal behaviour of the Sauce Grande River downstream from the Paso de las Piedras Dam. Patterns of river water temperature were quantified at multiple river sites deployed above and below the impoundment (Fig. 4.11), the upstream sites serving as reference of natural river thermal conditions. Analysis focused on a summer and a winter period to understand the complex response of river water temperature to (i) dam operation procedures inducing regulated patterns of flow, and (ii) hot (or cold) weather conditions inducing thermal stress. Note, results from summer water temperature assessment can be found in Casado *et al.* (2013).

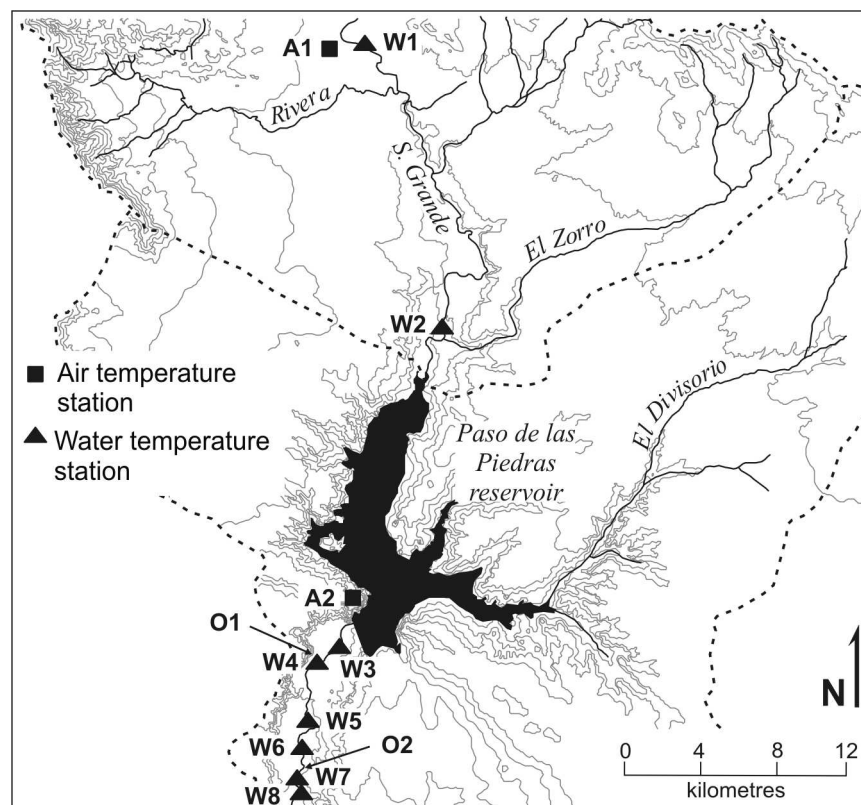
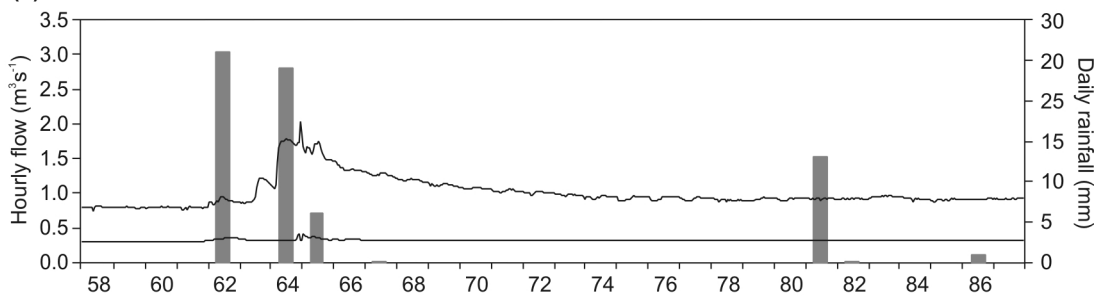


Figure 4.11: Map showing the location of air (A) and water (W) temperature gauging sites.

2.2.1. Changes in temporal patterns of river water temperature

Patterns of river water temperature were inspected for two sample periods of 30 day-length spanning varying atmospheric conditions during austral summer 2009 (day 58 to 87) and austral winter 2010 (day 173 to 202); these periods may be referred to as ‘summer’ and ‘winter’ to facilitate interpretation of results. Concurrent patterns of air temperature, rainfall and streamflow were inspected to evaluate meteorological and hydrological influence on river water temperature during each period. Note, flow variability over the monitoring periods was very low (Fig. 4.12) so that streamflow and rainfall series were excluded from the analysis. Rainfall during the summer period was 55 mm, and river flow averaged $1.01 \text{ m}^3 \text{ s}^{-1}$ upstream and $0.33 \text{ m}^3 \text{ s}^{-1}$ downstream, with little fluctuation ($\sigma = 0.21$ and $\sigma = 0.01 \text{ m}^3 \text{ s}^{-1}$, respectively); rainfall during the winter period was 24 mm, and river flow averaged $1.66 \text{ m}^3 \text{ s}^{-1}$ upstream and $0.29 \text{ m}^3 \text{ s}^{-1}$ downstream, with little fluctuation ($\sigma = 0.29$ and $\sigma = 0.01 \text{ m}^3 \text{ s}^{-1}$, respectively).

(a) Summer flow and rainfall series



(b) Winter flow and rainfall series

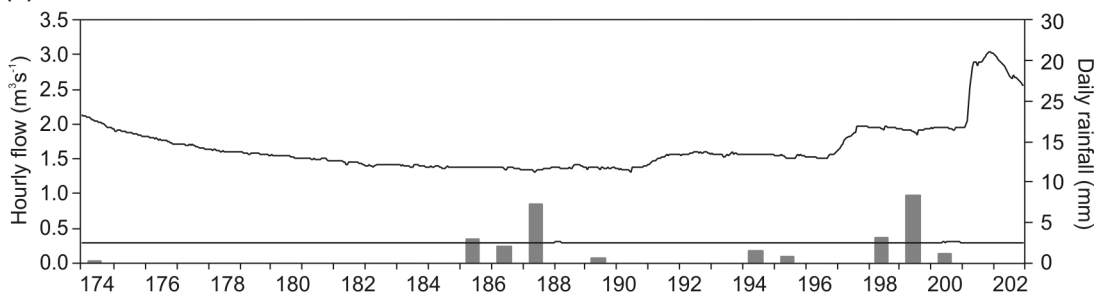


Figure 4.12: Series of hourly flow and daily rainfall over (a) the summer period and (b) the winter period.

Summer patterns of air and water temperature

Series of *air temperature* revealed strong seasonal and diurnal fluctuations (Fig. 4.13 Table 4.8). Four episodes of high daily temperature with short duration (2 consecutive days) occurred simultaneously at both sites A1 and A2. The hottest episode started on day 71, with the maximum daily temperature attained on day 72. Both sites cooled markedly on day 73, and daily temperature remained low over 4 consecutive days. A second episode of low daily temperature was observed on days 61-63, although with lower intensity. Maximum daily ranges were up to 18°C (A1) and 15°C (A2), and averaged 12°C and 10°C , respectively.

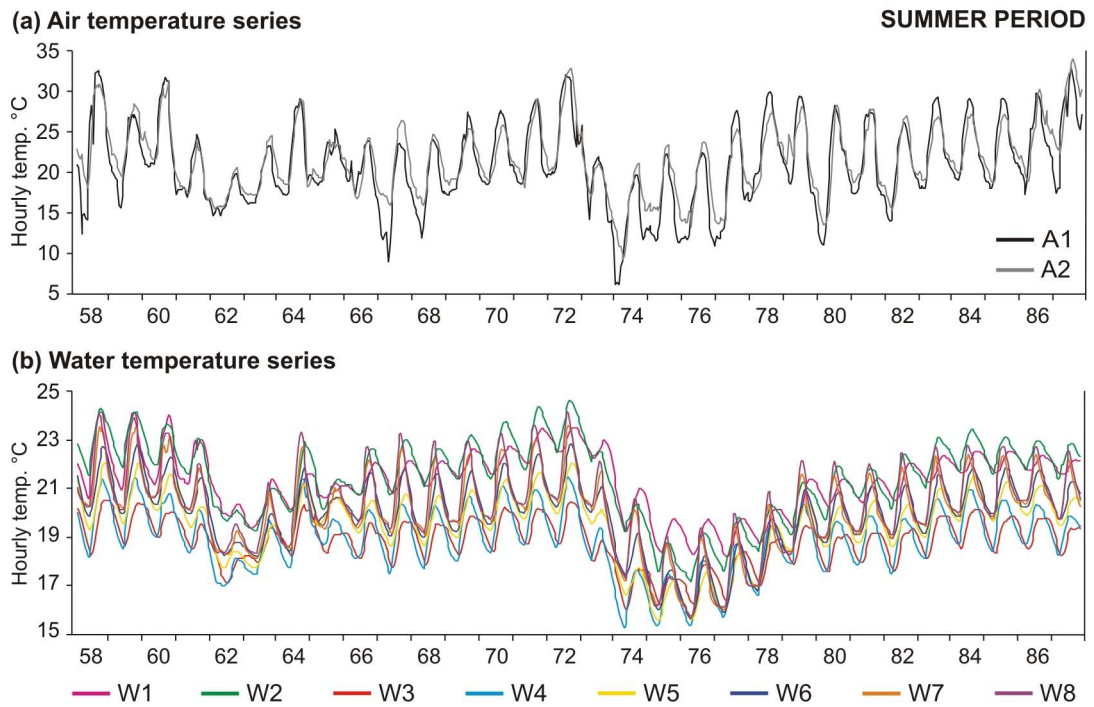


Figure 4.13: Time series of hourly air and water temperature over the 30-day summer period.

Table 4.8: Summer thermal patterns by (a) air temperature site and (b) water temperature site. Maximum values per metric in bold.

Temperature metrics (°C)	<i>(a) Air temp.</i>		<i>(a) Water temperature</i>							
	A1	A2	W1	W2	W3	W4	W5	W6	W7	W8
Minimum temp.	6.1	9.3	18.2	17.2	16.0	15.3	15.6	15.7	15.7	15.8
Low temp.	17.8	18.7	20.5	20.3	18.2	18.1	18.8	19.1	19.2	19.3
Median temp.	20.6	21.3	21.5	21.7	18.9	19.0	19.8	20.1	20.1	20.3
High temp.	24.5	24.6	22.2	22.6	19.5	19.9	20.4	20.9	21.0	21.4
Maximum temp.	33.0	34.1	25.3	24.6	20.5	21.5	22.0	22.9	23.6	24.2
Mean temp.	21.0	21.6	21.3	21.4	18.8	18.9	19.5	19.9	20.0	20.3
Area under the mean	0.5	0.4	0.4	0.4	1.0	1.0	1.0	1.0	0.9	0.8
Day of max. temp.	72	72	72	72	72	72	72	72	72	72
Day of min. temp.	73	73	76	76	74	74	75	76	76	76
Start of high temp.	58	58	58	58	58	58	58	58	58	58
	71	71	70	70	70	70	71	71	70	70
Start of low temp.	61	61	62	62	62	61	62	62	62	62
	73	73	74	74	73	73	73	73	73	73
Length of high temp.	2; 2	2; 2	3; 3	3; 3	3; 3	3; 3	3; 2	3; 2	3; 3	3; 3
Length of low temp.	2; 2	3; 1	2; 6	2; 6	1; 7	2; 6	2; 6	2; 6	2; 6	2; 6
Mean daily range	12.2	10.2	1.6	2.1	1.6	1.9	2.0	2.4	3.0	3.4

Note: days are expressed in Julian dates and durations are expressed in number of days.

Between-station differences in the absolute magnitude of air temperatures may be explained by the geographical situation of the sites (Fig. 4.11). Site A1 is at higher elevation than A2, which may explain the relatively cooler mean and median temperatures. Smaller diurnal ranges at site A2 are possibly due to close proximity to the reservoir and the moderating influence of the lake on air temperature.

Temporal variations in series of *water temperature* were synchronized broadly with those observed for air temperature (Fig. 4.13 Table 4.8). All water temperature sites attained daily maximum temperature on day 72 and cooled on day 73 (same as air temperature), except for sites W1 and W2 that cooled on day 74. Daily minimum temperatures were attained on days 74 to 76 (1 to 3 days lag compared with air temperature), and the period of time associated with low temperatures was longer and steadier than for air temperature sites (6 consecutive days).

Winter patterns of air and water temperature

Temporal fluctuations of *air temperatures* during the winter period showed a net tendency to cooling (Fig. 4.14 Table 4.9). The episodes of warmest temperature occurred during the first half of the sequence at both sites although with short duration (1 to 2 days); maximum temperature was attained simultaneously on day 179. The second half of the period was notably cooler, and episodes of low temperature had very long duration (8 days). The minimum temperature was attained on days 198 (A1) and 196 (A2). Diurnal fluctuations were slightly lower than those for the summer period in both sites, and averaged 10.4 °C in A1 and 9.1 °C in A2. Between-station differences revealed the effects of topography and proximity to the reservoir lake affecting the absolute magnitude of the thermographs same as for the summer series.

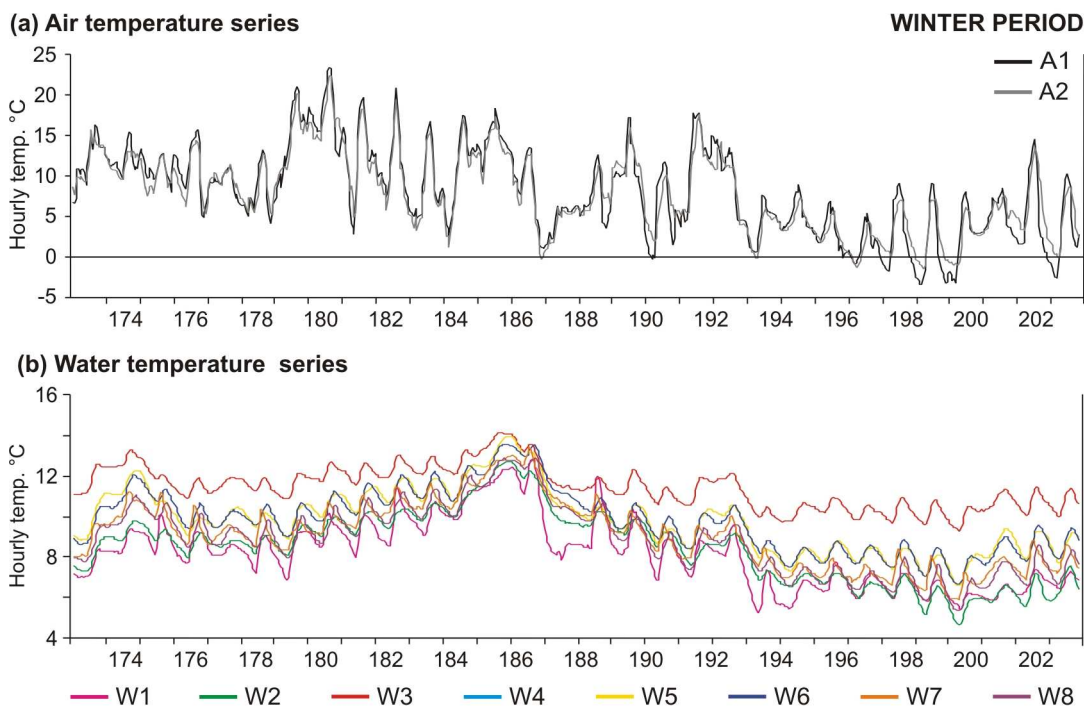


Figure 4.14: Time series of hourly air and water temperature over the 30-day winter period.

Synchrony in patterns of air and water temperature during the winter season was less apparent than that for the summer season. All *water temperature* sites warmed on day 181-182, and maximum daily temperature was attained simultaneously on day 185 (6 days lag compared to air temperature). The sites cooled on day 193 (except for W2 that cooled on day 195), and minimum temperatures were attained on days 198-199 (same as A1 but 2-3 days lag compared to A2). Episodes of high and low temperature showed durations longer than 6 consecutive days for all sites.

Table 4.9: Winter thermal patterns by (a) air temperature site and (b) water temperature site. Maximum values per metric in bold.

Temperature Metrics (°C)	<i>(a) Air temp.</i>		<i>(a) Water temperature</i>							
	A1	A2	W1	W2	W3	W4	W5	W6	W7	W8
Minimum temp.	0.7	1.6	6.0	5.6	10.0		7.5	7.6	6.7	6.3
Low temp.	4.6	4.4	6.7	6.8	10.5		8.4	8.4	7.6	7.3
Median temp.	7.9	8.2	8.2	8.7	11.4		9.9	9.9	9.2	9.1
High temp.	11.9	10.9	9.2	9.7	12.2		10.7	10.9	10.3	10.0
Maximum temp.	17.3	15.9	12.0	12.4	13.9		13.5	13.2	12.8	12.6
Mean temp.	8.0	7.8	8.2	8.5	11.4		9.8	9.8	9.1	8.9
Area under the mean	0.5	0.5	0.5	0.4	0.0	* Missing data *	0.2	0.2	0.3	0.4
Day of max. temp.	179	179	185	185	185		185	185	185	185
Day of min. temp.	198	196	199	199	199		199	199	199	199
Start of high temp.	173	173	180	181	173		174	174	174	174
	179	179	188	188	182		181	181	182	182
Start of low temp.	195	193	193	195	193		193	193	193	193
			202		202		202	202	202	202
Length of high temp.	2;3	1;3	6; 1	6; 1	2; 5		1; 6	1; 6	1; 6	1; 6
Length of low temp.	8	8	2; 5	8	7; 1		7; 1	8	8	8
Mean daily range	10.4	9.1	1.2	1.9	1.2		1.4	1.5	1.6	1.7

Note: days are expressed in Julian dates and durations are expressed in number of days.

Spatial variations in patterns of water temperature

Inter-comparison of water temperature sites revealed spatial differentiation in the absolute magnitude of the thermographs during both periods (Tables 4.8 and 4.9). Whilst differences in the thermal behaviour of sites W1 and W2 (above the dam) were negligible, water temperatures immediately below the dam were considerably cooler in summer and considerably warmer in winter. Furthermore, mean daily temperatures showed clear warming (summer) and cooling (winter) trends in the downstream direction (W3→W8), and the magnitude of daily fluctuations increased with distance from the dam during both periods.

Comparison between the thermal magnitude of the unregulated and the regulated river during the *summer period* evidenced the effect of the dam in depressing water

temperature downstream (Fig. 4.15). The difference in mean temperature between the dam outlet and site W2 (immediately upstream) was $-4.2\text{ }^{\circ}\text{C}$; below the dam, mean daily temperatures remained below the unregulated summer mean ($21.4\text{ }^{\circ}\text{C}$) over the entire monitoring period and for all sites, except for the distal sites W7 and W8 (Table 4.8).

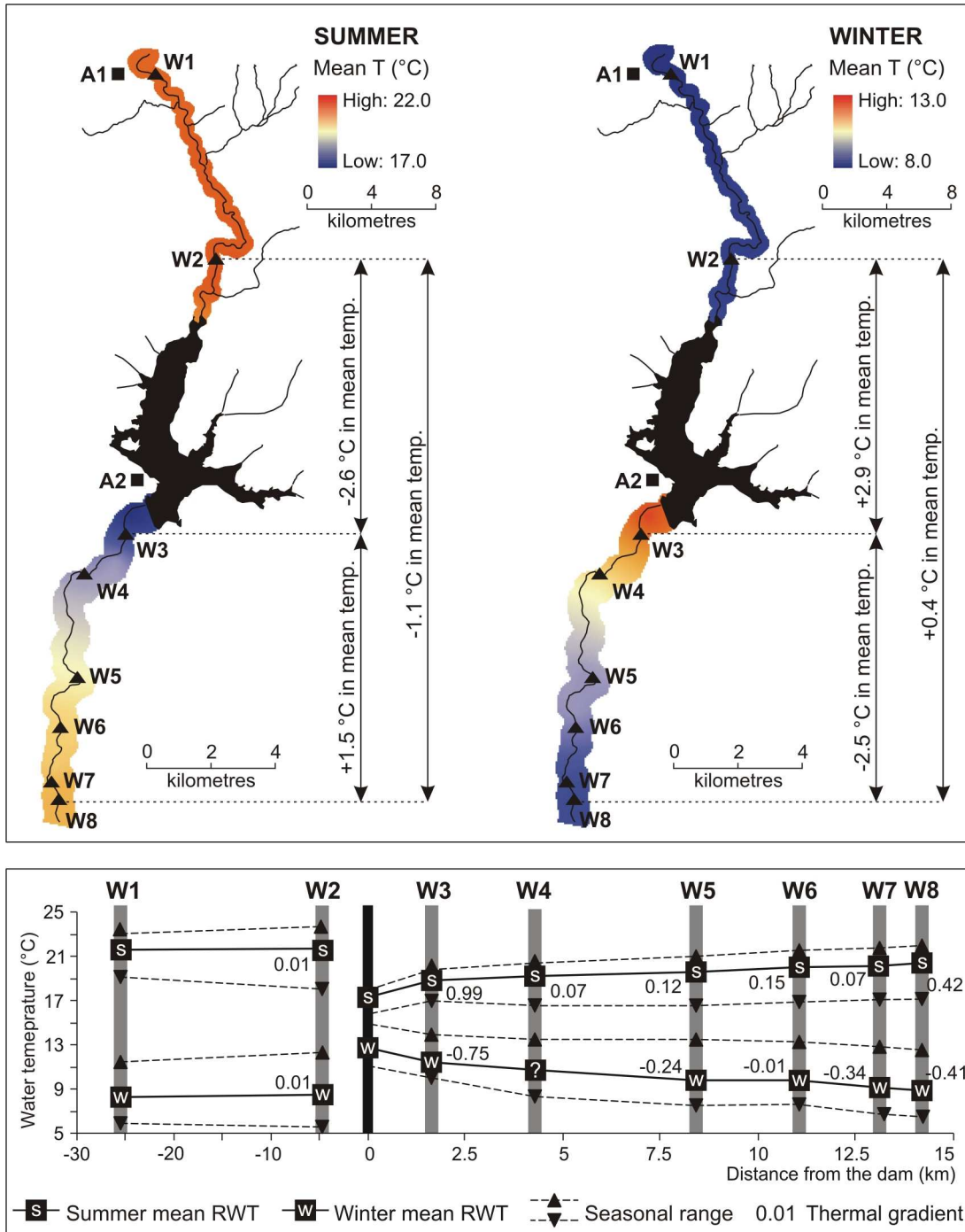


Figure 4.15: Spatial distribution of mean water temperature and longitudinal profile of mean, maximum and minimum water temperature by monitoring period. Dam outlet temperatures were recorded on the weir draining reservoir seepage into the river channel. The scale of representation of the river segment below the dam was increased by 2 times.

The summer warming trend in the downstream direction was clear. Warming rates between the dam outlet and site W3 (river kilometre 1.7) averaged 1.6 °C with maximum in 1.9 °C and minimum in 1.1 °C. Mean water temperature between sites W3 and W4 (river kilometre 4.2) remained relatively steady, although minimum temperature decreased by 0.2 °C.km⁻¹. Downstream from site W4, water temperatures described a steady increase with the exception of a small decline in minimum temperature between sites W4 and W5 (river kilometre 8.3).

Mean water temperature at the dam outlet during the *winter period* was 4.2 °C warmer than the mean water temperature recorded within the unregulated river over the same period (Table 4.9). As a result, the thermal magnitude of the regulated river was significantly higher than the thermal magnitude of the natural river upstream (Fig. 4.15), especially in the vicinity of the impoundment where mean daily temperatures rarely dropped below the unregulated winter mean (8.4 °C). Thermal gradients between the dam outlet and site W3 revealed substantial cooling in the downstream direction (-0.75 °C.km⁻¹), although the cooling trend declined with distance from site W3 to site W6 (river kilometre 11.1). Downstream from site W6 (-0.4 °C.km⁻¹), the cooling trend intensified and water temperatures at the distal sites were nearly as cool as those recorded upstream from the impoundment.

The warming (or cooling) trend in river water temperature below the dam was non linear, and rates of increase (or decrease) in water temperature were notably higher for sites located in the vicinity of the dam. It is beyond the scope of this research to understand inter-site thermal differences as a result of external control factors such as upland shading or groundwater influence; however, the potential effects of the stream structure on river water temperatures are evaluated briefly in further sections and discussed robustly in the Discussion section.

2.2.2. Changes in the magnitude and timing of diurnal water temperature regimes

Upstream-downstream shifts in the attributes of diurnal thermal regimes were evaluated using a classification approach based on the ‘shape’ (timing) and ‘magnitude’ (size) of diel cycles (RSMC; Hannah *et al.*, 2000). Despite series of air and water temperature during both periods were classified together, interpretation of results was performed for the summer and winter periods separately to inspect seasonal variations in the thermal impacts of the dam.

Prior to classification, air and water temperature data sets were inspected. The diurnal thermographs showed that the daily temperature minima occurred typically just before sunrise and the maxima after solar noon in both seasons. Hence, diurnal cycles were demarcated to begin at 0900 hours for all the station-days. This ensured that the rising limb, peak and falling limb of daily cycles were encapsulated on the ‘thermal response day’ for analysis. Regimes are referred to by the day in which they begin.

Diurnal regime shape (timing)

Inspection of the cluster dendrogram and agglomeration schedule plot suggested that

five clusters provided an informative classification of the data sets (Fig. 4.16). The regime shape classes were identified as follows:

- Class A* → Symmetrical diurnal cycle with gradual onset to a broad peak at 1800 hours and gentle cessation (225 station-days)
- Class B* → Steep rise towards an early peak at 1500 hours, short duration peak and rapid cessation (150 station-days)
- Class C* → Early peak at 1600 hours followed by extended recession (81 station-days)
- Class D* → Late rise into an extended peak at 2100 hours with gradual cessation (98 station days)
- Class E* → Multi-peak thermograph with highly fluctuating air temperatures during 8 winter days (16 station-days; not shown)

The main difference between regime shape classes was in the timing and duration of the diurnal peak. Whilst classes B and C exhibited early and steep peaks, classes A and D revealed gentle onset and cessation with a longer duration. Diurnal cycles for classes C and D appeared to be uneven across the day, indicative of a long-term (multi-day) cooling and a warming trend, respectively (Fig. 4.16).

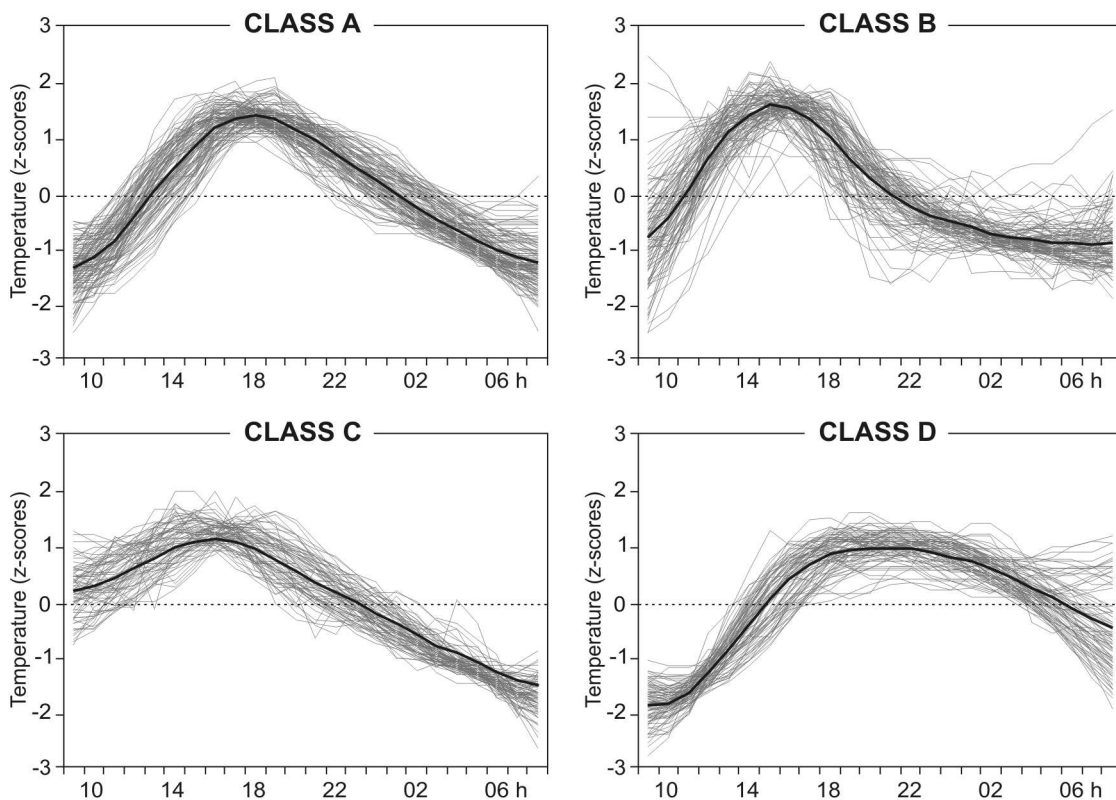


Figure 4.16: Standardised (z-scores) hourly records of air temperature (120 station-days) and water temperature (450 station-days) by regime shape class. The thick black line shows the average value for each shape class.

Analysis of class frequency by site (Table 4.10) revealed clear dominance of one single class for each site, suggesting that there is a ‘typical’ regime shape by site. Except for sites W1 and W3, all sites revealed the same dominant shape class during both the summer and the winter period and so interpretation of results is seasonally invariant; seasonal shifts in dominant regime shape classes for W1 and W3 respond to the channel morphology and materials at the sites and are evaluated robustly in the Discussion section.

Table 4.10: Frequency (as fractional proportion of days) of diurnal regime ‘shape’ classes by (a) air temperature site and (b) water temperature site. Class frequency is computed separately for the summer period and the winter period. Bold numbers indicate the dominant class by site.

<i>Summer series</i>										
Shape class	(a) Air temp.		(b) Water temperature							
	A1	A2	W1	W2	W3	W4	W5	W6	W7	W8
A	-	0.27	0.13	0.73	0.10	0.87	0.80	0.90	0.40	0.13
B	0.77	0.60	0.10	0.07	-	-	-	-	0.53	0.80
C	0.23	0.13	0.10	0.13	0.07	0.13	0.13	0.10	0.07	0.07
D	-	-	0.67	0.07	0.83	-	0.07	-	-	-
<i>Winter series</i>										
Shape class	(a) Air temp.		(b) Water temperature							
	A1	A2	W1	W2	W3	W4	W5	W6	W7	W8
A	-	-	0.47	0.40	0.53	-	0.47	0.60	0.10	0.07
B	0.60	0.57	0.10	0.07	0.17	-	-	-	0.63	0.60
C	0.13	0.17	0.10	0.20	0.10	-	0.23	0.20	0.20	0.13
D	-	-	0.33	0.33	0.20	-	0.30	0.20	0.07	0.20
E	0.27	0.27	-	-	-	-	-	-	-	-

Spatial correspondence of dominant regime shape classes permitted to assemble water temperature sites into groups of similar diurnal regime shape, especially for sites located below the dam. Class A was observed to dominate from site W4 to W6, revealing relative homogeneity in the river thermal behaviour after a distance of about 4 km below the dam and similarity with unregulated conditions (site A2). Spatial constancy in dominant classes of diurnal regime shape was also observed for sites W7 and W8, which revealed clear dominance of Class B similar to dominant patterns for air temperature. This indicated potential equilibration and synchronisation of distal water temperatures with the atmosphere.

Diurnal regime magnitude

Based on the cluster dendrogram and agglomeration schedule plot, three clusters provided a robust classification of the magnitude of air and water temperature diurnal regimes (Fig. 4.17). The magnitude classes can be arranged to give a relative temperature classification as follows:

- Class 1* → Cool day with the lowest minimum and maximum temperatures (148 station-days)
- Class 2* → Warm day with intermediate minimum and maximum temperatures (222 station-days)
- Class 3* → Hot day with the highest minimum and maximum temperatures (200 station-days)

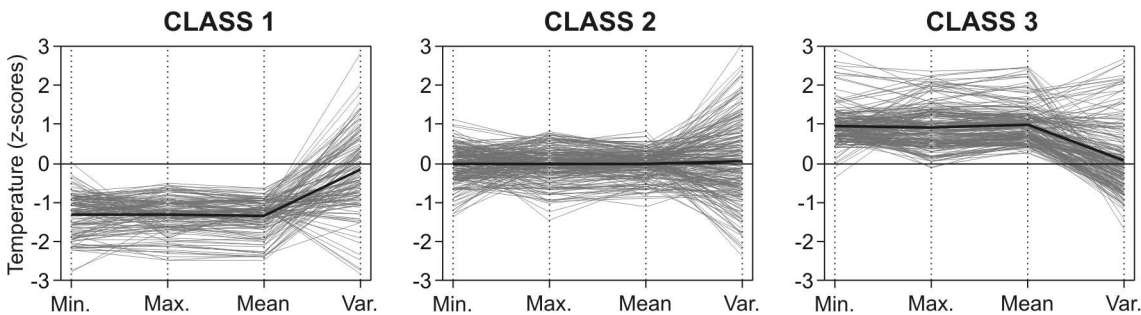


Figure 4.17: Standardised (z-scores) hourly records of air temperature (120 station-days) and water temperature (450 station-days) by regime shape class. The thick black line shows the average value for each magnitude class.

Magnitude classification did not reveal broad differences between sites (Table 4.11). The three classes exhibited broadly the same frequency across all the sites and during both periods, with a slightly preponderance of warm days (Class 2). This suggested sequencing and synchrony of change in the relative magnitude of diurnal regimes within and between sites regardless of temporal and spatial variations in absolute temperatures.

Composite classification

A composite classification was achieved by combining regime shape and magnitude classes. Because not all of the regime classes were present within air and water temperature series, both series were treated separately.

Series of *air temperature* showed 9 composite classes of diurnal regime during both the summer and the winter periods, whereas 12 and 15 class combinations were possible, respectively (Table 4.11). The dominance of Class B (early peak and steep daily fluctuations) over the full range of regime magnitude classes was evident in both periods (68 % in summer and 58 % in winter); during winter, the frequency of Class E (multi-peak cycles) was also significant (26 %).

Composite classification revealed that *water temperature regimes* were less stable (the full range of possible regime shape and magnitude combinations occurred; Table 4.11). Class A (symmetrical diurnal cycle) dominated clearly during both periods (50 % in summer and 45 % in winter), although hot days with high diurnal amplitude dominated in summer (Class 3A) and cool days with low diurnal amplitude dominated in winter (Class 1A). The remaining composite classes revealed similar frequencies with a slight predominance of Class 3B in summer (steep daily fluctuations with high magnitude) and Class 2C in winter (early peak with extended cessation and moderated magnitude).

Table 4.11: Frequency (as fractional proportion of days) of diurnal regime 'magnitude' classes by (a) air temperature site and (b) water temperature site. Class frequency is computed separately for the summer period and the winter period. Bold numbers indicate the dominant class by site.

<i>Summer series</i>										
Magnitude class	(a) Air temp.		(b) Water temperature							
	A1	A2	W1	W2	W3	W4	W5	W6	W7	W8
1	0.23	0.17	0.23	0.20	0.37	0.23	0.20	0.20	0.20	0.20
2	0.30	0.47	0.33	0.37	0.37	0.40	0.43	0.40	0.40	0.40
3	0.47	0.37	0.43	0.43	0.27	0.37	0.37	0.40	0.40	0.40
<i>Winter series</i>										
Magnitude class	(a) Air temp.		(b) Water temperature							
	A1	A2	W1	W2	W3	W4	W5	W6	W7	W8
1	0.23	0.23	0.30	0.33	0.30	-	0.30	0.33	0.33	0.33
2	0.40	0.37	0.40	0.33	0.40	-	0.43	0.40	0.37	0.43
3	0.37	0.40	0.30	0.33	0.30	-	0.27	0.27	0.30	0.23

Table 4.12: Frequency of composite regime shape and magnitude classes during summer and winter periods for (a) air temperature sites and (b) water temperature sites. Dominant composite class in bold.

<i>(a) Air temperature sites</i>										
Summer	1	2	3	Total	Winter	1	2	3	Total	
 A	1	4	3	8	 B	10	15	10	35	
 B	9	15	17	41	 C	2	3	4	9	
 C	2	4	5	11	 E	2	5	9	16	
Total	12	23	25	60	Total	14	23	23	60	
<i>(b) Water temperature sites</i>										
Summer	1	2	3	Total	Winter	1	2	3	Total	
 A	25	45	52	122	 A	38	31	26	95	
 B	9	12	24	45	 B	10	12	7	29	
 C	7	16	1	24	 C	7	23	7	37	
 D	14	20	15	49	 D	12	17	20	49	
Total	55	93	92	240	Total	67	83	60	210	

Analysis of the spatial distribution of dominant classes of composite regime (Fig. 4.18; 4.19) revealed similar behaviour for *air temperature* sites; warm to hot temperatures and steep diurnal cycles (Class 2B and 3B) dominated clearly in both periods. Conversely, comparison between *water temperature* sites showed great spatial contrast relative to river impoundment with seasonal variations in response to meteorological forcing.

SUMMER PATTERNS OF AIR AND WATER TEMPERATURE

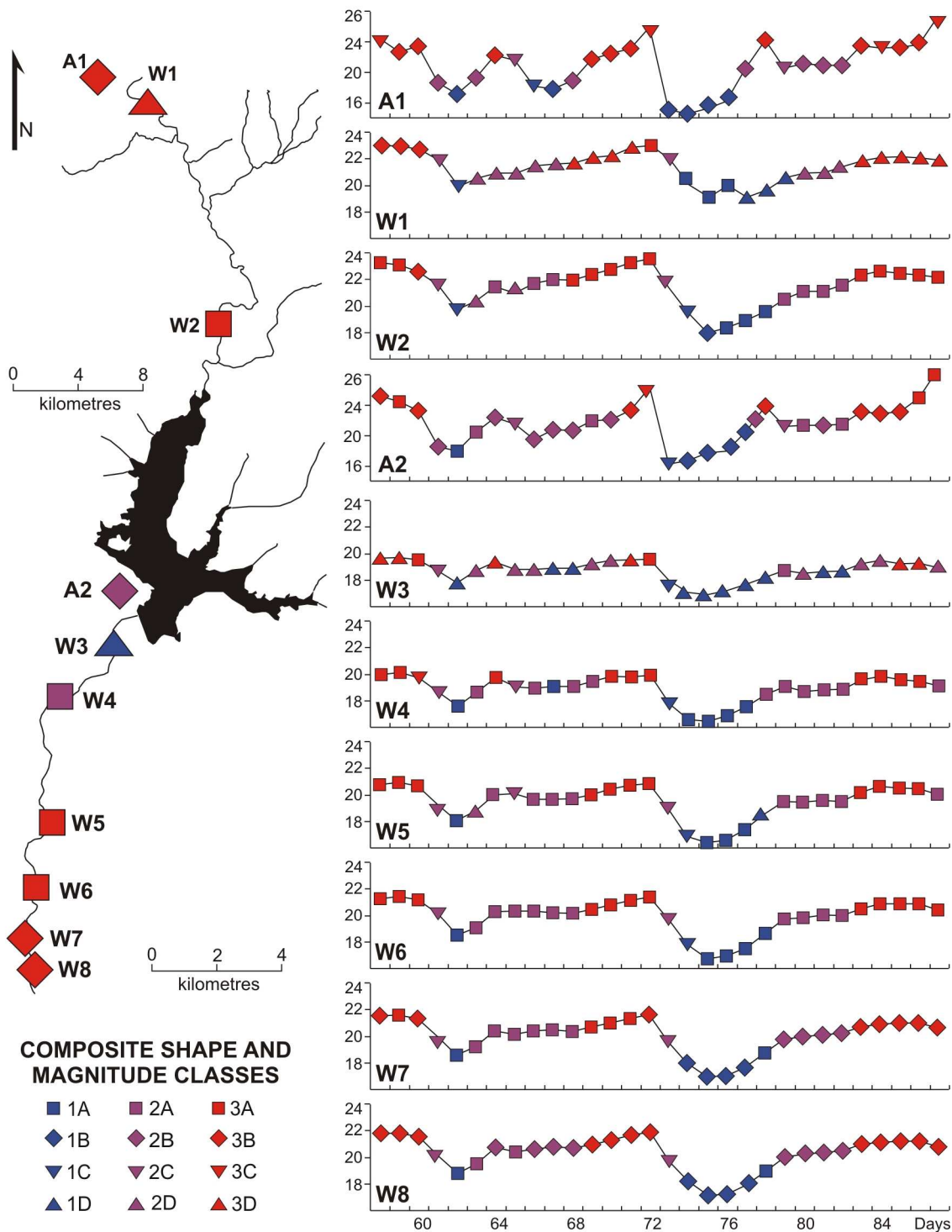


Figure 4.18: Distribution of composite shape and magnitude classes over curves of daily mean temperature by site (right) and spatial distribution of the dominant composite classes of air and water temperature regime (left). Summer period.

WINTER PATTERNS OF AIR AND WATER TEMPERATURE

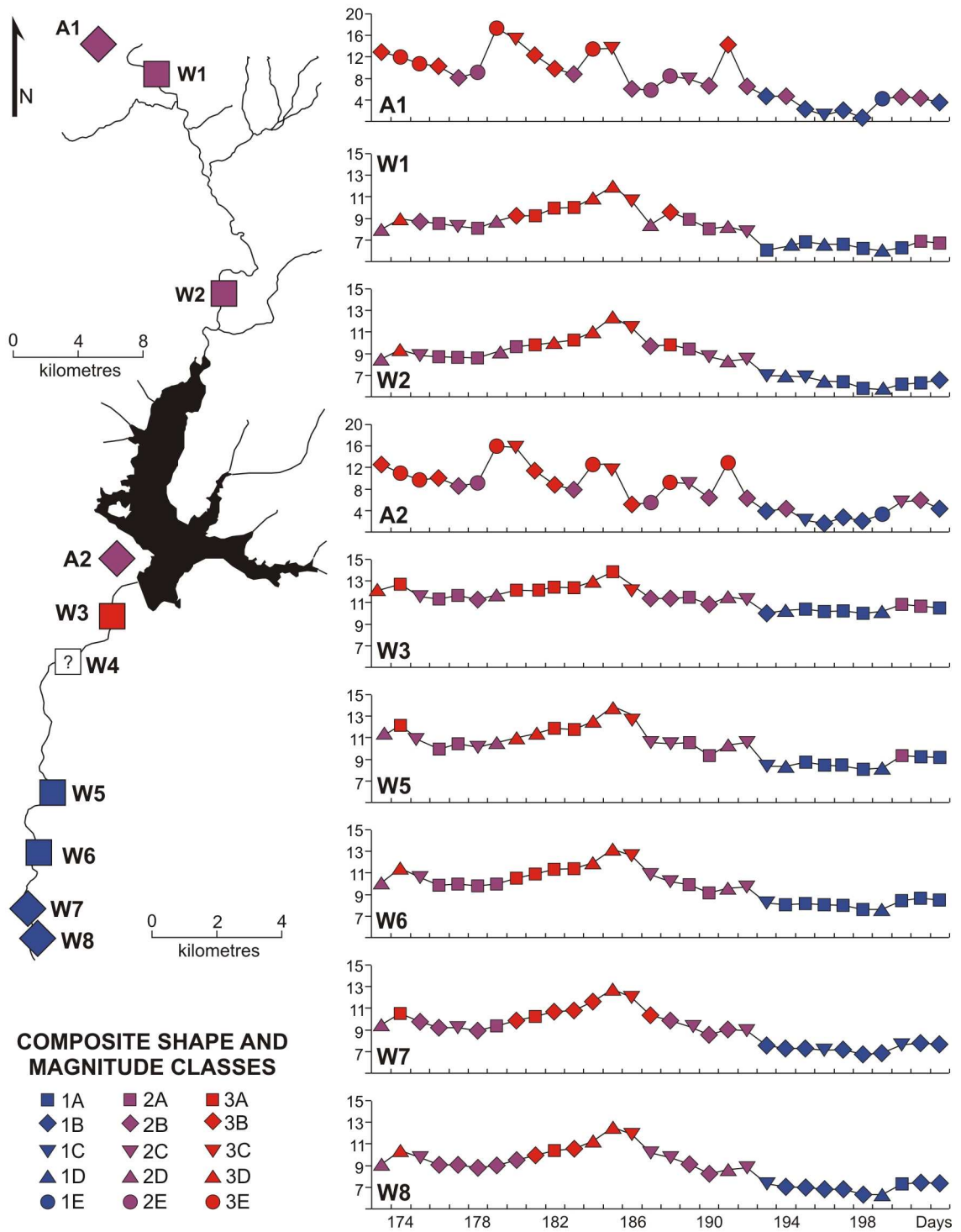


Figure 4.19: Distribution of composite shape and magnitude classes over curves of daily mean temperature by site (right) and spatial distribution of the dominant composite classes of air and water temperature regime (left). Winter period.

Upstream sites (W1 and W2) revealed similar behaviour of regime magnitude with high temperature and amplitude in summer and moderated temperature and amplitude in winter. Variations in the regime shape within each period were closely related to the channel morphology at each site (pool and riffle, respectively).

Dominant diurnal regimes below the impoundment revealed variations in shape with distance from the dam and inversions in magnitude during both periods of observation. Site W3 showed the greatest thermal shifts with respect to the unregulated river. Diurnal cycles revealed late and extended peaks with low magnitude in summer (Class 1D) and more symmetrical diel variations with high magnitude in winter (Class 3A). This is comparable to the seasonal thermal behaviour of site W1, although the magnitude of water temperatures in site W3 was comparatively out-of-phase. In addition, site W3 is riffle-shaped and so it should reveal thermal regimes closer to those of site W2. The cooling summer trend persisted over at least 4 km downstream; site W4 revealed a dominance of intermediate regime magnitude and symmetrical diurnal cycles (Class 2A). Winter temperature data for site W4 are missing so that any interpretation would remain a simple assumption. The predominance of symmetrical cycles with high (low) regime magnitude in summer (winter) within sites W5 and W6 matched unregulated thermal conditions and hence gave an expression of thermal recovery. However, the distal sites (W7 and W8) described dominant patterns similar to those of air temperature. This indicates that the thermal behaviour of the sites is highly dependent on the ambient conditions, and hence suggests great disruption in other natural paths of heat exchange due to flow regulation.

2.2.3. Temporal stability and climatic sensitivity of water temperature regimes

Building on analysis performed in the preceding sections, the temporal stability (day-to-day switching) of air and water temperature diurnal regimes was quantified using a regime Equitability Index (*EI*). Additionally, a Sensitivity Index (*SI*) was used to summarize the strength and direction of water-air temperature regime associations. These analyses were conducted for regime shape and magnitude separately (Table 4.13). Note, the Equitability Index provides a probability-based measure of regime stability and ranges from 0 to 1; the Sensitivity Index summarises the strength and direction of links between water and air temperature regimes and ranges from -1 to 1 where 0 indicates a sensitive situation (see Section 1.2.4, p. xxx).

Regime shape

Equitability and sensitivity indices for the regime shape defined two different scenarios for sites located above or below the dam clearly (Table 4.13, Fig. 4.20). Upstream and downstream scenarios were seasonally consistent in the direction of water-air temperature associations, although revealed seasonal variations in the level of climatic sensitivity of water temperature regimes.

Positive *SI* values for upstream sites indicated that water temperature regimes were more variable than air temperature regimes and hence, more equitable ($0.62 < EI_{Sum} < 0.72$; $0.85 < EI_{Win} < 0.89$). Moderate to high values of *EI* suggested that water regime

shape classes had roughly the same probability of occurrence during both seasons, with stronger equitability in winter.

Table 4.13: (a) Equitability (or stability) of diurnal regime shape and magnitude classes by air and water temperature site, and (b) climatic sensitivity of the shape and the magnitude of water temperature regimes to air temperature.

Site	(a) Equitability Index				(b) Sensitivity Index			
	Summer		Winter		Summer		Winter	
	Shape	Magn.	Shape	Magn.	Shape	Magn.	Shape	Magn.
A1	0.49	0.96	0.84	0.98	-	-	-	-
W1	0.72	0.97	0.85	0.99	0.42	-0.16	0.59	0.53
W2	0.62	0.96	0.89	1.00	0.30	-0.41	0.72	0.57
A2	0.84	0.93	0.91	0.98	-	-	-	-
W3	0.41	0.98	0.86	0.99	-0.70	0.46	-0.41	0.50
W4	0.28	0.96	-	-	-0.58	0.41	-	-
W5	0.45	0.96	0.76	0.98	-0.55	0.55	-0.41	0.51
W6	0.23	0.96	0.69	0.99	-0.71	0.47	-0.45	0.54
W7	0.44	0.96	0.74	1.00	-0.41	0.47	-0.36	0.56
W8	0.45	0.96	0.69	0.97	-0.51	0.47	-0.45	-0.46

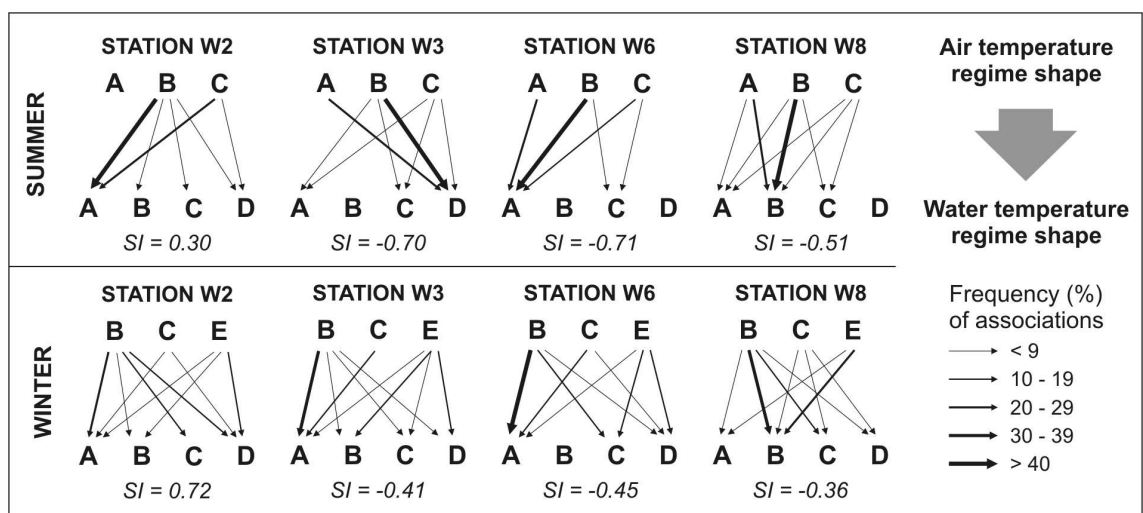


Figure 4.20: Direction and frequency of associations between air and water temperature regime *shape* during the summer and winter periods.

Negative SI values for downstream sites suggested that water temperature regimes were less variable than air temperature and so, more stable ($0.23 < EI_{Sum} < 0.45$; $0.69 < EI_{Win} < 0.86$). This indicated that a limited number of water temperature classes occurred under a range of air temperature regimes, especially in summer. Water temperature regime stability was less apparent in winter, but remained higher than that for air

temperature regimes.

Regardless of their sign, SI values revealed seasonal variations in the strength of water-air temperature associations (climatic sensitivity). Sites above the impoundment (positive scenario) showed low to moderate SI values in summer ($0.30 < SI_{Sum} < 0.42$) and moderate to high SI values in winter ($0.59 < SI_{Win} < 0.72$), i.e. variability in water temperature regimes was more sensitive to air temperature in summer than in winter. Conversely, the climatic sensitivity of downstream water temperature regimes (negative scenario) was stronger in winter ($-0.36 < SI_{Win} < -0.45$), the summer regime variability revealing an overall climatic insensitivity ($-0.41 < SI_{Sum} < -0.71$).

Regime magnitude

Water temperature *regime magnitude* showed the higher overall sensitivity to air temperature in both periods, and was stronger in summer (Table 4.13; Fig. 4.21). All sites showed low to moderate SI values, either positive ($0.41 < SI < 0.57$) or negative ($-0.16 < SI < -0.46$). This indicated that the relative magnitude of water temperatures was influenced by meteorological conditions even though absolute values were affected by impoundment.

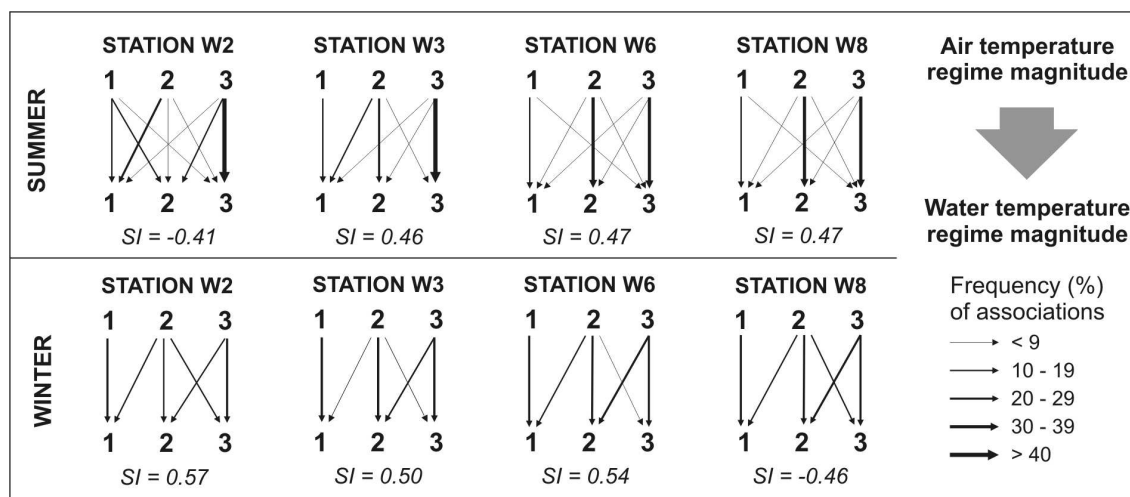


Figure 4.21: Direction and frequency of associations between air and water temperature regime *magnitude* during the summer and winter periods.

This interdependence could be expected, as air and water temperature regime magnitude revealed high seasonal equitability ($0.96 < EI < 1.0$) and hence, high seasonal variability. Moreover, the direction and frequency of water-air associations revealed strong links between similar regime magnitude classes. Spatial patterns based on values of the SI were unclear as expected given the relative classification of regime magnitude (see Methods section).

2.2.4. Other factors influencing river thermal variability

The potential influence of physical factors (other than air temperature) on the thermal

behaviour of the Sauce Grande River was evaluated based on a set of micro-scale channel characteristics measured for eight sample river reaches. Note, sample reaches were defined over a straight distance of 1500 m above each water temperature site; an overview of the characteristics of each site is presented in Figure 4.22. The variables measured for each sample reach included indicators of topographic, morphologic and streambed influence; results are summarized in Figure 4.23.

Topographic indicators include upland vegetation shading, stream altitude and stream orientation (Fig. 4.23). The relationship between channel orientation and altitude together with riparian vegetation height and density influences the balance between light and shadow affecting the effective stream insulation throughout the day (Poole and Berman, 2001; Broadmedow and Nisbet, 2004; Moore *et al.*, 2005; Caissie, 2006). The absolute altitude of the river reaches ranged from 219 to 118 m.s.l.; although the overall stream orientation is SSE, most reaches were orientated S (W2, W5), SSW (W3, W6, W7) and SW (W4). Riparian zones revealed two dominant cover types: (i) grasslands dominated by *Stipa* and important associations (sociability 5) of pampas grasses (*Cortaderia seollana*), and (ii) discontinuous galleries of trees dominated by willow (*Salix humboldtiana*) along the river margins and poplar (*Populus alba*) over the top portions of the river banks. The proportion of in-channel wood cover ranged from 21 to 71 % and defined three types of river reach clearly: (i) mainly grassy reaches (W1, W7 and W8), (ii) semi-wooded reaches (W2 and W6) and (iii), mainly wooded reaches (W3 to W5).

Morphologic indicators include longitudinal (slope, number of pools and riffles) and cross-sectional (width:depth ratio) channel characteristics (Fig. 4.23). The bed channel slope and the number of pools and riffles were used as indicators of thermal buffering resulting from variations in flow velocity and hyporheic flow (Poole and Berman, 2001; Moore *et al.*, 2005). Bed channel slope ranged from 1.1 to 4.8 % and showed clear relationships with altitude: the highest degrees of inclination were found within the upper reaches, except for site W1 that showed the lowest gradient. The number of pools and riffles was approximated from GIS analysis based on the relationship between the channel width and length (Richards, 1976), and hence increased with increasing flow sinuosity. The highest number of pools and riffles was observed upstream from site W5 (61) and site W6 (66); the average distance between riffles was of about 100 m and the reach sinuosity was 2.1 and 2.4, respectively. The channel width:depth ratio gave an expression of the stream channel shape and thermal capacity of the stream contributing to reduce or increase the air/water heat fluxes (Poole *et al.*, 2001; Caissie, 2006). Most reaches exhibited moderate to large width:depth ratios and moderate to low wetted area. Upstream from the dam, width:depth ratios increased with distance downstream; below the dam, the sites revealed an opposite tendency as the channel becomes deeper and narrower.

Inspection of thermal drivers at the *streambed-water interface* used measures of electrical conductivity as indicator of groundwater influence and hence of heat transfer between the water column and the alluvial aquifer. This relationship implies that the higher the rates of electrical conductivity, the greater the dominance of groundwater flow inputs over surface flow inputs and hence, the greater their potential to influence stream temperature variations (cooling or heating). *In situ* electrical conductivity revealed a marked increase in the downstream direction from 600 to 1060 $\mu\text{S}\cdot\text{cm}^{-1}$.

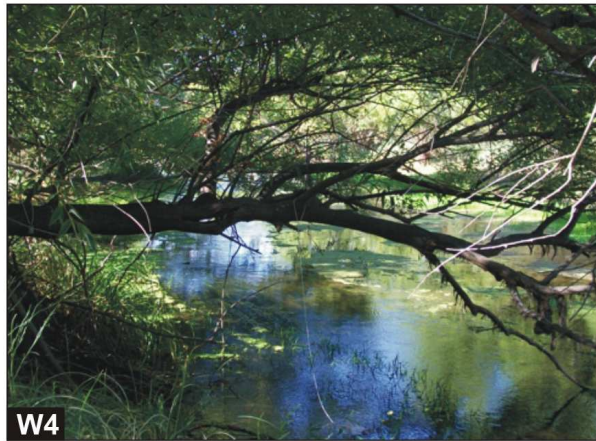


Figure 4.22: Overview of the channel characteristics at each water temperature sampling site.

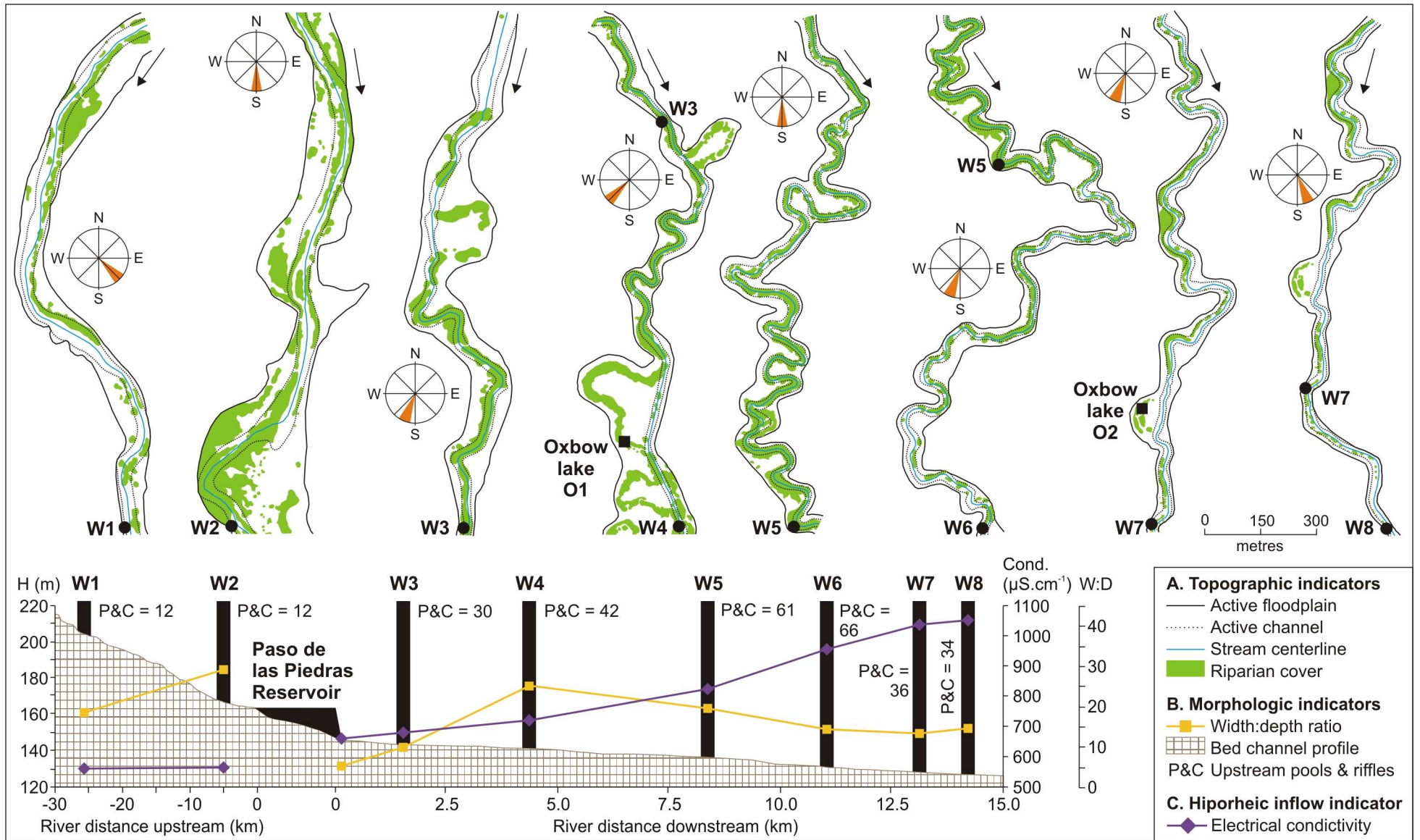


Figure 4.23: Indicators of topographic, morphologic and groundwater influence on water temperature by site and river reach. The downstream scale in the longitudinal plot was increased by 3 times. Note: reach W3 initiates below the dam; see Figure 4.11 for site location along the river course.

Principal components analysis

Principal component analysis (PCA) was conducted to inspect the influence exerted by the physical factors described above on patterns of river water temperature. The variables selected for PCA included seven indicators of potential topographic, morphologic and streambed control at the micro-scale. The value of each variable per site was calculated as mean (or percentage of coverage) of all observations available so that variables were considered seasonally constant. Prior to conduct principal component analysis, correlations between variables were inspected to avoid collinearity (Table 4.14). The correlation matrix showed absence of significant correlations for $\alpha = 0.05$ (two-tailed test), which implied that there was no redundancy in the variables selected for analysis.

Table 4.14: Pearson's correlation matrix between physical indicators of thermal control. In bold, significant values for $\alpha = 0.05$ (two-tailed test).

Indicator	Aspect	Rip. cover	Altitude	Slope	w:d ratio	P & R	Cond.
Stream aspect	1						
Riparian Cover	0.646	1					
Altitude	-0.642	-0.354	1				
Channel slope	0.609	0.618	-0.369	1			
Width-depth ratio	-0.048	0.227	0.501	0.260	1		
Pools & Riffles	0.407	0.467	-0.605	0.494	-0.304	1	
Conductivity	0.110	-0.360	-0.689	0.048	-0.538	0.448	1

PCA permitted to assemble the seven variables into two factors accounting for 77 % of the total variance (Fig. 4.24). The first factor (F1) was related to morphologic and topographic characteristics of the river reaches, whereas the second factor (F2) was linked to the channel shape, the riparian cover and the groundwater influence. F1 separated the sites into two groups clearly: sites influenced by the stream slope, aspect and the number of upland pools and riffles (W5 and W6), and sites influenced by the average altitude of the reach (W1). F2 separated sites into three groups defined by the width:depth ratio (W2), the riparian cover (W3 and W4) and the electrical conductivity of the stream (W7 and W8). The site arrangement defined by the factors is highly consistent with the spatial constancy in river thermal regimes identified above.

The upstream sites W1 and W2 were highly scattered from each other. This is consistent with previous results, which showed that the sites reflected distinct dominant thermal patterns (especially in summer) related to differences in the stream channel morphology. The influence of the channel shape in water temperature was particularly evident for site W2, which describes a wide and shallow channel with low thermal capacity. Shallow and large streams have greater potential for heat exchange at the air/water surface interface due to higher exposure to solar radiation and wind, and lesser influence of riparian shading on the water surface.

Below the dam, the sites were separated into three groups in the downstream direction clearly (Fig. 4.24). Sites W3 and W4 were strongly influenced by riparian vegetation

cover enhancing the thermal stability of the sites. Upland riparian cover was also significant in site W5 (71 %), although the overall stream characteristics of the site were more related to those of site W6. Both sites are orientated S and SSW, respectively, so that the light penetrates for much of the day. However, the factor that influences the stream temperature within these reaches is the overall reach morphology. Both sites exhibited the greatest sinuosity and hence, the longest length and the largest number of pools and riffles contributing to thermal buffering by increased groundwater influence and hiporheic flow. Sites W7 and W8 were separated clearly by high values of electrical conductivity indicating strong influence of groundwater inflows; the riparian cover arrow increasing in the opposite direction clearly suggest coupled exposure to ambient conditions.

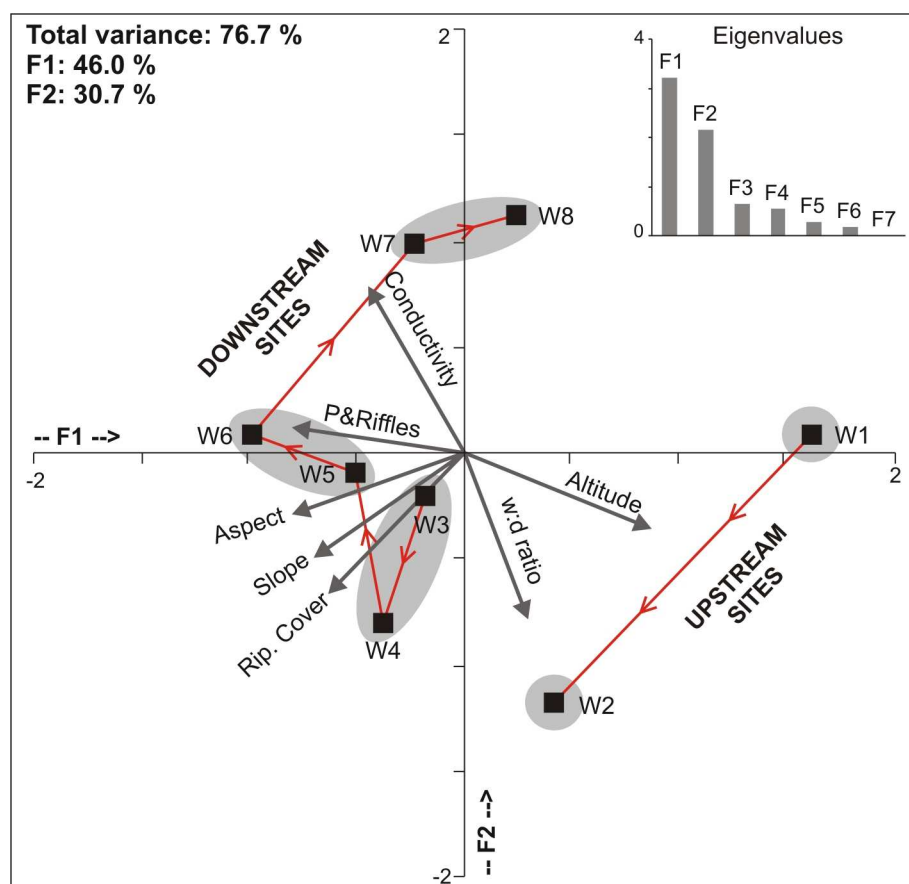


Figure 4.24: Structure and distribution of water temperature sites as a function of two factors axis (F1 and F2).

This chapter has evaluated in detail the effects of the Paso de las Piedras Dam on the flow regime and water temperature of the Sauce Grande River downstream from the impoundment. In addition to provide new information on the overall hydrology of the river system, this chapter provided the very first assessment of the broad-scale impacts of the dam by focusing on two variables of geomorphological and ecological relevance (Fig. 4.25).

The river flow regime is a key driver (Poff *et al.*, 1997; Leigh *et al.*, 2010) regulating geomorphic processes (Magilligan and Nislow, 2005; Graf, 2006) and diversity (Richter *et al.*, 1996; Bunn and Arthington, 2002) in river systems. The river flow regime also exert strong influence on the overall river water quality (Meybeck and Helmer, 1996) and particularly on the river water temperature regime by determining the thermal capacity of the stream (Ward, 1985; Webb, 1996; Poole and Berman, 2001; Caissie, 2006). In turn, the river water temperature is an indicator of both water quality (through influence on biological, chemical and physical reaction, Stevens *et al.*, 1975; Caissie, 2006; Haag and Luce, 2008) and habitat suitability (through influence on the structure, composition and distribution of aquatic organisms, Webb, 1996; Bonacci *et al.*, 2008; Olden and Naiman, 2010).

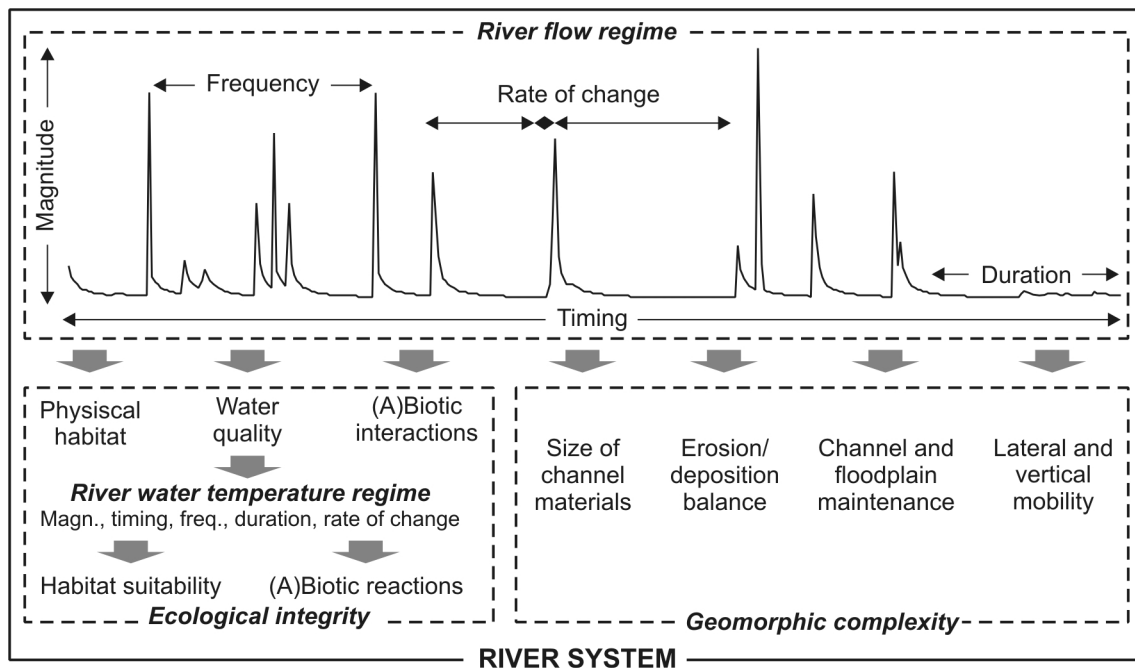


Figure 4.25: Significance of the river flow regime and water temperature regime for the ecological integrity and geomorphic complexity of the river system. Based on Richter *et al.* (1996), Poff *et al.* (1997) and Graf (2006).

The results from this investigation are discussed into two linked sections examining the natural attributes of the river flow and water temperature regimes, and the magnitude of change in such attributes within the river downstream from the impoundment.

3.1. CRITICAL ALTERATION OF THE RIVER FLOW REGIME

Results from flow regime analysis revealed that the dam has induced extreme changes in the hydrology of the regulated river. Changes attained the full range of flows and occurred to all components of the river flow regime; the most dramatic upstream-downstream shifts were decreased low- and high-flow magnitude, increased low-flow duration, flood suppression and altered flow seasonality. These changes are evaluated based on a prior understanding of the natural flow regime as discussed below.

3.1.1. The natural river flow regime

The river flow regime is complex

The flow regime of the Sauce Grande River is exclusively rainfed, which implies that the river variability depends directly on the rainfall regime. Inspection of the annual distribution of mean monthly flow (1956-2010) showed that the water year starts in winter (July) in connection to the dry season. Although the rainy season extends from spring to early autumn (October to April), the distribution of monthly flows over the water year described a complex regime with two annual peaks, one in spring and other in late summer-early autumn separated by an episode of low flow. This second episode of low flow was strongly related to the effects of evapotranspiration rates higher than the rainfall contribution during the summer months.

Conversely, previous studies reported that the water year starts in summer (January) and that winter flows are sustained by increased groundwater inflow following the rainy season (Gil, 2009). There are two possible explanations for such discrepancies in our results. First, the study of Gil (2009) is based on historic records of monthly runoff (1910-1947). Recent studies conducted at the national and regional scale gave evidence of increased annual rainfall amounts since the 1970s (e.g. Scian, 2000; Penalba and Vargas, 2004; Kruse and Laurencena, 2005; Núñez *et al.*, 2005; Penalba and Robledo, 2005; Forte-Lay *et al.*, 2008; Penalba and Llano, 2008), and meteorological studies conducted at the scale of SESA reported that such rainfall increase is related to increase in both the frequency and the magnitude of rainy days during the summer season (e.g. Nogués-Paegle and Mo, 1997; Liebmann *et al.*, 1999; Liebmann *et al.*, 2004). Hence, increased rainfall during the summer season could contribute to alter the timing of annual minimum flow, even if summer flows are reduced due to the effects of evapotranspiration. Second, flow regime analysis was based on simulated series of daily flow and thus is subject to many sources of uncertainty. For example, the model did not consider the effects of groundwater inflows in periods of base flow, the reliability of rainfall series used as input was moderate, and evapotranspiration estimates were calculated based on estimated series of air temperature (see Chapter 2).

The river flow regime is flashy and event-driven

The annual distribution of daily flows over the period of monitoring (1956-2010) revealed high coefficients of variation ($0.5 < CV < 8.7$) and moderate to low coefficients

of dispersion ($0.2 < CD < 1.0$). This indicated coupled variability and constancy in the river flow behaviour, where episodes of low-flow with long duration were alternated by episodes of high-flow with short duration and high magnitude. These aspects were evidenced by all parameters of regime measure, indicating a perennial flashy flow regime and an event-driven river configuration (Poff and Ward, 1989; Poff, 1996).

In spite of the moist sub-humid climate within the headwater areas, the river flow regime is characteristic of semi-arid regions (McMahon *et al.*, 1992; Dettinger and Diaz, 2000; Bull and Kirkby, 2002; McMahon *et al.*, 2007c), where rivers originate in relatively wet upland areas but flow for the majority of their course through semiarid regions that produce little or no additional discharge (allogenic rivers) and that induce high losses through evaporation and groundwater recharge (Thoms and Sheldon, 2000; Schmandt, 2010). Similar patterns of flow have been reported for a wide number of semiarid rivers worldwide, especially in Australia (e.g. Murray-Darling Basin, Walker, 1992; Thoms and Sheldon, 2000; Leigh *et al.*, 2010; LakeEyre Basin, Puckridge *et al.*, 2000; Bunn *et al.*, 2006; Leigh *et al.*, 2010), in USA (e.g. Sacramento-San Joaquin Basin, Kondolf and Batalla, 2005; Rio Grande, Schmandt, 2010), and in South Africa (e.g. Orange River, Blanchon and Bravard, 2007; Sabie River, Naiman *et al.*, 2008).

The river flow regime is highly variable with low flood predictability

Annual coefficients of variation were greater than 1 for 95 % of years of record and were highly scattered in time ($SD = 1.5$), suggesting that the magnitude of annual flow variations varied considerably from one year to another. The overall flow predictability was moderate to high (58 %), although the predictability of overbank flooding (i.e. the predictability of flows greater than the Q_2) was very low (28 %). This indicated that episodes of low flow were fairly uniform, constant and hence predictable, whilst floods were seasonally unpredictable. The distribution of environmental flow components over the monitoring period reflected this variability clearly; the frequency of low and extreme low flows was near as great as 75 %, whereas the frequency of floods was very small (less than 2 %) with unclear seasonality or timing. These aspects suggest a flood- and drought-dominated regime (*sensu* Warner, 1987; Erskine and Warner, 1998), where the flood magnitude and frequency are driven by alternated periods of humidity and dryness with return periods that may involve several years.

The contribution of ENSO events to flow variability is apparent but not systematic

Semiarid rivers are among the most variable in the world (Bunn *et al.*, 2006; Leigh *et al.*, 2010; Schmandt, 2010); some authors consider that inter-annual variations in flow (range and predictability) and flooding (frequency and predictability) within semiarid rivers represents the sixth facet of the five components of the river flow regime (Bunn *et al.*, 2006; Naiman *et al.*, 2008; Leigh *et al.*, 2010). According to Kondolf and Batalla (2005), such variability is comparable to Mediterranean rivers (e.g. Ebro River, Batalla *et al.*, 2004; Magdaleno and Fernandez, 2010), although the flood seasonality is highly less predictable (Poff and Ward, 1989).

Low flood predictability implies that the hydrograph is strongly influenced by rainfall

events responding to aseasonal factors (Walker *et al.*, 1995; Puckridge *et al.*, 2000; Leigh *et al.*, 2010); within semiarid rivers in the southern hemisphere, such variability is frequently associated to the effects of the El Niño Southern Oscillation (ENSO) phenomenon (McMahon *et al.*, 1992). To inspect this relationship within the area of interest, the distribution of environmental flow components (i.e. low flows, high flows and floods) was compared to the recurrence of ENSO events (Fig. 4.27). The ENSO phases were defined by 5-month running means of the SST 3.4 Index exceeding the ± 0.4 °C threshold over 6 consecutive months or more (Trenberth, 1997); positive (or negative) deviations of the SST 3.4 indicate El Niño (or La Niña) events, which for the region of interest are associated with heavy rainfall and floods (or drought and low flows).

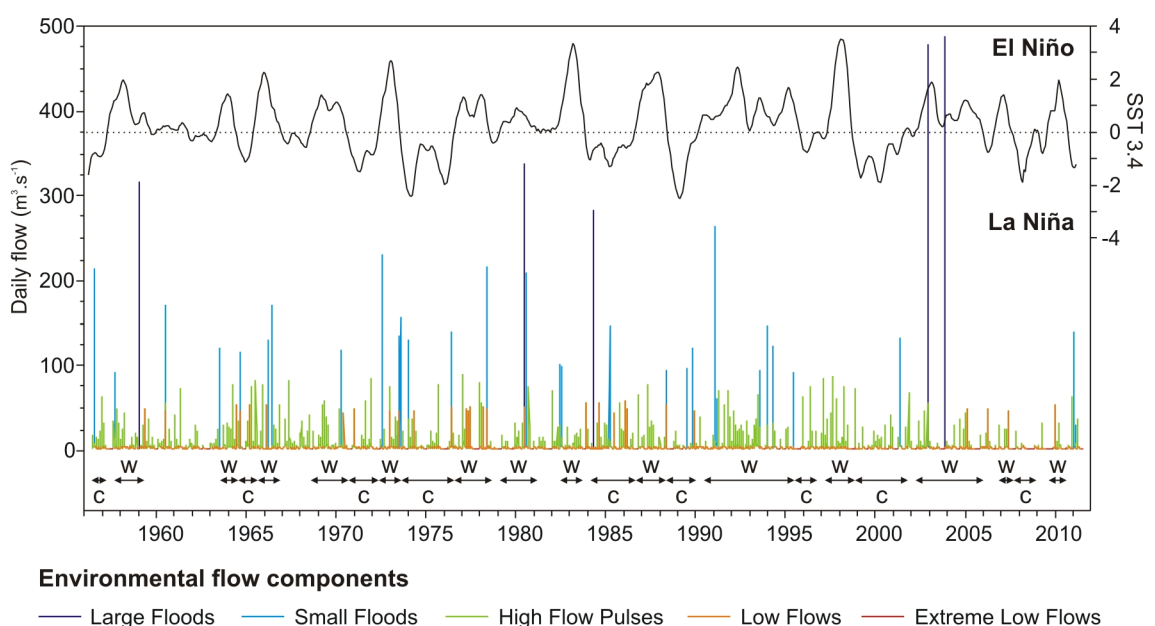


Figure 4.26: Daily flows classed by environmental flow component and 5-month running means of the SST 3.4 Index over the period 1956-2010. Phases of warm and cold ENSO were indicated by 'w' and 'c', respectively.

From Figure 4.27, the connection between flood episodes and warm phases of ENSO is apparent, although not systematic. For example, the large flood of 1984 occurred under La Niña conditions, and there were strong Niño signals with long duration during which no floods were observed (e.g. 1986-87, 1997-98). The connection between episodes of low flow and cold phases of ENSO was less clear. This is consistent with previous findings on reservoir inflow variability assessment, which indicated that, together, cold and warm ENSO episodes explain between 60 and 70 % of the seasonal rainfall and runoff variability within the river basin. The remaining percentage responds conceivably to the effects of other large-scale phenomena, although these aspects remain to be investigated directly (see Discussion section in Chapter 3).

3.1.2. Sources for flow within the regulated Sauce Grande River

The Paso de las Piedras Dam has impounded the middle river section since 1978 for

water supply to a population that today reaches about 400 000 people. Climate variability and population growth combine to generate low resilience to deficiencies in local water resources; accordingly, dam operational procedures seek to store and conserve a maximum volume of water to assure supply in periods of drought. Reservoir evacuation occurs only in periods of water excess (i.e. full reservoir), so that sources for downstream flow are intermittent and very scarce (Figure 4.27). Flow release is conducted either through the bottom gate (controlled hypolimnetic release) or through the overflow spillway (uncontrolled epilimnetic release). The reservoir overflowed only two times since dam closure (in 1984 and in 2002), so that downstream flow originates principally from flow released through the bottom gate. Controlled flow release can reach $10 \text{ m}^3\text{s}^{-1}$ for 0.15 m sluice gate (Schefer, 2004), although the historic mean of flow release is $5.3 \text{ m}^3\text{s}^{-1}$.

Where no reservoir release occurs, downstream flow originates from (i) reservoir seepage below the dam structure ($\sim 0.03 \text{ m}^3\text{s}^{-1}$), and (ii) leakage from the bottom gate ($\sim 0.07 \text{ m}^3\text{s}^{-1}$); flow discharge at Bajo San José averages $0.28 \text{ m}^3\text{s}^{-1}$. These measures suggest that the reservoir contributes to downstream flow by about 37 %; the remaining proportion is provided by groundwater inflow. Except for some short gullies, the Sauce Grande River receives no tributary inputs until its confluence with Cañada de los Leones creek (unsteady) in the lowest section.

3.1.3. Ecodeficit: a simplified measure of hydrological disruption in regulated rivers

Semiarid rivers are among the most regulated rivers in the world (W.C.D., 2000), because the need for water management in these regions is greatest due to extreme flow variability (Kondolf and Batalla, 2005). Given the dam purpose for water supply and the high scarcity of local water resources, flow release downstream is highly scattered in both magnitude and time. The eco-deficit concept of Vogel *et al.* (2007) provides an expression of the overall water loss within impounded rivers during the period following flow regulation; if water is gained, then ecosurplus occurs. Both eco-deficit and ecosurplus are identified from regions delineated between regulated and unregulated flow duration curves (FDC), and hence provide a simplified measure of the magnitude of hydrologic impacts of river impoundment

Flow duration curves were created from series of daily flow (1989-2010) for the regulated and unregulated Sauce Grande River (Fig. 4.28) The distribution of daily flow downstream from the dam was substantially steeper and skewed (skewness = 60.2) than that for the river upstream (skewness = 31.1), which in turn evidenced clearly the high variability of the natural flow regime. Note, the steep decline in the regulated FDC reflects the difference in magnitude between base flows and higher flows in periods of dam release.

FDC for the regulated and unregulated rivers determined two areas of eco-deficit coincident with both curve extremes, indicating that downstream low-flow and flood requirements were not met (at least over the period of observation). Conversely, the unregulated FDC on the high-flow area was below the regulated FDC, indicating that high-flow requirements were exceeded for about 15 % of all flows (ecosurplus). In spite

of the simplicity of the concept, the measure of ecodeficit and ecosurplus provide clear evidence of strong dam-induced hydrological alteration of the river downstream.

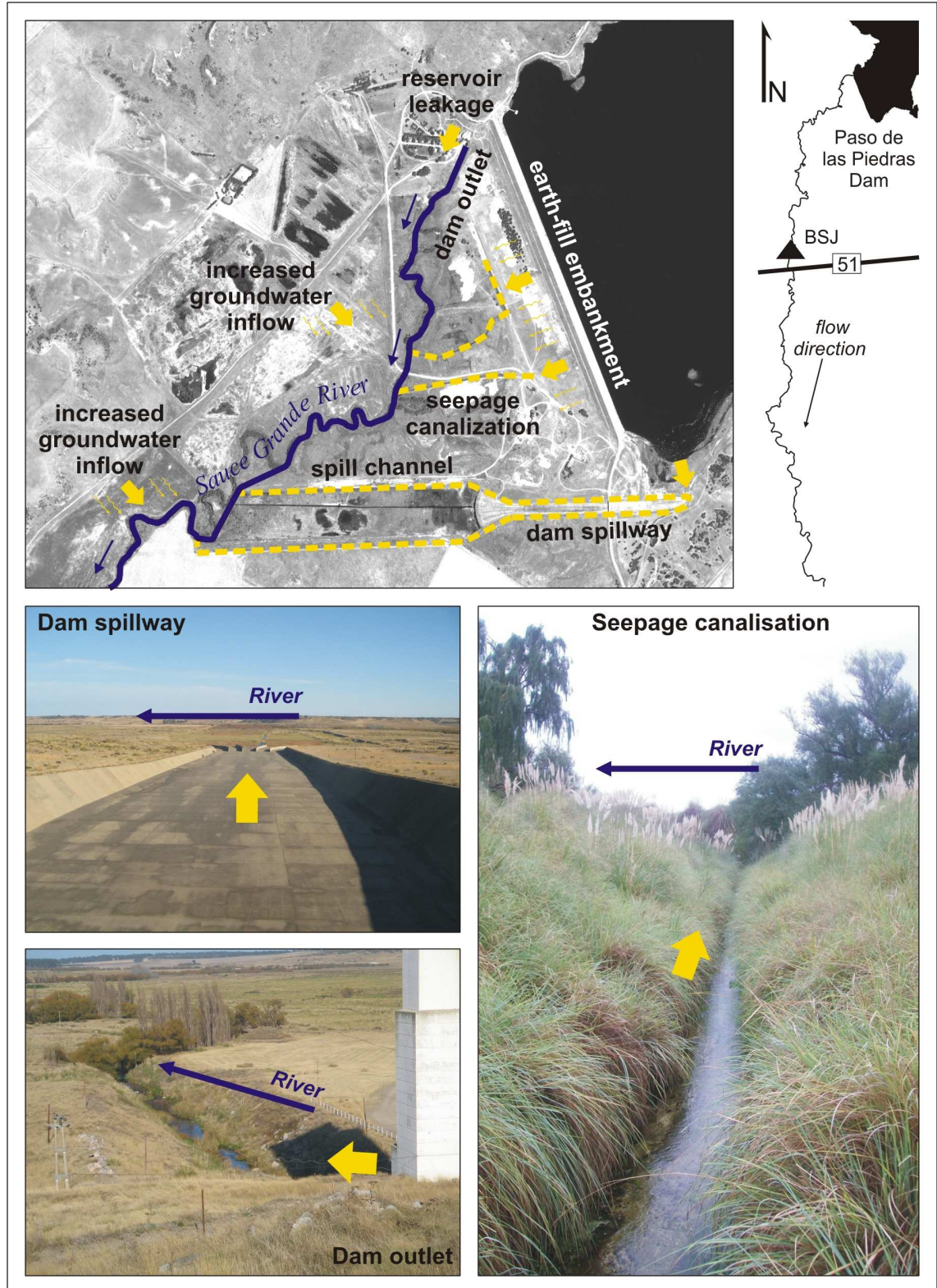


Figure 4.27: Scheme of downstream sources for flow.

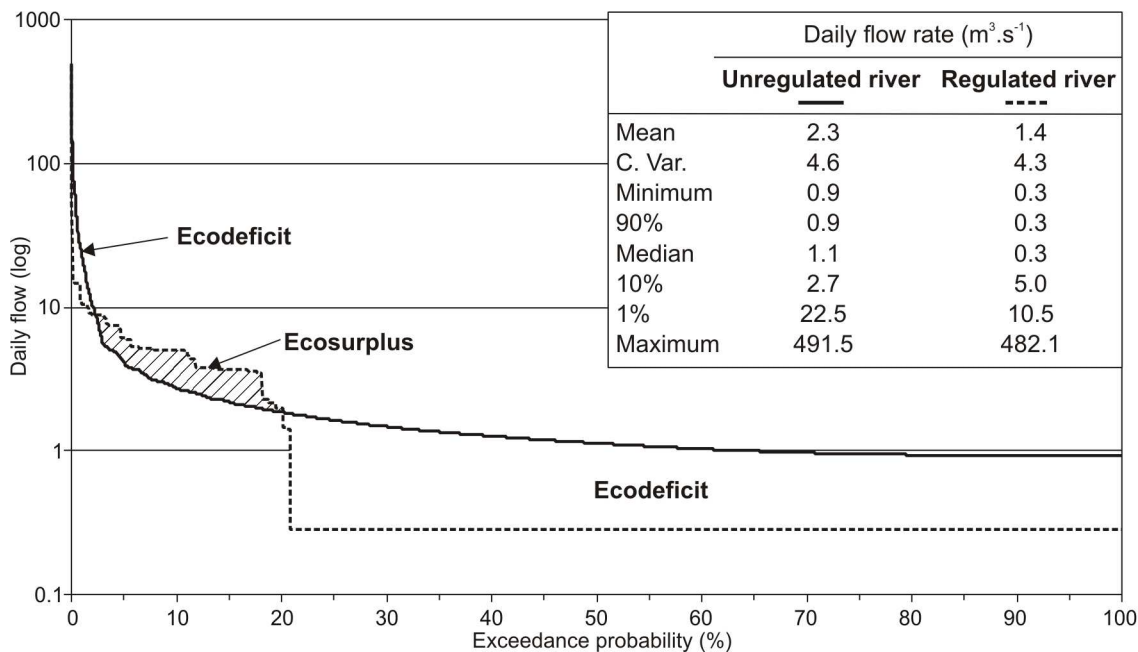


Figure 4.28: Ecodeficit and ecosurplus regions defined from areas between total-period flow duration curves for the regulated and the unregulated Sauce Grande River (1989-2010).

3.1.4. The degree of hydrological alteration of the regulated Sauce Grande River

The degree of hydrological alteration of the river downstream was examined in detail by inspection of upstream-downstream shifts for a suite of indicators (IHA) of river flow regime relative to natural ranges of flow variability (RVA). IHA and RVA approaches permitted to determine whether the state of the regulated river differed significantly from what it would have been in the absence of flow regulation (Richter *et al.*, 1996).

Results from this investigation demonstrated that the dam has induced substantial changes in all components of the river flow regime (Fig. 4.29). The relationship of expected to observed frequency within the middle RVA category was negative for all flow metrics (except for the date of maximum), indicating that very little flow values observed downstream fell within an acceptable range of variability for all flow regime components; the same tendency was observed within the higher thresholds of natural flow variability. Conversely, the frequency of flow values within the lowest thresholds of suitable variability was increased notably. From Figure 4.29, it is clear that the most dramatic shifts occurred in the flow seasonality, in the magnitude of annual minimum flows, in the duration and frequency of high pulses and in the rates of annual flow variability.

Changes in the flow seasonality

The distribution of monthly flows described a flattered hydrograph. Mean and median monthly flows were reduced for all months except for July (austral winter), and monthly coefficients of dispersion were reduced significantly. This indicated coupled reduction

in the flow magnitude and in the inter-annual variability of monthly flows, which ultimately contributed to alter the flow seasonality: summer peaks were suppressed, spring peaks were reduced and delayed, and winter minima were increased.

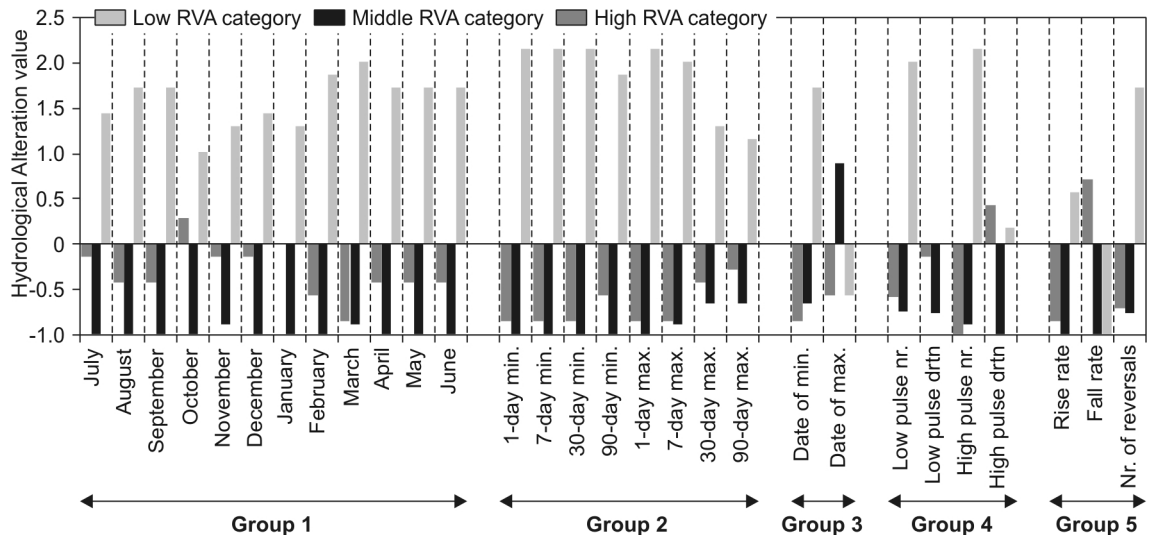


Figure 4.29: Degree of hydrological alteration by flow regime metric. RVA boundaries were defined automatically to provide three categories of equal size delineated by 17th percentiles from the median, where the middle RVA category contains all values falling in the range of the 34th to 67th percentiles. A positive (or negative) deviation indicates that annual parameter values fell inside the RVA target window more often (or less often) than expected (Richter *et al.*, 1998).

Altered seasonality of flow over the annual cycle is a common consequence of flow regulation by dams (Petts, 1984), and so has been reported for many regulated rivers worldwide regardless of the dam purpose (e.g. the Rhone River below several dams for hydropower, Edouard and Vivian, 1984 and Vivian, 1986; 1994; the River Murray below several dams for irrigation and water supply, Maheshwari *et al.*, 1995; the Dudhkumar River below Kurigram Dam for flood control, Hossain and Hossain, 2011). In semiarid regions, decreased summer peaks below reservoirs for water supply is a natural consequence of increased water demand (e.g. Snake River below Jackson Lake Dam, Marston *et al.*, 2005); however, semiarid rivers impounded for irrigation purposes may describe increased summer flow as a consequence of increased agricultural demand (e.g. Ebro River, Magdaleno and Fernández, 2010; Sacramento-San Joaquin River Basin, Kondolf and Batalla, 2005). Increased winter flow in the regulated sauce Grande River (the driest season) may be explained by the action of two coupled processes: (i) water requirements during winter are lowest, and (ii) a number of years recorded small and large floods during winter months, which conceivably contributed to fill the reservoir and hence to increase flow release in order to control the reservoir levels.

Changes in annual flow extremes

Other significant change induced by the Paso de las Piedras Dam was the reduction in the magnitude (-64 to -48 % for increasing duration windows) and frequency (-59 %) of low flows with substantial increase in the low-flow duration (+ 473 %). These findings

oppose those of most studies on regulated rivers, which report overall increase in the magnitude of annual minima as natural consequence of dam operational procedures for hydropower generation (Fergus, 1997; Shields *et al.*, 2000; Maingi and Marsh, 2002; Assani and Petit, 2004), flood control (Richard and Julien, 2003; Choi *et al.*, 2005), or irrigation (Kondolf and Batalla, 2005). Reduction in the low-flow magnitude and increase in the low-flow duration within the sauce Grande River are conceivably related to episodes of drought where the downstream river is sustained almost exclusively by groundwater inflows, reservoir leakage and seepage. Downstream, base flows may persist for much of the year or even for several consecutive years (Fig. 4.28); at present, the river has exhibited residual flows since April 2005.

In contrast to minimum flows that showed significant and consistent alteration trends with increasing flow durations ($HA = -1$ for all duration windows), annual maximum flows showed decreasing degree of alteration as the flow duration window increased. Annual maxima were reduced by 79 % for 1-day maximum and 34 % for 90-day maximum. Similar decreasing magnitudes and alteration trends were found by Magilligan and Nislow (2005) and Graf (2006) within 21 and 36 regulated rivers across USA, respectively. This suggests that reduction in annual peak flows is common to all dams, whereas their impacts on flows of lesser magnitude is less significant and so the hydrological alteration of flows averaged over the week, the month or the season decrease.

Particularly significant was the change in the timing of annual maxima, which fell during the winter season (water year). However, dates of annual maximum and minimum were highly scattered and so any interpretation of the results would be erroneous. One aspect to point out regarding the timing of annual maximum extremes is that any inflow greater than the Q_{10} has high probability of passing downstream whether the initial storage levels are high.

Changes in the flow pulsing and reversals

Besides altering the magnitude and seasonality of annual flows, the dam has reduced substantially the annual flow variability by increasing the flow constancy. This aspect was evidenced by a significant reduction in the frequency of both low- and high-flow pulsing (-59 % and -95 %, respectively) with significant increase in their duration (+473 % and +353 %, respectively), and by a significant reduction in the number of annual reversals (-71 %). Such changes imply a flattered hydrograph, where the duration of flows of similar magnitude was increased notably after river impoundment. Similar conditions were reported for many regulated rivers worldwide (e.g. Ebro River, Batalla *et al.*, 2004 and Magdaleno and Fernández, 2010). However, in years where large volumes of water were evacuated from the dam, the number of reversals of the downstream hydrograph was significantly greater than that for the unregulated flow upstream (e.g. 1993, 1994). This gives evidence of the pulsing character of flow releases inducing artificial variations in daily flows that are notably higher than that for the natural flows. Similar alternating patterns of dam-induced changes in downstream flow variability were found, for example, by Richter *et al.* (1998) within the Green and Colorado Rivers among many others.

3.1.5. Changes in environmental flow components

Extreme reduction in the magnitude and frequency of the full range of flows and substantial increase in the duration of similar flow conditions ultimately contributed to generate a homogeneous hydrograph sustained by subsidence flows and hence with very low variability. These conditions were observed for about 80 % of the observation period (Fig. 4.28), this is 17.6 years over the 22 years of monitoring. The remaining percent of time corresponded to episodes of flow release, where the magnitude and duration of high flows were greater than for natural flow conditions, yet the magnitude of annual extremes was reduced.

Inspection of the distribution of daily flows categorized as environmental flows provided a good expression of the degree of hydrologic alteration relative to the magnitude, timing, frequency, duration and variability of flow states that are critical for geomorphic and ecologic maintenance of the river system (Mathews and Richter, 2007). Results revealed that the most dramatic impact of the dam was the suppression of small floods and the extreme reduction in the frequency of large floods. During the 22 years of monitoring, only one flood episode occurred downstream; upstream, floods occurred 13 times. This single flood was related to the reservoir overflow of November 2002; more than 80 hm³ were evacuated downstream, and more than 200 000 ha were submerged under water (La Nueva Provincia, 12th November 2002).

In spite that reservoirs may be responsible for a reduction of 98 % in peak flows and flood events (Petts, 1977), the effects of the Paso de las Piedras Dam on downstream flooding were extreme compared to those reported in literature for similar dam purposes and environmental conditions. For example, small floods in the River Murray were reduced by 50 % and large floods were poorly affected (Maheshwari *et al.*, 1995). Phillips *et al.* (2005) found that changes in the hydrologic regime of the Trinity River after closure of the Livingston Dam (USA) were negligible; yet Sherrard and Erskine (1991) reported 94 % reduction in flooding in the Mangrove Creek below Mangrove Creek Dam. Within the Sauce Grande River, flood suppression is closely related to the large capacity of the reservoir relative to the hydrologic magnitude of reservoir inflows ($S/\mu = 3.63$). Since floods play an important role in structuring the morphology of river channels and in preventing vegetation encroachment (Richter *et al.*, 1998), flood suppression will have major implications for the morphology of the regulated Sauce Grande River.

On the other side of the scale, the magnitude of low flows was dramatically reduced (70 %) and the low-flow duration was increased notably (821 %); increased duration led to a reduction in the frequency of extreme low flows (33 %) due to increased persistence of similar flow conditions over time. As discussed above, reduced low flows were rarely reported in literature; within the area of interest, this phenomenon responds to the dam purpose for water supply and to the large proportion of reservoir yield relative to mean annual inflow (73 %). Reduced flow magnitude results in reduced stream energy to erode the channel and to transport sediment (Kondolf, 1997; Kondolf and Batalla, 2005), which may lead to channel aggradation and terrace formation within the former floodplain (Church, 1995). Ultimately, reduction of the flow magnitude and suppression of downstream flooding contribute to disconnect the river channel from its floodplain and aquifer (Petts, 1984, Ward and Stanford, 1995b; 1998).

3.2. CRITICAL ALTERATION OF THE RIVER WATER TEMPERATURE

The thermal effects of the dam were similar to those found for temperate rivers (Ward and Stanford, 1979; 1983; 1995a) and included (i) reduction of summer maxima, (ii) increase of winter minima, (iii) reduction in diurnal fluctuations, and (iv) increase in the seasonal constancy. These changes are evaluated relative to the natural river thermal regime *sensu* (Olden and Naiman, 2010) as discussed below.

3.2.1. The unregulated river thermal regime

The water temperature is a measure of the concentration of heat energy in a stream relative to the volume of water (Poole and Berman, 2001). Hence, the water temperature of streams and rivers is dependent on two principal factors: the river hydrology (surface and subsurface flow, and water sources; Ward, 1985), and the atmospheric conditions (dependent on latitude, altitude and continentality; Ward, 1985) determining the heat energy (Webb, 1996; Caissie, 2006). These factors are commonly referred to as drivers of water temperature (Poole and Berman, 2001; Poole *et al.*, 2001) because they influence both the heat load and the thermal capacity (volume of water) of the stream.

The thermal regime of streams and rivers is a measure of water temperature variability in space and time (Ward, 1985; Poole *et al.*, 2001; Caissie, 2006). Series of water temperature data available for the Sauce Grande River were too reduced to effectuate a thermal regime characterization. Nevertheless, water temperatures within the unregulated river upstream were collected during distinct calendar seasons (summer and winter) and for two distinct river sites in terms of channel morphology (pool-shaped and riffle-shaped sections). This procedure permitted to consider the effects of contrasting atmospheric conditions on unregulated patterns of water temperature for two river sections with different thermal capacity.

Overall, the thermal characteristic of the natural river were highly consistent with those of middle-sized temperate streams (Ward and Stanford, 1979; Ward, 1985; Caissie, 2006). Mean daily water temperature increased in the downstream direction during both the summer and the winter period at rates of between 0.006 and 0.013 °C.km⁻¹, respectively. Increase in water temperature with distance is closely related to decreasing groundwater influence as the stream order increases and the stream responds to atmospheric conditions and other local controls (Ward and Stanford, 1979).

Mean daily water temperature over the summer period was 21.4 °C with maximum in March (25 °C), and mean daily water temperature over the winter period was 8.4 °C with minimum in July (4.9 °C); the annual range was 20.1 °C. Despite that temperature data for the entire year are lacking, river thermal patterns during the summer and winter periods reflected the sinusoidal shape described by temperate rivers over the annual cycle (Ward, 1985). Note, the river did not freeze during winter, which is consistent with latitude (38° S).

Diurnal cycles of water temperature revealed moderated fluctuations in both sites. Mean daily ranges were about 1.8 °C in summer and 1.6 °C in winter, with maximum in February (4.7 °C) and July (4.5 °C). Diel fluctuations reached the minimum in the early

morning (at sunrise) and the maximum in late afternoon to early evening in both sites and during both periods; daily maxima were 3 to 6 hours lagged with respect to air temperature. Inter-site differences in the timing of the peak and duration of the recession limb were apparent and linked to differences in the stream morphology and hence to the stream thermal capacity at the sites. Diel cycles of water temperature in site W1 (pool) were more gradual and delayed than those in site W2 (riffle), because pools create a more stable thermal environment. Seasonal shifts in the timing of diel cycles in site W1 were closely related to the flow magnitude during each period; low summer flows contribute to increase the thermal inertia within the pool (due to increased water residence times), whereas higher flow during winter generate less stable thermal environments.

3.2.2. Changes in the absolute magnitude of the downstream thermographs

The suite of thermal metrics used in the assessment of water temperature time series revealed that river impoundment affected primarily the absolute magnitude of the thermographs, whilst the frequency, timing and duration of temperature extremes across sites were influenced by ambient conditions without significant differences between the unregulated and regulated river. Differences in summer (winter) temperature with respect to the unregulated river upstream were of $-2.6\text{ }^{\circ}\text{C}$ ($+2.9\text{ }^{\circ}\text{C}$) in daily means, $-4.1\text{ }^{\circ}\text{C}$ ($+1.5\text{ }^{\circ}\text{C}$) in daily maxima, $-1.2\text{ }^{\circ}\text{C}$ ($+4.4\text{ }^{\circ}\text{C}$) in daily minima, and $-0.5\text{ }^{\circ}\text{C}$ ($-0.7\text{ }^{\circ}\text{C}$) in mean daily ranges.

Comparable magnitudes of thermal change were reported, for example, in the Ain River below the Vouglans Dam, France ($-2\text{ }^{\circ}\text{C}$ in summer mean and $+1.0\text{ }^{\circ}\text{C}$ in winter mean, Poirel and Gailhard, 2010) and in the River Tyne below the Kielder Dam, UK ($-3\text{ }^{\circ}\text{C}$ in summer mean and $+4.0\text{ }^{\circ}\text{C}$ in winter mean, Archer, 2008). Also in the UK, Webb and Walling (1993; 1995; 1997) found that the main effects of the Wimbleball Dam upon the thermal regime of the upper Haddeo River were depressed summer maxima ($3\text{ }^{\circ}\text{C}$ on average), increased winter minima ($4\text{ }^{\circ}\text{C}$ on average), and reduced diurnal fluctuations in all seasons (up to 60 % reduction in maximum daily range).

In comparison to this study, significantly greater magnitudes of thermal change were reported for regulated rivers in Australia, which are comparable in terms of physical setting. For example, summer water temperature in the Macquarie River below the Burrendong Dam and in the Mitta Mitta River below the Dartmouth Dam was reduced by $8\text{ }^{\circ}\text{C}$ and by $10\text{ }^{\circ}\text{C}$, respectively (reviewed by Preece and Jones, 2002), and temperature maxima in the Naomi River below Keepit Dam was reduced by $5\text{ }^{\circ}\text{C}$ (Preece and Jones, 2002); winter temperatures were increased in all cases, and the annual cycles were delayed.

Extreme magnitudes of thermal change were reported within regulated rivers of western USA as well. Olden and Naiman (2010) found that mean summer temperatures in Green River (USA) below the Flaming Gorge Dam decreased from 17.2 to $5.7\text{ }^{\circ}\text{C}$ and winter temperatures increased by $5\text{ }^{\circ}\text{C}$, and Wright *et al.* (2005), reported $15\text{ }^{\circ}\text{C}$ summer decrease and $8\text{ }^{\circ}\text{C}$ winter increase in the temperature of the Colorado River below Glen Canyon Dam.

3.2.3. Changes in the relative magnitude and timing of diurnal regimes

Whilst there were significant differences in the absolute temperatures within and between sites, the regime shape and magnitude classification (RSMC) revealed that the thermal behaviour of the time series could be explained by the recurrence of four classes of regime shape (form of the diurnal cycle, timing and duration of the peak) and three different regime magnitudes (size of the thermograph). This suggests a strong similarity in the relative shape and magnitude of diurnal regimes of water temperature, regardless of their absolute magnitude.

The response of diurnal regimes of water temperature to regulated patterns of flow under extreme weather conditions showed dissimilarity regarding the shape and the magnitude of the thermographs, and similarity in such response during the two periods of monitoring. *Regime shape* analysis revealed strong class dominance by site regardless of the monitoring period (i.e. each site had a 'typical' form of diurnal regime), and clear differentiation in the spatial distribution of dominant classes downstream related systematically to the effects of the dam. Conversely, *regime magnitude* analysis revealed high within-site variability and strong between-site synchrony, i.e. changes in the relative magnitude of diurnal regimes occurred at the same time across all sites during both summer and winter periods. This revealed that water temperature regimes were more sensitive to change in the relative size than in the timing of the diurnal cycles, which in turn were affected by the impoundment.

Based on the frequency and the spatial distribution of dominating classes of regime shape and magnitude, the river thermal behaviour may be simplified into four combinations of composite classes of diurnal regime (Table 4.15) highlighting contrasts of major ecological significance (Harris *et al.*, 2000). Note, differences between summer and winter conditions were in the relative magnitude of the thermographs but not in the timing of the diurnal cycles, except for site W3.

The unregulated 'natural' river thermal regime revealed relatively symmetrical diurnal cycles and preponderance of sequencing of high temperatures in summer and moderated to low temperature in winter. These thermal patterns showed the major shift directly below the dam. Diurnal cycles in site W3 revealed a dominance of late and extended peaks in summer and more symmetrical diel variations in winter (Class *i*); this is comparable to the 'seasonal' thermal behaviour of site W1, although site W3 is riffle-shaped and so it should reveal thermal regimes closer to those of site W2.

Conceivably, this is related to the effects of upstream impoundment, as the thermal characteristics of waters going out from the reservoir have greater thermal inertia related to the impounded water mass (Webb, 1996, Olden and Naiman, 2010). Furthermore, the relative magnitude of diurnal thermographs at site W3 showed clear 'seasonal' inversion with respect to unregulated thermal conditions: water temperatures were substantially lower in summer and substantially higher in winter. Thermal inversion is closely related to the effects of upstream impoundment as well, as the temperature of waters running below stratified reservoirs is out-of-phase with respect to that of the unregulated river upstream (Ward and Stanford, 1979; Webb, 1996; Webb *et al.*, 2008).

Relative cool summer temperatures and warm winter temperatures persisted over about 4 river-kilometres downstream (class *ii*), although the dominant shape of diel cycles was more in synchrony with that of unregulated waters. Diurnal regimes recovered the ‘natural’ behaviour (class *iii*) after a distance of about 8 km, but changed again downstream from river kilometre 13 (class *iv*). Diurnal fluctuations in the distal sites were very steep for both periods, and were significantly higher in magnitude during summer than during winter. These aspects indicated stronger synchrony to air temperature regimes than to upstream unregulated thermal conditions.

Table 4.15: Simplified classes of diurnal regime of water temperature and spatial distribution along the regulated Sauce Grande River.

Class	Timing	Magnitude	Spatial distribution
Class <i>i</i> 	Late and extended peak at 2100 hours with gradual cessation in summer; symmetrical diurnal cycles with broad peak at 1800 in winter	Low magnitude in summer; high magnitude in winter	Site W3; river km 2 below the dam
Class <i>ii</i> 	Symmetrical diurnal cycles with broad peak at 1800 in summer; similar timing in winter (inferred)	Low magnitude in summer; moderated to high magnitude in winter (inferred)	Site W4; river km 4 below the dam
Class <i>iii</i> 	Symmetrical diurnal cycles with broad peak at 1800 hours in both periods	High magnitude in summer, low magnitude in winter	Sites W5 and W6; river km 8 to 11 below the dam
Class <i>iv</i> 	Steep and early peak at 1500 hours with rapid cessation in both periods	High magnitude in summer, low magnitude in winter	Sites W7 and W8; river km 13 to 15 below the dam

3.2.4. Causes of thermal change and downstream persistence

The main effects of the dam on downstream patterns of river water temperature were (i) decrease in summer temperature, (ii) increase in winter temperature, (iii) reduction of diurnal fluctuations, and (iv) changes in the timing of diurnal cycles; together, these changes contributed to increase the seasonal constancy of the river thermal regime. These changes are characteristic of regulated rivers in temperate regions of the world (Ward and Stanford, 1979) and respond to dam-induced changes in both components of the river water temperature downstream: (i) the heat load, due to thermal stratification of the reservoir and altered groundwater circulation downstream from the dam (Ward and Stanford, 1979; Ward, 1985; Webb and Walling, 1997; Olden and Naiman, 2010), and (ii) the stream thermal capacity, due to reduction in downstream flow discharge and hence, increased influence of groundwater inflows and atmospheric conditions on the thermal behaviour of the running waters (Webb, 1996; Poole and Berman, 2001).

In contrast to other dams where cooling (or warming) trends during summer (or winter) months are mostly related to deep release from thermally stratified reservoirs (e.g. Zhong and Power, 1996; Preece and Jones, 2002; Archer, 2008; Wright *et al.*, 2009;

Poirel *et al.*, 2010), the cooling/warming effect induced by the Paso de las Piedras Dam was mostly related to canalisation of reservoir leakage and seepage into the main river channel (Fig. 4.27); water release did not occur due to dam operations to maximise water storage in the context of prolonged drought and limited reservoir inflows over both monitoring periods. Furthermore, the cooling/warming effect of the dam was conceivably enhanced by increased groundwater inflow following river impoundment. Similar patterns of mixed inflow sources below dams (i.e. groundwater and reservoir outflow) have been found, for example, in the Upper Haddeo River below Wimbleball Lake (Webb and Walling, 1995; 1997), where groundwater inflows were relatively cooler and steadier than reservoir inflows for much of the summer season.

Downstream river summer cooling and winter warming persisted along the 15 km stretch monitored. During summer, the cooling effect of the dam was most marked over a distance of about 8 km and declined downstream thereafter; however, 30-day mean water temperature at site W8 (river km 15) was 1.3 °C cooler than that of the unregulated river. During winter, warm temperatures persisted over 11 km and declined steeply thereafter; water temperatures at site W8 were almost as cool as those recorded within the river upstream.

Similar patterns of spatial persistence of altered water temperatures were found by Webb and Walling (1988; 1993) for different river sites in south-west England (20 km; 40 km in conditions of hot weather) and by Cowx *et al.* (1987) for three river sites in Wales (30 km). However, the distance for thermal recovery below dams has been reported to vary considerably (e.g. 60 km, Archer, 2008; 100 km, Preece and Jones, 2002; 260 km, Zhong and Power, 1996) as it depends primarily on the dam structure and operational procedures (Ward and Stanford, 1979; Petts, 1984), on the energy contributions from the atmosphere, tributaries and the phreatic zone (Webb, 1996; Hannah *et al.*, 2004; Caissie, 2006; Webb *et al.*, 2008), and on a number of structural factors moderating heat exchange to and from the river.

3.2.5. Other potential drivers of river thermal change

Whilst the effects of the dam in altering the downstream thermographs were clear, patterns of thermal recovery with distance from the dam were non linear and reflected variations between the two periods of monitoring. These aspects indicated influence of other external factors controlling heat and water exchanges (in addition to the control exerted by the dam), as well as influence of the stream structure on such exchanges at the micro-scale.

Among all atmospheric thermal drivers, air temperature is the main factor affecting river water temperature (Ward, 1985; Webb, 1996; Ahmadi Nedushan *et al.*, 2007; Bonacci *et al.*, 2008). As air temperature provides a surrogate measure of net heat exchange (Webb *et al.*, 2008), water-air temperature relationships have been used widely either to predict (e.g. Caissie *et al.*, 2005; Ahmadi Nedushan *et al.*, 2007; Koch and Grünewald, 2010) or to evaluate (e.g. Mohseni and Stefan, 1999; Ozaki *et al.*, 2003; Webb *et al.*, 2003; Bonacci *et al.*, 2008) river thermal variability.

Inspection of patterns of water temperature revealed that temporal and diel variations were synchronized broadly with those observed for air temperature, especially during

the summer period. All water temperature sites warmed and cooled simultaneously, with lags of 0 to 3 days (in summer) and up to 6 days (in winter) relative to air temperature. Sensitivity analysis for water-air temperature associations revealed two contrasting scenarios for sites located above and below the impoundment, and temporal variations in the degree of climatic sensitivity of each scenario. The shape and the magnitude of diurnal water temperature regimes within the upstream, 'natural' river were climatically sensitive (especially in summer) and temporally equitable. Downstream from the dam, the form (timing) of water temperature regimes revealed overall climatic insensitivity during summer and moderate to high sensitivity during winter, the shape of diurnal regimes reflecting high stability during both periods. Water-air associations regarding the regime magnitude revealed higher sensitivity and equitability than the regime shape.

Overall, results suggested that the sequencing of size of response was broadly driven by prevailing weather conditions, although the timing and absolute size of the thermographs were affected by the dam. Water temperature regimes within the river downstream were highly stable regardless the temporal variations in the strength of water-air temperature associations; additionally, *SI* values close to 0 (sensitivity) were missing. In some cases, climatic insensitivity may be associated to the thermal effects of the dam (e.g. in site W3). However, many other reasons could be behind this overall water-air insensitivity.

The structural components of a stream act as moderators for heat exchanges at the air/water and streambed/water interfaces and hence, determine the stream resistance to warming or cooling. This study evaluated a set of indicators of topographic, morphologic and groundwater influence on river water temperatures (Table 4.16). The relationship between channel orientation and size, together with riparian vegetation height and density influence insulating processes to the stream (Poole and Berman, 2001; Moore *et al.*, 2005; Caissie, 2006), whereas the bed channel slope and bed shape control longitudinal thermal dispersion resulting from variations in flow velocity (Moore *et al.*, 2005) and hyporheic exchange (Poole and Berman, 2001; Hannah *et al.*, 2009). Finally, the electrical conductivity of running waters provided an indicator of groundwater influence driving heat exchanges through geothermal conduction (Hannah *et al.*, 2004; Caissie, 2006; Webb *et al.*, 2008). Note, heat exchange processes at the air-water and streambed-water interfaces have not been evaluated and hence, the energy budget of the river remains to be investigated directly.

The relative stream characteristics along the river stretch monitored permit to assemble water temperature sites into groups of similar stream structural influence on river water temperature. Upstream sites were clearly differentiated from each other as well as from the sites located below the impoundment. The main difference between sites was in the channel geometry moderating heat exchange at the air/water interface. Thermal inertia in site W1 (pool-shaped) was higher than in site W2 (riffle-shaped) because of the higher thermal capacity of the stream; thermal variations in site W2 were higher because the large size of the stream contributes to increase water/air heat exchange regardless of the effects of riparian shading. In spite of these differences, both sites revealed characteristics of intermediate streams, where groundwater influence is moderated relative to the flow capacity of the stream and where lateral tributaries may have strong thermal influence.

Table 4.16: Stream characteristics by water temperature site. Properties for each characteristic are relative to the entire river stretch monitored.

Site	Aspect	Riparian cover	Channel shape	Bed shape (P&R)	Channel slope	Electrical conductivity
W1	SE	Low	Intermediate	Low	Low	Low-mod.
W2	S	Moderate	Large	Low	High	Moderate
W3	SSW	Mod.-high	Small	Low-mod.	Mod.-high	Moderate
W4	SW	High	Int.-large	Low-mod.	Mod.-high	Mod.-high
W5	S	High	Intermediate	High	Moderated	High
W6	SSW	Mod.-high	Small-int.	High	High	High
W7	SSW	Low	Small-int.	Moderated	Low-mod.	Very high
W8	SSE	Low	Small-int.	Low-mod.	Low-mod.	Very high

Below the dam, thermal variations in sites W3 and W4 were strongly influenced by riparian shading exerted by dense willow associations growing along the river margins; depending on the channel size, willows may shade all or a great portion of the water surface. A large number of studies on river thermal dynamics within forested basins reported that riparian vegetation cover creates stable thermal environments (e.g. Osborne and Kovacic, 1993; Broadmedow and Nisbet, 2004; Johnson, 2004; Webb and Crisp, 2006; Malcolm *et al.*, 2008; Hannah *et al.*, 2008a). Thermal stability was evidenced clearly by low regime equitability and low gradients of thermal recovery between the sites, especially in summer.

The effects of upland shading in site W5 were also significant, although the overall stream characteristics of the site were more related to those of site W6. The overall reach morphology upstream from both sites exhibited the greatest sinuosity and hence the greater number of pools and riffles. Alternating pool and riffle sequences contribute to increase hiporheic flow (Poole and Berman, 2001; Moore *et al.*, 2005) and hence increase advective thermal exchange (Hannah *et al.*, 2009; Dallas and Rivers-Moore, 2011; Krause *et al.*, 2011). Furthermore, high stream sinuosity contributes to increase groundwater influence as the stream dissects piezometric levels.

Finally, thermal dynamics in sites W7 and W8 were strongly influenced by groundwater inflow as indicated by the high electrical conductivity of running waters. Geothermal waters typically moderate stream water temperature by cooling the stream in summer and warming the stream in winter (Webb and Walling, 1995; 1997; Hannah *et al.*, 2009; Duque *et al.*, 2010). However, in the absence of shading influence and in the presence of shallow channel conditions, water temperatures may trend rapidly toward atmospheric temperatures (Poole and Berman, 2001). This aspect was evidenced by high gradients of thermal recovery between both sites and dominant patterns of diurnal regimes strongly synchronized with air temperature.

3.3. APPLICABILITY OF THE METHODS USED IN ANALYSIS

Increasing concern on the hydrological alteration of regulated rivers on a global scale has led to the development of a wide range of methodologies to assess flow requirements for geomorphic and ecological integrity of river systems. The most complete evaluation of methods for environmental flow assessment can be found in the reviews of Arthington and Zalucki (1998) and Tharme (2003).

Among all methods available in literature, this study used coupled hydrological and holistic methodologies including the range of variability approach (Richter *et al.*, 1997) based on a set of indicators of hydrological alteration (Richter *et al.*, 1996), and the environmental flow components approach (Mathews and Richter, 2007). As the methodological suite is available within the Indicators of Hydrological Alteration program, it is frequently referred to as IHA. Some examples of the application of IHA to hydrological assessment of regulated rivers include, for example the case studies of Richter *et al.* (1996) on the Roanoke River (USA), Richter *et al.* (1998) on the Colorado and Green Rivers (USA), Maingi and Marsh (2002) on the Tana River (Kenya), Opperman (2006a; 2006b) on the Middle Fort and Patuca Rivers (USA), and Mathews and Richter (2007) on the Green River (USA). Examples of regional applications of the IHA suite include the studies of Assani and Tardif in Canada (2005), Magilligan and Nislow (2005) and Graf (2006) in USA, and Fernández *et al.* (2012) in Spain, among others. A good analysis of the applicability of the IHA method to flow regime assessment in Texas was performed by Hersh and Maidment (2006).

The suite of IHA methods was selected for a number of reasons. First, IHA is based on the paradigm of the natural flow regime (Poff *et al.*, 1997) and regime variability (Poff and Ward, 1989), providing an integrated measure of alteration in the flow attributes that are relevant for both the river morphology and the stream ecology. Second, the set of indicators of hydrological alteration provide the majority of information with the smallest population of indices (Olden and Poff, 2003), and allow minimizing redundant metrics based on hydrological understanding (Monk *et al.*, 2007). Third, the method uses thresholds and other parameters commonly used in hydrologic analysis, and it is flexible to adjust such parameters by the user. Fourth, the IHA Program is of free access and is compatible to independent software such as Microsoft Excel; in addition, the program only requires flow data to run, and calculates rapidly the entire set of metrics through a friendly interface.

Overall, IHA is best suited to assess hydrologic alteration (Hersh and Maidment, 2006) and has great potential to quantify impacts of dams and other projects for water management. The greatest limitation of the IHA method is that it has been conceived to quantify hydrological alteration based on the comparison between pre- and post-impact periods. Nevertheless, the method is flexible to evaluate the degree of alteration of a regulated system relative to a natural system used as reference, and to compare measured post-impact conditions to unaffected conditions predicted for the same period of time (Richter *et al.*, 1996).

The set of temperature metrics used to water temperature assessment was very helpful to evaluate temporal patterns of river water temperature at different sites. However, the thermal behaviour of the river has been evaluated using a temporally limited data set.

The lack of long-term detailed data was the greatest limitation to assess the river water temperature regime. Most studies solve this problem by predicting river water temperature based on regression models (Stefan and Preud'homme, 1993; Koch and Grünwald, 2010), deterministic models (Sinokrot *et al.*, 1995; Caissie *et al.*, 2005; Wright *et al.*, 2009) or stochastic models (Ahmadi-Nedushan *et al.*, 2007). Although physical modelling has provided very suitable results, most of models incorporate independent variables that for the area of interest were unavailable.

This study tested utility of the regime shape and magnitude classification approach (RSMC, Hannah *et al.*, 2000) to water temperature assessment. RSMC provided easily interpretable information on two key attributes of the river thermal regime influencing river ecology: the size and the timing of the thermograph. The method allows analysis of both key regime attributes either separately or jointly (Harris *et al.*, 2000; Kansakar *et al.*, 2004), so that aggregated patterns of water temperature regime can be identified simply. Additionally, the RSMC procedure is relative at a station, and so it provides information on the regime variability within (time) and between (space) observation sites. The major benefits of this technique are that (i) it may be applied to any variable exhibiting a cycle for a given time length and resolution (Harris *et al.*, 2000; Bower *et al.*, 2004), and (ii) the flexibility of the classification procedure allows modification for a range of applications (Hannah *et al.*, 2000). Thus, RSMC represents a potentially powerful tool to regime analysis of a variety of variables, contexts and time-scales.

RSMC classes provided a means for assessing the temporal regime stability at a station (Equitability Index, *EI*) and for quantifying the linkages between water and air temperature regimes (Sensitivity Index, *SI*). The use of the *SI* to assess the climatic sensitivity of water temperature regimes is novel, and provided useful summaries of the complex linkages between water temperature regimes, flow regulation and weather conditions during two critical periods of water and thermal stress. The major advantage of the *SI* is that it summarizes the strength and the direction of water-air temperature associations into a single, concise value that allows comparison in space and time. Arguably, the *SI* provides less information about the direction and frequency of single class associations. However, this may be evaluated by cross-tabulation of values of conditional entropy for a given location. By simply plotting these results, meaningful complementary information may be yielded. Furthermore, as the *SI* quantifies relationships between two variables subject to any nominal regime classification (Bower *et al.*, 2004), it may be applied to link classes for a wide range of variables affecting water quality and stream ecology (e.g. flow discharge; water conductivity; dissolved oxygen) and thus, it has great potential utility as a tool for ecohydrological analysis.

3.4. CONCLUSIONS

This study provided the very first assessment of the impacts of the Paso de las Piedras Dam on the flow regime and patterns of water temperature within the Sauce Grande River below the impoundment. As well as yielding new information on the impacts of flow regulation, this study represents the first assessment of natural hydrologic and thermal processes within the river basin. The greatest limitation for earlier assessment of these two critical variables for the integrity of the river system was strongly

conditioned by the lack of climatic and hydrologic data. In this regard, this investigation provides an important platform to enable further research to assess the health of the river ecosystem and to inform the sustainable management of water resources. In addition, this study has tested applicability of three different methods to flow and water temperature assessment within ungauged basins. This knowledge and the methods yielded herein are widely transferable to other river flow and water temperature studies over a range of spatial and temporal scales.

Results from this investigation revealed broad changes in the hydrology and thermal patterns of the regulated river. Floods were fully eliminated and the magnitude and frequency of high and low flow pulsing were dramatically reduced with substantial increase in the duration of similar flow conditions. Furthermore, summer temperatures were depressed, winter temperatures were increased and diurnal fluctuations were substantially altered in both magnitude and timing.

Assuming sediment retention greater than 99 %, the hydrological disruption induced by the dam reservoir may be schematized as shown in Figure 4.30. The equilibrium of longitudinal fluvial processes was seriously perturbed by parallel reduction in the two key hydrologic parameters, the flow discharge and the sediment load; however, reduction in the flow capacity to transport sediment was conceivably greater than the reduction in the flow competence due to flood suppression and extreme reduction in high- and low-flow conditions. In addition, the dam has induced upstream-downstream river thermal inversion during both periods of analysis, which ultimately impact on the seasonal quality of running waters with great implications for the stream ecology. Such disruption will lead to a suite of morphological and ecological adjustments of the downstream river channel and its floodplain. Implications of hydrological alteration for the morphology and the riverine landscape of the regulated river are evaluated robustly in the next chapter.

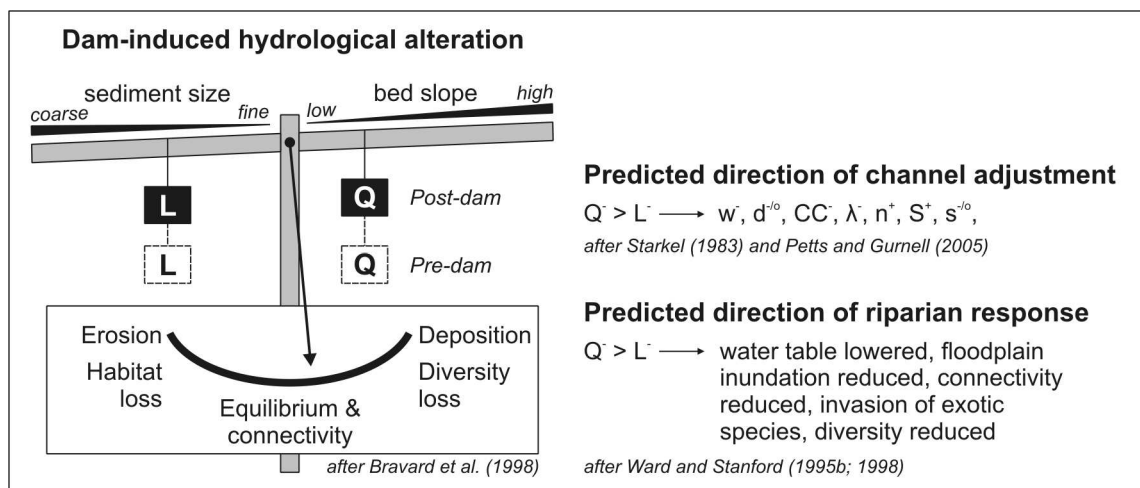


Figure 4.30: Dam-induced disruption of longitudinal fluvial processes and predicted morphological and ecological response of the river downstream.

CONTENTS

- 1 Methods
- 2 Results
 - Changes in the river morphology
 - Morphologic changes at the scale of the river segment*
 - Morphologic changes at the scale of the river reach*
 - Changes in the fluvial landscape
 - Changes in the landscape composition*
 - Changes in the landscape configuration*
- 3 Discussion and Conclusions

The previous chapter revealed strong dam-induced disturbance in the key variables of morphological and ecological control: the flow discharge, the sediment load and the water quality. The full range of flows was dramatically reduced, floods were suppressed and the duration of low flows was increased significantly; reductions in the sediment concentration of the stream (assumed as greater than 99 %) were considered of less importance given the extreme decrease in the transport capacity of flows. Furthermore, longitudinal inversion in patterns of river water temperature was observed during both the summer and the winter observation periods.

Disruption of the fluvial processes in the longitudinal dimension results in serial discontinuities (Ward and Stanford, 1983; 1995a; Stanford and Ward, 2001) within the river *continuum* (sensu Vannote *et al.*, 1980) affecting the strengths of lateral, vertical and longitudinal connectivity along the river corridor downstream. Upstream-downstream shifts in the river hydrology and water quality heterogeneity ultimately impact on the channel stability (Petts, 1984; Williams and Wolman, 1984), the ecological connectivity (Ward and Stanford, 1995b; Ward, 1998) and the overall biodiversity (Ward, 1998; Nilsson and Berggren, 2000; Bunn and Arthington, 2002) of the river downstream.

This chapter evaluates the dam impacts of second order involving the response of the river channel morphology and the associated riparian zone to altered patterns of flow, sediment and water quality over time. The river segment selected for analysis extends from the dam closure to the confluence of Los Cardales creek about 25 km south; a river segment extending over about 15 km upstream from the dam was selected as reference of unregulated conditions. A set of eight reference reaches along the entire river corridor was used to inspect channel stability.

Analysis of dam impacts on the river corridor was structured into two linked subsections. First, the chapter quantifies morphologic changes below the dam with focus on the lateral mobility and the channel capacity at the scale of the river segment, and on the channel stability at the scale of the river reach. Second, the chapter examines the evolution of the fluvial landscape at the scale of the quaternary floodplain with especial regard on the riparian zone and channel vegetation processes. As the river Sauce Grande is an agricultural stream, special attention was accorded to the dynamics in land use types within the river environment to identify their potential effects on the river channel morphology regardless of the effects of the dam.

The methods used coupled diachronic and synchronic analysis based on comparison of land cover types and fluvial forms between the regulated and the unregulated river over time. This permitted to quantify rates of change in two dimensions: the trajectory of changes since dam closure (time) and the distance of changes with respect to the dam (space).



Figure 5. 1: Actual state of the Sauce Grande River for two reference reaches located upstream and downstream from the Paso de las Piedras Dam.

1.1. SCALES OF ANALYSIS

Quantification of change in the river morphology and associated vegetation was based on a chronological sequence of historical aerial photographs and imagery spanning pre- and post-disturbance river conditions (Fig. 5.2). Historic spatial data were available for three time steps: (i) 17 years before dam closure (1961), (ii) 3 years after dam closure (1981), and (iii) 26 years after dam closure (2004). Geomorphic analysis for each time step focused on two sample river segments located above and below the impoundment. The upstream river segment extends from the town of Saldungaray to the top portion of the reservoir's lake; the downstream river segment extends from the dam closure to the confluence of Los Cardales Creek. Additionally, each river segment was subdivided into functional sectors (Petts and Amoros, 1996), or reaches in terms of Graff (2006) and Poole (2002), having similar geomorphic characteristics.

The length of the river segments, measured as 'bird eye', is ~15 km for the river segment upstream (26.3 km in river distance) and ~25 km for the river segment downstream (40.0 km in river distance). The length of the sample reaches is 1 km measured along the channel axis; this length was selected based on common distances suggested by guides of geomorphological survey (e.g. Thorne, 1993; Harrelson *et al.*, 1994; Rosgen, 1996) and relative to the total length of the river segments.

Based on Bravard *et al.* (1998), the width of the river segments and reaches was defined by three lateral edges including: (i) the *inactive floodplain*, or space of maximum mobility, (ii) the *active floodplain*, or space of functional mobility, and (iii) the *stream channel*, or space of minimum mobility (Fig. 5.2). The terms employed within this research are associated to standard concepts as specified below.

The *inactive floodplain* corresponds to the broad alluvial plain composed of fluvial deposits of Pleistocene and Holocene origin (Bravard *et al.*, 1998). The lateral edges of the inactive floodplain for the Sauce Grande River were defined by the Terrace 0, where visible, as it was recognized as the oldest fluvial feature associated to the river Sauce Grande (Borromei, 1991; Zavala and Quattrocchio, 2001; Quattrocchio *et al.*, 2008). In sectors where the oldest lateral break lines were hidden by agricultural practices, lateral edges were defined by contour lines.

The *active floodplain* refers to the area along the stream that is subject to occasional or frequent flooding (Junk *et al.*, 1989; Ward, 1998) and that supports the riparian zone (Steiger *et al.*, 2005), i.e. plants that grow close to the stream where the stream influences the growing conditions (Poole *et al.*, 2001). The edges of the active floodplain for the Sauce Grande River were identified easily by changes in vegetation type and density, and by changes in the land cover use from agricultural land use to semi-natural cover.

The *stream channel* refers to the area that is inundated frequently (Poole *et al.*, 2001) by flows of 2-yr return interval (bankfull flow, Dunne and Leopold, 1978). The edges for the stream channel were identified from cut banks and pointbars, and from changes in the vegetation density and bank materials.

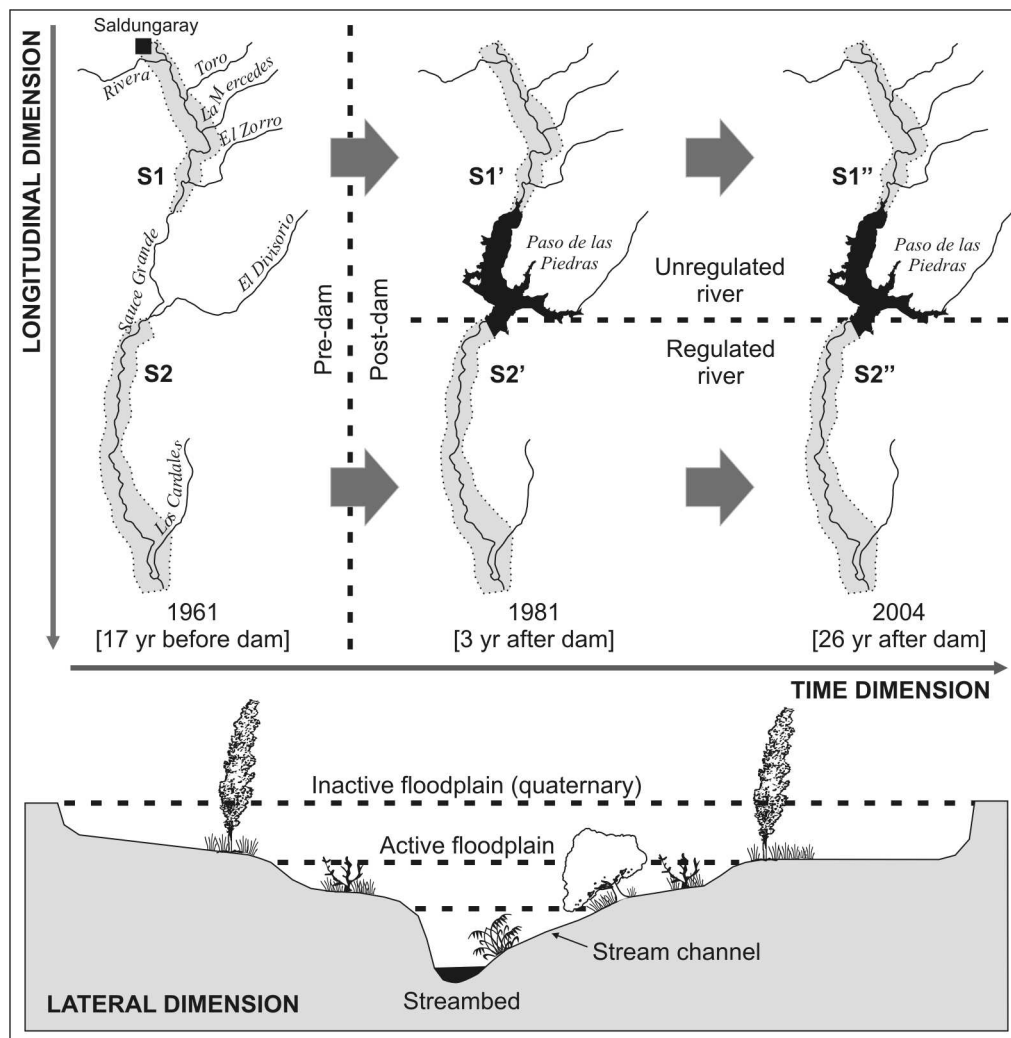


Figure 5.2: Longitudinal, lateral and temporal dimensions used in geomorphic analysis.

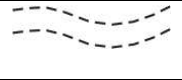
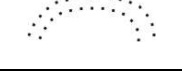
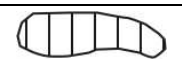
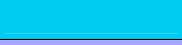
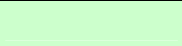
1.2. MAPPED SURFACES

Rivers and streams are hierarchic systems composed of a multitude of functional surfaces or *units* interacting at different spatial scales (Petts and Amoros, 1996; Poole, 2002; Graf, 2006). Functional units underlay a variety of dynamic environmental processes (Aspinall and Pearson, 2000; Fujihara and Kikuchi, 2005) influencing the river morphology and ecology (Phillips, 2009).

Functional units were mapped in ArcGIS based on rectified aerial photography and imagery for the three time steps considered in analysis (1961; 1981; 2004). Internal operations within ArcGIS permitted measuring the frequency and extent of functional surfaces for each time step and scale of observation (spatial structure and dynamics). Mapped surfaces were grouped into three major landscape categories including agricultural lands, fluvial forms and semi-natural vegetation cover (Table 5.1). Terms and representation colours of land cover types were adapted from the CORINE Land

Cover nomenclature (European Environmental Agency, 1994); terms and representation symbols of fluvial forms were based on Thorne (1993).

Table 5.1: Mapped surfaces and representation symbols by scale of observation.

Category	Level I	Level II	Description	Symbol
Fluvial morphology	Active floodplain	Terraces	Remnant of former floodplain no longer inundated	
		Abandoned channel	Old channel disconnected from the current main channel	
		Cut-offs	Abandoned bends; may contain oxbow lakes	
	Stream channel	Levees	Natural or artificial banks above the floodplain level	
		Stream centreline	Line representing the centre of the flow path along the channel	
		Islands	Sediment accumulation within the low-flow channel	
		Deposition banks	Depositional banks inside meander bends	
		Cut banks	Erosive banks outside meander bends	
Inland waters	Water surfaces		Surface occupied by water	
	Flooding areas		Surfaces inundated frequently	
Natural vegetation	Semi-natural mixed woodlands		Natural or artificial associations of trees dominated by willow and poplar	
	Grasslands		Low, medium and high herbs dominated by grasses and pampas grasses	
	Bare soils		Open spaces with little or no vegetation	
Agricultural areas	Crops		Rainfed production of cereals, oilseeds and forage	
	Pastures		Dense grass cover mainly used for grazing	
Artificial surfaces	Constructions		Urban fabric, farms, roads, bridges and other artificial surface areas	

Two scales of observation were defined (Table 5.1) based on combinations between the lateral dimension (quaternary floodplain, active floodplain, stream channel) and the longitudinal dimension (river segments and reaches); note, the degree of detail in mapped surfaces increases with the scale of observation. The Level I includes units at the broad scale of the inactive floodplain for the upstream and the downstream river segments, whereas the Level II focuses on functional surfaces at the scale of the active floodplain along the river reaches. The identification of functional units for both levels was supported by field survey including land use and vegetal species recognition,

measurements of active channel (floodplain) width and depth, and sediment observations. Mapped surfaces at the Level I provided the basis for conducting analysis of change in the fluvial landscape. Geomorphic analysis was conducted based on functional surfaces at Levels I and II.

1.3. QUANTIFICATION OF CHANGE IN THE FLUVIAL MORPHOLOGY

The influence of flow regulation on the river morphology downstream was evaluated based on the recognition of stream states above and below the impoundment for the pre-(1961) and post-disturbance (1981 and 2004) periods. Geomorphic analysis combined the two levels of observation described above with the Rosgen's (1994; 2001) geomorphic classification of natural rivers (Fig. 5.3).

Analysis at the Level I involved a broad geomorphic characterization of the river segments, whereas analysis at the Level II used detailed morphological descriptions of sample reaches. Inspection of the evolutionary stream state at both levels of analysis provided the basis for assessment of channel change with time.

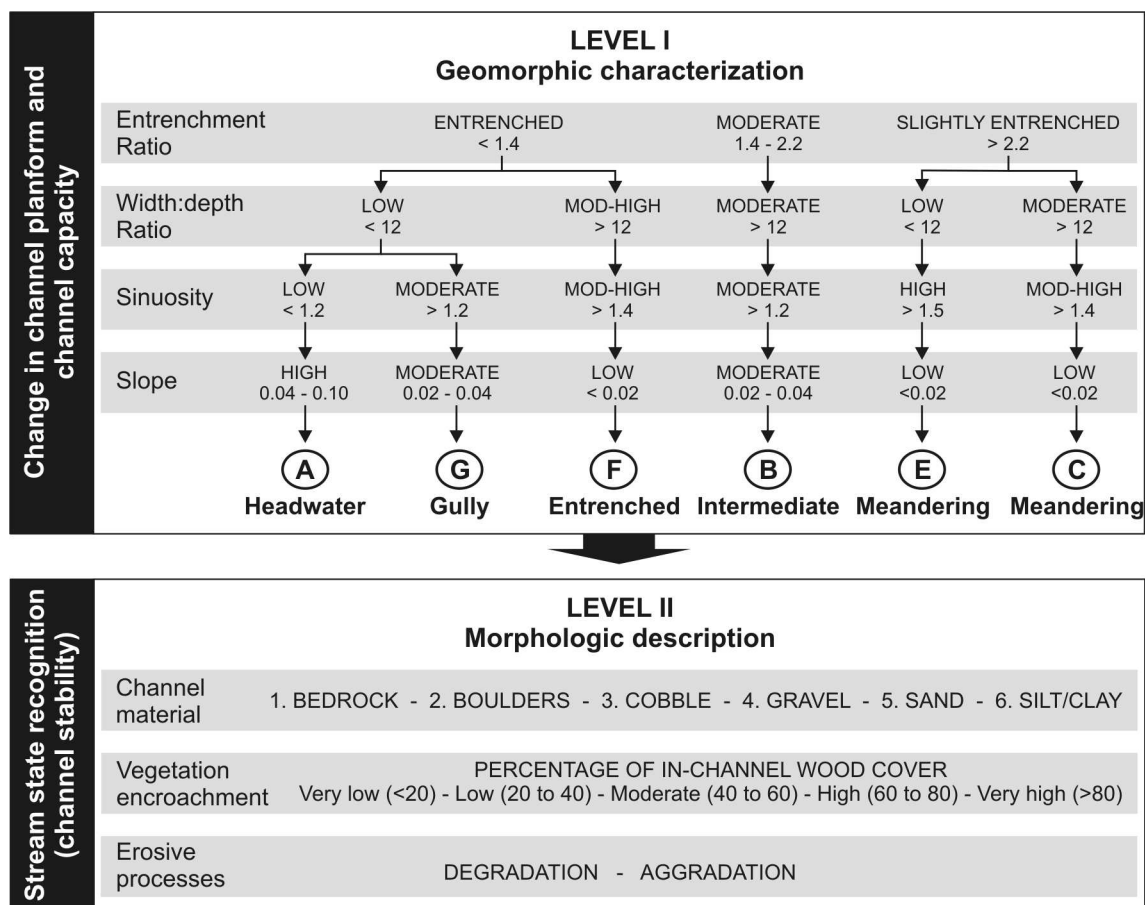


Figure 5.3: Hierarchic levels of geomorphic analysis delineated to quantify morphological changes. Modified from Rosgen (1994; 2001). Note, the stream type D (braided) was not illustrated.

1.3.1. Level I: geomorphic analysis at the scale of the river segment

Geomorphic analysis at Level I provided an expression of the stream type based on the stream classification scheme of Rosgen (1994). The stream type (A-G) for each river segment and for each time step was identified based on longitudinal, cross-sectional and plan view stream characteristics (Figure 5.3; Table 5.2).

Table 5.2: Quantitative and qualitative metrics used for morphologic description of the river segments and the reference reaches by time interval. Based on Thorne (1993), Gilvear and Bravard (1996), and Rosgen (1996) .

Measure	Dimension	Parameter	Level	Description
Quantitative	Plan view	Reach sinuosity	I; II	Ratio of the stream length to the valley length
		Meander wavelength	II	Average distance between consecutive meander inflexion points.
	Cross-section	Floodplain width and depth	I; II	Mean, maximum and minimum measures
		Bankfull channel width and depth	I; II	Mean, maximum and minimum measures
		Average channel capacity	I; II	Ratio of mean width to mean depth
		Entrenchment ratio	I; II	Ratio of mean floodplain width to mean bankfull width
	Longitudinal profile	Reach slope	I; II	Difference in height (m) between the highest and the lowest bed points divided by 1000.
	Stream efficiency	Hydraulic radius	II	Ratio of bankfull wetted area to wetted perimeter
		Stream velocity	II	Manning's relationship between channel efficiency, roughness and slope.
		Unit stream power	II	Relationship between slope, water weight and $Q_{1.5}$ to channel width.
Land cover	Vegetation encroachment	II	Percentage of in-channel tree cover	
Qualitative	Channel materials	Bank dominant material	II	Field survey observation of dominant materials
		Bed dominant material	II	
		Bank degradation	II	Identification of erosion/ deposition zones (aerial photography)
		Bank aggradation	II	

Longitudinal characteristics of the river segments were inferred from bed channel profiles derived from the TG10 DEM in ArcGIS (ArcHydro Tools). Note that bed channel profiles are temporally stationary. Bed features were predicted from bed slope indices presented by Rosgen (1994) and confronted to field observations.

The *average cross-sectional shape* for each river segment (i.e. narrow/wide and deep/shallow channel) was quantified using the width:depth ratio. The channel width was measured in GIS using cut lines separated by 500 metres along the channel bank lines. The average channel depth for shallow and deep channel sections was estimated from several field measures. The average entrenchment ratio was derived from GIS measures of the channel and floodplain widths over the cut lines cited above.

Finally, the *stream planform* categorization was defined by visual analysis coupled with measures of flow sinuosity. Flow sinuosity was computed as the ratio of the flow length to the channel length measured over a straight line along the river axis (Gilvear and Bravard, 1996). The total flow length for each river segment by time step was simply derived from GIS measures based on stream centreline layers.

1.3.2. Level II: geomorphic analysis at the scale of the river reach

Geomorphic analysis at the Level II was based on detailed morphological descriptions of a set of reference reaches of 1 km-length. Analysis included quantification of the channel slope and cross-sectional shape, stream sinuosity and efficiency, vegetation encroachment and channel materials (Table 5.2). Morphologic analysis was based on the stream reconnaissance scheme devised by Thorne (1993) to give continuity to previous geomorphological survey of the upper Sauce Grande (Gil and Campo, 2006; Gil, 2009); quantitative measures of the stream profile, cross-section and plan view were based on Rosgen (1996). Morphological features were digitized in ArcGIS for each time interval considered in analysis and superimposed to the corresponding land cover maps. Inspection of the present stream state was reinforced by field survey.

1.3.3. Quantification of geomorphic change

The ultimate objective of geomorphic and morphologic characterization was to quantify changes with time and distance from the dam closure, and to determine the stream stability state. Quantification of geomorphic changes focused on the channel planform and the channel width and was performed based on several metrics performed in ArcGIS for both levels of analysis. The effects of the dam on the river morphology were determined by simple comparison between rates of change in both parameters from the unregulated river upstream to the regulated river downstream.

a) Changes in the channel planform

Quantification of changes in the channel planform used coupled measures of channel activity and lateral migration based on Wellmeyer *et al.* (2005). Similar GIS-based analysis was also conducted by Shields *et al.* (2000), Downward *et al.* (1994) and Gilvear (2004), among many others.

The first method to inspect changes in the channel planform was based on the measure of *channel activity* for the time intervals 1961-1981 and 1981-2004. Overlay of channel outlines gave three classes of channel area: the area occupied during both time periods (stability), the area occupied only in the first photograph (channel abandon), and the area occupied only in the second photograph (channel creation). Rates of channel abandon and creation were derived by dividing the squared root of the total area for each process by the time elapsed during the time interval (20 and 23 years).

Quantification of *lateral migration* used digitized stream centrelines for each time step considered in analysis. Centrelines for two consecutive time steps T1 and T2 were superimposed within a single layer and then exported as polygons. If lateral migration occurred, then several polygons are created within the two lines; the surface area of the polygons gives a measure of the active migration area for the time interval considered. Based on Shields *et al.* (2000), the rate of channel migration may be quantified as follows:

$$\text{Active migration} = \frac{(\text{Active area} / \text{Length of T1})}{T1 - T2} \quad (5.1)$$

The total area of active migration is divided by the channel length measured during the time step T1. This procedure provides a linear measure of lateral migration. The migratory rate is determined by comparing this linear measure to the period of time elapsed during the time interval considered.

b) Changes in the channel width

Variations in the channel width with time were inspected as indicator of change in the channel capacity. Although most studies assessing changes in the channel capacity use linear regression analysis of the width:depth ratio to the drainage area (e.g. Gregory and Park, 1974), to the stream length (e.g. Petts, 1977) or to flow discharge and velocity (e.g. Knighton, 1977), variations in the channel capacity with time and distance from dam closure were simply evaluated by computing rates of change in the channel width between consecutive time steps. Similar procedures were performed by Fergus (1997), Surian (1999), Gilvear (2004) and Gordon and Meentemeyer (2006), among others.

Quantification of change in the channel width used the same GIS-based procedures that the quantification changes in the channel landform (i.e. stream channel overlay and cross-tabulation). Rates of channel widening indicated channel degradation by bank erosion, whereas rates of channel narrowing suggested lateral aggradation and vertical scour (Leopold, 1973). Longitudinal variations in the channel width were simply evaluated by comparison between the upstream and the downstream river segments.

c) Quantification of the channel stability

Among the wide range of methods to determine channel stability, we choose that of Simon and Downs (1995) because of its simplicity and compatibility to the stream reconnaissance methodology of Thorne (1993). The method is GIS-based and uses a two-step approach. First, it ranks a set of physical variables by their state of stability; second, it determines the geomorphic status of the stream by computation of the

Instability Index (I_i). The value of the Instability Index for a particular reach equals the sum of the values assigned to each variable at each site (Simon and Downs, 1995). High values of the Instability Index indicate unstable and degraded reaches with strong erosive activity.

1.4. QUANTIFICATION OF CHANGE IN THE FLUVIAL LANDSCAPE

Structure and dynamics in river channel and riparian vegetation were examined based on the Landscape Ecology approach (Forman and Godron, 1986; Forman, 1995; Burel and Baudry, 2000). The fundamental of Landscape Ecology is that functional surfaces are seen as a nested hierarchy of individual patches influencing interactions between structure (composition and configuration) and function in environmental landscapes. Hence, this approach provides a useful framework to assess complexity and dynamic within fluvial landscapes (Aspinall and Pearson, 2000; Poole, 2002; Graf, 2006).

Although analysis was conducted at all levels and dimensions of observation (Table 5.1); special attention was accorded to land cover types related to natural vegetation cover within the river channel and its riparian zone. The fluvial landscape structure for each time step was evaluated using a set of common metrics used in landscape ecology (Table 5.3) including measures of both the landscape composition (variety and abundance of patch types) and the landscape configuration (spatial distribution and arrangement of patches). Landscape metrics were computed within the FRAGSTATS software (McGarigal and Marks, 1994) based on GIS-derived land cover maps.

Table 5.3: Metrics used in the quantification of the landscape structure (composition and configuration) by time step considered in analysis.

	Metric	Type	Level	Unit	Description
LANDSCAPE COMPOSITION	Abundance/ Dominance	Class area	Class	Ha $0 \leq \infty$	Surface area occupied by each class
		Percentage of landscape	Class	% $0 \leq 100$	Surface area occupied by each class as a proportion of the total landscape
		Largest Patch Index	Class	% $0 \leq 100$	Percentage of landscape occupied by the largest patch
	Richness/ Diversity	Number of patches	Class/ Landscape	--- $0 \leq \infty$	Number of patches by class
		Patch richness	Landscape	--- $0 \leq \infty$	Number of patch classes within the landscape
		Shannon Index	Landscape	--- $0 \leq \infty$	Measure of diversity (equitability) of patches

Table 5.3: cont.

	Metric	Type	Level	Unit	Description
LANDSCAPE CONFIGURATION	Distribution	Mean, Variation	Class/ Landscape		Central tendency and variation of patch size by class
	Isolation/ Proximity	Cohesion Index	Class/ Landscape	% $0 \leq 100$	Physical connectivity of patch classes as proportion of the landscape
	Aggregation	Aggregation Index	Class/ Landscape	% $0 \leq 100$	Proportion of like adjacencies of patches by class and of classes within the landscape
	Fragmentation	Division Index	Class/ Landscape	--- $0 \leq 1$	Probability of no class adjacency between patch cells

Changes in the landscape structure (composition and configuration) over time (dynamics) were determined by comparison of landscape metrics between consecutive time steps. Additionally, cross tabulation and overlay between consecutive land cover maps (1961/1981 and 1981/2004) provided the basis to (i) compute rates of change as a measure of the total proportion (%) of landscape gained or lost by each land cover type, and (ii) construct transition diagrams to visualise the direction and strength of landscape changes.

In sum, these procedures provided a measure of change in the patch frequency and extent, in the spatial arrangement of patch types and in their evolutionary trends. Ultimately, this approach permitted identifying processes of environmental change such as fragmentation-simplification, expansion-contraction-stability or invasion-domination-succession, all having specific ecological and geomorphic implications (Forman, 1995).

2.1. CHANGES IN THE RIVER MORPHOLOGY

Geomorphic analysis builds on preceding hydrological analysis, which revealed substantial changes in the hydrology of the regulated river including flood elimination, reduction in the magnitude and frequency of low and high flows with increased low- and high-flow duration, and altered flow seasonality. On the other hand, this study assumed that sediment load inputs were reduced by 99 %. Although the reduction in flow discharge (Q) and sediment load (L) inputs below the dam was significant in both cases, decrease in the flow capacity to transport sediment was higher than the decrease in the amount of sediment available to transport.

This section quantifies the geomorphic response of the regulated river to major decrease in discharge and sediment inputs, and compares the direction of geomorphic changes to qualitative models of channel adjustment available in literature. Inspection of downstream channel changes since dam closure in 1978 builds on the understanding of natural geomorphic processes within the unregulated river upstream. Results are structured into two linked sections examining actual state and evolutionary trends in (i) broad geomorphic characteristics of the river segments, and (ii) morphologic conditions of a set of eight sample reaches situated above and below the dam.

2.1.1. Level I: Morphologic changes at the scale of the river segment

a) Geomorphic characteristics of the river segments

The broad geomorphic characteristics of the present river system were inspected prior to conduct analysis on natural and dam-induced change in the river morphology. Longitudinal, cross-sectional and plan view characteristics of the river segments upstream and downstream from the dam provided an expression of the overall stream type (Fig. 5.4). Both upstream and downstream rivers exhibit meandering patterns with low longitudinal gradients (0.014 and 0.006, respectively) and pool-riffle bed morphologies. The main differences between the river segments are in the stream sinuosity, in the cross-sectional shape (width:depth ratio) and in the degree of channel entrenchment, all of which contributes to classify the upstream stream as type *C* and the downstream stream as type *E* (Rosgen, 1994).

The *river upstream* exhibits a slightly entrenched channel (i.e. the average floodplain width is more than twice the average channel width) with well-defined meandering morphology and moderate to high sinuosity (Fig. 5.4). The average channel width:depth ratio is moderate to high (27.7) with high dispersion (15.1); width:depth ratios along the river segment range from 17.0 (narrow and deep channel) to 64.1 (wide and shallow channel). Mean stream channel depth is 1.9 m (± 0.3 m) and mean channel width is 52.9 m (± 19 m). The floodplain along the river course is well defined; the relative ceiling of the active floodplain (Terrace II; Borromei, 1991) is up to 8 m height with respect to the

channel bed, and the average floodplain width is 135.6 m with high variation (SD = 93.2 m).

The stream sinuosity within the *river downstream* increases (1.6), and the river channel is narrower and entrenched with respect to the river upstream. The average width:depth ratio is low (11.9); mean stream channel depth is 1.8 m (± 0.2 m) and mean channel width is 20.8 m with little variations (± 3.8 m). The relative ceiling of the active floodplain with respect to the channel bed decrease from 7 m immediately below the dam to 5.5 m about 15 km downstream; mean floodplain width is 52.5 m with high variations (± 31 m).

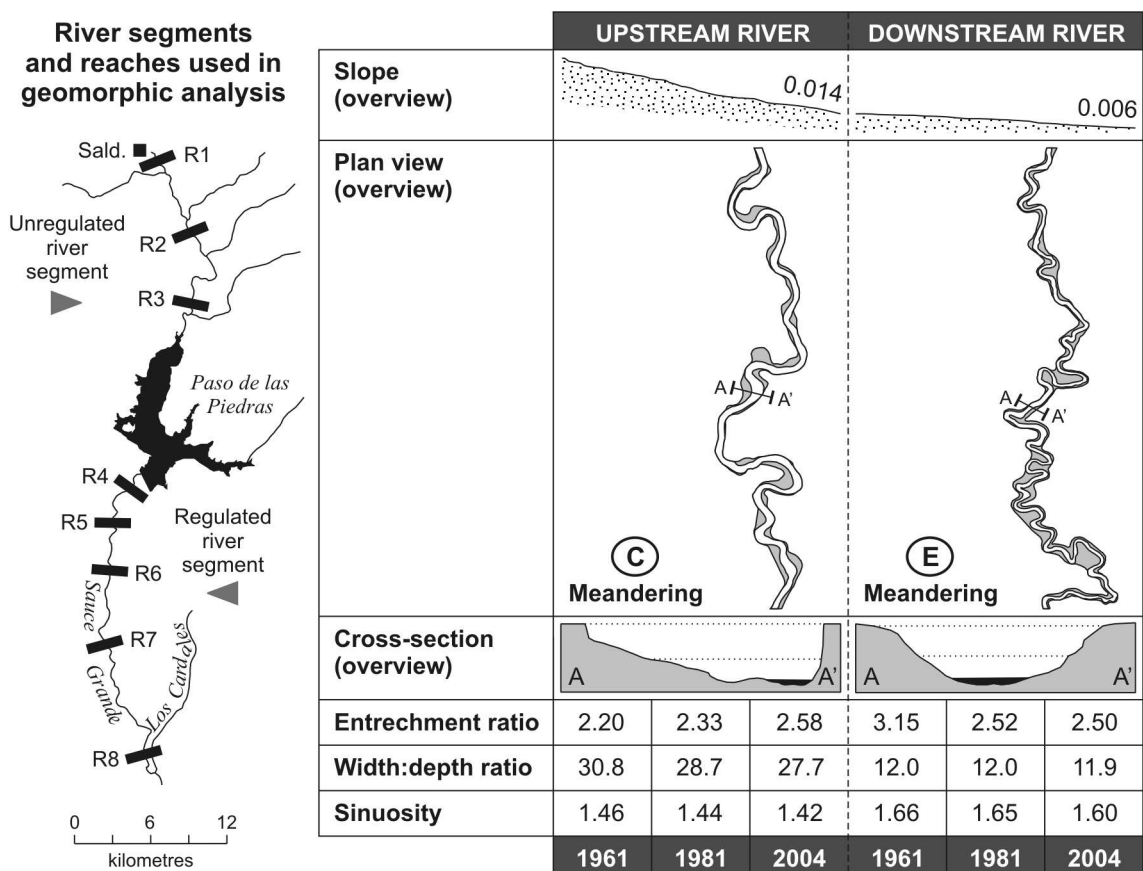


Figure 5.4: Longitudinal, cross-sectional and plan view characteristics of the river segments upstream and downstream from the dam by time interval used in analysis (1961, 1981 and 2004). Overviews correspond to present conditions.

Examples of characteristic channel cross sections within the upstream and downstream river segments are given in Figure 5.5 and 5.6; the floodplain and channel boundaries are indicated by a long and short dashed white line, respectively. Upstream river sections exhibit well-defined meander morphologies (asymmetric banks), with vertical and deep cut banks on the convex margins and medium (gravel) to fine (sand/silt) grain-sized sediment deposition on the concave margins (point-bars). In sections where the river exhibits lower sinuosity, the channel banks loss altitude and the floodplain enlarges considerably.

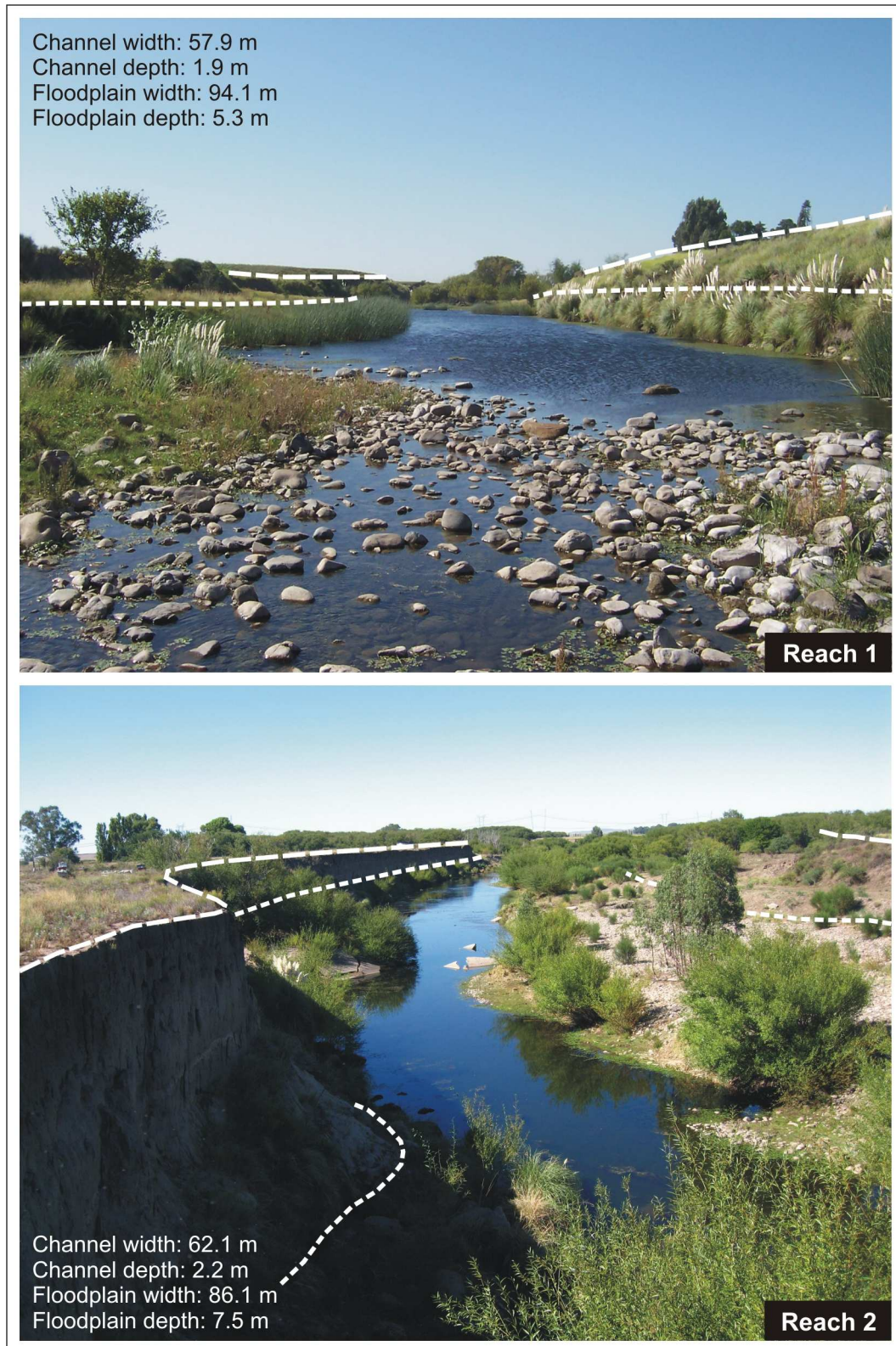


Figure 5.5: Characteristic cross sections within the upstream river segment (base flow stage). Photographs were taken on river reaches located about 24 km (Reach 1) and 18 km (Reach 2) upstream from the dam closure.

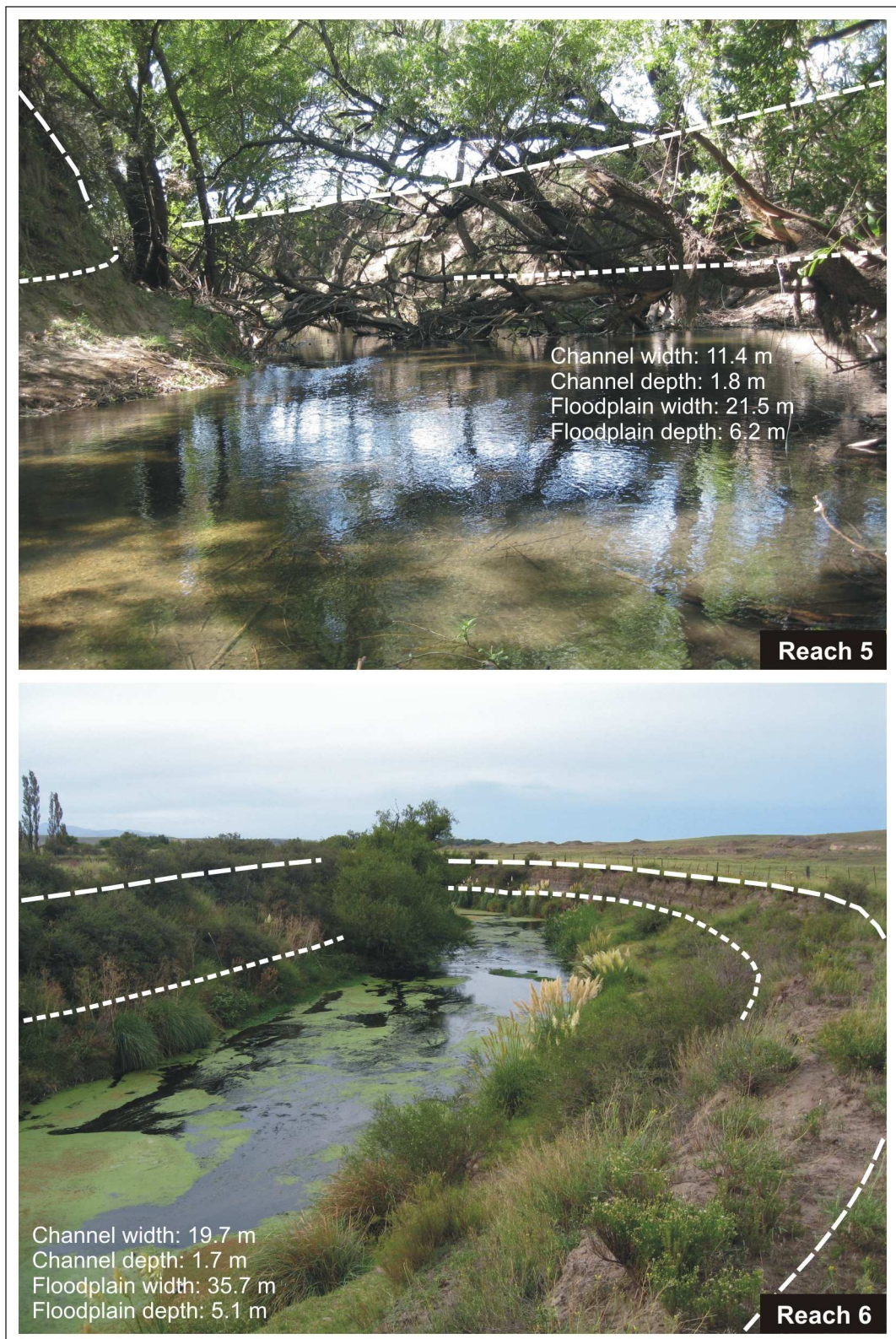


Figure 5.6: Characteristic cross sections within the downstream river segment (base flow stage). Photographs were taken on river reaches located about 5 km (Reach 5) and 8 km (Reach 6) downstream from the dam closure.

Overall, the river downstream flows through a narrow and relatively deep channel with stable, well vegetated banks. In contrast to upstream river sections, channel boundaries are unclear due to vegetation and the lateral limits of the active floodplain are often undefined due to intense human activities. Human-related channel and floodplain alteration (e.g. artificial levees, gravel extraction, and farming) were observed all along the downstream river corridor.

b) Changes with time and distance from dam closure

Quantification of morphologic change at the broad river scale used metrics of variation in the channel planform and channel width performed for three time steps spanning pre-disturbance river conditions (1961) and post-disturbance river conditions (1981 and 2004). Analysis built on field observations and GIS measurements based on aerial photography; the effects of the dam on the downstream river morphology were inferred by simple comparison between rates of change in planform and width parameters from the regulated river upstream to the regulated river downstream.

Changes in the channel planform

Comparison of the broad stream characteristics over the three time steps used in analysis revealed a slight decrease in the stream sinuosity with time for both river segments, the trend to decreasing sinuosity being slightly higher for the river downstream (Fig. 5.4). Changes in stream sinuosity underlie changes in rates of channel activity and lateral migration, both designating planform changes. Overall, the Sauce Grande River exhibited wide lateral activity within the river upstream and relative stability within the river downstream (Fig. 5.7). Upstream, channel activity was principally related to meander progression and cut-off, although the latter occurred in minor extent. Downstream, channel activity was mostly associated to artificial cut-offs and lateral migration was either absent or very low.

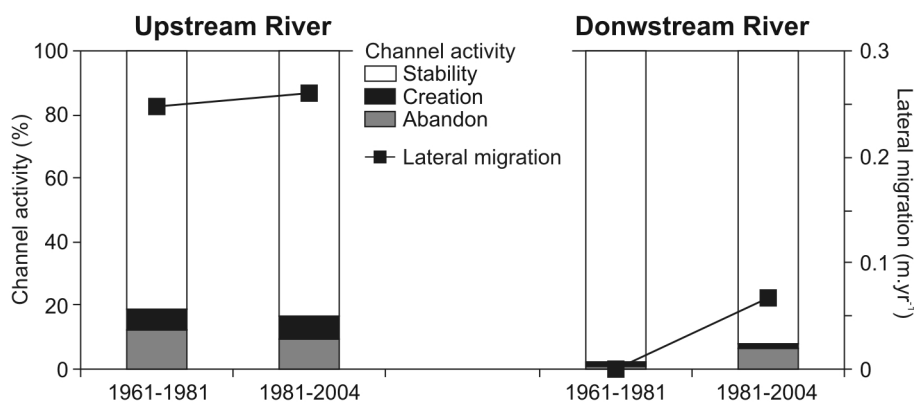


Figure 5.7: Rates of channel activity and lateral migration within the upstream and downstream rivers for the time intervals 1961-1981 and 1981-2004.

The first comparative period (1961–1981) is representative of pre-disturbance conditions and early regulated conditions due to dam construction in early 1970's, closure in 1978, and initial filling of the Paso de las Piedras Lake by late 1970's and

Conversely, the unregulated river upstream revealed lesser stability (82 %), and hence higher rates of channel abandon (21.3 m.yr⁻¹), channel creation (15.0 m.yr⁻¹) and lateral migration (0.25 m.yr⁻¹). Comparison of the channel state between 1961 and 1981 showed a tendency to meander progression in the downstream direction that in some cases led to meander cut-off (Fig. 5.8). Channel activity was more important within the upper and lower sections of the study river segment, there where slope gradients were stronger. Many bends in the upper section showed a general tendency to straightening; in the lowest section, there was a slight tendency to increasing meander amplitude coupled to avulsion processes.

The second comparative period (1981-2004) corresponds to post-disturbance river conditions. In spite that this period is climatically wetter than the preceding, the dominance of low flows over high flows was slightly higher (74.9 %), and the frequency of small floods decreased (1.6 %); nevertheless, this period recorded a suite of large floods that represented 0.4 % of all flow conditions over the time interval.

The river below the dam showed lesser stability than during the first period (92.5 %) due to increased rates of channel abandon (10.2 m.yr⁻¹). Although this aspect could be related to increased rainfall and runoff contributing to increased rates of water release downstream and hence increased stream power, inspection of imagery and field observations revealed that channel abandon was related to artificial cut-offs in the vicinity of the dam structure (Fig. 5.8). Conceivably, the river was artificially straightened to facilitate canalization of dam outlets and spills. Furthermore, construction of levees and other bank stability structures were also observed in the vicinity of the dam, which may be partially responsible for channel stability.

Upstream from the impoundment, the unregulated river revealed the same tendency to straightening that during the preceding period. However, rates of channel activity were lower than those observed for the time interval 1961-1981. Rates of channel abandon were 15.4 m.yr⁻¹ and were closely related to meander cut-off (Fig. 5.8), rates of channel creation were 13.7 m.yr⁻¹ and responded to coupled increasing meander amplitude and meander progression downstream. Decreased rates of channel activity and hence increased percent of channel stability (84.2 %) revealed a tendency to simplification of the meander complexity. Coupled increase in rates of lateral migration (0.26 m.yr⁻¹) indicates a tendency to in-channel stream wandering.

Changes in the channel width

Inspection of the width:depth [w:d] and entrenchment ratios by time step (Fig. 5.4) permits to make some early interpretations on change in the overall channel size; note, any change in these parameters with time will be directly related to changes in the width of the fluvial forms (depth values were averaged and were considered as temporally stationary). The average w:d ratio within the downstream river was very low for all time steps and revealed almost stable conditions with time (12.0 in 1961 to 11.9 in 2004); the average entrenchment ratio was low for all time steps, although increased with time from 3.2 (1961) to 2.5 (2004). Increase in the average entrenchment ratio for stable conditions in the channel width suggests contraction of the active floodplain; this aspect was evidenced all along the river corridor and was related to progressive farming activities. Conversely, the average w:d ratio within the river upstream decreased with time clearly from 30.8 in 1961 to 27.7 in 2004, and the average entrenchment ratio

decreased with time from moderate (2.2) to low (2.6). These aspects suggest coupled channel and floodplain activity, where the overall channel size contracted whilst the overall floodplain size enlarged.

Rates of change in the channel width between 1961 and 1981 and between 1981 and 2004 were inspected as indicator of changes in the channel capacity (Fig. 5.9). Note, rates of change lesser than 0.2 m.yr^{-1} were dismissed to avoid potential influence of error in rectification of the photographs and digitizing procedures affecting the results. Results were highly consistent with those obtained from planform change analysis (above). The river downstream from the dam reflected high lateral stability and so changes in the channel width were not apparent; nevertheless, an overall tendency to channel contraction was evidenced by increased vegetation within the active channel, especially in the vicinity of the impoundment. Upstream, coupled channel widening and narrowing occurred in the upper and lower river sections, there where rates of lateral activity were the strongest. An overall tendency to channel narrowing was evidenced during both periods.

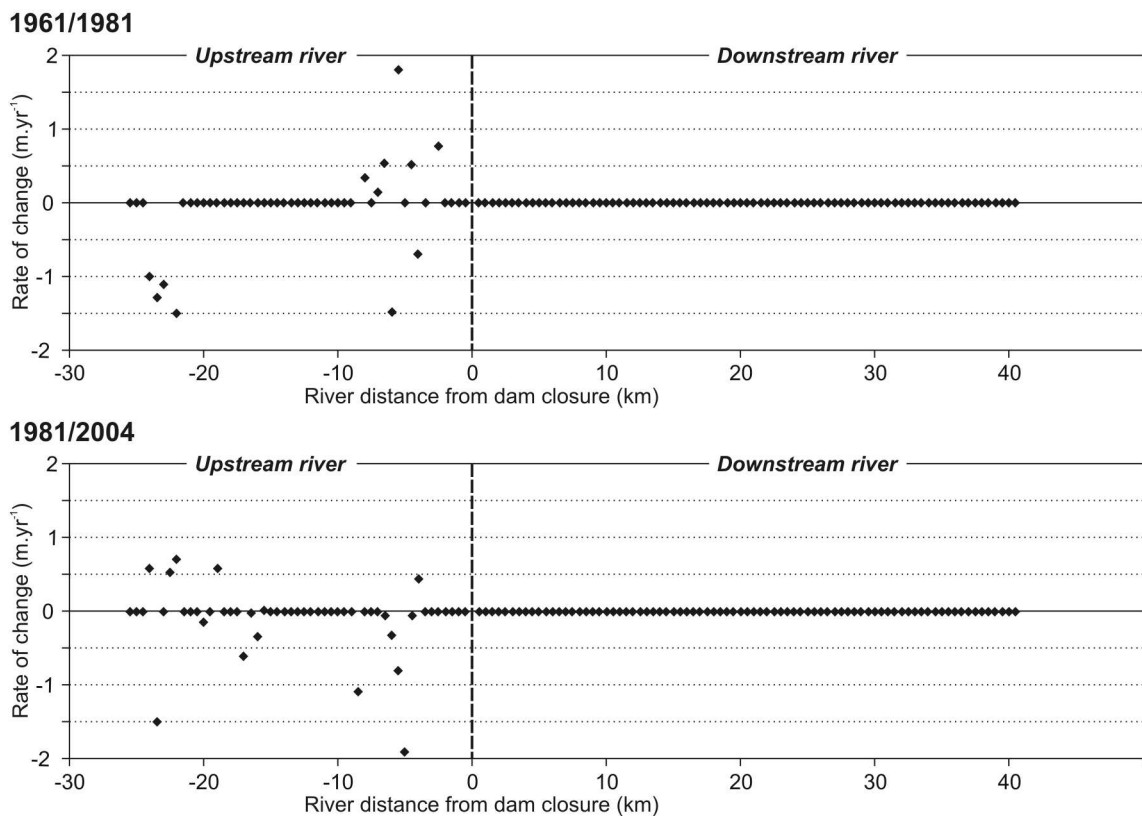


Figure 5.9: Rates of change in the channel width of the upstream and downstream rivers for the time intervals 1961-1981 and 1981-2004.

2.1.2. Level II: Morphologic changes at the scale of the river reach

Morphologic analysis at the Level II builds on quantitative and qualitative descriptions of a set of eight reference reaches distributed above (3 reaches) and below (5 reaches) the dam (Fig. 5.4). The total length of the reaches is 1 km measured as “bird eye” over

the channel axis; the lateral edge of the reaches was defined by the active floodplain. Although Thorne (1993) recommends the use of survey reaches separated by distances greater than 10 km, the distance between sample reaches within the river segment downstream from the dam is considerable lower to investigate morphologic changes with distance from the dam on a more detailed scale of observation. Analysis of morphologic change with time and present morphologic state used metrics of stream type, channel capacity, degree of meandering and stream efficiency (See Table 5.2 in the Methods section, p. 235). Results and the corresponding explanations are structured into three subsections based on Thorne (1993) and Rosgen (1994).

a) Stream types

Analysis at the broad geomorphic scale revealed that the Sauce Grande River exhibits an overall meandering morphology, although the river section below the dam is more tortuous than the river section above. Inspection of the river morphology at the scale of the river reach showed great contrast in the stream type along the river course (Table 5.4). Within the *river upstream*, only Reach 3 showed the stream type characteristic of the river segment (Type C); Reaches 1 and 2 were moderately entrenched ($1.63 < E < 2.18$) and so they classified as intermediate streams (Type B). The stream channel was riffle dominated, although the w:d ratio was considerably larger than that for intermediate streams ($23.3 < w:d < 28.4$) and the channel bed slope was considerable lower ($0.003 < S < 0.005$). As for the stream sinuosity, Reach 1 revealed moderate values (1.2) whereas Reach 2 was highly sinuous (1.6).

Variations in the stream type were also found for the *river downstream*, which classifies as stream type E (tortuously meandering). Type E was found for reaches 4, 5 and 8, which exhibited low entrenchment ratios ($2.9 < E < 3.4$), very low w:d ratios ($9.7 < w:d < 11.7$), low slope gradients ($0.001 < S < 0.004$), and very high sinuosity ($1.5 < S < 2.8$). Conversely, Reach 6 revealed moderate entrenchment (2.29), w:d ratio (14.1) and sinuosity (1.4), all characteristic of intermediate streams (B). Reach 7 was highly entrenched (1.4) and so it classified as stream type F, with high sinuosity (2.2).

b) Vertical and lateral relations of channel to valley

Measure of channel entrenchment and interpretation of channel planform and floodplain features permitted to infer the degree of vertical and lateral channel activity along the river course. Present geomorphic conditions revealed two contrasted scenarios for river reaches located above and below the dam (Table 5.4). Geomorphic sketch maps of some representative reaches with the upstream and downstream rivers are illustrated in Figures 5.10 and 5.11, respectively.

Upstream reaches

The reaches above the dam exhibited well-defined terraces which in most cases were related to lateral activity more than to channel incision (e.g. Reach 3, Fig. 5.10). Actual entrenchment ratios ranged from moderate ($1.6 < E < 2.2$) to very low (4.0), indicating that lateral processes dominate over vertical scouring. Nevertheless, the average bed channel depth with respect to the ceiling of the active floodplain is rather high (6.5 m),

and hence suggests that vertical activity was stronger in the past. In reaches 1 and 2 where the channel is more entrenched into its floodplain, vertical cut banks revealed up to 8 m height. Coarse lateral deposits and in-channel islands provided evidence of active aggradation processes (Fig. 5.12); overbank trash lines substantially separated from the actual stream gave evidence of the magnitude of peak flows and floods (Fig. 5.13).

Increased sinuosity in the downstream direction (1.2 in Reach 1 to 1.5 in Reach 3) suggests a transitional stream state from straight to meandering, with significant influence of local controls for lateral mobility (resistant metamorphic materials) as suggested by the recurrence of irregular meanders along the river segment (Reach 2, not shown). The meander amplitude increased with distance as well (Table 5.4); meander progression and avulsion processes were observed especially in Reaches 2 and 3.

Table 5.4: Morphologic characteristics of the sample reaches within (a) the upstream river segment and (b) the downstream river segment. See Table 5.2 for morphological variables correspondences.

<i>Parameter</i>	Units	<i>(a) Upstream reaches</i>			<i>(b) Downstream reaches</i>				
		1	2	3	4	5	6	7	8
Distance from dam closure	km	24.4	18.2	13.0	0.9	4.6	7.5	13.7	22.4
<i>Reach morphology</i>	Units	1	2	3	4	5	6	7	8
Entrenchment ratio (E)	-	2.2	1.6	4.0	2.98	3.4	2.2	1.4	3.0
Width:depth ratio (w:d)	-	28.4	23.3	28.1	9.7	11.6	14.1	13.1	11.7
Sinuosity (S)	-	1.2	1.6	1.5	1.5	2.8	1.4	2.2	1.6
Channel slope (s)	-	0.005	0.003	0.008	0.004	0.003	0.002	0.001	0.001
Bank material	-	6	6	6	6	6	6	6	6
Bed material	-	3-4	4-3	4-3	4-6	6-4	6-4	6-4	6
Stream type (Rosgen, 1994)	-	B3c	B4c	C4c	E4	E6	B6c	F6	E6
<i>Channel capacity</i>	Units	1	2	3	4	5	6	7	8
Width (w)	m	55.7	42.7	58.9	18.9	20.9	23.5	21.2	18.7
Depth (d)	m	2.0	1.8	2.1	2.0	1.8	1.7	1.6	1.6
Channel capacity (CC)	m ²	72.4	52.8	89.2	24.8	26.9	27.4	23.6	22.2
<i>Stream efficiency</i>	Units	1	2	3	4	5	6	7	8
Hydraulic radius (R)	-	0.65	0.62	0.76	0.65	0.64	0.58	0.55	0.58
Roughness (n)	-	0.09	0.09	0.08	0.11	0.08	0.07	0.06	0.06
Velocity (V)	m.s ⁻¹	0.62	0.42	0.91	0.44	0.54	0.51	0.27	0.37
Unit stream power (P)	W.m ⁻²	80.1	62.6	121.1	188.6	128.1	76.0	46.4	28.6
<i>Degree of meandering</i>	Units	1	2	3	4	5	6	7	8
Meander wavelength (λ)	m	151.9	292.2	614.0	111.2	106.3	158.5	169.3	180.6
Meander width (M_w)	m	20.1	36.2	203.5	24.3	54.7	48.9	59.7	51.0

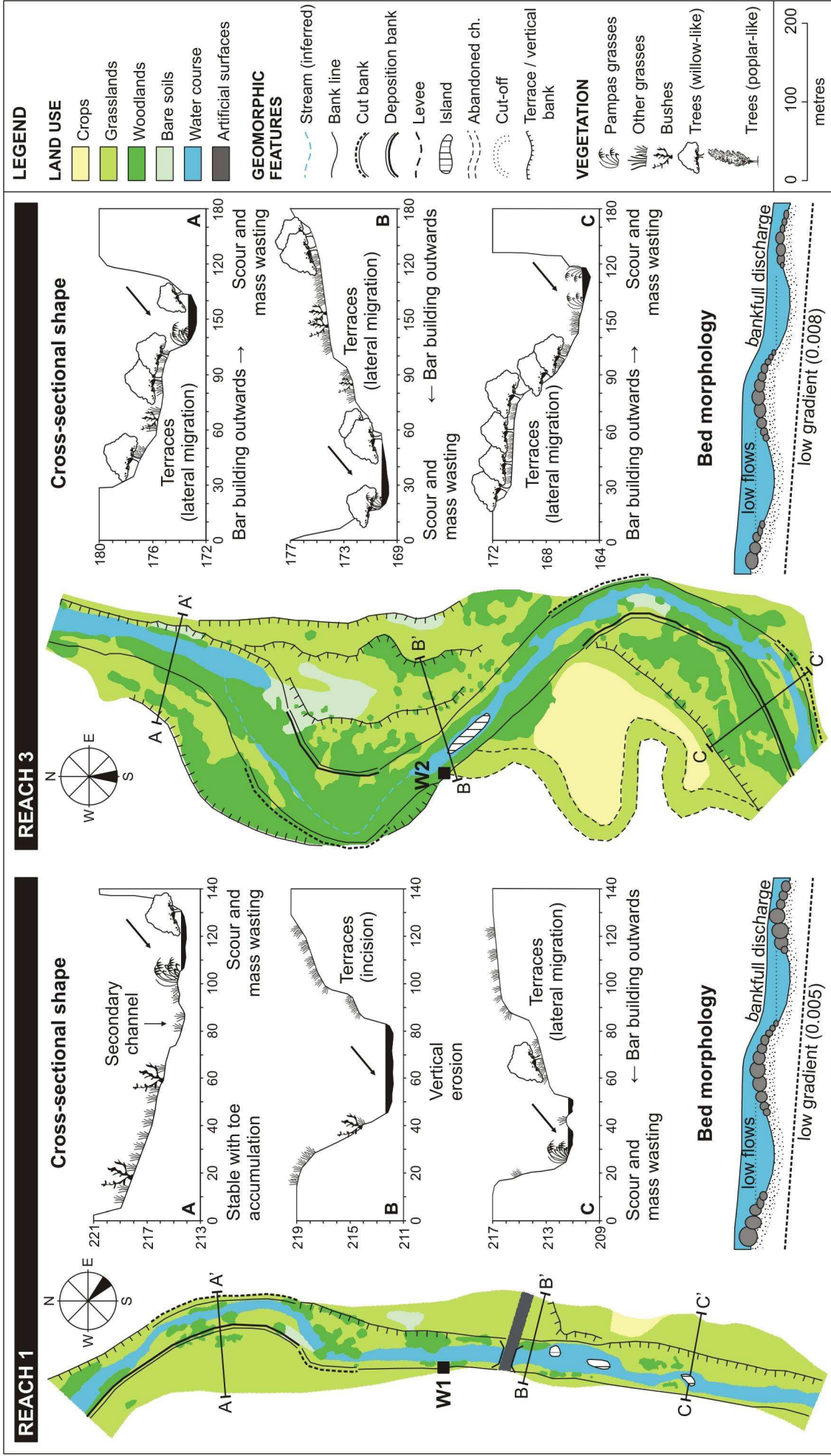


Figure 5.10: Geomorphologic sketch map, land use and representative cross sections for two sample reaches within the river upstream.

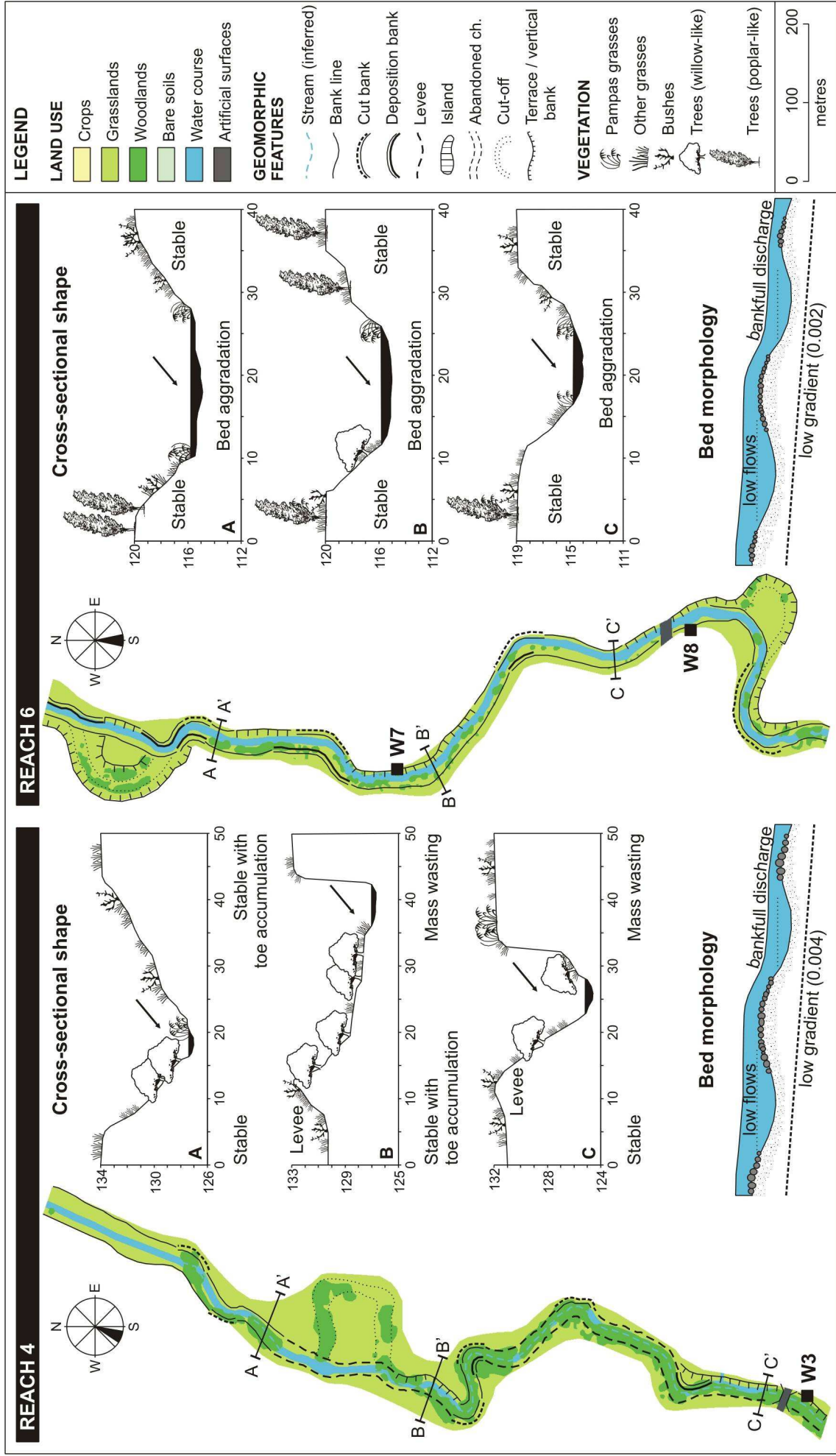


Figure 5.11: Geomorphic sketch map, land use and representative cross sections for two sample reaches within the river downstream.

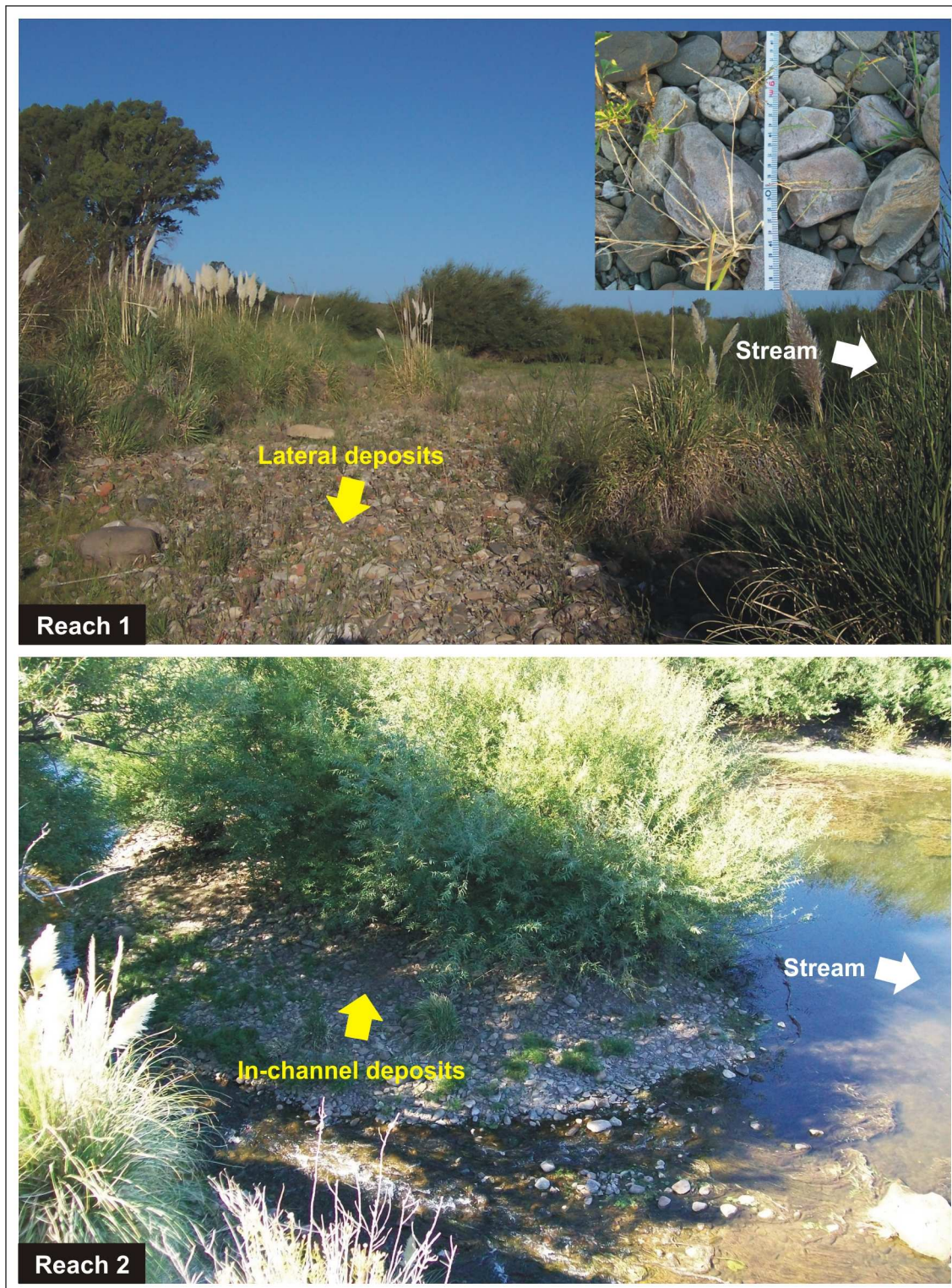


Figure 5.12: Evidence of channel activity within the river upstream. Photographs were taken on river reaches located about 24 km (Reach 1) and 18 km (Reach 2) upstream from the dam closure.



Figure 5.13: Evidence of flooding within the river upstream. Photographs were taken in Reach 1 (about 24 km upstream from the dam closure).

Downstream reaches

In opposition to what was expected, there was no clear evidence of channel scour within the river immediately below the dam. The river environment revealed strong human intervention. Artificial levees were observed all along the river course over at least 4 km below the dam (Reaches 4 and 5; Fig. 5.14), and were more frequent and extensive immediately downstream; in some sections, artificial levees were up to 2 m-height with respect to the top portions of the natural river banks. Field survey of channel bathymetry revealed that the channel depth in some river sections was notably deeper than that for the natural river (e.g. up to 1.6 m in Reach 4). However, evidence of artificial bed digging suggested that channel incision responded to human intervention more than to natural bed degradation.

Meander wavelength and width increased in the downstream direction significantly; however, the meander amplitude was notably small compared to that for the upstream reaches (Table 5.4). Meanders in Reaches 5 and 7 were very tortuous (not shown) and cut-offs were observed in Reaches 4, 6 and 8 (Fig. 5.11; 5.14). The cut-off morphology suggested that cut-offs were associated to human intervention more than to natural meander progression, at least in Reaches 4 and 6.

c) Channel description

The stream efficiency and hence, the channel size clearly separates reaches as located upstream or downstream from the impoundment. Such variations are related to the effects of decreasing slope more than to the hydrologic effects of the dam, the latter having potential implications for rates of channel aggradation and/or scour within the river downstream.

Upstream reaches

As presented above, upstream reaches exhibited broad and relatively shallow channels with moderate capacity ($53 \text{ m}^2 < CC < 89 \text{ m}^2$). Bed channel slope is low (Table 5.4), and so the stream velocity and the stream power of the Q_2 ($91 \text{ m}^3 \cdot \text{s}^{-1}$) per unit area were moderate. Human-related obstructions for flow were more important in Reach 1 due to urban fabrics (Saldungaray town), roads and bridges (old and new Road 72) and intense farming; obstructions in Reaches 2 and 3 were more related to vegetation and stream sinuosity. Human and natural obstructions for flow compensate to give similar values of channel roughness across the reaches (0.08 to 0.09).

The overall channel morphology was clearly meandering with alternating active cut banks and lateral deposits in point bars. The bed morphology is pool-riffled and base flow depths are shallow (Fig. 5.10); flow averages 30 to 40 cm-depth in riffles and 70 to 80 cm-depth in pools. Bed material in Reach 1 is coarse in riffles (cobbles and coarse gravel) and finer in pools (small gravels, silt and clay). As for natural rivers, the sediment grain-size decreases in the downstream direction; riffle bed material in Reaches 2 and 3 is composed of coarse to medium gravel with cobbles. Banks are composed either by non-cohesive deposits of silt/clay, gravels and cobbles in channel bars or by layered non-cohesive and cohesive alluvial –aeolian material of Holocene age in cut banks (Fig. 5.15).

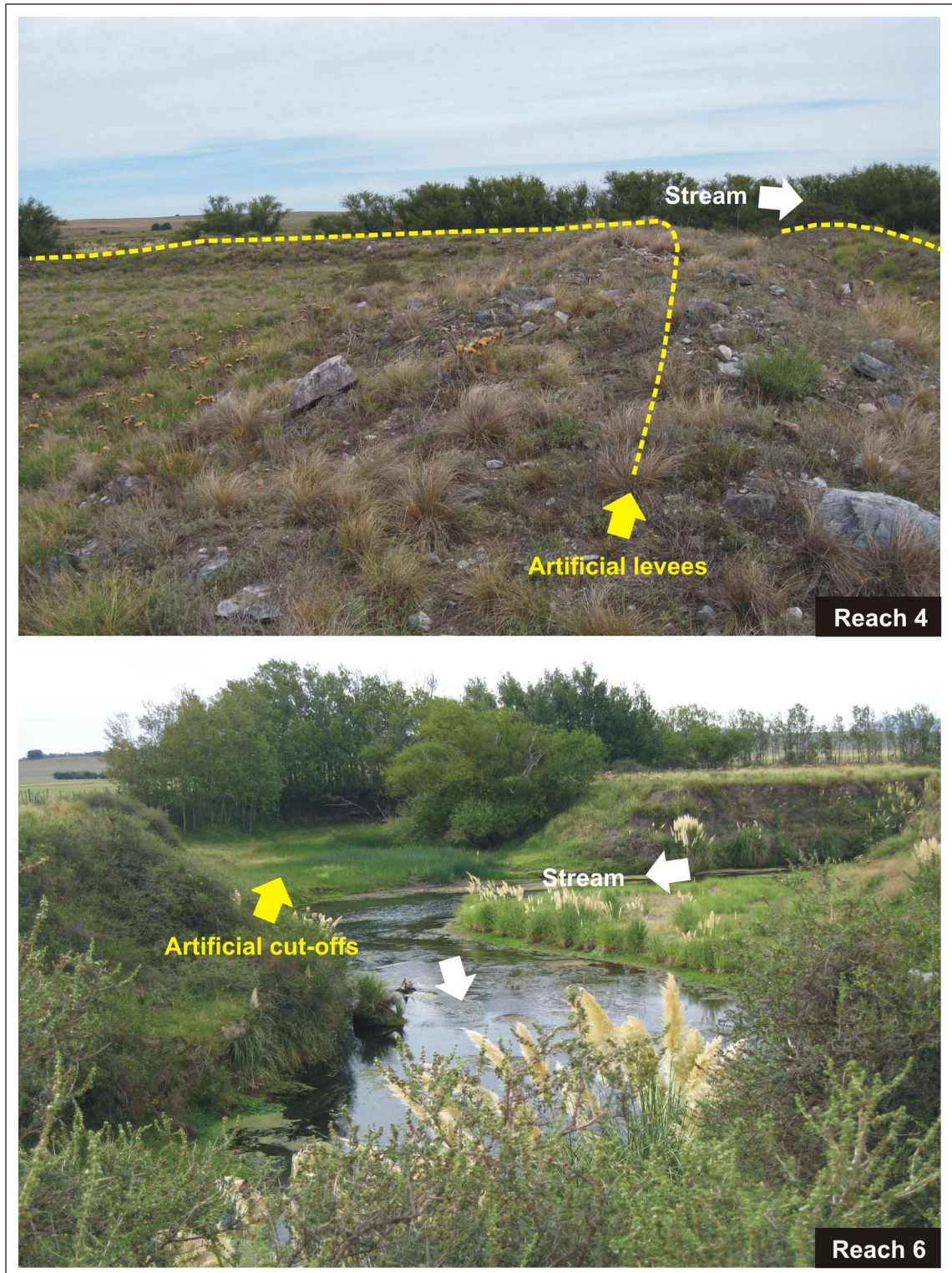


Figure 5.14: Evidence of human intervention within the river downstream. Photographs were taken on river reaches located about 1 km (Reach 4) and 8 km (Reach 6) downstream from the dam closure.

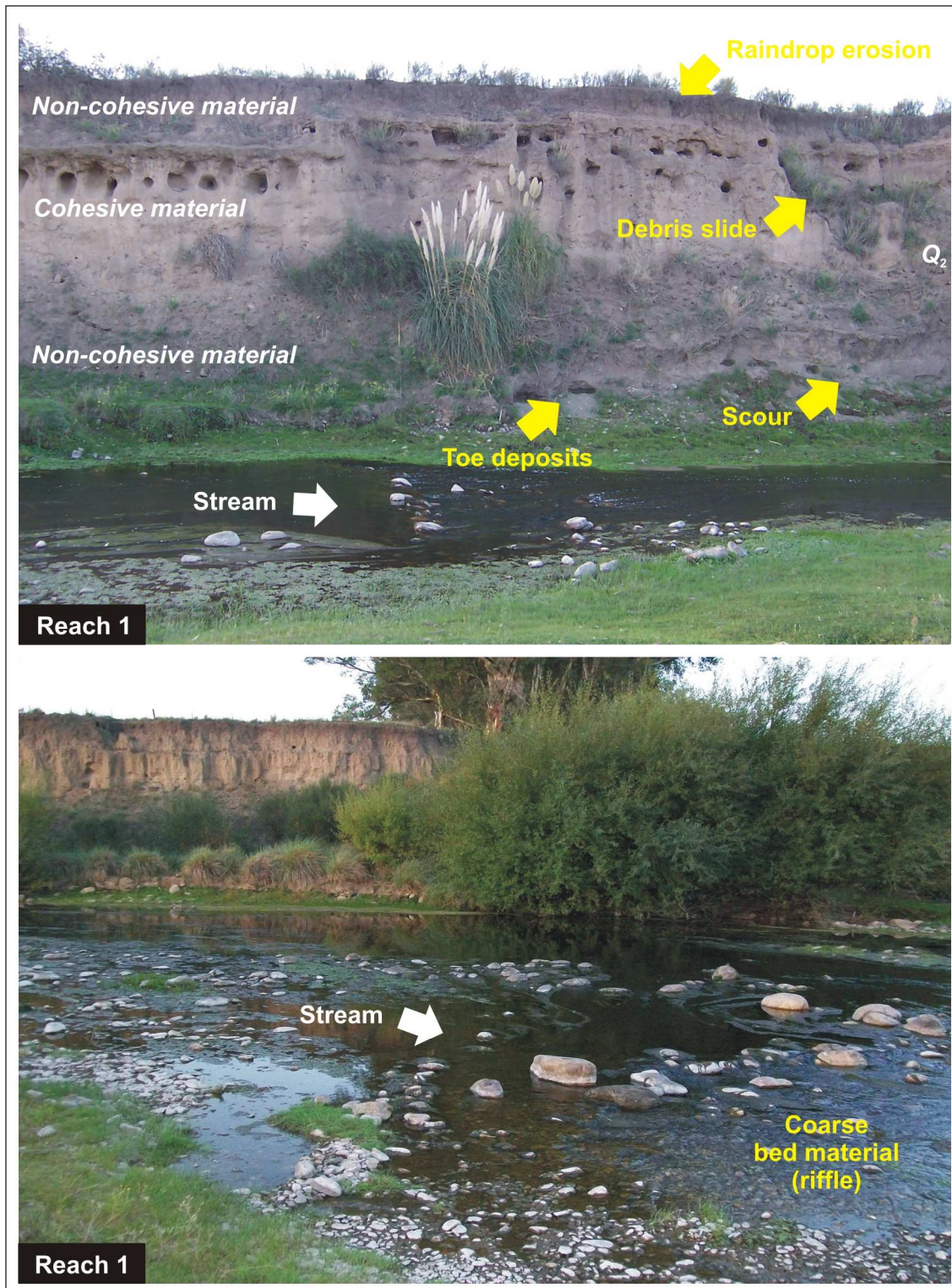


Figure 5.15: Channel materials and evidence of channel activity within the river upstream. Photographs were taken in Reach 1 (about 24 km upstream from the dam closure).

As shown in Figures 5.10 and 5.15, bank profiles reveal both aggradation and erosive processes. Eroding banks show evidence of bank undercut (especially in Reaches 1 and 2) and toe scour (especially in Reach 3); bank undercut and scour were frequently hidden by processes of mass wasting. Depositional banks are more stable, with toe sediment accumulation of a wide range of grain sizes.

Downstream reaches

The overall channel morphology of the reaches downstream reflects stable conditions. Slope gradients are very low ($0.004 < s < 0.001$) and hence the flow velocity is low to moderate ($0.27 \text{ m.s}^{-1} < V < 0.38 \text{ m.s}^{-1}$). The stream power for bankfull discharge decreases with distance downstream as a consequence of decreasing bed slope, although the stream power per unit area remains moderate to high due to the low channel capacity of the reaches ($22 \text{ m}^2 < CC < 27 \text{ m}^2$), especially regarding Reaches 4 and 5 (Table 5.4). Obstructions for flow are closely related to in-channel vegetation, especially in Reaches 4 to 6 ($0.07 < n < 0.11$). The high roughness of Reach 4 (0.11) is associated to both high vegetation in channel banks and strong human intervention (bridges and dam-related structures). Further downstream (Reaches 7 and 8), the tree galleries are less dense and continuous and so the channel roughness decreases (0.06).

The channel morphology is clearly tortuously-meandering (Table 5.4), with a narrow and deep channel ($9.7 < w:d < 14.1$) and a formerly well-developed floodplain now strongly reduced due to progressive farming. Same as the river upstream, the bed morphology is pool-riffled and base flows are shallow. Bank materials are composed of cohesive layers of silt and clay of Holocene origin; the grain size of bed and lateral deposits decreases considerably with respect to the river upstream. Bank profiles exhibited high stability all along the river stretch monitored. This aspect was evidenced by vegetation encroachment on the channel banks (Fig. 5.16) and by cross-sectional profiles showing stable conditions (Fig. 5.11). Evidence of lateral activity (narrowing and/or widening) was lacking for all reaches, at least regarding fluvial-related erosive and/or aggradation processes. Channel banks were in general highly stable, except for some sections in Reach 4 where mass wasting was observed in vertical banks with little vegetation cover. As for vertical channel activity, bed aggradation of very fine materials was observed all along the river course.

d) Channel stability

Morphologic analysis at the scale of the river reach provided the basis to inspect the degree of channel stability along the river course. Instability indices by river reach (Table 5.5) revealed overall channel stability for both the river upstream and downstream from the dam (potential instable channel conditions are indicated by values of the instability index greater than 20; Simon and Downs, 1995) with a slight tendency to less stable conditions in the downstream direction.

Despite apparent channel stability along the river course, there was great contrast in the overall geomorphic status between the river reaches located above and below the dam. Upstream, channel stability was related to dynamic geomorphic conditions adjusted to variations in the natural river flow regime; downstream, channel stability responded to moribund geomorphic conditions where actual channel forms result from processes that

operated in the past under conditions of higher energy. This contrast indicates extreme reduction in the stream energy after dam closure, and hence evidences the geomorphic effects of the dam clearly.



Figure 5.16: Evidence of channel stabilisation within the river downstream. Photographs were taken on river reaches located about 1 km (Reach 4) and 5 km (Reach 5) downstream from the dam closure.

Upstream dynamic stability was reflected by clear tendency to lateral mobility; cut banks and point bars were mostly active, and in-channel vegetation was, in general, in a pioneer state. Downstream, channel conditions were stable for all time intervals; the river downstream did not show evidence of channel activity, either lateral or vertical, but strong bank stabilisation by progressive vegetation encroachment. The present channel geometry and fluvial landforms are relics of a fluvial environment that no longer exists.

Table 5.5: Instability Index by river reach and description of the overall reach state.

Reach	Instability Index	Description	
<i>Upstream reaches</i>	1	11.2	Stable stream with alternate erosion/deposition of meander bends and mass wasting in convex top-banks. Coarse bed material, low channel constriction and moderate to high obstruction for flow (urbanisation, roads and bridges).
	2	12.7	Stable stream with alternate erosion/deposition of meander bends and mass wasting in convex top-banks. Gravel bed material, low channel constriction and high obstruction for flow (riparian vegetation).
	3	14.2	Stable stream with alternate erosion/deposition of meander bends and mass wasting in convex top-banks. Gravel bed materials, moderate to high channel constriction and high obstruction for flow (riparian vegetation).
<i>Downstream reaches</i>	4	15.5	Aggradational stream with little evidence of erosion; mass wasting observed in convex top-banks. Middle-sized bed material, low to moderate channel constriction and high obstruction for flow (riparian vegetation and dam-related structures).
	5	13.5	Aggradational stream with little evidence of erosion. Middle-sized to fine bed material, low to moderate channel constriction and moderate to high obstruction for flow (riparian vegetation).
	6	14.7	Aggradational stream with little evidence of erosion. Middle-sized to fine bed material, moderate to high channel constriction and low obstruction for flow.
	7	15.2	Aggradational stream with little evidence of erosion. Fine bed material, moderate to high channel constriction and low obstruction for flow.
	8	14.3	Aggradational stream with little evidence of erosion. Fine bed material, low to moderate channel constriction and moderate obstruction for flow (riparian vegetation).

2.2. CHANGES IN THE FLUVIAL LANDSCAPE

Dam-induced disruption in longitudinal fluvial processes has significant implications for the structure and composition of riparian communities as well. Reduction in the flow magnitude and variability, and reduction in the frequency and magnitude of flooding

plays in disrupting both the lateral and the vertical connectivity of the river system, which ultimately contributes to reduce riverine diversity. We used the Landscape Ecology approach (Forman and Godron, 1986; Forman, 1995; Burel and Baudry, 2000) to examine vegetation changes in terms of *dynamics* in the *structure*, *composition* and *function* of the riverine fluvial landscape. Inspection of dynamics in the regulated fluvial landscape within the regulated river from pre- to post-disturbance conditions was based on the understanding of natural landscape processes upstream.

2.2.1. Brief description of functional fluvial units

Besides considering primary types of natural vegetation cover, analysis incorporates land use types to inspect their potential effect on the river morphology independently than the effects of flow regulation induced by the dam. Seven functional fluvial units were selected for analysis; these units were grouped into three major categories of land cover: (i) semi-natural surfaces, (ii) agricultural lands and other artificial surfaces, and (iii) in-land waters.

- (i) *Semi-natural surfaces* include bare soils, grasslands and woodlands. Bare surfaces refer to open spaces with little vegetation and are mostly related to dynamic sediment deposits along and within the stream channel (point bars, bars, islands and cut banks). Natural grasslands are dominated by graminoid species (*Stipa ambigua*; *Stipa caudata*) and important associations (sociability 5) of pampas grasses (*Cortaderia seollana*). Secondary associations integrate various species of Asteraceae such as *Senecio* (*madagascariensis*; *bonariensis*), *Crepis*, *Ambrosia*, and thorny species of genus *Centaurea*, *Cirsium* and *Caduus* (Frangi and Bottino, 1995; Casado, 2006). Wood cover is clearly dominated by native species of willow (*Salix humboldtiana*) and bushy species of ‘brusquilla’ (*Discaria Americana*) and *Eupatorium bunifolium* (Frangi and Bottino, 1995; Barrera and Frangi, 1997). Exotic tree species such as poplar (*Populus alba*) may form extensive galleries along the top portions of the channel banks, especially within the river corridor downstream. Other exotic tree species of genus *Eucalyptus* and *Pinus* proliferate within artificially forested areas near farms and urban fabrics.
- (ii) *Agricultural lands* integrate crops and pastures. Agricultural activities within the river catchment are strongly related to rainfed cereal, corn and oilseed production and livestock grazing of unimproved grasslands (Aduriz *et al.*, 2003). Other *artificial surfaces* comprise discontinuous urban fabric, farms and roads.
- (iii) *Inland waters* refer mainly to the water course. The only water body within the area of interest corresponds to the reservoir lake.

2.2.2. Dynamics in the landscape composition

Analysis of the overall landscape composition was based on successive land cover maps to derive transition matrices and indices of variation that quantify and qualify directions and patterns of change (dynamics). Analysis was conducted for the upstream and the downstream river segments separately to allow for comparison between regulated and unregulated landscape conditions.

a) The overall fluvial landscape composition

The fluvial landscape was firstly evaluated at the coarse scale of the quaternary floodplain to inspect dynamics in land use susceptible of exerting influence in geomorphic processes. The spatial distribution of landscape units within both the upstream and downstream river segments revealed a clear dominance of agricultural lands over the three time steps used in analysis; artificial surfaces were much reduced, and semi-natural vegetation constrained to the river channel and its floodplain (Fig. 5.17; 5.18).

The landscape structure in 1961 (17 years before dam closure) was markedly agricultural. Crops covered 83 % (upstream) and 89 % (downstream) of the total landscape, and dominated over the fluvial and aeolian deposits (loess) within the inactive floodplain. The reduced number of patches indicates large cultivated surfaces. Natural vegetation occupied a much reduced landscape proportion and dominated clearly within the active floodplain. The overall landscape structure in 1981 and 2004 revealed similar patterns with minor shifts; the proportion of agricultural lands decreased by 15 % (upstream) and by 4 % (downstream) due to the advancement of impounded waters and progressive grazing activities over degraded lands in the vicinity of the dam. Upstream and downstream from the impoundment, the number of cultivated patches increased notably due to land subdivision. At this point, it should be noted that the lowest limit of the upstream river segment has been arbitrarily defined as the point where the surface covered by the reservoir lake in 1981 exceeded the quaternary floodplain. Grasslands and woodlands were almost exclusively confined to the river channel and its riparian zone in both river segments. Downstream, the proportion of semi-natural grasslands increased by 7 % due to vegetation growth over abandoned lands below the dam structure.

b) The riverine landscape composition

Inspection of the patch number and surface area of land cover types at the scale of the active floodplain revealed very different landscape composition relative to that of the quaternary landscape (Fig. 5.19). The fluvial corridor was clearly dominated by semi-natural vegetation; the domain of agricultural lands was restricted to sectors where abandoned braids provided benefits for farming activities. In 1961, natural grasslands dominated both the river upstream (62 %) and downstream (72 %) from the dam; the proportion of bare soils being higher upstream (16 % of the upstream landscape). Riparian trees formed sparse communities and occupied much reduced surfaces within both river segments (6 % upstream and 12 % downstream). In 1981, the proportion of grasslands and bare soils upstream decreased by 23 % and 50 %, respectively, as a consequence of progressive advance of water surfaces (+197 %). Downstream, grasslands contracted by 41 % due to advancing woodlands (+13 %). The riparian landscape in 2004 showed relatively equitable abundance of grasslands and woodlands within both river segments, although the rate of woodland progression within the river upstream was notably higher than that for the river downstream (+308 % and +70 %, respectively). Upstream, trees formed dense and continuous galleries along the river margins and proliferated in large groups over the riparian zone; tree galleries downstream were more discontinuous and were restrained to the channel margins.

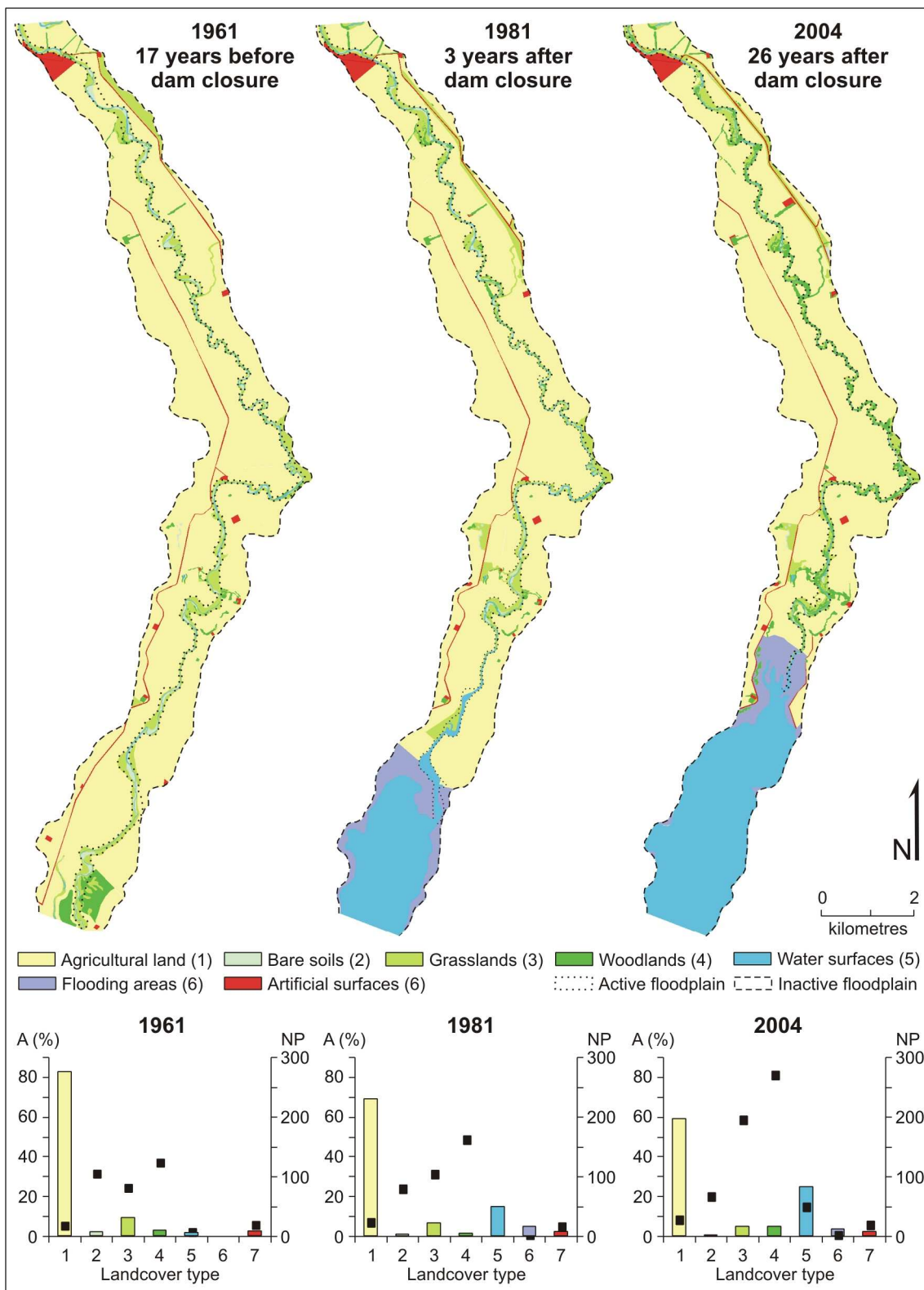


Figure 5.17: Spatial distribution of land cover types within the *upstream* river segment for the years 1961 (pre-disturbance), 1981 and 2004 (post-disturbance). The bar charts show the percent of surface area (A) by landcover type and time step; the corresponding number of patches (PN) is indicated by a black square.

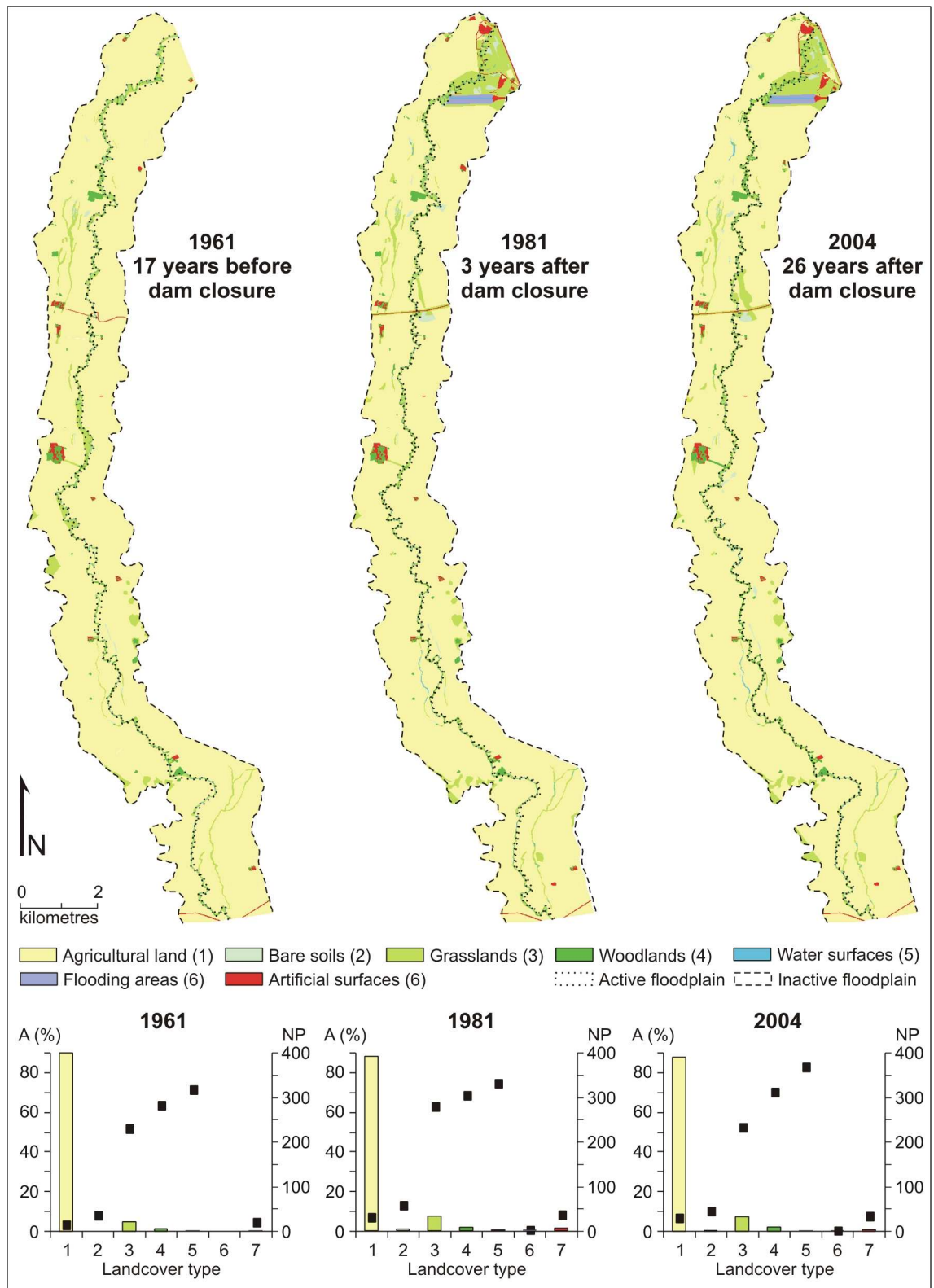
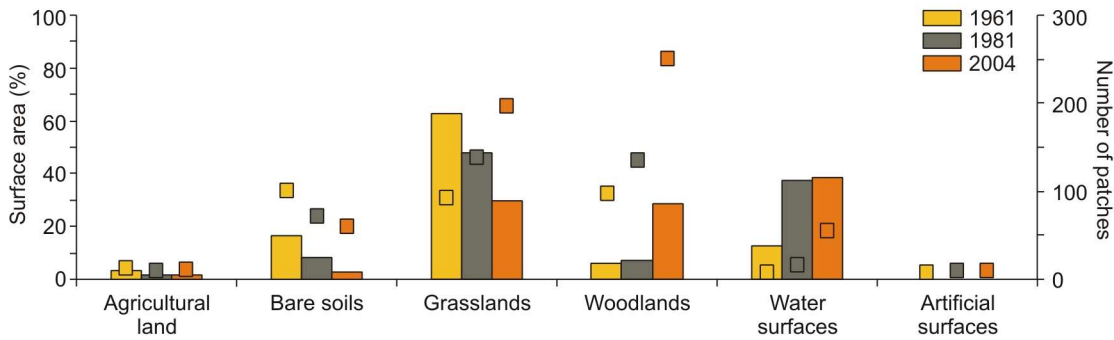
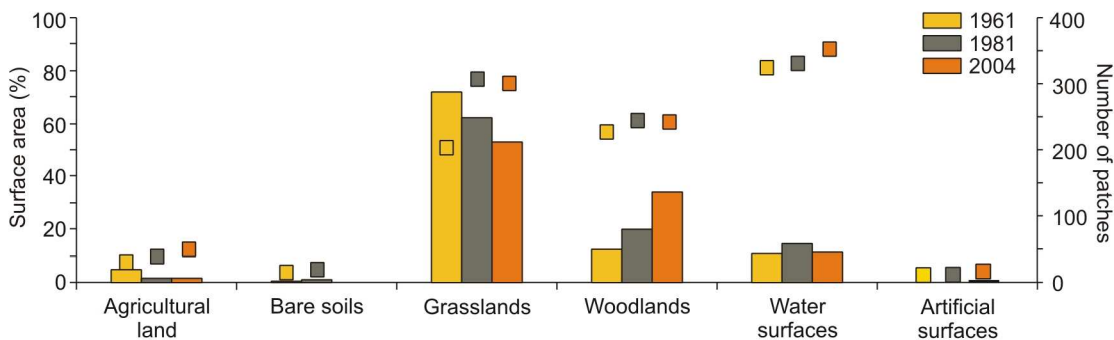


Figure 5.18: Spatial distribution of land cover types within the *downstream* river segment for the years 1961 (pre-disturbance), 1981 and 2004 (post-disturbance). The bar charts show the percent of surface area (A) by landcover type and time step; the corresponding number of patches (PN) is indicated by a black square.

[A] Upstream river segment

Land cover type	Surface (ha)			Difference (ha)		Rate of change (%)	
	1961	1981	2004	61 / 81	81 / 04	61 / 81	81 / 04
Agricultural land	12.6	1.0	7.7	-11.6	6.6	-91.9	648.9
Bare soils	66.1	33.3	10.9	-32.8	-22.4	-49.6	-67.3
Grasslands	250.2	192.7	121.8	57.5	-70.9	-23.0	-36.8
Woodlands	23.4	28.5	116.4	5.1	87.9	21.8	308.0
Water surfaces	50.4	149.9	157.3	99.4	7.4	197.1	4.9

[B] Downstream river segment

Land cover type	Surface (ha)			Difference (ha)		Rate of change (%)	
	1961	1981	2004	61 / 81	81 / 04	61 / 81	81 / 04
Agricultural land	12.7	2.5	2.7	-10.1	0.1	-80.0	4.6
Bare soils	1.0	2.1	0.0	1.1	-2.1	102.4	-100.0
Grasslands	191.3	113.4	96.5	-77.9	-16.9	-40.7	-14.9
Woodlands	32.4	36.6	62.0	4.2	25.4	12.9	69.3
Water surfaces	28.8	26.9	20.8	-1.9	-6.1	-6.6	-22.7

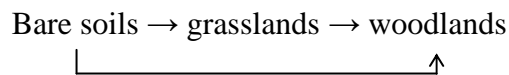
Figure 5.19: Number of patches by landcover type and class distribution as percentage of the fluvial corridor for the upstream and downstream river segments.

Inspection of landscape diversity by time step revealed an overall trend towards landscape diversification, especially within the river upstream where the number of patches (PN) increased by 83 %. As a result, the Shannon's Diversity Index increased from 1.1 to 1.3 within the river upstream and from 0.9 to 1.0 within the river downstream.

Analysis of patch abundance and dominance by class revealed that landscape diversification was strongly related to the progression of trees over bare soils and grasslands. Invasion of woodlands was particularly evident within both river segments due to (i) increased number of patches and spatial dominance of surfaces covered by

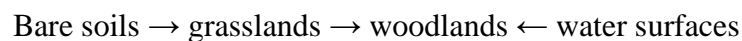
trees, (ii) increased number of patches over decreasing surfaces covered by grasslands (contraction and fragmentation), and (iii) decreased number of patches and surface area of bare soils (contraction). These aspects indicated that in both cases, landscape diversification was related to increasing number of landscape units resulting from landscape fragmentation more than to increasing number of land cover types.

Cross-tabulation of consecutive land cover maps revealed some differences in the evolutionary trends toward afforestation for the unregulated and regulated river corridors (Fig. 5.20). Upstream patterns of vegetal succession may be schematized as follows:



Transitions from bare soils to grasslands and from grasslands to woodlands occurred in both comparative periods, although they accelerated strongly between 1981 and 2004. The proportion of grass colonisation upon bare surfaces increased from 16 % between 1961/1981 to 31 % between 1981/2004; the proportion of colonisation of trees over grasslands increased from 3 % (1961/1981) to 31 % (1981/2004). A great proportion of wooded surfaces were observed to develop over bare surfaces directly. Successions from bare surfaces to woodlands between 1961/1981 were small (7 %), and intensified significantly during the last period (50 %). Given the ± 20 -yr interval between lands cover maps, we are unable to say whether these transitions involved intermediate states or not.

Patterns of succession of semi-natural vegetation within the downstream river corridor may be schematized as follows:



Transitions from bare soils to grasslands and from grasslands to woodlands were stronger between 1981 and 2004; the proportion of grass colonisation upon bare surfaces was of 73 % and the progression of tree communities over former grasslands was of 16 %. There were important transitions from water surfaces to woodlands during both comparative periods; such transitions intensified with time from 6 % to 32 %. Progression of tree cover upon water surfaces indicates that afforestation processes were circumscribed mainly to the stream channel.

2.2.3. Dynamics in the landscape configuration

Diversification of the landscape composition underlies changes in the landscape configuration. Building on previous results, analysis of landscape configuration focuses on the fluvial landscape at the scale of the active floodplain as it revealed the most interesting dynamics in the overall landscape structure; agricultural lands within the active floodplain were excluded from analysis because this class was not dominant and demonstrated very little change with time. Changes in the spatial arrangement of the landscape units with time were evaluated using measures of patch distribution, connectivity and aggregation. These measures provided the basis to inductive qualification of spatiotemporal landscape processes that generate ecological changes.

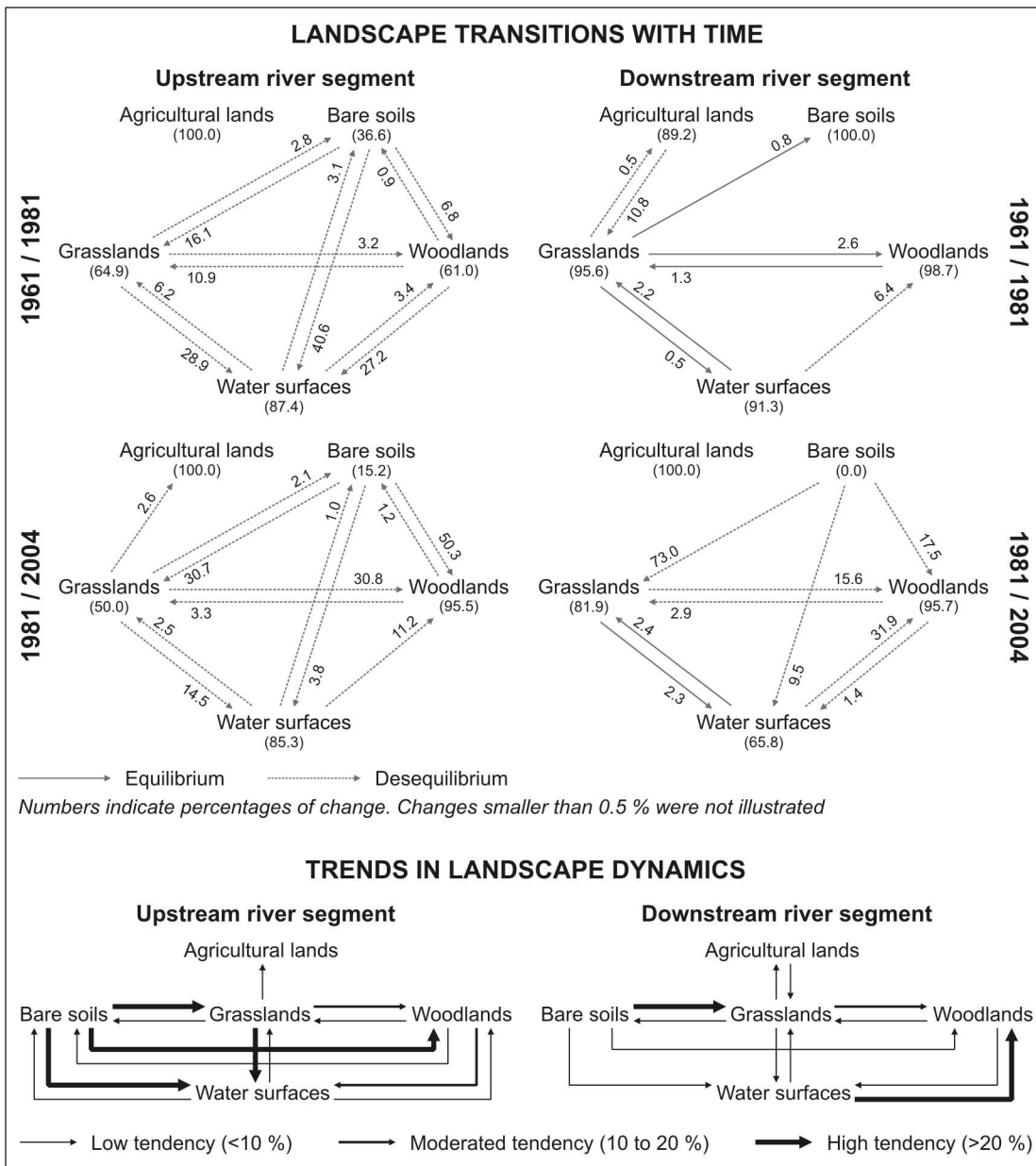


Figure 5.20: Transitions in the fluvial landscape with time and overall trends in landscape dynamics.

Measurement of the mean patch shape (MSH) and size (MPS) by class revealed a general tendency to landscape fragmentation by proliferation of trees over former grasslands and bare soils (Table 5.6). The average size of woody patches increased with time for both the upstream (+0.3 ha) and the downstream (+0.2 ha) river environments. Patch sizes diversified significantly, as revealed by increasing coefficients of variations (CV), and the average patch shape became slightly irregular. Small MPS and high CV suggest dominance of spare and little groups of trees. On the other hand, both upstream and downstream rivers showed contraction in the average size of surfaces covered by grasses (-2.1 ha; -0.6 ha), water (-5.3 ha; -0.2 ha) and bare soils (-0.5 ha; -0.2 ha), with increasing deviations in the mean patch size.

Table 5.6: Distribution of landscape units by landscape class for the years 1961, 1981 and 2004 within (a) the river segment upstream and (b) the river segment downstream.

<i>(a) Upstream river</i>												
Year	Grasslands			Woodlands			Water			Bare soils		
	MSH	MPS	CV	MSH	MPS	CV	MSH	MPS	CV	MSH	MPS	CV
1961	2.7	2.7	235	1.6	0.2	255	8.3	8.4	174	2.0	0.7	120
1981	2.3	1.4	249	1.7	0.2	160	4.7	8.8	285	2.0	0.5	93
2004	2.2	0.6	264	1.7	0.5	463	3.2	3.1	584	2.0	0.2	109

<i>(b) Downstream river</i>												
Year	Grasslands			Woodlands			Water			Bare soils		
	MSH	MPS	CV	MSH	MPS	CV	MSH	MPS	CV	MSH	MPS	CV
1961	2.1	0.9	372	1.7	0.1	140	1.8	0.1	263	1.7	0.1	476
1981	2.2	0.4	235	1.7	0.1	155	1.8	0.1	280	1.6	0.1	146
2004	2.1	0.3	242	1.8	0.3	237	1.6	0.1	405	-	-	-

MSH (mean patch shape); **MPS** (mean patch size [ha]); **CV** (coefficient of variation in the patch size).

Landscape fragmentation was particularly evident by measures of landscape division (DIV), that is, the degree to which the landscape is subdivided into separated patches. The Division Index equals 0 where the landscape consists of a single patch and reaches 1 where the landscape is maximally subdivided. As shown in Table 5.7, all classes showed high to very high DIV values for all years and, in the case of grasslands, DIV increased significantly with time (+0.4 upstream and +0.3 downstream). At the scale of the total landscape, DIV values increased from 0.7 (upstream) and 0.6 (downstream) in 1961 to 0.9 and 1.0 in 2004.

Values of the Aggregation Index were high for all classes (upstream and downstream) and for the three years, although revealed a slight decrease with time (Table 5.7). This indicates that individuals were spatially aggregated (high number of like-adjacencies) in large and compact spatial distributions, in spite of the overall tendency to landscape diversification and fragmentation. Patch aggregation is particularly important because it determines the potential for expansion, penetration, colonization and interference for dissemination between functional units.

Similarly, measures of landscape cohesion were close to 100 % for classes and time steps, which revealed strong connectivity between class-like units over time. Whereas division deals with the degree to which the landscape is fragmented, cohesion deals with the degree to which patches are spatially isolated from each other. Hence, class distributions may have identical levels of subdivision but very different levels of spatial isolation. High values of cohesion indicated that grasslands, woodlands and water surfaces, although subdivided, were close to each other and so spatially aggregated forming large and highly connected patches.

Table 5.7: Aggregation Index (AI) and Division Index (DIV) by landscape class for the years 1961, 1981 and 2004 within (a) the river upstream and (b) the river downstream.

<i>(a) Upstream river</i>										
Year	Grasslands		Woodlands		Water		Bare soils		Total landscape	
	AI	DIV	AI	DIV	AI	DIV	AI	DIV	AI	DIV
1961	92.2	1.0	84.3	1.0	78.5	1.0	88.9	1.0	89.6	1.0
1981	90.5	1.0	82.9	1.0	93.1	0.9	86.1	1.0	90.6	0.9
2004	87.2	1.0	86.5	1.0	94.0	0.9	78.6	1.0	89.4	0.9

<i>(b) Downstream river</i>										
Year	Grasslands		Woodlands		Water		Bare soils		Total landscape	
	AI	DIV	AI	DIV	AI	DIV	AI	DIV	AI	DIV
1961	88.3	1.0	77.1	1.0	63.9	0.8	69.6	1.0	84.5	0.9
1981	80.3	1.0	77.2	1.0	62.9	0.9	79.6	1.0	77.2	1.0
2004	79.3	1.0	81.2	1.0	64.3	1.0	87.3	1.0	78.4	1.0

2.2.4. Afforestation processes at the scale of the river reach

Previous analysis revealed an overall tendency to riparian vegetation growth for both the upstream and downstream river environments; during the last three decades, woody vegetation increased by 300 % upstream and by 70 % downstream. Vegetation growth was strongly related to the establishment of willows (*Salix humboldtiana*) over the channel banks forming continuous galleries along the river course which, in some cases, expanded laterally over the active floodplain. Other woody species observed within the channel and its riparian zone included weeping willows (*Salix sp.*) and poplars (*Populus alba, nigra*), although in minor extent. The second dominant woody species was the 'brusquilla' (*Discaria Americana*), a thorny bush of between 0.5 and 1.5 m height.

Willows and brusquilla are native species, and so they are well adapted to varying climate conditions. Conceivably, the dissemination of woody vegetation during the last decades is responding to the wetter climatic cycle documented since the 1970s. In opposition to what was expected, vegetation growth was considerably higher in terms of growth rate and significantly larger in terms of spatial distribution within the river upstream; below the dam, vegetation growth restrained to the active channel (Fig. 5.21).

a) Upstream reaches

Rates of vegetation growth and current woody cover within the reaches upstream revealed great contrasts between Reach 1, strongly anthropized and grass-dominated, and the semi-natural Reaches 2 and 3, strongly vegetated (Fig. 5.21). The current proportion of in-channel tree cover in Reach 1 is only 18.4 %, although this proportion is relatively high compared to the year 1961 (1.2 %). In Reaches 2 and 3, the percentage

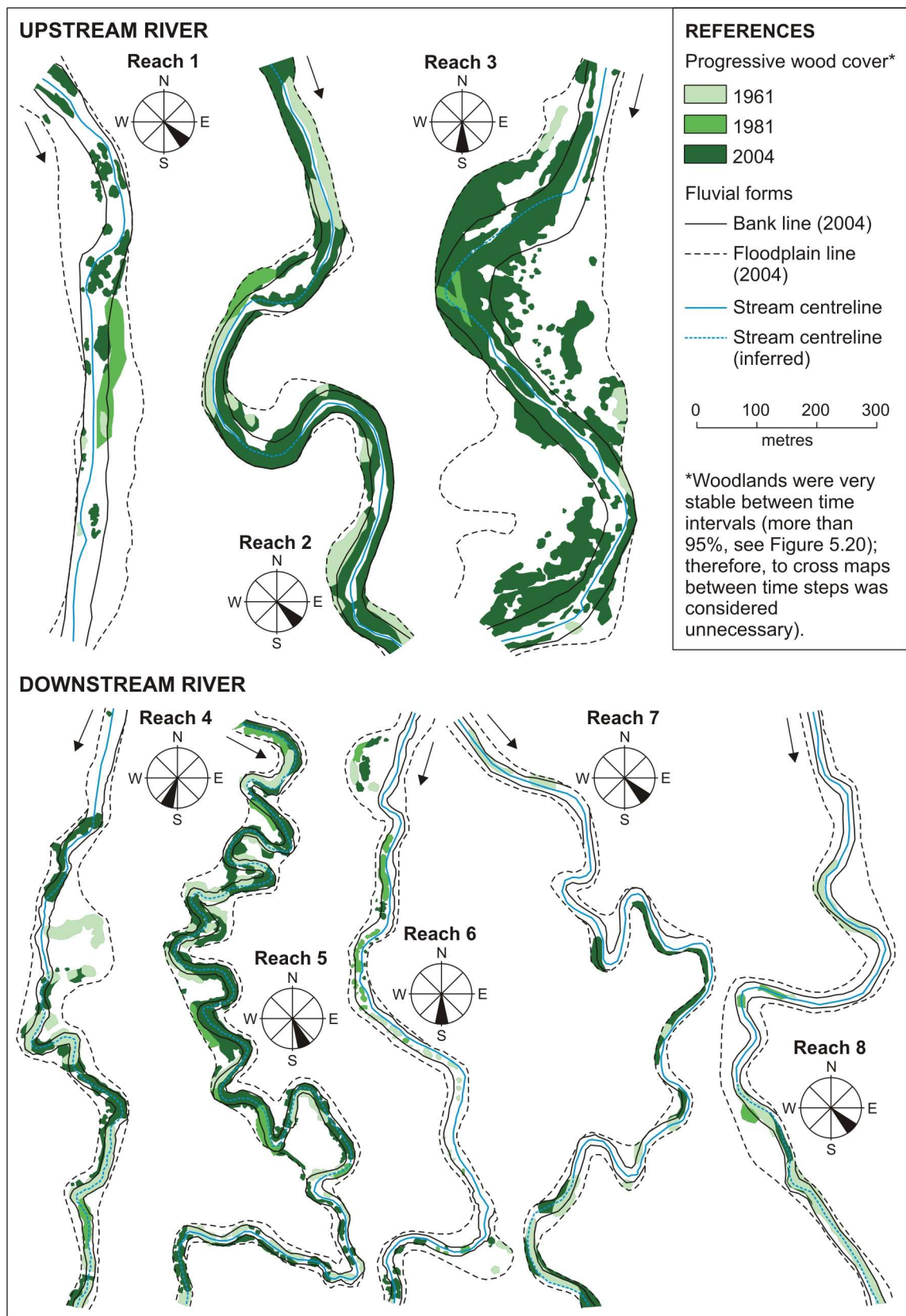


Figure 5.21: Progressive woody vegetation cover within the stream channel and the floodplain by river reach.

of in-channel trees increased from 17.2 % and 1 % in 1961 to 76.7 % and 86.5 % in 2004, respectively; rates of increase were considerably higher during the last comparative period. Except for Reach 1, the density of trees was high with very little spacing between clumps. This may induce good protection for bank erosion but also high resistance for flow. Willows form extensive and dense galleries over the river margins, and the age of individuals revealed that willows may be from a pioneer to a young-mature state. Examples of willow dissemination over channel banks are shown in Figure 5.22.



Figure 5.22: Examples of in-channel vegetation cover within the upstream river environment. Photographs were taken on river reaches located about 18 km (Reach 2) and 13 km (Reach 3) upstream from the dam closure.

b) Downstream reaches

Downstream, the current proportion of in-channel tree cover reflects a decreasing tendency in the downstream direction. The highest proportions of woody cover were found for reaches in the vicinity of the dam (62.8 % in Reach 4; 75 % in Reach 5); further downstream, the percentage of channel covered by trees decreased notably (22 % in Reach 6; 32 % in Reach 8). Growth rates for the period 1961-2004 were strong in Reach 5 (76.5 %) and Reach 6 (73.7 %), moderate in Reach 4 (49.1 %) and Reach 7 (45.8 %), and low in the distal Reach 8 (20.1 %). For all reaches, the highest rates of vegetation growth were documented within the last comparison period (1981-2004).

The density, extent (lateral and longitudinal) and spatial continuity of tree galleries decreased in the downstream direction as well. Tree galleries were dense, continuous and compact in reaches 4 and 5, whereas Reach 6 showed discontinuous single tree alienations and tree individuals in Reaches 7 and 8 were very sparse (Fig. 5.22; 5.24). The presence of old individuals in the upper reaches conceivably reflects the suppression of floods induced by the dam; individuals within reaches farther downstream were notably younger.



Figure 5.23: Examples of in-channel vegetation cover within the downstream river environment. The photograph was taken on a river reach located about 1 km downstream from the dam closure.

This chapter has evaluated changes in the morphology and vegetation cover of the Sauce Grande River downstream from the Paso de las Piedras Dam based on the understanding of geomorphic and vegetation processes within the unregulated river upstream. Despite the limited number of time steps for which spatial data were available and the considerable time lag between time steps (about 20 years), this study provided substantial information on geomorphic and vegetation dynamics from the natural pre-dam river state to the regulated post-dam river state. The methods used in analysis are widely available in literature and have been evaluated for a wide range of environments, applications and spatiotemporal scales. Results from this investigation are discussed below.

3.1. A THRESHOLD MATTER: A MATTER OF THRESHOLDS

Rivers are *systems* in *dynamic equilibrium* between erosion and deposition processes *adjusted* to present geologic, climatic and isostatic conditions (Schumm, 1977). A *threshold* is the point at which the dynamic behaviour of the fluvial system changes (Phillips, 2003a) in response to changes in *control factors* that may be external or internal to the system itself (Schumm, 1973; 1979). Research in fluvial geomorphology explains substantially the interconnections between the concepts cited above. In general terms, fluvial systems have the ability to adjust to external and internal factors so that a equilibrium state with some degree of stability is maintained; external or internal disturbance exceeding some critical threshold level results in instability and self-regulation to a new equilibrium state (Knighton, 1998).

The stability of fluvial systems is governed by the interactions between flow discharge and sediment load for a given type of channel material and degree of channel slope (Leopold *et al.*, 1964; Church, 1992; Bravard and Petit, 1997; Knighton, 1998; Robert, 2003). Interactions between these factors determine natural thresholds for physical processes (e.g. erosion, transport and deposition) and ecological processes (e.g. life cycles, species distribution, successions) within the river system (Church, 2002).

Dams represent the greatest source of human-related disturbance for fluvial stability (Petts and Gurnell, 2005), because they induce parallel disruption in both key control factors: flow magnitude and frequency, and sediment load and calibre (Petts, 1979). Although dam-induced changes in the stream competence contribute to exceed important geomorphic thresholds (e.g. rates of channel erosion, Chien, 1985; Kondolf, 1997) or ecologic thresholds (e.g. vegetation distribution, Hupp and Osterkamp, 1996), this thesis work deals with variations in flow discharge, the main driving force for both the geomorphic system (Knighton, 1998; Church, 2002; Robert, 2003) and the ecologic system (Poff *et al.*, 1997; Richter *et al.*, 1998).

Flow thresholds for the morphologic and ecologic functioning of fluvial systems are explicitly or implicitly considered in most baseline studies. For example, the incidence of flow events that form the channel varies systematically through the flow state

(Wolman and Miller, 1960), and the habitat heterogeneity and diversity patterns depend on the flow regime (Poff *et al.*, 1997), the flow persistence (Puckridge *et al.*, 2000) and the flow pulsing (Junk *et al.*, 1989; Tockner *et al.*, 2000) ensuring the longitudinal, vertical and lateral connectivity of the river system (Ward and Stanford, 1995b; Ward, 1998).

3.1.1. Altered flow thresholds below the Paso de las Piedras Dam

The hydrologic impacts of the Paso de las Piedras Dam were summarized (Table 5.9) based on flow states of major ecological and geomorphological significance: low flows ($< 1.2 \text{ m}^3 \cdot \text{s}^{-1}$), flow pulses ($> 12.8 \text{ m}^3 \cdot \text{s}^{-1}$) and floods ($> 91.1 \text{ m}^3 \cdot \text{s}^{-1}$). The effects of the dam on each flow state were quantified as fraction of averaged flow magnitude, frequency and duration within the river upstream over a 22-yr period of observation (1989-2010). Flow magnitude by flow state was calculated as means of all daily flows exceeding the flow state threshold, the number of times that daily flows exceeded such threshold provided a measure of the flow state frequency; the flow duration was calculated as the number of consecutive days where flows remained in the same flow category (including high-flow and flood recession).

Table 5.8: Dam-induced changes on three flow components of major geomorphic and ecologic significance. Changes are expressed as fraction of averaged upstream flow conditions (%). Numbers in parentheses show fraction of change relative to the flood of 2002 (single flood event observed downstream).

Flow state	Fraction of mean flow upstream (%)			Geomorphic implications	Ecologic implications
	Magnitude	Frequency	Duration		
Low flows	28	142	920	Far below limit for sediment transport and maintenance of the groundwater table	Far below limit for longitudinal connectivity, ecologic unsuitability
High flow pulses	58	55	590	Below limit for in-channel maintenance (erosion, deposition and vegetation)	May restore in-channel water quality and ecologic suitability
Over-bank floods	(154)	(8)	(720)	Far below limit for floodplain maintenance and riparian recruitment	Far below limit for lateral connectivity and nutrient exchange

Table 5.9 provides a good summary of the major hydrologic changes identified formerly in Chapter 4. The flow magnitude was reduced and the flow duration was increased substantially for all flow components; note, the apparent increase in the flood magnitude is given by the high magnitude of the single episode of downstream flooding observed during the period (reservoir overflow) relative to the averaged magnitude of floods observed upstream (13 episodes). The frequency of episodes of low-flow was increased notably (+140 %), whereas the frequency of high flows was reduced by 45 %; the

reduction in the flood frequency was dramatic (92 %). Reduced magnitude and frequency with increased duration of major flow states ultimately indicates a reduced and flatter hydrograph with very little variability.

3.1.2. Predicted direction of channel adjustment

Dam-induced reduction and homogenization of the downstream hydrograph combines to the sediment trapping efficiency of the reservoir to generate substantial changes in the balance between flow discharge and sediment load of the regulated Sauce Grande River. Both key control factors were dramatically reduced; however, reduction in the flow capacity to transport sediment [K] was conceivably greater than the reduction in the flow competence due to extreme reduction in the flow magnitude ($Q > L$).

A number of conceptual models have been developed to predict channel changes due to changes in flow discharge and sediment load inputs below dams. This research selected the predictive models of channel adjustment of Petts and Gurnell (2005) and Brandt (2000), and the qualitative model of change in the fluvial style of Surian and Rinaldi (2003). All these models predict the direction of channel adjustment in response to upstream impoundment; however, they are based on the conceptual models of Schumm (1969) and Lane (1955), respectively, and so provide complementary information on patterns of channel adjustment.

Based on the models cited above, the direction of channel adjustment to extreme reduction in flow discharge may be predicted as follows:

$$Q > L \text{ so that } L \sim K \rightarrow d^{0/-}, w^-, CC, n^+, s^{0/-}, S^+, \gamma, \\ \text{pool deposition, riffle erosion/deposition,} \\ \text{entrenchment, terrace formation.}$$

The channel response to extreme reduction in flow discharge will be associated to channel aggradation more than to degradation and armouring (Brandt, 2000; Petts and Gurnell, 2005). Although a combination of both aggradation and degradation processes may occur, riffles should not be subject to intensive scouring and deposition in pools should increase (Brandt, 2000). Rates of channel aggradation will depend strongly on (i) sediment supply by tributaries and/or channel resistance to erosion (Petts, 1984), and (ii) the proportion and size of the sediment available to transport relative to the capacity of the stream (Starkel, 1983). If the flow is overloaded, the exceeding material will be deposited in the channel bed and/or banks (e.g. Mangrove Creek below Mangrove Creek Dam, Australia, Sherrard and Erskine, 1991). Bed and lateral accretion ultimately contribute to reduce the channel capacity (e.g. Medjerda River below Sidi Salem Dam, Tunisia, Zahar *et al.*, 2008), and promote terrace and new floodplain formation on former channel banks (e.g. Peace River below Benett Dam, Canada, Church, 1995). Because flow will concentrate within the main stream channel, vegetation may develop over the banks increasing the channel stability and roughness (Mangrove Creek below Mangrove Creek Dam, Australia, Sherrard and Erskine, 1991; Dry Creek below Warm Springs Dam, California, Gordon and Meentemeyer, 2006). Sediment deposition on bars and islands may contribute substantially to vegetation encroachment (Benn and Erskine, 1994; Friedman *et al.*, 1998). The planform response may involve either

straightening and narrowing processes (e.g. Green River below Flaming Gorge Dam, Utah, Andrews, 1986; Grams and Schmidt, 2002) or wandering with consequent increased sinuosity (e.g. Yellow River below Sanmenxia Dam, Chien, 1985; Wang *et al.*, 2007).

3.2. CHANGES IN THE RIVER MORPHOLOGY

The geomorphic response of the Sauce Grande River to upstream impoundment may be schematized as follows:

$$Q > L \text{ so that } L \sim K \rightarrow d^{o/-}, w^{o/-}, CC^{o/-}, n^{+/o}, s^{o/-}, S, \\ \text{pool/riffle deposition of fines}$$

Except for a slight decrease in the stream sinuosity, which was also observed upstream from the dam, results showed no significant geomorphic change since dam closure (Fig. 5.24). Evidence of lateral and vertical activity was related to human intervention to facilitate evacuation of dam outlets and spills (e.g. bed digging, artificial meander cut-off and levees building) more than to natural adjustments to reduced flow discharge and sediment load (e.g. incision/deposition and narrowing). Another human-related change was related to the extreme reduction of the extent of the active floodplain. Conceivably, the suppression of flood has encouraged farmers to extend agricultural practices to the limits of the stream channel; at present, the lateral limits of the river floodplain are undefined for much of the river course.

In opposition to what was expected, there was no clear evidence of channel scour within the river immediately below the dam. Bank profiles exhibited high stability all along the stretch monitored; this aspect was evidenced by vegetation encroachment on the channel banks and by cross-sectional profiles showing stable conditions (Fig. 5.245). Bed deposition of very fine materials (clay and silt) was observed in both pools and riffles, although rates of pool deposition were notably higher. Possibly, bed aggradation led to some decrease in the channel capacity; however, rates of bed aggradation were negligible compared to those reported in literature (e.g. Lower Yellow River and Liu River below flood control reservoirs, China, Chien, 1985; Rio Grande below Elephant Butte Dam, New Mexico, Schmidt and Everitt, 2000).

Furthermore, channel contraction was inferred at some degree by vegetation growth within the stream channel, although the position of bank outlines, where visible, remained unchanged for the three time steps used in photo-interpretation analysis. Gordon and Meentemeyer (2006) also reported channel contraction due to expansion of vegetation within the main stream channel; however, most studies documenting channel narrowing indicate that this process is related to lateral accretion (e.g. Green River below Flaming Gorge Dam, Utah, Andrews, 1986; Grams and Schmidt, 2002; Mangrove Creek below Mangrove Creek Dam, Australia, Sherrard and Erskine, 1991) with vegetation invasion on lateral deposits (e.g. Cudgegong River below Windamere Dam, Australia, Benn and Erskine, 1994). Evidence of lateral accretion was not observed in the present Sauce Grande River, although stabilisation of channel banks by vegetation growth could hide former aggradation processes.

channel states with time showed lateral migration of meander bends across the floodplain coupled with meander progression and meander cut-off for the two time intervals (1961-1981; 1981-2004). Nevertheless, rates of lateral channel activity and average channel width decreased during the second comparative period suggesting an overall tendency to channel narrowing and simplification of the meander complexity.

Whereas the river upstream revealed dynamic geomorphic stability adjusted to variations in the natural river flow regime, geomorphic stability within the river downstream was related to stable channel conditions with apparent absence of erosion and/or aggradation processes (at least of natural origin) contributing to lateral and/or vertical channel activity. These findings evidence the geomorphic effects of the dam clearly: the dam has suppressed morphogenetic flows, and hence has induced stable (moribund) channel conditions downstream. At present, the downstream river reflects a slightly aggradational stream where the channel morphology is a relic of a fluvial environment created in the past under conditions of higher energy.

Besides the studies cited above, confrontation of the results to those reported elsewhere is limited to a few examples because, in our knowledge, moribund channel conditions were reported by very few studies abroad. Furthermore, the Sauce Grande River is a semiarid river, and the geomorphic response to upstream impoundment within semiarid fluvial systems remains poorly known (Blanchon and Bravard, 2007). The importance of confronting results to those reported for regulated systems within arid and semiarid regions of the world rely on the recent understanding that fluvial processes (and hence fluvial response to external change) within semiarid rivers may be very different from those generally accepted within more humid regions. The reviews of Thoms and Sheldon (2000) and Tooth (2000) on Australian rivers, for example, outline the distinctive characteristics of arid and semiarid fluvial environments relative to those of humid climate: arid and semiarid rivers are allogenic, subject to extreme temporal and spatial variations in rainfall, runoff and sediment transport, and depend on large floods as main control for channel morphology.

Dam-induced stability in the channel planform after dam construction has been reported by Blanchon and Bravard (2007) in the Orange River, South Africa; however, this comparison is poorly founded because (i) the morphology of the Orange River differs substantially from that of the Sauce Grande, and (ii) the Orange River has been impounded for different purposes (hydropower). In a more similar geomorphic and dam operational context although very different in terms of hydrologic magnitude, Thoms and Walker (1993) found that the coarse morphology of the regulated Murray River, Australia, remained unchanged due to the low stream energy and cohesive bank materials restricting the initiation of channel adjustment. In USA, Friedman *et al.* (1998) reported that the principal geomorphic response of meandering channels in the Great Plains was the reduction in migration rates, and Shields *et al.* (2000) found that the Missouri River downstream from Fort Peck Dam in Montana became slightly more sinuous after impoundment, although rates of channel activity were considerably higher prior to dam closure than afterwards. Similarly, Marston *et al.* (2005) reported that the Snake River below Jackson Lake Dam (Wyoming) experienced fewer avulsions and a decrease in sinuosity, although these patterns of response reversed close to the influence of tributaries.

3.2.2. Causes of unapparent geomorphic change

From his study on 14 regulated rivers in Britain, Petts (1979) found that the complex channel response within active meander systems could involve no change if the channel was lined by coarse sediments, cohesive material or if it was well vegetated, because the regulated flow may be below the threshold for sediment recovery and transport (e.g. Derwent River below Ladybower Reservoir). The author concluded that in such cases, floods of high magnitude would be required to exceed intrinsic geomorphic thresholds and hence initiate adjustments. Regardless that they were formulated within humid fluvial environments, these arguments could explain the unapparent geomorphic change of the Sauce Grande River.

Under natural, unregulated conditions, the channel morphology is influenced by peak flows and floods of high magnitude, short duration and very low predictability characteristic of most semiarid rivers (Warner, 1987; Erskine and Warner, 1998; Thoms and Sheldon, 2000; Tooth, 2000; Bull and Kirkby, 2002; McMahon and Finlayson, 2003; Schmandt, 2010). Hence, flood suppression and reduction in the frequency and magnitude of geomorphically effective flows is conceivably the greatest cause for downstream channel stability.

The river has been regulated since 1908 for water supply to the city of Bahía Blanca from La Toma Intake Station (see Chapter 1). Despite that the volume of water extracted from La Toma was 12.7 % the dam yield capacity, the station has probably altered the flood regime somehow. During the early steps of dam construction by early 1970's (Fig. 5.25) and after the filling of the Paso de las Piedras Reservoir initiated in 1978, dam operations increased the permanence of flow conditions below suitable geomorphic thresholds. Together, these aspects explain the apparent channel stability observed during both the first, 'pre-disturbance' comparative period (1961-1981) and the second, 'post-disturbance' comparative period (1981-2004).

Most studies on rivers subject to extreme reduction in flow discharge document channel aggradation at some level (e.g. Sherrard and Erskine, 1991; Thoms and Walker, 1993; Benn and Erskine, 1994; Grams and Schmidt, 2002); however, rates of bed aggradation within the Sauce Grande River were comparatively negligible, and the channel capacity remained relatively unchanged. As noted by Petts and Lewin (1979), reduction of the channel capacity due to channel aggradation requires either introduction of sediment by tributaries, redistribution of sediment within the channel, or both.

These arguments provide a double explanation for unapparent aggradation processes within the Sauce Grande. After the reservoir traps more than 99 % of the sediment yielded from headwater sources, sources for sediment supply downstream are very scarce. First, the river flows for the majority of its course without tributary influence. Second, redistribution of sediment within the channel is unlikely to occur because the reduced flow is incompetent to remove channel materials. The only mineral source downstream is the sediment delivered by lateral runoff along the river course. Combined to endogen production of organic matter, this process may explain deposition of fine materials in pools and riffles. Despite that the overall topography beyond the limits of the main stream channel is rather flat, sediment supply from lateral runoff is conceivably promoted by intensive agricultural use of the formerly active floodplain, especially in periods of fallow.



Figure 5.25: Operations for dam construction by early 1970's. Source: La Nueva Provincia (<http://www.lanueva.com/multimedia/nota/3855858f4a/173/18136.html>).

Although downstream flow has been reduced dramatically, some episodes of flow release occurred during the life history of the dam reservoir; they included high flow pulsing and one flood event in 2002. The question at this point may be formulated as

follows: why these episodes of high-flow did not initiate channel adjustments? There are two possible explanations to apparent channel stability during periods of high-flow. First, the river channel in the vicinity of the dam has been strongly altered. Man has done what the river should have done by itself; the difference was in that the sediment recovered from the channel bed and banks was not deposited further downstream but in the levees constructed along the river course to increase the channel capacity to evacuate flows and spills. Second, channel banks are composed of cohesive layers of Holocene fluvial deposits including sand, silt and clay (Borromei, 1991), which increases resistance to erosion and hence thresholds for flow effectiveness. The resistance to erosion of the channel materials is possibly exacerbated by vegetation encroachment, although vegetation growth within the regulated channel was dominated by herbaceous species more than woody species as discussed below.

3.3. CHANGES IN THE FLUVIAL LANDSCAPE

Fluvial landscapes are structural and functional units that integrate a variety of dynamic environmental and human processes (Aspinall and Pearson, 2000; Fujihara and Kikuchi, 2005) contributing to potential changes in geomorphic systems (Phillips, 2009). This study has evaluated parallel changes in land uses and natural vegetation cover at the scale of the quaternary floodplain and the riverine landscape (i.e. the active floodplain) to inspect (i) the potential effects of land use on the river morphology and vegetation regardless of the effects of flow regulation induced by the dam, and (ii) the potential effects of the dam on riparian and channel vegetation. Note that some interactions between fluvial landforms and vegetation dynamics were hypothesized, although these aspects require further attention to inspect the nature of the colonisations, the rate of vegetation growth and the feedbacks between hydrology, morphology and patterns of succession.

3.3.1. Dynamics in the landscape structure

Comparison of the structure and dynamics of the fluvial landscape at the scale of the quaternary floodplain showed minor shifts from the unregulated to the regulated river environment. Both river environments were clearly agricultural, with very little variation in types of land use over time. Overall, the agricultural landscape revealed temporal stability with a slight tendency to progression of crops over natural surfaces. This tendency was observed along the entire fluvial landscape regardless of the agricultural losses due to river impoundment (upstream flooding and downstream land degradation). Downstream from the dam, agricultural lands expanded over the active floodplain for much of the river course. This process was conceivably encouraged by the suppression of floods and has major implications for the morphology and vegetation cover of the river downstream, especially in terms of sediment supply (Liébault and Piégay, 2001; Owens and Walling, 2002; Liébault *et al.*, 2005) and vegetation establishment (Gordon and Meentemeyer, 2006).

The semi-natural landscape constrained to the active floodplain for both river segments. A strong tendency to vegetation growth was observed all along the fluvial corridor, with significant changes in the land cover from bare surfaces and herbaceous associations to shrub/wood communities. Upstream from the dam, the progression of grasslands and trees over bare surfaces occurred in both the stream channel and its riparian zone; downstream, vegetation growth was almost exclusively confined to the main stream channel. In terms of surface area, riparian trees increased by 397 % above the dam and by 91 % downstream; by 2004, the riparian surface occupied by woodlands was of 116 ha and 62 ha, respectively.

In opposition to what was expected, results revealed parallel landscape dynamics for the upstream and downstream river environments. Despite apparent differences in patterns of woodland expansion, the tendency to afforestation of the river corridor was clear for both river segments and accelerated significantly during the last decades. This suggests that the effects of flow regulation on the composition and configuration of the fluvial landscape downstream were conceivably coupled with the action of other drivers of change related to physical processes (e.g. climate change, channel morphology), human processes (e.g. advancing cultivated lands over the active floodplain), or both. These aspects underlie a wide range of processes as discussed below.

3.3.2. Processes in the fluvial landscape

Inspection of dynamics in the structure (composition and configuration) of the riverine landscape revealed an array of landscape transitions with time. However, a better understanding of environmental change requires the identification of spatiotemporal processes that are the basis of such transformations. Based upon the inductive model presented by Mendonça-Santos and Claramunt (2001), the main processes of change identified within the upstream and the downstream river environments may be schematized as shown in Figure 5.26.

Analysis of patch abundance and dominance at the scale of the total landscape revealed an overall tendency to landscape diversification. Landscape diversification was strongly related to the progression of trees over bare soils, grasslands and water surfaces, so that diversification processes were related to landscape fragmentation more than to increasing number of land cover types. Landscape fragmentation was particularly evident by measures of landscape division close to unity; however, inspection of the landscape aggregation and cohesion revealed that landscape patches were spatially aggregated in large and compact distributions despite the overall tendency to landscape fragmentation.

Analysis of transitions in landscape units revealed substantial stability (i.e. no change) in land use types, and an array of processes of change in the semi-natural vegetation cover (Fig. 5.26). The change the most apparent was the *expansion* of woodlands within the current river corridor, either above or below the impoundment. Expansion of woodlands led logically to a *contraction* of former landscape units such as grasslands, bare soils and water surfaces. Contraction processes were greater for the last two units, as they showed small rates of concomitant expansion. On the other hand, surfaces covered by grasslands revealed coupled processes of expansion-contraction, with

predominance of the latter. Except for the areas covered by water due to filling of the reservoir lake, contraction of woodlands towards other land cover types was negligible. This indicates high persistence of woody vegetation over time and underlies presence of old individuals, especially in the areas less affected by flood disturbance.

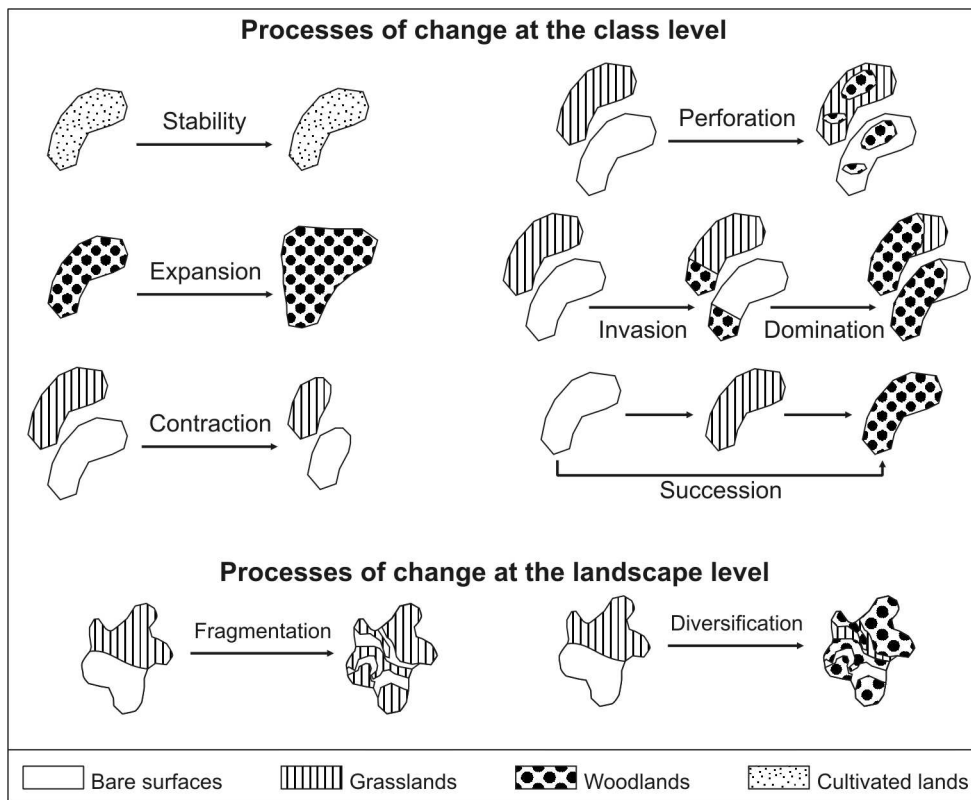


Figure 5.26: Conceptual scheme of processes of change at the class and landscape levels along the riverine landscape. Based on Mendonça-Santos and Claramunt (2001).

The remaining processes of change at the scale of landscape classes were related to the mechanisms in which woodlands and grasslands expanded over former surfaces. Two main processes of vegetal colonisation were observed: perforation and invasion. *Perforation* processes were related to growing of sparse trees by creating holes within homogeneous units, while *invasion* processes were associated to spreading of grasslands over bare soils and spreading of woodlands over both. Perforation and invasion processes were observed mainly during the first comparative period (1961/1981), and were represented by increasing number of woody and grassy patches greater than increasing surface area per class unit. As for *domination* processes (i.e. a class dominates an area formerly covered by another class), they were stronger during the period 1981/2004 and were associated to increasing woody surfaces over water surfaces, grasslands and bare soils.

In some cases, invasion/perforation and domination processes led to complete sequences of change (*succession*). Patterns of succession showed typical progressive sequences from a pioneer stage to a forested stage (bare soil → grasslands → woodlands), and rapid progressive sequences jumping intermediate stages (bare soil →

woodlands). Mechanisms of vegetal succession were not investigated and so we can not expand on the nature of evolutionary transitions. Nevertheless, results underscore a tendency to afforestation of the fluvial corridor. Afforestation processes were stronger within the river environment upstream, and intensified during the post-disturbance period for both the upstream and downstream fluvial landscapes. Given the considerable time interval between landcover maps (about 20 years) we are not able to expand on the continuity of vegetal successions neither. Conceivably, successions have not always been progressive as peak flows and floods have probably contributed to remove pioneer vegetation from the channel banks and the river floodplain. However and whatever the direction and temporal continuity in patterns of vegetation change, the expansion of woodlands was clear for both upstream and downstream river corridors.

3.3.3. Variations in the nature of afforestation processes along the river course

Channel afforestation and changes in the structure of the riparian landscape have been reported by a number of studies on impounded rivers for a variety of purposes and environments (e.g. Williams and Wolman, 1984; Walker and Thoms, 1993; Benn and Erskine, 1994; Fergus, 1997; Friedman *et al.*, 1998; Merritt and Cooper, 2000; Richard and Julien, 2003; Choi *et al.*, 2005; Marston *et al.*, 2005; Gordon and Meentemeyer, 2006). Although the effects of the dam on the fluvial landscape downstream were clear, afforestation processes within the regulated Sauce Grande River were less significant than those reported in literature and were less important than those observed within the unregulated river upstream. Petts and Gurnell (2005) argued that successional sequences on regulated river systems depend on a range of morphologic factors (e.g. pre-dam channel type and size) and hydrologic factors (e.g. actual sequences of flow and tributary influence) acting over different spatial and temporal scales. Overall, these factors combine to explain variations in the nature of afforestation processes within the regulated and the unregulated Sauce Grande River.

Synchrony in the expansion of woodlands all along the river course is conceivably related to the humid climate cycle documented since the 1970's (e.g. Scian, 2000; Penalba and Vargas, 2004; Kruse and Laurencena, 2005; Núñez *et al.*, 2005; Penalba and Robledo, 2005; Forte-Lay *et al.*, 2008; Penalba and Llano, 2008). Woodlands are dominated by willows, which is a native species. Willow alignments along the stream inspired English pioneers of late XIX Century to name the river (Widmann, 2012) - *Sauce* means willow in Spanish-, and way before that, hunter-gatherers used willow wood as combustion material (Brea *et al.*, 2001). Furthermore, willow debris were found in late Holocene fluvial deposits (Rabassa *et al.*, 1985; Rabassa *et al.*, 1991); ¹⁴C measurements dated the debris in 1150 ± 70 (Figini *et al.*, 1990). In sum, willows and grasslands are part of the fluvial landscape since geological times (Quattrocchio *et al.*, 2008) and hence are well adapted to respond quickly to climate fluctuations and consequent variations in moisture. These aspects could explain the overall tendency to afforestation of the river corridor during the last decades; however, differences in the nature and spatial domain of tree colonisations between the upstream and downstream river environments were evident and related to both hydrologic and geomorphic alteration of the river downstream.

During wet periods, flood pulses (*sensu* Junk *et al.*, 1989) increase connectivity (productivity and disturbance) between the river and its floodplain (Ward and Stanford, 1995b; Ward, 1998), promoting seedling establishment over the riparian zone (Friedman *et al.*, 1998). Reduction in the frequency, extent and duration of overbank flooding below dams contributes to isolate the river channel from its floodplain (Nilsson and Berggren, 2000) and to lowering the groundwater table (Petts, 1984; McCartney *et al.*, 2001), all of which disrupts the pathways of lateral and vertical connectivity of the fluvial system (Ward and Stanford, 1995b; Poff *et al.*, 1997; Ward, 1998).

Floods within the regulated Sauce Grande River were suppressed, so that the lateral connectivity promoting successful recruitment of tree seedling was truncated. As a result, there was great contrast in patterns of tree dissemination between the river upstream and downstream from the dam. Upstream, willows formed widespread galleries along the stream channel and extended over the floodplain forming dense associations; downstream, vegetation growth confined to the stream channel and, except for the river reach immediately below the dam, tree galleries were less extensive and more discontinuous than those observed upstream. Furthermore, flood suppression has encouraged farmers to extend their agricultural practices to the formerly active floodplain; at present, the natural riparian landscape is reduced or even absent for much of the river course.

Invasion of xeric species were reported for many regulated rivers (e.g. Green River below Flaming Gorge Dam, Merritt and Cooper, 2000), although in the case of the Sauce Grande changes in the composition of vegetal communities were not observed. Probably, this aspect is linked to the fact that native species are well adapted to cyclical changes in moisture; hence, reduced flows below the dam should not be a source of change different than that induced by dry climate cycles. Nevertheless, this study builds on field observations, and more detailed research on the biologic composition of riparian communities is required.

Finally, differences in the nature of tree colonisation are conceivably related to dam-induced channel stability. Channel migration promotes establishment of riparian pioneers by providing new bare and moist surfaces (e.g. point bars) suitable for seedling establishment (Friedman *et al.*, 1998; Shields *et al.*, 2000); within the river upstream, these aspects were evidenced by significant landscape transitions from bare surfaces to woodlands (50 % between 1981 and 2004). Downstream, lateral channel stability and so reduced rates of bank erosion and deposition decrease the frequency in which new channel suitable for vegetation establishment is created, which ultimately slows regeneration of pioneer species. Furthermore, the channel downstream is relatively narrow and deep, so that the channel area available for vegetation establishment is relatively small. Willows spread discontinuously over the lower portions of the channel banks, there where the bank slope decreases and the soil is moist. As a result, transitions from water surfaces to woodlands within the river downstream were significant, especially during the second time interval (30 %).

3.4. CONCLUSIONS

This chapter has presented detailed information on the morphology and landscape dynamics of the Sauce Grande River below the Paso de las Piedras Dam. The methods used to geomorphic and fluvial landscape assessment have been widely evaluated for a variety of environments and applications; hence discussion of the methods presented herein was considered unnecessary.

Results from this investigation revealed that the dam has induced moribund channel stability within the downstream river course. Lateral and vertical channel activity was related to human intervention to facilitate evacuation of dam outlets and spills more than to natural adjustments to reduced flow discharge and sediment load. After the reservoir retains the majority of discharge and sediment delivered from headwater sources, there are no supplementary sources for flow and sediment supply downstream. The reduced flow, even if sediment-free, is incompetent to work its channel and at present, the downstream river morphology is a relic of a fluvial environment created in the past under conditions of higher energy.

Parallel processes of vegetation encroachment over stable banks were observed, although for much river sections they were related to herbaceous communities more than to woody species. Patterns of woody colonisation downstream were strongly constrained by the flood suppression, the pre-dam channel morphology and the overall channel stability. Despite some relationships between vegetation and fluvial landforms were inferred, interactions between the channel morphology and vegetation cover require of further attention.

This thesis work has evaluated the degree to which the Paso de las Piedras Dam disrupts the hydrologic continuity of the Sauce Grande River, and has quantified the impacts of flow regulation on the hydrology, morphology and water temperature of the river downstream. Based on the understanding of natural fluvial processes upstream, this study provided the very first assessment of the broad-scale impacts of the dam on the river environment downstream. As well as yielding new information on the hydrologic, morphologic and thermal impacts of dam construction and reservoir operation, this study has generated new spatial, climatic and hydrologic data that provide an important platform on which to base further assessment of both the unregulated and the regulated rivers. Furthermore, this study has implemented a methodological framework to hydrological assessment within ungauged basins that has great potential to application to other ungauged basins in the regional context and other semiarid regions of the world.

1. METHODOLOGICAL FRAMEWORK

The greatest limitation to accomplish this investigation was the overall lack of climatic and hydrologic data, and the consequent lack of pre-existent knowledge on the complexity of hydrological processes playing within the river basin. Hence, the methodological framework implemented within this research combines (i) a set of methods used to data generation, and (ii) a set of methods used to hydrological, morphological and water temperature assessment.

Building on calculation and modelling of spatial and climatic data, this study developed and tested a hydrological model of the upper river basin based on simple empirical relationships between topography, climate and runoff processes. Despite that the model applicability to other ungauged basins requires to be evaluated and that the variables used in flow simulation require incorporating groundwater processes, results indicated that the model has great potential to generate flow data, especially within semiarid regions.

Assessment of the hydrological, thermal and morphological impacts of river impoundment built on a prior understanding of the degree of flow regulation induced by the dam. A Water Balance Model for the Paso de las Piedras Reservoir was developed and tested to predict variations in water storage (declines and raises). Based on the water balance equation, any component of the reservoir hydrology may be estimated from the relationships between the remaining components, which ultimately allow inspecting reservoir storage-yield-release relationships. Hence, the model has great utility as assessment tool from a management and scientific perspective.

The hydrologic impacts of dam operation over time were evaluated using the methodological suite included within the Indicators of Hydrological Alteration program (IHA). IHA is the best suited methodology to assess hydrologic alteration, and has great potential to quantify impacts of dams and other projects for water management.

Furthermore, this thesis work tests applicability of two novel approaches to river water temperature assessment: a regime shape and magnitude classification and a climatic Sensitivity Index. Combined, these approaches provided substantial information on temporal (in)stability, climatic sensitivity and spatial variability of water temperature regimes. Finally, this study provides an expression of the widely accepted utility of GIS-based chronological techniques to geomorphic and vegetation assessment.

2. PRINCIPAL RESEARCH FINDINGS

Building on a large basis of literature on impounded rivers and on previous knowledge of the river basin and its regional environment, research hypotheses stated that reservoir conservation storage policies exerted great disruption in the hydrologic continuity of river system, especially in periods of drought. Because droughts are recurrent and severe, the direction of change in the components of the river system downstream was hypothesized assuming (i) major decrease in flow discharge and sediment load inputs with altered water quality due to combination of reservoir outflows from the bottom layers of the reservoir and increased groundwater influence, and (ii) a tendency to channel aggradation (after an initial phase of bed degradation), bank stabilisation by progressive vegetation growth, and changes in the diversity and patterns of succession of the riparian landscape.

Results from this investigation revealed that the fluvial response to upstream impoundment was unique, complex and unpredictable. Reservoir inflows are driven by varying climate conditions inducing strong intra- and inter-annual fluctuations in the effective water available for storage purposes. Such fluctuations are linked to both ENSO and non-ENSO phenomena, and hence are highly unpredictable. On the other hand, reservoir outflows are constrained by the dam purpose for water supply; large volumes of water are yielded annually (73 % of the mean annual runoff) and the remaining volume is conserved within the reservoir for periods of drought. The reservoir storage capacity is almost four times the mean annual inflow volume, which implies great dam potential to absorb the full range of flows within its reservoir and the majority of the sediment delivered from the headwaters. Overall, results revealed that reservoir evacuation is very unlikely to occur and that, whether occurs, the fraction of inflow available to flow release downstream after the annual yield requirements were met is only 27 % the mean annual inflow.

Patterns of flow regulation have seriously affected the overall hydrology and water quality of the river downstream. The direction and magnitude of hydrologic and thermal change below the dam were similar to that reported for other regulated rivers in temperate regions of the world, although the magnitude of hydrologic change was sensibly higher than that reported elsewhere. Floods were fully eliminated and the magnitude and frequency of both high and low flows were dramatically reduced with substantial increase in the duration of similar flow conditions. Ultimately, these changes combine to alter the annual flow seasonality including suppression of summer peaks, reduction of spring peaks and increase in winter minima.

Furthermore, summer temperatures were depressed, winter temperatures were

increased, and diurnal fluctuations were substantially altered in both magnitude and timing. Although water release during the observation period did not occur, the thermal inversion of the river downstream relative to the unregulated river upstream was clear and linked to dam-induced changes in both components of the river water temperature: (i) the heat load, due to canalisation of reservoir seepage into the main channel, and (ii) the stream thermal capacity, due to reduction in downstream flow discharge.

Flood suppression and reduced flow magnitude over the full range of flows combine to reduce sediment concentration to generate substantial changes in the equilibrium of the regulated river downstream. Both key control factors were dramatically reduced, the flow discharge and the sediment load, although the reduction in flow discharge was extreme so that the reduction in the flow capacity to transport sediment was greater than the reduction in the amount of sediment available to transport.

Qualitative models of geomorphic response to extreme reduction in flow discharge predict reduction of the channel capacity due to vertical and lateral aggradation, reduction in the lateral migration, within-channel vegetation encroachment and disruption of the river-floodplain connectivity. In opposition to what was expected, results from geomorphic analysis revealed no significant change since dam closure.

Lateral and vertical channel activity was related to human intervention to facilitate evacuation of dam outlets and spills more than to natural adjustments to reduced flow discharge and sediment load (e.g. incision/deposition and narrowing). Bed deposition of very fine materials was observed in both pools and riffles, although rates of bed aggradation were negligible compared to those reported in literature. Bank profiles exhibited high stability all along the river segment monitored; channel contraction was inferred at some degree by vegetation growth within the stream channel, although the position of bank outlines, where visible, remained unchanged for the three time steps used in photo-interpretation analysis.

These findings indicate clearly that the dam has induced stable (moribund) river channel conditions downstream. After the reservoir retains the majority of discharge and sediment delivered from headwater sources, there are no supplementary sources for flow and sediment supply downstream (the river is allogenic). The reduced flow, even if sediment-free, is incompetent to work its channel and at present, the downstream river reflects a slightly aggradational and strongly altered stream where the channel morphology is a relic of a fluvial environment created in the past under conditions of higher energy.

The most significant change in the riverine landscape was related to the contraction of the active floodplain face to the progression of agricultural activities encouraged by the suppression of floods. An overall tendency to progression of woodlands within the river channel was also observed, although this process was comparatively less significant than that observed upstream and restrained to the vicinity of the dam. Patterns of woody colonisation downstream were strongly constrained by the channel morphology, where the channel form (narrow and deep) prevents for tree establishment and where the overall channel stability prevents for creation of new, suitable zones for vegetation establishment.

3. FURTHER RESEARCH AND PERSPECTIVES

The results from this investigation lead to a suite of additional issues that require further attention. For example, the river hydrology was evaluated based on simulated flow data. Although results from simulation were suitable and provided a consistent basis on which to base hydrological analysis, the rainfall-runoff model implemented herein is subject to many sources of error and uncertainty and requires further efforts of calibration and parameterization (e.g. incorporation of sub-surface hydrological components). River water temperature assessment used detailed and high-quality data sets that permitted to infer the potential thermal impacts of the dam robustly. Nevertheless, long-term series of water temperature data are required to inspect the effects of the dam over the full range of seasons, and for a variety of climate and hydrological conditions. Similarly, some relationships between vegetation and fluvial landforms were hypothesized, although these aspects require further attention to inspect the nature of tree colonisations, the rate of vegetation growth and the feedbacks between hydrology, morphology and vegetation.

A number of questions that emerge on a wider scale delineate specific areas of research as expressed below.

1. Which are the causes of the natural river flow variability?

This investigation showed that the ENSO phenomenon explains a considerable proportion of variability in local rainfall regimes and hence in the river flow regime, although not systematically. Many other large-scale phenomena may influence sequences of drought and flooding at the regional scale, and their potential influence within the river basin requires to be investigated directly. Dealing with this aspect is essential from a dam management perspective, and is at the basis of the establishment of future frameworks of water release downstream.

2. Which are the implications of flow regulation for the overall water quality of the river downstream?

This research has evaluated with the effects of the dam on the river water temperature as indicator of river water quality. However, many other physical, chemical and biological river water properties may be altered by river impoundment. At present, water quality studies concentrate their efforts on the reservoir limnology. Despite the indisputable value of these studies relative to the reservoir purpose, attention should be given to the quality of the waters flowing below the dam, as the river supplies water to meet human requirements, especially in periods of drought.

3. Which are the implications of hydrological and thermal alteration for the river ecology?

Considerable research has evaluated the effects of altered hydrology and water quality on the distribution, structure and life cycles of aquatic organisms within the regulated river downstream. This research provided substantial information on change in two ecologically-relevant variables: the river flow regime and the water temperature; however, the ecological implications of altered patterns of flow and water temperature

within the Sauce Grande River remain to be investigated directly. In this regard, this investigation provides an important platform to enable further research to assess the health of the river ecosystem and to inform the sustainable management of water resources.

4. Which are the implications of the dam for the river environment upstream?

Inspection of the impacts of the dam on the river environment downstream built on comparisons relative to unregulated fluvial processes upstream used as reference of 'natural' river conditions. Yet, a number of studies have demonstrated that river impoundment may affect the upstream river system as well, especially due to artificial change in the base level. The dam potential to alter the river environment upstream provides a completely new research field that requires further attention.

4. RESEARCH APPLICABILITY

This research provided consistent information on the overall hydrology, morphology and thermal patterns of the Sauce Grande River upstream and downstream from the Paso de las Piedras Dam. The new climatic, hydrologic and morphologic information yielded herein has double applicability. First, it informs dam management about the complex behaviour of the river system and about the broad-scale impacts of reservoir operation on the river downstream. This information and the data generated for analysis are made available of dam managers to contribute to establish reservoir operation policies that maintain the overall integrity of the river system without compromising the reservoir function for water supply. Second, this study provides a consistent scientific platform on which to base further research efforts conducting to an interdisciplinary framework of river restoration.

Proposals for river restoration are way beyond the purpose of this research. At present, most scientific and governmental efforts at the international scale are orientated to evaluate the costs and benefits of changing dam operating rules or even of dam removal to restore the hydrological and ecological integrity of impounded river systems. However, these actions are not a viable regarding the Paso de las Piedras Dam because of its vital purpose for water supply. On the other hand, patterns of flow regulation within reservoirs operating for water supply in semiarid regions represent the most serious threat for ecological suitability. The solution is then complex, and further restoration efforts require interdisciplinary research that conciliates the usual conflict between ecologic and human needs for freshwater from both a scientific and a water management perspective.

Cette recherche évalue le degré de régulation hydrologique induit par le barrage-réservoir Paso de las Piedras sur la Sauce Grande et quantifie les effets de cette régulation sur la hydrologie, la morphologie et la température de l'eau de la rivière en aval. Le travail de thèse consiste en une évaluation exhaustive et systématique des impacts du barrage-réservoir sur le système fluvial basée sur la compréhension des processus naturels qui se produisent en amont. En plus de fournir des informations sur les impacts hydrologiques, morphologiques et thermiques de la construction du barrage Paso de las Piedras et de l'exploitation de son réservoir, cette étude génère des séries de données climatiques et hydrologiques qui fournissent une base significative sur laquelle fonder des recherches futures. Par ailleurs, cette étude met en place un cadre méthodologique appliqué à l'analyse hydrogéomorphologique des bassins versants non jaugés qui a un grand potentiel d'application dans d'autres bassins de la région similaires ainsi que dans d'autres régions semi-arides du monde.

1. JUSTIFICATION DE L'ÉTUDE

Cette étude évalue les changements hydrologiques, thermiques et morphologiques de la rivière Sauce Grande en aval du barrage-réservoir Paso de las Piedras. Située dans la partie centrale de la région Sud-Ouest de Buenos Aires, Argentine, la rivière et le réservoir constituent la ressource en eau douce la plus importante de la région (Borromei 1991 ; Zavala et Quattrocchio, 2001; Schefer, 2004).

Même si le climat est du type tempéré sub-humide (Campo *et al.*, 2004), la variabilité interannuelle des précipitations est forte et liée à des phénomènes atmosphériques de grande échelle comme El Niño (ENSO) et des anomalies de circulation atmosphérique dans la Zone de Convergence de l'Atlantique Sud (Scian, 2000 ; Labraga *et al.*, 2002 ; Scian *et al.*, 2006). Les épisodes de sécheresse (ou d'inondation) sont fréquents (Campo *et al.*, 2009 ; Bohn *et al.*, 2011) et impactent sérieusement l'économie régionale (Troha et Forte Lay, 1993 ; Andrade *et al.*, 2009).

La région a très régulièrement connu des déficiences qualitatives et quantitatives dans l'approvisionnement d'eau potable (Andres *et al.*, 2009). La récurrence des sécheresses et l'augmentation de la demande en eau suite à la croissance de la population ont conduit à une série de crises hydriques qui, à leur tour, ont conduit à des avancées systématiques des pratiques locales de gestion de la ressource en eau.

Le barrage-réservoir Paso de las Piedras régule la rivière Sauce Grande depuis 1978 à des fins d'approvisionnement en eau potable. Aujourd'hui, la demande en eau concerne environ 350.000 habitants concentrés dans les villes de Bahía Blanca et Punta Alta. À pleine capacité, le réservoir a une superficie de 36 km², une profondeur de 25 mètres et une capacité de stockage utile de 328 hm³ (Schefer, 2004). La variabilité climatique et la croissance démographique se combinent pour engendrer une forte vulnérabilité des ressources en eau locales face au déficit hydrique. Par conséquent, les procédures de gestion du barrage-réservoir tendent à maximiser le stockage et la conservation d'eau

dans le réservoir pour assurer l'approvisionnement en eau potable au cours des périodes de sécheresse.

Malgré l'importance régionale de la Sauce Grande comme principale source d'eau potable et la grande capacité du réservoir Paso de las Piedras, l'hydrologie du bassin versant et les effets du barrage sur l'environnement fluvial restent très mal évalués. Le manque de connaissances intégrées sur le comportement complexe des ressources en eau locales s'est illustré au cours des dernières années du fait des effets dramatiques des événements extrêmes. Des séries de sécheresses et d'inondations ont gravement affecté la relation entre l'usage de l'eau et sa disponibilité, mettant en question les pratiques de gestion des ressources hydriques. Actuellement, la demande en eau potable dépasse la capacité d'approvisionnement du réservoir et, par conséquent, le barrage et son réservoir requièrent une attention toute particulière au niveau régional.

Cette étude fournit la toute première évaluation (i) de l'hydrologie du réservoir Paso de las Piedras, (ii) du degré de régulation hydrologique induit par le barrage et, (iii) de l'impact de cette régulation sur l'hydrologie, la morphologie et la température de l'eau de la Sauce Grande en aval du réservoir. En plus de fournir un nouvel exemple sur les effets des barrages sur les rivières régulées et de documenter les effets du Paso de las Piedras sur la Sauce Grande, cette étude génère des séries de données climatiques et hydrologiques et met en place un cadre méthodologique appliqué à l'analyse hydrologique des bassins non jaugés. Les contenus climatiques, hydrologiques et morphologiques assemblés dans cette recherche peuvent être appliqués dans un triple cadre :

- (i) ils informent l'organisme en charge de la gestion du barrage sur le comportement complexe du système fluvial,
- (ii) ils contribuent à l'amélioration des politiques de gestion du réservoir en respectant l'intégrité globale du système fluvial, et
- (iii) ils contribuent à construire une plate-forme scientifique cohérente sur laquelle fonder des efforts de recherche interdisciplinaire conduisant à des propositions de restauration fluviale.

2. CADRE THEORIQUE

Les systèmes fluviaux s'inscrivent dans un *continuum* des processus physiques et biologiques interdépendants (Vannote *et al.*, 1980) liés par des transferts longitudinaux, latéraux et verticaux d'énergie, de matière et d'êtres vivants (Petts et Amoros, 1996). Malgré la valeur indiscutable des barrages pour la gestion des ressources en eau (Magilligan et Nislow 2005 ; Petts et Gurnell, 2005), la construction de barrages et l'exploitation de réservoirs altèrent fortement la continuité longitudinale des processus fluviaux (Petts, 1984), ce qui provoque des discontinuités en série du *continuum* fluvial (Ward et Stanford, 1983 ; 1995a ; Stanford et Ward, 2001).

La préoccupation scientifique sur les impacts des barrages sur des systèmes fluviaux a augmenté en même temps que la construction de barrages s'est accélérée à travers le monde (Brandt, 2000). Les travaux de Graff (2005) et de Petts et Gurnell (2005), par

exemple, fournissent une revue très complète des progrès scientifiques dans la compréhension des effets des barrages sur les systèmes fluviaux en aval. Actuellement, la littérature sur l'impact hydrologique, géomorphologique et écologique des barrages est abondante et le nombre d'études qui ont inspiré cette recherche est trop élevé pour être cité dans ce résumé.

Cette étude est clairement basée sur la notion de discontinuité (Ward et Stanford, 1983 ; 1995a ; Stanford et Ward, 2001) et s'appuie largement sur les travaux de Petts (1979 ; 1984) et l'idée d'ordre de la réponse fluviale à des perturbations dans l'équilibre des processus fluviaux (Schumm, 1969). La base conceptuelle de cette recherche peut être simplifiée par une chaîne de processus de cause à effet. Dans leur état naturel, les rivières sont des systèmes dynamiques sous la dépendance de contrôles climatiques, topographiques et géologiques à l'échelle du bassin versant. La construction de barrages représente la source la plus importante de perturbation hydrologique induite par les activités humaines. La rétention de débit et de sédiments dans des réservoirs modifie trois éléments critiques du système fluvial en aval :

- (i) la capacité de la rivière à transporter des sédiments,
- (ii) la quantité de sédiment disponible pour le transport, et
- (iii) la qualité des eaux courantes.

Ensemble, ces changements engendrent une série d'ajustements fluviaux qui vont se poursuivre dans le temps jusqu'à ce que le système fluvial assimile la perturbation ou jusqu'à ce qu'il atteigne un nouvel état d'équilibre.

Les études effectuées sur des rivières régulées à travers le monde ont documenté une large gamme de changements morphologiques et écologiques en réponse à l'altération hydrologique. De telles transformations incluent des changements dans la géométrie du chenal (forme transversale, forme en plan et pente du lit), dans la diversité et les modèles de succession végétale et dans la structure et la fonction des organismes aquatiques. Pourtant, la direction, l'ampleur, la fréquence temporelle et l'étendue spatiale de tels changements peuvent varier considérablement d'une rivière à l'autre.

La réponse fluviale à la construction de barrages en amont est complexe et dépend d'un bon nombre de facteurs, y compris la taille et la fonction du barrage, l'histoire de gestion des ressources en eau et l'environnement du système fluvial imposant une certaine résistance au changement. Citant Phillips (2003b), *la seule généralisation globalement acceptée est que les effets des barrages sont souvent importants et vastes et varient d'une rivière à l'autre, au fil du temps et en fonction de la distance en aval.*

3. CONTEXTE DE RECHERCHE

3.1. Objectifs principaux

Ce travail de thèse a été fortement motivé par deux besoins parallèles. Tout d'abord, cette étude répond à la nécessité d'une évaluation intégrée de l'hydrologie du réservoir Paso de las Piedras et de ses effets sur la Sauce Grande en aval. Deuxièmement, cette

recherche répond à la nécessité de générer des ensembles de données climatiques et hydrologiques permettant d'évaluer des processus fluviaux à l'échelle du bassin versant et du corridor fluvial.

En fonction de ces aspects, l'objectif principal de cette étude vise à évaluer le degré de régulation hydrologique induit par le barrage-réservoir Paso de las Piedras sur le cours moyen de la rivière Sauce Grande et à quantifier les impacts sur l'hydrologie, la température de l'eau et la morphologie de la rivière en aval de l'aménagement. Le deuxième objectif est de générer des données de référence pour évaluer les variations spatio-temporelles des processus hydrologiques avec précision.

3.2. Hypothèses

La réponse de la Sauce Grande à la régulation hydrologique induite par le barrage Paso de las Piedras est évaluée à partir de quatre hypothèses :

- (i) le climat de type sub-humide à semi-aride induit des fortes variations annuelles et interannuelles dans l'eau disponible pour l'écoulement et le stockage,
- (ii) la zone d'étude se constitue de trois sections bien identifiées (lit amont, réservoir, lit aval),
- (iii) le réservoir constitue une perturbation, voire une rupture du *continuum* fluvial (ordre 6),
- (iv) le réservoir présente une grande capacité de stockage par rapport aux apports hydrologiques. Il est thermiquement stratifié, et son potentiel de rétention des sédiments est supérieur à 99%.

Sur la base de ces hypothèses, il résulte que la continuité hydrologique de la Sauce Grande a été fortement interrompue en raison des pratiques de gestion du réservoir, lesquelles tendent à maximiser le stockage d'eau pour assurer l'approvisionnement en temps de sécheresse.

En période de sécheresse, récurrente et liée à El Niño, la réduction de la fréquence et de l'ampleur des crues exerce une grande influence sur l'environnement de la rivière en aval affectant toutes les composantes du système fluvial. Les effets d'une telle régulation hydrologique incluent (i) l'altération de la qualité de l'eau due à l'influence accrue des eaux souterraines, (ii) la réduction de la capacité du chenal par des phénomènes de sédimentation et de croissance de la végétation dans le lit mineur et, (iii) une déconnection renforcée entre le chenal et sa plaine d'inondation.

En période humide, la fréquence et l'ampleur des crues en aval augmentent et donc la direction d'ajustement s'inverse. Les changements incluent (i) la modification de la qualité de l'eau par des apports provenant des couches les plus profondes du réservoir, (ii) l'augmentation de la capacité du chenal par des processus d'érosion verticale et / ou latérale et par l'enlèvement de la végétation et, (iii) le rétablissement de la connectivité entre le chenal et la plaine d'inondation.

3.3. Méthodes

La principale limite pour effectuer cette étude a été liée au manque général et au caractère discontinu des données climatiques et hydrologiques disponibles. De plus, les études sur la complexité de processus hydrologiques qui ont lieu au sein du bassin versant sont insuffisantes. Ainsi, cette étude incorpore un ensemble de méthodes appliquées à la génération de données et un ensemble de méthodes appliquées à l'étude des transformations hydrologiques, thermiques et morphologiques de la rivière en aval du barrage.

1. Cette étude développe tout d'abord un modèle hydrologique du haut bassin versant basé sur des relations empiriques simples entre la topographie, les précipitations et l'écoulement. Bien que l'application du modèle à d'autres bassins non jaugés reste à être évaluée et bien que le modèle nécessite d'intégrer des processus hydrogéologiques, les résultats ont montré qu'il a un grand potentiel pour générer des données d'écoulement, en particulier dans des régions semi-arides.
2. Ensuite, cette étude évalue le degré de régulation hydrologique induit par le barrage-réservoir. Le bilan hydrologique du réservoir a été calculé pour prédire les variations de stockage d'eau (diminutions et les augmentations) en fonction des variations des flux d'entrée et de sortie. Pour ce faire, un modèle hydrologique du réservoir a été développé et testé. Le modèle a permis (i) d'estimer n'importe quelle composante hydrologique à partir des relations entre les composantes restantes, (ii) de quantifier la relation entre le stockage, la performance du réservoir et les lâchés d'eau, et (iii) d'estimer le potentiel de décharge du réservoir en aval en fonction de sa capacité et de sa performance pour répondre aux exigences d'approvisionnement en eau. En ce sens, le modèle est très utile comme outil d'analyse et de gestion.
3. La quantification des impacts hydrologiques de la gestion du barrage-réservoir dans le temps s'est basée sur la suite méthodologique incluse dans le programme Indicators of Hydrological Alteration (IHA). IHA est l'une des méthodes les plus appropriées pour évaluer l'altération hydrologique des rivières régulées et donc pour quantifier les impacts des barrages et d'autres aménagements.

D'autre part, cette étude a évalué l'application des deux approches novatrices pour l'analyse de la température de l'eau : une classification hiérarchique basée sur la forme et le timing des régimes de température (RSMC) et un Indice de Sensibilité climatique (SI). Ensemble, ces approches ont fourni des informations importantes sur les régimes diurnes de température de l'eau, y compris leur stabilité temporelle, leur sensibilité aux conditions météorologiques et leur variabilité spatiale le long du cours d'eau.

4. Enfin, cette étude fournit une confirmation supplémentaire de l'utilité des SIG pour l'analyse chronologique des changements géomorphologiques et de la végétation. L'analyse s'est basée sur l'interprétation de photographies aériennes et des images satellitaires à haute résolution (Ikonos) pour trois pas de temps: 1961 (période de pré-impact), 1981 (trois ans après la mise en eau du réservoir) et 2004 (26 ans plus tard). La quantification des changements morphologiques a été basée sur la comparaison et la superposition de cartes du corridor fluvial acquises pour ces trois dates.

4. RESULTATS PRINCIPAUX

La séquence logique de causalités produisant l'impact peut être résumée comme suit:

Le barrage interrompt la continuité longitudinale des processus fluviaux → cette régulation modifie l'hydrologie de la rivière en aval → la configuration du chenal et de la plaine d'inondation change en réponse à cette altération hydrologique.

Cette séquence structure les résultats de cette étude au sein de trois chapitres explorant chaque partie de la séquence séparément (Chapitres 3 à 5).

Chapitre 3

Le Chapitre 3 quantifie le degré de régulation hydrologique induit par le barrage sur la base du bilan hydrologique du réservoir. Les résultats ont démontré que le fonctionnement du système hydrologique est unique, complexe et imprévisible. Les entrées du réservoir sont influencées par des conditions climatiques très variables tout au long de l'année ou sur plusieurs années. Ces fluctuations sont fortement liées au phénomène ENSO, mais aussi à d'autres phénomènes atmosphériques à grande échelle. Par conséquent, les ressources en eau fluctuent annuellement et interannuellement de façon imprévisible. D'autre part, les sorties d'eau régulées sont fortement influencées par la fonction du barrage pour l'approvisionnement en eau potable ; de grands volumes d'eau sont utilisés chaque année (73 % de l'écoulement annuel moyen) et le volume restant est conservé dans le réservoir pour les périodes de sécheresse. La capacité de stockage du réservoir est presque quatre fois le volume d'écoulement annuel moyen, ce qui indique le grand potentiel du barrage pour absorber dans son réservoir toute la gamme des flux d'entrée et la plupart des sédiments fournis par l'amont. Enfin, les résultats ont démontré que la probabilité de décharge du débit en aval est très faible et que, si une telle décharge se produit, la fraction d'eau disponible pour alimenter la rivière en aval une fois que les besoins annuels d'approvisionnement en eau potable sont satisfaits est seulement de 27 % de l'écoulement annuel moyen.

Chapitre 4

Le Chapitre 4 évalue les changements fluviaux de premier ordre, à savoir, les changements qui se sont produits immédiatement après la fermeture du barrage et qui dépendent directement des procédures de gestion des eaux. L'analyse porte sur deux des trois changements principaux documentés par Petts (1984), c'est à dire les changements affectant le régime d'écoulement et la qualité de l'eau courante. Concernant ce dernier changement, cette étude est centrée sur le régime thermique du cours d'eau.

Les résultats ont montré que les procédures de gestion du barrage ont sérieusement affecté le débit de la rivière et la qualité globale de l'eau en aval. La direction et l'ampleur des changements hydrologiques et thermiques sont similaires à celles documentées sur d'autres rivières régulées des régions tempérées du monde, même si l'ampleur du changement hydrologique est sensiblement plus élevée que celle rapportée ailleurs. Les crues ont été complètement éliminées et l'ampleur et la fréquence des débits de pointe ont été considérablement réduites. D'ailleurs, la durée des conditions

d'écoulement similaires a été augmentée substantiellement. Ensemble, ces changements ont contribué à modifier la saisonnalité du régime d'écoulement annuel : les pics d'été ont été supprimés, les débits de pointe de printemps ont été réduits et les débits d'étiage ont été augmentés.

D'autre part, la température de l'eau estivale (hivernale) a été diminuée (augmentée) significativement et les fluctuations diurnes ont été substantiellement modifiées en ampleur et en timing. Bien que pendant la période d'observation nulle évacuation en aval ne se soit produite, la température de l'eau de la rivière en aval a été inversée par rapport à la rivière amont non régulée. Ce processus témoigne de deux effets concurrents du barrage sur (i) la charge thermique de la rivière, suite aux apports provenant des fuites du fond du barrage, et (ii) la capacité thermique de la rivière, suite à la forte réduction du débit.

Chapitre 5

Enfin, le Chapitre 5 évalue les impacts des barrages de second ordre, c'est à dire la réponse de la morphologie du chenal et de la plaine d'inondation à la modification du régime d'écoulement et du budget sédimentaire. Le débit en aval du réservoir a été fortement réduit en ampleur et modifié radicalement en termes de fréquence, timing, durée et variation annuelle. La réduction du débit et la suppression des crues se combinent avec la rétention des sédiments dans le réservoir (supposée supérieure à 99 % de la charge fournie par les zones en amont) pour générer des changements importants dans l'équilibre de la rivière en aval. Les deux variables de contrôle (c.-à-d. le débit et la charge sédimentaire) ont été considérablement réduites ; cependant, la diminution du débit a été tellement forte que la réduction de la capacité de transport de la rivière est supérieure à la réduction de la charge sédimentaire disponible pour le transport.

Les modèles qualitatifs de réponse géomorphologique à la réduction extrême du débit indiquent (i) une réduction de la capacité du chenal suite à des processus de dépôt vertical et latéral et d'accroissement de la végétation sur les berges, les bancs et les îles, (ii) une réduction de la migration latérale du chenal, et (iii) une déconnexion entre le chenal et sa plaine d'inondation. Contrairement à ce qui était attendu, les résultats de l'analyse géomorphologique n'ont pas révélé des changements significatifs du chenal depuis la fermeture du barrage.

L'activité latérale et verticale du chenal est plus liée à des interventions humaines pour faciliter l'évacuation des lâchées du réservoir qu'à l'ajustement naturel du chenal en réponse à la réduction du débit liquide et solide (par exemple, des processus d'incision du lit et/ou de dépôt). Des dépôts de sédiments très fins dans les mouilles et rapides ont été observés, bien que les taux de sédimentation soient négligeables par rapport à ceux décrits dans la littérature. Les profils transversaux ont révélé que le chenal est fortement stable sur l'ensemble du tronçon de la rivière étudiée ; la croissance de végétation dans le lit mineur témoigne d'une contraction du chenal, bien que la position des berges soit restée inchangée au cours des trois intervalles de temps utilisés en photo-interprétation.

Ces résultats indiquent clairement que le barrage est responsable d'une morphologie moribonde en aval. La rivière à débit réduit est incompétente pour éroder son chenal et,

actuellement, le chenal en aval du réservoir présente, hors les tronçons à forte intervention humaine, des formes qui sont une relique d'un environnement fluvial créé dans le passé dans de conditions d'énergie plus élevée.

Finalement, les résultats de l'analyse du paysage fluvial indiquent que le changement le plus significatif est lié à la contraction de la plaine d'inondation active face à la progression des activités agricoles ; ce dernier processus étant fortement lié à la suppression de crues. Une tendance générale à la progression de végétation ligneuse dans le lit mineur a été également observée, notamment en amont du réservoir est dans les alentours du barrage. Plus en aval, les patrons de colonisation ligneuse sont plus fortement influencés par la morphologie du chenal (étroite et profonde), ce qui empêche la croissance d'arbres dans le lit mineur, et par la stabilité fluviale, ce qui implique l'absence de création de nouvelles zones propices à l'établissement de la végétation .

5. CONCLUSIONS

Ce travail de thèse fournit des informations originales et approfondies sur l'hydrologie, la morphologie et les patrons thermiques de la rivière Sauce Grande en amont et en aval du barrage-réservoir Paso de las Piedras. Les connaissances climatiques, hydrologiques et morphologiques produites par cette étude ont une double application. Premièrement, elles informent les organismes de gestion des eaux sur le comportement complexe du système fluvial et sur les impacts de l'exploitation du réservoir dans le temps. Les résultats de cette recherche et les données produites pour l'analyse sont mis à disposition des gestionnaires du barrage afin de contribuer à l'établissement de pratiques de gestion du réservoir qui maintiennent l'intégrité du système fluvial sans compromettre la fonction vitale du barrage. Deuxièmement, cette étude fournit une plate-forme scientifique robuste sur laquelle fonder des efforts de recherche interdisciplinaire visant à la restauration de la rivière.

Fournir des propositions de restauration fluviale est bien au-delà de la portée de cette recherche. Actuellement, la plupart d'efforts scientifiques et gouvernementaux à l'échelle internationale sont dirigés vers l'évaluation des avantages et des désavantages de la proposition de nouvelles politiques de gestion des barrages (voire leur suppression dans certains cas extrêmes) pour restaurer l'intégrité écologique et hydrologique des systèmes fluviaux régulés. Cependant, ces actions ne sont pas une option réaliste concernant le barrage-réservoir Paso de las Piedras en raison de sa fonction vitale pour l'approvisionnement en eau potable. D'autre part, la régulation hydrologique induite par les barrages pour l'approvisionnement en eau dans des régions semi-arides constitue la plus grande menace pour l'intégrité écologique des systèmes fluviaux en aval. La solution est donc complexe et les mesures de restauration fluviale nécessitent une recherche interdisciplinaire qui réconcilie le conflit habituel entre les besoins humains et écologiques des ressources en eau, autant sur le plan scientifique que de la gestion.

La presente investigación evalúa el grado en que el dique-embalse Paso de las Piedras ha interrumpido la continuidad hidrológica del río Sauce Grande y cuantifica los impactos de la regulación hidrológica sobre el régimen de caudal, la morfología y la temperatura del agua del río aguas abajo del embalse. El trabajo de tesis presenta una evaluación integral y sistémica de los impactos del dique-embalse basada en el entendimiento de los procesos fluviales que ocurren aguas arriba del mismo. Además de proveer información sobre los impactos hidrológicos, morfológicos y térmicos de la construcción y operación del dique-embalse, este estudio genera nuevas series de datos climáticos e hidrológicos que proporcionan una importante plataforma sobre la cual basar futuras investigaciones de la cuenca del Sauce Grande. Por otra parte, este estudio implementa un marco metodológico aplicado al análisis hidro-geomorfológico de cuencas no aforadas que tiene un gran potencial de aplicación en otras cuencas de la región y en otras regiones semiáridas del mundo.

1. JUSTIFICACIÓN DEL ESTUDIO

El presente estudio evalúa los efectos hidrológicos, térmicos y morfológicos del dique-embalse Paso de las Piedras sobre el río Sauce Grande aguas abajo del mismo. Localizados en la llanura pampeana, Argentina, en el suroeste de la provincia de Buenos Aires, el río y el embalse constituyen uno de los recursos de agua dulce más importantes de la región (Borromei, 1991; Zavala y Quattrocchio, 2001; Schefer, 2004).

A pesar de que el clima regional es de tipo templado sub-húmedo (Campo *et al.*, 2004), la variabilidad interanual de las precipitaciones es alta y vinculada a fenómenos atmosféricos a gran escala como El Niño-Oscilación del Sur (ENOS) y anomalías en la circulación atmosférica dentro de la Zona de Convergencia del Atlántico Sur (Scian, 2000; Labraga *et al.*, 2002; Scian *et al.*, 2006). Los episodios de sequía (o inundación) son frecuentes (Campo *et al.*, 2009; Bohn *et al.*, 2011) e impactan seriamente en la economía regional (Troha y Forte Lay, 1993; Andrade *et al.*, 2009).

La región ha conocido periódicamente deficiencias cualitativas y cuantitativas en el abastecimiento de agua potable (Andrés *et al.*, 2009). La recurrencia de sequías y el aumento de la demanda de agua posterior al crecimiento de la población condujeron a una serie de crisis hídricas que, a su vez, se transfirieron en avances sistemáticos para las prácticas locales de gestión del agua.

El dique Paso de las Piedras embalsa la sección media del río Sauce Grande desde 1978 para suministro de agua potable. La demanda concierne una población que hoy alcanza aproximadamente los 350.000 habitantes concentrados principalmente en las ciudades de Bahía Blanca y Punta Alta. A máxima capacidad, el embalse tiene una superficie de 36 km², una profundidad de 25 metros y una capacidad de almacenamiento activo de 328 hm³ (Schefer, 2004). La variabilidad climática y el crecimiento demográfico se combinan para generar alta vulnerabilidad de los recursos hídricos locales frente al déficit hídrico; en consecuencia, los procedimientos de gestión del dique-embalse

tienden a maximizar el almacenamiento y la conservación del máximo volumen de agua posible dentro del embalse para asegurar el abastecimiento de agua potable en períodos de sequía.

Pese a la importancia regional del río Sauce Grande como principal fuente de abastecimiento de agua potable y la gran capacidad del embalse Paso de las Piedras, tanto la hidrología de la cuenca como los efectos de la represa sobre el ambiente fluvial han sido muy poco evaluados. La falta de conocimiento integrado sobre el comportamiento complejo de los recursos hídricos locales se ha hecho evidente en los últimos años debido a los efectos dramáticos de eventos climáticos extremos. Series de episodios de sequía e inundación repercutieron gravemente sobre la relación entre el uso del agua y el agua disponible para uso, poniendo en tela de juicio las prácticas de gestión hídrica. A la fecha, la demanda de agua supera la capacidad de oferta del embalse y, por lo tanto, el dique y su entorno revisten especial atención regional.

Este estudio proporciona la primera evaluación (i) de la hidrología del embalse Paso de las Piedras, (ii) del grado de regulación hidrológica inducida por la represa y, (iii) de los efectos de tal regulación sobre la hidrología, la morfología y la temperatura del agua del río Sauce Grande aguas abajo del embalse. Además de proporcionar nueva información sobre patrones de respuesta y ajuste de ríos regulados y sobre los efectos del dique Paso de las Piedras sobre el río Sauce Grande en concreto, este estudio genera nuevas series de datos climáticos e hidrológicos y pone en práctica un marco metodológico aplicado al análisis hidrológico de cuencas no aforadas. La nueva información climática, hidrológica y morfológica contenida en la presente investigación es aplicable en un triple marco:

- (i) informa a los organismos de gestión del dique acerca del comportamiento complejo del sistema fluvial,
- (ii) contribuye a mejorar las políticas de gestión del embalse respetando la integridad general del sistema fluvial y,
- (iii) proporciona una plataforma científica consistente sobre la cual basar nuevos esfuerzos de investigación interdisciplinaria que conduzcan a propuestas de restauración fluvial.

2. MARCO TEÓRICO

Los sistemas fluviales existen como un continuo de procesos físicos y biológicos interrelacionados (Vannote *et al.*, 1980) que dependen de transferencias longitudinales, laterales y verticales de energía, materia y biota (Petts y Amoros, 1996). A pesar del valor indiscutible de las represas para la gestión de recursos hídricos (Magilligan y Nislow, 2005; Petts y Gurnell, 2005), la construcción y operación de diques y embalses altera fuertemente la continuidad longitudinal de los procesos fluviales a lo largo del río (Petts, 1984) provocando discontinuidades en serie en el continuo fluvial (Ward y Stanford, 1983; 1995a; Stanford y Ward, 2001).

La preocupación científica internacional por los impactos de represas sobre sistemas fluviales ha crecido tanto como la construcción de represas se incrementó en el mundo

(Brandt, 2000). Los trabajos de Graff (2005) y de Petts y Gurnell (2005), por ejemplo, proporcionan una revisión exhaustiva de los avances en el entendimiento científico de los efectos de represas sobre sistemas fluviales aguas debajo de las mismas. En la actualidad, la bibliografía especializada en impacto hidrológico, geomorfológico y ecológico es abundante y el número de estudios en los que se basó esta investigación es demasiado elevado como para ser citado en este epígrafe.

Este estudio se basa claramente en el concepto de discontinuidad (Ward y Stanford, 1983, 1995a; Stanford y Ward, 2001) y se inspira fuertemente en la obra de Petts (1979, 1984) y la idea de órdenes de respuesta fluvial a disrupciones en el equilibrio de los procesos fluviales (Schumm, 1969). La base conceptual de esta investigación puede simplificarse en una serie de procesos de causa-efecto. En su estado natural, los ríos son sistemas tridimensionales en equilibrio dinámico dependiente de controladores climáticos, topográficos y geológicos a la escala de la cuenca. El embalse de ríos por represas representa la mayor fuente de disrupción hidrológica inducida por actividades humanas. La retención de agua y sedimento en embalses modifica tres elementos críticos del sistema fluvial aguas abajo:

- (i) la capacidad del río para transportar sedimentos,
- (ii) la cantidad de sedimento disponible para transporte y,
- (iii) la calidad de las aguas corrientes.

En conjunto, estas transformaciones desencadenan una serie de ajustes fluviales que se prolongarán en el tiempo hasta que el sistema fluvial se acomode a la perturbación o hasta que alcance un nuevo estado de equilibrio.

Estudios sobre ríos regulados del mundo documentaron una amplia gama de ajustes morfológicos y ecológicos en respuesta a la alteración hidrológica. Tales cambios incluyen cambios en la geometría del cauce (forma de la sección transversal, forma en planta y pendiente), cambios en la diversidad y los patrones de sucesión de las comunidades vegetales y cambios en la estructura y función de los organismos acuáticos. Sin embargo, la dirección, magnitud, frecuencia temporal y extensión espacial de los cambios fluviales puede variar sustancialmente de un río regulado a otro.

La respuesta fluvial a la construcción de represas aguas arriba es compleja y depende de un gran número de factores relacionados con el tamaño de la represa, el propósito de la misma, la historia de gestión de los recursos hídricos y del entorno ambiental del sistema fluvial que impone una mayor o menor resistencia al cambio. Citando a Phillips (2003b), la única generalización aceptada es que *los efectos de las represas son generalmente significativos y con frecuencia extensivos y varían de un río a otro, con el tiempo y con la distancia aguas abajo.*

3. CONTEXTO DE INVESTIGACIÓN

3.1. Objetivos principales

Esta investigación se fundamenta en un doble propósito. Primero, responde a la

necesidad de realizar una evaluación integrada de la hidrología del embalse Paso de las Piedras y de los efectos de la regulación hidrológica inducida por el mismo sobre el río Sauce Grande aguas abajo. Segundo, a la necesidad de generar series de datos climáticos e hidrológicos para análisis hidrológico a la escala de la cuenca en sí misma, del corredor fluvial y de la represa.

Por lo expuesto, el objetivo general del trabajo de tesis consiste en evaluar el grado de regulación hidrológica inducida por el dique-embalse Paso de las Piedras sobre la sección media del río Sauce Grande y en cuantificar sus impactos sobre el régimen de caudal, la temperatura del agua y la morfología del río aguas abajo. Un segundo objetivo es generar datos de base que permitan evaluar las variaciones espacio-temporales de los procesos hidrológicos con precisión.

3.2. Hipótesis

La respuesta del río Sauce Grande a la regulación hidrológica inducida por el dique-embalse Paso de las Piedras es evaluada asumiendo:

- (iv) condiciones climáticas de tipo sub-húmedo a semiárido con fuertes variaciones anuales e interanuales en el agua disponible para procesos de escorrentía y almacenamiento,
- (v) un continuo fluvial con tres secciones bien definidas a lo largo del curso del río,
- (vi) una interrupción del continuo fluvial por embalse de la sección media,
- (vii) un embalse con gran capacidad de almacenamiento en relación con la magnitud hidrológica de los flujos de entrada, térmicamente estratificado y con un potencial de retención de sedimentos mayor que el 99 %.

Sobre la base de estos supuestos, la hipótesis a probar en la presente investigación establece que el dique-embalse Paso de las Piedras interrumpe fuertemente la continuidad hidrológica del río Sauce Grande debido a prácticas de gestión del embalse que maximizan el almacenamiento de agua para garantizar el suministro en épocas de sequía.

En periodos de sequía, que son recurrentes y están relacionados con el fenómeno ENOS, la frecuencia y la magnitud de crecidas y avenidas aguas abajo se reducen significativamente. Los impactos de la regulación hidrológica incluyen (i) la alteración de la calidad del agua por una mayor influencia de aguas subterráneas, (ii) la reducción de la capacidad del cauce por fenómenos de deposición de sedimento y crecimiento de vegetación en el cauce principal y (iii) la desconexión entre el cauce principal y la llanura de inundación.

En períodos húmedos, la frecuencia y la magnitud de crecidas y avenidas aguas abajo se incrementan y los ajustes fluviales cambian de dirección. Los impactos de la regulación hidrológica incluyen (i) la alteración de la calidad del agua por liberación de flujo de fondo, (ii) el incremento de la capacidad del cauce por procesos de erosión vertical y/o lateral y remoción de la vegetación y (iii) el reestablecimiento de la conectividad entre el cauce y la llanura de inundación.

3.3. Métodos

La mayor limitación para llevar a cabo esta investigación fue la discontinuidad de datos climáticos e hidrológicos y la consiguiente falta de conocimiento pre-existente sobre la complejidad de procesos hídricos que tienen lugar dentro de la cuenca. Por lo tanto, el marco metodológico implementado dentro del presente estudio combina un conjunto de métodos utilizados para la generación de datos y un conjunto de métodos utilizados para la evaluación de las transformaciones hidrológicas, térmicas y morfológicas del río aguas abajo del embalse.

1. Este estudio desarrolla e implementa un modelo hidrológico de la cuenca superior basado en relaciones empíricas simples entre topografía, precipitación y escorrentía. A pesar de que la aplicación del modelo a otras cuencas no aforadas requiere ser evaluada y a pesar de que las variables utilizadas en la simulación de caudal requieren incorporar procesos hidrogeológicos, los resultados demostraron que el modelo tiene un gran potencial para generar datos de caudal, especialmente en regiones semiáridas.
2. Los impactos hidrológicos, térmicos y morfológicos del embalse fueron evaluados sobre la base del entendimiento previo del grado de regulación hidrológica inducida por el dique-embalse. Se evaluó el balance hidrológico del embalse para predecir variaciones en el almacenamiento de agua (descensos e incrementos) y se desarrolló un modelo hidrológico como herramienta de gestión. El modelo hidrológico permitió (i) estimar cualquier componente hidrológico a partir de las relaciones entre los componentes restantes, (ii) cuantificar las relaciones entre almacenamiento, rendimiento y liberación de aguas y (iii) estimar el potencial de regulación hidrológica en relación con la capacidad del embalse y el rendimiento del mismo para cumplir con los requerimientos de suministro de agua. En este sentido, el modelo tiene gran utilidad como herramienta de evaluación desde una perspectiva tanto científica como de gestión hídrica.
3. Los impactos hidrológicos de la gestión del dique en el tiempo se evaluaron mediante el uso del paquete metodológico incluido dentro del programa Indicators of Hydrological Alteration (IHA). IHA es una de las metodologías más adecuada para evaluar la alteración hidrológica de ríos regulados y tiene un gran potencial para cuantificar los impactos de represas y otras obras de gestión de aguas.

Además, este estudio evaluó la aplicación de dos enfoques novedosos al análisis de la temperatura del agua: una clasificación jerárquica basada en la forma y la variación temporal de regímenes de temperatura (RSMC) y un Índice de Sensibilidad climática de los mismos (SI). Combinados, estos enfoques proporcionaron información sustancial sobre la estabilidad temporal, la sensibilidad climática y la variabilidad espacial de los regímenes diurnos de temperatura del agua.

4. Finalmente, este estudio proporciona una nueva expresión de la gran utilidad de los SIG para el análisis cronológico de cambio geomorfológico y de la vegetación. El análisis se basó en la interpretación de fotografías aéreas (ortorectificadas) e imágenes satelitales de alta resolución (Ikonos) para tres pasos temporales: 1961 (periodo de pre-impacto), 1981 (3 años luego del impacto) y 2004 (26 años luego

del impacto). La cuantificación de cambios se realizó por superposición de mapas entre pasos de tiempo.

4. PRINCIPALES RESULTADOS

La secuencia lógica de causalidad entre variables de impacto y de respuesta fluvial puede ser resumida como sigue:

La represa interrumpe la continuidad longitudinal de los procesos fluviales → ello altera la hidrología general del río aguas abajo → el cauce del río y la llanura de inundación se transforman en respuesta a la alteración hidrológica.

En consecuencia, los resultados del presente estudio se articulan en tres capítulos que prueban cada parte de la secuencia por separado (Capítulos 3 a 5).

Capítulo 3

El Capítulo 3 cuantifica el grado de regulación hidrológica inducido por la represa sobre la base del entendimiento previo del balance hidrológico del embalse. Los resultados revelaron que el funcionamiento del sistema hídrico es único, complejo e imprevisible. Los flujos de entrada al embalse son influenciados por condiciones climáticas fluctuantes, ya sea a lo largo del año o a lo largo de varios años. Estas fluctuaciones están fuertemente relacionadas con el fenómeno ENOS y con otros fenómenos atmosféricos a gran escala altamente impredecibles. Por otro lado, los flujos de salida están limitados por la función de la represa para abastecimiento de agua potable; grandes volúmenes de agua son erogados cada año (73 % de la escorrentía media anual) y el volumen restante se conserva en el embalse para períodos de sequía. La capacidad de almacenamiento del embalse es casi cuatro veces el volumen medio de escorrentía anual, lo que indica el gran potencial de la represa para absorber toda la gama de flujos de entrada y la mayoría de los sedimentos transportados desde las zonas de cabecera. Finalmente, los resultados demostraron que la evacuación de flujo aguas abajo es muy poco probable que ocurra y que, de producirse, la fracción de agua disponible para liberar aguas abajo luego de que las necesidades anuales de aprovisionamiento de agua se cumplan es sólo del 27 % de la escorrentía media anual.

Capítulo 4

El Capítulo 4 evalúa los impactos fluviales de primer orden, a saber, los cambios que se produjeron inmediatamente después de la construcción de la represa y que dependen directamente de los procedimientos de gestión hídrica. El análisis se centra en dos de los tres cambios principales reconocidos por Petts (1984), a saber, los cambios en el régimen de caudal y en la calidad del agua. Respecto a éste último, este estudio se centra en el régimen térmico del río.

Los resultados indicaron que los patrones de regulación de caudal han afectado gravemente el caudal del río y la calidad general de las aguas por debajo del embalse. La dirección y la magnitud de los cambios hidrológicos y térmicos fueron similares a

aquéllas documentados en otros ríos regulados de regiones templadas del mundo, aunque la magnitud del cambio hidrológico fue sensiblemente mayor que la documentada en otros lugares. Las avenidas fueron completamente eliminadas y la magnitud y la frecuencia de crecidas se redujeron drásticamente con un aumento sustancial de la duración de condiciones de caudal similares. En conjunto, estos cambios contribuyeron a modificar la estacionalidad anual del régimen de caudal incluyendo supresión de los picos de verano, reducción de los picos de primavera y aumento de los caudales mínimos de invierno.

Por otra parte, la temperatura del agua fue disminuida durante el verano e incrementada durante el invierno y las fluctuaciones diurnas fueron alteradas sustancialmente tanto en magnitud como en momento. Si bien durante el período de observación no se produjo erogación de caudal aguas abajo, los patrones de temperatura del agua del río aguas abajo fueron invertidos en relación con el río no regulado aguas arriba. La inversión térmica a lo largo del curso del río responde a dos efectos paralelos inducidos por la represa: (i) cambios en la carga de calor debido a los aportes provenientes de filtraciones del embalse y (ii) cambios en la capacidad térmica de la corriente debido a la reducción de caudal.

Capítulo 5

Por último, el Capítulo 5 evalúa los impactos de represas de segundo orden, es decir, la respuesta de la morfología del cauce y la llanura de inundación a la alteración de los patrones de caudal y sedimento. Aguas abajo del embalse, el caudal fue reducido fuertemente en magnitud y alterado drásticamente en términos de frecuencia, momento, duración y variación anual. Reducción de caudal y supresión de avenidas se combinan con la retención de sedimentos en el embalse (asumida como mayor que el 99 % de la carga aportada por las cabeceras) para generar cambios sustanciales en el equilibrio fluvial aguas abajo. Ambos factores de control clave, caudal y sedimento, se redujeron drásticamente; sin embargo, la disminución de caudal fue tal que la reducción de la capacidad de la corriente para el transporte de sedimentos se asume mayor que la reducción en la cantidad de sedimento disponible para transporte.

Los modelos cualitativos de respuesta geomorfológica a la reducción extrema de caudal predicen (i) una reducción de la capacidad del cauce debido a procesos de agradación vertical y lateral e invasión de vegetación sobre bancos e islas, (ii) una reducción de la migración lateral del cauce y (iii) una interrupción de la conectividad entre el cauce y la llanura de inundación. En oposición a lo que se esperaba, los resultados de análisis geomorfológico no revelaron cambios significativos desde la inauguración de la represa.

Los cambios laterales y verticales del cauce guardan más relación con la intervención humana para facilitar la evacuación de las erogaciones que con ajustes naturales en respuesta a una reducción de caudal y sedimento (por ejemplo, incisión / deposición y estrechamiento). Se midió deposición de sedimento muy fino en el lecho sobre ambos, rápidos y mojados, aunque las tasas de deposición son insignificantes en comparación con las documentadas en la literatura. Series de perfiles transversales mostraron una alta estabilidad a lo largo de todo el tramo del río estudiado. La contracción del cauce se infirió en cierta medida por el crecimiento abundante de la vegetación en el lecho menor, aunque la posición en planta de los bancos se mantuvo sin cambios durante los

tres intervalos de tiempo utilizados en fotointerpretación.

Estos hallazgos indican claramente que el dique indujo una fuerte estabilidad geomorfológica aguas abajo del mismo. La corriente reducida, aun sin carga sedimentaria, es incompetente para erosionar el cauce. En la actualidad, el río aguas abajo exhibe una corriente ligeramente agradacional y fuertemente alterada, donde la morfología del cauce es una reliquia de un ambiente fluvial creado en el pasado en condiciones de mayor energía.

Finalmente, los resultados indicaron que el cambio más significativo en el paisaje fluvial se relaciona con la contracción de la zona inundable activa debido a la progresión de actividades agrícolas sobre la llanura de inundación; este último proceso guarda una fuerte relación con la eliminación de crecidas e inundaciones. También se observó una tendencia general a la progresión de árboles dentro del cauce principal, aunque este proceso fue comparativamente menos significativo que el observado aguas arriba y se restringió al cauce lindante con la represa. Aguas abajo, los patrones de colonización leñosa son restringidos por la morfología del cauce (estrecho y profundo), lo cual impide el establecimiento de árboles y por la estabilidad general del cauce, lo cual implica la falta de creación de zonas adecuadas para el establecimiento de nueva vegetación.

5. CONCLUSIONES

El presente estudio proporciona información original y consistente sobre la hidrología, la morfología y los patrones térmicos del río Sauce Grande aguas arriba y aguas abajo del dique-embalse Paso de las Piedras. Los contenidos climáticos, hidrológicos y morfológicos generados en esta tesis poseen doble aplicabilidad. En primer lugar, este estudio informa a los organismos de gestión hídrica sobre el comportamiento complejo del sistema fluvial y sobre el impacto a gran escala de la operación del embalse en el tiempo. Los resultados de esta investigación y los datos generados para el análisis se ponen a disposición de los gestores del dique para contribuir al planeamiento de prácticas de gestión del embalse que mantengan la integridad del sistema fluvial sin comprometer la función vital de la represa. En segundo lugar, este estudio proporciona una plataforma científica coherente y consistente sobre la cual basar futuros esfuerzos de investigación interdisciplinaria orientados a la restauración fluvial.

Las propuestas de restauración fluvial están más allá del propósito de esta investigación. En la actualidad, la mayoría de los esfuerzos científicos y gubernamentales a escala mundial se orientan a evaluar los costos y los beneficios de los cambios de políticas de gestión de represas (o incluso la remoción de diques) para restaurar la integridad hidrológica y ecológica de sistemas fluviales regulados. Sin embargo, estas acciones no son una opción viable para el dique-embalse Paso de las Piedras debido a su propósito vital para abastecimiento de agua potable. Por otra parte, los patrones de regulación de caudal ejercidos por diques para suministro de agua en regiones semiáridas representan la mayor amenaza para la integridad ecológica de los sistemas regulados. La solución es entonces compleja y las medidas de restauración fluvial requieren de investigaciones interdisciplinarias que concilien el conflicto habitual entre las necesidades ecológicas y

humanas de agua dulce, tanto desde una perspectiva científica como de gestión del recurso hídrico.

- Aceituno P., 1988. On the functioning of the Southern Oscillation in the South American sector. Part I: Surface climate, *Monthly Weather Review*, 116:505-524.
- Aduriz M. A., Gargano A. O., Chimeno P., Saldungaray M. C., Conti V. P., 2003. Caracterización de los agrosistemas predominantes de la cuenca del río Sauce Grande, *RIA*, 32:3-26.
- Ahmadi Nedushan B., St Hilaire A., Ouarda T. B. M. J., Bilodeau L., Robichaud E., Thiémonge N., Bobée B., 2007. Predicting river water temperatures using stochastic models: case study of the Moisie River (Québec, Canada), *Hydrological Processes*, 21:21-34.
- Almeira G., Scian B., 2006. Some atmospheric and oceanic indices as predictors of seasonal rainfall in the Del Plata Basin of Argentina, *Journal of Hydrology*, 329:350-359.
- Anderson A. M., 1989. *Predicted effects of flow regulation on the Oldman River zoobenthos*, Report 0070z, Alberta Environment, Environmental Assessment Division, Alberta, 32 p.
- Andrade M. I., Laporta P., Iezzi L., 2009. Sequías en el Sudoeste Bonaerense: vulnerabilidad e incertidumbre, *Geograficando*, 5:213-231.
- André H., Audinet M., Mazeran G., Richer C., 1976. *Hydrométrie pratique des cours d'eau*, Eyrolles, Paris, 259 p.
- Andreoli R. V., Kayano M. T., 2005. ENSO-related rainfall anomalies in South America and associated circulation features during warm and cold Pacific decadal oscillation regimes, *International Journal of Climatology*, 25:2017-2030.
- Andrés F., Bambill E., Bandoni A., Campaña H., Carrica J., Cifuentes O., Parodi E. R., Piccolo M. C., Poggio J., Varela H., Schefer J. C., 2009. *Informe técnico sobre aspectos relevantes de la problemática del agua en la región de Bahía Blanca*, Technical report of the Universidad Tecnológica Nacional - Universidad Nacional del Sur, Bahía Blanca, 41 p.
- Andrews E. D., 1986. Downstream effects of Flaming Gorge Reservoir on the Green River, Colorado and Utah, *Geological Society of America Bulletin*, 97:1012-1028.
- Angilletta M. J., Steel E. A., Bartz K. K., Kingsolver J. G., Scheuerell M. D., Beckman B. R., Crozier L. G., 2008. Big dams and salmon evolution: changes in thermal regimes and their potential evolutionary consequences, *Evolutionary Applications*, 1:286-299.
- Arcement G. J., Schneider V. R., 1989. *Guide for selecting Manning's roughness coefficients for natural channels and flood plains*, USGS Water-supply Paper 2339, 67 p.

- Archer D., 2008. The influence of river regulation at Kielder Water on the thermal regime of the River North Tyne, *Proceedings of the BHS 10th National Hydrology Symposium*, Exeter, 35-41.
- Arthington A. H., Zalucki J. M., 1998. *Comparative evaluation of environmental flow assessment techniques: review of methods*, Land and Water Resources Research and Development Corporation, Canberra, 149 p.
- Aspinall R., Pearson D., 2000. Integrated geographical assessment of environmental condition in water catchments: linking landscape ecology, environmental modelling and GIS, *Journal of Environmental Management*, 59:299-319.
- Assani A., Petit F., 2004. Impact of hydroelectric power releases on the morphology and sedimentology of the bed of the Warche River (Belgium), *Earth Surface Processes and Landforms*, 29:133-143.
- Assani A., Tardif S., 2005. Classification, caractérisation et facteurs de variabilité spatiale des régimes hydrologiques naturels au Québec (Canada). Approche éco-géographique, *Revue des Sciences de l'Eau*, 18:247-266.
- Auge M., 2004. *Regiones hidrogeológicas de la Republica Argentina y provincias de Buenos Aires, Mendoza y Santa Fe*, Universidad de Buenos Aires, La Plata, Argentina, 111 p.
- Barrera M. D., Frangi J. L., 1997. Modelo de estados y transiciones de la arbustificación de pastizales de Sierra de la Ventana, Argentina, *Ecotrópicos*, 10:161-166.
- Barros V., Doyle M. E., 2002. Midsummer low-level circulation and precipitation in subtropical South America and related sea surface temperature anomalies in the South Atlantic, *Journal of Climate*, 15:3394-3410.
- Barros V., Gonzalez M., Liebmann B., Camilloni I., 2000. Influence of the South Atlantic Convergence Zone and South Atlantic Sea surface temperature on inter-annual summer rainfall variability in Southeastern South America, *Theoretical and Applied Climatology*, 67:123-133.
- Barrucand M. G., Vargas W. M., Rusticucci M. M., 2007. Dry conditions over Argentina and the related monthly circulation patterns, *Meteorology and Atmospheric Physics*, 98:99-114.
- Batalla R. J., Gomez C. M., Kondolf G. M., 2004. Reservoir-induced hydrological changes in the Ebro River basin (NE Spain), *Journal of Hydrology*, 290:117-136.
- Beauger A., 2012. *The impacts of Paso de las Piedras Dam on the distribution of benthic diatoms along the Sauce Grande River*, Technical Report, GEOLAB UMR 6042, CNRS - Université Blaise Pascal, Clermont-Ferrand, 6 p.
- Benn P. C., Erskine W. D., 1994. Complex channel response to flow regulation: Cudgegong River below Windamere Dam, Australia, *Applied Geography*, 14:153-168.
- Bennett N. D., Newham L. T. H., Croke B. F. W., Jakeman A. J., 2007. Patching and disaccumulation of rainfall data for hydrological modelling, *Proceedings of the International Congress on Modelling and Simulation New Zealand*, 2520-2526.

- Beven K. J., 2001. *Rainfall-runoff modelling: the primer*, Wiley, Chichester, UK, 377 p.
- Beven K. J., Kirkby M. J., 1979. A physically based, variable contributing area model of basin hydrology, 24:43-69.
- Blanchon D., Bravard J.-P., 2007. La stabilité des formes fluviales de l'Orange, entre variabilité naturelle et impacts des grands barrages (secteur Boegoeberg-Augrabies, Afrique du Sud), *Géographie physique et Quaternaire*, 61:21-37.
- Boehrer B., Schultze M., 2008. Stratification of lakes, *Reviews of Geophysics*, 46:1-27.
- Bohn V. Y., Piccolo M. C., Perillo G. M. E., 2011. Análisis de los periodos secos y húmedos en el sudoeste de la provincia de Buenos Aires (Argentina), *Revista de Climatología*, 11:31-43.
- Bonacci O., Trninić D., Roje Bonacci T., 2008. Analysis of the water temperature regime of the Danube and its tributaries in Croatia, *Hydrological Processes*, 22:1014-1021.
- Boonstra J., 1994. Estimating peak runoff rates. In: Ritzema H. P. (Editor), *Drainage principles and applications*, IILRI - International Institute for Land Reclamation and Improvement, Wageningen, 111-144.
- Borromei A. M., 1991. Geología y palinología de los depósitos cuaternarios en el valle del río Sauce Grande. *Doctoral Thesis*, Universidad Nacional del Sur, Bahía Blanca, 199 p.
- Bower D., Hannah D. M., 2002. Spatial and temporal variability of UK river flow regimes, *Proceedings of the Fourth International FRIEND Conference*, Cape Town, South Africa, 457-464.
- Bower D., Hannah D. M., McGregor G. R., 2004. Techniques for assessing the climatic sensitivity of river flow regimes, *Hydrological Processes*, 18:2515-2543.
- Box G. E. P., Jenkins G. M., 1970. *Time series analysis: forecasting and control*, Holden-Day, San Francisco, 533 p.
- Brandt S. A., 2000. Classification of geomorphological effects downstream of dams, *Catena*, 40:375-401.
- Bravard J.-P., Petit F., 1997. *Les cours d'eau. Dynamique du système fluvial*, Armand Colin Masson, Paris, 222 p.
- Bravard J.-P., Piégay H., Héroin E., Ramez P., 1998. *Détermination de l'espace de liberté des cours d'eau*, Guide Technique N°2, SDAGE RHONE MEDITERRANEE CORSE, 42 p.
- Brea M., Zucol A. F., Mazzanti D., 2001. Determinación de combustibles vegetales en Cueva El Abra, provincia de Buenos Aires, *Arqueología Argentina en los Inicios de un Nuevo Siglo. Tomo 3, Cap. 31: Estado actual de las investigaciones arqueobotánicas*, Rosario, 693-697.
- Broadmedow S., Nisbet T. R., 2004. The effects of riparian forest management on the freshwater environment: a literature review of best management practice, *Hydrology and Earth System Sciences*, 8:286-305.

- Bruniard E. D., 1982. La diagonal árida argentina: un límite climático real (The Argentinian arid diagonal: a real climatic boundary), *Revista Geográfica del Instituto Panamericano de Geografía e Historia*, 95:5-20.
- Bull L. J., Kirkby M. J., 2002. *Dryland rivers. Hydrology and geomorphology of semi-arid channels*, John Wiley & Sons, Chichester, 398 p.
- Bunn S. E., Arthington A. H., 2002. Basic principles and ecological consequences of altered flow regimes for aquatic biodiversity, *Environmental Management*, 30:492–507.
- Bunn S. E., Thoms M. C., Hamilton S. K., Capon S. J., 2006. Flow variability in dryland rivers: boom, bust and the bits between, *River Research and Applications*, 22:179-186.
- Buraschi J., Bustinza J., Schmoll S., 1999. Evaluación del escurrimiento en la fundación del dique Paso de las Piedras, *Proceedings of the MECOM 99*, Mendoza, Argentina, 11.
- Burel F., Baudry J., 2000. *Ecologie du paysage. Concepts, méthodes et applications*, Tec & Doc, Paris, 355 p.
- Caissie D., 2006. The thermal regime of rivers: a review, *Freshwater Biology*, 51:1389-1406.
- Caissie D., Satish M. G., El Jabi N., 2005. Predicting river water temperatures using the equilibrium temperature concept with application on Miramichi River catchments (New Brunswick, Canada), *Hydrological Processes*, 19:2137-2159.
- Campo A. M., Capelli A., Diez P., 2004. *El clima del Suroeste bonaerense*, UNS, Bahía Blanca, 99 p.
- Campo A. M., Ramos M. B., Zapperi P., 2009. Análisis de las variaciones anuales de precipitación en el Suroeste bonaerense, Argentina, *Proceedings of the XII Encuentro de Geógrafos de América Latina*, Montevideo, Uruguay,
- Capelli de Steffens A., Campo A. M., 1994. *La transición climática en el sudoeste bonaerense*, SIGEO, Bahía Blanca, 75 p.
- Carrara A., Bitelli G., Carla R., 1997. Comparison of techniques for generating digital terrain models from contour lines, *International Journal of Geographical Information Science*, 11:451-473.
- Casado A., 2006. Modelo digital para la prevención de incendios forestales en el área de Villa Ventana. *Bachelor Thesis*, Universidad Nacional del Sur, Bahía Blanca, 120 p.
- Casado A., Gentili J., Campo A. M., Peiry J.-L., 2010. Evaluación de la calidad de modelos digitales de elevación derivados de curvas de nivel para aplicaciones hidrológicas, *Tecnologías de la Información Geográfica del sur argentino*, UNS, Bahía Blanca, 102-116.
- Casado A., Hannah D. M., Peiry J.-L., Campo A. M., 2013. Influence of dam-induced hydrological regulation on summer water temperature: Sauce Grande River, Argentina, *Ecohydrology*. Online. DOI: 10.1002/eco.1375

- Castañeda M., Gonzalez M., 2008. Statistical analysis of the precipitation trends in the Patagonia region in Southern South America, *Atmosfera*, 21:303-317.
- Chapman D., 1992. *Water Quality Assessments: A guide to the use of biota, sediments and water in environmental monitoring*, E & FN SPON, London, 653 p.
- Chen F.-W., Liu C.-W., 2012. Estimation of the spatial rainfall distribution using inverse distance weighting (IDW) in the middle of Taiwan, *Paddy and Water Environment*.
- Chien N., 1985. Changes in river regime after the construction of upstream reservoirs, *Earth Surface Processes and Landforms*, 10:143-159.
- Choi S., Yon B., Woo H., 2005. Effects of dam-induced flow regime change on downstream river morphology and vegetation cover in the Hwang River, Korea, *River Research and Applications*, 21:315-325.
- Chow V. T., 1994. *Hidrología aplicada*, McGraw-Hill Interamericana, Bogota, 584 p.
- Chu C., Jones N. E., Allin L., 2010. Linking the thermal regimes of streams in the Great Lakes Basin, Ontario, to landscape and climate variables, *River Research and Applications*, 26:221-241.
- Church M., 1992. Channel morphology and typology. In: Carlow P., Petts G. E. (Editors), *The River's Handbook*, Blackwell Science, Oxford, 126-143.
- Church M., 1995. Geomorphic response to river flow regulation: case studies and time scales, *Regulated Rivers: Research & Management*, 11:3-22.
- Church M., 2002. Geomorphic thresholds in riverine landscapes, *Freshwater Biology*, 47:541-557.
- Collier M., Webb R. H., Schmidt J. C., 1996. *Dams and rivers. A primer on the downstream effects of dams*, U.S. Geological Survey Circular 1126, 94 p.
- Cowx I. G., Young W. O., Booth P., 1987. Thermal characteristics of two regulated rivers in mid-Wales, U.K., *Regulated Rivers: Research & Management*, 1:85-91.
- Crisp D. T., 1987. Thermal 'Resetting' of Streams by Reservoir Releases with Special Reference to Effects on Salmonid Fishes *Regulated Streams: Advances in Ecology*, Plenum Press, New York, 163-182.
- Dallas H. F., Rivers Moore N. A., 2011. Micro-scale heterogeneity in water temperature, *Water S.A.*, 37:505-512.
- Del Cogliano D., Napal E., Di Croche N., Aldalur B., Napal P., De Aduris A., Martinez M., 1998. Topographic control with GPS, *International Society of Photogrammetry and Remote Sensing*, 32:142-147.
- Dettinger M. D., Diaz H. F., 2000. Global characteristics of stream flow seasonality and variability, *Journal of Hydrometeorology*, 1:289-310.
- Dijkstra H. A., 2006. The ENSO phenomenon: theory and mechanisms, *Advances in Geosciences*, 6:3-15.

- Downward S. R., Gurnell A. M., Brookes A., 1994. A methodology for quantifying river channel planform change using GIS, *Proceedings of the International Association of Hydrological Sciences Publication, Variability in Stream Erosion and Sediment Transport*, Canberra, 449-456.
- Droque G., Pfister L., Leviandier T., Humbert J., Hoffmann L., Idrissi A. E., Iffly J.-F., 2002. Using 3D dynamic cartography and hydrological modelling for linear streamflow mapping, *Computers & Geosciences*, 28:981-994.
- Dunne T., Leopold L. B., 1978. *Water in environmental planning*, W. H. Freeman & Co., San Francisco, 818 p.
- Duque C., Calvache M. L., Engesgaard P., 2010. Investigating river-aquifer relations using water temperature in an anthropized environment (Motril-Salobreña aquifer), *Journal of Hydrology*, 381:121-133.
- Echenique R., Ferrari L., González D., 2001. Cyanobacterial blooms in Paso de las Piedras Reservoir (Buenos Aires, Argentina), *Harmful Algae News*, 22:3.
- Echenique R., Giannuzzi L., Ferrari L., 2007. Drinking water: problems related to water supply in Bahía Blanca, Argentina, *Acta Toxicológica Argentina*, 14:23-30.
- Edouard J.-L., Vivian H., 1984. Une hydrologie naturelle dans les Alpes du Nord?, *Revue de Géographie Alpine*, 72:165-188.
- Endreny T. A., Wood E. F., Lettenmaier D. P., 2000. Satellite-derived digital elevation model accuracy: hydrogeomorphological analysis requirements, *Hydrological Processes*, 14:1-20.
- Erskine W. D., Warner R. F., 1998. Further assessment of flood- and drought-dominated regimes in south-eastern Australia, *Australian Geographer*, 29:257-261.
- Estrada V., Parodi E. R., Díaz M. S., 2002. Advances in simultaneous strategies for dynamic process optimization, *Chemical Engineering Science*, 57:575-593.
- Estrada V., Parodi E. R., Díaz M. S., 2008. A simultaneous dynamic optimization approach to address restoration policies in reservoirs, *Mecánica Computacional*, 27:301-308.
- Estrela T., Marcuello C., Iglesias A., 1996. *Water resources problems in Southern Europe*, Report of the European Topic Centre on Inland Waters, European Environment Agency, Copenhagen, 49 p.
- European Environmental Agency E., 1994. *CORINE Landcover Nomenclature*, Commission of the European Communities, 165 p.
- Feddema J. J., 2005. A revised Thornthwaite-type global climate classification, *Physical Geography*, 26:442-466.
- Felicísimo A. M., 1994. Modelos Digitales del Terreno. Introducción y aplicaciones en las ciencias ambientales, 122 p.
- Fergus T., 1997. Geomorphological response of a river regulated for hydropower: River Fortun, Norway, *Regulated Rivers: Research & Management*, 13:449-461.

- Fernández C., Parodi E. R., Cáceres E. J., 2009. Limnological characteristics and trophic state of Paso de las Piedras Reservoir: An inland reservoir in Argentina, *Lakes & Reservoirs: Research and Management*, 14:85-101.
- Fernández C., Parodi E. R., Cáceres E. J., 2011. Phytoplankton structure and diversity in the eutrophic-hypereutrophic reservoir Paso de las Piedras, Argentina, *Limnology*, Online. DOI 10.1007/s10201-011-0347-3.
- Fernández J. A., Martínez C., Magdaleno F., 2012. Application of indicators of hydrologic alterations in the designation of heavily modified water bodies in Spain, *Environmental Science and Policy*, 16:31-43.
- Ferrer F. J., 1993. *Recomendaciones para el cálculo hidrometeorológico de avenidas*, Ministerio de Obras Públicas, Madrid, 75 p.
- Ferrera I. M., Alamo M., 2010. La Problemática del agua en el sudoeste bonaerense: la ciudad de Bahía Blanca, *Proceedings of the III Congreso Pampeano del Agua*, Santa Rosa, Argentina, 191-199.
- Figini A. J., Carbonari J. E., Huarte R. A., 1990. Museo de la Plata radiocarbon measurements, *Radiocarbon*, 32:197-208.
- Fisher P. F., Tate N. J., 2006. Causes and consequences of error in digital elevation models, *Progress in Physical Geography*, 30:467-489.
- Forman R., 1995. *Land mosaics. The ecology of landscapes and regions*, Cambridge University Press, Cambridge, 605 p.
- Forman R., Godron M., 1986. *Landscape Ecology*, John Wiley & Sons, New York, 619 p.
- Forte Lay J., Scarpati O., Capriolo A., 2008. Precipitation variability and soil water content in Pampean Flatlands (Argentina), *Geofísica Internacional*, 47:341-354.
- Frangi J. L., Bottino O. J., 1995. Comunidades vegetales de Sierra de la Ventana, provincia de Buenos Aires, Argentina, *Revista de la Facultad de Agronomía*, 71:93-133.
- Friedman J. M., Osterkamp W. R., Scott M. L., Auble G. T., 1998. Downstream effects of dams on channel geometry and bottomland vegetation: Regional patterns in the Great Plains, *Wetlands*, 18:619-633.
- Frimpong E. A., Sutton T. M., Lim K. J., Hrodey P. J., Engel B. A., Simon T. P., Lee J. G., Master D. C. L., 2005. Determination of optimal riparian forest buffer dimensions for stream biota-landscape association models using multimetric and multivariate responses, *Canadian Journal of Fisheries and Aquatic Sciences*, 62:1-6.
- Fujihara M., Kikuchi T., 2005. Changes in the landscape structure of the Nagara River Basin, central Japan, *Landscape and Urban Planning*, 70:271-281.
- Gabella J. I., Zapperi P., Campo A. M., 2010. Distribución estacional de las precipitaciones en el Suroeste Bonaerense, *Proceedings of the VII Jornadas Nacionales de Geografía Física de la República Argentina*, Posadas, Argentina, 87-94.

- Gan M. A., Kousky V. E., Ropelewski C. F., 2004. The South America Monsoon circulation and its relationship to rainfall over west-central Brazil, *Journal of Climate*, 17:47-66.
- Gao J., 1997. Resolution and accuracy of terrain representation by grid DEMs at a micro-scale, *International Journal of Geographical Information Sciences*, 11:199-212.
- Garreaud R. D., Aceituno P., 2007. Atmospheric circulation and climatic variability. In: Veblen T. *et al.* (Editors), *The Physical Geography of South America*, Oxford University Press, Oxford, 45-66.
- Garreaud R. D., Vuille M., Compagnucci R., Marengo J. A., 2009. Present-day South American climate, *Palaeogeography, Palaeoclimatology, Palaeoecology*, 281:180-195.
- Gaspari F. J., Rodriguez Vagaría A. M., Sensiterra G. E., Delgado M. I., 2008. Determinación espacio-temporal del índice de agresividad de precipitaciones en el sistema serrano de Ventania. Provincia de Buenos Aires-Argentina, *Revista Geográfica Venezolana*, 49:57-66.
- Gil V., 2009. Hidrogeomorfología de la cuenca alta del río Sauce Grande aplicada al peligro de crecidas. *Doctoral Thesis*, Universidad Nacional del Sur, Bahía Blanca, 287 p.
- Gil V., Campo A. M., 2006. Caracterización morfológica sectorizada del río Sauce Grande, provincia de Buenos Aires, Argentina, *Revista Geográfica de Valparaíso*, 38:19-28.
- Gil V., Zapperi P., Campo A. M., Iuorno M. V., Ramborger M. A., 2008. Análisis de las precipitaciones de otoño y primavera en el Suroeste bonaerense, *Proceedings of the VII Jornadas de Geografía Física*, San Salvador de Jujuy, Argentina,
- Gilard O., Oberlin G., 1998. *Guide pratique de la méthode inondabilité*, Etude Inter-Agences N° 60, Agences de l'eau, 158 p p.
- Gilvear D. J., 2004. Patterns of channel adjustment to impoundment of the upper River Spey, Scotland (1942–2000), *River Research and Applications*, 20:151-165.
- Gilvear D. J., Bravard J.-P., 1996. Geomorphology of temperate rivers. In: Petts G., Amoros C. (Editors), *Fluvial Hydrosystems*, Chapman & Hall, London, 68-97.
- Gordon E., Meentemeyer R. K., 2006. Effects of dam operation and land use on stream channel morphology and riparian vegetation, *Geomorphology*, 82:412-429.
- Graf W. L., 1999. Dam Nation: a geographic census of American dams and their large-scale hydrologic impacts, *Water Resources Research*, 35:1305-1311.
- Graf W. L., 2005. Geomorphology and American dams: The scientific, social, and economic context, *Geomorphology*, 71:3-26.
- Graf W. L., 2006. Downstream hydrologic and geomorphic effects of large dams on American rivers, *Geomorphology*, 79:336-360.

- Grams P. E., Schmidt J. C., 2002. Streamflow regulation and multi-level flood plain formation: channel narrowing on the aggrading Green River in the eastern Uinta Mountains, Colorado and Utah, *Geomorphology*, 44:337-360.
- Gregory K. J., Park C., 1974. Adjustment of River Channel Capacity Downstream From a Reservoir, *Water Resources Research*, 10:870-873.
- Grimm A. M., 2011. Interannual climate variability in South America: impacts on seasonal precipitation, extreme events, and possible effects of climate change, *Stochastic Environmental Research and Risk Assessment* 25:537-554.
- Grimm A. M., Barros V., Doyle M. E., 2000. Climate variability in southern South America associated with El Niño and La Niña events, *Journal of Climate*, 13:35-58.
- Grimm A. M., Vera C. S., Mechoso C. R., 2005. The South American monsoon system. In: Chang C.-P. *et al.* (Editors), *The global monsoon system: research and forecast*, WMO/TD 1266-TMRP 70, 219–238.
- Grippio S. B., Visciarelli S. M., 2005. Inversiones en servicios públicos y dinámica del espacio urbano, *Scripta Nova*, 9:1-14.
- Groom J. D., Dent L., Madsen L. J., 2011. Stream temperature change detection for state and private forests in the Oregon Coast Range, *Water Resources Research*. Online. DOI: 10.1029/2009WR009061
- Güntner A., Krol M. S., de Araújo J. C., Bronstert A., 2004. Simple water balance modelling of surface reservoir systems in a large data-scarce semiarid region, *Hydrological Sciences Journal*, 49:901-918.
- Gumbel E. J., 1958. *Statistics of extremes*, Columbia University Press, New York, 375 p.
- Guttman N. B., 1999. Accepting the Standardized Precipitation Index: a calculation algorithm, *Journal of the American Water Resources Association*, 35:311-322.
- Haag I., Luce A., 2008. The integrated water balance and water temperature model LARSIM-WT, *Hydrological Processes*, 22:1046-1056.
- Haines A. T., Finlayson B. L., McMahon T. A., 1988. A global classification of river regimes, *Applied Geography*, 8:255-272.
- Hancock G. R., 2005. The use of digital elevation models in the identification and characterization of catchments over different grid scales, *Hydrological Processes*, 19:1727-1749.
- Hannah D. M., Kansakar S. R., Gerrard J., Rees G., 2005. Flow regimes of Himalayan rivers of Nepal: nature and spatial patterns, *Journal of Hydrology*, 308:18-32.
- Hannah D. M., Malcolm I. A., Bradley C., 2009. Seasonal hyporheic temperature dynamics over riffle bedforms, *Hydrological Processes*, 23:2178-2194.
- Hannah D. M., Malcolm I. A., Soulsby C., Youngson A. F., 2004. Heat exchanges and temperatures within a salmon spawning stream in the Cairngorms, Scotland: Seasonal and sub-seasonal dynamics, *River Research and Applications*, 20:635-652.

- Hannah D. M., Malcolm I. A., Soulsby C., Youngson A. F., 2008a. A comparison of forest and moorland stream microclimate, heat exchanges and thermal dynamics, *Hydrological Processes*, 22:919-940.
- Hannah D. M., Smith B. P. G., Gurnell A. M., McGregor G. R., 2000. An approach to hydrograph classification, *Hydrological Processes*, 14:317-338.
- Hannah D. M., Webb B. W., Nobilis F., 2008b. Preface: River and stream temperature: dynamics, processes, models and implications, *Hydrological Processes*, 22:899-901.
- Harrelson C. C., Rawlins C. L., Potyondy J. P., 1994. *Stream channel reference sites: an illustrated guide to field technique*, General Technical Report RM-245, United States Department of Agriculture - Forest Service, 67 p.
- Harris N. M., Gurnell A. M., Hannah D. M., Petts G. E., 2000. Classification of river regimes: a context for hydroecology, *Hydrological Processes*, 14:2831-2848
- Hengl T., Gruber S., Shrestha D., 2004. Reduction of errors in digital terrain parameters used in soil-landscape modelling, *International Journal of Applied Earth Observation*, 5:97-112.
- Hersh E. S., Maidment D. R., 2006. *Assessment of hydrologic alteration software*, TWDB Project #2005-483-029 - Final Report, Center for Research in Water Resources, University of Texas, Austin, USA, 114 p.
- Hilldale R. C., Raff D., 2008. Assessing the ability of airborne LiDAR to map river bathymetry, *Earth Surface Processes and Landforms*, 33:773-783.
- Hoff H., Swartz C., Tielborger K., Yates D. (Editors), 2007. Water management under extreme water scarcity: scenario analyses for the Jordan river basin, using WEAP21. Water saving in Mediterranean agriculture and future research needs. CIHEAM, Bari, 321-331.
- Holzman M. E., Rivas R. E., 2011. ENSO effects on hydric conditions of La Pampa Region: a preliminary evaluation using LST and EVI, *Proceedings of the XV Simposio Brasileiro de Sensoriamento Remoto*, Curitiba, Brasil, 2242-2249.
- Hossain M. M., Hossain M. J., 2011. Instream flow requirement of Dudhkumar River in Bangladesh, *Asian Transactions on Engineering*, 01:21-49. DOI: ATE-80109039
- Hupp C. R., Osterkamp W. R., 1996. Riparian vegetation and fluvial geomorphic processes, *Geomorphology*, 14:277-295.
- Hutchinson M. F., 1988. Calculation of hydrologically sound digital elevation models, *Proceedings of the Third International Symposium on Spatial Data Handling* Sidney, Australia, 117-133.
- Hutchinson M. F., 1989. A new procedure for gridding elevation and stream line data with automatic removal of spurious pits, *Journal of Hydrology*, 106:211-232.
- Hutchinson M. F., Dowling T. I., 1991. A continental hydrological assessment of a new grid-based digital elevation model of Australia, *Hydrological Processes*, 5:45-58.

- Ibrahim A. B., Cordery I., 1995. Estimation of recharge and runoff volumes from ungauged catchments in eastern Australia, *Hydrological Sciences*, 40:499-515.
- Islam N., Doscher C., Davies T., 2000. Estimating missing daily maximum and minimum temperatures for Mount Cook, South Island, New Zealand, using a statistical model and 'aiNet' neural network models, *Journal of Hydrology (NZ)*, 39:83-106.
- Jeffrey S. J., Carter J. O., Moodie K. B., Beswick A. R., 2001. Using spatial interpolation to construct a comprehensive archive of Australian climate data, *Environmental Modelling & Software*, 16:309-330.
- Johnson S. L., 2004. Factors influencing stream temperatures in small streams: substrate effects and a shading experiment, *Canadian Journal of Fisheries and Aquatic Sciences*, 61:913-923.
- Junk W. J., Bayley P. B., Sparks R. E., 1989. The flood pulse concept in river-floodplain systems, *Canadian Journal of Fisheries and Aquatic Sciences*, 106:110-127.
- Kansakar S. R., Hannah D. M., Gerrard J., Rees G., 2004. Spatial pattern in the precipitation regime of Nepal, *International Journal of Climatology*, 24:1645-1659.
- Kayano M. T., Andreoli R. V., 2007. Relations of South American summer rainfall inter-annual variations with the Pacific Decadal Oscillation, *International Journal of Climatology*, 27:531-540.
- Kemp W. P., Burnell D. G., Everson D. O., Thomson A. J., 1983. Estimating missing daily maximum and minimum temperatures, *Journal of Climate and Applied Meteorology*, 22:1587-1593.
- Kendall M., Dickinson Gibbons J., 1990. *Rank correlation methods (5th ed.)*, Oxford University Press, New York, 260 p.
- Kennard M. J., Pusey B. J., Olden J. D., MacKay S. J., Stein J. L., Marsh N., 2010. Classification of natural flow regimes in Australia to support environmental flow management, *Freshwater Biology*, 55:171-193.
- Kenward T., Lettenmaier D. P., Wood E. F., Fielding E., 2000. Effects of Digital Elevation Model Accuracy on Hydrologic Predictions, *Remote Sensing & Environment*, 74:432-444.
- Kerby W. S., 1959. Time of concentration for overland flow, *Civil Engineering*, 29:174.
- Kim S., Lee H., 2004. A digital elevation analysis: a spatially distributed flow apportioning algorithm, *Hydrological Processes*, 18:1777-1794.
- King J., Cambray J. A., Impson N. D., 1998. Linked effects of dam-released floods and water temperature on spawning of the Clanwilliam yellowfish *Barbus capensis*, *Hydrobiologia*, 384:245-265.
- Kirpich Z. P., 1940. Time of concentration of small agricultural watersheds, *Civil Engineering*, 10:362.

- Knighton A. D., 1977. Short-term changes in hydraulic geometry. In: Gregory J. K. (Editor), *River Channel Changes*, John Wiley & Sons, Chichester, 101-119.
- Knighton D., 1998. *Fluvial forms and processes. A new perspective*, Arnold, London, 383 p.
- Ko C., Cheng Q., 2004. GIS spatial modeling of river flow and precipitation in the Oak Ridges Moraine area, Ontario, *Computers & Geosciences*, 30:379-389.
- Koch H., Grünewald U., 2010. Regression models for daily stream temperature simulation: case studies for the river Elbe, Germany, *Hydrological Processes*. Online. DOI: 10.1002/hyp.7814
- Kondolf G. M., 1997. Hungry Water: Effects of Dams and Gravel Mining on River Channels, *Environmental Management*, 21:533-551.
- Kondolf G. M., Batalla R. J., 2005. Hydrological effects of dams and water diversions on rivers of Mediterranean-climate regions: examples from California. In: Garcia C., Batalla R. J. (Editors), *Catchment Dynamics and River Processes: Mediterranean and Other Climate Regions*, Elsevier, 197-211.
- Krasovskaia I., 1995. Quantification of the stability of river flow regimes, *Hydrological Sciences*, 40:587-598.
- Krasovskaia I., 1996. Sensitivity of the stability of river flow regimes to small fluctuations in temperature, *Hydrological Sciences*, 41:251-264.
- Krasovskaia I., Saelthun N. R., 1997. Sensitivity of the stability of Scandinavian river flow regimes to a predicted temperature rise, *Hydrological Sciences*, 42:693-711.
- Krause S., Hannah D. M., Blume T., 2011. Interstitial pore-water temperature dynamics across a pool-riffle-pool sequence, *Ecohydrology*, 4:549-563.
- Kruse E., Forte Lay J. A., Aiello J. L., Basualdo A., Heinzenknecht G., 2001. Hydrological processes on large flatlands: case study in the northwest region of Buenos Aires Province (Argentina), *Proceedings of the Remote Sensing and Hydrology Symposium*, Santa Fe, USA, 531-535.
- Kruse E., Laurencena P., 2005. Aguas superficiales. Relación con el régimen subterráneo y fenómenos de anegamiento, *Proceedings of the XVI Congreso Geológico Argentino*, La Plata, Argentina,
- Labraga J. C., Scian B., Frumento O., 2002. Anomalies in the atmospheric circulation associated with the rainfall excess or deficit in the Pampa Region in Argentina, *Journal of Geophysical Research*, 107:4666-4681.
- Lane E. W., 1955. The importance of fluvial morphology in hydraulic engineering, *Proceedings of the American Society of Civil Engineers*, 1-17.
- Lastra J., Fernández E., Díez Herrero A., Marquínez J., 2008. Flood hazard delineation combining geomorphological and hydrological methods: an example in the Northern Iberian Peninsula, *Natural Hazards*, 45:277-293.

- Lavis M. E., Smith K., 1972. Reservoir storage and the thermal regime of rivers, with special reference to the river Lune, Yorkshire, *The Science of The Total Environment*, 1:81-90.
- Lehmkuhl D. M., 1972. Change in thermal regime as a cause of reduction of benthic fauna downstream of a reservoir, *Journal Fisheries Research Board of Canada*, 29:1329-1332.
- Leigh C., Sheldon F., Kingsford R. T., Arthington A. H., 2010. Sequential floods drive 'booms' and wetland persistence in dryland rivers: a synthesis, *Marine & Freshwater Research*, 61:896-908.
- Leopold L. B., 1973. River channel change with time: an example, *Geological Society of America Bulletin*, 84:1845-1860.
- Leopold L. B., Wolman M. G., Miller J. P., 1964. *Fluvial processes in geomorphology*, W. H. Freeman and Co., San Francisco, 522 p.
- Liébault F., Gomez B., Page M., Marden M., Peacock D., Richard D., Trotter C., 2005. Land-use change, sediment production and channel response in upland regions, *River Research and Applications*, 21:739-756.
- Liébault F., Piégay H., 2001. Assessment of channel changes due to long-term bedload supply decrease, Roubion River, France, *Geomorphology*, 36:167-186.
- Liebmann B., Kiladis G. N., Marengo J. A., Ambrizzi T., Glick J. D., 1999. Submonthly convective variability over South America and the South Atlantic Convergence Zone, *Journal of Climate*, 12:1877-1891.
- Liebmann B., Vera C., Carvalho L. M. V., Camilloni I., Hoerling M. P., Barros V. R., Báez J., Bidegain M., 2004. An observed trend in Central South American precipitation, *Journal of Climate*, 17:4357-4367.
- Liquid Gold Team, 2002. *Drainage research in farmer's fields: analysis of data*, Report of the International Institute for Land Reclamation and Improvement (ILRI), Wageningen, The Netherlands, 69 p.
- Llano M. P., Penalba O. C., 2011. A climatic analysis of dry sequences in Argentina, *International Journal of Climatology*, 31:504-513.
- Lloyd Hughes B., Saunders M. A., 2002. A drought climatology for Europe, *International Journal of Climatology*, 22:1571-1592.
- López N. C., Alioto R., Schefer J. C., Belleggia F., Sinischaldi A., Parodi E. R., 2006. Diseño de un humedal artificial para remoción de nutrientes de un afluente del embalse paso de las piedras (Argentina), *Proceedings of the Congreso Interamericano de Ingeniería Sanitaria y Ambiental*, Punta del Este, 1-7.
- Lorenzo Lacruz J., Vicente Serrano S. M., López Moreno J. I., Beguería S., García Ruiz J. M., Cuadra J. M., 2010. The impact of droughts and water management on various hydrological systems in the headwaters of the Tagus River (central Spain), *Journal of Hydrlogy*, 386:13-26. DOI: 10.1016/j.jhydrol.2010.01.001

- Lowe L. D., Webb J. A., Nathan R. J., Etchells T., Malano H. M., 2009. Evaporation from water supply reservoirs: an assessment of uncertainty, *Journal of Hydrology*, 376:261-274.
- Luque J. A., Paoloni J. D., Bonorino G. A., 1979. Estudio hidrológico e hidrogeológico de la cuenca del río Sauce Grande, *Serie Hidrología*, 3:64 p.
- Maestro Cano I. C., Pardo Pascual J. E., Porres de la Haza M. J., 2003. Mejoras en la extracción automática de redes de drenaje aplicando el modelo área-pendiente, *Proceedings of the IX Conferencia Iberoamericana de SIG*, Cáceres, España,
- Magdaleno F., Fernandez A., 2010. Hydromorphological alteration of a large Mediterranean river: relative role of high and low flows on the evolution of riparian forests and channel morphology, *River Research and Applications*. Online. DOI: DOI: 10.1002/rra.1368
- Magilligan F. J., Nislow K. H., 2005. Changes in hydrologic regime by dams, *Geomorphology*, 71:61-78.
- Maheshwari B. L., Walker K. F., McMahon T. A., 1995. Effects of regulation on the flow regime of the river Murray, Australia, *Regulated Rivers: Research & Management*, 10:15-38.
- Mainigi J. K., Marsh S. E., 2002. Quantifying hydrologic impacts following dam construction along the Tana River, Kenya, *Journal of Arid Environments*, 50:53-79.
- Mair A., Fares A., 2011. Comparison of rainfall Interpolation methods in a mountainous region of a tropical island, *Journal of Hydrologic Engineering*, on line. DOI: 10.1061/(ASCE)HE.1943-5584.0000330
- Malcolm I. A., Soulsby C., Hannah D. M., Bacon P. J., Youngson A. F., Tetzlaff D., 2008. The influence of riparian woodland on stream temperatures: implications for the performance of juvenile salmonids, *Hydrological Processes*, 22:968-979.
- Marek M. A., 2011. *Hydraulic design manual*, Texas Department of Transportation, Texas, 478 p.
- Marengo J. A., Liebmann B., Grimm A. M., Misra V., Silva Dias P. L., Cavalcanti I. F. A., Carvalho L. M. V., Berbery E. H., Ambrizzi T., Vera C. S., Saulo A. C., Nogués Paegle J., Zipser E., Sethk A., Alvese L. M., 2010. Review: Recent developments on the South American monsoon system, *International Journal of Climatology*, Published online in Wiley Online Library.
- Marengo J. A., Seluchi M. E., 1998. Tropical mid-latitude exchange of air masses in South America. Part I: Some climatic aspects, *Proceedings of the X Congresso Brasileiro de Meteorologia*, Brasilia, Brasil,
- Marini F., 2009. *Evolución de la superficie ocupada por agua en el Dique Paso de las Piedras durante 2008*, Technical Report, Instituto Nacional de Tecnología Agropecuaria (INTA), Bordenave, 5 p.
- Marston R. A., Mills J. D., Wrazien D. R., Bassett B., Splinter D. K., 2005. Effects of Jackson Lake Dam on the Snake River and its floodplain, Grand Teton National Park, Wyoming, USA, *Geomorphology*, 71:79-98.

- Mathews R., Richter B. D., 2007. Application of the indicators of hydrologic alteration software in environmental flow setting, *Journal of the American Water Resources Association*, 1400-1413.
- Matsunaga K., Nakaya T., Sugai T., 2009. Simple DEM-Based Methods to Delineate Channel Networks for Hydrogeomorphological Mapping, *Transactions in GIS*, 13:87-103.
- Mazvimavi D., Burgers S. L., Stein A., 2006. Identification of basin characteristics influencing spatial variation of river flows, *International Journal of Applied Earth Observation and Geoinformation*, 8:165-172.
- MBB, 2000. *Plan Estratégico Bahía Blanca*, Bahía Blanca, 269 p.
- McCabe G. J., Markstrom S. L., 2007. A monthly water-balance model driven by a graphical user interface. U.S. Geological Survey, Virginia, U.S.
- McCartney M. P., Sullivan C., Acreman M. C., 2001. *Ecosystem impacts of large dams*, Background Paper Nr. 2, UNEP - United Nations Foundation - IUCN, 76 p.
- McCuen R. H., 1973. The role of sensitivity analysis in hydrologic modelling, *Journal of Hydrology*, 18:37-53.
- McGarigal K., Marks B. J., 1994. *Spatial pattern analysis program for quantifying landscape structure*, General Technical Report of the, USDA Forest Service, Covallis, 141 p.
- McKee T. B., Doesken N. J., Kleist J., 1993. The relationship of drought frequency and duration to time scales, *Proceedings of the Eighth Conference on Applied Climatology*, Anaheim, USA,
- McMahon T. A., Adeloje A. J., 2005. *Water resources yield*, Water Resources Publications, Highlands Ranch, Colorado, 234 p.
- McMahon T. A., Adeloje A. J., Zhou S.-L., 2006. Understanding performance measures of reservoirs, *Journal of Hydrology*, 324:359-382.
- McMahon T. A., Finlayson B. L., 2003. Droughts and anti-droughts: the low flow hydrology of Australian rivers, *Freshwater Biology*, 48:1147-1160.
- McMahon T. A., Finlayson B. L., Haines A. T., Srikanthan R., 1992. *Global runoff: continental comparisons of annual flows and peak discharges*, Catena Verlag, Cremlingen, 166 p.
- McMahon T. A., Mein R. G. (Editors), 1978. Reservoir capacity and yield. *Developments in Water Science 9*. Elsevier, Amsterdam, 213.
- McMahon T. A., Peel M. C., Vogel R. M., Pegram G. G. S., 2007c. Global streamflows. Part 3: Country and climate zone characteristics, *Journal of Hydrology*, 347:272-291.
- McMahon T. A., Pegram G. G. S., Vogel R. M., Peel M. C., 2007d. Revisiting reservoir storage–yield relationships using a global streamflow database, *Advances in Water Resources*, 30:1858-1872.

- McMahon T. A., Vogel R. M., Pegram G. G. S., Peel M. C., Etkin D., 2007b. Global streamflows. Part 2: Reservoir storage-yield performance, *Journal of Hydrology*, 347:260-271.
- Mendonça Santos M. L., Claramunt C., 2001. An integrated landscape and local analysis of land cover evolution in an alluvial zone, *Computers, Environments and Urban Systems*, 25:557-577.
- Merritt D. M., Cooper D. J., 2000. Riparian vegetation and channel change in response to river regulation: a comparative study of regulated and unregulated streams in the Green River Basin, USA, *Regulated Rivers: Research & Management*, 16:543-564.
- Merwade V., Cook A., Coonrod J., 2008. GIS techniques for creating river terrain models for hydrodynamic modeling and flood inundation mapping, *Environmental Modelling & Software*, 23:1300-1311.
- Meybeck M., Helmer R., 1996. Chapter 1 - An introduction to water quality. In: Chapman D. (Editor), *Water Quality Assessments - A Guide to Use of Biota, Sediments and Water in Environmental Monitoring, 2nd Edition*, E & FN Spon, London, 1-22.
- Meybeck M., Kuusisto E., Mäkelä A., Mälkki E., 1996. Water quality. In: Bartram J., Ballance R. (Editors), *Water Quality Monitoring - A Practical Guide to the Design and Implementation of Freshwater Quality Studies and Monitoring Programmes*, UNEP/WHO, London, 22.
- Minetti J. L., Vargas W. M., Vega B., Costa M. C., 2007. Las sequías en La Pampa Húmeda: impacto en la productividad del maíz, *Revista Brasileira de Meteorologia*, 22:218-232.
- Mockus V., 1972. *National Engineering Handbook, Section 4: Hydrology*, USDA Soil Conservation Service (Natural Resources Conservation Service, NRCS), 127 p.
- Modallaldoust S., 2010. Evaluating optimized digital elevation precipitation model using IDW method, *Desert*, 15:5-14.
- Mohseni O., Stefan H. G., 1999. Stream temperature/air temperature relationship: a physical interpretation, *Journal of Hydrology*, 218:128-141.
- Monk W. A., Wood P. J., Hannah D. M., Wilson D. A., 2007. Selection of river flow indices for the assessment of hydroecological change, *River Research and Applications*, 23:113-122.
- Moore R. D., Spittlehouse D. L., Story A., 2005. Riparian microclimate and stream temperature response to forest harvesting: a review, *Journal of the American Water Resources Association*, 41:813-834.
- Morris G. L., Fan J., 1997. *Reservoir sedimentation handbook*, McGraw-Hill, New York, 805 p.
- Naiman R. J., Latterell J. J., Pettit N. L., Olden J. D., 2008. Flow variability and the biophysical vitality of river systems, *Comptes Rendus Geoscience*, 340:629-643.

- Nash J. E., Sutcliffe J. E., 1970. River flow forecasting through conceptual models. Part 1. A discussion of principles, *Journal of Hydrology*, 10:282-290.
- Nilsson C., Berggren K., 2000. Alterations of riparian ecosystems caused by river regulation, *BioScience*, 50:783-792.
- Nogués Paegle J., Mechoso C. R., R.Fu, Berbery E. H., Chao W. C., Chen T.-C., Cook K., Diaz A. F., Enfield D., Ferreira R., Grimm A. M., Kousky V., Liebmann B., Marengo J. A., Mo K. C., Neelin J. D., Paegle J., Robertson A. W., Seth A., Vera C. S., Zhou J., 2002. Understanding the South American monsoon, *Progress in Pan American CLIVAR research*, 27:3-32.
- Nogués Paegle J., Mo K. C., 1997. Alternating Wet and Dry Conditions over South America during Summer, *Monthly Weather Review*, 125:279-291.
- NRCS, 1986. *Urban Hydrology for Small Watersheds*, TR-55, United States Department of Agriculture, 160 p.
- NRCS, 2004. *Chapter 9: Hydrologic soil-cover complexes*, National Engineering Handbook, Part 630: Hydrology, USDA, 20 p.
- NRCS, 2007a. *Chapter 7: Hydrologic Soil Groups*, National Engineering Handbook, Part 630: Hydrology, USDA, 14 p.
- NRCS, 2007b. *Chapter 16: Hydrographs*, National Engineering Handbook, Part 630: Hydrology, USDA, 50 p.
- NRCS, 2010. *Chapter 15: Time of concentration*, National Engineering Handbook, Part 630: Hydrology, USDA, 29 p.
- Núñez S. E., Núñez L. N., Podestá G. P., Skansi M. M., 2005. El Índice Estandarizado de Precipitación como herramienta para la caracterización y el monitoreo de la sequía: una prueba de concepto, *Proceedings of the CONGREGMET IX, 9th Argentine Congress of Meteorology*, Buenos Aires, Argentina,
- Olden J. D., Naiman R. J., 2010. Incorporating thermal regimes into environmental flows assessments: modifying dam operations to restore freshwater ecosystem integrity, *Freshwater Biology*, 55:86-107.
- Olden J. D., Poff N. L., 2003. Redundancy and the choice of hydrologic indices for characterizing streamflow regimes, *River Research and Applications*, 19:101-121.
- Oosterbaan R. J., 1994. Frequency and regression analysis. In: Ritzema H. P. (Editor), *Drainage principles and applications*, IILRI - International Institute for Land Reclamation and Improvement, Wageningen, 175-223.
- Opperman J., 2006a. *Preliminary IHA analysis for the Middle Fork Willamette River at Jasper OR*, Technical Report, The Nature Conservancy, 5 p.
- Opperman J., 2006b. *Indicators of Hydrologic Alteration Analysis for the Patuca River*, Technical Report, The Nature Conservancy, 19 p.
- Osborne L. L., Kovacic D. A., 1993. Riparian vegetated buffer strips in water quality restoration and stream management, *Freshwater Biology*, 29:243-258.

- Owens P. N., Walling D. E., 2002. Changes in sediment sources and floodplain deposition rates in the catchment of the river Tweed, Scotland, over the last 100 years: the impact of climate and land use change, *Earth Surface Processes and Landforms*, 27:403-423.
- Ozaki N., Fukushima T., Harasawa H., Kojiri T., Kawashima K., Ono M., 2003. Statistical analyses on the effects of air temperature fluctuations on river water qualities, *Hydrological Processes*, 17:2837-2853.
- Ozdemir H., Bird D., 2008. Evaluation of morphometric parameters of drainage networks derived from topographic maps and DEM in point of floods, *Environmental Geology*. Online. DOI: 10.1007/s00254-008-1235-y.
- Paoloni J. D., Tjuchneider O. C., Luque J. A., 1972. Caracterización hidrológica de la cuenca del río Sauce Grande en primera fase, *Investigaciones Agropecuarias Serie 3: Clima y Suelo*, 9:127-146.
- Pardé M., 1933. *Fleuves et rivières*, Armand Colin, Paris, 224 p.
- Pardo Pascual J. E., Acosta Matarredona P., Porres de la Haza M. J., 2002. Quality assesment of Digital Elevation Models deduced from digital cartography for hydrogeomorphological applications, *Proceedings of the 3^a Asamblea Hispano Portuguesa de Geodesia y Geofísica*, 1746-1750.
- Parodi E. R., Estrada V., Trobbiani N., Argañaraz Bonini G., 2004. Análisis del estado trófico del Embalse Paso de las Piedras, *Proceedings of the II Reunión Binacional de Ecología*, Mendoza,
- Pedraza J., 1996. *Geomorfología. Principios, métodos y aplicaciones*, Rueda, Madrid, 414 p.
- Peiry J.-L., Girel J., Pautou G., 1999. Hydroelectric developments, environmental impact. In: Alexander D. E., Fairbridge R. W. (Editors), *Encyclopedia of environmental sciences*, Kluwer Academic Publishers, Dordrecht, 332-336.
- Peiry J.-L., Salvador P.-G., Nouguier F., 1994. L'incision des rivières dans les Alpes du nord : état de la question, *Revue de Géographie Alpine*, 69:47-56.
- Pellarin T., Delrieu G., Saulnier G.-M., 2002. Hydrologic visibility of weather radar systems operating in mountainous regions: case study for the Ardèche Catchment (France), *American Meteorological Society*, 3:539-555.
- Penalba O. C., Llano M. P., 2008. Contribución al estudio de las secuencias secas en la zona agropecuaria de Argentina, *Meteorológica* 32:51-64.
- Penalba O. C., Robledo F., 2005. Frequency of precipitation in the Humid Pampa of Argentina, *Proceedings of the 15th Conference on Applied Climatology*, Savannah, USA,
- Penalba O. C., Vargas W. M., 2004. Interdecadal and Interannual variations of annual and extreme precipitation over central-northeastern Argentina, *International Journal of Climatology*, 24:1565-1580.
- Petts G. E., 1977. Channel response to flow regulation: the case of the River Derwent,

- Derbyshire. In: Gregory K. J. (Editor), *River Channel Changes*, J. Wiley & Sons Ltd, Chichester, 145-164.
- Petts G. E., 1979. Complex response of river channel morphology subsequent to reservoir construction, *Progress in Physical Geography*, 3:529-632.
- Petts G. E., 1980a. Long-term consequences of upstream impoundment, *Environmental Conservation*, 7:325-332.
- Petts G. E., 1980b. Implications of the fluvial process—channel morphology interaction below British reservoirs for stream habitats *The Science of The Total Environment*, 16:149-163.
- Petts G. E., 1984. *Impounded Rivers*, John Wiley & Sons, Chichester, 326 p.
- Petts G. E., Amoros C., 1996. The fluvial hydrosystem. In: Petts G. E., Amoros C. (Editors), *Fluvial Hydrosystems*, Chapman & Hall, London, 1-12.
- Petts G. E., Gurnell A. M., 2005. Dams and geomorphology: Research progress and future directions, *Geomorphology*, 71:22-47.
- Petts G. E., Lewin J., 1979. Physical effects of reservoirs on river systems. In: Hollis G. E. (Editor), *Man's impact on the hydrological cycle in the United Kingdom*, Geo Abstracts, Norwich, 79-91.
- Phillips J. D., 2003a. Sources of nonlinearity and complexity in geomorphic systems, *Progress in Physical Geography*, 27:1-23. DOI: 10.1191/0309133303pp340ra
- Phillips J. D., 2003b. Toledo Bend Reservoir and geomorphic response in the Lower Sabine River, *River Research and Applications*, 19:137-159.
- Phillips J. D., 2009. Landscape evolution space and the relative importance of geomorphic processes and controls, *Geomorphology*, 109:79-85.
- Phillips J. D., Slattery M. C., Musselman Z. A., 2005. Channel adjustments of lower Trinity River, Texas, downstream of Livingston Dam, *Earth Surface Processes and Landforms*, 30:1419-1439.
- Piccolo M. C., Capella de Steffens A., Campo A. M., 2002. La sequía de 1995 en el sur de la región pampeana argentina. In: Hubp Lugo J., Inbar M. (Editors), *Desastres Naturales en América Latina*, Fondo de Cultura económica, 189-206.
- Poff N. L., 1996. A hydrogeography of unregulated streams in the United States and an examination of scale-dependence in some hydrological descriptors, *Freshwater Biology*, 36:71-91.
- Poff N. L., Allan J. D., Bain M. B., Karr J. R., Prestegard K. L., Richter B. D., Sparks R. E., Stromberg J. C., 1997. The Natural Flow Regime. A paradigm for river conservation and restoration, *BioScience*, 47:769-784.
- Poff N. L., Hart D. D., 2002. How dams vary and why it matters for the emerging science of dam removal, *BioScience*, 52:659-734.
- Poff N. L., Ward J. V., 1989. Implications of streamflow variability and predictability for lotic community structure: a regional analysis for streamflow patterns, *Canadian Journal of Fisheries and Aquatic Sciences*, 46:1805-1817.

- Poirel A., Gailhard J., Capra H., 2010. Influence des barrages-réservoirs sur la température de l'eau : exemple d'application au bassin versant de l'Ain, *La Houille Blanche*, 4:72-79.
- Poole G. C., 2002. Fluvial landscape ecology: addressing uniqueness within the river discontinuum, *Freshwater Biology*, 47:641-660.
- Poole G. C., Berman C. H., 2001. An ecological perspective on in-stream temperature: Natural heat dynamics and mechanisms of human-caused thermal degradation, *Environmental Management*, 27:787-802.
- Poole G. C., Risley J., Hicks M., 2001. *Spatial and temporal patterns of stream temperature*, Issue Paper 3, United States Environmental Protection Agency, 35 p.
- Prats J., Armengol J., Marcé R., Sanchez Juny M., Dolz J., 2011. Dams and reservoirs in the lower Ebro River and its effects on the river thermal cycle *The Handbook of Environmental Chemistry*, 13:77-95.
- Prats J., Val R., Armengol J., Dolz J., 2010. Temporal variability in the thermal regime of the lower Ebro River (Spain) and alteration due to anthropogenic factors, *Journal of Hydrology*, 387:105-118.
- Prats J., Val R., Dolz J., Armengol J., 2012. Water temperature modelling in the Lower Ebro River (Spain): Heat fluxes, equilibrium temperature, and magnitude of alteration caused by reservoirs and thermal effluent, *Water Resources Research*. Online. 10.1029/2011WR010379
- Preece R. M., Jones H. A., 2002. The effect of Keepit Dam on the temperature regime of the Naomi River, Australia, *River Research and Applications*, 18:397-414.
- Puckridge J. T., Walker K. F., Costello J. F., 2000. Hydrological persistence and the ecology of dryland rivers, *Regulated Rivers: Research & Management*, 16:385-402.
- Quattrocchio M. E., Borromei A. M., Deschamps C. M., Grill S., Zavala C., 2008. Landscape evolution and climate changes in the Late Pleistocene–Holocene, southern Pampa (Argentina): Evidence from palynology, mammals and sedimentology, *Quaternary International*, 181:123-138.
- Quattrocchio M. E., Deschamps C. M., Zavala C., Borromei A. M., Grill S., Guerslein R., 1993. Cuaternario del Sur de la provincia de Buenos Aires: Estratigrafía e inferencias paleoambientales. In: Iriondo M. (Editor), *El Holoceno en Argentina*, CADINQUA, 2:22-34.
- Rabassa J., 1982. Variación regional y significado geomorfológico de la densidad de drenaje en la cuenca del río Sauce Grande, provincia de Buenos Aires, *Revista de la Asociación Geológica Argentina*, 37:268-284.
- Rabassa J., 1989. Geología de los depósitos del Pleistoceno Superior y Holoceno en las cabeceras del río Sauce Grande, provincia de Buenos Aires, *Proceedings of the I Jornadas Geológicas Bonaerenses*, 765-790.

- Rabassa J., Heusser C., Salemme M., Politis G., Stuckenrath R., 1991. Troncos de *Salix humboldtiana* en depósitos aluviales del Holoceno tardío, Río Sauce Grande (Provincia de Buenos Aires, Argentina), *Cuadernos de Geografía*, 3:221-236.
- Rabassa J., Salemme M., Heusser C., 1985. Hallazgo de los troncos fósiles (*Salix humboldtiana*) en sedimentos aluviales del río Sauce Grande, Provincia de Buenos Aires, *Proceedings of the I Jornadas Geológicas Bonaerenses*, Tandil,
- Ramusson E. M., Wallace J. M., 1983. Meteorological aspects of El Niño/Southern Oscillation, *Science*, 222:1195-12020.
- Raskovsky L., 2009. *Embalse Paso de las Piedras: Estado de situación*, Autoridad del Agua, Departamento Preservación y Mejoramiento de los Recursos, Buenos Aires, 17 p.
- Rausch D. L., Heinemann H. G., 1975. Controlling Reservoir Trap Efficiency, *Transactions of the ASAE*, 18:1105-1113.
- Réménieras G., 1986. *L'hydrologie de l'ingénieur*, Editions Eyrolles, Paris, 456 p.
- Richard G., Julien P., 2003. Dam impacts on and restoration of an alluvial river -Rio Grande, New Mexico, *International Journal of Sediment Research*, 18:89-96.
- Richards K. S., 1976. The morphology of riffle-pool sequences, *Earth Science Reviews*, 1:71-88.
- Richter B. D., Baumgartner J. V., Braun D. P., Powell J., 1998. A spatial assessment of hydrologic alteration within a river network, *Regulated Rivers: Research & Management*, 14:329-340.
- Richter B. D., Baumgartner J. V., Powell J., Braun D. P., 1996. A method for assessing hydrologic alteration within ecosystems, *Conservation Biology*, 10:1163-1174.
- Richter B. D., Baumgartner J. V., Wigington R., Braun D. P., 1997. How much water does a river need?, *Freshwater Biology*, 37:231-249.
- Rieger W., 1998. A phenomenon-based approach to upslope contributing area and depressions in DEMs, *Hydrological Processes*, 12:857-872.
- Rippl W., 1883. The capacity of storage-reservoirs for water-supply, *Proceedings of the Institute of Civil Engineering*, 71:270-278.
- Robert A., 2003. *River processes. An introduction to fluvial dynamics*, Arnold, London, 214 p.
- Roche M., 1963. *Hydrologie de surface*, Gauthier-Villars, Paris, 431 p.
- Ropelewski C. F., Halpert M. S., 1987. Global and regional scale precipitation patterns associated with the El Niño/Southern Oscillation, *Monthly Weather Review*, 115:1606-1626.
- Ropelewski C. F., Halpert M. S., 1989. Precipitation patterns associated with the High Index Phase of the Southern Oscillation, *Journal of Climate*, 2:268-284.
- Ropelewski C. F., Halpert M. S., 1996. Quantifying Southern Oscillation-precipitation relationships, *Journal of Climate*, 9:1043-1059.

- Rosgen D. L., 1994. A classification of natural rivers, *Catena*, 22:169-199.
- Rosgen D. L., 1996. Field survey procedures for characterization of river morphology.
- Rosgen D. L., 2001. A stream channel stability assessment methodology, *Proceedings of the 7th Federal Interagency Sedimentation Conference*, Reno, USA,
- Roussel M. C., Thompson D. B., Fang X., Cleveland T. G., Garcia C. A., 2005. *Time-parameter estimation for applicable Texas watersheds*, Lamar University, Beaumont, Texas,
- Ruibal Conti A. L., Guerrero J. M., Regueira J. M., 2005. Levels of microcystins in two Argentinean reservoirs used for water supply and recreation: differences in the implementation of safe levels, *Environmental Toxicology*, 20:263-269.
- Rusticucci M. M., Marengo J. A., Penalba O. C., 2010. An intercomparison of model-simulated in extreme rainfall and temperature events during the last half of the twentieth century. Part 1: mean values and variability, *Climatic Change*, 98:493-508.
- Sanders B. F., 2007. Evaluation of on-line DEMs for flood inundation modeling, *Advances in Water Resources*, 30:1831-1843.
- Saulnier G.-M., Le Lay M., 2009. Sensitivity of flash-flood simulations on the volume, the intensity, and the localization of rainfall in the Cévennes-Vivarais region (France) *Water Resources Research*, 45:W10425, 9 pp.
- Saulo A. C., Seluchi M. E., Nicolini M., 2004. A case study of a Chaco low-level jet event, *Monthly Weather Review*, 132:2669-2683.
- Schefer J. C., 2004. *Los recursos hídricos y el abastecimiento de agua*, CEPADE, Bahía Blanca, 133 p.
- Schmandt J., 2010. Rivers in semi-arid lands: impact of dams, climate and people, *Proceedings of the 2nd International Conference: Climate, Sustainability and Development in Semi-arid Regions*, Fortaleza - Ceara, Brazil, 21.
- Schmidt J. C., Everitt B. L., 2000. Hydrology and geomorphology of the Rio Grande/Rio Bravo between Fort Quitman and Amistad Reservoir and implications for river restoration, *Proceedings of the Rio Grande/Rio Bravo Binational Symposium, US Department of the Interior, Mexico Secretariat of Environment and Natural Resources, International Boundary and Water Commission Juarez, Mexico*,
- Schneider T., 2001. Analysis of incomplete climate data: estimation of mean values and covariance matrices and imputation of missing values, *Journal of Climate*, 14:853-871.
- Schumm S. A., 1969. River metamorphosis, *Proceedings of the American Society of Civil Engineers, Journal of the Hydraulics Division HY1*, 255-273.
- Schumm S. A. (Editor), 1973. *Geomorphic thresholds and complex response of drainage systems. Fluvial Geomorphology*. State University of New York, Binghamton, 299-310.

- Schumm S. A., 1977. *The fluvial system*, John Wiley & Sons, New York, 338 p.
- Schumm S. A., 1979. Geomorphic thresholds: the concept and its applications, *Transactions of the Institute of British Geographers*, 4:485-515.
- Scian B., 2000. Episodios ENSO y su relación con las anomalías de precipitación en la pradera pampeana, *Geoacta*, 25:23-40.
- Scian B., Labraga J. C., Reimers W., Frumento O., 2006. Characteristics of large-scale atmospheric circulation related to extreme monthly rainfall anomalies in the Pampa Region, Argentina, under non-ENSO conditions, *Theoretical and Applied Climatology*, 85:89-106.
- Sear D. A., 1995. Morphological and sedimentological changes in a gravel-bed river following 12 years of flow regulation for hydropower, *Regulated Rivers: Research & Management*, 10:247-264.
- Selvi H. Z., Bildirici O., 2008. The accuracy and reliability of digital elevation models created from the contour lines of paper maps, *Proceedings of the 2nd International Conference on Cartography and GIS*, Borovest, Bulgaria, 7.
- Serio L., Martin P., Murphy G., 2010. Evaluación de una metodología de pronóstico estadístico para la condición hídrica del suelo en la región pampeana argentina, *Agriscientia*, 27:11-17.
- Sharma A., Tiwari K. N., Bhadoria P. B. S., 2009. Measuring the Accuracy of Contour Interpolated Digital Elevation Models, *J. Indian Soc. Remote Sens.*, 37:139-146.
- Sherrard J. J., Erskine W. D., 1991. Complex response of a sand-bed stream to upstream impoundment, *Regulated Rivers: Research & Management*, 6:53-70.
- Shields F. D., Simon A., Steffen L. J., 2000. Reservoir effects on downstream river channel migration, *Environmental Conservation*, 27:54-66.
- Sili M., 2000. *Los espacios de la crisis rural : geografía de una pampa olvidada*, EdiUNS, Bahía Blanca, 179 p.
- Silva R. P. D., Dayawansa N. D. K., Ratnasiri M. D., 2007. A comparison of methods used in estimating missing rainfall data, *The Journal of Agricultural Sciences*, 3:101-108.
- Simon A., Downs P. W., 1995. An interdisciplinary approach to evaluation of potential instability in alluvial channels, *Geomorphology*, 12:215-232.
- Sinokrot B. A., Stefan H. G., McCormick J. H., Eaton J. G., 1995. Modeling of climate change effects on stream temperatures and fish habitats below dams and near groundwater inputs, *Climatic Change*, 30:181-200.
- Smith K., 1972. River water temperatures: an environmental review, *Scottish Geographical Magazine*, 88:211-220. DOI: 10.1080/00369227208736229
- Sokolov A. A., Chapman T. G., 1974. *Methods for water balance computations. An international guide for research and practice* The Unesco Press, Paris, 124 p.
- Stanford J. A., Ward J. V., 2001. Revisiting the serial discontinuity concept, *Regulated Rivers: Research & Management*, 17:303-310.

- Starkel L., 1983. The reflection of hydrologic changes in the fluvial environment of the temperate zone during the last 15,000 years. In: Gregory K. J. (Editor), *Background to Palaeohydrology*, Wiley, Chichester, 213-235.
- Steel E. A., Lange I. A., 2007. Using wavelet analysis to detect changes in water temperature regimes at multiple scales: effects of multi-purpose dams in the Willamette River Basin, *River Research and Applications*, 23:351-359.
- Stefan H. G., Preud'homme E. B., 1993. Stream temperature estimation from air temperature, *Water Resources Bulletin*, 29:27-45.
- Steiger J., Tabacchi E., Dufour S., Corenblit D., Peiry J.-L., 2005. Hydrogeomorphic processes affecting riparian habitat within alluvial channel-floodplain river systems: a review for the temperate zone, *River Research and Applications*, 21:719-737.
- Stevens H. H., Ficke J. F., Smoot G. F., 1975. *Water temperature-influential factors, field measurement, and data presentation*, Techniques of Water-Resources Investigations, U.S. Geological Survey, Arlington, 70 p.
- Strahler A., 1981. *Geografía Física*, Ediciones Omega, Barcelona, 770 p.
- Surian N., 1999. Channel changes due to river regulation: the case of the Piave River, Italy, *Earth Surface Processes and Landforms*, 24:1135-1151.
- Surian N., Rinaldi M., 2003. Morphological response to river engineering and management in alluvial channels in Italy, *Geomorphology*, 50:307-326.
- Tharme R. E., 2003. A global perspective on environmental flow assessment: emerging trends in the development and application of environmental flow methodologies for rivers, *River Research and Applications*, 19:397-441.
- Thomas H. A., Burden R. P., 1963. *Operations research in water quality management*, Harvard water Resources Group, Cambridge, 208 p.
- Thoms M. C., Sheldon F., 2000. Lowland rivers: an Australian introduction, *Regulated Rivers: Research & Management*, 16:375-383.
- Thoms M. C., Walker K. F., 1993. Channel changes associated with two adjacent weirs on a regulated lowland alluvial river, *River Research and Applications*, 8:271-284. DOI: 10.1002/rrr.3450080306
- Thorne C. R., 1993. *Guidelines for the use of stream reconnaissance record sheets in the field*, U.S. Army Corps of Engineers, Washington, 91 p.
- Thorntwaite C. W., 1948. An approach toward a rational classification of climate, *Geographical Review*, 38:55-94.
- Tockner K., Malard F., Ward J. V., 2000. An extension of the flood pulse concept, *Hydrological Processes*, 14:2861-2883.
- Tooth S., 2000. Process, form and change in dryland rivers: a review of recent research, *Earth Science Reviews*, 51:67-107.
- Trenberth K. E., 1997. The definition of El Nino, *Bulletin of the American Meteorological Society*, 78:2771-2777.

- Troha A., Forte Lay J. A., 1993. Análisis de las principales sequías edáficas ocurridas en la provincia de Buenos Aires, *Geoacta*, 20:79-85.
- Tucker G. E., Catani F., Rinaldo A., Bras R. L., 2001. Statistical analysis of drainage density from digital terrain data, *Geomorphology*, 36:187-202.
- USACE, 1991. *Optimization of multiple-purpose reservoir system operations: a review of modeling and analysis approaches*, Research Document No. 34, U.S. Army Corps of Engineers, Davis, 89 p.
- USDA S. S. S., 1999. *Soil Taxonomy. A Basic System of Soil Classification for Making and Interpreting Soil Surveys*, United States Department of Agriculture (USDA), Washington, 871 p.
- van Kreveld M., 1997. Digital elevation models and TIN algorithms. In: van Kreveld M. et al. (Editors), *Algorithmic Foundations of Geographic Information Systems*, Springer-Verlag, Berlin, 37-38.
- Vannote R. L., Minshall G. W., Cummins K. W., Sedell J. R., Cushing C. E., 1980. The river continuum concept, *Canadian Journal of Fisheries and Aquatic Sciences*, 37:130-137.
- Vera C., Higgins W., Amador J., Ambrizzi T., Garreaud R. D., Gochis D., Gutzler D., Lettenmaier D., Marengo J. A., Mechoso C. R., Nogués Paegle J., Silva P. L., Zhang C., 2006. Toward a Unified View of the American Monsoon Systems, *Journal of Climate*, 19:4977-5000.
- Vincendon B., Ducrocq V., Saulnier G.-M., Bouilloud L., Chancibault K., Habets F., Noilhan J., 2010. Benefit of coupling the ISBA land surface model with a TOPMODEL hydrological model version dedicated to Mediterranean flash-floods, *Journal of Hydrology*, 394:256-266.
- Vivian H., 1986. Un exemple de régime influencé: hydrologie et hydroélectricité dans les cours d'eau des Alpes du Nord, *Hydrologie Continentale*, 1:63-78.
- Vivian H., 1994. L'hydrologie artificialisée de l'Isère en amont de Grenoble. Essai de quantification des impacts des aménagements, *Revue de Géographie Alpine*, 82:97-112.
- Vogel R. M., Lane M., Ravindiran R. S., Kirshen P., 1999. Storage reservoir behavior in the United States, *Journal of Water Resources Planning and Management*, 125:245-264.
- Vogel R. M., Sieber J., Archfield S. A., Smith M. P., Apse C. D., Huber Lee A., 2007. Relations among storage, yield, and instream flow, *Water Resources Research*, 43:W05403. DOI: 10.1029/2006WR005226
- W.C.D., 2000. *Dams and development. A new framework for decision-making*, Earthscan Publications, London, 356 p.
- Walker J. P., Willgoose G., 1999. On the effect of digital elevation model accuracy on hydrology and geomorphology, *Water Resources Research*, 35:2259-2268.
- Walker K. F., 1992. A semi-arid lowland river: The River Murray, Australia. In: Calow P. A., Petts G. E. (Eds), *The River's Handbook*, Blackwell, Oxford, 472-492.

- Walker K. F., Sheldon F., Puckridge J. T., 1995. A perspective on dryland river ecosystems, *Regulated Rivers: Research & Management*, 11:85-104.
- Walker W. W., 1979. Use of Hypolimnetic Oxygen Depletion Rate as a Trophic State Index for Lakes, *Water Resources Research*, 15:1463-1470.
- Wang M., Hjelmfelt A. T., Garbrecht J., 2000. DEM aggregation for watershed modeling, *Journal of the American Water Resources Association*, 36:579-584.
- Wang X., Yin Z.-Y., 1998. A comparison of drainage networks derived from digital elevation models at two scales, *Journal of Hydrology*, 210:221-241.
- Wang Z.-Y., Wu B., Wang G., 2007. Fluvial processes and morphological response in the Yellow and Weihe Rivers to closure and operation of Sanmenxia Dam, *Geomorphology*, 91:65-79.
- Ward J. V., 1985. Thermal characteristics of running waters, *Hydrobiologia*, 125:31-46.
- Ward J. V., 1998. Riverine landscapes: biodiversity patterns, disturbance regimes, and aquatic conservation, *Biological Conservation*, 83:269-278.
- Ward J. V., Stanford J. A., 1979. Ecological factors controlling stream zoobenthos with emphasis on thermal modification of regulated streams. In: Ward J. V., Stanford J. A. (Editors), *The Ecology of Regulated Streams, Proceedings of the First International Symposium on Regulated Streams*, Plenum Press, New York, 35-55.
- Ward J. V., Stanford J. A., 1982. Thermal responses in the evolutionary ecology of aquatic insects, *Annual Review of Entomology*, 27:97-117.
- Ward J. V., Stanford J. A., 1983. The serial discontinuity concept of lotic ecosystems. In: Fontaine T. D., Bartell S. M. (Editors), *Dynamics of lotic ecosystems*, Ann Arbor Scientific Publishers, Ann Arbor, 29-42.
- Ward J. V., Stanford J. A., 1995a. The serial discontinuity concept: extending the model to floodplain rivers, *Regulated Rivers: Research & Management*, 10:159-168.
- Ward J. V., Stanford J. A., 1995b. Ecological connectivity in alluvial river ecosystems and its disruption by flow regulation, *Regulated Rivers: Research & Management*, 11:105-119.
- Warner R. F., 1987. The impacts of alternating flood- and drought-dominated regimes on channel morphology at Penrith, New South Wales, Australia, *Proceedings of the Vancouver Symposium - The Influence of Climate Change and Climatic Variability on the Hydrologic Regime and Water Resources* Wallingford, 327-338.
- Webb B. W., 1996. Trends in stream and river temperature, *Hydrological Processes*, 10:205-226.
- Webb B. W., Clack P. D., Walling D. E., 2003. Water-air temperature relationships in a Devon river system and the role of flow, *Hydrological Processes*, 17:3069-3084.
- Webb B. W., Crisp D. T., 2006. Afforestation and stream temperature in a temperate maritime environment, *Hydrological Processes*, 20:51-66.

- Webb B. W., Hannah D. M., Moore D., Brown L. E., Nobilis F., 2008. Recent advances in stream and river temperature research, *Hydrological Processes*, 22:902-918.
- Webb B. W., Walling D. E., 1988. Modification of temperature behaviour through regulation of a British river system, *Regulated Rivers: Research & Management*, 2:103-116.
- Webb B. W., Walling D. E., 1992. Long term water temperature behaviour and trends in a Devon, UK, river system, *Hydrological Sciences*, 37:567-580.
- Webb B. W., Walling D. E., 1993a. Temporal variability in the impact of river regulation on thermal regime and some biological implications, *Freshwater Biology*, 29:167-182.
- Webb B. W., Walling D. E., 1995. The long-term thermal impact of reservoir operation and some ecological implications, *Proceedings of the Man's Influence on Freshwater Ecosystems and Water*, 245-257.
- Webb B. W., Walling D. E., 1997. Complex summer water temperature behaviour below a UK regulating reservoir, *Regulated Rivers: Research & Management*, 13:463-477.
- Wellmeyer J. L., Slattery M. C., Phillips J. D., 2005. Quantifying downstream impacts of impoundment on flow regime and channel planform, lower Trinity River, Texas, *Geomorphology*, 69:1-13.
- Wetzel R. G., 1975. *Limnology*, Saunders, Philadelphia, 743 p.
- Widmann L., 2012. *Twigs of a tree, a family tale: from a priest defrocked by the French revolution to English pioneering on the Pampas*, Authorhouse, Bloomington, 356 p.
- Williams G. P., Wolman M. G., 1984. *Downstream effects of dams on alluvial rivers*, US Government Printing Office, Washington, 83 p.
- Wise S. M., 2000. Assessing the quality for hydrological applications of digital elevations models derived from contours, *Hydrological Processes*, 14:1909-1929.
- Wise S. M., 2007. Effect of differing DEM creation methods on the results from a hydrological model, *Computers & Geosciences*, 33:1351-1365.
- Wolman M. G., Miller J. P., 1960. Magnitude and frequency of forces in geomorphic processes, *Journal of Geology*, 68:54-74.
- Wood J. D., Fisher P. F., 1993. Assessing interpolation accuracy in elevation models, *IEEE Computer Graphics and Applications*, 13:48-56.
- Wright S. A., Anderson C. R., Voichick N., 2009. A simplified water temperature model for the Colorado River below Glen Canyon dam, *River Research and Applications*, 25:675-686.
- Wu S., Li J., Huang G. H., 2008. A study on DEM-derived primary topographic attributes for hydrologic applications: Sensitivity to elevation data resolution, *Applied Geography*, 28:210-223.

- Wurbs R. A., 2005. Modeling river/reservoir system management, water allocation, and supply reliability, *Journal of Hydrology*, 300:100-113.
- Xu J., 1996. Channel pattern change downstream from a reservoir: An example of wandering braided rivers, *Geomorphology*, 15:147-158.
- Yeung C. W., 2004. *Rainfall-Runoff and Water-Balance Models for Management of the Fena Valley Reservoir*, Scientific Investigations Report - 5287, U.S. Geological Survey, 64 p.
- Zahar Y., Ghorbel A., Albergel J., 2008. Impacts of large dams on downstream flow conditions of rivers: Aggradation and reduction of the Medjerda channel capacity downstream of the Sidi Salem dam (Tunisia), *Journal of Hydrology*, 351:318-330.
- Zamboni L., 2008. Seasonal variability of precipitation over South Eastern South America: its relationship with upper level circulation as physical base for predictions, Università degli Studi di Trieste, Trieste, 109 p.
- Zamboni L., Mechoso C. R., Kucharski F., 2010. Relationships between Upper-Level Circulation over South America and Rainfall over Southeastern South America: A Physical Base for Seasonal Predictions, *Journal of Climate*, 23:3300-3315.
- Zapperi P., Casado A., Gil V., Campo A. M., 2006. Caracterización de las precipitaciones invernales en el Suroeste bonaerense. In: Cazzaniga N., Vaquero M. (Editors), *Ambiente natural, campo y ciudad: Estrategias de uso y conservación en el Sudoeste Bonaerense*, Ediciones UNS, Bahía Blanca, 63-68.
- Zapperi P., Ramos B., Gil V., Campo A. M., 2007. Caracterización de las precipitaciones estivales en el Suroeste bonaerense, *Contribuciones Científicas*, GAEA, Posadas, x a x.
- Zavala C., Quattrocchio M. E., 2001. Estratigrafía y evolución geológica del río Sauce Grande (Cuaternario), provincia de Buenos Aires, Argentina, *Revista de la Asociación Geológica Argentina*, 56(1):25-37.
- Zhong Y., Power G., 1996. Environmental effects of hydroelectric projects on fish resources in China, *Regulated Rivers: Research & Management*, 12:81-98. DOI: 10.1002/(SICI)1099-1646(199601)12:1
- Zhou J., Lau K.-M., 1998. Does a Monsoon Climate Exist over South America?, *Journal of Climate*, 11:1020-1040.
- Ziadat F. M., 2007. Effect of Contour Intervals and Grid Cell Size on the Accuracy of DEMs and Slope Derivatives, *Transactions in GIS*, 11:67-81.



CHAPTER 1: Research Context

Figure 1.1: Dams constructed by world's region over the period 1900-2000 and regional distribution of large dams at the end of the 20th Century.....	13
Figure 1.2: Orders of change of impounded river systems relative to the dam purpose and the reservoir size.....	14
Figure 1.3: Common types of flow regulation and implications for the flow regime of the river downstream	15
Figure 1.4: Stratification of deep temperate reservoirs and implications for the water quality of the river downstream	18
Figure 1.5: Drivers of river water temperature and insulating/buffering processes within a hypothetical stream.....	19
Figure 1.6: Dam-induced disruption for sediment transport.....	22
Figure 1.7. [A] Scenarios of channel adjustment in response to relative changes in flow discharge and sediment load, and [B] trajectory of geomorphic changes following dam closure.....	24
Figure 1.8: Qualitative scheme of change in the fluvial style.....	25
Figure 1.9: Potential changes in the channel morphology following altered inputs of flow and sediment below dams.....	27
Figure 1.10: Linked processes influencing the relationship between use and management of water resources within the Sauce Grande River Basin and its regional context	32
Figure 1.11: Spatial distribution of surface and underground water resources within the central south-western Buenos Aires.....	33
Figure 1.12: Patterns of atmospheric circulation and rainfall over South America and adjacent oceans during austral summer and austral winter.....	35
Figure 1.13: Distribution of mean annual rainfall for the periods 1941-1970 and 1971-2001 across the Buenos Aires province.....	36
Figure 1.14: Long-term climographs for eight locations across SWBA.....	37
Figure 1.15: Recurrence of dry (or wet) years within SWBA and ENSO episodes for the period 1950-2010.....	39
Figure 1.16: Major geomorphologic features within the Sauce Grande Basin based on elevation ranges and terrain slope, and longitudinal profile of the river from the headwaters to the mouth.....	41
Figure 1.17: Quaternary geology of the Sauce Grande River.....	42
Figure 1.18: [A] Urban centres and [B] major land uses within the six departments (grey area) linked to the Sauce Grande River Basin (yellow area).....	44

Figure 1.19: Population density and rates of population growth by department for 11 time steps between 1869 and 2010.....	45
Figure 1.20: Population growth and advances in water management practices along the 20th Century	47
Figure 1.21: Waterworks for water supply in central SWBA.....	48
Figure 1.22: Paso de las Piedras Complex scheme.....	50
Figure 1.23: Reservoir volume by water level and level-related threats for water reserves.....	52
Figure 1.24: Sequence of extreme dry (wet) evens documented within the area of interest during the last decade.....	54
Figure 1.25: Hypothesized effects of the Paso de las Piedras Dam on the hydrology of the Sauce Grande River downstream and expected response of the river environment.....	59
Figure 1.26: Scheme of the structure of the thesis manuscript	61
Figure 1.27: Conceptual scheme of synchronic and diachronic analysis	63

CHAPTER 2: Generation of baseline data

Figure 2.1: Terrain parameters and series of climatic and hydrologic data required for analysis.....	68
Figure 2.2: Series of climatic and hydrologic data available for analysis.	70
Figure 2.3: Distribution of meteorological and flow gauging stations within the upper river basin and nearby areas.....	71
Figure 2.4: RainOff-empirical model for streamflow simulation.	75
Figure 2.5: Distribution of meteorological and flow gauging stations within the river basin downstream from the dam and nearby areas.....	75
Figure 2.6: [A] Overview and spatial situation of the river sections selected for stream stage reading (hydrometric stations); [B] field techniques used to flow gauging; [C] field techniques used to measurement of the channel geometry	75
Figure 2.7: Sample area for the twelve contour-derived Digital Elevation Models.....	75
Figure 2.8: Overview of the 10 m-resolution DTMs by interpolation technique	75
Figure 2.9: Relative accuracy of the 10-m resolution DEMs by interpolation technique	75
Figure 2.10: [A] Annual rainfall distribution and [B] monthly rainfall distribution in Nonthué, Sierra de la Ventana, Saldungaray and Paso de las Piedras over the period 1971-2010.	75
Figure 2.11: Frequency, return period and inter-annual variability of annual	

rainfall modules by site over the period 1971-2010	75
Figure 2.12: Long-term series (1971-2010) of monthly rainfall for [A] the upper river basin and [B] Paso de las Piedras	75
Figure 2.13: Error residuals from estimation of maximum daily temperature [Tmax] and minimum daily temperature [Tmin] in Saldungaray and Paso de las Piedras over the year 2010	75
Figure 2.14: Long-term series (1971-2010) of mean daily temperature in Saldungaray and Paso de las Piedras	75
Figure 2.15: Long-term series (1971-2010) of mean monthly potential evapotranspiration for [A] Saldungaray and [B] Paso de las Piedras	75
Figure 2.16: Short-term series (2009-2011, with blanks) of daily evaporation from the surface of the reservoir lake	75
Figure 2.17: Correlation between monthly evaporation and monthly potential evapotranspiration for Paso de las Piedras over the period 2009-2011	75
Figure 2.18: Hydrological Response Units (HRU) within the upper Sauce Grande Basin	75
Figure 2.19: Rainfall-runoff relationships by runoff curve number	75
Figure 2.20: Unit Hydrograph for 1 mm-depth rainfall excess within the upper Sauce Grande Basin	75
Figure 2.21: Comparison between measured and simulated daily flow rates for the upper Sauce Grande River over the calibration period	75
Figure 2.22: Rates of daily flow simulated from daily rainfall over the period 1956-2011	75
Figure 2.23: Scheme of the parameters used in estimation of the channel roughness	75
Figure 2.24: Mean daily flow rates for Bajo San José over the period 2009-2012 (above) and long-term series (1989-2012) of daily flow rates estimated for the river downstream.....	75
Figure 2.25: Parameters and measures used in estimation of rates of reservoir seepage	75
Figure 2.26: Overview of the procedures performed to generate data for hydrological assessment of the Sauce Grande River and series of data achieved.....	75

CHAPTER 3: The Water Balance of the Dam Reservoir

Figure 3.1: Annual water budget of the Paso de las Piedras Reservoir	119
Figure 3.2: Conceptual scheme of the reservoir capacity-yield-performance approach	125

Figure 3.3: Components of the water balance of the Paso de las Piedras Reservoir	128
Figure 3.4: Reservoir volume as function of water level and maps of reservoir coverage for three water level heights	129
Figure 3.5: Measured and simulated month-end reservoir volume over the period 2009-2010 (verification period).....	131
Figure 3.6: Original and corrected series of hourly flow data (gauged) for the upper Sauce Grande River over the years 2009 and 2010	133
Figure 3.7: Measured and simulated month-end reservoir volume over the period 2009-2010 (verification period) based on corrected series of gauged and simulated streamflow data	134
Figure 3.8: Temporal trends and descriptive statistics of monthly series of inflow volume by inflow component over the period 1989-2010	135
Figure 3.9: Correlograms of monthly series of inflow volume by inflow component showing autocorrelation functions at 66 lags.....	136
Figure 3.10: Temporal trends and descriptive statistics of monthly series of outflow volume by outflow component over the period 1989-2010	137
Figure 3.11: Temporal trends in water withdrawal based on [A] series of measured data over the period 2009-2010, and [B] historic records of annual water demand	138
Figure 3.12: Correlograms of monthly series of outflow volume by outflow component showing autocorrelation functions at 66 lags.....	139
Figure 3.13: Temporal trends, descriptive statistics and correlogram of series of monthly reservoir volume over the period 1989-2010.....	140
Figure 3. 14: Storage-yield relationships for the Paso de las Piedras Reservoir based on historic inflow data over the year 1978-2010	141
Figure 3.15: Storage-release relationships for the Paso de las Piedras reservoir as fraction of varying annual inflow volumes.....	143
Figure 3.16: Annual Impounded Runoff Index [QI] and Yield Index [YI] showing the degree of hydrologic regulation of the Sauce Grande River after closure of the Paso de las Piedras Dam in 1978	145
Figure 3.17: Monthly variations in the components of the reservoir water balance over the period 1989-2010.....	148
Figure 3.18: Relationship between annual rainfall [P] and evapotranspiration [PET] for the upper river basin and the area near the Paso de las Piedras Reservoir	150
Figure 3.19: Deviations of averaged series of the SPI and SRI for the WE season (Nov0-Feb1) and the CE season (jun-dec).....	153
Figure 3.20: Deviations of mean annual SRI/SPI indices (1971-2010) and mean annual reservoir water level elevation (1989-2010)	155

CHAPTER 4: Dam Impacts of First Order

Figure 4.1: Actual state of the Sauce Grande River for two reference reaches located upstream and downstream from the Paso de las Piedras Dam	164
Figure 4.2: Conceptual scheme of the Range of Variability Approach (RVA).....	167
Figure 4.3: Conceptual scheme of the Environmental Flow Components approach (EFC)	168
Figure 4.4: Conceptual illustration describing the direction and the level of meteorological sensitivity of water temperature regimes	173
Figure 4.5: Annual distribution of mean monthly flow within the unregulated Sauce Grande River over the period 1956-2010	176
Figure 4.6: Annual distribution of mean monthly flow within the regulated river over the period 1989-2010	176
Figure 4.7: Magnitude of annual flow extremes for different durations within the unregulated river (1956-2010) and the regulated river (1989-2010)	178
Figure 4.8: Number of annual flow reversals within the unregulated river (1956-2010) and the regulated river (1989-2010)	181
Figure 4.9: Flood magnitude and frequency within the upper Sauce Grande River (1956-2011).....	182
Figure 4.10: Environmental flow components within the unregulated river (1956-2011) and the regulated river (1989-2011).....	183
Figure 4.11: Map showing the location of air (A) and water (W) temperature gauging sites.....	185
Figure 4.12: Series of hourly flow and daily rainfall over (a) the summer period and (b) the winter period	186
Figure 4.13: Time series of hourly air and water temperature over the 30-day summer period.....	187
Figure 4.14: Time series of hourly air and water temperature over the 30-day winter period	188
Figure 4.15: Spatial distribution of mean water temperature and longitudinal profile of mean, maximum and minimum water temperature by monitoring period.....	190
Figure 4.16: Standardised (z-scores) hourly records of air temperature (120 station-days) and water temperature (450 station-days) by regime shape class	192
Figure 4.17: Standardised (z-scores) hourly records of air temperature (120 station-days) and water temperature (450 station-days) by regime magnitude class	194

Figure 4.18: Distribution of composite shape and magnitude classes over curves of daily mean temperature by site (right) and spatial distribution of the dominant composite classes of air and water temperature regime (left). Summer period.....	196
Figure 4.19: Distribution of composite shape and magnitude classes over curves of daily mean temperature by site (right) and spatial distribution of the dominant composite classes of air and water temperature regime (left). Winter period	197
Figure 4.20: Direction and frequency of associations between air and water temperature regime shape during the summer and winter periods	199
Figure 4.21: Direction and frequency of associations between air and water temperature regime magnitude during the summer and winter periods.....	200
Figure 4.22: Overview of the channel characteristics at each water temperature sampling site	202
Figure 4.23: Indicators of topographic, morphologic and groundwater influence on water temperature by site and river reach	203
Figure 4.24: Structure and distribution of water temperature sites as a function of two factors axis (F1 and F2)	205
Figure 4.25: Significance of the river flow regime and water temperature regime for the ecological integrity and geomorphic complexity of the river system.....	206
Figure 4.26: Daily flows classed by environmental flow component and 5-month running means of the SST 3.4 Index over the period 1956-2010.....	209
Figure 4.27: Scheme of downstream sources for flow.....	211
Figure 4.28: Ecodeficit and ecosurplus regions defined from areas between total-period flow duration curves for the regulated and the unregulated Sauce Grande River (1989-2010).....	211
Figure 4.29: Degree of hydrological alteration by flow regime metric	211
Figure 4.30: Dam-induced disruption of longitudinal fluvial processes and predicted morphological and ecological response of the river downstream	211

CHAPTER 5: Dam Impacts of Second Order

Figure 5.1: Actual state of the Sauce Grande River for two reference reaches located upstream and downstream from the Paso de las Piedras Dam	230
Figure 5.2: Longitudinal, lateral and temporal dimensions used in geomorphic analysis.....	232

Figure 5.3: Hierarchic levels of geomorphic analysis delineated to quantify morphological changes.....	234
Figure 5.4: Longitudinal, cross-sectional and plan view characteristics of the river segments upstream and downstream from the dam by time interval used in analysis (1961, 1981 and 2004).....	241
Figure 5.5: Characteristic cross sections within the upstream river segment (base flow stage).....	242
Figure 5.6: Characteristic cross sections within the downstream river segment (base flow stage)	243
Figure 5.7: Rates of channel activity and lateral migration within the upstream and downstream rivers for the time intervals 1961-1981 and 1981-2004.....	244
Figure 5.8: Examples of change in the channel planform within the upstream and downstream river segments for the time intervals 1961-1981 and 1981-2004	245
Figure 5.9: Rates of change in the channel width of the upstream and downstream rivers for the time intervals 1961-1981 and 1981-2004	247
Figure 5.10: Geomorphic sketch map, land use and representative cross sections for two sample reaches within the river upstream	- 250 -
Figure 5.11: Geomorphic sketch map, land use and representative cross sections for two sample reaches within the river downstream.....	- 251 -
Figure 5.12: Evidence of channel activity within the river upstream	252
Figure 5.13: Evidence of flooding within the river upstream	253
Figure 5.14: Evidence of human intervention within the river downstream.....	255
Figure 5.15: Channel materials and evidence of channel activity within the river upstream	256
Figure 5.16: Evidence of channel stabilisation within the river downstream	258
Figure 5.17: Spatial distribution of land cover types within the upstream river segment for the years 1961 (pre-disturbance), 1981 and 2004 (post-disturbance).....	262
Figure 5.18: Spatial distribution of land cover types within the downstream river segment for the years 1961 (pre-disturbance), 1981 and 2004 (post-disturbance).....	263
Figure 5.19: Number of patches by landcover type and class distribution as percentage of the fluvial corridor for the upstream and downstream river segments	264
Figure 5.20: Transitions in the fluvial landscape with time and overall trends in landscape dynamics.....	266

Figure 5.21: Progressive woody vegetation cover within the stream channel and the floodplain by river reach	269
Figure 5.22: Examples of in-channel vegetation cover within the upstream river environment	270
Figure 5.23: Examples of in-channel vegetation cover within the downstream river environment	271
Figure 5.24: Overview of the principal morphologic characteristics of the unregulated and the regulated rivers	276
Figure 5.25: Operations for dam construction by early 1970's	279
Figure 5.26: Conceptual scheme of processes of change at the class and landscape levels along the riverine landscape.....	282



CHAPTER 1: Research Context

Table 1.1: Hydrologic impacts of dams reported worldwide by dam purpose	16
Table 1.2: Examples of changes in the thermal regime of regulated rivers worldwide.....	20
Table 1.3: Examples of dam-induced geomorphic changes by world region	29
Table 1.4: Morphometric characteristics of the Sauce Grande Basin for the upper, middle and lower river sections	42
Table 1.5: Water use within the departments of Bahía Blanca and Coronel Rosales along the 20th Century.....	42
Table 1.6: Characteristics and main features integrating the Paso de las Piedras Complex	42

CHAPTER 2: Generation of baseline data

Table 2.1: Set of documents used in analysis.	69
Table 2.2: Absolute error (m) of the terrain models by interpolating method (TIN, IDW, TG, OK) and output grid size (50, 25 and 10 m resolution)	75
Table 2.3: Monthly pluviometric coefficients (%) for Nonthué [N], Sierra de la Ventana [SV], Saldungaray [S] and Paso de las Piedras [PP] based on long-term (1971-2010) averaged monthly rainfall.....	75
Table 2.4: Runoff Curve Number (CN) by Hydrological response Unit (HRU) identified within the upper river basin	75
Table 2.5: Areal-weighted runoff curve number (CN) by Hydrological Response Unit (HRU)	75
Table 2.6: Errors from simulation of daily flow rates for the upper Sauce Grande River over (a) the calibration period, and (b) the verification period.....	75

CHAPTER 3: The Water Balance of the Dam Reservoir

Table 3.1: Monthly and annual volumes of water withdrawal (hm ³) over the period 2009-2010. Mean monthly and annual volumes in bold.	137
Table 3.2: Patterns in inflow and outflow components of the water balance of the Paso de las Piedras Reservoir.....	146
Table 3.3: Correlation coefficients between components of the reservoir water balance.....	148

Table 3.4: Recurrence and duration (in months) of Warm and Cold ENSO episodes since 1970.....	152
Table 3.5: Frequency (%) of positive and negative anomalies of averaged SPI and SRI values occurring under ENSO conditions (WE, CE) and non-ENSO conditions (N) during (a) the WE season and (b) the CE season.....	154
 CHAPTER 4: Dam Impacts of First Order	
Table 4.1: Descriptive statistics of flow included within the IHA method and implications of each metric for the river morphology and the stream ecology.....	166
Table 4.2: Environmental Flow Components and implications for the river morphology, ecology and water quality.....	168
Table 4.3: Metrics used in the characterization of air and water temperature series.....	171
Table 4.4: Changes in the magnitude of mean monthly flow ($\text{m}^3.\text{s}^{-1}$) from the unregulated river upstream to the regulated river downstream over the period 1989-2010	177
Table 4.5: Changes in the magnitude of annual extreme flows ($\text{m}^3.\text{s}^{-1}$) from the unregulated river upstream to the regulated river downstream over the period 1989-2010	179
Table 4.6: Changes in the frequency and duration of high- and low-flow pulses from the unregulated river upstream to the regulated river downstream over the period 1989-2010.....	180
Table 4.7: Changes in the attributes of Environmental Flow Components (EFC) from the unregulated river upstream to the regulated river downstream over the period 1989-2010.....	184
Table 4.8: Summer thermal patterns by (a) air temperature site and (b) water temperature site	187
Table 4.9: Winter thermal patterns by (a) air temperature site and (b) water temperature site	189
Table 4.10: Frequency (as fractional proportion of days) of diurnal regime 'shape' classes by (a) air temperature site and (b) water temperature site	193
Table 4.11: Frequency (as fractional proportion of days) of diurnal regime 'magnitude' classes by (a) air temperature site and (b) water temperature site	195
Table 4.12: Frequency of composite regime shape and magnitude classes during summer and winter periods for (a) air temperature sites and (b) water temperature sites	195

Table 4.13: (a) Equitability (or stability) of diurnal regime shape and magnitude classes by air and water temperature site, and (b) climatic sensitivity of the shape and the magnitude of water temperature regimes to air temperature..... 199

Table 4.14: Pearson’s correlation matrix between physical indicators of thermal control 204

Table 4.15: Simplified classes of diurnal regime of water temperature and spatial distribution along the regulated Sauce Grande River..... 211

Table 4.16: Stream characteristics by water temperature site..... 211

CHAPTER 5: Dam Impacts of Second Order

Table 5.1: Mapped surfaces and representation symbols by scale of observation..... 233

Table 5.2: Quantitative and qualitative metrics used for morphologic description of the river segments and the reference reaches by time interval 235

Table 5.3: Metrics used in the quantification of the landscape structure (composition and configuration) by time step considered in analysis 238

Table 5.4: Morphologic characteristics of the sample reaches within (a) the upstream river segment and (b) the downstream river segment 249

Table 5.5: Instability Index by river reach and description of the overall reach state 259

Table 5.6: Distribution of landscape units by landscape class for the years 1961, 1981 and 2004 within (a) the river segment upstream and (b) the river segment downstream 267

Table 5.7: Aggregation Index (AI) and Division Index (DIV) by landscape class for the years 1961, 1981 and 2004 within (a) the river upstream and (b) the river downstream 268

Table 5.8: Dam-induced changes on three flow components of major geomorphic and ecologic significance 273



TABLE OF CONTENTS

INTRODUCTION.....	1
CHAPTER 1: Research Context	
1. The effects of dams on alluvial fluvial systems	13
1.1. First-order changes: regulated inputs below dams.....	14
1.1.1. <i>Changes in the river flow regime</i>	14
1.1.2. <i>Changes in the river water quality</i>	17
1.1.3. <i>Changes in the sediment load</i>	21
1.2. Second-order changes: the response of the river morphology	22
1.2.1. <i>The direction of geomorphic change</i>	23
1.2.2. <i>The magnitude of geomorphic vegetation change</i>	27
1.2.3. <i>Variability of changes with time and distance from the dam</i>	31
2. The Paso de las Piedras Dam on the Sauce Grande River	32
2.1. The vulnerability of local water resources	33
2.1.1. <i>The climate variability within SWBA</i>	34
2.1.2. <i>The topographic setting: landforms and materials</i>	40
2.1.3. <i>Linked physical processes and fluctuations in water resources</i>	43
2.2. The water demand: agriculture, population, and industry.....	44
2.3. Practices and policies of water management	46
2.3.1. <i>Advances in water management practices</i>	47
2.3.2. <i>The Paso de las Piedras Complex</i>	49
2.4. Water use and management face to the variability of water resources	53
3. Research purpose, hypothesis and structure.....	57
3.1. Research purpose	57
3.2. Research hypothesis	58
3.2.1. <i>Dam-induced hydrological regulation</i>	58
3.2.2. <i>Changes in hydrological conditions downstream</i>	59
3.2.3. <i>The response of the river downstream</i>	60
3.3. Articulation of the thesis manuscript	61
3.4. Working scales	62
3.4.1. <i>The spatial dimension</i>	62
3.4.2. <i>The temporal dimension</i>	62

CHAPTER 2: Generation of baseline data

Introduction.....	67
1. Methods.....	68
1.1. Assemblage of pre-existing data.....	68
1.1.1. <i>Processing and classification of documents and imagery</i>	68
1.1.2. <i>Time series assemblage</i>	69
1.2. Terrain modelling.....	71
1.3. Generation of climatic data.....	73
1.3.1. <i>Filling of rainfall series</i>	73
1.3.2. <i>Assemblage of rainfall series</i>	73
1.3.3. <i>Filling of air temperature series</i>	74
1.3.4. <i>Estimation of potential evapotranspiration and evaporation</i>	74
1.4. Hydrological modelling of the upper river basin.....	74
1.4.1. <i>Delineation of Hydrologic Response Units (HRU)</i>	74
1.4.2. <i>Estimation of direct runoff rates</i>	75
1.4.3. <i>Estimation of the time of concentration</i>	75
1.5. Simulation of flow within the unregulated river.....	76
1.5.1. <i>The RainOff-empirical model</i>	76
1.5.2. <i>Model calibration and verification</i>	79
1.6. Estimation of flow within the regulated river.....	80
1.6.1. <i>Computation of the downstream hydrograph</i>	80
1.6.2. <i>Inspection of rates of reservoir seepage</i>	83
2. Results.....	84
2.1. The terrain model of the river basin.....	84
2.1.1. <i>The quality of the sample models</i>	84
2.1.2. <i>Model selection and running</i>	87
2.2. Climatic data series.....	87
2.2.1. <i>Long-term series of rainfall</i>	88
2.2.2. <i>Long-term series of air temperature</i>	92
2.2.3. <i>Temperature-derived time series</i>	93
2.3. The hydrological model of the upper river basin.....	96
2.3.1. <i>Physiographic characteristics of the drainage basin</i>	96
2.3.2. <i>Hydrological Response Units</i>	98
2.3.3. <i>Direct runoff depth</i>	99
2.3.4. <i>Temporal distribution of runoff</i>	100
2.4. Daily flow rates for the unregulated river.....	101

2.5. Daily flow rates for the regulated river	104
2.5.1. Daily flow rates over the period 2009-2012	104
2.5.2. Daily flow rates over the long term	104
2.5.3. The sources for downstream flow	106
3. Discussion and Conclusions.....	107
3.1. Spatial data.....	107
3.2. Climatic data	110
3.2.1. Rainfall data.....	110
3.2.2. Air temperature data	111
3.3. Hydrologic data.....	112
3.3.1. The hydrology of the river basin	112
3.3.2. Rainfall-runoff modelling.....	113
3.4. Conclusions.....	114

CHAPTER 3: The Water Balance of the Dam Reservoir

Introduction.....	119
1. Methods.....	121
1.1. The Water Balance Model of the reservoir	121
1.1.1. Time series assemblage.....	121
1.1.2. Model running	123
1.2.3. Model verification	123
1.2. Time series assessment	124
1.3. Determining the reservoir size and performance	124
1.3.1. Question 1: measuring storage-yield relationships	125
1.3.2. Question 2: measuring the reservoir performance	125
1.3.3. Predicting scenarios of inflow volume and reservoir response	126
1.4. Quantification of the degree of impoundment	127
2. Results	128
2.1. The Water Balance Model of the Paso de las Piedras Reservoir	128
2.1.1. Reservoir volume-surface area-elevation relationships	128
2.1.2. Model running and verification	130
2.1.3. Flow data recalibration	132
2.1.4. Water Balance Model re-running	133
2.2. Patterns in the reservoir hydrology	134
2.2.1. Patterns in inflow components	134
2.2.2. Patterns in outflow components	136
2.2.3. Patterns in water storage	139

2.3. Reservoir size-yield-performance	140
2.3.1. Storage-yield relationships	140
2.3.2. Storage-release relationships	142
2.4. The degree of impoundment	144
3. Discussion and Conclusions.....	146
3.1. Patterns in the reservoir hydrology	146
3.1.1. Synchrony in the seasonality of inflows and outflows.....	146
3.1.2. Inter-annual variability vs inter-annual reliability.....	147
3.1.3. The causes of inter-annual variability in inflow components	151
3.2. Drought and water demand: constraints for reservoir management	154
3.3. The degree of impoundment of the Sauce Grande River.....	156
3.4. Applicability of the methods used in analysis	157
3.5. Conclusions.....	159

CHAPTER 4: Dam Impacts of First Order

Introduction.....	163
1. Methods.....	165
1.1. Quantifying dam impacts on the river flow regime	165
1.1.1. Computing flow statistics	165
1.1.2. Assessing the range of flow variability	167
1.1.3. Evaluating Environmental Flow Components	167
1.1.4. Assessment of the river flow predictability	169
1.1.5. Quantification of the degree of hydrologic alteration	169
1.2. Quantifying dam impacts on the river water temperature.....	170
1.2.1. Temperature data collection	170
1.2.2. Time series assessment and thermal metrics	170
1.2.3. Classification of diurnal regimes of air and water temperature	171
1.2.4. Quantification of the climatic sensitivity of diurnal water temperature regimes	172
1.2.5. Inspection of structural characteristics of the stream	173
2. Results.....	175
2.1. Dam impacts on the downstream river flow regime	175
2.1.1. Changes in the attributes of the river flow regime.....	175
2.1.2. Changes in environmental flow components	182
2.1.3. Flow predictability.....	184
2.2. Dam impacts on the river water temperature	185
2.2.1. Changes in temporal patterns of river water temperature	186

2.2.2. <i>Changes in the magnitude and timing of diurnal water temperature regimes</i>	191
2.2.3. <i>Temporal stability and climatic sensitivity of water temperature regimes</i>	198
2.2.4. <i>Other factors influencing river thermal variability</i>	200
3. Discussion and Conclusions.....	206
3.1. Critical alteration of the river flow regime	207
3.1.1. <i>The natural river flow regime</i>	207
3.1.2. <i>Sources for flow within the regulated Sauce Grande River</i>	209
3.1.3. <i>Ecodeficit: a simplified measure of hydrological disruption in regulated rivers</i>	210
3.1.4. <i>The degree of hydrological alteration of the regulated Sauce Grande River</i>	212
3.1.5. <i>Changes in environmental flow components</i>	215
3.2. Critical alteration of the river water temperature.....	216
3.2.1. <i>The unregulated river thermal regime</i>	216
3.2.2. <i>Changes in the absolute magnitude of the downstream thermographs</i>	217
3.2.3. <i>Changes in the relative magnitude and timing of diurnal regimes</i>	218
3.2.4. <i>Causes of thermal change and downstream persistence</i>	219
3.2.5. <i>Other potential drivers of river thermal change</i>	220
3.3. Applicability of the methods used in analysis.....	223
3.4. Conclusions	224

CHAPTER 5: Dam Impacts of Second Order

Introduction	229
1. Methods.....	231
1.1. Scales of analysis	231
1.2. Mapped surfaces.....	232
1.3. Quantification of change in the fluvial morphology	234
1.3.1. <i>Level I: geomorphic analysis at the scale of the river segment</i>	235
1.3.2. <i>Level II: geomorphic analysis at the scale of the river reach</i>	236
1.3.3. <i>Quantification of geomorphic change</i>	236
1.4. Quantification of change in the fluvial landscape.....	238
2. Results	240
2.1. Changes in the river morphology	240
2.1.1. <i>Level I: Morphologic changes at the scale of the river segment</i>	240
2.1.2. <i>Level II: Morphologic changes at the scale of the river reach</i>	247

2.2. Changes in the fluvial landscape.....	259
2.2.1. <i>Brief description of functional fluvial units</i>	260
2.2.2. <i>Dynamics in the landscape composition</i>	260
2.2.3. <i>Dynamics in the landscape configuration</i>	265
2.2.4. <i>Afforestation processes at the scale of the river reach</i>	268
3. Discussion and Conclusions.....	272
3.1. A threshold matter: a matter of thresholds.....	272
3.1.1. <i>Altered flow thresholds below the Paso de las Piedras Dam</i>	273
3.1.2. <i>Predicted direction of channel adjustment</i>	274
3.2. Changes in the river morphology.....	275
3.2.1. <i>Between dynamic and moribund stability</i>	276
3.2.2. <i>Causes of unapparent geomorphic change</i>	278
3.3. Changes in the fluvial landscape.....	280
3.3.1. <i>Dynamics in the landscape structure</i>	280
3.3.2. <i>Processes in the fluvial landscape</i>	281
3.3.3. <i>Variations in the nature of afforestation processes along the river</i> <i>course</i>	283
3.4. Conclusions.....	285
 CONCLUSIONS AND PERSPECTIVES	 287
Résumé.....	293
Resumen.....	303
Reference List	313
List of Figures	341
List of tables.....	349

ABSTRACT

Despite the regional importance of the Sauce Grande River as main source for water supply and the large capacity of the Paso de las Piedras Reservoir, both the hydrology of the river basin and the effects of the impoundment on the river environment remain poorly evaluated. This study provides the very first assessment of the degree of flow regulation induced by the Paso de las Piedras Dam on the middle section of the Sauce Grande River, and quantifies its impacts on the hydrology, morphology and patterns of water temperature of the river downstream from the impoundment. In addition to providing new information on the response of regulated rivers to upstream impoundment and on the effects of impoundment on the Sauce Grande River specifically, this study generates spatial, climatic and hydrologic data and implements a methodological framework to hydrological assessment of ungauged basins.

The methods include a set of procedures performed to generate data and a set of procedures performed to hydrological and morphological assessment. Methods used to generate data include (i) terrain modelling of the river basin, (ii) filling and modelling of climatic data, (iii) hydrological modelling of the upper river basin, and (iv) flow simulation and calculation. Methods used for hydrological and morphological assessment include (i) inspection of the water balance of the dam reservoir and quantification of the reservoir size-yield-performance relationships, (ii) quantification of the degree of hydrological alteration of the river downstream, (iii) classification of diurnal regimes of water temperature and quantification of their climatic sensitivity, and (iv) GIS-based diachronic analysis of change in the fluvial forms and the fluvial landscape.

Results revealed that reservoir inflows are driven by varying climate conditions, whereas reservoir outflows are constrained by the dam purpose for water supply. Large volumes of water are yielded annually (73 % of the mean annual runoff) and the remaining volume is conserved within the reservoir for periods of drought. These patterns of flow regulation have seriously affected the hydrology and water quality of the river downstream. Floods were fully eliminated and the magnitude and frequency of high and low flows were reduced dramatically, with substantial increase in the duration of similar flow conditions. Furthermore, summer temperatures were depressed, winter temperatures were increased, and diurnal fluctuations were altered in both magnitude and timing. Analysis of the geomorphic response to altered hydrology revealed fluvial stability. Lateral and vertical channel activity was related to human intervention to facilitate the evacuation of dam outlets and spills more than to natural adjustments to reduced flow discharge and sediment load. The reduced flow, even if sediment-free, is incompetent to work its channel and at present, the downstream channel morphology is a relic of a fluvial environment created in the past under conditions of higher energy.

The new climatic, hydrologic and morphologic information yielded herein has triple applicability: (i) it informs dam managers about the complex behaviour of the river system, (ii) it contributes to improve reservoir operation procedures while maintaining the overall integrity of the river system, and (iii) it provides a consistent scientific platform on which to base further research efforts conducting to an interdisciplinary framework of river restoration. Furthermore, the methods implemented in this research are widely transferable to hydrological assessment of ungauged basins worldwide, with special applicability to semiarid regions.